frontiers | Research Topics

Astrocytic synaptic plasticity in epilepsy: From synapses to circuits

Edited by
Sandra Henriques Vaz, Vincenzo Crunelli, Giuseppe Di Giovanni and Ana Maria Sebastiao

Coordinated by
Tatiana P. Morais

Published in
Frontiers in Molecular Neuroscience

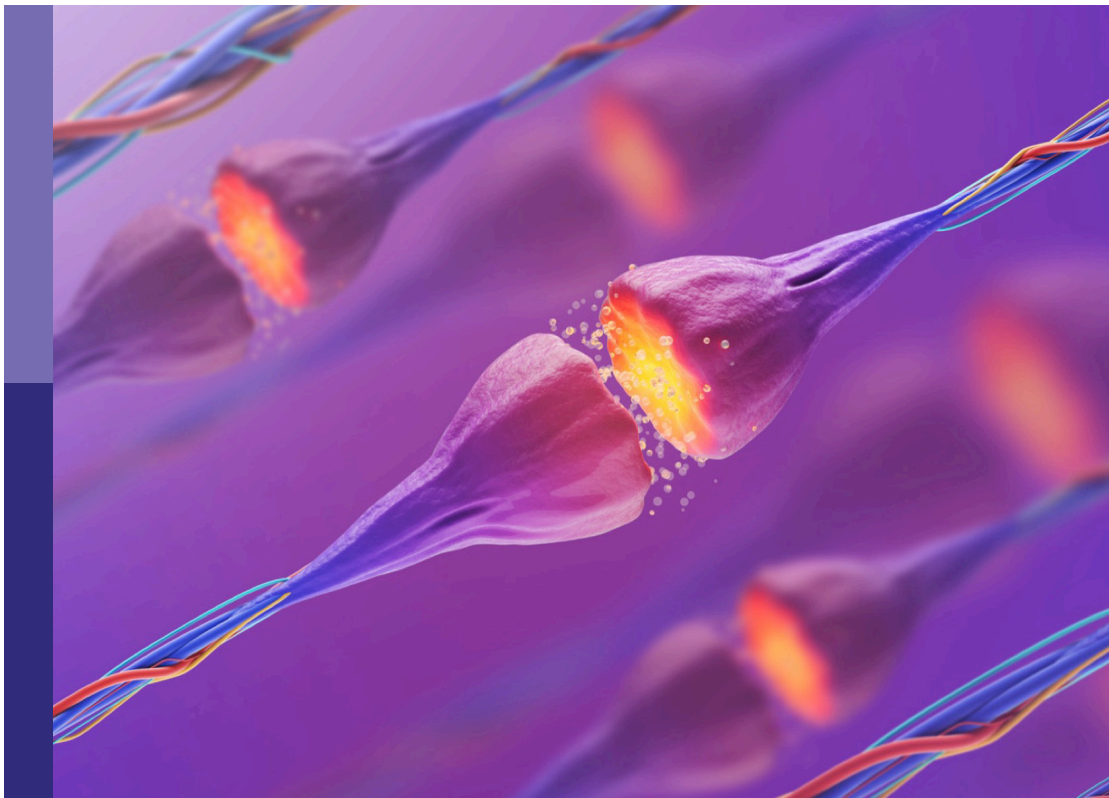

ISSN 1664-8714
ISBN 978-2-8325-3736-7
DOI 10.3389/978-2-8325-3736-7

About Frontiers

Frontiers is more than just an open access publisher of scholarly articles: it is a pioneering approach to the world of academia, radically improving the way scholarly research is managed. The grand vision of Frontiers is a world where all people have an equal opportunity to seek, share and generate knowledge. Frontiers provides immediate and permanent online open access to all its publications, but this alone is not enough to realize our grand goals.

Frontiers journal series

The Frontiers journal series is a multi-tier and interdisciplinary set of open-access, online journals, promising a paradigm shift from the current review, selection and dissemination processes in academic publishing. All Frontiers journals are driven by researchers for researchers; therefore, they constitute a service to the scholarly community. At the same time, the *Frontiers journal series* operates on a revolutionary invention, the tiered publishing system, initially addressing specific communities of scholars, and gradually climbing up to broader public understanding, thus serving the interests of the lay society, too.

Dedication to quality

Each Frontiers article is a landmark of the highest quality, thanks to genuinely collaborative interactions between authors and review editors, who include some of the world's best academicians. Research must be certified by peers before entering a stream of knowledge that may eventually reach the public - and shape society; therefore, Frontiers only applies the most rigorous and unbiased reviews. Frontiers revolutionizes research publishing by freely delivering the most outstanding research, evaluated with no bias from both the academic and social point of view. By applying the most advanced information technologies, Frontiers is catapulting scholarly publishing into a new generation.

What are Frontiers Research Topics?

Frontiers Research Topics are very popular trademarks of the *Frontiers journals series*: they are collections of at least ten articles, all centered on a particular subject. With their unique mix of varied contributions from Original Research to Review Articles, Frontiers Research Topics unify the most influential researchers, the latest key findings and historical advances in a hot research area.

Find out more on how to host your own Frontiers Research Topic or contribute to one as an author by contacting the Frontiers editorial office: frontiersin.org/about/contact

Astrocytic synaptic plasticity in epilepsy: From synapses to circuits

Topic editors
Sandra Henriques Vaz — Universidade de Lisboa, Portugal
Vincenzo Crunelli — Cardiff University, United Kingdom
Giuseppe Di Giovanni — University of Malta, Malta
Ana Maria Sebastiao — University of Lisbon, Portugal

Topic coordinator
Tatiana P. Morais — University of Malta, Malta

Citation
Vaz, S. H., Crunelli, V., Di Giovanni, G., Sebastiao, A. M., Morais, T. P., eds. (2023). *Astrocytic synaptic plasticity in epilepsy: From synapses to circuits*. Lausanne: Frontiers Media SA. doi: 10.3389/978-2-8325-3736-7

Table of contents

frontiers in Molecular Neuroscience

ORIGINAL RESEARCH
published: 21 March 2022
doi: 10.3389/fnmol.2022.829506

Hemisynapse Formation Between Target Astrocytes and Cortical Neuron Axons *in vitro*

*Zenghui Teng and Kurt Gottmann**

Institute of Neuro- and Sensory Physiology, Medical Faculty, Heinrich Heine University Düsseldorf, Düsseldorf, Germany

One of the most fundamental organizing principles in the mammalian brain is that neurons do not establish synapses with the other major cell type, the astrocytes. However, induced synapse formation between neurons and astrocytes appears conceivable, because astrocytes are well known to express functional ionotropic glutamate receptors. Here, we attempted to trigger synapse formation between co-cultured neurons and astrocytes by overexpressing the strongly synaptogenic adhesion protein LRRTM2 in astrocytes physically contacted by cortical axons. Interestingly, control experiments with immature cortical astrocytes without any overexpression resulted in the induction of synaptic vesicle clustering in contacting axons (hemisynapse formation). This synaptogenic activity correlated with the endogenous expression of the synaptogenic protein Neuroligin1. Hemisynapse formation was further enhanced upon overexpression of LRRTM2 in cortical astrocytes. In contrast, cerebellar astrocytes required overexpression of LRRTM2 for induction of synaptic vesicle clustering in contacting axons. We further addressed, whether hemisynapse formation was accompanied by the appearance of fully functional glutamatergic synapses. We therefore attempted to record AMPA receptor-mediated miniature excitatory postsynaptic currents (mEPSCs) in innervated astrocytes using the whole-cell patch-clamp technique. Despite the endogenous expression of the AMPA receptor subunits GluA2 and to a lesser extent GluA1, we did not reliably observe spontaneous AMPA mEPSCs. In conclusion, overexpression of the synaptogenic protein LRRTM2 induced hemisynapse formation between co-cultured neurons and astrocytes. However, the formation of fully functional synapses appeared to require additional factors critical for nano-alignment of presynaptic vesicles and postsynaptic receptors.

Keywords: target astrocytes, synapse formation, hemisynapse, synaptogenic protein, LRRTM2

OPEN ACCESS

Edited by:
Christian Henneberger,
University of Bonn, Germany

Reviewed by:
Janosch P. Heller,
Dublin City University, Ireland
Christian Lohr,
University of Hamburg, Germany

***Correspondence:**
Kurt Gottmann
Kurt.Gottmann@uni-duesseldorf.de

Specialty section:
This article was submitted to Molecular Signalling and Pathways, a section of the journal Frontiers in Molecular Neuroscience

Received: *05 December 2021*
Accepted: *08 February 2022*
Published: *21 March 2022*

Citation:
Teng Z and Gottmann K (2022) Hemisynapse Formation Between Target Astrocytes and Cortical Neuron Axons in vitro. Front. Mol. Neurosci. 15:829506. doi: 10.3389/fnmol.2022.829506

INTRODUCTION

Synapse formation is an essential neurodevelopmental process that enables neurons to transfer, process, and store information in highly connected cellular networks. Molecular interactions between pre- and postsynaptic partner neurons are thought to be needed to establish exactly aligned pre- and postsynaptic compartments (Südhof, 2018; Sanes and Zipursky, 2020; Südhof, 2021).

A relatively simple, but fundamental molecular mechanism might be the transsynaptic interaction of pre- and postsynaptically localized transmembrane receptor proteins (Südhof, 2008; Shen and Scheiffele, 2010; Siddiqui and Craig, 2011). These transsynaptic adhesion molecules would then initiate pre- and postsynaptic signaling pathways ultimately resulting in both presynapse formation and postsynaptic differentiation (Takahashi and Craig, 2013; Südhof, 2017; Gomez et al., 2021).

A number of transsynaptic adhesion molecules that induce synaptic vesicle clustering in "presynaptic" neurons have been identified and have been termed synaptogenic proteins (Shen and Scheiffele, 2010; Siddiqui and Craig, 2011; de Wit and Ghosh, 2014; Südhof, 2017). In a landmark study, Scheiffele et al. (2000) demonstrated that expression of the postsynaptic adhesion protein Neuroligin1 in non-neural HEK293 cells induced synaptic vesicle clustering in contacting axons reminiscent of presynapse formation. Other neuronal adhesion proteins such as e.g., SynCAM1 (Biederer et al., 2002), NGL-3 (Woo et al., 2009), Slitrks (Yim et al., 2013), and LRRTM2 (de Wit et al., 2009; Ko et al., 2009; Linhoff et al., 2009) were subsequently described to exhibit a similar synaptogenic activity with LRRTM2 showing a particularly strong vesicle clustering effect. These induced vesicle clusters were capable of releasing vesicles resulting in postsynaptic currents when glutamate receptors were highly overexpressed in non-neural cells (Biederer et al., 2002; Fu et al., 2003; Sara et al., 2005; de Wit et al., 2009; Linhoff et al., 2009). However, this type of forced presynaptic differentiation was not accompanied by the formation of an organized postsynaptic specialization, and therefore the term hemisynapse formation was coined (Craig et al., 2006) to describe this partial synapse formation. Hemisynapse formation does not only occur with postsynaptic adhesion proteins acting on contacting neurons, but also with presynaptic adhesion proteins acting on neurons that serve as postsynaptic targets (Siddiqui and Craig, 2011; Südhof, 2017). As an example, expression of beta-neurexin in fibroblasts induced postsynaptic differentiation in neurons contacted by these fibroblasts (Graf et al., 2004; Craig and Kang, 2007).

Overexpression of these synaptogenic proteins in neurons contacting other neurons in standard neuronal cell cultures led to the induction of additional *bona fide* synapses consisting of both pre- and postsynaptic specializations. This has been demonstrated for prototypical synaptogenic proteins such as Neuroligin1, SynCAM1, and LRRTM2 (Chih et al., 2005; Sara et al., 2005; de Wit et al., 2009; Ko et al., 2009; Dagar and Gottmann, 2019). In addition, these induced synapses were fully functional as demonstrated by patch-clamp recordings of miniature excitatory postsynaptic currents (mEPSCs) that were mediated by AMPA receptors (Sara et al., 2005; Wittenmayer et al., 2009; Stan et al., 2010). From these observations, it appears conceivable that synaptogenic proteins might also be able to induce *bona fide* functional synapses if expressed in the second major neural cell type, the astrocytes. Cortical and cerebellar astrocytes are well known to endogenously express functional AMPA receptors (e.g., Sontheimer et al., 1988; von Blankenfeld and Kettenmann, 1991; Burnashev et al., 1992; Gallo et al., 1994; David et al., 1996; Ceprian and Fulton, 2019), but do not form synapses with neurons *in vivo*. In line with a potential of astrocytes to form artificial synapses with neurons, non-standard glial cell types, i.e., NG2 cells (Bergles et al., 2010; Sakry et al., 2011) and some glioblastoma cells (Venkataramani et al., 2019; Venkatesh et al., 2019) have been described to establish functional, AMPA receptor containing synapses with presynaptic neurons. However, whether artificial *bona fide* synapse formation is induced by expression of synaptogenic proteins in cultured astrocytes, which are in physical contact with neuronal axons, has not been investigated.

In this paper, we used expression of the postsynaptic adhesion protein LRRTM2 in cultured cortical and cerebellar astrocytes that were contacted by cortical axons to study whether artificial formation of fully functional synapses can occur in neuron-astrocyte pairs. Unexpectedly, we found that immature cortical astrocytes induced synaptic vesicle clusters in contacting axons even without LRRTM2 expression, while cerebellar astrocytes required LRRTM2 expression for induction of synaptic vesicle clustering. This finding correlated with the expression of Neuroligin1 in cortical astrocytes. Because both types of cultured astrocytes expressed AMPA receptor subunits, we expected to observe functional synapses in LRRTM2 expressing astrocytes. However, patch-clamp recordings in LRRTM2 expressing astrocytes contacted by axons did not reliably reveal AMPA receptor-mediated mEPSCs This indicates that although hemisynapse formation is induced by a single type of synaptogenic protein, artificial formation of fully functional synapses in neuron-astrocyte pairs requires additional molecular mechanisms.

MATERIALS AND METHODS

All experiments were done in accordance with the relevant guidelines.

Cell Culture

Co-cultures of cortical explants and dissociated astrocytes or dissociated cortical neurons (positive controls) were done as described previously (Gottmann et al., 1997; Mohrmann et al., 1999). In brief, cortical and cerebellar astrocytes were obtained from newborn (P0) mouse cortex and P7 mouse cerebellum (brains from C57BL/6 wildtype mice) by mechanical dissociation after trypsin treatment, and further cultivation for 10–12 days in flasks with BME medium (Gibco) containing 10% FBS, L-glutamine (2 mM), glucose (20 mM), insulin transferrin selenium A (ITS) and penicilline-streptomycine (1%). This pre-cultivation step of dissociated cells was done to increase the number of astrocytes and to obtain cultures dominated by proliferating astrocytes. In cerebellar cultures, this might have led to a relative loss of Bergmann glial cells as indicated by the high percentage of GluA2 expressing astrocytes (see section "Results"). As positive controls, dissociated cortical neurons were prepared by dissociating the cortical tissue from cortices of E18-19 embryos (C57BL/6 wildtype mice) after trypsin treatment.

Cortical explants were prepared by cutting the occipital cortex from cortices of E18-19 embryos (C57BL/6 wildtype mice) into

tissue blocks of 0.5–0.8 mm diameter. These explants were placed in the center of polyornithine-coated glass coverslips, and cultured for 5 days with Neurobasal (NB) medium (Gibco) containing 2% B27 supplement, 0.5% Glutamax-1 supplement (Gibco) and 1% penicilline-streptomycine. For co-cultures, re-dissociated astrocytes or freshly dissociated neurons were added to the explant cultures and were further co-cultured for 12 days (see **Figure 1**).

Magnetofection and Plasmids

Magnetic nanoparticles (NeuroMag; OZ Biosciences) were used to transfect the co-cultured astrocytes using a previously described transfection procedure (van Stegen et al., 2017). In brief, mixed complexes including plasmid DNA and magnetic nanoparticles in NB medium without supplements were incubated for 20 min at room temperature. After that, the DNA/NeuroMag-complexes were added to the cultures in 6-well plates for 30 min at 37°C. An oscillating magnetic plate (Magnetofection^{TM}, magnefect LT; nanoTherics) was used to enhance the transfection efficiency. Fresh NB medium was added after transfection. The plasmids pEGFP-N1 (Clontech) and myc-LRRTM2 (gift from Dr. J. de Wit, Leuven, Belgium) were used. Co-expression of myc-LRRTM2 and EGFP in astrocyte co-transfection experiments was confirmed by immunocytochemical staining for the myc tag (**Supplementary Figure 1**).

Immunocytochemistry

Immunocytochemistry was performed using a standard staining protocol as described previously (Nieweg et al., 2015). The following primary antibodies were used: Anti-vGlut1 (Guinea pig polyclonal, 1:1,000, Synaptic Systems Cat# 135304, RRID: AB_887878, Göttingen, Germany); Anti-GFAP (Chicken polyclonal, 1:1,000, Millipore Cat# AB5541, RRID: AB_177521, Burlington, MA), United States; Anti-MAP2 (Chicken polyclonal, 1:1,000, Abcam Cat# Ab92434, RRID: AB_2138147, Cambridge, United Kingdom); Anti-Tau (Monoclonal mouse, 1:1,000, Synaptic Systems Cat# 314011, RRID: AB_10805762, Göttingen, Germany). Anti-NLG1 (Rabbit polyclonal, 1:1,000, Synaptic Systems Cat# 129003, RRID: AB_887746, Göttingen, Germany); Anti-GluA1 (Rabbit polyclonal, 1:1,000, Sigma-Aldrich Cat# AB 1504, RRID: AB_2113602, St. Louis, MO, United States); Anti-GluA2 (Guinea pig polyclonal, 1:500, Synaptic Systems Cat# 182105, RRID: AB_2619875, Göttingen, Germany). Anti-myc (Monoclonal mouse, 1:1,000, Thermo Fisher Cat#_46-0603, RRID: AB_2556560, MA, United States). The GluA1 and GluA2 antibodies were validated in this study by staining standard cultures of mouse cortical neurons.

The secondary antibodies used were: AF555 goat anti-mouse (1:1,000, Cat# A-21424, RRID: AB_1417801), AF555 goat anti-pig (1:1,000, Cat# A-21435, RRID: AB_2535856), AF555 goat anti-rabbit (1:1,000, Cat# A-21429, RRID: AB_2535850), AF555 goat anti-chicken (1:1,000, Cat# A-21437, RRID: AB_2535858); AF488 goat anti-mouse (1:1,000, Cat# A-11029, RRID: AB_2534088), AF488 goat anti-guinea pig (1:1,000, Cat# A-11073, RRID: AB_2534117), AF488 goat anti-rabbit (1:1,000, Cat# A-11034, RRID: AB_2576217), AF488 goat anti-chicken (1:1,000, Cat# A-11039, RRID: AB_2534096), all from Life Technologies (Carlsbad, CA, United States). We routinely performed negative controls without addition of primary antibodies to validate the specificity of the immunostainings.

Fluorescence Imaging and Data Analysis

Wide-field fluorescence imaging was performed using an inverted motorized Axiovert 200 M microscope (Zeiss) as described previously (Nieweg et al., 2015; van Stegen et al., 2017) to image the cultured astrocytes that exhibited a very flat morphology on the plane cover slips. In brief, fluorescence images were obtained with a 12 bit CoolSnap ES2 CCD camera (Photometrics) using VisiView software (Visitron Systems). The following filter sets (Zeiss) were used: (1) excitation 485/20 nm, beam splitter 510 nm, emission 515/565 nm (GFAP; MAP2; EGFP); (2) excitation 545/25 nm, beam splitter 570 nm, emission 605/70 nm (Tau; vGlut1; NLG1; GluA1; GluA2). For data analysis, images were thresholded using ImageJ software. vGlut1 puncta located on cortical or cerebellar astrocytes were identified by analyzing overlay images (**Supplementary Figure 2**).

Electrophysiology and Data Analysis

Whole-cell voltage-clamp recordings were obtained from the target astrocytes or neurons at room temperature using an Axopatch 200B patch-clamp amplifier and pClamp 11.0.3 software (Molecular Devices, SanJose, CA) as described previously (Mohrmann et al., 1999). The patch pipette was filled with intracellular solution containing (in mM): 110 KCl, 20 HEPES, 10 EGTA, 0.25 CaCl2 with pH adjusted to 7.3. The standard extracellular solution contained (in mM) 130 NaCl, 3 KCl, 2.5 $CaCl_2$, 1 $MgCl_2$, and 20 HEPES, with pH adjusted to 7.3. The high [K^+] extracellular solution contained (in mM) 112 NaCl, 40 KCl, 2.5 $CaCl_2$, 1 $MgCl_2$, and 20 HEPES, with pH adjusted to 7.3. AMPA receptor-mediated miniature EPSCs (1 μM TTX, 10μM gabazine added) were recorded at a holding potential of -60 mV.

Statistics

All data are given as means ± SEM. Statistical significance was determined by Student's *t*-test, if applicable, or by one-way ANOVA in combination with Tuckey's *post-hoc* test by using SigmaPlot 11 software.

RESULTS

Cortical Neuron Axons Physically Contact Immature Astrocytes in Culture

To study synaptogenic events occurring between presynaptic axons and astrocytes, we used a co-culture system consisting of mouse cortical explants (embryonic day 18–19) with axon outgrowth and added dissociated astrocytes (**Figures 1A,B**). Using dissociated neurons as postsynaptic cells, a similar co-culture system has previously been described to enable efficient functional synapse formation (Gottmann et al., 1997; Mohrmann et al., 1999; **Figure 1C**). Two types of

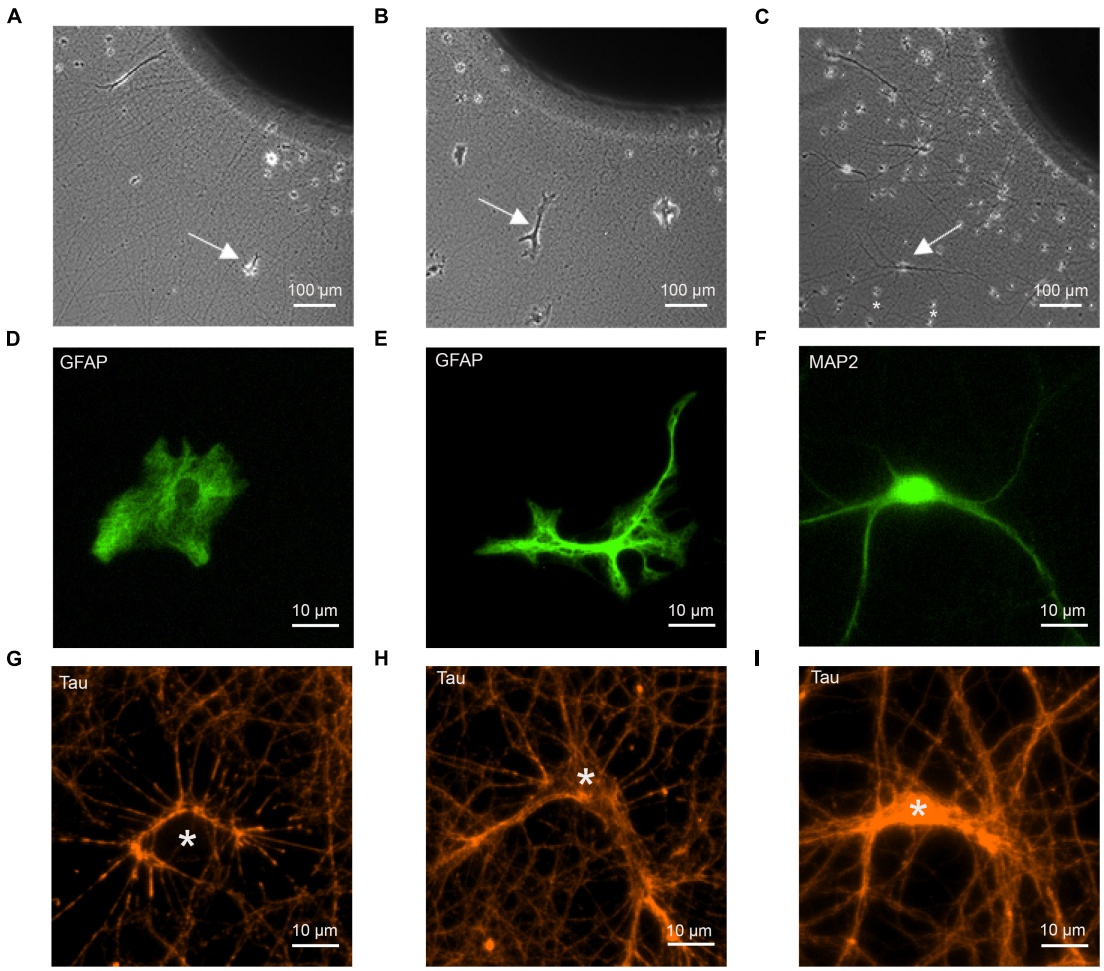

FIGURE 1 | Co-cultures of cortical explants with axon outgrowth and immature astrocytes as target cells. The following target cells were added to explants: **(A,D,G)** cortical astrocytes; **(B,E,H)** cerebellar astrocytes; **(C,F,I)** cortical neurons (control). **(A–C)** Photomicrographs of co-cultures of cortical explants with axon outgrowth and target cells (white arrows indicate target cells). 12 days of co-culture for target cells. Explants were cultured 5 days before addition of dissociated target cells. In C small cells (marked by *) that occasionally migrated out of the explant (presumably microglia cells) are present in addition to co-cultured neurons. These cells were clearly distinguished from neurons and astrocytes by their different morphology. **(D–F)** Immunostaining of target cells for GFAP **(D,E)** and MAP2 **(F)** to visualize the morphology of target cells. **(G–I)** Immunostaining of outgrowing axons for tau to demonstrate formation of physical contacts between axons and target cells. White stars indicate the cell bodies of target cells. Cells in **(D–I)** are not identical.

immature astrocytes were used as potential target cells for cortical axons: GFAP-immunopositive astrocytes from newborn (P0) mouse cortex, and GFAP-immunopositive astrocytes from P7 mouse cerebellum. At 12 days in co-culture, cerebellar astrocytes showed a more ramified morphology (**Figure 1E**) as compared to the processes-lacking morphology of cortical astrocytes (**Figure 1D**), suggesting that cortical astrocytes were more immature. As positive control for synapse formation, dissociated MAP2-immunopositive neurons from embryonic day 18–19 mouse cortex were used as target cells (**Figure 1F**). To study whether cortical axons physically contacted immature astrocytes in a way comparable to contacting cortical neurons, we immunostained axons for tau protein, and imaged axon-astrocyte contacts (**Figures 1G,H**). We observed that cortical axons physically contacted both, cortical and cerebellar astrocytes in a way qualitatively comparable to contacting neurons (**Figure 1I**). This indicates that the basic physical contacts required for synapse formation between axons and immature astrocytes were established in culture.

Immature Cortical Astrocytes Induce Synaptic Vesicle Clustering in Contacting Axons

We next wanted to study, whether physical contact between axons and immature astrocytes is accompanied by clustering of synaptic vesicles in contacting axons similar to synaptogenesis in neurons. We visualized synaptic vesicle clusters in axons by immunostaining for the synaptic vesicle protein vGlut1. We analyzed the resulting fluorescent puncta in explant axons with and without contact to target cells by determining vGlut1

puncta area as a quantitative measure of vesicle clustering (**Supplementary Figure 2**). Unexpectedly, vGlut1 puncta in axons on immature cortical astrocytes (co-stained for GFAP) were significantly larger as compared to vGlut1 puncta in axons not contacting target cells (**Figure 2A**). Using control neurons as target cells (co-stained for MAP2), we observed a similar significant difference between vGlut1 puncta in axons on neurons and vGlut1 puncta in non-contacting axons (**Figure 2C**). In contrast, vGlut1 puncta in axons on cerebrellar astrocytes were not significantly different as compared to vGlut1 puncta in non-contacting axons (**Figure 2B**). We further directly compared puncta areas in axons on cortical astrocytes, cerebellar astrocytes, and control neurons after normalization to the mean puncta area in non-contacting axons. Mean puncta areas in both, axons on cortical astrocytes and axons on control neurons were significantly larger as compared to the mean puncta area in axons on cerebellar astrocytes (**Figure 2D**). There was no significant difference between mean puncta areas in axons on cortical astrocytes and in axons on neurons. These results unexpectedly indicated that immature cortical astrocytes have a similar vesicle clustering effect on contacting axons as control cortical neurons.

Expression of the postsynaptic adhesion protein Neuroligin1 is well known to induce synaptic vesicle clustering in contacting axons (Scheiffele et al., 2000; Biederer et al., 2002; Dagar and Gottmann, 2019). Because expression of Neuroligins has recently been described in cortical astrocytes (Stogsdill et al., 2017), we qualitatively studied the expression of Neuroligin1 in the target astrocytes in our co-culture system. Immunostaining for Neuroligin1 revealed prominent expression of Neuroligin1 in immature cortical astrocytes (**Figure 2E**; 82% of GFAP-co-stained cells were immunopositive), whereas the vast majority of cerebellar astrocytes did not exhibit expression of Neuroligin1 (**Figure 2F**; only 26% of GFAP-co-stained cells were immunopositive). This result suggests that expression of Neuroligin1 selectively by immature cortical astrocytes might underlie the synaptogenic effect of cortical astrocytes on contacting axons.

AMPA Receptor Subunit Expression in Innervated Immature Astrocytes

We next wanted to study the expression of AMPA receptor subunits in immature cortical and cerebellar astrocytes that served as target cells. Therefore, we performed immunocytochemical co-stainings for GFAP and either GluA1 or GluA2 in astrocytes contacted by explant axons at 12 days in co-culture. In immature cortical astrocytes expression of GluA1 was almost completely absent (**Figures 3A,F**), while in cerebellar astrocytes a small fraction (around 10%) of cells expressed GluA1 (**Figures 3B,C,F**). In contrast to GluA1, GluA2 was expressed in almost all immature cortical (**Figures 3D,G**) and cerebellar astrocytes (**Figures 3E,G**) contacted by explant axons. This is in line with previous studies describing expression of GluA2 and GluA1 in cultured astrocytes (Backus et al., 1989; Condorelli et al., 1993).

LRRTM2 Expression in Immature Astrocytes Induces Vesicle Clustering in Contacting Axons

In a further approach intended to induce synaptogenic events, we used overexpression of the synaptogenic adhesion protein LRRTM2 (de Wit et al., 2009; Ko et al., 2009; Linhoff et al., 2009) in immature cortical and cerebellar astrocytes that were contacted by cortical explant axons. Sparse transfection of individual astrocytes with LRRTM2 was done at 10 days of explant co-culture using plasmid carrying magnetic beads (van Stegen et al., 2017). To identify transfected neurons EGFP was co-expressed. 2 days after transfection, immunostaining for vGlut1 was performed and vGlut1 puncta on astrocytes were quantitatively analyzed (**Figure 4**). As expected from the results shown above in **Figure 2**, control immature cortical astrocytes (expressing only EGFP) exhibited a significantly increased area of vGlut1 puncta as compared to the area of vGlut1 puncta on axons not contacting target cells (**Figure 4A**), indicating a retrograde induction of synaptic vesicle clustering. Immature cortical astrocytes overexpressing LRRTM2 also showed a significantly increased area of vGlut1 puncta as compared to vGlut1 puncta on axons not contacting target cells. Interestingly, the increase in puncta area appeared to be much stronger in cortical astrocytes overexpressing LRRTM2 (**Figure 4B**). Control cerebellar astrocytes (expressing only EGFP) did not exhibit a significantly different area of vGlut1 puncta as compared to the area of vGlut1 puncta on non-contacting axons (**Figure 4C**). In contrast, cerebellar astrocytes overexpressing LRRTM2 showed a significantly increased area of vGlut1 puncta as compared to the area of vGlut1 puncta on non-contacting axons (**Figure 4D**), thus indicating an induction of synaptic vesicle clustering by LRRTM2 expression. To statistically compare effect sizes of LRRTM2 expression, we normalized mean vGlut1 puncta areas on different astrocytes to the respective mean area of vGlut1 puncta on axons not contacting target cells (**Figures 4E–G**). We observed a significantly increased mean relative vGlut1 puncta area in both immature cortical and cerebellar astrocytes expressing LRRTM2, when compared to their respective control astrocytes (expressing only EGFP). In summary, our results demonstrate that overexpression of LRRTM2 in immature cortical astrocytes led to an enhancement of the vesicle clustering activity of untransfected astrocytes. In cerebellar astrocytes, which lacked a basal vesicle clustering activity, overexpression of LRRTM2 led to an appearance of synaptogenic activity.

AMPA Receptor Subunit Expression in Innervated, LRRTM2 Expressing Astrocytes

After having established the formation of presynaptic vesicle clusters on astrocytes by LRRTM2 expression, we wanted to study whether LRRTM2 expression in addition leads to an enhanced expression of AMPA receptor subunits. This might be expected, because LRRTM2 deficient neurons have been described to exhibit reduced AMPA receptor function and plasticity (Soler-Llavina et al., 2013; Bhouri et al., 2018).

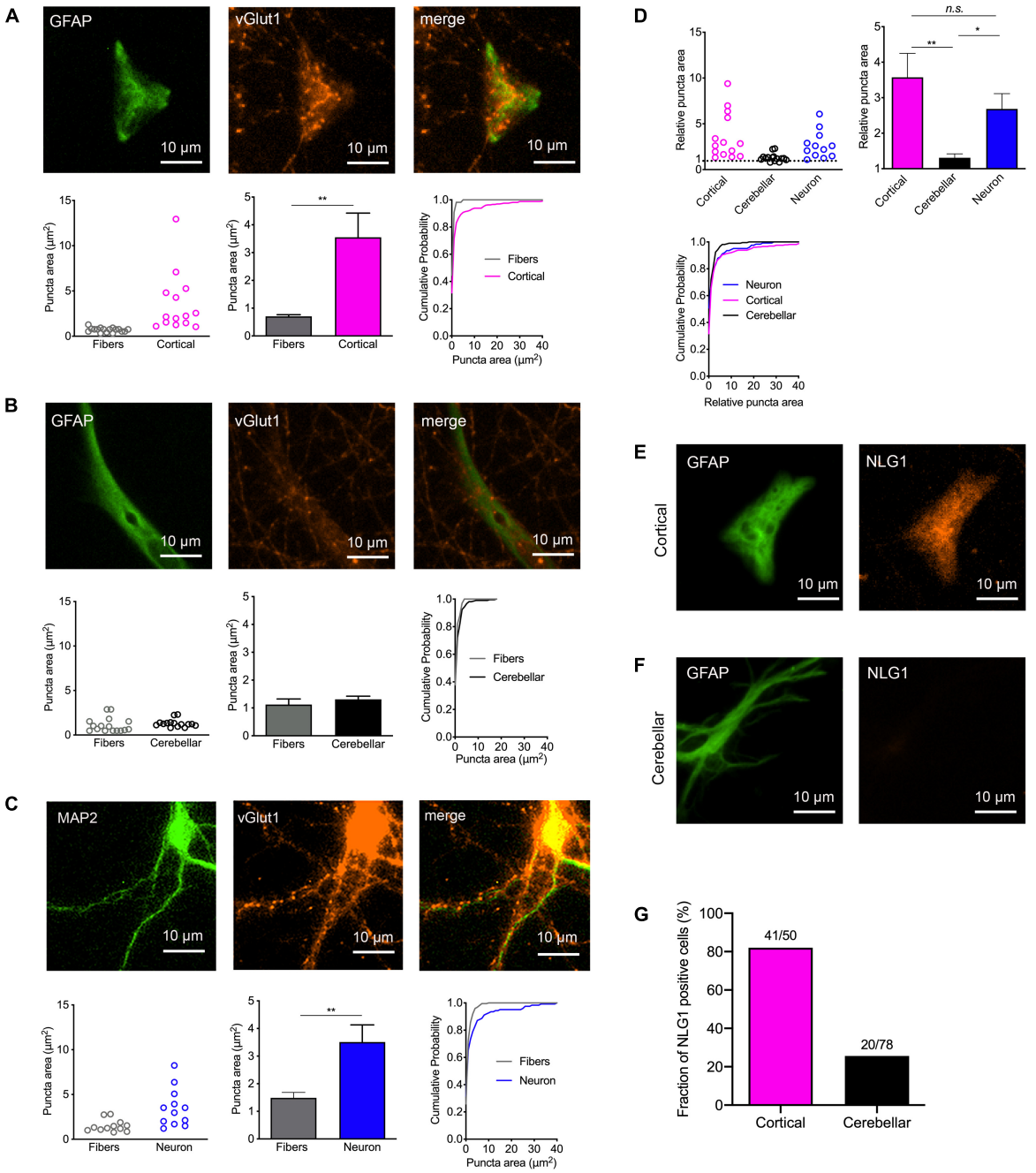

FIGURE 2 | Induction of synaptic vesicle clusters in axons by immature cortical astrocytes. **(A–D)** Immunostaining for vGlut1 revealed induction of vesicle clusters in axons by target cells. **(A)** Upper panel: Immunostaining of immature cortical astrocytes for GFAP (left image), vGlut1 (middle image), and merge image. Lower panel: Quantification of vesicle cluster area [left: means of individual cells (n = 14/14); middle: means of cells ± SEM; right: cumulative distribution of the areas of all puncta (110/326)]. **(B)** Upper panel: Immunostaining of cerebellar astrocytes for GFAP (left image), vGlut1 (middle image), and merge image. Lower panel: Quantification of vesicle cluster (vGlut1 puncta) area [left: means of individual cells (n = 15/15); middle: means of cells ± SEM; right: cumulative distribution of the areas of all puncta (66/211)]. **(C)** Upper panel: Immunostaining of control neurons for MAP2 (left image), vGlut1 (middle image), and merge image. Lower panel: Quantification of vesicle cluster area [left: means of individual cells (n = 12/12); middle: means of cells ± SEM; right: cumulative distribution of the areas of all puncta (224/124)]. $^{**}P < 0.01$, Student's t-test. **(D)** Direct quantitative comparison of relative vGlut1 puncta area [normalized to respective mean puncta area in non-contacting axons (fibers)] in immature cortical astrocytes, in cerebellar astrocytes, and in control neurons. Upper left: means of individual cells; upper right: means of cells ± SEM; lower left: cumulative distribution of the areas of all puncta. $^{*}P < 0.05$, $^{**}P < 0.01$, one-way-ANOVA with Tuckey's *post-hoc* test. **(E–G)** Immunostainings for GFAP (left image) and Neuroligin1 (NLG1) in immature cortical astrocytes **(E)** and in cerebellar astrocytes **(F)** as target cells. Note the prominent expression of Neuroligin1 in immature cortical astrocytes. **(G)** Quantification of the fraction of Neuroligin1 expressing cortical and cerebellar astrocytes.

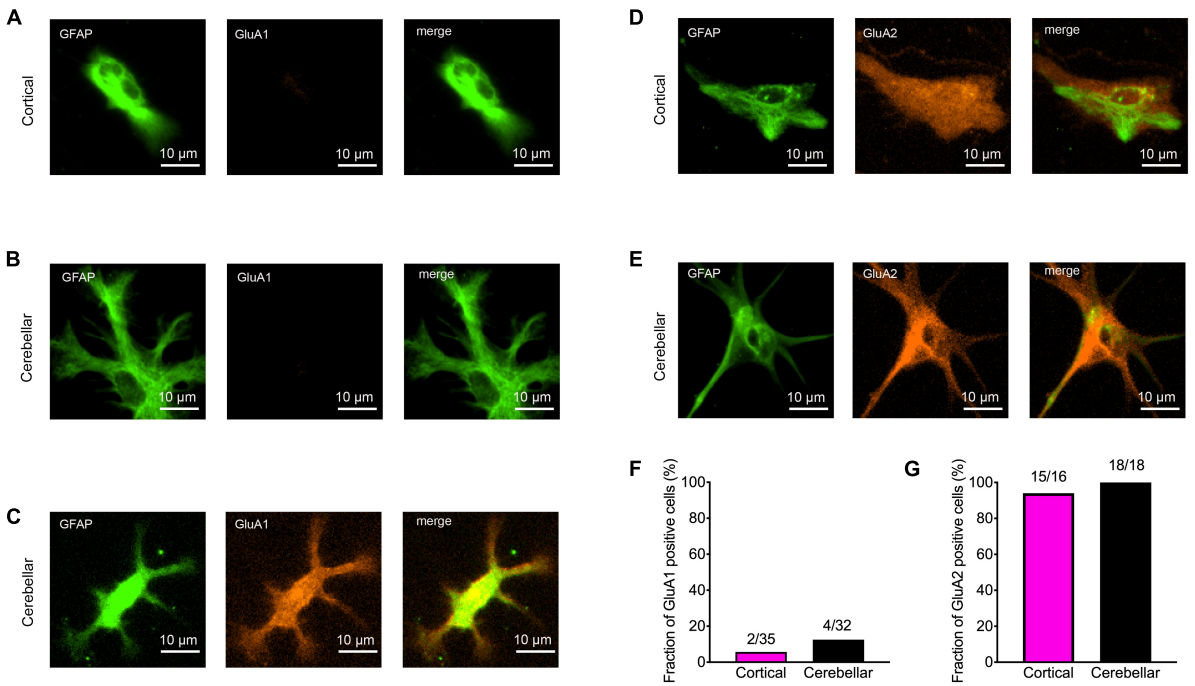

FIGURE 3 | Expression of AMPA receptor subunits GluA1 and GluA2 in immature cortical and cerebellar astrocytes contacted by explant axons. **(A–C)** Co-immunostainings for GFAP (green) and GluA1 (red) in immature cortical astrocytes **(A)** and in cerebellar astrocytes **(B,C)**. Scale bars: 10 µm. **(D,E)** Co-immunostainings for GFAP (green) and GluA2 (red) in immature cortical astrocytes **(D)** and in cerebellar astrocytes **(E)**. **(F,G)** Quantification of GluA1 **(F)** and GluA2 **(G)** positive astrocytes contacted by explant axons.

To qualitatively analyze AMPA receptor subunit expression, we performed immunocytochemistry for GluA1 and GluA2 in LRRTM2 (and EGFP) transfected, immature cortical and cerebellar astrocytes that were innervated by explant axons (12 days in co-culture). We observed a slight increase in the fraction of target cells immunopositive for GluA1 in both immature cortical and cerebellar astrocytes upon expression of LRRTM2 (**Figures 5A2,B2,C**). This parallel increase in GluA1 expressing cells might indicate an enhancing effect of LRRTM2 on AMPA receptor expression in astrocytes. However, the majority of transfected target astrocytes did not exhibit detectable GluA1 expression (**Figures 5A1,B1,C**). Qualitative immunocytochemical analysis for GluA2 subunit expression revealed that almost all transfected target astrocytes expressed GluA2 independent of LRRTM2 expression (**Figures 5D–F**).

Lack of Miniature Excitatory Postsynaptic Currents in Innervated, LRRTM2 Expressing Astrocytes

We next wanted to study, whether AMPA receptor mediated postsynaptic responses can be observed in astrocytes innervated by explant axons. We attempted to record spontaneous AMPA receptor-mediated miniature excitatory postsynaptic currents (AMPA mEPSCs) from axon-contacted astrocytes by whole-cell patch-clamp recording. We used recording conditions with i) standard (3 mM) extracellular [K^+] and with ii) elevated (40 mM) extracellular [K^+] to stimulate vesicle release. In control cortical neurons innervated by explant axons at 12 days of co-culture typical spontaneous AMPA mEPSCS were present at both conditions in all 18 neurons recorded (**Figure 6C**). In immature cortical astrocytes (n = 16 cells) no AMPA mEPSCs were detectable (**Figure 6A**) despite the presence of presynaptic vesicle clusters and the expression of GluA2 subunits. Similar, in cerebellar astrocytes expressing LRRTM2 (n = 16 cells) AMPA mEPSCs were not detectable except for three individual mEPSC-like events (**Figure 6B**). Again, AMPA mEPSCs were largely absent despite the presence of presynaptic vesicle clusters and the expression of both GluA1 and GluA2 in about 1/3 of cerebellar astrocytes. In summary, expression of a single type of synaptogenic protein, LRRTM2, was not sufficient to reliably induce functional synapses characterized by postsynaptic currents in astrocytes.

DISCUSSION

In this paper, we analyzed as a first step the synaptogenic effects of co-cultured cortical and cerebellar astrocytes on axons growing out from cortical explants. Unexpectedly, we found that immature cortical astrocytes strongly increased presynaptic vesicle clustering in contacting cortical axons. By contrast, cerebellar astrocytes did not induce a comparable hemisynapse formation. Interestingly, the ability to induce hemisynapse formation correlated with the expression of Neuroligin1 in immature cortical astrocytes. Because Neuroligin1

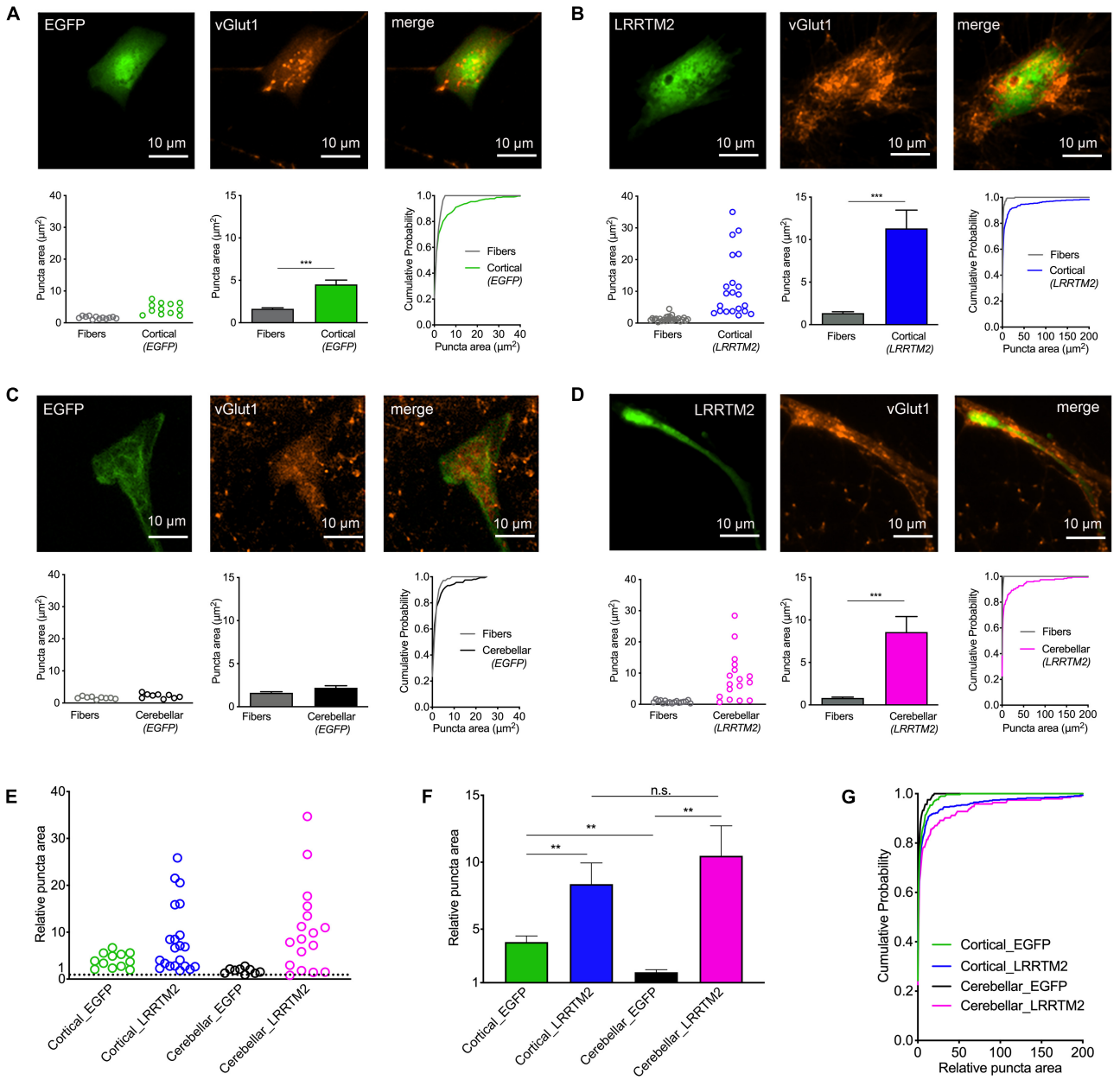

FIGURE 4 | Induction of synaptic vesicle clusters in axons by LRRTM2 expression in immature cortical and cerebellar astrocytes. **(A–D)** Immunostaining for vGlut1 revealed induction of vesicle clusters in axons by LRRTM2 expression in target cells. **(A)** Expression of only EGFP (control) in immature cortical astrocytes. Upper panel: EGFP fluorescence (left image), immunocytochemistry for vGlut1 (middle image), and merge image. Lower panel: Quantification of vesicle cluster area on target cells (green) and in non-contacting axons (fibers) [left: means of individual cells (n = 12/12); middle: means of cells ± SEM; right: cumulative distribution of the areas of all puncta (86/300)]. **(B)** Expression of LRRTM2 + EGFP (co-transfection) in immature cortical astrocytes. Upper panel: EGFP fluorescence (left image), immunocytochemistry for vGlut1 (middle image), and merge image. Lower panel: Quantification of vesicle cluster area on target cells (blue) and in non-contacting axons (fibers) [left: means of individual cells (n = 21/21); middle: means of cells ± SEM; right: cumulative distribution of the areas of all puncta (177/462)]. **(C)** Expression of only EGFP (control) in cerebellar astrocytes. Upper panel: EGFP fluorescence (left image), immunocytochemistry for vGlut1 (middle image), and merge image. Lower panel: Quantification of vesicle cluster area on target cells (black) and in non-contacting axons (fibers) [left: means of individual cells (n = 9/9); middle: means of cells ± SEM; right: cumulative distribution of the areas of all puncta (72/163)]. **(D)** Expression of LRRTM2 + EGFP (co-transfection) in cerebellar astrocytes. Upper panel: EGFP fluorescence (left image), immunocytochemistry for vGlut1 (middle image), and merge image. Lower panel: Quantification of vesicle cluster area on target cells (magenta) and in non-contacting axons (fibers) [left: means of individual cells (n = 17/17); middle: means of cells ± SEM; right: cumulative distribution of the areas of all puncta (113/194)]. **(E–G)** Quantitative comparison of the effect sizes of EGFP (control) and LRRTM2 + EGFP expression in immature cortical and cerebellar astrocytes (calculated from data in **A–D**). vGlut1 puncta areas on target cells were normalized to the respective mean puncta area in non-contacting axons. **(E)** Means of normalized puncta areas of individual cells. **(F)** Means of cells ± SEM. **(G)** Cumulative distributions of the normalized areas of all puncta. ***$P < 0.001$; Student's t-test **(A–D)**; **$P < 0.01$; one-way ANOVA with Tuckey's *post-hoc* test **(F)**.

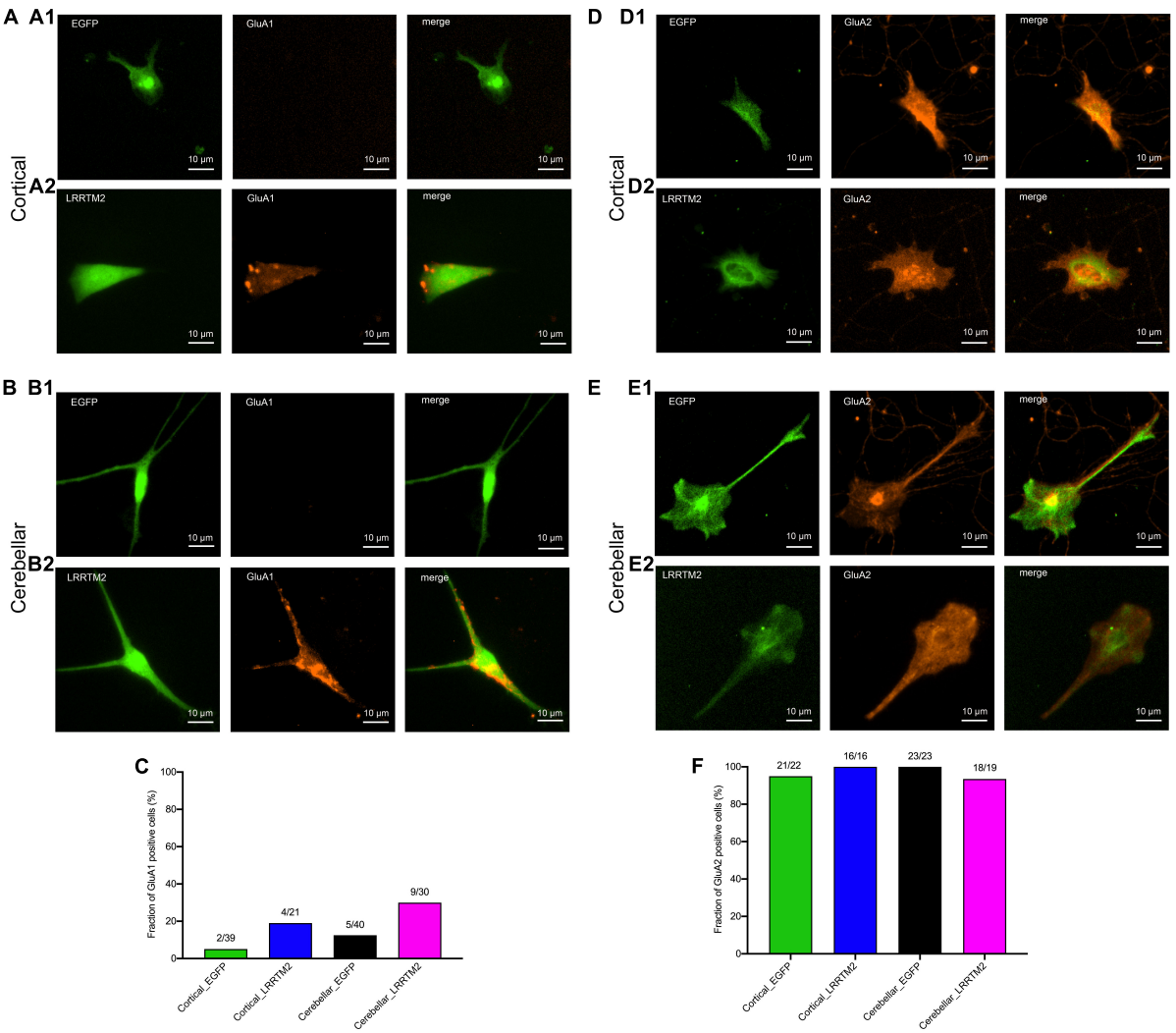

FIGURE 5 | Effects of LRRTM2 expression on AMPA receptor subunit GluA1 and GluA2 expression in immature cortical and cerebellar astrocytes contacted by explant axons. **(A,B)** Fluorescence images of transfected astrocytes (EGFP (control) and LRRTM2 + EGFP, green) and immunostainings for GluA1 (red) in immature cortical astrocytes **(A1,A2)** and in cerebellar astrocytes **(B1,B2)**. Scale bars: 10 µm. **(C)** Quantification of the fraction of GluA1 positive astrocytes. **(D,E)** Fluorescence images of transfected astrocytes (EGFP (control) and LRRTM2 + EGFP, green) and immunostainings for GluA2 (red) in immature cortical astrocytes **(D1,D2)** and in cerebellar astrocytes **(E1,E2)**. **(F)** Quantification of the fraction of GluA2 positive astrocytes.

is a well-established postsynaptic adhesion molecule with strong synaptogenic properties (Scheiffele et al., 2000; Biederer et al., 2002; Dagar and Gottmann, 2019), the expression of Neuroligin1 might underly the observed synaptogenic effect of immature cortical astrocytes. Expression of Neuroligins in cortical astrocytes in culture and *in vivo* has been well described (Zhang et al., 2014; Stogsdill et al., 2017), and has been shown to play an important role in astrocyte morphogenesis and neuronal synaptogenesis (Stogsdill et al., 2017).

In a second step, we expressed the synaptogenic protein LRRTM2 in immature cortical and in cerebellar astrocytes contacted by co-cultured explant axons. LRRTM2 has been shown to exhibit strong synaptogenic activity as indicated by presynaptic vesicle clustering (de Wit et al., 2009; Ko et al., 2009; Linhoff et al., 2009; Dagar and Gottmann, 2019), and to bind to presynaptic neurexins thereby inducing hemisynapse formation on the presynaptic side (de Wit et al., 2009; Ko et al., 2009; Siddiqui et al., 2010). As expected, we found an enhanced hemisynapse formation in immature cortical astrocytes upon expression of LRRTM2. Importantly, we further observed a strong induction of vesicle clustering in axons contacting cerebellar astrocytes, which did not induce hemisynapse formation without expression of LRRTM2.

To investigate functional synapse formation between explant axons and co-cultured astrocytes, we used whole-cell patch-clamp recording of AMPA receptor mediated miniature EPSCs. Recording of mEPSCs represents a highly sensitive method to detect spontaneous vesicle release, if functional AMPA

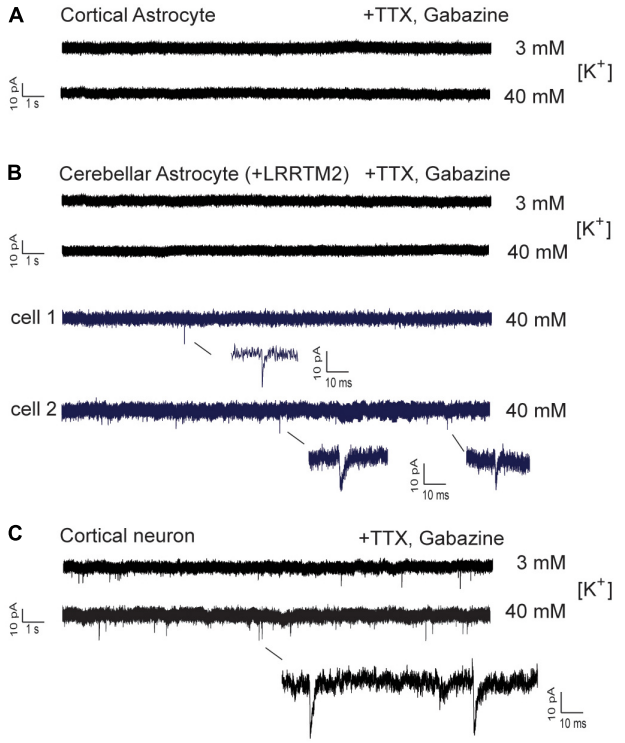

FIGURE 6 | Whole-cell patch-clamp recordings in immature cortical astrocytes and in cerebellar astrocytes expressing LRRTM2. AMPA receptor-mediated miniature EPSCs (AMPA mEPSCs) were pharmacologically isolated by addition of TTX (1 μM) and gabazine (10 μM). Holding potential: -60 mV. Extracellular solution contained standard (3 mM) or elevated (40 mM) $[K^+]$ as indicated. **(A)** Lack of spontaneous AMPA mEPSCs in immature cortical astrocytes contacted by explant axons. n = 16 cells. **(B)** Lack of spontaneous AMPA mEPSCs in cerebellar astrocytes expressing LRRTM2 and contacted by explant axons. In a total of 16 cells only three individual mEPSC-like events were detected and are shown enlarged (blue). **(C)** Typical AMPA mEPSCs were routinely recorded in cortical neurons innervated by explant axons. All cells recorded at 12 days in explant co-culture.

receptors are expressed spatially aligned on the postsynaptic side. In GluR2 (GluA2) subunit overexpressing HEK293 cells contacted by presynaptic axons, spontaneous mEPSCs have been described upon expression of Neuroligin1 to induce presynaptic differentiation (Biederer et al., 2002; Fu et al., 2003; Sara et al., 2005). Unexpectedly, we did not observe spontaneous AMPA mEPSCs in immature cortical and in cerebellar astrocytes, although these cells strongly expressed GluA2 subunits and expressed synaptogenic proteins such as Neuroligin1 and LRRTM2 that induced presynaptic vesicle clustering. Only extremely few AMPA mEPSC-like events were found in very few astrocytes despite high $[K^+]$ induced depolarization. This lack of functional synapse formation between explant axons and co-cultured astrocytes might be due to presynaptic or postsynaptic reasons, as will be discussed below.

Presynaptically, the vesicle clusters induced by co-cultured astrocytes in contacting axons might not be capable of spontaneously releasing vesicles. However, this appears highly unlikely, because vesicle clusters induced by heterologous expression of Neuroligin1 (Biederer et al., 2002; Fu et al., 2003; Sara et al., 2005) and of LRRTM2 (de Wit et al., 2009; Linhoff et al., 2009) in HEK293 cells have been described to spontaneously release transmitter. Moreover, it is well known that even axonal vesicle clusters not in contact with a postsynaptic cell are capable of vesicle release (Matteoli et al., 1992; Kraszewski et al., 1995). Nevertheless, a lack of spontaneous vesicle release cannot be completely excluded, however, this potential explanation would require yet unknown factors from the co-cultured astrocytes that strongly inhibit spontaneous vesicle release.

Postsynaptically, we observed prominent expression of the AMPA receptor subunit GluA2 (GluR2) in co-cultured cortical and cerebellar astrocytes, and also expression of GluA1 (GluR1) in a fraction of LRRTM2 expressing astrocytes. Nevertheless, the co-cultured astrocytes might not express AMPA receptors on their plasma membrane resulting in a lack of postsynaptic currents. However, this appears highly unlikely, because functional surface AMPA receptors in cultured astrocytes have been well described in a large number of studies (e.g., Sontheimer et al., 1988; von Blankenfeld and Kettenmann, 1991; Burnashev et al., 1992; Gallo et al., 1994; David et al., 1996; Ceprian and Fulton, 2019). A hypothetical lack of surface AMPA receptors would require that the assembly machinery of AMPA receptors in the ER is not functional for example due to dysfunction of accessory proteins (e.g., ABHD6, TARPs and others; Schwenk and Fakler, 2021). Furthermore, in HEK293 cells expression of GluR2 (GluA2) subunits has been demonstrated to be sufficient to observe AMPA receptor mediated ion currents (Biederer et al., 2002; Sara et al., 2005). HEK293 cells most likely express AMPA receptor subunits encoded on plasmids at a high level, possibly resulting in the presence of functional AMPA receptors on the entire surface membrane. This might be the reason why miniature-like postsynaptic currents are readily observed in HEK293 cells. In contrast, in astrocytes AMPA receptor surface expression is likely to be more restricted by mechanisms regulating endogenous AMPA receptor expression.

Postsynaptic AMPA receptors have a relatively low affinity for binding glutamate as compared to NMDA receptors (for review see Traynelis et al., 2010). Therefore, a relatively high concentration of glutamate (mM) must be reached to activate AMPA receptor-mediated ion currents. In addition, AMPA receptors show strong desensitization thus requiring that such relatively high glutamate concentrations are reached within a millisecond (Lisman et al., 2007). Because miniature EPSCs are postsynaptic responses to the spontaneous release of just one synaptic vesicle, it appears to be critical that presynaptic vesicle release and postsynaptic AMPA receptors are spatially highly aligned to enable fast rising, high glutamate concentrations at the postsynaptic AMPA receptors (Lisman et al., 2007).

In line with this classic view, it has been found using modern super-resolution techniques that postsynaptic AMPA receptors are clustered in nanoscale subdomains ("slots") that restrict their diffusional mobility in the plane of the

postsynaptic membrane (for review see Opazo et al., 2012; Choquet and Hosy, 2020). Moreover, it has been described recently that molecularly defined presynaptic vesicle release sites are tightly aligned to these postsynaptic AMPA receptor nanoclusters thus forming a transsynaptic unit or nanocolumn (Tang et al., 2016; Biederer et al., 2017; Heine and Holcman, 2020). This delicate transsynaptic molecular architecture of functional synapses is presumably not established in the *in vitro* axon-astrocyte contacts studied in our present paper. The absence of transsynaptic nanocolumns might be the molecular reason, why we do not observe spontaneous AMPA mEPSCs despite the presence of presynaptic vesicle clusters and the expression of postsynaptic AMPA receptor subunits. In line with this idea, it has been demonstrated experimentally that interfering with the nanoscale spatial coupling of the presynapse-organizing protein Neuroligin1 and AMPA receptor nanodomains results in a significant decrease in AMPA mEPSC amplitudes (Haas et al., 2018).

We conclude that *in vitro* physical contacts of cortical neuron axons and target astrocytes enable the formation of hemisynapses, i.e., presynaptic differentiation in the contacting axons. This appears to require the expression of synaptogenic proteins such as Neuroligin1 and LRRTM2 by the astrocytes. However, AMPA mEPSCs, which are characteristic of fully functional synapses, were not observed despite the expression of AMPA receptor subunits in the target astrocytes. The lack of AMPA mEPSCs might indicate the absence of transsynaptic nanocolums tightly aligning vesicle release sites and AMPA receptor nanodomains at the molecular level.

DATA AVAILABILITY STATEMENT

The raw data supporting the conclusions of this article will be made available by the authors, without undue reservation.

ETHICS STATEMENT

The animal study was reviewed and approved by the Tierschutzbeauftragter University Düsseldorf.

AUTHOR CONTRIBUTIONS

ZT performed the experiments and wrote the manuscript. KG designed the research and wrote the manuscript. Both authors contributed to the article and approved the submitted version.

FUNDING

This work was supported by grants from the Deutsche Forschungsgemeinschaft.

ACKNOWLEDGMENTS

We want to thank Joris de Wit for providing the LRRTM2 expression vector. We also want to thank Sabine Ueberschär for excellent technical assistance.

SUPPLEMENTARY MATERIAL

The Supplementary Material for this article can be found online at: https://www.frontiersin.org/articles/10.3389/fnmol.2022.829506/full#supplementary-material

Supplementary Figure 1 | Validation of co-expression of myc-tagged LRRTM2 and EGFP in transfected astrocytes. Standard cultures of astrocytes without explants were co-transfected with EGFP and myc-LRRTM2 plasmids. **(A,C)** Co-expression of EGFP and myc-tagged LRRTM2 in cultured cortical **(A)** and cerebellar **(C)** astrocytes was confirmed by EGFP fluorescence (EGFP) and by immunocytochemical staining with myc-antibodies (myc). Overlay of images (merge) to demonstrate co-expression. **(B,D)** Control experiments, in which cultured cortical **(B)** and cerebellar **(D)** astrocytes were only transfected with EGFP, did not exhibit any myc fluorescence signal.

Supplementary Figure 2 | Quantitative analysis of vGlut1-immunopositive puncta area. **(A,D)** Merged images of vGlut1 (red) and GFAP (green) immunofluorescence of an immature cortical astrocyte innervated by explant fibers **(A)** and of a cerebellar astrocyte innervated by explant fibers **(D)**. The astrocyte is outlined in red. The blue square demarcates the area in which vGlut1 puncta on explant fibers were analyzed at 12 days in co-culture. Scale bars: 10 μm. **(B,E)** Negative images of vGlut1 immunofluorescence that were thresholded to obtain the images shown in **(C,F)**. **(C,F)** Astrocyte outline (red) and explant fiber area (blue) were transferred onto thresholded negative images of vGlut1 immunofluorescence. Regions of interest (ROIs) were created around black puncta, and puncta area was determined separately for astrocytes (red outline) and explant fibers (blue square). ImageJ software was used for image analysis.

REFERENCES

Backus, K. H., Kettenmann, H., and Schachner, M. (1989). Pharmacological characterization of the glutamate receptor in cultured astrocytes. *J. Neurosci. Res.* 22, 274–282. doi: 10.1002/jnr.490220307

Bergles, D. E., Jabs, R., and Steinhäuser, C. (2010). Neuron-glia synapses in the brain. *Brain Res. Rev.* 63, 130–137. doi: 10.1016/j.brainresrev.2009.12.003

Bhouri, M., Morishita, W., Temkin, P., Goswami, D., Kawabe, H., Brose, N., et al. (2018). Deletion of LRRTM1 and LRRTM2 in adult mice impairs basal AMPA receptor transmission and LTP in hippocampal CA1 pyramidal neurons. *Proc. Natl. Acad. Sci. U. S. A.* 115, E5382–E5389. doi: 10.1073/pnas.1803280115

Biederer, T., Kaeser, P. S., and Blanpied, T. A. (2017). Transcellular Nanoalignment of Synaptic Function. *Neuron* 96, 680–696. doi: 10.1016/j.neuron.2017.10.006

Biederer, T., Sara, Y., Mozhayeva, M., Atasoy, D., Liu, X., Kavalali, E. T., et al. (2002). SynCAM, a synaptic adhesion molecule that drives synapse assembly. *Science* 297, 1525–1531. doi: 10.1126/science.1072356

Burnashev, N., Khodorova, A., Jonas, P., Helm, P. J., Wisden, W., Monyer, H., et al. (1992). Calcium-permeable AMPA-kainate receptors in fusiform cerebellar glial cells. *Science* 256, 1566–1570. doi: 10.1126/science.1317970

Ceprian, M., and Fulton, D. (2019). Glial Cell AMPA Receptors in Nervous System Health, Injury and Disease. *Int. J. Mol. Sci.* 20:2450. doi: 10.3390/ijms20102450

Chih, B., Engelman, H., and Scheiffele, P. (2005). Control of excitatory and inhibitory synapse formation by neuroligins. *Science* 307, 1324–1328. doi: 10.1126/science.1107470

Choquet, D., and Hosy, E. (2020). AMPA receptor nanoscale dynamic organization and synaptic plasticities. *Curr. Opin. Neurobiol.* 63, 137–145. doi: 10.1016/j.conb.2020.04.003

Condorelli, D. F., Dell'Albani, P., Corsaro, M., Barresi, V., and Giuffrida, S., A.M. (1993). AMPA-selective glutamate receptor subunits in astroglial cultures. *J. Neurosci. Res.* 36, 344–356. doi: 10.1002/jnr.490360312

Craig, A. M., Graf, E. R., and Linhoff, M. W. (2006). How to build a central synapse: clues from cell culture. *Trends Neurosci.* 29, 8–20. doi: 10.1016/j.tins.2005.11.002

Craig, A. M., and Kang, Y. (2007). Neurexin-neuroligin signaling in synapse development. *Curr. Opin. Neurobiol.* 17, 43–52. doi: 10.1016/j.conb.2007.01.011

Dagar, S., and Gottmann, K. (2019). Differential Properties of the Synaptogenic Activities of the Neurexin Ligands Neuroligin1 and LRRTM2. *Front. Mol. Neurosci.* 12:269. doi: 10.3389/fnmol.2019.00269

David, J. C., Yamada, K. A., Bagwe, M. R., and Goldberg, M. P. (1996). AMPA receptor activation is rapidly toxic to cortical astrocytes when desensitization is blocked. *J. Neurosci.* 16, 200–209. doi: 10.1523/JNEUROSCI.16-01-00200.1996

de Wit, J., and Ghosh, A. (2014). Control of neural circuit formation by leucine-rich repeat proteins. *Trends Neurosci.* 37, 539–550. doi: 10.1016/j.tins.2014.07.004

de Wit, J., Sylwestrak, E., O'Sullivan, M. L., Otto, S., Tiglio, K., Savas, J. N., et al. (2009). LRRTM2 interacts with Neurexin1 and regulates excitatory synapse formation. *Neuron* 64, 799–806. doi: 10.1016/j.neuron.2009.12.019

Fu, Z., Washbourne, P., Ortinski, P., and Vicini, S. (2003). Functional excitatory synapses in HEK293 cells expressing neuroligin and glutamate receptors. *J. Neurophysiol.* 90, 3950–3957. doi: 10.1152/jn.00647.2003

Gallo, V., Patneau, D. K., Mayer, M. L., and Vaccarino, F. M. (1994). Excitatory amino acid receptors in glial progenitor cells: molecular and functional properties. *Glia* 11, 94–101. doi: 10.1002/glia.440110204

Gomez, A. M., Traunmüller, L., and Scheiffele, P. (2021). Neurexins: molecular codes for shaping neuronal synapses. *Nat. Rev. Neurosci.* 22, 137–151. doi: 10.1038/s41583-020-00415-7

Gottmann, K., Mehrle, A., Gisselmann, G., and Hatt, H. (1997). Presynaptic control of subunit composition of NMDA receptors mediating synaptic plasticity. *J. Neurosci.* 17, 2766–2774. doi: 10.1523/JNEUROSCI.17-08-02766.1997

Graf, E. R., Zhang, X., Jin, S. X., Linhoff, M. W., and Craig, A. M. (2004). Neurexins induce differentiation of GABA and glutamate postsynaptic specializations via neuroligins. *Cell* 119, 1013–1026. doi: 10.1016/j.cell.2004.11.035

Haas, K. T., Compans, B., Letellier, M., Bartol, T. M., Grillo-Bosch, D., Sejnowski, T. J., et al. (2018). Pre-post synaptic alignment through neuroligin-1 tunes synaptic transmission efficiency. *Elife* 7:e31755. doi: 10.7554/eLife.31755

Heine, M., and Holcman, D. (2020). Asymmetry Between Pre- and Postsynaptic Transient Nanodomains Shapes Neuronal Communication. *Trends Neurosci.* 43, 182–196. doi: 10.1016/j.tins.2020.01.005

Ko, J., Fuccillo, M. V., Malenka, R. C., and Südhof, T. C. (2009). LRRTM2 functions as a neurexin ligand in promoting excitatory synapse formation. *Neuron* 64, 791–798. doi: 10.1016/j.neuron.2009.12.012

Kraszewski, K., Mundigl, O., Daniell, L., Verderio, C., Matteoli, M., and De Camilli, P. (1995). Synaptic vesicle dynamics in living cultured hippocampal neurons visualized with CY3-conjugated antibodies directed against the lumenal domain of synaptotagmin. *J. Neurosci.* 15, 4328–4342. doi: 10.1523/JNEUROSCI.15-06-04328.1995

Linhoff, M. W., Laurén, J., Cassidy, R. M., Dobie, F. A., Takahashi, H., Nygaard, H. B., et al. (2009). An unbiased expression screen for synaptogenic proteins identifies the LRRTM protein family as synaptic organizers. *Neuron* 61, 734–749. doi: 10.1016/j.neuron.2009.01.017

Lisman, J. E., Raghavachari, S., and Tsien, R. W. (2007). The sequence of events that underlie quantal transmission at central glutamatergic synapses. *Nat. Rev. Neurosci.* 8, 597–609. doi: 10.1038/nrn2191

Matteoli, M., Takei, K., Perin, M. S., Südhof, T. C., and De Camilli, P. (1992). Exo-endocytotic recycling of synaptic vesicles in developing processes of cultured hippocampal neurons. *J. Cell Biol.* 117, 849–861. doi: 10.1083/jcb.117.4.849

Mohrmann, R., Werner, M., Hatt, H., and Gottmann, K. (1999). Target-specific factors regulate the formation of glutamatergic transmitter release sites in cultured neocortical neurons. *J. Neurosci.* 19, 10004–10013. doi: 10.1523/JNEUROSCI.19-22-10004.1999

Nieweg, K., Andreyeva, A., van Stegen, B., Tanriöver, G., and Gottmann, K. (2015). Alzheimer's disease-related amyloid-β induces synaptotoxicity in human iPS cell-derived neurons. *Cell Death Dis.* 6:e1709. doi: 10.1038/cddis.2015.72

Opazo, P., Sainlos, M., and Choquet, D. (2012). Regulation of AMPA receptor surface diffusion by PSD-95 slots. *Curr. Opin. Neurobiol.* 22, 453–460. doi: 10.1016/j.conb.2011.10.010

Sakry, D., Karram, K., and Trotter, J. (2011). Synapses between NG2 glia and neurons. *J. Anat.* 219, 2–7. doi: 10.1111/j.1469-7580.2011.01359.x

Sanes, J. R., and Zipursky, S. L. (2020). Synaptic Specificity, Recognition Molecules, and Assembly of Neural Circuits. *Cell* 181, 536–556. doi: 10.1016/j.cell.2020.04.008

Sara, Y., Biederer, T., Atasoy, D., Chubykin, A., Mozhayeva, M. G., Südhof, T. C., et al. (2005). Selective capability of SynCAM and neuroligin for functional synapse assembly. *J. Neurosci.* 25, 260–270. doi: 10.1523/JNEUROSCI.3165-04.2005

Scheiffele, P., Fan, J., Choih, J., Fetter, R., and Serafini, T. (2000). Neuroligin expressed in nonneuronal cells triggers presynaptic development in contacting axons. *Cell* 101, 657–669. doi: 10.1016/s0092-8674(00)80877-6

Schwenk, J., and Fakler, B. (2021). Building of AMPA-type glutamate receptors in the endoplasmic reticulum and its implication for excitatory neurotransmission. *J. Physiol.* 599, 2639–2653. doi: 10.1113/JP279025

Shen, K., and Scheiffele, P. (2010). Genetics and cell biology of building specific synaptic connectivity. *Annu. Rev. Neurosci.* 33, 473–507. doi: 10.1146/annurev.neuro.051508.135302

Siddiqui, T. J., and Craig, A. M. (2011). Synaptic organizing complexes. *Curr. Opin. Neurobiol.* 21, 132–143. doi: 10.1016/j.conb.2010.08.016

Siddiqui, T. J., Pancaroglu, R., Kang, Y., Rooyakkers, A., and Craig, A. M. (2010). LRRTMs and neuroligins bind neurexins with a differential code to cooperate in glutamate synapse development. *J. Neurosci.* 30, 7495–7506. doi: 10.1523/JNEUROSCI.0470-10.2010

Soler-Llavina, G. J., Arstikaitis, P., Morishita, W., Ahmad, M., Südhof, T. C., and Malenka, R. C. (2013). Leucine-rich repeat transmembrane proteins are essential for maintenance of long-term potentiation. *Neuron* 79, 439–446. doi: 10.1016/j.neuron.2013.06.007

Sontheimer, H., Kettenmann, H., Backus, K. H., and Schachner, M. (1988). Glutamate opens Na+/K+ channels in cultured astrocytes. *Glia* 1, 328–336. doi: 10.1002/glia.440010505

Stan, A., Pielarski, K. N., Brigadski, T., Wittenmayer, N., Fedorchenko, O., Gohla, A., et al. (2010). Essential cooperation of N-cadherin and neuroligin-1 in the transsynaptic control of vesicle accumulation. *Proc. Natl. Acad. Sci. U. S. A.* 107, 11116–11121. doi: 10.1073/pnas.0914233107

Stogsdill, J. A., Ramirez, J., Liu, D., Kim, Y. H., Baldwin, K. T., Enustun, E., et al. (2017). Astrocytic neuroligins control astrocyte morphogenesis and synaptogenesis. *Nature* 551, 192–197. doi: 10.1038/nature24638

Südhof, T. C. (2008). Neuroligins and neurexins link synaptic function to cognitive disease. *Nature* 455, 903–911. doi: 10.1038/nature07456

Südhof, T. C. (2017). Synaptic Neurexin Complexes: a Molecular Code for the Logic of Neural Circuits. *Cell* 171, 745–769. doi: 10.1016/j.cell.2017.10.024

Südhof, T. C. (2018). Towards an Understanding of Synapse Formation. *Neuron* 100, 276–293. doi: 10.1016/j.neuron.2018.09.040

Südhof, T. C. (2021). The cell biology of synapse formation. *J. Cell Biol.* 220:e202103052. doi: 10.1083/jcb.202103052

Takahashi, H., and Craig, A. M. (2013). Protein tyrosine phosphatases PTPδ, PTPσ, and LAR: presynaptic hubs for synapse organization. *Trends Neurosci.* 36, 522–534. doi: 10.1016/j.tins.2013.06.002

Tang, A. H., Chen, H., Li, T. P., Metzbower, S. R., MacGillavry, H. D., and Blanpied, T. A. (2016). A trans-synaptic nanocolumn aligns neurotransmitter release to receptors. *Nature* 536, 210–214. doi: 10.1038/nature19058

Traynelis, S. F., Wollmuth, L. P., McBain, C. J., Menniti, F. S., Vance, K. M., Ogden, K. K., et al. (2010). Glutamate receptor ion channels: structure, regulation, and function. *Pharmacol. Rev.* 62, 405–496. doi: 10.1124/pr.109.002451

van Stegen, B., Dagar, S., and Gottmann, K. (2017). Release activity-dependent control of vesicle endocytosis by the synaptic adhesion molecule N-cadherin. *Sci. Rep.* 7:40865. doi: 10.1038/srep40865

Venkataramani, V., Tanev, D. I., Strahle, C., Studier-Fischer, A., Fankhauser, L., Kessler, T., et al. (2019). Glutamatergic synaptic input to glioma cells drives brain tumour progression. *Nature* 573, 532–538. doi: 10.1038/s41586-019-1564-x

Venkatesh, H. S., Morishita, W., Geraghty, A. C., Silverbush, D., Gillespie, S. M., Arzt, M., et al. (2019). Electrical and synaptic integration of glioma into neural circuits. *Nature* 573, 539–545. doi: 10.1038/s41586-019-1563-y

von Blankenfeld, G., and Kettenmann, H. (1991). Glutamate and GABA receptors in vertebrate glial cells. *Mol. Neurobiol.* 5, 31–43. doi: 10.1007/BF02935611

Wittenmayer, N., Körber, C., Liu, H., Kremer, T., Varoqueaux, F., Chapman, E. R., et al. (2009). Postsynaptic Neuroligin1 regulates presynaptic maturation. *Proc. Natl. Acad. Sci. U. S. A.* 106, 13564–13569. doi: 10.1073/pnas.0905819106

Woo, J., Kwon, S. K., Choi, S., Kim, S., Lee, J. R., Dunah, A. W., et al. (2009). Trans-synaptic adhesion between NGL-3 and LAR regulates the formation of excitatory synapses. *Nat. Neurosci.* 12, 428–437. doi: 10.1038/nn.2279

Yim, Y. S., Kwon, Y., Nam, J., Yoon, H. I., Lee, K., Kim, D. G., et al. (2013). Slitrks control excitatory and inhibitory synapse formation with LAR receptor protein tyrosine phosphatases. . *Proc. Natl. Acad. Sci. U. S. A.* 110, 4057–4062. doi: 10.1073/pnas.1209881110

Zhang, Y., Chen, K., Sloan, S. A., Bennett, M. L., Scholze, A. R., O'Keeffe, S., et al. (2014). An RNA-sequencing transcriptome and splicing database of glia, neurons, and vascular cells of the cerebral cortex. *J. Neurosci.* 34, 11929–11947. doi: 10.1523/JNEUROSCI.1860-14.2014

Conflict of Interest: The authors declare that the research was conducted in the absence of any commercial or financial relationships that could be construed as a potential conflict of interest.

Publisher's Note: All claims expressed in this article are solely those of the authors and do not necessarily represent those of their affiliated organizations, or those of the publisher, the editors and the reviewers. Any product that may be evaluated in this article, or claim that may be made by its manufacturer, is not guaranteed or endorsed by the publisher.

frontiers in Molecular Neuroscience

ORIGINAL RESEARCH
published: 31 March 2022
doi: 10.3389/fnmol.2022.817996

Preventing Phosphorylation of the $GABA_AR$ β3 Subunit Compromises the Behavioral Effects of Neuroactive Steroids

Thuy N. Vien[1], Michael A. Ackley[2], James J. Doherty[2], Stephen J. Moss[1] and Paul A. Davies[1]**

[1] Department of Neuroscience, Tufts University School of Medicine, Boston, MA, United States, [2] Research and Non-clinical Development, Sage Therapeutics, Inc., Cambridge, MA, United States

OPEN ACCESS

Edited by:
Stephen Brickley,
Imperial College London,
United Kingdom

Reviewed by:
Istvan Mody,
University of California, Los Angeles,
United States
Petrine Wellendorph,
University of Copenhagen, Denmark

***Correspondence:**
Stephen J. Moss
Stephen.moss@tufts.edu
Paul A. Davies
paul.davies@tufts.edu

Specialty section:
This article was submitted to Molecular Signalling and Pathways, a section of the journal Frontiers in Molecular Neuroscience

Received: 18 November 2021
Accepted: 09 March 2022
Published: 31 March 2022

Citation:
Vien TN, Ackley MA, Doherty JJ, Moss SJ and Davies PA (2022) Preventing Phosphorylation of the $GABA_AR$ β3 Subunit Compromises the Behavioral Effects of Neuroactive Steroids. Front. Mol. Neurosci. 15:817996. doi: 10.3389/fnmol.2022.817996

Neuroactive steroids (NASs) have potent anxiolytic, anticonvulsant, sedative, and hypnotic actions, that reflect in part their efficacy as $GABA_AR$ positive allosteric modulators (PAM). In addition to this, NAS exert metabotropic effects on GABAergic inhibition *via* the activation of membrane progesterone receptors (mPRs), which are G-protein coupled receptors. mPR activation enhances the phosphorylation of residues serine 408 and 409 (S408/9) in the β3 subunit of $GABA_ARs$, increasing their accumulation in the plasma membrane leading to a sustained increase in tonic inhibition. To explore the significance of NAS-induced phosphorylation of $GABA_ARs$, we used mice in which S408/9 in the β3 subunit have been mutated to alanines, mutations that prevent the metabotropic actions of NASs on $GABA_AR$ function while preserving NAS allosteric potentiation of GABAergic current. While the sedative actions of NAS were comparable to WT, their anxiolytic actions were reduced in S408/9A mice. Although the induction of hypnosis by NAS were maintained in the mutant mice the duration of the loss of righting reflex was significantly shortened. Finally, ability of NAS to terminate diazepam pharmacoresistant seizures was abolished in S408/9A mice. In conclusion, our results suggest that S408/9 in the $GABA_AR$ β3 subunit contribute to the anxiolytic and anticonvulsant efficacy of NAS, in addition to their ability to regulate the loss of righting reflex.

Keywords: neurosteroids, GABAergic inhibition, drug-resistant seizures, anxiety, loss of consciousness

INTRODUCTION

Endogenous neuroactive steroids (NAS) are synthesized in the brain from cholesterol and play a central role in regulating behavior *via* their potent anxiolytic, anticonvulsant, sedative, and hypnotic actions (Belelli et al., 2009). Accordingly, modifications in the levels of NASs contribute to anxiety, autism spectrum disorders, depression, epilepsy, neurodevelopmental disorders, and premenstrual syndrome (Belelli and Lambert, 2005; Belelli et al., 2009, 2021; Maguire, 2019; Antonoudiou et al., 2022). Significantly, NASs may also be central mediators in the efficacy

of antidepressants as selective serotonin reuptake inhibitors and tricyclic antidepressants both act to increase allopregnanolone levels in the brain (Uzunova et al., 2004; Marx et al., 2006; Lüscher and Mohler, 2019). Thus, it is of fundamental importance to understand the signaling mechanism by which NASs modify neuronal excitability and the impact these processes have on behavior.

Classical mechanistic studies initially identified that NASs, in common with benzodiazepines and barbiturates, act as positive allosteric modulators (PAM) of γ-aminobutyric type A receptors (GABA$_A$R), the principal sites of fast neuronal inhibition in the brain (Paul and Purdy, 1992; Mitchell et al., 2008). GABA$_A$Rs are pentameric Cl^- selective ligand gated ion channels assembled from homologous subunits that share a common structure consisting of a large extracellular domain, four transmembrane domains (TM) with a large intracellular loop between TMs 3 and 4. GABA$_A$R subunits can be divided into nine subunit classes, some with multiple members; α1-6, β1-3, γ1-3, δ, ε, ⊖, p, π, and ρ (Rudolph and Mohler, 2006). Consensus opinion suggests that in the brain, benzodiazepine sensitive synaptic GABA$_A$Rs that mediate phasic inhibition are composed of α1-3, β1-3, and γ2 subunits. In contrast to this, specialized populations of extrasynaptic GABA$_A$Rs, which are largely insensitive to benzodiazepines, but highly sensitive to NASs, are composed of α4-6, β1-3, with or without δ subunits (Bencsits et al., 1999; Mortensen and Smart, 2006; Brickley and Mody, 2012; Parakala et al., 2019).

In addition to allosteric modulation, sustained exposure to NASs can have profound effects on the expression levels of GABA$_A$Rs, which are in part dependent upon the activity of protein kinase C (PKC; Hodge et al., 2002; Harney et al., 2003; Lambert et al., 2009). Consistent with this we have established that NASs act to increase the phosphorylation of serine 443 (S443) in the α4 subunit and serines 408 and 409 (S408/9) in the β3 subunit that are independent of their allosteric actions (Abramian et al., 2010, 2014). NAS-dependent phosphorylation promotes GABA$_A$R insertion into the plasma membrane leading to sustained elevations in their accumulation on the cell surface. In both cultured neurons and hippocampal brain slices these events correlate with sustained increases in the efficacy of tonic inhibition (Abramian et al., 2010, 2014; Adams et al., 2015; Modgil et al., 2017). Phosphorylation of the β3 subunit can induce spontaneous channel openings of α4β3δ receptors which have an impact upon agonist/antagonist pharmacology and neuronal excitability (Wlodarczyk et al., 2013; O'Neill and Sylantyev, 2018; Dalby et al., 2020; Sexton et al., 2021).

Recently, we have demonstrated that the metabotropic actions of NASs on tonic inhibition are mediated through membrane progesterone receptor (mPR)-dependent modulation of GABA$_A$R phosphorylation (Parakala et al., 2019). Furthermore, substitution of β3 Ser-408/9 to alanine residues (S408/9A) prevented the effects of NAS and mPR activation on tonic current while leaving the positive allosteric effects of NASs intact.

However, to date the physiological significance of this metabotropic signaling mechanism and its role in mediating the behavioral effects of NAS remains to be examined.

MATERIALS AND METHODS

Mice

Ten- to twelve-week-old male S408/9A mice and the corresponding WT littermates were housed in a 12-h light/dark cycle with standard rodent food and water *ad libitum*. S408/9A mice (C57BL/6J background) were generated by gene targeting in murine ES cells as previously described in Vien et al. (2015). For behavioral testing, animals were acclimatized to the testing room for 1 h before the start of all procedures. Because of the confounds of studying behavioral effects of neurosteroids in female mice, only male mice were used in the current study (Martin et al., 2021). This study was carried out in accordance with the recommendations of the Institutional Animal Care and Use Committee of Tufts University and Tufts Medical Center. The protocol was approved by the Institutional Animal Care and Use Committee of Tufts University and Tufts Medical Center.

Drug Formulation

SGE-516 [3α-Hydroxy-3β-methyl-21-(1′,2′,3′-triazol-2′-yl)-19-nor-5β-pregnan-20-one, Sage Therapeutics, Inc.] (Martinez Botella et al., 2015), and THDOC (tetrahydrodeoxycorticosterone, Sigma-Aldrich, St. Louis, MO, United States, cat. # P2016) was dissolved in vehicle (four parts saline to one part cremophor, MilliporeSigma, St. Louis, MO, United States, cat. # C5135). Diazepam (Dash Pharmaceuticals, Upper Saddle River, NJ, United States) was dissolved in vehicle. All drugs were delivered intraperitoneally, (*i.p.*) at doses specified in the text.

Open Field Test

Individual mice were placed in the center of a 40 cm × 40 cm arena, and their movement was digitally tracked (EthoVision XT 7.0, Noldus Information Technology). WT and S408/9A mice were dosed *i.p.* with vehicle, SGE-516, or THDOC. As controls, the actions of 0.25–1 mg/kg diazepam were compared in WT and S408/9A mice. After 10 min following injections, the mice were placed in the center and the total distance traveled in the open field was compared to vehicle-treated control. Total distance traveled in 60 min was calculated.

Light-Dark Box

Box has equally sized chambers (each chamber is 21 cm × 21 cm), individual mice *i.p.* injected with vehicle (four parts saline to one part cremophor), diazepam, SGE-516, or 10 mg/kg THDOC. After 10 min, mice were placed in the dark chamber and allowed to freely roam between the dark and light chambers. Movement and time spent in the different chambers was digitally tracked and calculated (EthoVision XT 7.0, Noldus Information Technology).

Loss and Return of the Righting Reflex

Anesthetic sensitivity was assayed behaviorally with the loss of righting reflex according to published protocols (Jurd et al., 2003; Sun et al., 2006). Mice 11–38 weeks of age were used only once in each study and received a single injection of THDOC (100 mg/kg, *i.p.*) formulated in four

parts saline to one part cremophor. As loss of righting reflex was instantaneous upon intravenous injection, mice were placed supine in a V-shaped trough with a heating pad set to 37°C to maintain body temperature during the anesthetic state. The time until return of the righting reflex was recorded by an experimenter. All studies were conducted between ZT6 and ZT8.

Electroencephalogram Recordings and Seizures

Electroencephalograms (EEG) were performed as previously described (Vien et al., 2015). Age-matched male littermates, aged 10–12 weeks, were used for recording EEGs in awake, behaving animals. Mice were deeply anesthetized and implanted with prefabricated head mounts containing six-pin connectors with two electromyogram reference electrodes (Pinnacle Technology) 2.0 mm posterior to the bregma, along the midsagittal suture, and 2 mm below the dura. Following a 1-week recovery period, EEG activity was monitored using the Pinnacle Technology turnkey system with a 100 × amplifier and were sampled at 2 kHz and high-pass-filtered at 1 Hz (Power-Labs; AD Instruments). A 30-min baseline was obtained before an *i.p.* injection of 20 mg.kg^{-1} kainic acid (Tocris), followed by continuous EEG monitoring for an additional 120 min. Epileptiform activity was defined as electrographic events with amplitudes greater than twofold the standard deviation of the averaged baseline that last a minimum of 10 s and are separated from another event by greater than 10 s. Epileptiform activity was additionally confirmed by an increase in the power and frequency of high-amplitude events. *Status epilepticus* (SE) was defined as epileptiform activity lasting longer than 5 min with no silent period greater than 10 s. The onset of SE was defined as the time at which the gap between continuous epileptiform activity was less than 2 min. The durations of individual epileptiform events were measured from the start of the epileptiform discharge until return to baseline. Epileptiform activity was quantified using LabChart, version 7 (AD Instruments). Fast Fourier transformation was used to compare seizure power between treatments at frequencies of 1–100 Hz (Vien et al., 2015).

Sixty minutes following the onset of SE mice were given an *i.p.* injection of diazepam, THDOC, SGE-516, or the equivalent amount of vehicle consisting of four parts saline to one part cremophor. Data was converted from the time domain to the frequency domain to generate power spectral density plots [8K FFT size, Hann (cosine-bell), 87.50% window overlap]. Total power 60 s preceding drug injection were quantified and compared to the total power at 10 min after drug injection.

Statistics

Statistical analysis for the Open Field test and Light-dark test was conducted using one-way ANOVA with *post hoc* comparison test using Holm-Sidak's multiple comparison test. An unpaired *t*-test was used for analysis of induction and duration of loss of righting reflex, and percent change in EEG power. All analyses were done using Prism software (GraphPad).

RESULTS

The biochemical and electrophysiological data shown here and in previous publications (Abramian et al., 2010, 2014; Adams et al., 2015; Modgil et al., 2017; Parakala et al., 2019) collectively demonstrate that in addition to the positive allosteric modulation, NAS action at mPRs increase α4 and β3 phosphorylation leading to enhanced extrasynaptic GABA$_A$R membrane insertion and stability resulting in increased tonic inhibition. To determine whether preventing β3 phosphorylation may lead to a modified responsiveness to the anxiolytic, hypnotic/anesthetizing and anti-convulsant properties of neurosteroids, we assessed the behavioral responses of S408/9A and WT controls to acute neurosteroid treatment.

S408/9 Contributes to the Anxiolytic but Not Sedative Actions of Neuroactive Steroids

Neuroactive steroids are potent anxiolytics, and sedatives (Lambert et al., 2009). We have previously found that there were no significant differences between WT and S408/9A mice in motor activity and anxiety-like behavior (Vien et al., 2015). An increase in exploratory behavior in the open field test following a drug treatment is typically indicative of an increase in exploratory activity whereas a decrease in distance traveled would indicate a sedative effect of the drug used. We measured the total distance traveled in the open field in 60 min following *i.p.* doses of diazepam (DZ), SGE-516, and THDOC compared to vehicle-treated control, in WT and S408/9A mice.

There was no difference in distance traveled with WT vehicle treated controls (n = 9) compared to S408/9A vehicle controls (p = 0.24, n = 8). In both WT and S408/9A mice there were no significant change in distance traveled in mice at low dose (0.25 mg/kg, n = 10) of DZ compared with vehicle control (p = 0.6 for both WT and S408/9A, n = 9, **Figure 1A**). In WT mice SGE-516 had a significant effect on exploration at 0.5 mg/kg (n = 5, p = 0.003), 1 mg/kg (n = 8, $p < 0.0001$) and 3 mg/kg doses (n = 14, $p < 0.0001$, **Figure 1B**). In contrast, there was no significant increase in distance traveled following treatment with 0.5 mg/kg (n = 5, p = 0.7), 1 mg/kg (n = 12, p = 0.5), and 3 mg/kg SGE-516 (n = 12, p = 0.64, **Figure 1B**) in S408/9A mice. No dose of THDOC showed a significant increased travel in WT mice although there was a trend to increased travel with 10 and 20 mg/kg (p = 0.27, p = 0.09 for 10 and 20 mg/kg, respectively, n = 8, **Figure 1C**). No dose of THDOC in S408/9A mice significantly increased distance traveled (10 mg/kg, n = 10, p = 0.58: 20 mg/kg, n = 10, p = 0.75, **Figure 1C**).

At higher doses benzodiazepines and NASs become sedative. At 0.5 and 1 mg/kg, diazepam was strongly sedative, significantly reducing the distance traveled compared to vehicle control in WT (n = 8–9, $p < 0.0001$ for both 0.5 and 1 mg/kg) and S408/9A mice (n = 9–10, $p < 0.0001$ for both 0.5 and 1 mg/kg, **Figure 1A**). SGE-516 exerted sedative effects at 5 mg/kg in WT (n = 9, $p < 0.0001$), but in S408/9A mice, the decrease in exploration did not reach significance (n = 12, p = 0.08) compared to vehicle, but distance

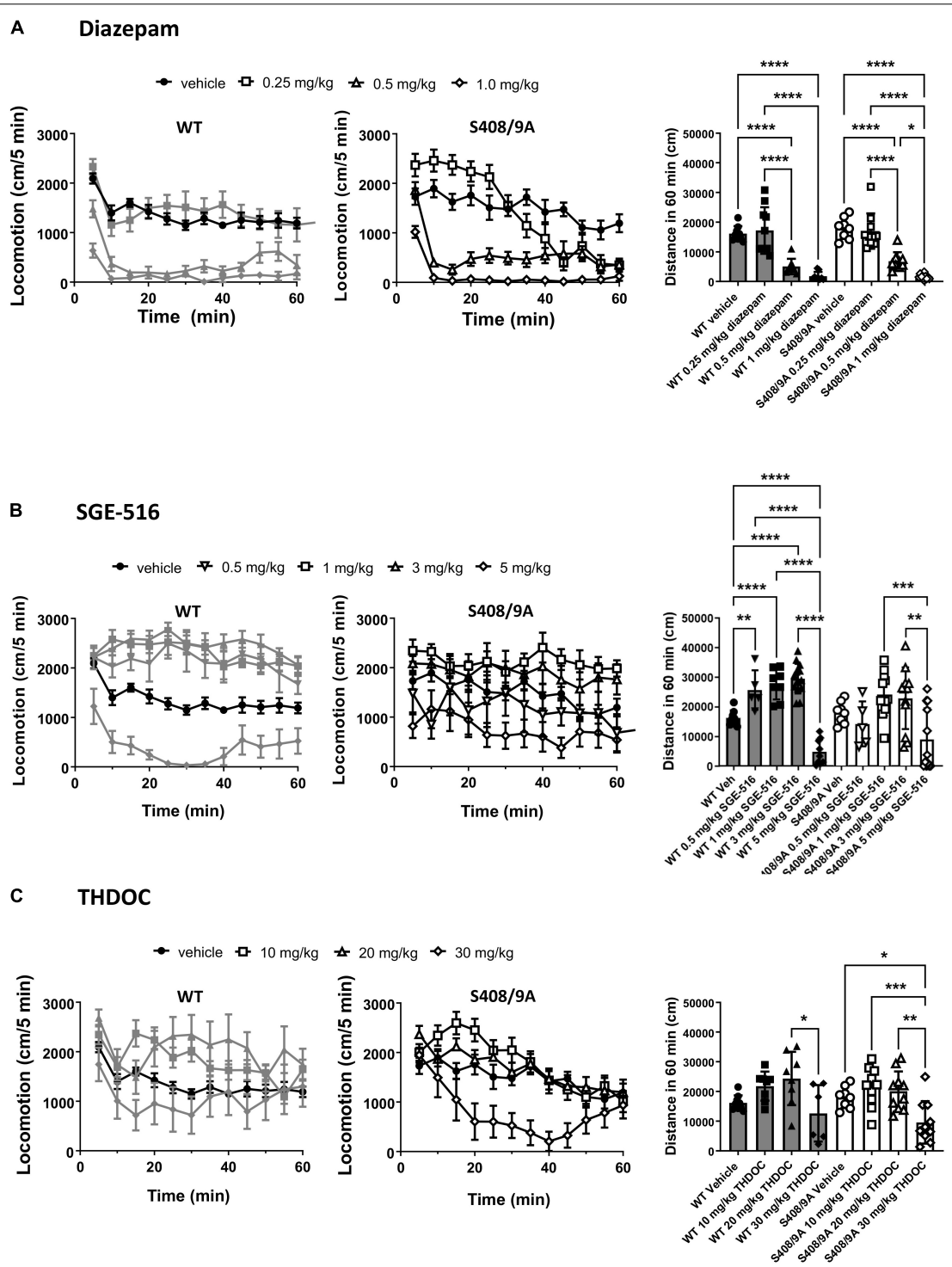

FIGURE 1 | S408/9A is not critical for sedative actions of NASs in the Open Field test. WT (black bars) and S408/9A (white bars) mice were injected *i.p.* with vehicle, 0.25–1 mg/kg Diazepam **(A)**, 1–5 mg/kg SGE-516 **(B)**, or 10–30 mg/kg THDOC **(C)**. 30 min later total distance traveled was measured for 60 min. All data represent mean ± S.D., $^*p \leq 0.03$, $^{**}p \leq 0.003$, $^{***}p \leq 0.001$, $^{****}p < 0.0001$.

traveled at 5 mg/kg was significant reduced compared to 1 and 3 mg/kg SGE-616 (1 mg/kg $p = 0.0009$, $n = 12$; 3 mg/kg $p = 0.003$, $n = 12$, **Figure 1B**). THDOC (30 mg/kg) reduced distance traveled in WT compared to at 20 mg/kg ($n = 6$, $p = 0.02$). A significant sedative effect was observed with 30 mg/kg THDOC compared to vehicle in S408/9A mice ($n = 10$, $p = 0.03$, **Figure 1C**).

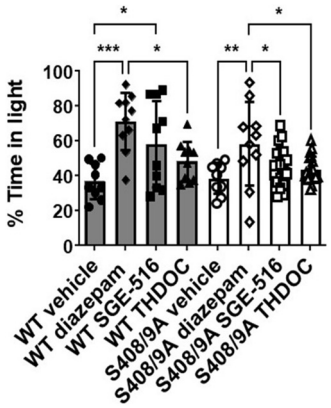

FIGURE 2 | S408/9A selectively impairs the anxiolytic effects of neuroactive steroids. Time spent in the light arena of the light-dark box assay was determined for WT (black bars) and S408/9A (white bars) mice with vehicle, diazepam (0.25 mg/kg), SGE-516 (1 mg/kg), or THDOC (10 mg/kg) treatment. In both genotypes, diazepam significantly increased the amount of time spent in the light arena. THDOC was ineffective at increasing time spent in the light whereas SGE-516 increased time in light area only in WT mice. $^*p \leq 0.04$, $^{**}p = 0.004$, $^{***}p = 0.0006$; $n = 9$–20.

To further test the anxiolytic efficacy of NASs, the behavior of both strains was examined in the light/dark box test, using non-sedating doses of diazepam (0.25 mg/kg), THDOC (10 mg/kg), and SGE-516 (1 mg/kg). For vehicle-treated mice, WT and S408/9A mice spent equal time, approximately 37% of the time, in the light (WT 221.0 ± 20.6 s, $n = 9$: S408/9A 230.5 ± 18.0 s, $n = 9$, $p = 0.99$). However, when examining the % time spent in the light 10 min following *i.p.* injection of drug there was a significant difference between genotypes (**Figure 2**). As expected from previous work detailing their anxiolytic actions, diazepam and the NASs increased the time in the light box. In WT mice the % time spent in the light was significantly increased with diazepam (71 ± 5%, $n = 10$, $p = 0.0001$), and SGE-516 (58 ± 8%, $n = 10$, $p = 0.02$) compared to vehicle control (37 ± 3%, $n = 9$). There was a small but insignificant increase in the % time spent in the light following THDOC treatment in WT mice (48 ± 4%, $n = 10$, $p = 0.33$).

In S408/9A mice, only diazepam significantly increased % time spent in the light (58 ± 8%, $n = 10$, $p = 0.004$) compared to vehicle control (38 ± 3%, $n = 9$). The NASs THDOC (44 ± 2%, $n = 20$, $p = 0.67$) and SGE-516 (45 ± 3%, $n = 19$, $p = 0.47$) did not significantly increase % time in the light box indicating an absence of anxiolytic effect of the NASs in S408/9A mice.

Hypnotic Properties of Neuroactive Steroids Are Reduced in S408/9A Mice

The ability of neurosteroids to cause a loss of consciousness has long been known and one neurosteroid, alphaxalone, is used as a veterinarian general anesthetic. GABA$_A$Rs-mediated currents are potently enhanced by the positive allosteric actions of general anesthetics (Hemmings et al., 2019). Extrasynaptic GABA$_A$Rs are particularly sensitive to positive allosteric actions of NASs and are believed to be the primary mediators of the hypnotic endpoint of general anesthetics (Belelli and Lambert, 2005; Kretschmannova et al., 2013). Furthermore, the β3 subunit is known to be critical for hypnotic actions of general anesthetics (Jurd et al., 2003). Given that NAS activation of mPRs leads to the phosphorylation of β3 S408/9 to bring about an increase in tonic current, we hypothesized that this increase in receptor expression would, in turn, be allosterically potentiated by the NAS to produce a hypnotic effect. Given that extrasynaptic-like GABA$_A$Rs containing the β3 S408/9A mutation are as sensitive to potentiation by THDOC as WT receptors (Adams et al., 2015) we have examined NAS-mediated loss of righting reflex (LORR) in S408/9A mice to examine the role of β3 subunit phosphorylation and receptor trafficking in NAS-mediated hypnosis.

Only ∼55% of the S408/9A mice responded to 80 mg/kg *i.p.* THDOC by becoming ataxic, compared to 100% of WT controls. Of the S408/9A mice that underwent LORR, there were no statistical differences in latency of LORR compared to WT controls (WT, 9 ± 1 min, $n = 6$; S408/9A, 9 ± 1 min, $n = 5$, $p = 0.6$, **Figure 3A**). However, the S408/9A mice that responded to THDOC injections exhibited a striking decrease in the duration of LORR compared to WT controls (WT, 31 ± 4 min, $n = 6$: S408/9A, 17 ± 4 min, $n = 5$; $P = 0.03$; **Figure 3B**). This result indicates that the inability of NASs to phosphorylate β3-containing GABA$_A$Rs reduces the hypnotic duration of NASs but not the induction.

S408/9 Determines the Ability of Neuroactive Steroids to Terminate Pharmacoresistant Seizures

Studies in animals suggest that NASs are efficacious in terminating pharmacoresistant seizures (Rogawski et al., 2013). We explored if the ability of NASs to arrest pharmacoresistant seizures is dependent upon their ability to phosphorylate β3 subunits, by comparing the anticonvulsant efficacy of NASs in WT, and S408/9A mice using EEG recording. While these mice do not appear to exhibit overt spontaneous seizures, they are more sensitivity to kainite-induced *Status epilepticus* than WT, as reflected by a reduced latency to the onset of SE, coupled with enhanced seizure severity (Vien et al., 2015).

To examine the role that S408/9 plays in the ability of NASs to terminate pharmacoresistant seizures we implanted WT and S408/9A mice (2–4 months of age) with EEG/EMG electrodes and allowed them to recover for 7 days (Vien et al., 2015). During experiments, baseline EEGs were recorded for 30 min prior to *i.p.* injection of 20 mg/kg kainate which resulted in the development of SE approximately 35–40 min after kainate injection. Sixty min after entrance into SE, mice were treated *i.p.* with the prototypic benzodiazepine, diazepam (DZ, 20 mg/kg), THDOC (100 mg/kg), or SGE-516 (3 mg/kg). Seizure activity 10 min following treatment was compared to 30 s prior to drug treatment.

Sixty minutes after entrance into SE, *i.p.* injection of DZ did not terminate seizure activity and EEG power tended to increase following DZ injection in WT mice (128 ± 58%, $n = 11$). S408/9A mice readily entered SE and DZ resistance was evident following treatment (2 ± 14%, $n = 7$; **Figure 4**). In WT mice, THDOC

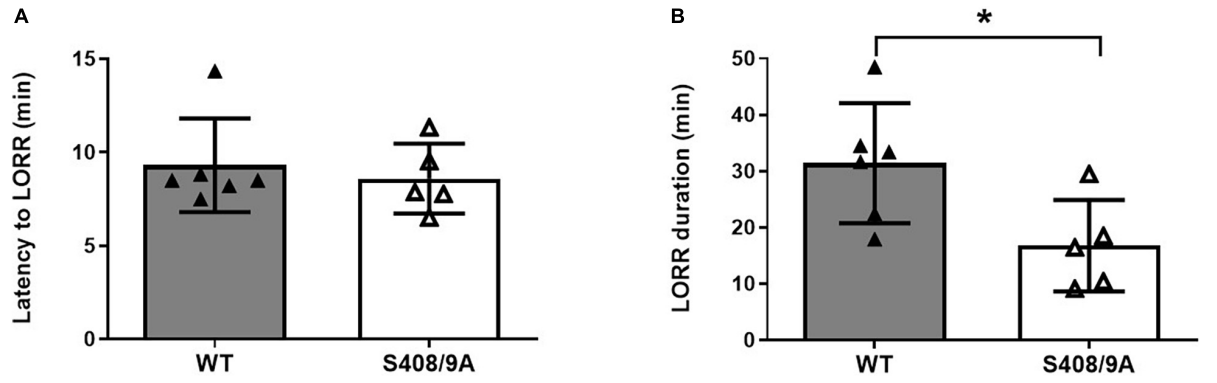

FIGURE 3 | Hypnotic actions of THDOC are decreased in S408/9A mice. Hypnotic action of THDOC was measured using the loss of righting reflex assay, 44% of S408/9A mice tested did not lose their righting reflex with THDOC. Bars represent only the responders. **(A)** Induction of LORR with *i.p.* injection of 80 mg/kg THDOC was similar in WT and S408/9A mice. **(B)** The S408/9A mice spent a significantly shorter duration of loss of righting reflex compared to WT controls following THDOC (*p = 0.03; t-test; n = 5–6).

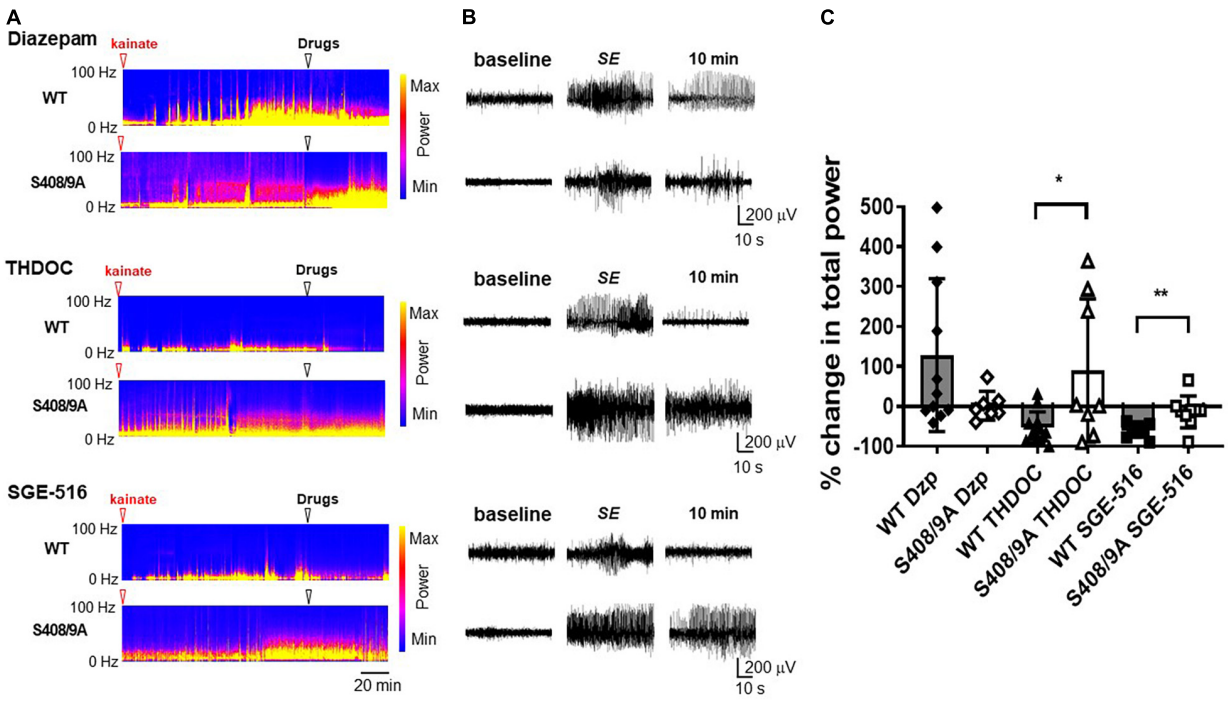

FIGURE 4 | Neuroactive steroids are ineffective in terminating diazepam resistant seizures in S408/9A mice. **(A)** EEG spectrograms from WT and S408/9A mice following injection with 20 mg/kg kainate (red arrowhead) to induce *Status Epilepticus* (SE). 60 min after entrance into SE, mice were then injected *i.p.* (white arrowhead) with diazepam (Dzp, 20 mg/kg), THDOC (100 mg/kg), or SGE-516 (3 mg/kg). **(B)** EEG recordings from WT and S408/9A mice during baseline, SE, 10 min following drug administration demonstrating diazepam resistant seizures that are suppressed with THDOC or SGE-516 in WT but not S408/9A mice. **(C)** The % change in total EEG power (1–100 Hz) 10 min after drug treatment compared to 30 s prior to treatment. All data represent mean ± S.D., *p = 0.015, **p = 0.004; n = 7–12 mice.

dramatically reduced seizure activity and EEG power 10 min after administration by −52 ± 39%, n = 12 (**Figure 4**). In contrast to WT mice, THDOC were unable to terminate pharmacoresistant SE in S408/9A mice (90 ± 63%, n = 8, p = 0.015, **Figure 4**). Similarly, the reduction in EEG power by SGE-516 treatment (−59 ± 5%, n = 10) in WT mice was significantly reduced in S408/9A mice (−14 ± 13%, n = 9, p = 0.004).

DISCUSSION

Pregnane neurosteroids such as allopregnanolone and tetrahydrodeoxycorticosterone (THDOC), and their synthetic neuroactive steroids, have long been known to have anxiolytic, sedative, hypnotic, and anticonvulsant properties (Belelli et al., 2020). Conventionally, it was thought that these pharmacological

endpoints were a result of a positive allosteric modulation (PAM) of GABA$_A$Rs, whereby neurosteroids bind to the GABA$_A$R causing a conformational structural change to prolong channel open times and enhance Cl^- flow through the channel. Both synaptic and extrasynaptic GABA$_A$Rs are sensitive to the PAM activity of neurosteroids (Belelli and Lambert, 2005). However, it has been documented that neurosteroids have long-lasting GABA$_A$R modulatory effects, outlasting the presence of neurosteroids and thus negating any allosteric modulation. We have investigated additional mechanisms that could explain these long-term neurosteroid effects on GABA$_A$Rs and have demonstrated that in the dentate gyrus of the hippocampus the actions of neurosteroids increase the intracellular trafficking and plasma membrane stability of extrasynaptic GABA$_A$Rs in a phosphorylation-dependent manner (Jacob et al., 2008; Abramian et al., 2010, 2014; Comenencia-Ortiz et al., 2014). Furthermore, neurosteroids evoke this change in the phosphorylated state of α4 and β3 subunits *via* a metabotropic mechanism involving the activation of membrane Progesterone Receptors (mPRs) leading to an increase in PKC and PKA activity (Parakala et al., 2019).

Neurosteroids are known to facilitate their persistent effects, through phosphorylation-dependent mechanism (Fancsik et al., 2000; Lambert et al., 2001a,b; Brussaard and Koksma, 2003; Harney et al., 2003; Herd et al., 2007; Mitchell et al., 2008; Vithlani and Moss, 2009; Abramian et al., 2010, 2014; Kia et al., 2011; Comenencia-Ortiz et al., 2014). Therefore, an understanding of the mechanisms through which neurosteroids exert their effects on extrasynaptic GABA$_A$Rs may promote the development of therapies to alleviate neurological disorders. In this study, we investigated the contribution of β3 subunit phosphorylation in mediating the effects of neurosteroids on GABA$_A$R activity at the behavioral level.

Neuroactive steroids have long been demonstrated to have anxiolytic effects in several animal models of anxiety (Schule et al., 2014). Increases of NAS levels in the hippocampus are correlated with lower anxiety and increased exploratory behavior (Koonce et al., 2012). Here, we examined if this anxiolytic effect was due to allosteric or metabotropic mediated pathways. We have previously shown that β3S408/9A mice do not exhibit any deficits in locomotor activity and exhibit comparable behavior in the open field compared to WT animals (Vien et al., 2015). Similarly, we found no basal differences between WT and S408/9A mice in the open field and light-dark box. We initially examined the open field apparatus and saw an increase in exploratory behavior with SGE-516 and THDOC in WT mice that was absent in β3S408/9A mice. At high doses of THDOC and diazepam both WT and β3S408/9A mice became sedated suggesting positive allosteric modulation of GABA$_A$Rs underlies the sedating actions of NASs. In agreement with this, sedation brought on by administration of general anesthetics is believed to be through positive allosteric modulation of GABA$_A$Rs containing the β2 subunit (Reynolds et al., 2003).

To explore NAS anxiolytic effects, we used the light-dark box and examined the time spent in the light. In accordance with its anxiolytic properties, diazepam increased time spent in the light in both WT and β3S408/9A mice. Only SGE-516 showed anxiolytic effects in WT mice at the dose tested and no anxiolytic effect was observed in β3S408/9A mice demonstrating the requirement to activate the metabotropic pathway for NASs anxiolysis. While there was a trend for an anxiolytic effect with THDOC, it did not reach significance. Previous studies have described anxiolytic effects with THDOC (Crawley et al., 1986; Wieland et al., 1991; Rodgers and Johnson, 1998), the differences in past and present observations could be due to timing of the test following THDOC administration, dose of THDOC, different mouse strain, and different tests of anxiety employed.

A large percentage of β3S408/9A mice did not respond to the hypnotic actions of THDOC. Those mice that did eventually lose consciousness, induction of hypnosis was no different to WT mice. However, loss of righting reflex duration was significantly reduced in β3S408/9A mice. β3 subunit containing GABA$_A$Rs are known to play an essential role in the hypnotic actions of intravenous general anesthetics (Jurd et al., 2003; Belelli et al., 2005; Belelli and Lambert, 2005; Ferguson et al., 2007). Additionally, phosphorylation of the β3 subunit is important for propofol mediated hypnosis (Nikaido et al., 2017) leading to the suggestion that modulation of phosphorylation and membrane trafficking of GABA$_A$Rs could be targeted to enhance hypnotic endpoint of general anesthetics and reduce the dose of anesthetic needed for hypnosis and reduce their unwanted side effects.

Status Epilepticus (SE) in humans and rodent chemical-convulsant models, progressively becomes insensitive to arrest by benzodiazepines, the current standard of care. Development of benzodiazepine pharmacoresistance leads to a dramatic increase in mortality and morbidity (DeLorenzo et al., 1995; Lowenstein and Alldredge, 1998; Jones et al., 2002). Pharmacoresistant epilepsy accounts for approximately one third of all epileptic patients (Laxer et al., 2014). Not only have neuroactive steroids been shown to be anticonvulsant but ALLO and SGE-516 have been demonstrated to be effective at stopping pharmacoresistant epilepsy in refractory SE models (Rogawski et al., 2013; Althaus et al., 2017; Hammond et al., 2017). Both THDOC and SGE-516 terminated diazepam resistant SE in WT mice but these NASs were ineffective in β3S408/9A mice. Because NAS are still capable of acting as a PAM of tonic current in β3S408/9A mice (Adams et al., 2015), the allosteric actions of NASs which have typically been used to explain their anticonvulsant properties in pharmacoresistant epilepsy are at odds with our observations. While the S408/9A mice have increased sensitivity to kainite induced seizures (Vien et al., 2015), our results demonstrate that S408/9 or their phosphorylation status contribute to the efficacy of NAS to terminate pharmaco-resistant SE.

Great effort has been devoted to the development of GABA$_A$Rs PAMs with the aim of producing more efficacious and potent anxiolytic, hypnotic and anticonvulsant therapies. Recognition of the metabotropic pathways whereby NASs can increase the trafficking of GABA$_A$Rs and enhance neuronal inhibition without allosterically causing sedation will allow novel therapies to be developed. The S408/9A mutation altered the anxiolytic, hypnotic/anesthetizing, and anticonvulsant response to acute neurosteroid treatment while leaving the sedative response in S408/9A mice unaltered. We propose

that the mechanism that determines neurosteroid-mediated anxiolysis, duration of LORR, and termination of pharmaco-resistant seizures involves β3 S408/9 phosphorylation and the subsequent trafficking and stabilization of extrasynaptic GABA$_A$Rs.

DATA AVAILABILITY STATEMENT

The original contributions presented in the study are included in the article/supplementary material, further inquiries can be directed to the corresponding authors.

ETHICS STATEMENT

The animal study was reviewed and approved by the Institutional Animal Care and Use Committee of Tufts University and Tufts Medical Center.

AUTHOR CONTRIBUTIONS

TV, MA, JD, SM, and PD contributed to the conception and design of the study. TV and PD acquired, analyzed, and interpreted the data and wrote the first draft of the manuscript. All authors contributed to manuscript revision, read, and approved the submitted version.

FUNDING

This work was supported by the Sage Therapeutics, Inc., this funder contributed to the conception and design of the study. This study also received support from National Institutes of Health (NIH), National Institute of Neurological Disorders and Stroke Grants NS051195 (SM), NS056359 (SM), NS081735 (SM), NS087662 (SM), NS108378 (SM and PD), R21NS080064 (SM), R21NS111338 (PD), and R21NS111064 (PD), NIH, United States, and National Institute of Mental Health Grant MH097446 (SM and PD).

REFERENCES

Abramian, A. M., Comenencia-Ortiz, E., Modgil, A., Vien, T. N., Nakamura, Y., Moore, Y. E., et al. (2014). Neurosteroids promote phosphorylation and membrane insertion of extrasynaptic GABAA receptors. *Proc. Natl. Acad. Sci. U S A* 111, 7132–7137. doi: 10.1073/pnas.1403285111

Abramian, A. M., Comenencia-Ortiz, E., Vithlani, M., Tretter, E. V., Sieghart, W., Davies, P. A., et al. (2010). Protein kinase C phosphorylation regulates membrane insertion of GABAA receptor subtypes that mediate tonic inhibition. *J. Biol. Chem.* 285, 41795–41805. doi: 10.1074/jbc.M110.149229

Adams, J. M., Thomas, P., and Smart, T. G. (2015). Modulation of neurosteroid potentiation by protein kinases at synaptic- and extrasynaptic-type GABAA receptors. *Neuropharmacology* 88, 63–73. doi: 10.1016/j.neuropharm.2014.09.021

Althaus, A. L., McCarren, H. S., Alqazzaz, A., Jackson, C., McDonough, J. H., Smith, C. D., et al. (2017). The synthetic neuroactive steroid SGE-516 reduces status epilepticus and neuronal cell death in a rat model of soman intoxication. *Epilepsy Behav.* 68, 22–30. doi: 10.1016/j.yebeh.2016.12.024

Antonoudiou, P., Colmers, P. L. W., Walton, N. L., Weiss, G. L., Smith, A. C., Nguyen, D. P., et al. (2022). Allopregnanolone Mediates Affective Switching Through Modulation of Oscillatory States in the Basolateral Amygdala. *Biol. Psychiatry* 91, 283–293. doi: 10.1016/j.biopsych.2021.07.017

Belelli, D., Harrison, N. L., Maguire, J., Macdonald, R. L., Walker, M. C., and Cope, D. W. (2009). Extrasynaptic GABAA receptors: form, pharmacology, and function. *J. Neurosci.* 29, 12757–12763.

Belelli, D., Hogenkamp, D., Gee, K. W., and Lambert, J. J. (2020). Realising the therapeutic potential of neuroactive steroid modulators of the GABAA receptor. *Neurobiol. Stress* 12:100207. doi: 10.1016/j.ynstr.2019.100207

Belelli, D., and Lambert, J. J. (2005). Neurosteroids: endogenous regulators of the GABA(A) receptor. *Nat. Rev. Neurosci.* 6, 565–575. doi: 10.1038/nrn1703

Belelli, D., Peden, D. R., Rosahl, T. W., Wafford, K. A., and Lambert, J. J. (2005). Extrasynaptic GABAA receptors of thalamocortical neurons: a molecular target for hypnotics. *J. Neurosci.* 25, 11513–11520.

Belelli, D., Phillips, G. D., Atack, J. R., and Lambert, J. J. (2021). Relating neurosteroid modulation of inhibitory neurotransmission to behaviour. *J. Neuroendocrinol.* 2021:e13045. doi: 10.1111/jne.13045

Bencsits, E., Ebert, V., Tretter, V., and Sieghart, W. (1999). A significant part of native gamma-aminobutyric AcidA receptors containing alpha4 subunits do not contain gamma or delta subunits. *J. Biol. Chem.* 274, 19613–19616. doi: 10.1074/jbc.274.28.19613

Brickley, S. G., and Mody, I. (2012). Extrasynaptic GABA(A) receptors: their function in the CNS and implications for disease. *Neuron* 73, 23–34. doi: 10.1016/j.neuron.2011.12.012

Brussaard, A. B., and Koksma, J. J. (2003). Conditional regulation of neurosteroid sensitivity of GABAA receptors. *Ann. N. Y. Acad. Sci.* 1007, 29–36. doi: 10.1196/annals.1286.003

Comenencia-Ortiz, E., Moss, S. J., and Davies, P. A. (2014). Phosphorylation of GABAA receptors influences receptor trafficking and neurosteroid actions. *Psychopharmacology* 231, 3453–3465. doi: 10.1007/s00213-014-3617-z

Crawley, J. N., Glowa, J. R., Majewska, M. D., and Paul, S. M. (1986). Anxiolytic activity of an endogenous adrenal steroid. *Brain Res.* 398, 382–385. doi: 10.1016/0006-8993(86)91500-3

Dalby, N. O., Falk-Petersen, C. B., Leurs, U., Scholze, P., Krall, J., Frølund, B., et al. (2020). Silencing of spontaneous activity at α4β1/3δ GABAA receptors in hippocampal granule cells reveals different ligand pharmacology. *Br. J. Pharmacol.* 177, 3975–3990. doi: 10.1111/bph.15146

DeLorenzo, R. J., Pellock, J. M., Towne, A. R., and Boggs, J. G. (1995). Epidemiology of status epilepticus. *J. Clin. Neurophysiol.* 12, 316–325.

Fancsik, A., Linn, D. M., and Tasker, J. G. (2000). Neurosteroid modulation of GABA IPSCs is phosphorylation dependent. *J. Neurosci.* 20, 3067–3075. doi: 10.1523/JNEUROSCI.20-09-03067.2000

Ferguson, C., Hardy, S. L., Werner, D. F., Hileman, S. M., Delorey, T. M., and Homanics, G. E. (2007). New insight into the role of the beta3 subunit of the GABAA-R in development, behavior, body weight regulation, and anesthesia revealed by conditional gene knockout. *BMC Neurosci.* 8:85. doi: 10.1186/1471-2202-8-85

Hammond, R. S., Althaus, A. L., Ackley, M. A., Maciag, C., Martinez Botella, G., Salituro, F. G., et al. (2017). Anticonvulsant profile of the neuroactive steroid. SGE-516, in animal models. *Epilepsy Res.* 134, 16–25. doi: 10.1016/j.eplepsyres.2017.05.001

Harney, S. C., Frenguelli, B. G., and Lambert, J. J. (2003). Phosphorylation influences neurosteroid modulation of synaptic GABAA receptors in rat CA1 and dentate gyrus neurones. *Neuropharmacology* 45, 873–883. doi: 10.1016/s0028-3908(03)00251-x

Hemmings, H. C. Jr., Riegelhaupt, P. M., Kelz, M. B., Solt, K., Eckenhoff, R. G., Orser, B. A., et al. (2019). Towards a Comprehensive Understanding of Anesthetic Mechanisms of Action: a Decade of Discovery. *Trends Pharmacol. Sci.* 40, 464–481. doi: 10.1016/j.tips.2019.05.001

Herd, M. B., Belelli, D., and Lambert, J. J. (2007). Neurosteroid modulation of synaptic and extrasynaptic GABA(A) receptors. *Pharmacol. Ther.* 116, 20–34. doi: 10.1016/j.pharmthera.2007.03.007

Hodge, C. W., Raber, J., McMahon, T., Walter, H., Sanchez-Perez, A. M., Olive, M. F., et al. (2002). Decreased anxiety-like behavior, reduced stress hormones, and neurosteroid supersensitivity in mice lacking protein kinase Cepsilon. *J. Clin. Invest.* 110, 1003–1010. doi: 10.1172/JCI15903

Jacob, T. C., Moss, S. J., and Jurd, R. (2008). GABA(A) receptor trafficking and its role in the dynamic modulation of neuronal inhibition. *Nat. Rev. Neurosci.* 9, 331–343. doi: 10.1038/nrn2370

Jones, D. M., Esmaeil, N., Maren, S., and Macdonald, R. L. (2002). Characterization of pharmacoresistance to benzodiazepines in the rat Li-pilocarpine model of status epilepticus. *Epilepsy Res.* 50, 301–312. doi: 10.1016/s0920-1211(02)00085-2

Jurd, R., Arras, M., Lambert, S., Drexler, B., Siegwart, R., Crestani, F., et al. (2003). General anesthetic actions *in vivo* strongly attenuated by a point mutation in the GABA(A) receptor beta3 subunit. *FASEB J.* 17, 250–252. doi: 10.1096/fj.02-0611fje

Kia, A., Ribeiro, F., Nelson, R., Gavrilovici, C., Ferguson, S. S., and Poulter, M. O. (2011). Kindling alters neurosteroid-induced modulation of phasic and tonic GABAA receptor-mediated currents: role of phosphorylation. *J. Neurochem.* 116, 1043–1056. doi: 10.1111/j.1471-4159.2010.07156.x

Koonce, C. J., Walf, A. A., and Frye, C. A. (2012). Type 1 5alpha-reductase may be required for estrous cycle changes in affective behaviors of female mice. *Behav. Brain Res.* 226, 376–380. doi: 10.1016/j.bbr.2011.09.028

Kretschmannova, K., Hines, R. M., Revilla-Sanchez, R., Terunuma, M., Tretter, T., Jurd, R., et al. (2013). Enhanced tonic inhibition influences the hypnotic and amnestic actions of the intravenous anesthetics etomidate and propofol. *J. Neurosci.* 33, 7264–7273. doi: 10.1523/JNEUROSCI.5475-12.2013

Lambert, J. J., Belelli, D., Harney, S. C., Peters, J. A., and Frenguelli, B. G. (2001a). Modulation of native and recombinant GABA(A) receptors by endogenous and synthetic neuroactive steroids. *Brain Res. Brain Res. Rev.* 37, 68–80. doi: 10.1016/s0165-0173(01)00124-2

Lambert, J. J., Cooper, M. A., Simmons, R. D., Weir, C. J., and Belelli, D. (2009). Neurosteroids: endogenous allosteric modulators of GABA(A) receptors. *Psychoneuroendocrinology* 34(Suppl. 1), S48–S58. doi: 10.1016/j.psyneuen.2009.08.009

Lambert, J. J., Harney, S. C., Belelli, D., and Peters, J. A. (2001b). Neurosteroid modulation of recombinant and synaptic GABAA receptors. *Int. Rev. Neurobiol.* 46, 177–205. doi: 10.1016/s0074-7742(01)46063-6

Laxer, K. D., Trinka, E., Hirsch, L. J., Cendes, F., Langfitt, J., Delanty, N., et al. (2014). The consequences of refractory epilepsy and its treatment. *Epilepsy Behav.* 37, 59–70. doi: 10.1016/j.yebeh.2014.05.031

Lowenstein, D. H., and Alldredge, B. K. (1998). Status epilepticus. *N. Engl. J. Med.* 338, 970–976. doi: 10.1056/NEJM199804023381407

Lüscher, B., and Mohler, H. (2019). Brexanolone, a neurosteroid antidepressant, vindicates the GABAergic deficit hypothesis of depression and may foster resilience. *F1000Res.* 8:F1000. doi: 10.12688/f1000research.18758.1

Maguire, J. (2019). Neuroactive Steroids and GABAergic Involvement in the Neuroendocrine Dysfunction Associated With Major Depressive Disorder and Postpartum Depression. *Front. Cell Neurosci.* 13:83. doi: 10.3389/fncel.2019.00083

Martin, E. L., Doncheck, E. M., Reichel, C. M., and McRae-Clark, A. L. (2021). Consideration of sex as a biological variable in the translation of pharmacotherapy for stress-associated drug seeking. *Neurobiol. Stress* 15:100364. doi: 10.1016/j.ynstr.2021.100364

Martinez Botella, G., Salituro, F. G., Harrison, B. L., Beresis, R. T., Bai, Z., Shen, K., et al. (2015). Neuroactive steroids. 1. Positive allosteric modulators of the (γ-aminobutyric acid) a receptor: structure-activity relationships of heterocyclic substitution at C-21. *J. Med. Chem.* 58, 3500–3511. doi: 10.1021/acs.jmedchem.5b00032

Marx, C. E., Shampine, L. J., Khisti, R. T., Trost, W. T., Bradford, D. W., Grobin, A. C., et al. (2006). Olanzapine and fluoxetine administration and coadministration increase rat hippocampal pregnenolone, allopregnanolone and peripheral deoxycorticosterone: implications for therapeutic actions. *Pharmacol. Biochem. Behav.* 84, 609–617. doi: 10.1016/j.pbb.2006.07.032

Mitchell, E. A., Herd, M. B., Gunn, B. G., Lambert, J. J., and Belelli, D. (2008). Neurosteroid modulation of GABAA receptors: molecular determinants and significance in health and disease. *Neurochem. Int.* 52, 588–595.

Modgil, A., Parakala, M. L., Ackley, M. A., Doherty, J. J., Moss, S. J., and Davies, P. A. (2017). Endogenous and synthetic neuroactive steroids evoke sustained increases in the efficacy of GABAergic inhibition *via* a protein kinase C-dependent mechanism. *Neuropharmacology* 113, 314–322. doi: 10.1016/j.neuropharm.2016.10.010

Mortensen, M., and Smart, T. G. (2006). Extrasynaptic alphabeta subunit GABAA receptors on rat hippocampal pyramidal neurons. *J. Physiol.* 577(Pt 3), 841–856. doi: 10.1113/jphysiol.2006.117952

Nikaido, Y., Furukawa, T., Shimoyama, S., Yamada, J., Migita, K., Koga, K., et al. (2017). Propofol Anesthesia Is Reduced in Phospholipase C-Related Inactive Protein Type-1 Knockout Mice. *J. Pharmacol. Exp. Ther.* 361, 367–374. doi: 10.1124/jpet.116.239145

O'Neill, N., and Sylantyev, S. (2018). Spontaneously opening GABAA receptors play a significant role in neuronal signal filtering and integration. *Cell Death Dis.* 9:813. doi: 10.1038/s41419-018-0856-7

Parakala, M. L., Zhang, Y., Modgil, A., Chadchankar, J., Vien, T. N., Ackley, M. A., et al. (2019). Metabotropic, but not allosteric, effects of neurosteroids on GABAergic inhibition depend on the phosphorylation of GABA. *J Biol Chem* 294, 12220–12230. doi: 10.1074/jbc.RA119.008875

Paul, S. M., and Purdy, R. H. (1992). Neuroactive steroids. *FASEB J.* 6, 2311–2322.

Reynolds, D. S., Rosahl, T. W., Cirone, J., O'Meara, G. F., Haythornthwaite, A., Newman, R. J., et al. (2003). Sedation and anesthesia mediated by distinct GABA(A) receptor isoforms. *J. Neurosci.* 23, 8608–8617. doi: 10.1523/JNEUROSCI.23-24-08608.2003

Rodgers, R. J., and Johnson, N. J. (1998). Behaviorally selective effects of neuroactive steroids on plus-maze anxiety in mice. *Pharmacol. Biochem. Behav.* 59, 221–232. doi: 10.1016/s0091-3057(97)00339-0

Rogawski, M. A., Loya, C. M., Reddy, K., Zolkowska, D., and Lossin, C. (2013). Neuroactive steroids for the treatment of status epilepticus. *Epilepsia* 54(Suppl. 6), 93–98. doi: 10.1111/epi.12289

Rudolph, U., and Mohler, H. (2006). GABA-based therapeutic approaches: GABAA receptor subtype functions. *Curr. Opin. Pharmacol.* 6, 18–23. doi: 10.1016/j.coph.2005.10.003

Schule, C., Nothdurfter, C., and Rupprecht, R. (2014). The role of allopregnanolone in depression and anxiety. *Prog. Neurobiol.* 113, 79–87. doi: 10.1016/j.pneurobio.2013.09.003

Sexton, C. A., Penzinger, R., Mortensen, M., Bright, D. P., and Smart, T. G. (2021). Structural determinants and regulation of spontaneous activity in GABAA receptors. *Nat. Commun.* 12:5457. doi: 10.1038/s41467-021-25633-0

Sun, Y., Chen, J., Pruckmayr, G., Baumgardner, J. E., Eckmann, D. M., Eckenhoff, R. G., et al. (2006). High throughput modular chambers for rapid evaluation of anesthetic sensitivity. *BMC Anesthesiol.* 6:13. doi: 10.1186/1471-2253-6-13

Uzunova, V., Wrynn, A. S., Kinnunen, A., Ceci, M., Kohler, C., and Uzunov, D. P. (2004). Chronic antidepressants reverse cerebrocortical allopregnanolone decline in the olfactory-bulbectomized rat. *Eur. J. Pharmacol.* 486, 31–34. doi: 10.1016/j.ejphar.2003.12.002

Vien, T. N., Modgil, A., Abramian, A. M., Jurd, R., Walker, J., Brandon, N. J., et al. (2015). Compromising the phosphodependent regulation of the GABAAR β3 subunit reproduces the core phenotypes of autism spectrum disorders. *Proc. Natl. Acad. Sci. U S A* 112, 14805–14810. doi: 10.1073/pnas.1514657112

Vithlani, M., and Moss, S. J. (2009). The role of GABAAR phosphorylation in the construction of inhibitory synapses and the efficacy of neuronal inhibition. *Biochem. Soc. Trans.* 37(Pt 6), 1355–1358. doi: 10.1042/BST0371355

Wieland, S., Lan, N. C., Mirasedeghi, S., and Gee, K. W. (1991). Anxiolytic activity of the progesterone metabolite 5α-pregnan-3α-ol-20-one. *Brain Res.* 565, 263–268. doi: 10.1016/0006-8993(91)91658-n

Wlodarczyk, A. I., Sylantyev, S., Herd, M. B., Kersanté, F., Lambert, J. J., Rusakov, D. A., et al. (2013). GABA-independent GABAA receptor openings maintain tonic currents. *J. Neurosci.* 33, 3905–3914. doi: 10.1523/JNEUROSCI.4193-12.2013

Conflict of Interest: MA and JD were employed by Sage Therapeutics, Inc. SM serves as a consultant for Sage Therapeutics, Inc., and AstraZeneca, relationships that are regulated by Tufts University.

The remaining authors declare that the research was conducted in the absence of any commercial or financial relationships that could be construed as a potential conflict of interest.

Publisher's Note: All claims expressed in this article are solely those of the authors and do not necessarily represent those of their affiliated organizations, or those of the publisher, the editors and the reviewers. Any product that may be evaluated in this article, or claim that may be made by its manufacturer, is not guaranteed or endorsed by the publisher.

frontiers | Frontiers in Molecular Neuroscience

REVIEW
published: 05 July 2022
doi: 10.3389/fnmol.2022.937789

Taurine and Astrocytes: A Homeostatic and Neuroprotective Relationship

*Sofía Ramírez-Guerrero[1], Santiago Guardo-Maya[1], Germán J. Medina-Rincón[1], Eduardo E. Orrego-González[1], Ricardo Cabezas-Pérez[2] and Rodrigo E. González-Reyes[1]**

[1] Grupo de Investigación en Neurociencias (NeURos), Centro de Neurociencias Neurovitae-UR, Instituto de Medicina Traslacional (IMT), Escuela de Medicina y Ciencias de la Salud, Universidad del Rosario, Bogotá, Colombia, [2] Grupo de Investigación en Ciencias Biomédicas GRINCIBIO, Facultad de Medicina, Universidad Antonio Nariño, Bogotá, Colombia

Taurine is considered the most abundant free amino acid in the brain. Even though there are endogenous mechanisms for taurine production in neural cells, an exogenous supply of taurine is required to meet physiological needs. Taurine is required for optimal postnatal brain development; however, its brain concentration decreases with age. Synthesis of taurine in the central nervous system (CNS) occurs predominantly in astrocytes. A metabolic coupling between astrocytes and neurons has been reported, in which astrocytes provide neurons with hypotaurine as a substrate for taurine production. Taurine has antioxidative, osmoregulatory, and anti-inflammatory functions, among other cytoprotective properties. Astrocytes release taurine as a gliotransmitter, promoting both extracellular and intracellular effects in neurons. The extracellular effects include binding to neuronal $GABA_A$ and glycine receptors, with subsequent cellular hyperpolarization, and attenuation of *N*-methyl-D-aspartic acid (NMDA)-mediated glutamate excitotoxicity. Taurine intracellular effects are directed toward calcium homeostatic pathway, reducing calcium overload and thus preventing excitotoxicity, mitochondrial stress, and apoptosis. However, several physiological aspects of taurine remain unclear, such as the existence or not of a specific taurine receptor. Therefore, further research is needed not only in astrocytes and neurons, but also in other glial cells in order to fully comprehend taurine metabolism and function in the brain. Nonetheless, astrocyte's role in taurine-induced neuroprotective functions should be considered as a promising therapeutic target of several neuroinflammatory, neurodegenerative and psychiatric diseases in the near future. This review provides an overview of the significant relationship between taurine and astrocytes, as well as its homeostatic and neuroprotective role in the nervous system.

Keywords: taurine, astrocytes, hypotaurine, glia, neuron, neuroprotection, brain

OPEN ACCESS

Edited by:
Alexander A. Mongin, Albany Medical College, United States

Reviewed by:
Rodrigo Franco, University of Nebraska-Lincoln, United States
Yujie Chen, Army Medical University, China
Carme Auladell, University of Barcelona, Spain

****Correspondence:***
Rodrigo E. González-Reyes
rodrigo.gonzalez@urosario.edu.co

Specialty section:
This article was submitted to Molecular Signalling and Pathways, a section of the journal Frontiers in Molecular Neuroscience

Received: *06 May 2022*
Accepted: *17 June 2022*
Published: *05 July 2022*

Citation:
Ramírez-Guerrero S, Guardo-Maya S, Medina-Rincón GJ, Orrego-González EE, Cabezas-Pérez R and González-Reyes RE (2022) Taurine and Astrocytes: A Homeostatic and Neuroprotective Relationship. Front. Mol. Neurosci. 15:937789. doi: 10.3389/fnmol.2022.937789

INTRODUCTION

More than 900 natural amino acids are currently known, although only around 2% of them are encoded in the genetic code of eukaryotes and used to synthesize proteins, thereby called "proteinogenic amino acids" (Yamane et al., 2010). The other 98% correspond to "non-proteinogenic" or "non-coded" amino acids, such as taurine, which are not coded into the DNA

and are therefore not involved in protein synthesis, but have important physiological functions (Popova and Koksharova, 2016; Fichtner et al., 2017). Taurine is considered the most abundant free amino acid present in the brain, retina, and muscle (Ripps and Shen, 2012). For example, human levels of taurine can range from 1 to 20 μmol/g in the brain, 30 to 40 μmol/g in the retina, and around 50 to 100 μmol/L in plasma (Wójcik et al., 2010).

The word taurine comes from the Latin *taurus*, meaning bull, the species from which it was first isolated (Caspi et al., 2018). Taurine (2-aminoethanesulfonic acid) is a beta-amino acid, with a molecular weight of 125.15 g/mol and a wide distribution in animal tissues (Caspi et al., 2018). It differs from other amino acids, due to the position of its amino group on the beta-carbon and the presence of a sulfonic acid group with a low pKa instead of the conventional carboxylic acid group (Hayes and Sturman, 1981). Taurine is endogenously synthesized in mammalian tissues, especially in the brain, heart, retina, and liver cells as part of the L-cysteine and L-methionine metabolic pathway (Huxtable, 1992). This process requires vitamin B6 as an enzyme cofactor; therefore, its dietary deficiency can lead to taurine depletion (Park and Linkswiler, 1970; Spinneker et al., 2007). Even though there are endogenous mechanisms for taurine production, an exogenous supply of taurine is required to meet physiological needs, especially in infants, in which taurine is a conditionally essential amino acid (Papet et al., 2019; Wu, 2020). Moreover, taurine is highly enriched in meat, seafood, fish, and milk (Froger et al., 2014), and a major component of energy drinks, along with caffeine and B-group vitamins (Piccioni et al., 2021). Taurine uptake by tissues is predominantly mediated by the chloride sodium-dependent taurine transporter (TauT) encoded by the *SLC6A6* gene (Baliou et al., 2020). However, taurine and hypotaurine transport has also been described through the GABA transporter 2 (GAT-2) in the blood-brain barrier (BBB) (Nishimura et al., 2018). Although TauT transporter predominates in the plasma membrane, studies with mouse fibroblasts models have identified its presence in the nucleus (Voss et al., 2004), whereas other models with HeLa cells propose its existence within the mitochondria (Suzuki et al., 2002).

Taurine has diverse functions in the cells, particularly cytoprotective actions through its antioxidative and anti-inflammatory effects (Schaffer and Kim, 2018). This amino acid neutralizes hypochlorous acid through the formation of taurine chloramine, a more stable molecule, and thus, diminishes the generation of reactive oxygen species (ROS) (Weiss et al., 1982). Similarly, taurine conjugates with a tRNA to enhance the expression of the nicotinamide adenine dinucleotide (NAD)-ubiquinone oxidoreductase chain 6, a subunit of the respiratory chain complex I, associated with the reduction of oxidative stress (Jong et al., 2012; Schaffer et al., 2014). Furthermore, taurine deficiency in heart tissue reduces glucose oxidation due to a decrease in pyruvate followed by an increase in lactate (Schaffer et al., 2016). Such a rise in lactate levels increases the $NADH/NAD^+$ ratio and decreases pyruvate dehydrogenase activity, inducing a reduction in total ATP production. Moreover, taurine deficiency leads to reduced fatty acid metabolism, downregulating the expression of peroxisome proliferator-activated receptor alpha (PPARα), an important nuclear receptor protein that promotes the fatty acid β-oxidation (Wen et al., 2019). These results highlight the essential role of taurine in the effective maintenance of cellular energy processes.

On the other hand, taurine works as a gene and transcription factor regulator in different models, including human hepatoma cells HepG2 (Park et al., 2006) and rodent heart (Schaffer et al., 2016). Genes regulated by taurine are involved in amino acid metabolism and protein synthesis. For instance, taurine depletion can provoke abnormal protein folding, thereby affecting longevity and cellular senescence (Ito et al., 2014). Cell injury and mitochondrial oxidative stress causes an imbalance between degradation and biosynthesis/folding of proteins, leading to the accumulation of unfolded or misfolded proteins, activating the unfolded protein response pathway (UPR) (Gharibani et al., 2015; Jong et al., 2015). By suppressing the UPR, taurine diminishes protein degradation, activation of chaperones, autophagy, and apoptosis that attenuates endoplasmic reticulum (ER) stress (Gharibani et al., 2013; Ito et al., 2015). This depicts taurine's role in the protein quality control systems of the cells and its anti-senescence function.

After its uptake, hypotaurine is oxidized into taurine by the hypotaurine dehydrogenase (Vitvitsky et al., 2011). Extracellular taurine binds to $GABA_A$ and glycine receptors augmenting its inhibitory effect (Jia et al., 2008). On the other hand, intracellular taurine concentrations are higher than extracellular levels, making it an organic osmolyte that contributes to the osmotic stress regulation in the cell (Oja and Saransaari, 2017). Moreover, taurine inhibits calcium release from internal stores, such as mitochondria, enhancing intracellular calcium modulation (Wu et al., 2005; Ramila et al., 2015). Other mechanisms described for taurine regulation of calcium influx include actions directed toward calbindin, calreticulin, and the Na^+/Ca^{2+} exchanger in the outer cell membrane (Schaffer et al., 2002; Junyent et al., 2010).

Thus, due to its multiple physiological functions in cells, taurine has been proposed as a novel therapeutic agent for many human diseases including stroke, epilepsy, neurodegenerative diseases like Alzheimer's disease (AD), retinal degeneration, heart failure, and mitochondrial diseases, such as mitochondrial encephalopathy with lactic acidosis and stroke-like episodes (MELAS), among others (Schaffer and Kim, 2018). Despite previous research regarding taurine's effect in different tissues, its role in the nervous system, particularly the functional relationship with astrocytes, remains to be further elucidated. This aspect is important, as astrocytes are considered the main producers of taurine in the central nervous system (CNS) (Vitvitsky et al., 2011). Astrocytes also release taurine as a gliotransmitter, acting on other cells, mainly in neurons. Hence, a deeper understanding of taurine's effect in astrocytes can contribute to a better insight of its physiological effects, which could potentially be used to ameliorate the course of several nervous system pathologies. This review, therefore, will provide an overview of the significant relationship between taurine and astrocytes, as well as its homeostatic and neuroprotective role in the pathologies of the nervous system.

TAURINE AND BRAIN

Taurine is one of the most abundant amino acids in the human brain, although, its concentration declines with age, with decreasing values that range from 4–20 μmol/g during development to 1–9 μmol/g at adulthood (Wójcik et al., 2010; Roysommuti and Wyss, 2015). A study in adult male Wistar rats identified heterogeneous concentrations of taurine among different brain regions, showing higher levels in the pyriform cortex, caudate-putamen, cerebellum, and supraoptic nucleus, and lower concentrations in the midbrain reticular formation (Palkovits et al., 1986). During the rat's postnatal growth, there is an increase in GABA, taurine and hypotaurine levels, which progressively decline until adulthood, in which its concentration reaches a plateau (Kontro et al., 1984). Moreover, a study in aged and young Wistar rats evidenced a significant decrease in the levels of taurine in the cerebellum, cortex, nucleus accumbens, and striatum of the aged animals (Benedetti et al., 1991). This suggests that taurine is required for an optimal postnatal brain development, which is supported by previous research evidencing disturbed maturation and migration of neurons, and a decreased number of astrocytes, in cat and monkey's brains with taurine deficiency (Sturman, 1992; Pasantes-Morales, 2017).

Taurine Synthesis and Transport

Synthesis of taurine in the brain follows a similar enzymatic pathway compared with other tissues, such as muscle, adipose tissue and liver, however, the rate of production differs from one to another (Roysommuti and Wyss, 2015). This explains the slight differences in taurine concentrations between the brain and other tissues, reporting 9 μmol/g in the adult brain compared to 6 μmol/g in heart, 5 μmol/g in skeletal muscle, 2 μmol/g in the liver, and up to 40 μmol/g in retina (Wójcik et al., 2010). Three main pathways have been described for taurine synthesis in the brain (Hayes and Sturman, 1981). The first, and most common, depends on cysteine as its primary substrate, which is oxidized by cysteine dioxygenase to form cysteine sulfinic acid (CAD), and finally transformed to hypotaurine by cysteine sulfinic acid decarboxylase (CSAD) (Pasantes-Morales, 2017). The second pathway uses extracellular methionine as primary substrate, which undergoes different enzymatic reactions to form cysteine, which then follows the first pathway. The third pathway consists in the degradation of coenzyme-A yielding cysteamine, which is later transformed to hypotaurine by 2-aminoethanethiol dioxygenase (Banerjee et al., 2008). All three pathways form hypotaurine, which can be either transformed into taurine and released as such, or be released as hypotaurine and undergo its conversion to taurine in another cell, such as neurons (Roysommuti and Wyss, 2015; **Figure 1**).

Regarding neural cells, taurine predominates in astrocytes and neurons, demonstrated by the presence of specific enzymatic machinery needed for its synthesis (Ripps and Shen, 2012). Moreover, a metabolic coupling between astrocytes and neurons has been reported, in which astrocytes provide neurons with hypotaurine as a substrate for taurine production (Vitvitsky et al., 2011). Given the fact that neurons lack CSAD (Tappaz et al., 1994), they are unable to synthetize hypotaurine from cysteine, and thus, rely on astrocytic hypotaurine supply (Brand et al., 1997). A possible rationale behind the absence of a complete taurine synthetic pathway in neurons is that it spares cysteine for glutathione synthesis, prioritizing sulfur use for ROS buffering and xenobiotic detoxification in neurons (Banerjee et al., 2008). This suggests that *de novo* synthesis of taurine occurs predominantly in astrocytes, whereas neuronal concentration of taurine mostly depends on extracellular hypotaurine provided by astrocytes, and its conversion to taurine through intracellular enzymatic and non-enzymatic reactions. Furthermore, this explains why there is a lower concentration of both hypotaurine and taurine in neurons compared to that in astrocytes (Vitvitsky et al., 2011).

The cells in the brain can synthetize taurine from cysteine or methionine as mentioned above (Peck and Awapara, 1967), or import it *via* sodium and chloride dependent transporters TauT1 and TauT2 (Banerjee et al., 2008). TauT1 transporters predominate in cerebellar Purkinje cells and in bipolar cells in the retina, whereas TauT2 is associated with astrocytes and CA1 pyramidal cells in the hippocampus (Pow et al., 2002). In terms of regulation, Kang et al. (2002) used an *in vitro* BBB model to demonstrate TauT transporter upregulation in response to cellular damage, osmolality and declining taurine concentrations. Other factors such as hyperglycemia and oxidative stress also contribute to the TauT transporter regulation (Baliou et al., 2020).

Taurine Release, Degradation, and Effects on Cellular Receptors

Taurine has a high transcellular gradient, with larger intracellular than extracellular concentrations, making it susceptible to changes in ionic concentrations (Oja and Saransaari, 2017). Furthermore, taurine's molecular characteristics makes it more hydrophilic and less capable of trespassing biological membranes due to its sulfonyl group, resulting in a slower spontaneous efflux (Saransaari and Oja, 1992). Therefore, taurine release from the nerve terminal depends mostly on neuronal depolarization (Kamisaki et al., 1996). This is supported by a study by Saransaari and Oja (1991), which demonstrated taurine release by activation of *N*-methyl-D-aspartic acid (NMDA) and kainate receptors in a rat model. Nonetheless, the existence of taurine synaptic vesicles has not been completely confirmed, therefore it is suspected that its release relies on calcium-independent mechanisms, including volume-sensitive organic anion channels and TauT reverse transport (Kilb and Fukuda, 2017).

The existence of a specific taurine receptor in the human brain remains a controversial matter. Some authors have not ruled out its existence (Wu et al., 1992; Jakaria et al., 2019), while other evidence still questions it (Ripps and Shen, 2012). Several experimental studies in animals have explored, though not confirmed, the presence of the receptor (Kudo et al., 1988; López-Colomé et al., 1991; Frosini et al., 2003). Other authors have further proposed inhibition of the taurine receptor by guanosine-5′-triphosphate (GTP) in a dose-dependent way, implying not only its existence, but also the type of receptor as a metabotropic taurine receptor (mTauR) coupled to inhibitory G-proteins

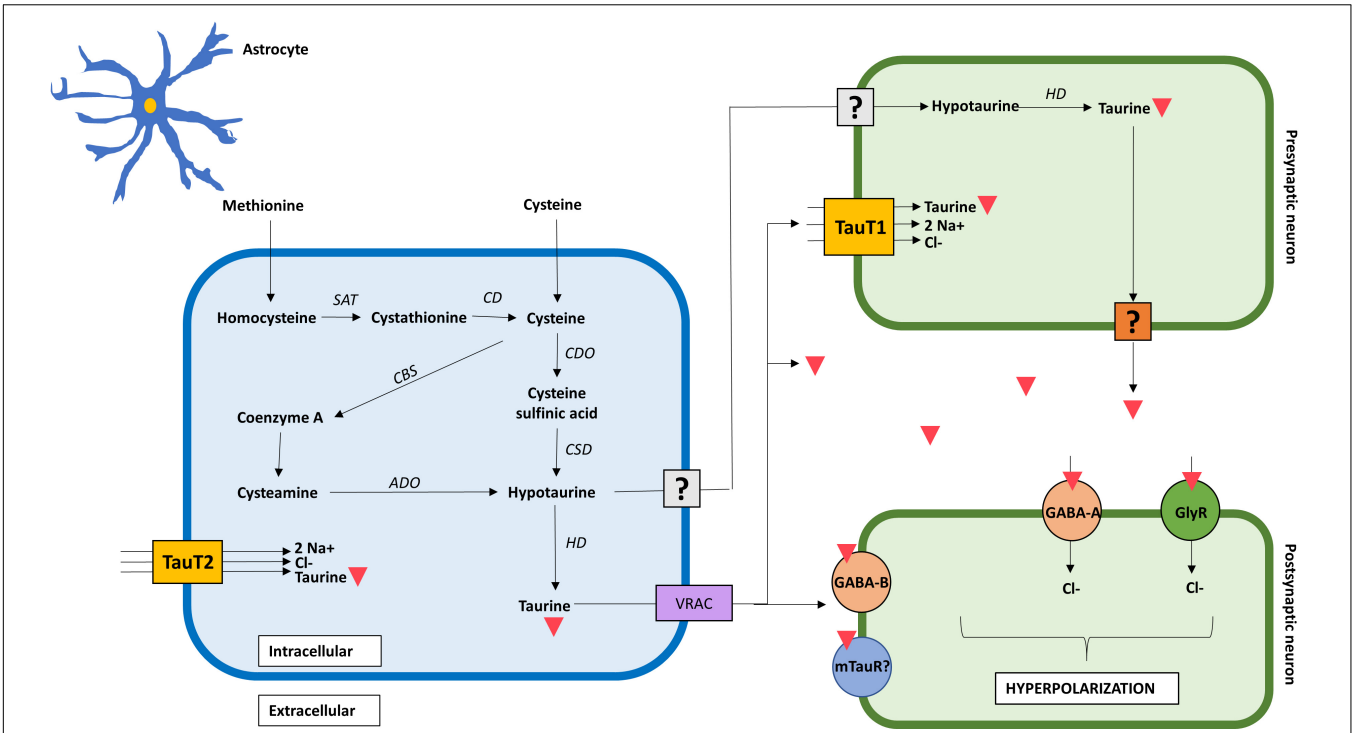

FIGURE 1 | Mechanistic action of taurine in the brain. Taurine is synthesized in astrocytes from extracellular methionine and cysteine through three distinct pathways. It is exported as hypotaurine or taurine into the extracellular space; however, the mechanism in which hypotaurine exits the astrocyte and enters the neuron remains uncertain. Transport of taurine depends on TauT1 and TauT2 transporters, for neurons and astrocytes, respectively. The mechanism in which taurine exits the pre-synaptic neuron remains to be confirmed. Taurine acts as a full agonist for $GABA_A$, $GABA_B$, and glycine receptors in the post-synaptic neuron, increasing chloride conductance, and thus, hyperpolarizing the cell. The presence of a post-synaptic taurine receptor remains controversial. Taurine is represented by an inverted red triangle. ADO, aminoethanethiol dioxygenase; CBS, 2-cystathionine ß-synthase; CD, cysteine desulfurase/γ-cystathionase; CDO, cysteine dioxygenase; CSD, cysteine sulfinate decarboxylase; GlyR, glycine receptor; HD, hypotaurine dehydrogenase; TauT1, taurine transporter type 1; TauT2, taurine transporter type 2; SAT, S-adenosyl transferase; uncertain receptor/transporter–represented by a question mark.

(Wu and Prentice, 2010). Nonetheless, future research is needed in order to corroborate the existence or not of the receptor, not only in neurons but also in other cell types such as glial cells. Further research showed taurine's inhibitory effect on the protein kinase C (PKC), thereby blocking the phosphorylation and activation of voltage-gated calcium channels (VGCC), and therefore, decreasing calcium influx (Ohno and Nishizuka, 2002). Some authors propose that mTauR, if present, may have a similar effect as $GABA_B$ receptors, so that its activation by taurine may lead to the activation of coupled inhibitory G-proteins, such as Go/Gi, which result in the inhibition of L-, N-, and P/Q-type VGCC (Leon et al., 2009; Traynelis et al., 2010; Wu and Prentice, 2010). Thus, the activation of mTauR and inhibitory G-proteins, leads to inhibition of phospholipase C (PLC), reduction in IP3 levels and consequently, inhibition of IP3-mediated release of Ca^{2+} from the internal storage pools (Leon et al., 2009; Traynelis et al., 2010; Wu and Prentice, 2010; **Figure 2**).

Taurine resembles the structure of the neurotransmitter GABA (Kletke et al., 2013; Ochoa-de la Paz et al., 2019). Such resemblance explains taurine's ability to bind to $GABA_A$ receptor ($GABA_AR$), presumably at the interface of α/β subunits binding site. Moreover, taurine has been proposed as an endogenous agonist of the $GABA_B$ receptors ($GABA_BR$) in adult mouse brains (Albrecht and Schousboe, 2005). The same study also evidenced, through immunocytochemical analysis, that $GABA_BR$, to which taurine binds, is located extrasynaptically. Taurine has been shown to activate both $GABA_A$ and glycine receptors (GlyR) at a 0.1 mM concentration (Song et al., 2012). Despite this, Wu et al. (2008) evidenced in adult rats that taurine's activation of $GABA_AR$ and GlyR varies among brain regions and is concentration-dependent. These authors observed that taurine at moderate concentrations (0.3 mM) activated GlyR, whereas at high concentrations (3 mM), acted as a weak agonist to $GABA_AR$ in neurons within the *substantia gelatinosa*. One explanation for this phenomenon may be the structural variability of these receptors due to the broad variety of combinations among its five subunits (Sigel and Steinmann, 2012).

In *Xenopus* oocytes research, a comparison of native and recombinant selected types of $GABA_AR$, showed that taurine acts as a full agonist at $\alpha_1\beta_3$ receptors and as a partial agonist at $\alpha_1\beta_3\gamma_2$ receptor and GlyR, which causes an increase in chloride influx into the cell, and thus hyperpolarizes the post-synaptic neuron (Kletke et al., 2013; Ahring et al., 2016). Therefore, taurine enhancement of post-synaptic neuronal inhibition represents one of its most important neuroprotective mechanisms against excitotoxicity. Furthermore, experiments on

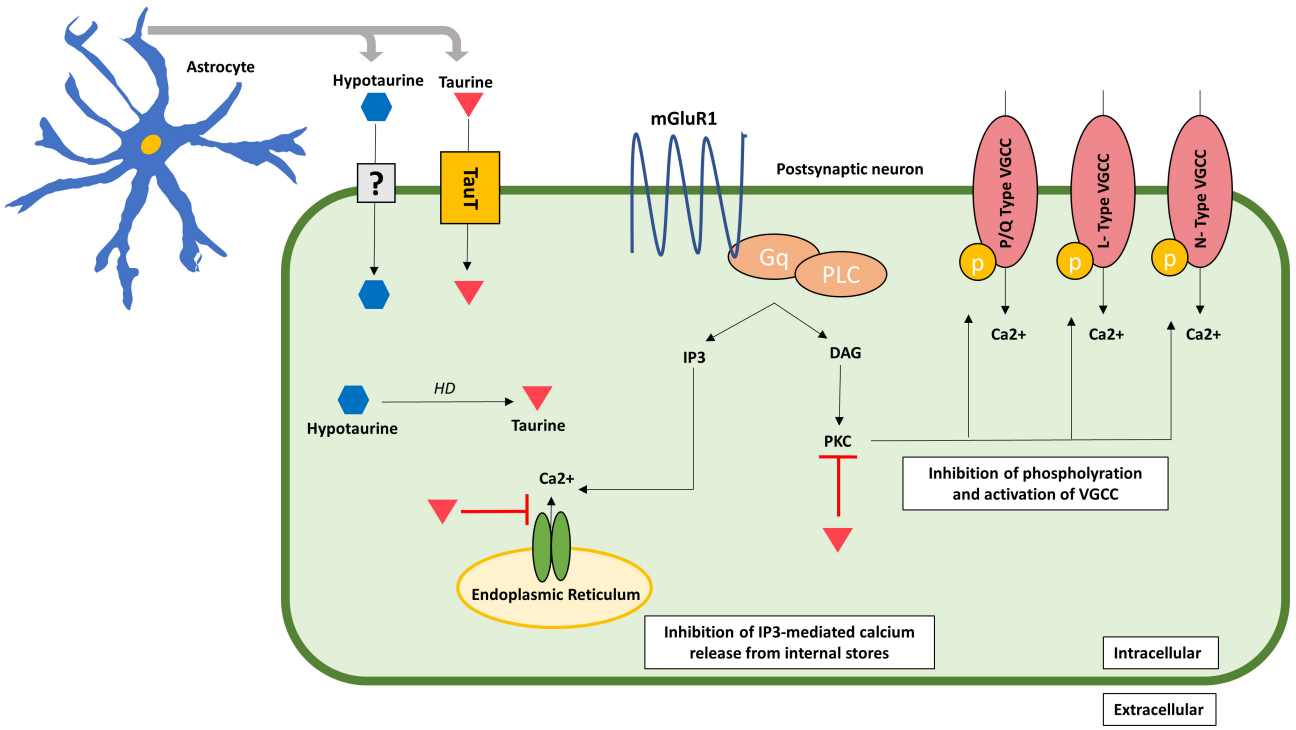

FIGURE 2 | Acute neuroprotective effects of taurine in the post-synaptic neuron. Taurine inhibits calcium influx by inhibiting the IP3-mediated calcium release from internal storages and blocking PKC activity, which inhibits phosphorylation and activation of VGCC consequently decreasing calcium entry through these channels. Taurine is represented by an inverted red triangle, while hypotaurine is represented by a blue hexagon. DAG, diacylglycerol; IP3, inositol trisphosphate; mGluR1, metabotropic glutamate receptor type 1; PLC, phospholipase C; PKC, protein kinase C; TauT, taurine transporter; uncertain receptor/transporter–represented by a question mark; VGCC, voltage-gated calcium channels.

amyloid beta (Aβ) models of neurotoxicity were carried out in chicks and rats, demonstrating that picrotoxin, a $GABA_A$ antagonist, blocked taurine's neuroprotective inhibitory effect (Louzada et al., 2004; Paula-Lima et al., 2005). Similarly, it has been proposed that the influx of chloride caused by taurine's agonist action over $GABA_AR$ and GlyR, counteracts glutamate-induced excitotoxicity (Paula-Lima et al., 2005). However, taurine does not interact directly with the binding site for glutamate or glycine of the NMDA receptor (Foos and Wu, 2002). Therefore, it is assumed that taurine effects on NMDA intracellular signaling are indirect.

Excitotoxicity induced by glutamate has been well established experimentally, both *in vitro* and *in vivo*, mainly in epilepsy and stroke models (Lai et al., 2014). Glutamate binds to NMDA receptor, which leads to significant increases in intracellular calcium loads and catabolic enzyme activities, triggering mitochondrial membrane depolarization, caspase activation, ROS production, apoptosis, and necrosis (Dong et al., 2009). *In vitro* experiments of rat cultured neurons showed that in the presence of taurine, glutamate failed to increase intracellular calcium levels, showing a reduction of more than 50% in the presence of 25 mM of taurine (Chen et al., 2001; Wu et al., 2009). Actions of taurine on neurons might be related to the Na^+/Ca^{2+} exchanger, which is a bidirectional ion transporter that couples the Na^+ in one direction with that of Ca^{2+} in the opposite direction, depending on the electrochemical gradient of Na^+ across the membrane (Blaustein, 1988; Blaustein et al., 1991; Takuma et al., 1994). During depolarization, the exchanger adopts a reverse mode, which promotes calcium influx. Taurine acts inhibiting the Na^+/Ca^{2+} exchanger through the following mechanisms: increasing the phospholipid *N*-methyltransferase activity over the exchanger, enhancing the calcium efflux from the cell, and increasing the intracellular calcium close to the exchanger (Schaffer et al., 2003, 2010). Leon et al. (2009) studied the presence of taurine in rat cultured neurons exposed to glutamate, identifying an increase in anti-apoptotic Bcl-2 together with a downregulation of Bax which works in favor of apoptosis. Taurine administration showed a 60% increase in the Bcl-2:Bax ratio, meaning an overall inhibition of programmed cell death (Elmore, 2007; Khodapasand et al., 2015; Dorstyn et al., 2018). Furthermore, taurine inhibits caspase-9 and calpain activity as part of its anti-apoptotic mechanisms (Leon et al., 2009).

After its release, taurine undergoes three different processes for its degradation including transamination, oxidation and oxygenation (Caspi et al., 2018). The process of transamination consists in the formation of L-alanine and sulfoacetaldehyde from taurine and pyruvate (Shimamoto and Berk, 1979). Oxidation involves the formation of isethionate (2-hydroxyethane sulfonate) from taurine (Kondo et al., 1971). The oxygenation

process consists of the use of taurine as a sulfur source by the sulfoacetaldehyde acetyltransferase, and finally into acetyl-CoA by the phosphate acetyltransferase (Eichhorn et al., 1997).

Taurine has been proposed as a neurotransmitter in the mammalian CNS (Huxtable, 1989; Wu and Prentice, 2010; Ripps and Shen, 2012; Kumari et al., 2013; Oja and Saransaari, 2017). This proposal has been based on the fact that taurine can be produced and released by pre-synaptic neurons, and exerts effects on post-synaptic neurons. However, for a substance to be considered a neurotransmitter it must meet the following criteria: (i) its synthesizing enzyme is present in the neuron; (ii) it is released upon neuron depolarization; (iii) it acts on a post-synaptic receptor; (iv) it causes a biological response on the post-synaptic neuron; and (v) it has an inactivation process after its release (Purves et al., 2001). So far, taurine complies with all but one of the mentioned criteria to be considered a neurotransmitter, which is the confirmation of the presence of a taurine specific receptor on the post-synaptic neuron. Furthermore, the intracellular gradient of taurine (around 400) has an intermediate position between established neurotransmitters (around 2000) and non-neurotransmitter aminoacids (less than 100) (Lerma et al., 1986; Oja and Saransaari, 2017).

TAURINE IN ASTROCYTES

The cysteine dependent pathway is believed to be the main pathway for taurine biosynthesis in the brain (Banerjee et al., 2008). The cellular localization of CSAD has yielded controversial results *in vivo*. Nevertheless, incorporation of the radioactive 35S from cysteine into taurine has confirmed the presence of CSAD in astrocytes (Vitvitsky et al., 2011), making them fully capable of synthesis and accumulation of taurine (Hertz, 1979). In contrast, low CSAD activity, if any, is found in neurons (Pasantes-Morales, 2017), making neurons dependent on astrocytes for provision of hypotaurine and/or taurine (Banerjee et al., 2008). When co-cultured with neurons in a rat model, astrocytic hypotaurine decreased and taurine levels increased, revealing the crosstalk between these cell types for regulation of taurine synthesis (Brand et al., 1997). Although astrocytes have the enzymatic machinery for taurine synthesis, taurine can also be transported into the astrocyte through TauT2 transporters from interstitial fluid (Pow et al., 2002; Junyent et al., 2011). TauT has 12 hydrophobic transmembrane domains with cytosolic N- and C- terminals, and for each taurine molecule to be passed across the membrane, two Na^+ ions and one Cl^- ion are required as a cotransport mechanism (Han et al., 2006).

Taurine has long been known to have an osmoregulatory role in the mammalian brain (Oja and Saransaari, 2017). Its release from neurons and astrocytes is directly proportional to a decrease in osmolarity (Pasantes-Morales and Schousboe, 1997). It has been shown that the replacement of 50 mM sodium ions by potassium evokes taurine release from rat's cerebellar astrocytes (Schousboe and Pasantes-Morales, 1989). The same study evidenced that taurine release in a hyperosmotic media is decreased from both cerebellar astrocytes and granule cells, even when 50 mM of potassium is added. This is supported by Vitvitsky et al. (2011), who demonstrated that exposure to hypertonic conditions increases taurine levels in astrocytes up to 14% in 48 h. Contrastingly, there are other release mechanisms described for taurine, namely, a dose-dependent taurine release mediated by glutamate and kainate in animal cultured cerebellar astrocytes (Dutton et al., 1991). Such different release mechanisms of taurine from astrocytes support an astrocytic high concentration gradient and high affinity transport systems.

Astrocytic taurine concentration can vary according to different neurotoxic stimuli. Morken et al. (2005), working in mice, reported that when exposed to methylmercury (MeHg), the concentration of taurine increased in astrocytic monocultures, whereas it decreased in neurons in co-cultures. This suggests that there is a compensatory increase in levels of taurine in astrocytes in response to toxic stimuli, depicting another important neuroprotective effect of astrocytic taurine. Taurine release in neurons and astrocytes share similarities, including a delayed onset of taurine release after stimulation, however, some level of discrepancy exists between them. For example, exposure to tetrodotoxin and dihydropyridines inhibit neuronal taurine release, whereas taurine release from astrocytes remains intact despite the presence of a sodium or calcium channel blocker, respectively (Dutton et al., 1991).

Different studies have shown that taurine is released from astrocytes through the volume-regulated anion channels (VRACs) (Choe et al., 2012; Schober et al., 2017). These channels, discovered in 2014, are structured as an hetero-hexamer complex formed by the leucine-rich repeat-containing 8 (LRRC8) proteins (the essential LRRC8A and complementary LRRC8B to E), which are also involved in the release of other metabolites like glutamate and aspartate (Qiu et al., 2014; Voss et al., 2014). For instance, a recent study in mice showed that cerebral ischemia increased neuronal LRRC8A-dependent VRAC activity in the hippocampus, suggesting that VRAC contributed to increased glutamatergic release during ischemic damage (Zhou et al., 2020). Importantly, VRAC channels mediate swelling-activated Cl^- currents during decreases in systemic osmolarity and have been extensively studied in astrocytes, neurons and other non-neuronal cells like pituicytes and retinal Müller cells (Choe et al., 2012; Qiu et al., 2014; Mongin, 2016; Netti et al., 2018). Furthermore, it has been shown that primary rat astrocytes express LRRC8A, and that knockdown of astrocytic LRRC8A expression inhibits swelling-activated release of taurine (Hyzinski-García et al., 2014; Mongin, 2016; Schober et al., 2017). Expression of LRRC8A has been observed in rat astrocytes from brain regions such as cortex and hippocampus (Hyzinski-García et al., 2014; Formaggio et al., 2019). Thus, VRAC, LRRC8A, and taurine, seem to play a critical role in astrocytic homeostasis. Moreover, previous studies have shown that the highest levels of taurine in the brain are found in cerebral cortex, hippocampus, caudate-putamen, cerebellum, and in hypothalamic supraoptic nucleus (Hussy et al., 1997, 2000; Hatton, 2002). VRAC and VRAC-like currents have been reported in mice and rats in several brain regions including cervical sympathetic ganglions, CA1 region of the hippocampus, cerebral cortex, hypothalamus,

and cerebellum (Leaney et al., 1997; Patel et al., 1998; Inoue et al., 2005; Sato et al., 2011; Zhang et al., 2011). For example, in the study by Choe et al. (2012), whole-cell voltage clamp recording demonstrated the absence of VRACs in rat's neurons from the supraoptic nucleus, while confirming its presence in cultured astrocytes from the same site. This suggests that astrocytes, in contrast to neurons, may be the main responsible cells for the VRAC-mediated taurine release in the brain. However, the relation of this channel with taurine in humans and in other neural cells such as oligodendrocytes, NG2 glia, or microglia, has not been completely clarified (Wang et al., 2022). Moreover, some reports have shown that taurine acts as a potent GlyR and GABA agonist, reducing the release of vasopressin and oxytocin in magnocellular neurons (Deleuze et al., 1998; Song and Hatton, 2003). In rats, these two hormones regulate taurine secretion from pituicytes, thus creating a loop of paracrine intercellular communication (Rosso et al., 2004). Regarding its effects as a GlyR agonist, it has been shown that taurine activates GlyR through binding with homomeric subunits αH1 and αH2 in both animal and human cells (De Saint Jan et al., 2001). Consequently, transport inhibition of endogenous amino acids, such as taurine, contributes to the preservation of tonic activity in glycine receptors as well as in inhibitory neurons in the hippocampus (Mori et al., 2002), suggesting that taurinergic gliotransmission enhances inhibition on neurons.

As previously mentioned, taurine is mainly produced and released by astrocytes in the CNS. Therefore, metabolic and physiological aspects of taurine depend on an adequate function of these glial cells. This includes the communication between astrocytes and other cells, in particular, neurons. As mentioned above, astrocytes release hypotaurine, which then becomes the precursor for neuronal taurine production (Vitvitsky et al., 2011). Astrocytic taurine acts on GABA and GlyR favoring inhibitory activity in neurons (Song et al., 2012; Ochoa-de la Paz et al., 2019). Furthermore, taurine helps to control intracellular calcium levels and reduces the risk of developing excitotoxicity and apoptosis (Leon et al., 2009; Wu et al., 2009). Although not tested in co-culture with astrocytes, rat neurons treated with taurine increased both the incidence of synapse formation and the efficacy of synaptic transmission (Mersman et al., 2020). This suggests astrocytes may be involved in taurine-related neuronal synaptogenesis, as astrocytes have been reported to play a central role in synapse formation, function, and elimination (Chung et al., 2015). However, taurine metabolic coupling between astrocytes and neurons may be affected by external factors. For instance, *in vitro* treatment with manganese induced an increase in astrocytic taurine and a decrease in neuronal and astrocytic-neuronal co-culture taurine (Zwingmann et al., 2003). Another *in vitro* study in rat astrocytes, reported that rapid taurine accumulation is enhanced by hyperosmotic conditions (Beetsch and Olson, 1998). Despite these observations, it is still not clear whether other important coupling functions between astrocytes and neurons, such as the astrocyte-neuron lactate shuttle, or purinergic signaling, are affected by taurine.

Despite the controversy regarding taurine's condition as a neurotransmitter, its categorization as a gliotransmitter can be clearly elucidated. For instance, for a substance to be considered an astrocyte gliotransmitter it must comply with the following criteria: (i) be synthesized and/or stored in astrocytes, (ii) have a physiologically triggered release, (iii) activate rapid responses in adjacent cells, and (iv) influence physiological processes (Volterra and Meldolesi, 2005). Other authors have proposed that substances that act as gliotransmitters can be released by calcium-independent non-exocytotic ways, as happens with taurine (Malarkey and Parpura, 2008; Hussaini and Jang, 2018). Taurine has proven to be synthesized and released from astrocytes, execute an inhibitory effect on neurons and influence multiple physiological processes. Therefore, taurine's status as a gliotransmitter can be confirmed. However, whether its main effect is directly over the pre-synaptic or post-synaptic neuron, remains to be established.

Other aspects merit further exploration such as if any difference in taurine takes place in the functional regions of the astrocytes (i.e., endfeet vs. soma), in astrocytic subtypes (i.e., protoplasmatic gray matter vs. fibrous white matter astrocytes), and if taurine is somehow involved in the function of glymphatic system.

NEUROPROTECTIVE EFFECTS OF TAURINE RELEASED FROM ASTROCYTES

As mentioned above, taurine acts as a gliotransmitter with a neuroprotective role in the brain. When released from astrocytes, it can either bind to neuronal post-synaptic receptors such as $GABA_AR$ and GlyR (Wu and Prentice, 2010), or enter the neuron *via* TauT1 and TauT2 transport proteins where it triggers intracellular signaling pathways. However, taurine's overall inhibitory effects combine both extracellular and intracellular processes.

Regarding the extracellular effects of taurine, it involves binding to neuronal $GABA_AR$ and GlyR, augmenting chloride conductance, thereby hyperpolarizing the cell and neutralizing NMDA-mediated glutamate excitotoxicity (Wu and Prentice, 2010). Furthermore, taurine release from the cells decreases Ca^{2+} entry by limiting the available Na^+ needed for the adequate functioning of the Na^+/Ca^{2+} exchanger in the cell membrane (Schaffer and Kim, 2018).

On the other hand, intracellular effects of taurine released from astrocytes involve direct and indirect actions on calcium homeostatic pathways in neurons. By reducing calcium overload, taurine prevents excitotoxicity, mitochondrial stress, and activation of apoptotic pathways (Junyent et al., 2010). Studies with cultured neurons treated with glutamate showed a significant increase in intracellular calcium levels, however, when taurine was added, such calcium elevation returned to near basal levels (Foos and Wu, 2002). As glutamate binds to its metabotropic receptor, IP3 increases, as does IP3-mediated calcium release from internal storages. However, when taurine was added, there was no increase in IP3 nor in intracellular calcium levels (Foos and Wu, 2002). This suggests taurine's neuroprotective effect toward glutamate-induced

calcium overload and consequent excitotoxicity. Furthermore, authors have proposed that taurine activates coupled inhibitory G-proteins, which in turn, inhibit phosphorylation of VGCC, thus preventing its activation induced by glutamate (Wu and Prentice, 2010). Therefore, by inhibiting calcium influx from VGCC, taurine provides another mechanism for regulation of intracellular calcium concentrations.

In a type II diabetes mellitus rat model, intracellular taurine has proven to inhibit neuronal apoptosis in the brain, more specifically in the hippocampal CA1 pyramidal cells by acting on the NGF/Akt/Bad pathway (Wu et al., 2020). The addition of taurine to rat's hippocampal cultured neurons increased the expression of nerve growth factor (NGF) and augmented phosphorylation of the NGF receptor, tyrosine kinase receptor type A (TrkA), activating an important anti-apoptotic pathway. Furthermore, hippocampal rat neurons treated with taurine showed a decreased expression of Bax, a diminished release of cytochrome C and a reduction in caspase-3 and caspase-8 activity, thereby contributing to neuronal survival by inhibiting apoptotic signaling pathways (Li et al., 2017). Finally, some evidence has emerged suggesting that taurine concentration may be related with the development of Parkinson's disease (PD) (Zhang et al., 2016; Che et al., 2018). For example, a study with 110 PD treated and untreated patients, found that PD patients exhibited lower levels of plasma taurine than control individuals (51.01 $\pm$ 29.07 vs. 133.83 $\pm$ 45.91 μmol/L, $p < 0.001$) (Zhang et al., 2016). Moreover, in a mice PD model, using primary neuron-glia cultures, it was found that taurine administration (150 mg/kg), attenuated the aggregation of α-synuclein, decreased the inflammatory response by microglia and provided dopaminergic neuroprotection (Che et al., 2018). Furthermore, a study in C57Bl/6j male mice showed that taurine administration significantly decreased the total number of ionized calcium-binding adapter molecule 1 (Iba1)-expressing microglia in the dentate gyrus supporting its anti-inflammatory role (Gebara et al., 2015). These combined results suggest the importance of taurine neuroprotection in neurodegenerative diseases such as PD. Moreover, as astrocytes are the main taurine releasing cells in the CNS, we suggest most of these neuroprotective effects may be attributed to astrocytes (**Figure 3**).

TAURINE AS A THERAPEUTIC ALTERNATIVE IN NERVOUS SYSTEM PATHOLOGIES

Taurine's neuroprotective role in neurons and astrocytes represent a novel potential therapeutic approach toward several nervous system diseases. By augmenting neuronal inhibition mediated by $GABA_AR$ and GlyR, taurine has proven to enhance neuronal inhibition, which remains useful in diseases such as epilepsy, characterized by a hypersynchronous and hyperexcitable neuronal circuit. Winkler et al. (2019) identified that the addition of 0.5 μmol/L of taurine significantly increased the anticonvulsant effect of 100–200 μmol/L of pentobarbital in mice. Kainic acid administration is one of the most frequently used models to mimic human temporal lobe epilepsy in animals. Either subcutaneous or intraperitoneal injection of taurine, preceding kainic acid administration, resulted in seizure prevention and significant reduction in neuronal cell death in the hippocampus of male mice (El Idrissi et al., 2003; Junyent et al., 2009). This suggests that taurine's action as a positive modulator of $GABA_AR$ could be considered as part of epilepsy therapy. In humans with epilepsy, including in children (Fukuyama and Ochiai, 1982), the effects of taurine oral administration on seizures has been examined (as reviewed by Oja and Saransaari, 2013). Most of these studies were conducted in the 70's and 80's, and showed a wide variation in the results. For instance, some reported disappearance of seizures in patients with intractable epilepsy, while others failed to show any improvement, despite comparable dosages. However, these clinical trials had many issues, such as a small number of participants, diverse range of epilepsy types and no control groups, among others. According to the webpage, clinicaltrials.gov, no clinical trial examining effects of taurine on epilepsy is currently ongoing. Therefore, novel and much better designed clinical trials examining taurine effects on epilepsy should be proposed in the future. On the other hand, taurine's role in the inhibition of neuronal apoptotic pathways and attenuation of oxidative stress, could represent a potential adjuvant therapy, particularly in neurodegenerative diseases such as AD. It has been shown that small concentrations of taurine in neuronal cultures from chick embryo retinas can decrease Aβ peptide aggregation and the underlying neuronal death (Louzada et al., 2004). In APP/PS1 AD transgenic mice, taurine administration was shown to bind oligomeric Aβ peptides and improve cognition (Jang et al., 2017). Moreover, decreased taurine levels, as detected by ion exchange in the temporal cortices of patients with AD could lead to higher aggregation and more rapid disease progression, highlighting the potential role of taurine as co-adjuvant in the delaying of neurodegenerative processes (Arai et al., 1985; Chen et al., 2019).

Taurine's neuroinflammatory modulation represents another viable mechanism in which it can be implemented in therapeutic approaches toward diseases such as traumatic brain injury and ischemic stroke, characterized by enhanced neuroinflammatory processes. By decreasing the expression of proinflammatory cytokines through the inactivation of microglia-mediated NOX2-NF-κB cascade, taurine may contribute to the amelioration of inflammatory changes (Che et al., 2018; Bhat et al., 2020; Tian et al., 2020). For example, administration of high doses of taurine in a rat model of intracerebral hemorrhage resulted in inactivation of proinflammatory pathways, thereby limiting neuronal damage and white matter injury, accompanied by a decrease in neutrophil infiltration and glial activation (Zhao et al., 2018). Furthermore, in an *in vitro* model for ischemic stroke, 88% of neurons pretreated with taurine survived after being exposed to high levels of glutamate (Prentice et al., 2017). Similarly, in the same study, the administration of taurine in an *in vivo* rat stroke model resulted in the inhibition of components within the ER stress pathway, reducing neuronal glutamate excitotoxicity. Therefore, taurine could have a beneficial effect in neuroinflammatory diseases and ischemic or traumatic brain injury.

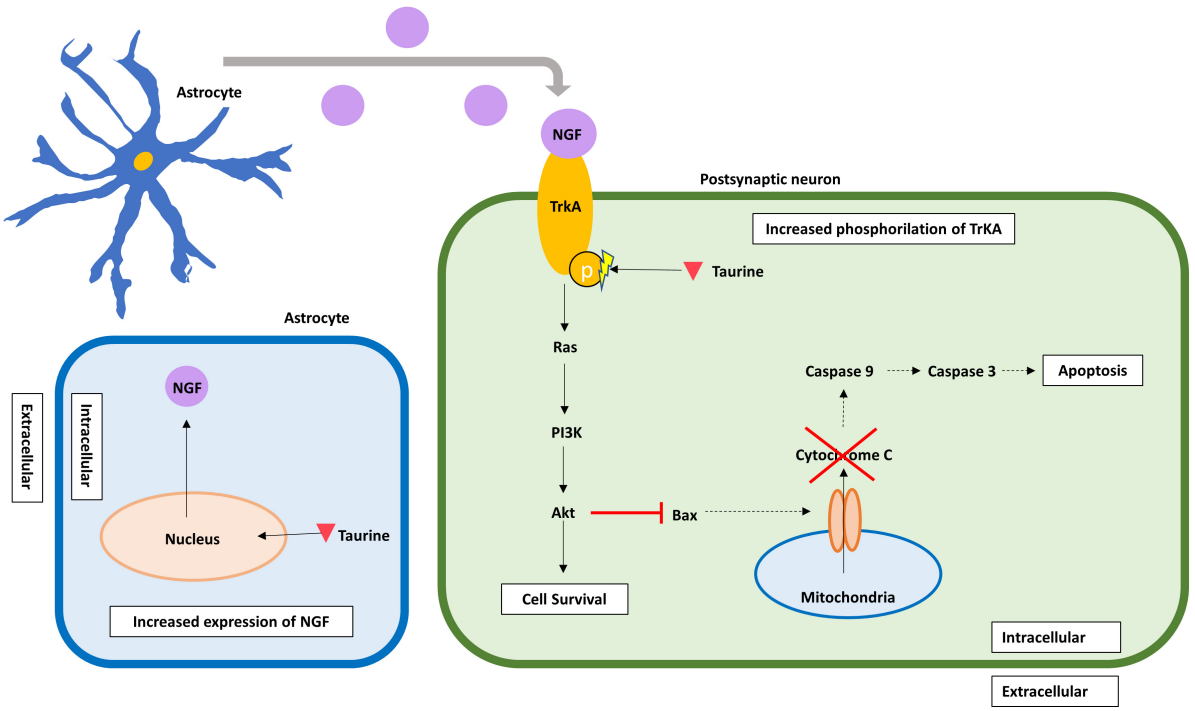

FIGURE 3 | Delayed neuroprotective effects of taurine in the post-synaptic neuron. Taurine increases the expression of NGF, presumably in astrocytes from where it is released. Additionally, intracellular taurine increases phosphorylation of TrkA, a specific receptor for NGF, thus enhancing the NGF/Akt/Bad anti-apoptotic pathway. By activating this pathway, taurine enhances Bax inhibition, which blocks Cytochrome C release from mitochondria, and inhibits caspase-mediated apoptotic pathways. Taurine is represented by an inverted red triangle, while NGF is represented by a magenta circle. HD, hypotaurine dehydrogenase; NGF, nerve growth factor; PI3K, phosphatidylinositol 3-kinase; TrkA, tropomyosin receptor kinase A.

The development of biological markers, or biomarkers, for nervous system diseases is actually one of the most important research topics in the field of neuroscience. The interest in the development of biomarkers is based on several current challenges these group of diseases pose, such as the lack of comprehension of the pathological mechanism, together with difficulties in the prevention, in particular early interventions, confirmatory diagnosis and treatment. According to the most accepted definition, a biomarker should be objectively measured or evaluated, and must be able to indicate (and differentiate) physiological activity from pathological processes or from pharmacological responses (Strimbu and Tavel, 2010). In addition, ideal biomarkers should benefit from being less invasive and fast to measure, providing results in minutes or hours, rather than days or weeks. Therefore, many biomarkers are explored in blood, saliva, or urine samples, as well as in imaging techniques including magnetic resonance or positron emission tomography (PET) (Young et al., 2020; Zetterberg and Schott, 2022). In fact, live imaging of brain metabolism is currently proposed as an interesting biomarker method both in preclinical and clinical settings (Zhu et al., 2018). Therefore, as taurine plays and important role in brain metabolism, and is mainly produced in astrocytes (the principal homeostatic regulators in the SNC), taurine can be suggested as a possible brain biomarker.

Several techniques exist to determine the metabolic activity of the brain in living individuals. The most commonly used in humans are functional magnetic resonance imaging (fMRI), PET, magnetic resonance spectroscopy (MRS) and metabolomics in tissue samples (Barros et al., 2018). Taurine is one of the metabolites that can be determined through MRS thus possibly serving as a biomarker. For instance, taurine concentrations, determined through MRS, were measured in primitive neuroectodermal tumors (PNT) of pediatric patients, finding a significant increase of this metabolite, which helped to differentiate PNT from other tumors (Kovanlikaya et al., 2005). Metabolic profiling of taurine has also been extended to other neural derived tumors such as medulloblastoma, neuroblastoma, and retinoblastoma (Kohe et al., 2018). Recently, a brain MRS study in cannabinoid users, found that taurine concentration was directly correlated with glutamate, and with the frequency of cannabinoid use (Newman et al., 2022). Furthermore, MRS measurements determined elevated concentrations of taurine in the cerebellar vermis of bipolar patients (Magnotta et al., 2022), and levels of taurine were significantly related to the duration of illness in schizophrenic patients (Shirayama et al., 2010). Hence, taurine MRS measurements can be applied to a large extent of neurological and neuropsychiatric diseases.

Taurine values have also been examined in biological samples such as blood and cerebrospinal fluid (CSF). A recent study found that taurine plasma levels correlated with the strength-duration time constant, an axonal excitability indicator, established to predict survival in amyotrophic lateral sclerosis

(ALS) (Nakazato et al., 2022). Furthermore, taurine was selected as a biomarker metabolite that helps to distinguish between patients with amnestic mild cognitive impairment and healthy controls (Sun et al., 2020). Plasmatic taurine has also been used as a predictor of poor outcome in patients with subarachnoid hemorrhage, finding that those patients with a sixfold increase in taurine at admission ended with a poor outcome, compared with those with a favorable outcome who had only a twofold increase (Barges-Coll et al., 2013). Similar findings were observed in the CSF of severe brain-injured patients, where taurine was significantly increased in subdural or epidural hematomas, contusions and generalized brain edema (Stover et al., 1999). Elevated concentrations of taurine in plasma have also been reported in psychiatric diseases, such as depression (Altamura et al., 1995). Similar findings have been observed in preclinical models. Song et al. (2021) studied a rat model treated with 20 mg/kg of fluoxetine daily, evidencing that repeated doses of fluoxetine, a selective serotonin reuptake inhibitor, led to decreased concentrations of taurine and other astrocytic metabolites in the medial prefrontal cortex. Moreover, Wu et al. (2017) reported that taurine pre-administration in a rat depression model counteracts the rise in glutamate and inflammatory mediators such as corticosterone. Furthermore, in the same study, the administration of taurine prevented the reduction in substances such as 5-hydroxytryptamine (5-HT), dopamine, noradrenaline, and even upregulated the expression of neurotrophic factors like fibroblast growth factor-2 (FGF-2), vascular endothelial growth factor (VEGF), and brain derived neurotrophic factor (BDNF), that tend to fall under stress conditions. This suggests taurine's compensatory effects in response to stress-induced depression, demonstrating that taurine's antidepressant properties could possibly contribute to neuropsychiatric disease therapeutics.

An important question about the possible use of taurine as a therapeutic option in nervous system pathologies refers to the delivery mode in the organism. Oral delivery is the most common and easy method of taurine administration, and most trials in humans use this form of delivery. In fact, oral taurine administration, up to 4 grams in healthy adults or up to 6 grams daily for 6 months in children with fatty liver, has been given without toxic side effects (Obinata et al., 1996; Ghandforoush-Sattari et al., 2010). However, despite encouraging results in many preclinical works, some reports in animal studies have shown that oral administration is not as effective as taurine injection, and that prolonged consumption may even produce some negative effects in rats (Eppler et al., 1999; El Idrissi et al., 2003). Therefore, the need to explore additional and more efficient administration routes. For instance, intravenous delivery of taurine (up to five grams) has been given safely to patients during myocardial revascularization (Milei et al., 1992). However, intravenous delivery of taurine has not been tested in humans with neurological or neuropsychiatric diseases. In addition to oral and intravenous delivery, other systemic administration routes such as intraperitoneal injection may be implemented, although they tend to be more invasive and risky, increasing the possibility of bleeding or infection. Systemic administration is also limited by the BBB, which restricts taurine passage into CNS parenchyma. Furthermore, the BBB transport of taurine into the brain can be affected by the presence of cytokines such as tumor necrosis factor (TNF) (Kang et al., 2002; Lee and Kang, 2004). Therefore, novel methods that bypass the BBB should be tested. For instance, intranasal delivery of medications have been shown to be a practical and non-invasive method to evade the BBB and reach the CNS (Hanson and Frey, 2008). In mice, intranasal delivery of taurine produced anxiolytic effects in animals treated with strychnine, picrotoxin, yohimbine, or isoniazid (Jung and Kim, 2019). Another strategy may involve the use of taurine nanocarriers aimed at CNS cells. Recently, a functionalized nanoparticle with taurine and graphene oxide was designed, and tested successfully in rats (Pan et al., 2021).

CONCLUSION

There is compelling evidence of taurine's neuroprotective and homeostatic effects in the CNS, including maintenance of cellular energy processes, intracellular calcium modulation, osmotic stress regulation, and protection against glutamate-induced excitotoxicity, among others. The metabolic coupling for taurine synthesis and degradation between astrocytes and neurons, evidence neuronal dependence on astrocytes for the adequate functioning of the mentioned effects in the brain. Finally, it could be relevant to explore the effects of taurine in other glial cells such as microglia or oligodendrocytes, in functions such as antioxidative protection and demyelination and its association with astrocytes. Therefore, the astrocyte's role in taurine-induced neuroprotective functions should be considered as a promising therapeutic target in the management of several neurodegenerative and neuropsychiatric diseases in the near future.

AUTHOR CONTRIBUTIONS

SR-G: literature review, writing the manuscript, and making the figures. SG-M, GM-R, and EO-G: literature review and writing the manuscript. RC-P: writing and editing the manuscript. RG-R: original draft preparation and writing and editing the manuscript. All authors contributed to the article and approved the submitted version.

FUNDING

Funds received for open access publication fees from Universidad del Rosario.

ACKNOWLEDGMENTS

We thank Universidad del Rosario for the administrative support with this publication.

REFERENCES

Ahring, P. K., Bang, L. H., Jensen, M. L., Strøbæk, D., Hartiadi, L. Y., Chebib, M., et al. (2016). A pharmacological assessment of agonists and modulators at α4β2γ2 and α4β2δ GABAA receptors: the challenge in comparing apples with oranges. *Pharmacol. Res.* 111, 563–576. doi: 10.1016/j.phrs.2016.05.014

Albrecht, J., and Schousboe, A. (2005). Taurine interaction with neurotransmitter receptors in the CNS: an update. *Neurochem. Res.* 30, 1615–1621. doi: 10.1007/s11064-005-8986-6

Altamura, C., Maes, M., Dai, J., and Meltzer, H. Y. (1995). Plasma concentrations of excitatory amino acids, serine, glycine, taurine and histidine in major depression. *Eur. Neuropsychopharmacol.* 5, 71–75. doi: 10.1016/0924-977x(95)00033-l

Arai, H., Kobayashi, K., Ichimiya, Y., Kosaka, K., and Iizuka, R. (1985). Free amino acids in post-mortem cerebral cortices from patients with Alzheimer-type dementia. *Neurosci. Res.* 2, 486–490. doi: 10.1016/0168-0102(85)90020-3

Baliou, S., Kyriakopoulos, A. M., Goulielmaki, M., Panayiotidis, M. I., Spandidos, D. A., and Zoumpourlis, V. (2020). Significance of taurine transporter (TauT) in homeostasis and its layers of regulation (Review). *Mol. Med. Rep.* 22, 2163–2173. doi: 10.3892/mmr.2020.11321

Banerjee, R., Vitvitsky, V., and Garg, S. K. (2008). The undertow of sulfur metabolism on glutamatergic neurotransmission. *Trends Biochem. Sci.* 33, 413–419. doi: 10.1016/j.tibs.2008.06.006

Barges-Coll, J., Pérez-Neri, I., Avendaño, J., Mendez-Rosito, D., Gomez-Amador, J. L., and Ríos, C. (2013). Plasma taurine as a predictor of poor outcome in patients with mild neurological deficits after aneurysmal subarachnoid hemorrhage. *J. Neurosurg.* 119, 1021–1027. doi: 10.3171/2013.4.JNS121558

Barros, L. F., Bolaños, J. P., Bonvento, G., Bouzier-Sore, A.-K., Brown, A., Hirrlinger, J., et al. (2018). Current technical approaches to brain energy metabolism. *Glia* 66, 1138–1159. doi: 10.1002/glia.23248

Beetsch, J. W., and Olson, J. E. (1998). Taurine synthesis and cysteine metabolism in cultured rat astrocytes: effects of hyperosmotic exposure. *Am. J. Physiol.* 274, C866–C874. doi: 10.1152/ajpcell.1998.274.4.C866

Benedetti, M. S., Russo, A., Marrari, P., and Dostert, P. (1991). Effects of ageing on the content in sulfur-containing amino acids in rat brain. *J. Neural Transm. Gen. Sect.* 86, 191–203. doi: 10.1007/BF01250705

Bhat, M. A., Ahmad, K., Khan, M. S. A., Bhat, M. A., Almatroudi, A., Rahman, S., et al. (2020). Expedition into taurine biology: structural insights and therapeutic perspective of taurine in neurodegenerative diseases. *Biomolecules* 1: 863. doi: 10.3390/biom10060863

Blaustein, M. P. (1988). Calcium transport and buffering in neurons. *Trends Neurosci.* 11, 438–443. doi: 10.1016/0166-2236(88)90195-6

Blaustein, M. P., Goldman, W. F., Fontana, G., Krueger, B. K., Santiago, E. M., Steele, T. D., et al. (1991). Physiological roles of the sodium-calcium exchanger in nerve and muscle. *Ann. N. Y. Acad. Sci.* 639, 254–274. doi: 10.1111/j.1749-6632.1991.tb17315.x

Brand, A., Richter-Landsberg, C., and Leibfritz, D. (1997). Metabolism of acetate in rat brain neurons, astrocytes and cocultures: metabolic interactions between neurons and glia cells, monitored by NMR spectroscopy. *Cell. Mol. Biol.* 43, 645–657.

Caspi, R., Billington, R., Fulcher, C. A., Keseler, I. M., Kothari, A., Krummenacker, M., et al. (2018). The MetaCyc database of metabolic pathways and enzymes. *Nucleic Acids Res.* 46, D633–D639. doi: 10.1093/nar/gkx935

Che, Y., Hou, L., Sun, F., Zhang, C., Liu, X., Piao, F., et al. (2018). Taurine protects dopaminergic neurons in a mouse Parkinson's disease model through inhibition of microglial M1 polarization. *Cell Death Dis.* 9:435. doi: 10.1038/s41419-018-0468-2

Chen, C., Xia, S., He, J., Lu, G., Xie, Z., and Han, H. (2019). Roles of taurine in cognitive function of physiology, pathologies and toxication. *Life Sci.* 231:116584. doi: 10.1016/j.lfs.2019.116584

Chen, W. Q., Jin, H., Nguyen, M., Carr, J., Lee, Y. J., Hsu, C. C., et al. (2001). Role of taurine in regulation of intracellular calcium level and neuroprotective function in cultured neurons. *J. Neurosci. Res.* 66, 612–619. doi: 10.1002/jnr.10027

Choe, K. Y., Olson, J. E., and Bourque, C. W. (2012). Taurine release by astrocytes modulates osmosensitive glycine receptor tone and excitability in the adult supraoptic nucleus. *J. Neurosci.* 32, 12518–12527. doi: 10.1523/JNEUROSCI.1380-12.2012

Chung, W.-S., Allen, N. J., and Eroglu, C. (2015). Astrocytes control synapse formation, function, and elimination. *Cold Spring Harb. Perspect. Biol.* 7:a020370. doi: 10.1101/cshperspect.a020370

De Saint Jan, D., David-Watine, B., Korn, H., and Bregestovski, P. (2001). Activation of human alpha1 and alpha2 homomeric glycine receptors by taurine and GABA. *J. Physiol.* 535, 741–755. doi: 10.1111/j.1469-7793.2001.t01-1-00741.x

Deleuze, C., Duvoid, A., and Hussy, N. (1998). Properties and glial origin of osmotic-dependent release of taurine from the rat supraoptic nucleus. *J. Physiol.* 507, 463–471. doi: 10.1111/j.1469-7793.1998.463bt.x

Dong, X.-X., Wang, Y., and Qin, Z.-H. (2009). Molecular mechanisms of excitotoxicity and their relevance to pathogenesis of neurodegenerative diseases. *Acta Pharmacol. Sin.* 30, 379–387. doi: 10.1038/aps.2009.24

Dorstyn, L., Akey, C. W., and Kumar, S. (2018). New insights into apoptosome structure and function. *Cell Death Differ.* 25, 1194–1208. doi: 10.1038/s41418-017-0025-z

Dutton, G. R., Barry, M., Simmons, M. L., and Philibert, R. A. (1991). Astrocyte taurine. *Ann. N. Y. Acad. Sci.* 633, 489–500. doi: 10.1111/j.1749-6632.1991.tb15638.x

Eichhorn, E., van der Ploeg, J. R., Kertesz, M. A., and Leisinger, T. (1997). Characterization of alpha-ketoglutarate-dependent taurine dioxygenase from *Escherichia coli*. *J. Biol. Chem.* 272, 23031–23036. doi: 10.1074/jbc.272.37.23031

El Idrissi, A., Messing, J., Scalia, J., and Trenkner, E. (2003). Prevention of epileptic seizures by taurine. *Adv. Exp. Med. Biol.* 526, 515–525. doi: 10.1007/978-1-4615-0077-3_62

Elmore, S. (2007). Apoptosis: a review of programmed cell death. *Toxicol. Pathol.* 35, 495–516. doi: 10.1080/01926230701320337

Eppler, B., Patterson, T. A., Zhou, W., Millard, W. J., and Dawson, R. Jr. (1999). Kainic acid (KA)-induced seizures in Sprague-Dawley rats and the effect of dietary taurine (TAU) supplementation or deficiency. *Amino Acids* 16, 133–147. doi: 10.1007/BF01321532

Fichtner, M., Voigt, K., and Schuster, S. (2017). The tip and hidden part of the iceberg: proteinogenic and non-proteinogenic aliphatic amino acids. *Biochim. Biophys. Acta Gen. Subj.* 1861(1 Pt A), 3258–3269. doi: 10.1016/j.bbagen.2016.08.008

Foos, T. M., and Wu, J.-Y. (2002). The role of taurine in the central nervous system and the modulation of intracellular calcium homeostasis. *Neurochem. Res.* 27, 21–26. doi: 10.1023/a:1014890219513

Formaggio, F., Saracino, E., Mola, M. G., Rao, S. B., Amiry-Moghaddam, M., Muccini, M., et al. (2019). LRRC8A is essential for swelling-activated chloride current and for regulatory volume decrease in astrocytes. *FASEB J.* 33, 101–113. doi: 10.1096/fj.201701397RR

Froger, N., Sahel, J.-A., and Picaud, S. (2014). "Taurine Deficiency and the Eye," in *Handbook of Nutrition, Diet and the Eye*, ed. V. R. Preedy (San Diego, CA: Academic Press), 505–513. doi: 10.1016/b978-0-12-401717-7.00051-4

Frosini, M., Sesti, C., Saponara, S., Ricci, L., Valoti, M., Palmi, M., et al. (2003). A specific taurine recognition site in the rabbit brain is responsible for taurine effects on thermoregulation. *Br. J. Pharmacol.* 139, 487–494. doi: 10.1038/sj.bjp.0705274

Fukuyama, Y., and Ochiai, Y. (1982). Therapeutic trial by taurine for intractable childhood epilepsies. *Brain Dev.* 4, 63–69. doi: 10.1016/S0387-7604(82)80103-4

Gebara, E., Udry, F., Sultan, S., and Toni, N. (2015). Taurine increases hippocampal neurogenesis in aging mice. *Stem Cell. Res.* 14, 369–379. doi: 10.1016/j.scr.2015.04.001

Ghandforoush-Sattari, M., Mashayekhi, S., Krishna, C. V., Thompson, J. P., and Routledge, P. A. (2010). Pharmacokinetics of oral taurine in healthy volunteers. *J. Amino Acids* 2010:346237. doi: 10.4061/2010/346237

Gharibani, P. M., Modi, J., Pan, C., Menzie, J., Ma, Z., Chen, P.-C., et al. (2013). The mechanism of taurine protection against endoplasmic reticulum stress in an animal stroke model of cerebral artery occlusion and stroke-related conditions in primary neuronal cell culture. *Adv. Exp. Med. Biol.* 776, 241–258. doi: 10.1007/978-1-4614-6093-0_23

Gharibani, P., Modi, J., Menzie, J., Alexandrescu, A., Ma, Z., Tao, R., et al. (2015). Comparison between single and combined post-treatment with S-Methyl-N,N-diethylthiolcarbamate sulfoxide and taurine following transient focal cerebral ischemia in rat brain. *Neuroscience* 300, 460–473. doi: 10.1016/j.neuroscience.2015.05.042

Han, X., Patters, A. B., Jones, D. P., Zelikovic, I., and Chesney, R. W. (2006). The taurine transporter: mechanisms of regulation. *Acta Physiol.* 187, 61–73. doi: 10.1111/j.1748-1716.2006.01573.x

Hanson, L. R., and Frey, W. H. II (2008). Intranasal delivery bypasses the blood-brain barrier to target therapeutic agents to the central nervous system and treat neurodegenerative disease. *BMC Neurosci.* 9(Suppl. 3):S5. doi: 10.1186/1471-2202-9-S3-S5

Hatton, G. I. (2002). Glial-neuronal interactions in the mammalian brain. *Adv. Physiol. Educ.* 26, 225–237. doi: 10.1152/advan.00038.2002

Hayes, K. C., and Sturman, J. A. (1981). Taurine in metabolism. *Annu. Rev. Nutr.* 1, 401–425. doi: 10.1146/annurev.nu.01.070181.002153

Hertz, L. (1979). Functional interactions between neurons and astrocytes I. Turnover and metabolism of putative amino acid transmitters. *Prog. Neurobiol.* 13, 277–323. doi: 10.1016/0301-0082(79)90018-2

Hussaini, S. M. Q., and Jang, M. H. (2018). New roles for old glue: astrocyte function in synaptic plasticity and neurological disorders. *Int. Neurourol. J.* 22(Suppl. 3), S106–S114. doi: 10.5213/inj.1836214.107

Hussy, N., Deleuze, C., Desarménien, M. G., and Moos, F. (2000). Osmotic regulation of neuronal activity: a new role for taurine and glial cells in a hypothalamic neuroendocrine structure. *Prog. Neurobiol.* 62, 113–134. doi: 10.1016/S0301-0082(99)00071-4

Hussy, N., Deleuze, C., Pantaloni, A., Desarménien, M. G., and Moos, F. (1997). Agonist action of taurine on glycine receptors in rat supraoptic magnocellular neurones: possible role in osmoregulation. *J. Physiol.* 502, 609–621. doi: 10.1111/j.1469-7793.1997.609bj.x

Huxtable, R. J. (1989). Taurine in the central nervous system and the mammalian actions of taurine. *Prog. Neurobiol.* 32, 471–533. doi: 10.1016/0301-0082(89)90019-1

Huxtable, R. J. (1992). Physiological actions of taurine. *Physiol. Rev.* 72, 101–163. doi: 10.1152/physrev.1992.72.1.101

Hyzinski-García, M. C., Rudkouskaya, A., and Mongin, A. A. (2014). LRRC8A protein is indispensable for swelling-activated and ATP-induced release of excitatory amino acids in rat astrocytes. *J. Physiol.* 592, 4855–4862. doi: 10.1113/jphysiol.2014.278887

Inoue, H., Mori, S.-I., Morishima, S., and Okada, Y. (2005). Volume-sensitive chloride channels in mouse cortical neurons: characterization and role in volume regulation. *Eur. J. Neurosci.* 21, 1648–1658. doi: 10.1111/j.1460-9568.2005.04006.x

Ito, T., Miyazaki, N., Schaffer, S., and Azuma, J. (2015). Potential anti-aging role of taurine via proper protein folding: a study from taurine transporter knockout mouse. *Adv. Exp. Med. Biol.* 803, 481–487. doi: 10.1007/978-3-319-15126-7_38

Ito, T., Yoshikawa, N., Inui, T., Miyazaki, N., Schaffer, S. W., and Azuma, J. (2014). Tissue depletion of taurine accelerates skeletal muscle senescence and leads to early death in mice. *PLoS One* 9:e107409. doi: 10.1371/journal.pone.0107409

Jakaria, M., Azam, S., Haque, M. E., Jo, S.-H., Uddin, M. S., Kim, I.-S., et al. (2019). Taurine and its analogs in neurological disorders: focus on therapeutic potential and molecular mechanisms. *Redox Biol.* 24:101223. doi: 10.1016/j.redox.2019.101223

Jang, H., Lee, S., Choi, S. L., Kim, H. Y., Baek, S., and Kim, Y. (2017). Taurine directly binds to oligomeric amyloid-β and recovers cognitive deficits in Alzheimer model mice. *Adv. Exp. Med. Biol.* 975, 233–241. doi: 10.1007/978-94-024-1079-2_21

Jia, F., Yue, M., Chandra, D., Keramidas, A., Goldstein, P. A., Homanics, G. E., et al. (2008). Taurine is a potent activator of extrasynaptic GABA(A) receptors in the thalamus. *J. Neurosci.* 28, 106–115. doi: 10.1523/JNEUROSCI.3996-07.2008

Jong, C. J., Azuma, J., and Schaffer, S. (2012). Mechanism underlying the antioxidant activity of taurine: prevention of mitochondrial oxidant production. *Amino Acids* 42, 2223–2232. doi: 10.1007/s00726-011-0962-7

Jong, C. J., Ito, T., and Schaffer, S. W. (2015). The ubiquitin-proteasome system and autophagy are defective in the taurine-deficient heart. *Amino Acids* 47, 2609–2622. doi: 10.1007/s00726-015-2053-7

Jung, J. H., and Kim, S.-J. (2019). Anxiolytic action of taurine via intranasal administration in mice. *Biomol. Ther.* 27, 450–456. doi: 10.4062/biomolther.2018.218

Junyent, F., De Lemos, L., Utrera, J., Paco, S., Aguado, F., Camins, A., et al. (2011). Content and traffic of taurine in hippocampal reactive astrocytes. *Hippocampus* 21, 185–197. doi: 10.1002/hipo.20739

Junyent, F., Romero, R., de Lemos, L., Utrera, J., Camins, A., Pallàs, M., et al. (2010). Taurine treatment inhibits CaMKII activity and modulates the presence of calbindin D28k, calretinin, and parvalbumin in the brain. *J. Neurosci. Res.* 88, 136–142. doi: 10.1002/jnr.22192

Junyent, F., Utrera, J., Romero, R., Pallàs, M., Camins, A., Duque, D., et al. (2009). Prevention of epilepsy by taurine treatments in mice experimental model. *J. Neurosci. Res.* 87, 1500–1508. doi: 10.1002/jnr.21950

Kamisaki, Y., Wada, K., Nakamoto, K., and Itoh, T. (1996). Release of taurine and its effects on release of neurotransmitter amino acids in rat cerebral cortex. *Adv. Exp. Med. Biol.* 403, 445–454. doi: 10.1007/978-1-4899-0182-8_48

Kang, Y.-S., Ohtsuki, S., Takanaga, H., Tomi, M., Hosoya, K., and Terasaki, T. (2002). Regulation of taurine transport at the blood-brain barrier by tumor necrosis factor-α, taurine and hypertonicity: regulation of the BBB taurine transporter. *J. Neurochem.* 83, 1188–1195. doi: 10.1046/j.1471-4159.2002.01223.x

Khodapasand, E., Jafarzadeh, N., Farrokhi, F., Kamalidehghan, B., and Houshmand, M. (2015). Is Bax/Bcl-2 ratio considered as a prognostic marker with age and tumor location in colorectal cancer? *Iran Biomed. J.* 19, 69–75. doi: 10.6091/ibj.1366.2015

Kilb, W., and Fukuda, A. (2017). Taurine as an essential neuromodulator during perinatal cortical development. *Front. Cell. Neurosci.* 11:328. doi: 10.3389/fncel.2017.00328

Kletke, O., Gisselmann, G., May, A., Hatt, H., and Sergeeva, O. A. (2013). Partial agonism of taurine at gamma-containing native and recombinant GABAA receptors. *PLoS One* 8:e61733. doi: 10.1371/journal.pone.0061733

Kohe, S. E., Bennett, C. D., Gill, S. K., Wilson, M., McConville, C., and Peet, A. C. (2018). Metabolic profiling of the three neural derived embryonal pediatric tumors retinoblastoma, neuroblastoma and medulloblastoma, identifies distinct metabolic profiles. *Oncotarget* 9, 11336–11351. doi: 10.18632/oncotarget.24168

Kondo, H., Anada, H., Ohsawa, K., and Ishimoto, M. (1971). Formation of sulfoacetaldehyde from taurine in bacterial extracts. *J. Biochem.* 69, 621–623.

Kontro, P., Marnela, K. M., and Oja, S. S. (1984). GABA, taurine and hypotaurine in developing mouse brain. *Acta Physiol. Scand. Suppl.* 537, 71–74.

Kovanlikaya, A., Panigrahy, A., Krieger, M. D., Gonzalez-Gomez, I., Ghugre, N., McComb, J. G., et al. (2005). Untreated pediatric primitive neuroectodermal tumor *in vivo*: quantitation of taurine with MR spectroscopy. *Radiology* 236, 1020–1025. doi: 10.1148/radiol.2363040856

Kudo, Y., Akiyoshi, E., and Akagi, H. (1988). Identification of two taurine receptor subtypes on the primary afferent terminal of frog spinal cord. *Br. J. Pharmacol.* 94, 1051–1056. doi: 10.1111/j.1476-5381.1988.tb11621.x

Kumari, N., Prentice, H., and Wu, J.-Y. (2013). Taurine and its neuroprotective role. *Adv. Exp. Med. Biol.* 775, 19–27. doi: 10.1007/978-1-4614-6130-2_2

Lai, T. W., Zhang, S., and Wang, Y. T. (2014). Excitotoxicity and stroke: identifying novel targets for neuroprotection. *Prog. Neurobiol.* 115, 157–188. doi: 10.1016/j.pneurobio.2013.11.006

Leaney, J. L., Marsh, S. J., and Brown, D. A. (1997). A swelling-activated chloride current in rat sympathetic neurones. *J. Physiol.* 501, 555–564. doi: 10.1111/j.1469-7793.1997.555bm.x

Lee, N.-Y., and Kang, Y.-S. (2004). The brain-to-blood efflux transport of taurine and changes in the blood-brain barrier transport system by tumor necrosis factor-alpha. *Brain Res.* 1023, 141–147. doi: 10.1016/j.brainres.2004.07.033

Leon, R., Wu, H., Jin, Y., Wei, J., Buddhala, C., Prentice, H., et al. (2009). Protective function of taurine in glutamate-induced apoptosis in cultured neurons. *J. Neurosci. Res.* 87, 1185–1194. doi: 10.1002/jnr.21926

Lerma, J., Herranz, A. S., Herreras, O., Abraira, V., and Martín del Río, R. (1986). *In vivo* determination of extracellular concentration of amino acids in the rat hippocampus. A method based on brain dialysis and computerized analysis. *Brain Res.* 384, 145–155. doi: 10.1016/0006-8993(86)91230-8

Li, S., Yang, L., Zhang, Y., Zhang, C., Shao, J., Liu, X., et al. (2017). Taurine ameliorates arsenic-induced apoptosis in the hippocampus of mice through intrinsic pathway. *Adv. Exp. Med. Biol.* 975(Pt .1), 183–192. doi: 10.1007/978-94-024-1079-2_16

López-Colomé, A. M., Fragoso, G., and Salceda, R. (1991). Taurine receptors in membranes from retinal pigment epithelium cells in culture. *Neuroscience* 41, 791–796. doi: 10.1016/0306-4522(91)90369-y

Louzada, P. R., Paula Lima, A. C., Mendonca-Silva, D. L., Noël, F., De Mello, F. G., and Ferreira, S. T. (2004). Taurine prevents the neurotoxicity of beta-amyloid

and glutamate receptor agonists: activation of GABA receptors and possible implications for Alzheimer's disease and other neurological disorders. *FASEB J.* 18, 511–518. doi: 10.1096/fj.03-0739com

Magnotta, V. A., Xu, J., Fiedorowicz, J. G., Williams, A., Shaffer, J., Christensen, G., et al. (2022). Metabolic abnormalities in the basal ganglia and cerebellum in bipolar disorder: a multi-modal MR study. *J. Affect. Disord.* 301, 390–399. doi: 10.1016/j.jad.2022.01.052

Malarkey, E. B., and Parpura, V. (2008). Mechanisms of glutamate release from astrocytes. *Neurochem. Int.* 52, 142–154. doi: 10.1016/j.neuint.2007.06.005

Mersman, B., Zaidi, W., Syed, N. I., and Xu, F. (2020). Taurine promotes neurite outgrowth and synapse development of both vertebrate and invertebrate central neurons. *Front. Synaptic Neurosci.* 12:29. doi: 10.3389/fnsyn.2020.00029

Milei, J., Ferreira, R., Llesuy, S., Forcada, P., Covarrubias, J., and Boveris, A. (1992). Reduction of reperfusion injury with preoperative rapid intravenous infusion of taurine during myocardial revascularization. *Am. Heart J.* 123, 339–345. doi: 10.1016/0002-8703(92)90644-B

Mongin, A. A. (2016). Volume-regulated anion channel-a frenemy within the brain. *Pflugers Arch.* 468, 421–441. doi: 10.1007/s00424-015-1765-6

Mori, M., Gähwiler, B. H., and Gerber, U. (2002). Beta-alanine and taurine as endogenous agonists at glycine receptors in rat hippocampus *in vitro*. *J. Physiol.* 539(Pt. 1), 191–200. doi: 10.1113/jphysiol.2001.013147

Morken, T. S., Sonnewald, U., Aschner, M., and Syversen, T. (2005). Effects of methylmercury on primary brain cells in mono- and co-culture. *Toxicol. Sci.* 87, 169–175. doi: 10.1093/toxsci/kfi227

Nakazato, T., Kanai, K., Kataura, T., Nojiri, S., Hattori, N., and Saiki, S. (2022). Plasma taurine is an axonal excitability-translatable biomarker for amyotrophic lateral sclerosis. *Sci Rep.* 12:9155. doi: 10.1038/s41598-022-13397-6

Netti, V., Pizzoni, A., Pérez-Domínguez, M., Ford, P., Pasantes-Morales, H., Ramos-Mandujano, G., et al. (2018). Release of taurine and glutamate contributes to cell volume regulation in human retinal Müller cells: differences in modulation by calcium. *J. Neurophysiol.* 120, 973–984. doi: 10.1152/jn.00725.2017

Newman, S. D., Schnakenberg Martin, A. M., Raymond, D., Cheng, H., Wilson, L., Barnes, S., et al. (2022). The relationship between cannabis use and taurine: a MRS and metabolomics study. *PLoS One* 17:e0269280. doi: 10.1371/journal.pone.0269280

Nishimura, T., Higuchi, K., Yoshida, Y., Sugita-Fujisawa, Y., Kojima, K., Sugimoto, M., et al. (2018). Hypotaurine is a substrate of GABA transporter family members GAT2/Slc6a13 and TAUT/Slc6a6. *Biol. Pharm. Bull.* 41, 1523–1529. doi: 10.1248/bpb.b18-00168

Obinata, K., Maruyama, T., Hayashi, M., Watanabe, T., and Nittono, H. (1996). Effect of taurine on the fatty liver of children with simple obesity. *Adv. Exp. Med. Biol.* 403, 607–613. doi: 10.1007/978-1-4899-0182-8_67

Ochoa-de la Paz, L., Zenteno, E., Gulias-Cañizo, R., and Quiroz-Mercado, H. (2019). Taurine and GABA neurotransmitter receptors, a relationship with therapeutic potential? *Expert Rev. Neurother.* 19, 289–291. doi: 10.1080/14737175.2019.1593827

Ohno, S., and Nishizuka, Y. (2002). Protein kinase C isotypes and their specific functions: prologue. *J. Biochem.* 132, 509–511. doi: 10.1093/oxfordjournals.jbchem.a003249

Oja, S. S., and Saransaari, P. (2013). Taurine and epilepsy. *Epilepsy Res.* 104, 187–194. doi: 10.1016/j.eplepsyres.2013.01.010

Oja, S. S., and Saransaari, P. (2017). Significance of taurine in the brain. *Adv. Exp. Med. Biol.* 975(Pt. 1), 89–94. doi: 10.1007/978-94-024-1079-2_8

Palkovits, M., Elekes, I., Láng, T., and Patthy, A. (1986). Taurine levels in discrete brain nuclei of rats. *J. Neurochem.* 47, 1333–1335. doi: 10.1111/j.1471-4159.1986.tb00761.x

Pan, H., Yu, Y., Li, L., Liu, B., and Liu, Y. (2021). Fabrication and characterization of taurine functionalized graphene oxide with 5-fluorouracil as anticancer drug delivery systems. *Nanoscale Res. Lett.* 16:84. doi: 10.1186/s11671-021-03541-y

Papet, I., Rémond, D., Dardevet, D., Mosoni, L., Polakof, S., Peyron, M.-A., et al. (2019). "Sulfur amino acids and skeletal muscle," in *Nutrition and Skeletal Muscle*, ed. S. Walrand (Cambridge, MA: Academic Press), 335–363. doi: 10.1016/b978-0-12-810422-4.00020-8

Park, S.-H., Lee, H., Park, K. K., Kim, H. W., Lee, D. H., and Park, T. (2006). Taurine-induced changes in transcription profiling of metabolism-related genes in human hepatoma cells HepG2. *Adv. Exp. Med. Biol.* 583, 119–128. doi: 10.1007/978-0-387-33504-9_12

Park, Y. K., and Linkswiler, H. (1970). Effect of vitamin B6 depletion in adult man on the excretion of cystathionine and other methionine metabolites. *J. Nutr.* 100, 110–116. doi: 10.1093/jn/100.1.110

Pasantes-Morales, H. (2017). Taurine homeostasis and volume control. *Adv. Neurobiol.* 16, 33–53. doi: 10.1007/978-3-319-55769-4_3

Pasantes-Morales, H., and Schousboe, A. (1997). Role of taurine in osmoregulation in brain cells: mechanisms and functional implications. *Amino Acids* 12, 281–292. doi: 10.1007/bf01373008

Patel, A. J., Lauritzen, I., Lazdunski, M., and Honoré, E. (1998). Disruption of mitochondrial respiration inhibits volume-regulated anion channels and provokes neuronal cell swelling. *J. Neurosci.* 18, 3117–3123. doi: 10.1523/JNEUROSCI.18-09-03117.1998

Paula-Lima, A. C., De Felice, F. G., Brito-Moreira, J., and Ferreira, S. T. (2005). Activation of GABA(A) receptors by taurine and muscimol blocks the neurotoxicity of beta-amyloid in rat hippocampal and cortical neurons. *Neuropharmacology* 49, 1140–1148. doi: 10.1016/j.neuropharm.2005.06.015

Peck, E. J. Jr., and Awapara, J. (1967). Formation of taurine and isethionic acid in rat brain. *Biochim. Biophys. Acta* 141, 499–506. doi: 10.1016/0304-4165(67)90178-x

Piccioni, A., Covino, M., Zanza, C., Longhitano, Y., Tullo, G., Bonadia, N., et al. (2021). Energy drinks: a narrative review of their physiological and pathological effects. *Intern. Med. J.* 51, 636–646. doi: 10.1111/imj.14881

Popova, A. A., and Koksharova, O. A. (2016). Neurotoxic non-proteinogenic amino Acid β-N-Methylamino-L-alanine and its role in biological systems. *Biochemistry* 81, 794–805. doi: 10.1134/S0006297916080022

Pow, D. V., Sullivan, R., Reye, P., and Hermanussen, S. (2002). Localization of taurine transporters, taurine, and (3)H taurine accumulation in the rat retina, pituitary, and brain. *Glia* 37, 153–168. doi: 10.1002/glia.10026

Prentice, H., Pan, C., Gharibani, P. M., Ma, Z., Price, A. L., Giraldo, G. S., et al. (2017). Analysis of neuroprotection by taurine and taurine combinations in primary neuronal cultures and in neuronal cell lines exposed to glutamate excitotoxicity and to hypoxia/re-oxygenation. *Adv. Exp. Med. Biol.* 975(Pt. 1), 207–216. doi: 10.1007/978-94-024-1079-2_18

Purves, D., Augustine, G. J., Fitzpatrick, D., Katz, L. C., LaMantia, A.-S., McNamara, J. O., et al. (2001). "What defines a neurotransmitter?," in *Neuroscience*, 2nd Edn, ed. D. Purves (Sunderland, MA: Sinauer Associates).

Qiu, Z., Dubin, A. E., Mathur, J., Tu, B., Reddy, K., Miraglia, L. J., et al. (2014). SWELL1, a plasma membrane protein, is an essential component of volume-regulated anion channel. *Cell* 157, 447–458. doi: 10.1016/j.cell.2014.03.024

Ramila, K. C., Jong, C. J., Pastukh, V., Ito, T., Azuma, J., and Schaffer, S. W. (2015). Role of protein phosphorylation in excitation-contraction coupling in taurine deficient hearts. *Am. J. Physiol. Heart Circ. Physiol.* 308, H232–H239. doi: 10.1152/ajpheart.00497.2014

Ripps, H., and Shen, W. (2012). Review: taurine: a "very essential" amino acid. *Mol. Vis.* 18, 2673–2686.

Rosso, L., Peteri-Brunbäck, B., Poujeol, P., Hussy, N., and Mienville, J.-M. (2004). Vasopressin-induced taurine efflux from rat pituicytes: a potential negative feedback for hormone secretion. *J. Physiol.* 554, 731–742. doi: 10.1113/jphysiol.2003.056267

Roysommuti, S., and Wyss, J. M. (2015). "The effects of taurine exposure on the brain and neurological disorders," in *Bioactive Nutraceuticals and Dietary Supplements in Neurological and Brain Disease*, eds R. R. Watson and V. R. Preedy (Cambridge, MA: Academic Press), 207–213. doi: 10.1016/b978-0-12-411462-3.00022-9

Saransaari, P., and Oja, S. S. (1991). Excitatory amino acids evoke taurine release from cerebral cortex slices from adult and developing mice. *Neuroscience* 45, 451–459. doi: 10.1016/0306-4522(91)90240-o

Saransaari, P., and Oja, S. S. (1992). Release of GABA and taurine from brain slices. *Prog. Neurobiol.* 38, 455–482. doi: 10.1016/0301-0082(92)90046-h

Sato, K., Numata, T., Saito, T., Ueta, Y., and Okada, Y. (2011). V_2 receptor-mediated autocrine role of somatodendritic release of AVP in rat vasopressin neurons under hypo-osmotic conditions. *Sci. Signal.* 4:ra5. doi: 10.1126/scisignal.2001279

Schaffer, S. W., Jong, C. J., Ito, T., and Azuma, J. (2014). Role of taurine in the pathologies of MELAS and MERRF. *Amino Acids* 46, 47–56. doi: 10.1007/s00726-012-1414-8

Schaffer, S. W., Jong, C. J., Ramila, K. C., and Azuma, J. (2010). Physiological roles of taurine in heart and muscle. *J. Biomed. Sci*. 17(Suppl. 1):S2. doi: 10.1186/1423-0127-17-S1-S2

Schaffer, S. W., Shimada-Takaura, K., Jong, C. J., Ito, T., and Takahashi, K. (2016). Impaired energy metabolism of the taurine-deficient heart. *Amino Acids* 48, 549–558. doi: 10.1007/s00726-015-2110-2

Schaffer, S. W., Solodushko, V., and Kakhniashvili, D. (2002). Beneficial effect of taurine depletion on osmotic sodium and calcium loading during chemical hypoxia. *Am. J. Physiol. Cell. Physiol.* 282, C1113–C1120. doi: 10.1152/ajpcell.00485.2001

Schaffer, S., and Kim, H. W. (2018). Effects and mechanisms of taurine as a therapeutic agent. *Biomol. Ther.* 26, 225–241. doi: 10.4062/biomolther.2017.251

Schaffer, S., Azuma, J., Takahashi, K., and Mozaffari, M. (2003). Why is taurine cytoprotective? *Adv. Exp. Med. Biol.* 526, 307–321. doi: 10.1007/978-1-4615-0077-3_39

Schober, A. L., Wilson, C. S., and Mongin, A. A. (2017). Molecular composition and heterogeneity of the LRRC8-containing swelling-activated osmolyte channels in primary rat astrocytes. *J. Physiol.* 595, 6939–6951. doi: 10.1113/JP275053

Schousboe, A., and Pasantes-Morales, H. (1989). Potassium-stimulated release of [3H]taurine from cultured GABAergic and glutamatergic neurons. *J. Neurochem.* 53, 1309–1315. doi: 10.1111/j.1471-4159.1989.tb07429.x

Shimamoto, G., and Berk, R. S. (1979). Catabolism of taurine in *Pseudomonas aeruginosa*. *Biochim. Biophys. Acta*. 569, 287–292. doi: 10.1016/0005-2744(79)90064-0

Shirayama, Y., Obata, T., Matsuzawa, D., Nonaka, H., Kanazawa, Y., Yoshitome, E., et al. (2010). Specific metabolites in the medial prefrontal cortex are associated with the neurocognitive deficits in schizophrenia: a preliminary study. *Neuroimage* 49, 2783–2790. doi: 10.1016/j.neuroimage.2009.10.031

Sigel, E., and Steinmann, M. E. (2012). Structure, function, and modulation of GABA(A) receptors. *J. Biol. Chem.* 287, 40224–40231. doi: 10.1074/jbc.R112.386664

Song, N.-Y., Shi, H.-B., Li, C.-Y., and Yin, S.-K. (2012). Interaction between taurine and GABA(A)/glycine receptors in neurons of the rat anteroventral cochlear nucleus. *Brain Res.* 1472, 1–10. doi: 10.1016/j.brainres.2012.07.001

Song, T., Chen, W., Chen, X., Zhang, H., Zou, Y., Wu, H., et al. (2021). Repeated fluoxetine treatment induces transient and long-term astrocytic plasticity in the medial prefrontal cortex of normal adult rats. *Prog. Neuropsychopharmacol. Biol. Psychiatry* 107:110252. doi: 10.1016/j.pnpbp.2021.110252

Song, Z., and Hatton, G. I. (2003). Taurine and the control of basal hormone release from rat neurohypophysis. *Exp. Neurol.* 183, 330–337. doi: 10.1016/S0014-4886(03)00105-5

Spinneker, A., Sola, R., Lemmen, V., Castillo, M. J., Pietrzik, K., and González-Gross, M. (2007). Vitamin B_6 status, deficiency and its consequences - an overview. *Nutr. Hosp.* 22, 7–24.

Stover, J. F., Morganti-Kosmann, M. C., Lenzlinger, P. M., Stocker, R., Kempski, O. S., and Kossmann, T. (1999). Glutamate and taurine are increased in ventricular cerebrospinal fluid of severely brain-injured patients. *J. Neurotrauma* 16, 135–142. doi: 10.1089/neu.1999.16.135

Strimbu, K., and Tavel, J. A. (2010). What are biomarkers? *Curr. Opin. HIV AIDS* 5, 463–466. doi: 10.1097/COH.0b013e32833ed177

Sturman, J. (1992). Review: taurine deficiency and the cat. *Adv. Exp. Med. Biol.* 315, 1–5. doi: 10.1007/978-1-4615-3436-5_1

Sun, C., Gao, M., Wang, F., Yun, Y., Sun, Q., Guo, R., et al. (2020). Serum metabolomic profiling in patients with Alzheimer disease and amnestic mild cognitive impairment by GC/MS. *Biomed. Chromatogr.* 34:e4875. doi: 10.1002/bmc.4875

Suzuki, T., Suzuki, T., Takeshi, W., Kazuhiko, S., and Kimitsuna, W. (2002). Taurine as a constituent of mitochondrial tRNAs: new insights into the functions of taurine and human mitochondrial diseases. *EMBO J.* 21, 6581–6589. doi: 10.1093/emboj/cdf656

Takuma, K., Matsuda, T., Hashimoto, H., Asano, S., and Baba, A. (1994). Cultured rat astrocytes possess Na(+)-Ca2+ exchanger. *Glia* 12, 336–342. doi: 10.1002/glia.440120410

Tappaz, M., Almarghini, K., and Do, K. (1994). Cysteine sulfinate decarboxylase in brain: identification, characterization and immunocytochemical location in astrocytes. *Adv. Exp. Med. Biol.* 359, 257–268. doi: 10.1007/978-1-4899-1471-2_26

Tian, T., Zhang, B. Y., Wang, K. D., Zhang, B. F., and Huang, M. (2020). [Protective effects of taurine on neurons and microglia in Parkinson's disease-like mouse model induced by paraquat]. *Zhonghua Lao Dong Wei Sheng Zhi Ye Bing Za Zhi* 38, 801–808. doi: 10.3760/cma.j.cn121094-20200121-00036

Traynelis, S. F., Wollmuth, L. P., McBain, C. J., Menniti, F. S., Vance, K. M., Ogden, K. K., et al. (2010). Glutamate receptor ion channels: structure, regulation, and function. *Pharmacol. Rev.* 62, 405–496. doi: 10.1124/pr.109.002451

Vitvitsky, V., Garg, S. K., and Banerjee, R. (2011). Taurine biosynthesis by neurons and astrocytes. *J. Biol. Chem.* 286, 32002–32010. doi: 10.1074/jbc.M111.253344

Volterra, A., and Meldolesi, J. (2005). Astrocytes, from brain glue to communication elements: the revolution continues. *Nat. Rev. Neurosci.* 6, 626–640. doi: 10.1038/nrn1722

Voss, F. K., Ullrich, F., Münch, J., Lazarow, K., Lutter, D., Mah, N., et al. (2014). Identification of LRRC8 heteromers as an essential component of the volume-regulated anion channel VRAC. *Science* 344, 634–638. doi: 10.1126/science.1252826

Voss, J. W., Pedersen, S. F., Christensen, S. T., and Lambert, I. H. (2004). Regulation of the expression and subcellular localization of the taurine transporter TauT in mouse NIH3T3 fibroblasts. *Eur. J. Biochem.* 271, 4646–4658. doi: 10.1111/j.1432-1033.2004.04420.x

Wang, Z., Li, Y., Zeng, Z., Guo, S., Chen, W., and Luo, Y. (2022). The potential role of leucine-rich repeat-containing protein 8A in central nervous system: current situation and prospect. *Neuroscience* 488, 122–131. doi: 10.1016/j.neuroscience.2022.03.001

Weiss, S. J., Klein, R., Slivka, A., and Wei, M. (1982). Chlorination of taurine by human neutrophils. evidence for hypochlorous acid generation. *J. Clin. Invest.* 70, 598–607. doi: 10.1172/jci110652

Wen, C., Li, F., Zhang, L., Duan, Y., Guo, Q., Wang, W., et al. (2019). Taurine is involved in energy metabolism in muscles, adipose tissue, and the liver. *Mol. Nutr. Food Res.* 63:e1800536. doi: 10.1002/mnfr.201800536

Winkler, P., Luhmann, H. J., and Kilb, W. (2019). Taurine potentiates the anticonvulsive effect of the GABA agonist muscimol and pentobarbital in the immature mouse hippocampus. *Epilepsia* 60, 464–474. doi: 10.1111/epi.14651

Wójcik, O. P., Koenig, K. L., Zeleniuch-Jacquotte, A., Costa, M., and Chen, Y. (2010). The potential protective effects of taurine on coronary heart disease. *Atherosclerosis* 208, 19–25. doi: 10.1016/j.atherosclerosis.2009.06.002

Wu, G. (2020). Important roles of dietary taurine, creatine, carnosine, anserine and 4-hydroxyproline in human nutrition and health. *Amino Acids* 52, 329–360. doi: 10.1007/s00726-020-02823-6

Wu, G.-F., Ren, S., Tang, R.-Y., Xu, C., Zhou, J.-Q., Lin, S.-M., et al. (2017). Antidepressant effect of taurine in chronic unpredictable mild stress-induced depressive rats. *Sci. Rep.* 7:4989. doi: 10.1038/s41598-017-05051-3

Wu, H., Jin, Y., Wei, J., Jin, H., Sha, D., and Wu, J.-Y. (2005). Mode of action of taurine as a neuroprotector. *Brain Res.* 1038, 123–131. doi: 10.1016/j.brainres.2005.01.058

Wu, J. Y., Tang, X. W., and Tsai, W. H. (1992). Taurine receptor: kinetic analysis and pharmacological studies. *Adv. Exp. Med. Biol.* 315, 263–268. doi: 10.1007/978-1-4615-3436-5_31

Wu, J., Kohno, T., Georgiev, S. K., Ikoma, M., Ishii, H., Petrenko, A. B., et al. (2008). Taurine activates glycine and gamma-aminobutyric acid A receptors in rat substantia gelatinosa neurons. *Neuroreport* 19, 333–337. doi: 10.1097/WNR.0b013e3282f50c90

Wu, J.-Y., and Prentice, H. (2010). Role of taurine in the central nervous system. *J. Biomed. Sci.* 17(Suppl. 1):S1. doi: 10.1186/1423-0127-17-S1-S1

Wu, J.-Y., Wu, H., Jin, Y., Wei, J., Sha, D., Prentice, H., et al. (2009). Mechanism of neuroprotective function of taurine. *Adv. Exp. Med. Biol.* 643, 169–179. doi: 10.1007/978-0-387-75681-3_17

Wu, P., Shi, X., Luo, M., Inam-U-Llah, Li, K., Zhang, M., et al. (2020). Taurine inhibits neuron apoptosis in hippocampus of diabetic rats and high glucose exposed HT-22 cells via the NGF-Akt/Bad pathway. *Amino Acids* 52, 87–102. doi: 10.1007/s00726-019-02810-6

Yamane, H., Konno, K., Sabelis, M., Takabayashi, J., Sassa, T., and Oikawa, H. (2010). "Chemical defence and toxins of plants," in *Comprehensive Natural Products II*, eds H.-W. Liu and L. Mander (Amsterdam: Elsevier), 339–385. doi: 10.1016/b978-008045382-8.00099-x

Young, P. E. N., Estarellas, M., Coomans, E., Srikrishna, M., Beaumont, H., Maass, A., et al. (2020). Imaging biomarkers in neurodegeneration: current and future practices. *Alzheimers Res. Ther.* 12:49. doi: 10.1186/s13195-020-00612-7

Zetterberg, H., and Schott, J. M. (2022). Blood biomarkers for Alzheimer's disease and related disorders. *Acta Neurol. Scand*. online ahead of print, doi: 10.1111/ane.13628

Zhang, H., Cao, H. J., Kimelberg, H. K., and Zhou, M. (2011). Volume regulated anion channel currents of rat hippocampal neurons and their contribution to oxygen-and-glucose deprivation induced neuronal death. *PLoS One* 6:e16803. doi: 10.1371/journal.pone.0016803

Zhang, L., Yuan, Y., Tong, Q., Jiang, S., Xu, Q., Ding, J., et al. (2016). Reduced plasma taurine level in Parkinson's disease: association with motor severity and levodopa treatment. *Int. J. Neurosci*. 126, 630–636. doi: 10.3109/00207454.2015.1051046

Zhao, H., Qu, J., Li, Q., Cui, M., Wang, J., Zhang, K., et al. (2018). Taurine supplementation reduces neuroinflammation and protects against white matter injury after intracerebral hemorrhage in rats. *Amino Acids* 50, 439–451. doi: 10.1007/s00726-017-2529-8

Zhou, J.-J., Luo, Y., Chen, S.-R., Shao, J.-Y., Sah, R., and Pan, H.-L. (2020). LRRC8A-dependent volume-regulated anion channels contribute to ischemia-induced brain injury and glutamatergic input to hippocampal neurons. *Exp. Neurol*. 332:113391. doi: 10.1016/j.expneurol.2020.113391

Zhu, X.-H., Lu, M., and Chen, W. (2018). Quantitative imaging of brain energy metabolisms and neuroenergetics using *in vivo* X-nuclear 2 H, 17 O and 31 P MRS at ultra-high field. *J. Magn. Reson*. 292, 155–170. doi: 10.1016/j.jmr.2018.05.005

Zwingmann, C., Leibfritz, D., and Hazell, A. S. (2003). Energy metabolism in astrocytes and neurons treated with manganese: relation among cell-specific energy failure, glucose metabolism, and intercellular trafficking using multinuclear NMR-spectroscopic analysis. *J. Cereb. Blood Flow Metab*. 23, 756–771. doi: 10.1097/01.WCB.0000056062.25434.4D

Conflict of Interest: The authors declare that the research was conducted in the absence of any commercial or financial relationships that could be construed as a potential conflict of interest.

Publisher's Note: All claims expressed in this article are solely those of the authors and do not necessarily represent those of their affiliated organizations, or those of the publisher, the editors and the reviewers. Any product that may be evaluated in this article, or claim that may be made by its manufacturer, is not guaranteed or endorsed by the publisher.

frontiers | Frontiers in Molecular Neuroscience

TYPE Original Research
PUBLISHED 05 August 2022
DOI 10.3389/fnmol.2022.924534

OPEN ACCESS

EDITED BY
Sulagna Das,
Albert Einstein College of Medicine,
United States

REVIEWED BY
Wayne S. Sossin,
McGill University, Canada
Tilmann Achsel,
University of Lausanne, Switzerland

*CORRESPONDENCE
Magdalena Dziembowska
m.dziembowska@cent.uw.edu.pl

SPECIALTY SECTION
This article was submitted to Neuroplasticity and Development, a section of the journal Frontiers in Molecular Neuroscience

RECEIVED 20 April 2022
ACCEPTED 18 July 2022
PUBLISHED 05 August 2022

CITATION
Kuzniewska B, Rejmak K, Nowacka A, Ziółkowska M, Milek J, Magnowska M, Gruchota J, Gewartowska O, Borsuk E, Salamian A, Dziembowski A, Radwanska K and Dziembowska M (2022) Disrupting interaction between miR-132 and *Mmp9* 3′UTR improves synaptic plasticity and memory in mice.
Front. Mol. Neurosci. 15:924534.
doi: 10.3389/fnmol.2022.924534

Disrupting interaction between miR-132 and *Mmp9* 3′UTR improves synaptic plasticity and memory in mice

Bozena Kuzniewska[1], Karolina Rejmak[1], Agata Nowacka[2], Magdalena Ziółkowska[2], Jacek Milek[1], Marta Magnowska[1], Jakub Gruchota[3], Olga Gewartowska[3], Ewa Borsuk[4], Ahmad Salamian[2], Andrzej Dziembowski[3,4], Kasia Radwanska[2] and Magdalena Dziembowska[1]*

[1]Laboratory of Molecular Basis of Synaptic Plasticity, Centre of New Technologies, University of Warsaw, Warsaw, Poland, [2]Laboratory of Molecular Basis of Behavior, Nencki Institute of Experimental Biology of Polish Academy of Sciences, Warsaw, Poland, [3]Laboratory of RNA Biology, International Institute of Molecular and Cell Biology, Warsaw, Poland, [4]Faculty of Biology, University of Warsaw, Warsaw, Poland

As microRNAs have emerged to be important regulators of molecular events occurring at the synapses, the new questions about their regulatory effect on the behavior have araised. In the present study, we show for the first time that the dysregulated specific targeting of miR132 to *Mmp9* mRNA in the mouse brain results in the increased level of Mmp9 protein, which affects synaptic plasticity and has an effect on memory formation. Our data points at the importance of complex and precise regulation of the Mmp9 level by miR132 in the brain.

KEYWORDS

microRNA, miR132, *Mmp9*, synaptic plasticity, behavior, brain

Introduction

MicroRNAs (miRNAs) are important regulators of gene expression. These small, non-coding RNAs target mRNAs mainly through base pairing between the miRNA seed region and partially complementary sites in the 3′UTR (untranslated region) of the target mRNA. Such binding of miRNA to its target leads to translational repression and accelerated mRNA decay (Naeli et al., 2022).

Although cell culture models can provide mechanistic insight into the role of miRNAs in the regulation of the physiology of neurons, only animal models allow for understanding the impact of miRNA-mediated regulation at the organismal level. Animal models with knockdown or overexpression of genes encoding for selected miRNAs provided a valuable approach to study the role of miRNAs, primarily allowing identification of potential miRNA target genes *in vivo*. Such functional studies

demonstrated the profound role of miRNAs in the regulation of brain development, physiology and animal behavior and suggested the contribution of miRNAs to neuropsychiatric and neurological disorders (Brennan and Henshall, 2020; Narayanan and Schratt, 2020). Still, one should keep in mind that miRNAs can exist singly or as clusters of different miRNA sequences, and a single miRNA can simultaneously regulate hundreds of mRNA target transcripts. The median number of potential targets for a given neuronal miRNA in the hippocampus was estimated as 500, ranging from 30 to more than 1,000 (Sambandan et al., 2017). Thus, targeted knock-out of one selected miRNA or even the whole miRNA cluster will have obvious implications for the dysregulation of hundreds of mRNA targets. Because of that, it is difficult to dissect the physiological role of specific miRNA-target interactions in the regulation of biological processes *in vivo*.

MicroRNA 132 (miR-132) is an experience-induced microRNA that is rapidly upregulated in model conditions of the synaptic plasticity, e.g., in the mouse primary visual cortex after eye-opening (Mellios et al., 2011), during long-term potentiation (LTP) in the rat hippocampus or upon brain-derived neurotrophic factor stimulation of primary cortical mouse neurons (Remenyi et al., 2010). MiR132 regulates dendritic arborization and neurite outgrowth during the development of hippocampal neurons and modulates dendritic spine morphology and synaptic transmission (Magill et al., 2010; Vo et al., 2010; Siegel et al., 2011; Wanet et al., 2012; Remenyi et al., 2013).

Matrix metalloproteinase 9 (Mmp9) is an endopeptidase involved in extracellular matrix remodeling. In the brain, Mmp9 plays a pivotal role in the regulation of dendritic spine morphology, synaptic plasticity, and learning and memory (Rivera et al., 2010; Michaluk et al., 2011; Huntley, 2012). Mmp9 expression, as well as its local translation at synapses, is induced by neuronal stimulation (Szklarczyk et al., 2002; Dziembowska et al., 2012).

Our previous study provided evidence for a direct link between those two essential regulators of synaptic plasticity: miR132 and Mmp9. We have shown that miR132 regulate the structural plasticity of dendritic spines through interaction with the *Mmp9* mRNA 3′UTR in primary hippocampal neurons (Jasinska et al., 2016).

The most reliable approach for confirming particular miRNA-target interaction and investigating its importance is to disrupt the miRNA-binding site within the endogenous target gene. Several attempts have been made to mutate miRNA binding sites *in vivo*, primarily using *Caenorhabditis elegans* as a model organism (Ecsedi et al., 2015; McJunkin and Ambros, 2017). Additionally, three mouse models with disrupted seed-match sequences in 3′UTRs of Socs1, Aicda, and Cdkn1b genes were created to study the role of miR155 and miR142 in the immune system (Dorsett et al., 2008; Lu et al., 2015; Mildner et al., 2017). However, there have been no reports of studying specific miRNA-target interaction *in vivo* in the mouse brain so far.

In the current manuscript, we elucidated the physiological consequences of miR132-*Mmp9* mRNA interaction *in vivo*. To address this question, we created a new knock-in mouse model with a disrupted miR132 binding site in *Mmp9* mRNA 3′UTR (*Mmp9* UTRmut). This approach allowed us to examine the implications of the resulting de-repression of the target mRNA at the organismal level. We detected elevated levels of Mmp9 protein in the hippocampus of *Mmp9* UTRmut mice, but the miR132 and *Mmp9* mRNA expression was not changed in this brain structure in course of development of the mutant mice. The *Mmp9* UTRmut mice displayed altered morphology of dendritic spines, which were more dense and shorter. Moreover, the hippocampal CA3-CA1 LTP was enhanced in *Mmp9* UTRmut mice. All the described changes in *Mmp9* UTRmut mouse neurons physiology impacted animal behavior since the mice exhibited enhanced learning in the hippocampus-dependent contextual fear-conditioning paradigm. In aggregate, in the present study, we show that an increased level of Mmp9 in the hippocampus resulting from lack of posttranscriptional regulation by miR132 affects the morphology of dendritic spines, synaptic plasticity and has an effect on memory formation in mice.

Materials and methods

Generating mouse model harboring mutation in *Mmp9* 3′UTR

A new mouse line B6.CBA *Mmp9*^{em1Iimcb}/Tar (“*Mmp9* UTRmut”) was generated by the Mouse Genome Engineering Facility.[1] All mice were bred and maintained in the animal house of Faculty of Biology, University of Warsaw under a 12-h light/dark cycle with food and water available *ad libitum*. The animals were treated in accordance with the EU Directive 2010/63/EU for animal experiments.

Basing on Mouse genome (GRCm38/mm10 Assembly) single guide RNA (sgRNA) was designed using Online CRISPR tool[2] Chosen sequence did not show any major off-targets while calculated efficiency was high. For sgRNA synthesis two oligodeoxynucleotides (ODN) carrying T7 polymerase promoter, guide sequence (Mmp9_UTR_sgRNA_f) and sgRNA scaffold (Univ_IVsgRNA_rev) were used to form dsDNA template for *in vitro* transcription using in-house T7 Polymerase.

In a survey, 120 bp oligonucleotide Mmp9_UTRmut_O1 carrying point mutations to replace the wild-type miR132

1 www.crisprmice.eu

2 http://crispr.mit.edu

seed match site in *Mmp9* 3′UTR was designed to introduce a unique. *Hpa*I (*Ksp*AI) restriction site for rapid and cost-effective genotyping. Cas9 mRNA was *in vitro* transcribed from Addgene pX458 plasmid using T7 RNA Polymerase, poly(A) tail and m7Gppp5′N Cap were added.

Injection cocktail (20 ng/μl Mmp9_UTR sgRNA IVT, 40 ng/μl Cas9 mRNA IVT, 50 ng/μl Mmp9_UTRmut_O1) was introduced into mice zygotes *via* microinjections. After 24–48 h of incubation embryos were implanted into surrogate mice.

Genotyping

Pups were genotyped at age of 4 weeks. DNA from tail or ear tips was isolated with Genomic Mini kit (A&A Biotechnology, Gdansk, Poland). DNA was amplified with Mmp9_seq_1fw/1rev primer pair and amplicons were digested with HspaI (*Ksp*AI, Thermo Scientific, Waltham, MA, United States). In all assays Sanger sequencing-confirmed homozygous, heterozygous and wild-type DNA was used as controls.

Primers used in the study are shown in **Table 1**.

Nissl-staining

Mouse brains were fixed in 4% paraformaldehyde in PBS overnight at 4°C, then the brains were cryoprotected in 20% sucrose in PBS at 4°C for 48 h and frozen in −80°C. Next, the brains were cut coronally on cryostat (Cryostat Leica CM 1860) on 40-μm slices. Coronal sections were air dried on slides and stained with 0.1% cresyl violet solution (containing 3% acetic acid) for 5 min, washed, dehydrated, cleared in xylene, and coverslipped.

RNA isolation and qRT-PCR

Hippocampi were dissected and frozen in −80°C. RNA was extracted using TRIzol (Thermo Fisher Scientific), DNA contamination was removed by 2 U of TURBO DNase (AM2238, Ambion, Austin, TX, United States) in the supplied buffer in 37°C for 30 min. Next, RNA was re-isolated with phenol/chloroform, precipitated with ethanol, and resuspended in 50 μl of RNase free water. Concentration was measured with Spectrophotometer DeNovix, Wilmington, DE, United States DS-11 at 260 nm.

Reverse transcription and qPCR of miR132 was performed using TaqMan MicroRNA Reverse Transcription Kit (4366596, Applied Biosystems), according to the manufacturer's recommendations. RNA was diluted to 50 ng/μl and 250 ng was reverse transcribed using RT hsa-miR-132 primer (RT: 000457). Obtained products were diluted 2x and 2 μl of template was amplified using TaqMan MicroRNA Assays with has-miR-132 probe (TM: 000457) in a final reaction volume of 15 μl using Light Cycler 480 Probes Master Mix (Roche, Indianapolis, IN, United States) in a LightCycler480 (Roche).

To study the levels of *Mmp9* mRNA, RNA samples were reverse transcribed using random primers (GeneON, Ludwigshafen am Rhein, Germany; #S300; 200 ng/RT reaction) and SuperScript IV Reverse Transcriptase (Thermo Fisher Scientific). Next, the cDNA samples were amplified using custom sequence-specific primers and TaqMan MGB probes in a final reaction volume of 15 μl, using Light Cycler 480 Probes Master Mix (Roche) in a LightCycler480 (Roche).

Following TaqMan Gene Expression Assays (Thermo Fisher Scientific) were used: *Mmp9* (Mm00442991_m1), *Gapdh* (Mm99999915_g1), *Psd95* (Mm00492193_m1). Fold changes in expression were determined using the ΔΔ Ct (where Ct is the threshold cycle) relative quantification method. Values were normalized to the relative amounts of *Gapdh* mRNA.

Gelatin zymography

Gelatin zymography was performed as previously described (Szklarczyk et al., 2002). Briefly, hippocampi were homogenized in buffer containing 10 mM $CaCl_2$, 0.25% Triton X-100 and protease inhibitors (cOmplete EDTA-free Protease Inhibitor Cocktail, Roche). Homogenates were centrifuged at 6000 × *g* for 30 min at 4°C, the supernatant was removed and the pellet was resuspended in a buffer II (50 mM Tris, pH, 7.5; 0.1 m$CaCl_2$, protease inhibitors), heated for 15 min at 60°C and then centrifuged at 10,000 × *g* for 30 min at 4°C. Supernatant was collected and stored in −80°C. Protein concentrations were measured using BCA protein assay (Thermo Fisher Scientific) and 30 μg of proteins were precipitated with 4 volumes of cold acetone overnight at −80°C. Next, the samples were centrifuged at 10,000 × g for 10 min at 4°C, the pellets were air-dried for 5 min at room temperature and resuspended in 20 μl of 2 × sample buffer in the absence of reducing reagents (Novex, Invitrogen, Carlsbad, CA, United States) and incubated for 30 min at 38°C with gentle shaking. Next, the samples were separated on 8% SDS-polyacrylamide gels containing 2 mg/ml gelatin. The gels were washed twice with 2.5% Triton X-100 for 30 min at room temperature and incubated in developing buffer (50 mM Tris-Cl, pH 7.5, 10 mM $CaCl_2$, 1 μM $ZnCl_2$, 1% Triton X-100, 0.02% NaN_3) for 48 h at 37°C. Following staining with Coomassie brilliant blue, the gelatinolytic activities of Mmp9 and Mmp2 were detected as clear bands against a blue background and was quantified with ImageJ program. The intensity of Mmp9 bands was normalized to the Mmp2 bands.

DiI staining of brain slices

To visualize morphology of dendritic spines 1,1'-dioctadecyl-3,3,3,3'-tetramethylindocarbocyanine perchlorate (DiI) staining was performed. Wild-type and *Mmp9* UTRmut

TABLE 1 Sequences of primers used in the study.

Name	Sequence	Description
Mmp9_UTRmut guide RNA	5′ TGCCCACCGTCCTTTCTTGT 3′	Guide RNA for CRISPR-based generation of mutation in *Mmp9* 3′ UTR
Mmp9_UTR_sgRNA_f	5′GAAATTAATACGACTCACTATAGGGtgcccaccgt ccttttcttgtGTTTTAGAGCTAGAAATAGCAAGTTAAAATAAGGC 3′	Forward primer (inc. T7 Pol RNA promoter) for generation of sgRNA
Univ_IVsgRNA_rev	5′AAAAAGCACCGACTCGGTGCCACTTTTTCAAGTTGATA ACGGACTAgccttattttaacttgctatttctagctcta 3′	Reverse primer for construction of sgRNAs
Mmp9_UTRmut_O1	5′AGATAAGCTGATTGACTAAAGTAGCTGGAAAAGGTTGGG GATCCGTGTTTATTAGAAgtgagttAACAAGAAAGGACGGTGGGCA GAGAGAGCCCTGCCTGCCTCCACTCCTTCCCAGTC 3′	ODN donor for CRISPR-based generation of *Mmp9* UTRmut mice
Mmp9_seq_1fw	5′ GCGTGTGAGTTTCCAAAATG 3′	Forward sequencing primer for *Mmp9* UTRmut mice genotyping
Mmp9_seq_1rev	5′ TATTTATGCAGCGGTTGGAG 3′	Reverse sequencing primer for *Mmp9* UTRmut mice genotyping

mice at the age of 28 days (postnatal day 28, P28) were anesthetized with isoflurane and decapitated. The brains were quickly removed and both hemispheres were fixed with 4% paraformaldehyde in phosphate-buffered saline (PFA; 60 min at 4°C) and kept in cold PBS until further procedures were performed. Hemispheres were cut into 150 μm coronal slices with a vibratome (Leica VT 1000S). Random dendrite labeling was performed using 1.3 μm tungsten particles (Bio-Rad, Hercules, CA, United States) that were coated with propelled lipophilic fluorescent dye (DiI; Invitrogen, Carlsbad, CA, United States) that was delivered to the cells by gene gun (Bio-Rad) bombardment. Images of dendrites (50–200 μm) from the cell soma of the CA1 field of the hippocampus were acquired under 561 nm fluorescent illumination using a confocal microscope (Zeiss LSM 700) (63 × objective, 1.4 NA) at a pixel resolution of 1024 × 1024 with a 1.40 zoom, resulting in a 0.07 μ m pixel size.

Morphometric analysis of dendritic spines

The analysis of dendritic spine morphology was performed as described previously (Magnowska et al., 2016). The images that were acquired from the CA1 field of the hippocampus were processed using ImageJ software (National Institutes of Health, Bethesda, MD, United States) and analyzed semi-automatically using custom-written SpineMagick software[3] (Ruszczycki et al., 2012). The analyzed dendritic spines belonged to secondary and ternary dendrites to reduce possible differences in spine morphology that are caused by the location of spines on dendrites with different ranks. The recorded parameters were the spine length, head width and the spine area. We also used a scale-free parameter (length/width ratio), which reflects spine shape. Dendritic segments of 4 animals per genotype were morphologically analyzed resulting in 67–79 images with 8890–9900 spines counted per experimental group. To determine spine density, approximately 4900–5000 μm of dendritic length was analyzed per genotype. Groups of dendritic spines were compared using nested unpaired Student's *t*-test in case of spine morphology, in spine density analysis an unpaired Student's *t*-test was used. The analysis was performed in a blinded fashion.

Dendritic spine clustering

The virtual skeletons of dendritic spines were obtained in SpineMagick. Spine length was calculated as the length of the path from the spine top to the dendrite along the virtual skeleton of the spine. To analyze the shapes of spines, the virtual skeleton of each spine from an individual image was transformed to form a straight line. The images were then rescaled to normalize the spine area. For each spine diameter, we defined width as a function of distance from the dendrite, denoted d(h).

We classified 18,941 spines according to shape from WT and *Mmp9*UTRmut mice using a two-step procedure (Jasinska et al., 2016). First, all 18,941 d(h) functions were clustered into 36 clusters. Second, the clusters were manually sorted into three groups (i.e., mushroom, stubby, and long spines) based on visual inspection of clustered spines. The data analysis was performed using custom scripts that were written in Python. using NumPy and SciPy (Oliphant, 2007; Perez and Granger, 2007) and Matplotlib (Hunter, 2007).

Electrophysiology

Mice were deeply anesthesized with isoflurane, decapitated and the brains were rapidly dissected and transfered into ice-cold cutting artificial cerebrospinal fluid (ACSF) consisting of (in mM): 87 NaCl, 2.5 KCl, 1.25 NaH_2PO_4, 25 $NaHCO_3$,

3 https://rdcu.be/cj5fb

0.5 $CaCl_2$, 7 $MgSO_4$, 20 D-glucose, 75 sacharose equilibrated with carbogen (5% CO_2/95% O_2). The brain was cut to two hemispheres and 350 μm thick coronal brain slices were cut in ice-cold cutting ACSF with Leica VT100S vibratome. Slices were then incubated for 15 min in cutting ACSF at 32°C. Next the slices were transferred to recording ACSF containing (in mM): 125 NaCl, 2.5 KCl, 1.25 NaH_2PO_4, 25 $NaHCO_3$, 2.5 $CaCl_2$, 1.5 $MgSO_4$, 20 D-glucose equilibrated with carbogen and incubated for minimum 1 h at RT.

Extracellular field potential recordings were recorded in a submerged chamber perfused with recording ACSF in RT. The potentials were evoked with a custom built stimulus isolator with a concentric bipolar electrode (FHC, CBARC75) placed in the stRad of CA3. The stimulating pulses were delivered every 15 s and the pulse duration was 0.2 ms. The intensity of stimulation was adjusted to evoke 50% of maximal fEPSP. Recording electrodes (resistance 1–4 MΩ) were pulled from borosilicate glass (WPI, 1B120F-4) with a micropipette puller (Sutter Instruments, P-1000) and filled with recording ACSF. The recording electrode was placed in stRad of the dorsal CA1 area. Simultaneously, a second recording electrode was placed in the stPyr to measure population spikes. Recordings were acquired with MultiClamp 700B (Molecular Devices, CA, United States), Digidata 1550B (Molecular Devices, CA, United States) and Clampex 10.0 software (Molecular Devices, CA, United States). Input/output curves were obtained by increasing stimulation intensity by 25 μA in the range of 0–300 μA. The relative amplitude of fEPSP, population spikes and fiber volley were measured.

During LTP experiments a 20 min baseline was recorded. High frequency stimulation consisted of 1 train or 4 trains of 100 pulses at 100 Hz with 15 s intervals between consecutive trains. Then the recordings were carried out for another 60 min. For the sake of analysis 4 sweeps per minute were averaged. The results were normalized to average amplitude of fEPSP during baseline. The mean amplitude of fEPSP during 20 min baseline recording was compared with the mean amplitude of fEPSP during first 10 min after HFS (STP) and mean amplitude of fEPSP during the last 10 min of recording (LTP). Electrophysiology data was analyzed with AxoGraph 1.7.4 software (Axon Instruments, United States).

Fear conditioning

A contextual fear conditioning paradigm was used to train the mice. Mice were trained in a Med Associates Inc. Fear Conditioning Chamber (St Albans, United States) connected to a computer running Video Freeze software. Mice were placed in the chamber on a metal grid platform and after 2.5 min of habituation, received three electric shocks (US, 2 s, 0.7 mA) with 90 s intervals. The animals were taken out from the experimental chamber 30 s after the last shock and put in the homecage. The training lasted 6 min between animals cage was cleaned with 70% ethanol solution and was readied for the next animal. The fear memory of the context, defined as a level of freezing in the context, was assessed for 5 min in the same experimental chamber 24 h and 1 week after training. All animals were trained, tested and sacrificed during the light phase of animals' day (between 09.00 and 16.00 h). The training and testing times were counterbalanced between the groups.

Preparation of synaptoneurosomes

Synaptoneurosomes were prepared as described previously (Scheetz et al., 2000; Dziembowska et al., 2012; Kuzniewska et al., 2018). Before tissue dissection Krebs buffer (2.5 mM $CaCl_2$, 1.18 mM KH_2PO_4, 118.5 mM NaCl, 24.9 mM $NaHCO_3$, 1.18 mM $MgSO_4$, 3.8 mM $MgCl_2$, 212.7 mM glucose) was aerated with an aquarium pump for 30 min at 4°C. Next, the pH was lowered to 7.4 using dry ice. The buffer was supplemented with 1 × protease inhibitor cocktail cOmplete EDTA-free (Roche) and 60 U/ml RNase Inhibitor (RiboLock, Thermo Fisher Scientific). Animals were euthanized by cervical dislocation, hippocampi and a part of cortex adjacent to the hippocampus were dissected. Tissue from one hemisphere (∼50 mg) was homogenized in 1.5 ml Krebs buffer using Dounce homogenizer with 10–12 strokes. All steps were kept ice-cold to prevent stimulation of synaptoneurosomes. Homogenates were loaded into 20 ml syringe and passed through a series of pre-soaked (with Krebs buffer) nylon mesh filters consecutively 100, 60, 30, and 10 μm (Merck Millipore, Kenilworth, NJ, United States) in cold room to 50 ml polypropylene tube, centrifuged at 1000 g for 15 min at 4°C, washed and the pellet was used for RNA-IP or frozen in −80°C for further RNA isolation.

RNA coimmunoprecipitation (RNA-IP)

Immunoprecipitation was performed as previously described (Janusz et al., 2013), according to the modified protocol of Brown et al. (2001). Synaptoneurosomes from WT, *Mmp9* UTRmut and *Fmr1* KO mice (∼1600 μg of total protein) were resuspended in 1,200 μl of precipitation buffer (10 mm HEPES, pH 7.4, 400 mm NaCl, 30 mm EDTA, and 0.5% Triton X-100) supplemented with protease inhibitor cocktail (Sigma-Aldrich, St. Louis, MO, United States) and 100 U/ml RiboLock (Fermentas, Thermo Scientific, Waltham, MA, United States), then precleared with 120 μl of Dynabeads A for 2.5 h. Afterward, ∼50 μl of each supernatant was saved as input fraction for WB and RNA isolation. Precipitation was performed overnight in 4°C with 120 μl of antibody-bound Dynabeads Protein A, blocked beforehand with either anti-FMRP antibody (7G1–1-c) or normal mouse IgGs. Next, 1/6

of the beads was boiled with sample buffer for WB. From the remaining beads, total RNA was isolated with TRIzol (Invitrogen). For the quantitative real-time (qRT)-PCR, RNA was suspended in 11 μl of RNase free H2O Then the RNA was reverse-transcribed and the cDNA samples were amplified using custom sequence-specific primers and TaqMan MGB probes as described above. Fold changes were determined using the ΔΔ Ct (where Ct is the threshold cycle) relative quantification method. Values were normalized to the relative amounts of analyzed mRNA in IgG sample and compared to the abundance of mRNA in *Fmr1* KO samples.

Quantification and statistical analysis

Unless otherwise noted, statistical analysis was performed using GraphPad Prism 7.0 (GraphPad Software, Inc.). Statistical details of experiments, including the statistical tests used and the value of n, are noted in figure legends.

Results

Knock-in mice with a mutation in miR132 binding site in *Mmp9* UTR does not display developmental abnormalities

To dissect the effect of miR132 interaction with a single target site in *Mmp9* mRNA, we generated a mouse with a mutation in the 3′UTR of *Mmp9* gene using genome editing technology. A new knock-in mouse with a disrupted miR132 binding site in *Mmp9* mRNA 3′UTR was named "*Mmp9* UTRmut" (**Figures 1A–D**). The homozygous *Mmp9* UTRmut mice did not present any visibly harmful phenotype, were viable, fertile, gave similar litter sizes, and their survival was similar to WT mice. To verify whether the introduced mutation affects brain development, we looked at the general brain histology using the Nissl staining on coronal brain sections of wild-type (WT) and *Mmp9* UTRmut mice at postnatal day 32 (P32) (**Figure 1E**). Compared to their WT littermates, no alterations of overall brain morphology or individual brain structures, particularly hippocampus and cortex, were observed in *Mmp9* UTRmut animals.

Mutated miR132 binding site in the *Mmp9* UTR did not affect mRNA levels and interactions with FMRP during hippocampus development

Since the expression of both miR132 and *Mmp9* genes is induced by neuronal activity (Nudelman et al., 2010), we decided to elucidate their levels in the developing hippocampus of *Mmp9* UTRmut and wild-type mice. In the hippocampus, synaptic connections start to be established around birth with the extensive growth of axons and dendrites during the first two postnatal weeks and intensive synaptogenesis leading to adult patterns and integrative functions by the end of the first postnatal month (young adolescent mice) (Ben-Ari, 2001). Therefore, we evaluated the miR132 and *Mmp9* mRNA expression levels in the developing hippocampus of *Mmp9* UTRmut and WT mice at several postnatal stages: P8, P15, P22, P26, and P49, using qRT-PCR. We discovered that the expression of miR132 was induced in the second week of postnatal development and gradually increased till adulthood in both genotypes (**Figure 2A**). *Mmp9* mRNA expression analyzed in the same samples was highest at postnatal day eight (P8) and decreased already at P15 until adulthood in both *Mmp9* UTRmut and wild-type mice (**Figure 2B**).

Altogether, we found that the level of miR132 expression increases in the hippocampus development by 6 times when comparing P8 and P49. Contrary to miR132, the *Mmp9* mRNA level was decreased in the development of hippocampus. No significant differences were observed between the two studied genotypes suggesting that miR132 does not induce *Mmp9* mRNA degradation.

Our previous work (Jasinska et al., 2016) revealed that miR132 interacts with *Mmp9* mRNA. Also, we and others have shown that both *Mmp9* mRNA and miR132 associate with Fragile X mental retardation protein–FMRP (Edbauer et al., 2010; Janusz et al., 2013), an RNA binding protein primarily characterized for its role in regulating synaptic protein synthesis (Bassell and Warren, 2008; Darnell and Klann, 2013). FMRP can bind to G-rich sequences in RNA, and such motif in *Mmp9* 3′UTR is located in the proximity to the miR132 seed match site (**Supplementary Figure 1A**). We tested the hypothesis that the reversible repression of *Mmp9* mRNA translation by miR132 is regulated by FMRP protein. In order to determine whether disruption of miR132 seed match sequence in *Mmp9* 3′UTR affects the association of *Mmp9* mRNA with FMRP, we performed RNA coimmunoprecipitation on synaptoneurosomes isolated from the cerebral cortex and hippocampi of WT, Mmp9 UTRmut and Fmr1 KO mice (**Supplementary Figure 1B**). As shown in **Supplementary Figure 1C**, FMRP was immunoprecipitated by the 7G1-1 anti-FMRP antibody from WT and *Mmp9* UTRmut synaptoneurosomes, while it was not detected in the *Fmr1* KO immunoprecipitates (IP). Next, we performed qRT-PCR on immunoprecipitated fractions to assess levels of *Mmp9* mRNA and control mRNAs bound to FMRP. As previously reported, *Mmp9* mRNA (Janusz et al., 2013) as well as *Psd95* mRNA, a known target of FMRP (Muddashetty et al., 2007; Zalfa et al., 2007), were significantly enriched in the IPs from the WT mice compared with the *Fmr1* KO (**Supplementary Figures 1D,E**). However, we did not observe any significant differences in the levels of *Mmp9* mRNA in *Mmp9* UTRmut immunoprecipitates

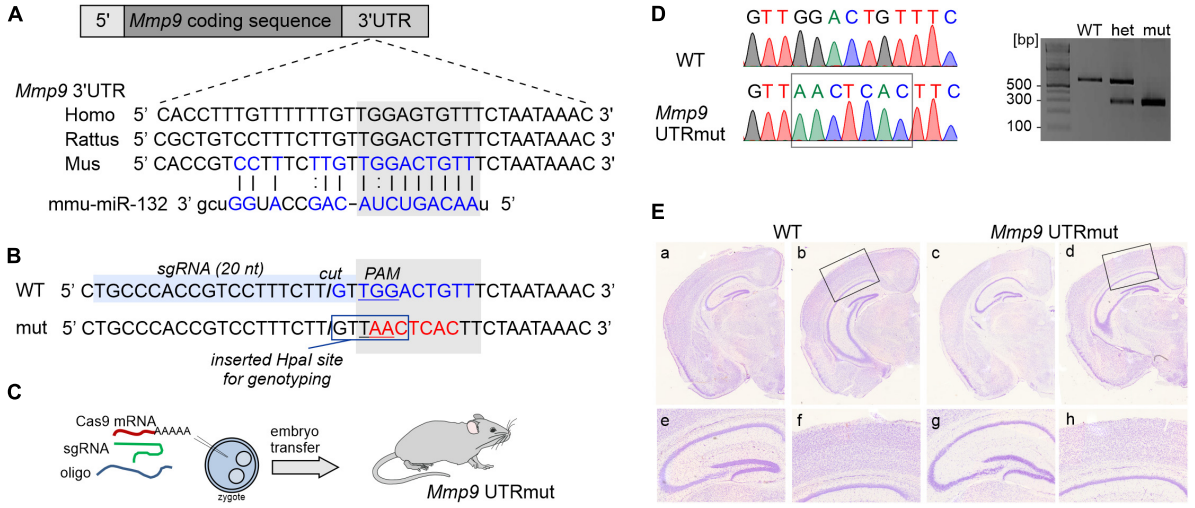

FIGURE 1

Generating mouse model harboring mutation in miR132 binding site in 3'UTR of *Mmp9* gene. **(A)** Schematic illustration of *Mmp9* allele, which contains coding sequence (dark gray) and untranslated regions (UTR, shown in light gray). The sequence of 3'UTR fragment that contains miR132 binding site is depicted in blue and aligned with human and rat sequences. Sequence of miR132 is aligned with its binding site. **(B)** Sequence of *Mmp9* 3'UTR fragment. The position of miR132-binding site (seed match) is marked with a gray box (WT seed match in blue and mutated in red). Position of the single-guide RNA (sgRNA) target is indicated with light-blue box. PAM, protospacer adjacent motif and the "cut" position is marked. To facilitate the detection of mutations, restriction site for *Hpa*I was introduced. **(C)** Schematic illustration of the strategy to introduce a knock-in mutations into the *Mmp9* locus using CRISPR/Cas9 strategy. **(D)** Alignment of chromatograms covering miR132 seed match site in *Mmp9*: wild-type (WT, top) and mutant (*Mmp9* UTRmut, bottom). Right panel, genotyping results of wild-type, heterozygous, and mutant mice based on *Hpa*I (*Ksp*AI) digestion of PCR amplicons covering miR132 seed match site in *Mmp9*. **(E)** Nissl-stained coronal sections of brains from wild-type (a, b, e, f) and mutant (c, d, g, h) mice. No neuroanatomical differences were observed in the WT and *Mmp9* UTRmut brains (a–d). Also, no abnormalities were found within the hippocampus (e, g) or in the cortex (f, h) of *Mmp9* UTRmut mice.

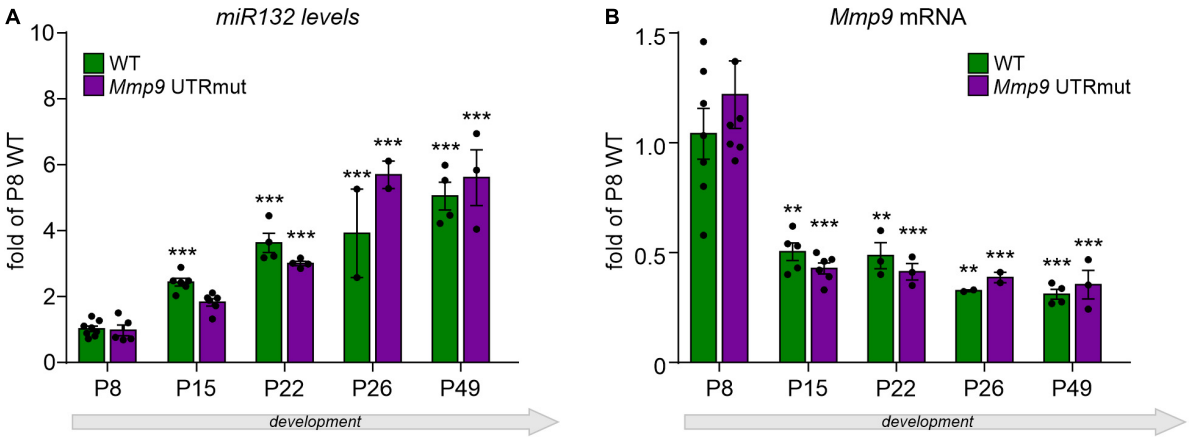

FIGURE 2

Relative expression of mature miR132 **(A)** and *Mmp9* mRNA **(B)** in the course of hippocampal development in *Mmp9* UTRmut and WT mice assessed by qRT-PCR. Generally, no significant differences in miR132 **(A)** and *Mmp9* mRNA **(B)** levels were observed among the two genotypes at any developmental stage. A two-way ANOVA revealed that there was statistically significant interaction between the effects of genotype and developmental stage on miR132 levels [**(A)** $F_{(4,34)} = 3.61$; $p = 0.015$], but not on Mmp9 mRNA levels [**(B)** $F_{(4,32)} = 0.59$; $p = 0.68$] in the hippocampus. Simple main effects analysis showed that genotype did not have a statistically significant effect neither on miR132 levels [$F_{(1,34)} = 1.05$; $p = 0.31$], nor on Mmp9 mRNA levels [$F_{(1,32)} = 0.12$; $p = 0.74$]. However, developmental stage did have a statistically significant effect on both miR132 [$F_{(4,34)} = 69.53$; $p < 0.0001$] and on Mmp9 mRNA [$F_{(4,32)} = 23.35$; $p < 0.0001$] levels. **(A)** Expression of miR132 was increased gradually and significantly during the development of the hippocampus at P15, P22, and P26 till adulthood (P49) in both genotypes (as compared to P8; ***$p < 0.001$; *post hoc* Sidak's multiple comparisons test). **(B)** *Mmp9* mRNA levels were reduced by half already at P15 hippocampus and stayed on the same low level till adulthood (as compared to P8; **$p < 0.01$, ***$p < 0.001$; *post hoc* Sidak's multiple comparisons test). Data is presented as mean ± SEM, normalized to P8 WT levels, dots correspond to single animals. *Mmp9* mRNA level was normalized to *Gapdh* mRNA.

as compared to WT (Supplementary Figure 1D). Taken together, our data suggest that the mutation in the miR132 target site of *Mmp9* 3′UTR does not alter FMRP-*Mmp9* mRNA interaction. The levels of *Gapdh* mRNA, used as a control, did not differ between any IP fractions (Supplementary Figure 1F). Also, total mRNA levels of *Mmp9* and *Psd95* mRNAs were not significantly different between WT, *Mmp9* UTRmut and *Fmr1* KO synaptoneurosomes (Supplementary Figures 1G,H).

Upregulation of Mmp9 protein in young adolescent *Mmp9* UTRmut mice correlates with altered structural plasticity of dendritic spines

MicroRNA fine-tuning of their target mRNAs may occur at the level of translational regulation. Since we did not observe any apparent alterations in *Mmp9* mRNA levels in *Mmp9* UTRmut mice, as a next step, we analyzed the level of Mmp9 protein in the hippocampus at various developmental stages. The level of Mmp9 protein in the brain is relatively low; therefore, it is poorly detectable with antibodies in western blotting. We used gel zymography, a proven and sensitive assay to quantify Mmp9 protein levels in the brain (Kleiner and Stetler-Stevenson, 1994; Snoek-van Beurden and Von den Hoff, 2005), which enables the visualization of Mmp2 and Mmp9 enzymatic activity in the polyacrylamide gel (Figure 3A).

We observed increased Mmp9 protein level in the hippocampus of young adolescent *Mmp9* UTRmut mice (postnatal day 28, P28; Figure 3B; $p = 0.0444$). In the juvenile mice (P7 and P14), no significant difference between genotypes was detected (Figure 3B).

MMP9 is secreted on dendritic spines in response to synaptic stimulation and has a well-documented effect on their structural plasticity (Wilczynski et al., 2008; Michaluk et al., 2011). We detected increased levels of MMP9 protein in the hippocampus of *Mmp9* UTRmut mice at P28, a developmental period of intense synapse formation and maturation. Therefore, we investigated the morphology and density of dendritic spines in the CA1 field of the hippocampus in the young adolescent (P28) *Mmp9* UTRmut and WT mice. Analysis was performed based on the DiI staining of coronal brain slices from four mice per genotype. Exemplary microphotographs of DiI stained dendrites are shown in Figure 3C. Using this approach, we demonstrated a significant increase in dendritic spine density in *Mmp9* UTRmut mice compared to WT (Figure 3D, $p = 0.0022$). Moreover, *Mmp9* UTRmut mice displayed changes in spine morphology. Dendritic spines in mutant mice had altered shape (Figure 3E, smaller spine length/head width ratio; $p < 0.0001$), were shorter (Figure 3F, smaller spine length; $p < 0.0001$), and had smaller spine area (Figure 3G; $p = 0.0057$). The spine head width remained unchanged (Figure 3H; $p = 0.096$). To further understand changes in dendritic spine shape, spines were clustered into three categories: long, stubby and mushroom. *Mmp9* UTRmut mice exhibited a significant decrease in the population of long spines as compared to WT mice (Figures 3I,J). Altogether in the hippocampus of *Mmp9* UTRmut mice, we observed shorter, however more dense dendritic spines, without a change in average spine head width, when compared to their wild-type littermates.

Mmp9 UTRmut mice show enhanced hippocampal long-term potentiation

The morphological changes in dendritic spine density and shape influence the electrophysiological properties of neurons. Having observed altered morphology and density of dendritic spines in the hippocampus of *Mmp9* UTRmut mice, we sought to determine its effect on electrophysiological activity of hippocampal circuits. Mmp9 is required for late-phase LTP stabilization in the hippocampus (Nagy et al., 2006). Interestingly, both Mmp9 knock-out mice, as well as rats with Mmp9 overexpression show decreased LTP in CA3-CA1 hippocampal projections (Nagy et al., 2006; Wiera et al., 2015; Magnowska et al., 2016), whereas transgenic mice overexpressing Mmp9 display prolonged LTP maintenance (Fragkouli et al., 2012). All this data indicate that balanced, fine-tuned Mmp9 levels are required for proper synaptic plasticity.

To examine the effect of mutation introduced in the non-coding region of *Mmp9* mRNA on the synaptic function, we measured basal synaptic transmission and synaptic plasticity at CA1 stratum radiatum synapses while stimulating Shaffer collaterals from CA3 hippocampal area, in acute brain slices from *Mmp9* UTRmut and wild-type mice (Figure 4A). Basal synaptic transmission in CA1 neurons, determined as the amplitude of fEPSP over a stimulation range 25–300 μA, was similar in slices from *Mmp9* UTRmut and WT mice (Figure 4B). Next, we induced LTP by high-frequency stimulation (HFS, 4 trains of 100 pulses at 100 Hz). This type of synaptic plasticity is long-lasting and was shown to be protein synthesis dependent (Frey et al., 1988; Impey et al., 1996). We recorded fEPSP for the next 60 min. The mean amplitude of fEPSP during the first 10 min after HFS, which corresponds to the short-term plasticity induced by stimulation (STP) was similar in both analyzed genotypes (Figures 4C,D). However, the mean amplitude of fEPSP during the last 10 min of recording, which corresponds to long-term plasticity (LTP) was significantly induced in both wild type and *Mmp9* UTRmut mice. Notably, the LTP was strongly enhanced in *Mmp9* UTRmut hippocampal slices, as compared to WT slices (Figures 4C–E). We also examined the LTP evoked by a weaker stimulus (1 × 100 Hz) in *Mmp9* UTRmut and WT mice hippocampi (Supplementary Figure 2). This weak protocol produces a synaptic potentiation that is shorter and not protein synthesis dependent (Frey et al., 1993). There was

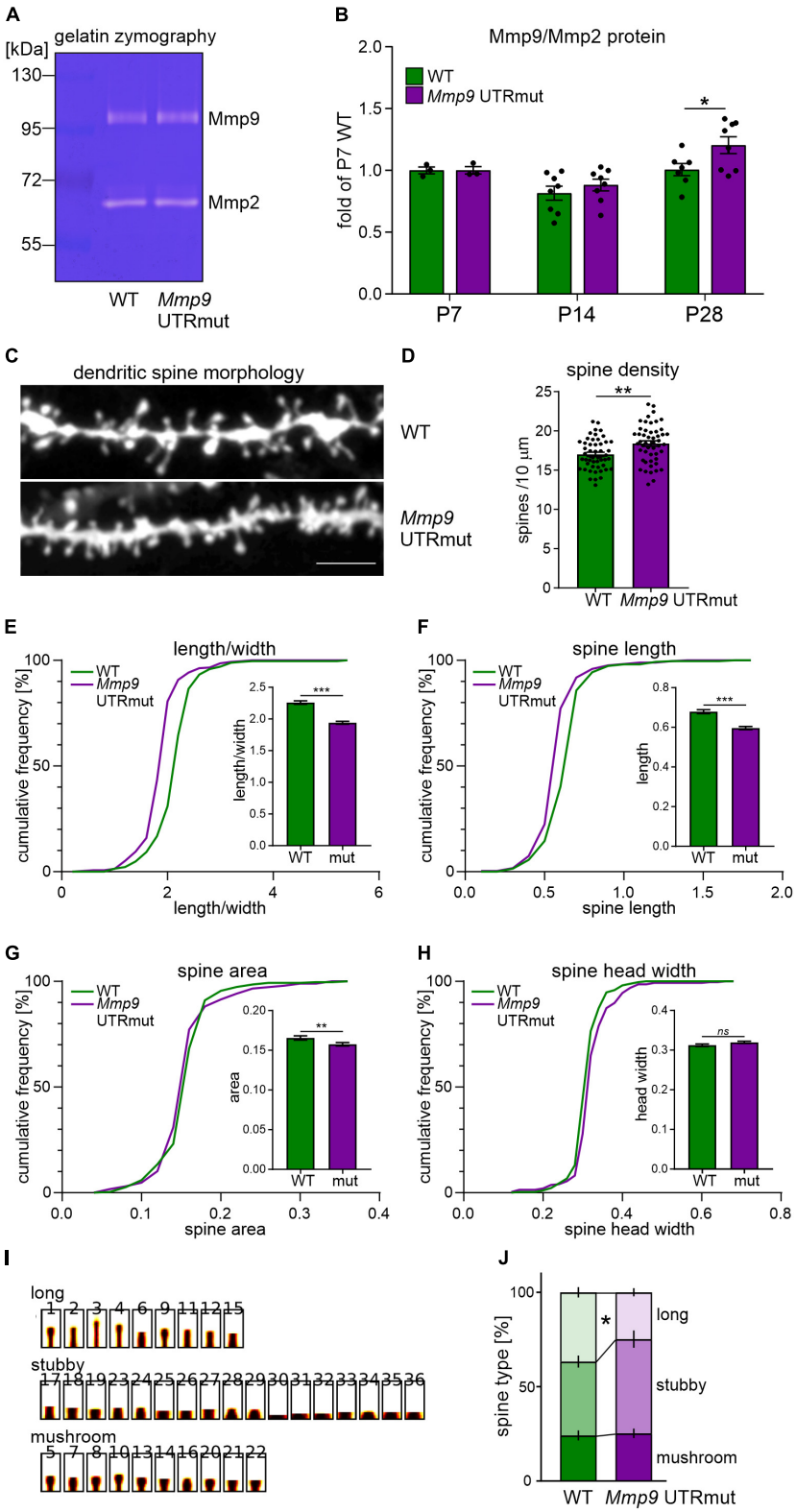

FIGURE 3
Mmp9 UTRmut mice display increased Mmp9 protein levels in the hippocampus and have shorter and more dense dendritic spines in the CA1 area. **(A)** Representative zymography gel revealing enzymatic activity of gelatinases from mouse hippocampus. Mmp9 and Mmp2 were identified as bright bands at ~95 kDa and ~65 kDa, respectively. **(B)** Two-way ANOVA did not reveal significant interaction between "genotype" and "development" factors [$F_{(2,31)}$ = 1.23; p = 0.3063], however, "development" factor had significant effect [$F_{(2,31)}$ = 11.62; p = 0.0002].
(Continued)

FIGURE 3
A significant increase of Mmp9 protein level was observed in the hippocampus of *Mmp9* UTRmut mice at P28 (*post hoc* Sidak's multiple comparisons test; $^{*}p = 0.0444$; *post hoc* Bonferroni's multiple comparisons test; $^{*}p = 0.0450$). Data is presented as mean ± SEM. Mmp9 levels were normalized to Mmp2 levels and presented as relative to WT P7. Dots correspond to single animals. **(C)** Examples of DiI-stained dendrites in the CA1 area of the hippocampus of wild-type (WT) and Mmp9 UTRmut mice. **(D)** Increased dendritic spine density in *Mmp9* UTRmut mice as compared to WT (unpaired Student's *t*-test; $^{**}p = 0.0022$). Data is presented as mean ± SEM. Dots correspond to mean density from single image, $n = 50$ images/genotype; dendritic segments of four animals per genotype were analyzed. **(E–H)** Morphology of dendritic spines is altered in *Mmp9* UTRmut mice. Data is presented as cumulative frequency of analyzed parameters and as mean ± SEM. Significant differences in the spine shape parameter: decreased length/width [**(E)** $^{***}p < 0.0001$], spine length [**(F)** $^{***}p < 0.0001$] and spine area [**(G)** $^{**}p = 0.0057$] were found in *Mmp9* UTRmut mice as compared to wild-types. Spine head width was unchanged in *Mmp9* UTRmut mice [**(H)** *ns* $p = 0.096$]. Nested unpaired Student's *t*-test was performed (dendritic segments of four animals per genotype were analyzed resulting in 67–79 images with 8890–9900 spines per experimental group). The analysis was performed in a blinded fashion. **(I,J)** Spines were clustered into three categories: long, stubby, and mushroom. *Mmp9* UTRmut mice exhibited a significant decrease in the population of long spines as compared with WT mice ($^{*}p = 0.0399$; two-way ANOVA, *post hoc* Sidak's multiple comparisons test).

no significant difference between LTP recorded from WT and *Mmp9* UTRmut animals.

Dysregulated specific targeting of miR132 to *Mmp9* mRNA enhances fear memory in mice

We demonstrated that blocking miR132-*Mmp9* mRNA interaction *in vivo* is sufficient to modulate Mmp9 protein levels in the developing brain and influence synaptic and structural plasticity in the hippocampus. With this in mind, we aimed at establishing the consequences of such dysregulation on mice behavior. Given the importance of both miR132 and Mmp9 in learning and memory formation, we verified whether these processes are impaired in *Mmp9* UTRmut mice. We tested the mice in the hippocampus-dependent contextual fear-conditioning task, in which animals learn to associate novel context (experimental chamber) with an aversive stimulus (electrical foot shock). The mice were trained with three-foot shocks and subsequently tested for contextual long-term fear memory at 24 h and 7 days after training (**Figure 5A**). The memory was scored as a freezing response to the context. Using this approach we found that *Mmp9* UTRmut mice showed improved contextual fear memory as demonstrated by enhanced freezing when exposed to the experimental chamber at 24 h and 7 days after the training (**Figure 5B**).

Discussion

In the present study, we show for the first time that the dysregulated specific targeting of miR132 to *Mmp9* mRNA in the mouse brain *in vivo* results in the increased level of Mmp9 protein, which affects the function and structure of glutamatergic synapses and has an effect on mice memory formation. Our data points at the importance of complex and precise regulation of Mmp9 level by miR132 in the brain.

There is growing evidence to suggest that miRNAs are involved in social and anxiety-related behaviors and are dysregulated in the pathophysiology of human neuropsychiatric and neurodevelopmental disorders [Konopka et al., 2010 and reviewed by Smith and Kenny (2018) and Narayanan and Schratt (2020)]. However, so far the data implicating the role of miRNAs in animal behavior was obtained in miRNA overexpressing or miRNA knock-out mouse models. As miRNAs regulate many target mRNAs simultaneously, miRNA up- or downregulation results in modulation of entire cellular pathways. Therefore, although such functional studies are valuable to investigate the potential role of selected miRNA in the context of the whole organism, they do not allow for the examination of specific miRNA-target interaction. Furthermore, the role of miRNAs in human neurological disorders was based on miRNA profiling studies or genetic association studies, and the results are mainly correlative. Here we show for the first time a functional study of selected, specific miRNA-target interaction in the context of brain physiology and animal behavior. So far, attempts to create mouse models with disrupted seed-match sequences in 3′UTRs of selected genes were sparse (Dorsett et al., 2008; Lu et al., 2015; Mildner et al., 2017), and were never used to evaluate the effect of miRNA-target interaction on animal behavior. In the present study we created a unique mouse model to study the effect of single microRNA-mRNA interaction. We show that an increased level of Mmp9 in the hippocampus resulting from lack of posttranscriptional regulation by miR132 affects the morphology of dendritic spines, synaptic plasticity and has an effect on memory formation in mice. The observed changes of steady-state Mmp9 protein levels were not very pronounced in the hippocampus in Mmp9 UTRmut mice, pointing to its fine-tuning mode of regulation.

As miRNAs interaction with their target mRNAs seed region can lead to degradation of their target mRNA or translational inhibition, we aimed to elucidate whether the ablation of miR132 seed match in *Mmp9* 3′UTR *in vivo* will affect *Mmp9* levels. MiR132 expression progressively increases during mouse postnatal brain development in the hippocampus, olfactory bulb, and striatum (Nudelman et al., 2010). In addition, robust miR132 upregulation was induced in the primary visual cortex

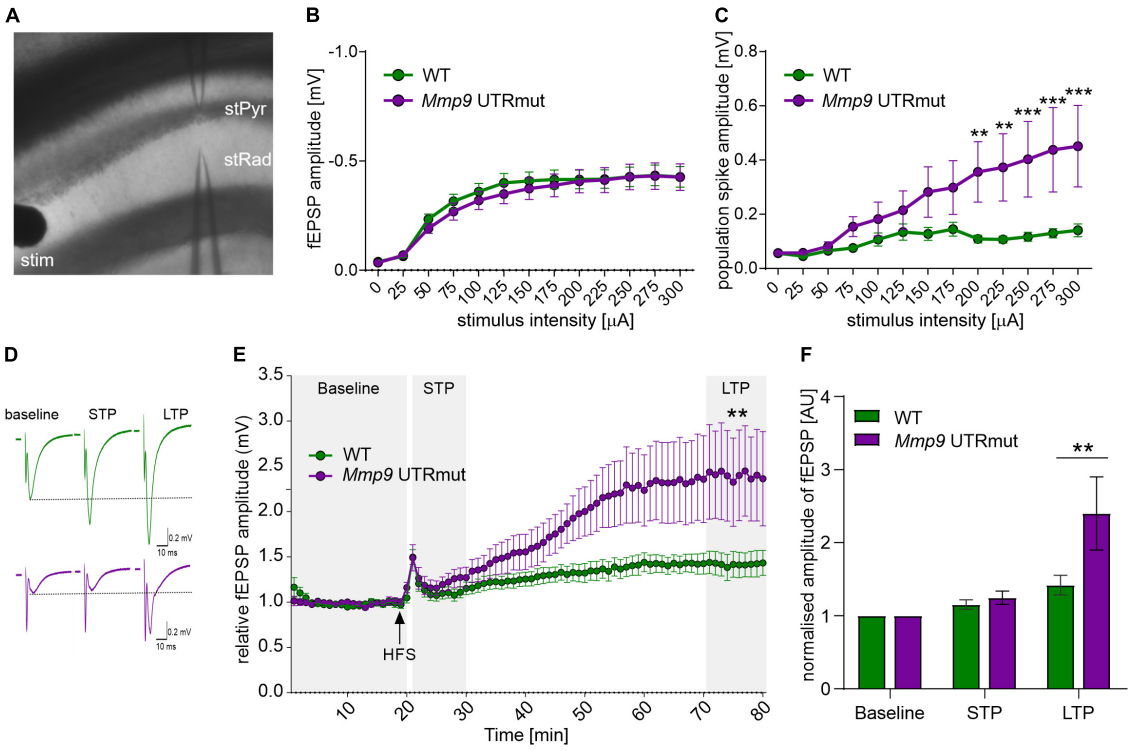

FIGURE 4
Mmp9 UTRmut mice show enhanced hippocampal long-term potentiation. **(A)** Electrophysiological recordings setup depicting positions of stimulating (stim) and recording (rec1, rec2) electrodes in CA1 and CA3 fields of the hippocampus (stPyr–*stratum pyramidale*, stRad–*stratum radiatum*). **(B)** Input/output curve of fEPSP amplitude. Data is represented as mean ± SEM (n: WT 18 slices/5 mice, *Mmp9* UTRmut 18 slices/5 mice; two-way ANOVA with Bonferroni *post hoc* test). **(C)** Amplitude of population spikes measured in the CA1 *stratum pyramidale* during increasing intensity stimulation of Schaffer collaterals (n: WT-13 slices/5 mice, *Mmp9* UTRmut 9 slices/5 mice; two-way ANOVA with Bonferroni *post hoc* test; $^{**}p < 0.01$, $^{***}p < 0.001$). **(D–F)** LTP induction at CA3–CA1 hippocampal synapses. High frequency stimulation (HFS) consisted of 4 trains of 100 pulses at 100 Hz with 15 s intervals between consecutive trains. Data is represented as mean of fEPSP amplitudes normalized to mean of baseline fEPSP amplitude ± SEM (n: WT 9 slices/5 mice, *Mmp9* UTRmut 9 slices/5 mice; repeated-measures two-way ANOVA with Bonferroni *post hoc* test; $^{**}p < 0.01$). **(F)** Bar graph of the means ± SEM of normalized fEPSP amplitude calculated from the data in panel **(E)**. Averaged amplitudes of fEPSP during 20 min baseline, 10 min after HFS (STP), and last 10 min of the recording (LTP) were plotted (n: WT 9 slices/5 mice, *Mmp9* UTRmut 9 slices/5 mice; repeated-measures two-way ANOVA with Bonferroni *post hoc* test; $^{**}p < 0.01$).

by the eye-opening during the critical period of its plasticity (Mellios et al., 2011). In accordance with those data, we also observed a significant increase in miR132 expression during the postnatal development of hippocampus in wild type and *Mmp9* UTRmut mice (**Figure 2A**).

Mmp9 plays an essential role in the developmental plasticity of hippocampus (Lepeta and Kaczmarek, 2015), and tight regulation of Mmp9 activity is critical for its function (Reinhard et al., 2015; Beroun et al., 2019). Mmp9 expression is also neuronal activity-dependent and is tightly regulated during brain development. In the hippocampus *Mmp9* expression levels are highest during the first postnatal week and decrease in adulthood (Aujla and Huntley, 2014). A similar pattern of *Mmp9* expression was observed in course of hippocampal development of wild-type and *Mmp9* UTRmut mice (**Figure 2B**).

The function of miRNA is highly context-dependent and may vary from the robust mRNA degradation during brain development to the subtle local effects on mRNA translation during dendritic spines remodeling (Schratt et al., 2006). Here we show that disrupting miR132 target sequence in the 3′UTR of *Mmp9* mRNA does not influence *Mmp9* mRNA levels in the hippocampus, indicating that miR132 recruitment to *Mmp9* does not promote mRNA degradation (**Figure 2**). Nevertheless, we demonstrate upregulation of Mmp9 protein levels in the brain of *Mmp9* UTRmut mice at different stages of development (**Figure 3**). Statistically significant results were observed in the hippocampus at P28. Taken together, our data points toward a translational regulation of *Mmp9* mRNA by miR132, which results with elevated Mmp9 protein level in the hippocampus of adolescent mice. In physiological conditions, Mmp9 is expressed at low levels in the brain and is induced by neuronal activity, particularly strongly in pathological conditions such as epilepsy, stroke, TBA (Konopacki et al., 2007; Wilczynski et al., 2008; Pijet et al., 2018, 2019). Mmp9 expression and activity is tightly regulated

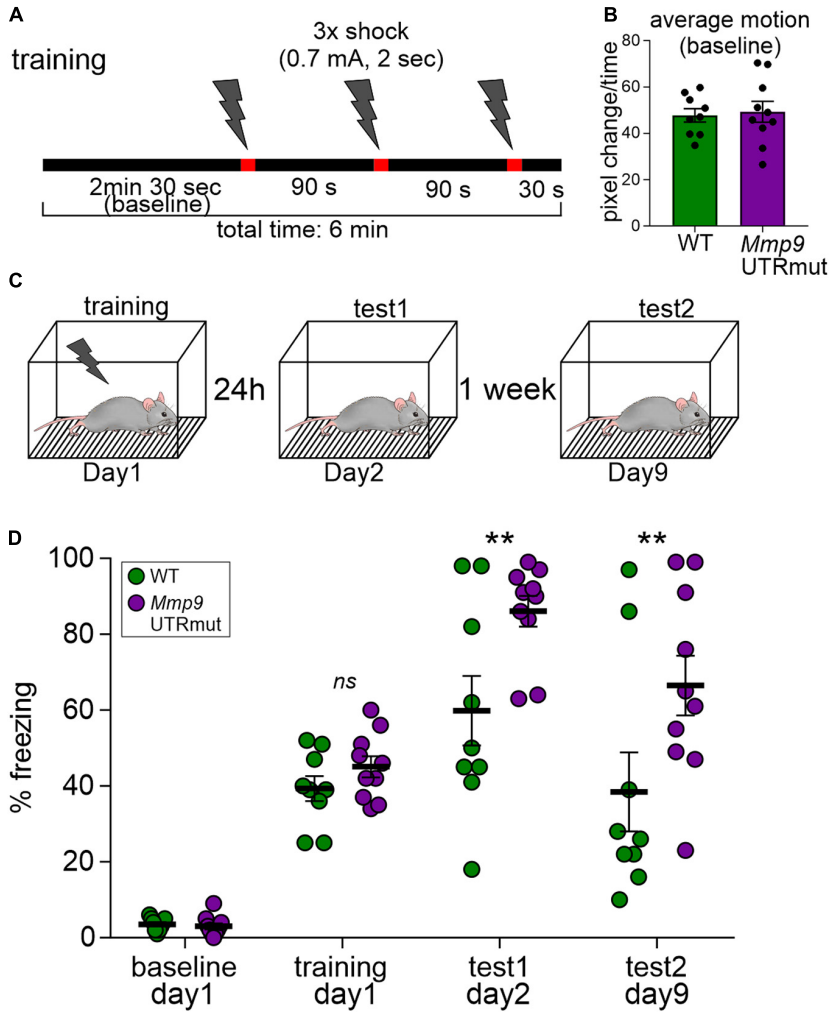

FIGURE 5
Learning is enhanced in contextual fear conditioning in the Mmp9 UTRmut mice. **(A)** Training protocol for fear conditioning indicating the number and timing of footshocks (lightning bolts). **(B)** Mouse activity within the conditioning chamber before the experiments was registered and quantified as an index of motion. **(C)** Scheme showing the experimental design. **(D)** Mice were conditioned according to the protocol and their freezing was recorded before the training–"baseline," during the "training" and 24 h later–"test1." Seven days after the training, the mice were exposed to the experimental chamber again and their freezing was recorded ("test2"). *Mmp9* UTRmut mice showed enhanced freezing in the test1 as compared to WT (**p = 0.0099). After 1 week *Mmp9* UTRmut mice still displayed enhanced freezing levels (** p = 0.0051). Data is presented as mean ± SEM. Dots correspond to single animals. Repeated-measures two-way ANOVA, *post hoc* Sidak's multiple comparisons test.

at the level of transcription, mRNA dendritic translocation, and local translation as well as protein activation of the enzyme [reviewed by Dziembowska and Wlodarczyk (2012)]. Both miR132 and Mmp9 are transported to the synapses where they can act to regulate synaptic function. Our results show that *Mmp9* UTRmut mice display relatively small, however significant upregulation of Mmp9 levels in the hippocampus (**Figure 3B**). In physiological conditions Mmp9 is expressed at a very low level in the brain and is induced by neuronal activity. Similarly, miR132 is an experience-dependent microRNA, that is rapidly upregulated in conditions of the synaptic plasticity. Therefore, presumably the mode of miR132-*Mmp9* interaction is also activity dependent, transient and local, restricted to the synaptic compartment. However, the activity-dependent regulation of *Mmp9* mRNA translation in *Mmp9* UTRmut mice needs to be addressed in the future. In this study the newly established mouse model *Mmp9* UTRmut mice allowed us to show that dysregulated specific targeting of miR132 to *Mmp9* mRNA has a functional relevance for the synaptic plasticity in the brain and can influence memory formation.

Dendritic spines are dynamic structures which exhibit morphological plasticity during brain development, learning and memory. Mmp9 is an extracellularly acting enzyme

responsible for their structural plasticity (Michaluk et al., 2011; Szepesi et al., 2014). Similarly miR-132 can affect dendritic spine shape (Edbauer et al., 2010; Luikart et al., 2011; Mellios et al., 2011). Previously we have shown that miR-132-dependent regulation of *Mmp9* mRNA in neurons resulted in structural changes of dendritic spines. In the present study we observed more dense but shorter and smaller dendritic spines in the hippocampus of *Mmp9* UTRmut mice (**Figure 3**).

The morphological changes in dendritic spine density and shape was also shown to influence the electrophysiological properties of neurons (Tonnesen and Nagerl, 2016). In the CA1 field of *Mmp9* UTRmut mice hippocampus dendritic spines were smaller, but their head size did not differ from wild-type littermates, what can suggests that the average synapse strength is affected. However, more dense dendritic spines in *Mmp9* UTRmut mice point toward an increased number of synapses, implying enhanced complexity of neuronal circuits in the *Mmp9* UTRmut mice hippocampus. This hypothesis is supported by further data obtained in the current study, indicating that disrupting miR132-Mmp9 interaction *in vivo* has an apparent effect on long-term potentiation, explicitly enhancing its late phase (LTP) without significant changes of the basal synaptic strength (**Figure 4**). For the late phase of LTP the induction of gene expression and local protein synthesis is required and pharmacological inhibitors of translation block long-lasting forms of LTP without affecting early stages of LTP expression (Frey et al., 1988). In *Mmp9* UTRmut hippocampi only the long lasting LTP induced by 4 × 100 Hz stimulation was increased and not the early 1 × 100 HZ induced one, indicating translational regulation of MMP-9. Our data is consistent with previous reports showing that Mmp9 is required and upregulated during the late phase of LTP (Nagy et al., 2006; Huntley, 2012; Gorkiewicz et al., 2015). Pharmacological inhibition of Mmp9 blocks the induction of LTP and *Mmp9* knock-out mice display impaired, smaller LTP (Nagy et al., 2006). On the contrary, it was also shown that excessive Mmp9 activity in transgenic rats impairs both the induction and maintenance of LTP (Magnowska et al., 2016), pointing toward tight regulation of Mmp9 levels that are required for the proper synaptic transmission and plasticity.

Furthermore, we demonstrate that dysregulation of miR132 targeting to *Mmp9* mRNA has evident consequences for long-term memory. We show enhanced cognitive performance of *Mmp9* UTRmut mice in the fear-conditioning learning and memory task, without significant changes of mice activity before the training (**Figure 5**). Our data is in line with the previous reports describing impairments in a fear-conditioning memory task in Mmp9 knock-out mice (Nagy et al., 2006) and enhanced cognitive performance of Mmp9 overexpressing mice (Fragkouli et al., 2012). Both miR132 and Mmp9 were reported to be upregulated after fear conditioning (Ganguly et al., 2013; Wang et al., 2013). Consistently, knocking down miR132 in the hippocampus impaired the acquisition of fear memory in mice (Wang et al., 2013; Hansen et al., 2016). Altogether, we provide complementary evidence to the previous studies showing the involvement of both miR132 and Mmp9 in long-term hippocampus-dependent fear-conditioning memory tasks. We demonstrate that, above all, their interaction is pivotal in this learning paradigm.

In summary, we conclude that translational dysregulation of *Mmp9* mRNA expression by the lack of miR132 binding in the 3′UTR results in enhanced synaptic plasticity and influences memory formation.

Data availability statement

The raw data supporting the conclusions of this article will be made available by the authors, without undue reservation.

Ethics statement

The animal study was reviewed and approved by 1st Local Ethical Committee for Animal Experiments in Warsaw, Poland Pasteur St. 3 02-093 Warsaw, Poland.

Author contributions

EB, OG, and JG developed the mouse model. BK, KRe, and JM collected tissue samples for the experiments. BK and KRe performed Nissl staining and gelatin zymography. BK extracted RNA, performed qRT-PCR analysis and IP experiments, analyzed dendritic spines, and prepared figures. MM prepared the DiI-stained brain slices and imaging. AN and AS performed the electrophysiological recordings. MZ performed the fear conditioning behavior. MD, AD, KRa, and BK designed experiments, analyzed the results, and wrote the manuscript. MD secured funding and supervised the project. All authors contributed to the article and approved the submitted version.

Funding

This work was mainly supported by NCN grant OPUS 2014/15/B/NZ3/01054 for MD and TEAM TECH CORE FACILITY/2017-4/5 to AD.

Conflict of interest

The authors declare that the research was conducted in the absence of any commercial or financial relationships that could be construed as a potential conflict of interest.

Publisher's note

Supplementary material

The Supplementary Material for this article can be found online at: https://www.frontiersin.org/articles/10.3389/fnmol.2022.924534/full#supplementary-material

SUPPLEMENTARY FIGURE 1
Mutation of miR132 binding site in 3′UTR of *Mmp9* gene does not affect FMRP-binding to *Mmp9* mRNA. **(A)** The sequence of mouse, rat, and human *Mmp9* 3′UTR fragment that contains miR132 binding site (seed) is marked with a gray box. MiR132 seed is depicted in blue and aligned with miR132 sequence. Position of G-quartet motif that forms quadraduplex structures and may be bound by FMRP is marked with a yellow box. **(B)** Scheme showing FMRP-*Mmp9* mRNA-miR132 complex. **(C–F)** RNA-immunoprecipitation using antibody on mouse synaptoneurosomal samples. **(C)** Western blot analysis of the immunoprecipitated FMRP from mouse synaptoneurosomes shows FMRP protein precipitated by the anti-FMRP 7G1-1 antibody in WT and *Mmp9* UTRmut mice. *Fmr1* KO mice and IgG IPs were used as negative controls. **(D–F)** qRT-PCR analysis of *Mmp9* mRNA, *Psd95* mRNA (positive control), and *Gapdh* mRNA (negative control) levels in immunoprecipitated samples from WT, *Mmp9* UTRmut, and *Fmr1* KO mice. **(D)** *Mmp9* mRNA associates with FMRP in synaptoneurosomes of WT (**p = 0.0057) and *Mmp9* UTRmut (**p = 0.0084) mice to the same extent, regardless of miR132 seed mutation. **(E)** As expected, *Psd95* mRNA also associates with FMRP in WT (**p = 0.0058) and *Mmp9* UTRmut (**p = 0.0046) synaptoneurosomes. **(F)** *Gapdh* mRNA does not associate with FMRP. Data is presented as mean ± SEM, n = 3 mice/genotype, One-way ANOVA, *post hoc* Dunnett's multiple comparisons test. **(G,H)** *Mmp9* mRNA and *Psd95* mRNA levels in synaptoneurosomes isolated from WT and *Mmp9* UTRmut mice. *Gapdh* mRNA was used as endogenous control.

SUPPLEMENTARY FIGURE 2
Mmp9 UTRmut mice show no significant differences in hippocampal early-LTP. **(A)** LTP induction at CA3–CA1 hippocampal synapses. High frequency stimulation (HFS) consisted of 1 train of 100 pulses at 100 Hz. Data is represented as mean of fEPSP amplitudes normalized to mean of baseline fEPSP amplitude ± SEM (WT, n = 6 slices; *Mmp9* UTRmut, n = 5 slices; repeated-measures two-way ANOVA with Bonferroni *post hoc* test; $p > 0.8$). **(B)** Bar graph of the means ± SEM of normalized fEPSP amplitude calculated from panel **(A)**. Averaged amplitudes of fEPSP during 20 min baseline, 10 min after HFS (STP), and last 10 min of the recording (LTP) were plotted (repeated-measures two-way ANOVA with Bonferroni *post hoc* test p = 0.0883).

References

Aujla, P. K., and Huntley, G. W. (2014). Early postnatal expression and localization of matrix metalloproteinases-2 and -9 during establishment of rat hippocampal synaptic circuitry. *J. Comp. Neurol.* 522, 1249–1263. doi: 10.1002/cne.23468

Bassell, G. J., and Warren, S. T. (2008). Fragile X syndrome: Loss of local mRNA regulation alters synaptic development and function. *Neuron* 60, 201–214. doi: 10.1016/j.neuron.2008.10.004

Ben-Ari, Y. (2001). Developing networks play a similar melody. *Trends Neurosci.* 24, 353–360. doi: 10.1016/S0166-2236(00)01813-0

Beroun, A., Mitra, S., Michaluk, P., Pijet, B., Stefaniuk, M., and Kaczmarek, L. (2019). MMPs in learning and memory and neuropsychiatric disorders. *Cell Mol. Life Sci.* 76, 3207–3228. doi: 10.1007/s00018-019-03180-8

Brennan, G. P., and Henshall, D. C. (2020). MicroRNAs as regulators of brain function and targets for treatment of epilepsy. *Nat. Rev. Neurol.* 16, 506–519. doi: 10.1038/s41582-020-0369-8

Brown, V., Jin, P., Ceman, S., Darnell, J. C., O'Donnell, W. T., Tenenbaum, S. A., et al. (2001). Microarray identification of FMRP-associated brain mRNAs and altered mRNA translational profiles in fragile X syndrome. *Cell* 107, 477–487. doi: 10.1016/S0092-8674(01)00568-2

Darnell, J. C., and Klann, E. (2013). The translation of translational control by FMRP: therapeutic targets for FXS. *Nat. Neurosci.* 16, 1530–1536. doi: 10.1038/nn.3379

Dorsett, Y., McBride, K. M., Jankovic, M., Gazumyan, A., Thai, T. H., Robbiani, D. F., et al. (2008). MicroRNA-155 suppresses activation-induced cytidine deaminase-mediated Myc-Igh translocation. *Immunity* 28, 630–638. doi: 10.1016/j.immuni.2008.04.002

Dziembowska, M., Milek, J., Janusz, A., Rejmak, E., Romanowska, E., Gorkiewicz, T., et al. (2012). Activity-dependent local translation of matrix metalloproteinase-9. *J. Neurosci.* 32, 14538–14547. doi: 10.1523/JNEUROSCI.6028-11.2012

Dziembowska, M., and Wlodarczyk, J. (2012). MMP9: A novel function in synaptic plasticity. *Int. J. Biochem. Cell Biol.* 44, 709–713. doi: 10.1016/j.biocel.2012.01.023

Ecsedi, M., Rausch, M., and Grosshans, H. (2015). The let-7 microRNA directs vulval development through a single target. *Dev. Cell* 32, 335–344. doi: 10.1016/j.devcel.2014.12.018

Edbauer, D., Neilson, J. R., Foster, K. A., Wang, C. F., Seeburg, D. P., Batterton, M. N., et al. (2010). Regulation of synaptic structure and function by FMRP-associated microRNAs miR-125b and miR-132. *Neuron* 65, 373–384. doi: 10.1016/j.neuron.2010.01.005

Fragkouli, A., Papatheodoropoulos, C., Georgopoulos, S., Stamatakis, A., Stylianopoulou, F., Tsilibary, E. C., et al. (2012). Enhanced neuronal plasticity and elevated endogenous sAPPalpha levels in mice over-expressing MMP9. *J. Neurochem.* 121, 239–251. doi: 10.1111/j.1471-4159.2011.07637.x

Frey, U., Huang, Y. Y., and Kandel, E. R. (1993). Effects of cAMP simulate a late stage of LTP in hippocampal CA1 neurons. *Science* 260, 1661–1664. doi: 10.1126/science.8389057

Frey, U., Krug, M., Reymann, K. G., and Matthies, H. (1988). Anisomycin, an inhibitor of protein synthesis, blocks late phases of LTP phenomena in the hippocampal CA1 region in vitro. *Brain Res.* 452, 57–65. doi: 10.1016/0006-8993(88)90008-X

Ganguly, K., Rejmak, E., Mikosz, M., Nikolaev, E., Knapska, E., and Kaczmarek, L. (2013). Matrix metalloproteinase (MMP) 9 transcription in mouse brain induced by fear learning. *J. Biol. Chem.* 288, 20978–20991. doi: 10.1074/jbc.M113.457903

Gorkiewicz, T., Balcerzyk, M., Kaczmarek, L., and Knapska, E. (2015). Matrix metalloproteinase 9 (MMP-9) is indispensable for long term potentiation in the central and basal but not in the lateral nucleus of the amygdala. *Front. Cell Neurosci.* 9:73. doi: 10.3389/fncel.2015.00073

Hansen, K. F., Sakamoto, K., Aten, S., Snider, K. H., Loeser, J., Hesse, A. M., et al. (2016). Targeted deletion of miR-132/-212 impairs memory and alters the hippocampal transcriptome. *Learn Mem.* 23, 61–71. doi: 10.1101/lm.039578.115

Hunter, J. D. (2007). Matplotlib: A 2D graphics environment. *Comput. Sci. Eng.* 9, 90–95. doi: 10.1109/MCSE.2007.55

Huntley, G. W. (2012). Synaptic circuit remodelling by matrix metalloproteinases in health and disease. *Nat. Rev. Neurosci.* 13, 743–757. doi: 10.1038/nrn3320

Impey, S., Mark, M., Villacres, E. C., Poser, S., Chavkin, C., and Storm, D. R. (1996). Induction of CRE-mediated gene expression by stimuli that generate long-lasting LTP in area CA1 of the hippocampus. *Neuron* 16, 973–982. doi: 10.1016/S0896-6273(00)80120-8

Janusz, A., Milek, J., Perycz, M., Pacini, L., Bagni, C., Kaczmarek, L., et al. (2013). The Fragile X mental retardation protein regulates matrix metalloproteinase 9 mRNA at synapses. *J. Neurosci.* 33, 18234–18241. doi: 10.1523/JNEUROSCI.2207-13.2013

Jasinska, M., Milek, J., Cymerman, I. A., Leski, S., Kaczmarek, L., and Dziembowska, M. (2016). miR-132 regulates dendritic spine structure by direct targeting of matrix metalloproteinase 9 mRNA. *Mol. Neurobiol.* 53, 4701–4712. doi: 10.1007/s12035-015-9383-z

Kleiner, D. E., and Stetler-Stevenson, W. G. (1994). Quantitative zymography: detection of picogram quantities of gelatinases. *Anal. Biochem.* 218, 325–329. doi: 10.1006/abio.1994.1186

Konopacki, F. A., Rylski, M., Wilczek, E., Amborska, R., Detka, D., Kaczmarek, L., et al. (2007). Synaptic localization of seizure-induced matrix metalloproteinase-9 mRNA. *Neuroscience* 150, 31–39. doi: 10.1016/j.neuroscience.2007.08.026

Konopka, W., Kiryk, A., Novak, M., Herwerth, M., Parkitna, J. R., Wawrzyniak, M., et al. (2010). MicroRNA loss enhances learning and memory in mice. *J. Neurosci.* 30, 14835–14842. doi: 10.1523/JNEUROSCI.3030-10.2010

Kuzniewska, B., Chojnacka, M., Milek, J., and Dziembowska, M. (2018). Preparation of polysomal fractions from mouse brain synaptoneurosomes and analysis of polysomal-bound mRNAs. *J. Neurosci. Methods* 293, 226–233. doi: 10.1016/j.jneumeth.2017.10.006

Lepeta, K., and Kaczmarek, L. (2015). Matrix Metalloproteinase-9 as a Novel Player in Synaptic Plasticity and Schizophrenia. *Schizophr. Bull.* 41, 1003–1009. doi: 10.1093/schbul/sbv036

Lu, L. F., Gasteiger, G., Yu, I. S., Chaudhry, A., Hsin, J. P., Lu, Y., et al. (2015). A Single miRNA-mRNA interaction affects the immune response in a context- and cell-type-specific manner. *Immunity* 43, 52–64. doi: 10.1016/j.immuni.2015.04.022

Luikart, B. W., Bensen, A. L., Washburn, E. K., Perederiy, J. V., Su, K. G., Li, Y., et al. (2011). miR-132 mediates the integration of newborn neurons into the adult dentate gyrus. *PLoS One* 6:e19077. doi: 10.1371/journal.pone.0019077

Magill, S. T., Cambronne, X. A., Luikart, B. W., Lioy, D. T., Leighton, B. H., Westbrook, G. L., et al. (2010). microRNA-132 regulates dendritic growth and arborization of newborn neurons in the adult hippocampus. *Proc. Natl. Acad. Sci. U.S.A.* 107, 20382–20387. doi: 10.1073/pnas.1015691107

Magnowska, M., Gorkiewicz, T., Suska, A., Wawrzyniak, M., Rutkowska-Wlodarczyk, I., Kaczmarek, L., et al. (2016). Transient ECM protease activity promotes synaptic plasticity. *Sci. Rep.* 6:27757. doi: 10.1038/srep27757

McJunkin, K., and Ambros, V. (2017). A microRNA family exerts maternal control on sex determination in C. elegans. *Genes Dev.* 31, 422–437. doi: 10.1101/gad.290155.116

Mellios, N., Sugihara, H., Castro, J., Banerjee, A., Le, C., Kumar, A., et al. (2011). miR-132, an experience-dependent microRNA, is essential for visual cortex plasticity. *Nat. Neurosci.* 14, 1240–1242. doi: 10.1038/nn.2909

Michaluk, P., Wawrzyniak, M., Alot, P., Szczot, M., Wyrembek, P., Mercik, K., et al. (2011). Influence of matrix metalloproteinase MMP-9 on dendritic spine morphology. *J. Cell Sci.* 124, 3369–3380. doi: 10.1242/jcs.090852

Mildner, A., Chapnik, E., Varol, D., Aychek, T., Lampl, N., Rivkin, N., et al. (2017). MicroRNA-142 controls thymocyte proliferation. *Eur. J. Immunol.* 47, 1142–1152. doi: 10.1002/eji.201746987

Muddashetty, R. S., Kelic, S., Gross, C., Xu, M., and Bassell, G. J. (2007). Dysregulated metabotropic glutamate receptor-dependent translation of AMPA receptor and postsynaptic density-95 mRNAs at synapses in a mouse model of fragile X syndrome. *J. Neurosci.* 27, 5338–5348. doi: 10.1523/JNEUROSCI.0937-07.2007

Naeli, P., Winter, T., Hackett, A. P., Alboushi, L., and Jafarnejad, S. M. (2022). The intricate balance between microRNA-induced mRNA decay and translational repression. *FEBS J* [Epub ahead of print]. doi: 10.1111/febs.16422

Nagy, V., Bozdagi, O., Matynia, A., Balcerzyk, M., Okulski, P., Dzwonek, J., et al. (2006). Matrix metalloproteinase-9 is required for hippocampal late-phase long-term potentiation and memory. *J. Neurosci.* 26, 1923–1934. doi: 10.1523/JNEUROSCI.4359-05.2006

Narayanan, R., and Schratt, G. (2020). miRNA regulation of social and anxiety-related behaviour. *Cell Mol. Life Sci.* 77, 4347–4364. doi: 10.1007/s00018-020-03542-7

Nudelman, A. S., DiRocco, D. P., Lambert, T. J., Garelick, M. G., Le, J., Nathanson, N. M., et al. (2010). Neuronal activity rapidly induces transcription of the CREB-regulated microRNA-132, in vivo. *Hippocampus* 20, 492–498. doi: 10.1002/hipo.20646

Oliphant, T. E. (2007). Python for scientific computing. *Comput. Sci. Eng.* 9, 10–20. doi: 10.1109/MCSE.2007.58

Perez, F., and Granger, B. E. (2007). IPython: a system for interactive scientific computing. *Comput. Sci. Eng.* 9, 21–29. doi: 10.1109/MCSE.2007.53

Pijet, B., Stefaniuk, M., and Kaczmarek, L. (2019). MMP-9 contributes to dendritic spine remodeling following traumatic brain injury. *Neural Plast.* 2019:3259295. doi: 10.1155/2019/3259295

Pijet, B., Stefaniuk, M., Kostrzewska-Ksiezyk, A., Tsilibary, P. E., Tzinia, A., and Kaczmarek, L. (2018). Elevation of MMP-9 levels promotes epileptogenesis after traumatic brain injury. *Mol. Neurobiol.* 55, 9294–9306. doi: 10.1007/s12035-018-1061-5

Reinhard, S. M., Razak, K., and Ethell, I. M. (2015). A delicate balance: role of MMP-9 in brain development and pathophysiology of neurodevelopmental disorders. *Front. Cell Neurosci.* 9:280. doi: 10.3389/fncel.2015.00280

Remenyi, J., Hunter, C. J., Cole, C., Ando, H., Impey, S., Monk, C. E., et al. (2010). Regulation of the miR-212/132 locus by MSK1 and CREB in response to neurotrophins. *Biochem. J.* 428, 281–291. doi: 10.1042/BJ20100024

Remenyi, J., van den Bosch, M. W., Palygin, O., Mistry, R. B., McKenzie, C., Macdonald, A., et al. (2013). miR-132/212 knockout mice reveal roles for these miRNAs in regulating cortical synaptic transmission and plasticity. *PLoS One* 8:e62509. doi: 10.1371/journal.pone.0062509

Rivera, S., Khrestchatisky, M., Kaczmarek, L., Rosenberg, G. A., and Jaworski, D. M. (2010). Metzincin proteases and their inhibitors: foes or friends in nervous system physiology?. *J. Neurosci.* 30, 15337–15357. doi: 10.1523/JNEUROSCI.3467-10.2010

Ruszczycki, B., Szepesi, Z., Wilczynski, G. M., Bijata, M., Kalita, K., Kaczmarek, L., et al. (2012). Sampling issues in quantitative analysis of dendritic spines morphology. *BMC Bioinformatics* 13:213. doi: 10.1186/1471-2105-13-213

Sambandan, S., Akbalik, G., Kochen, L., Rinne, J., Kahlstatt, J., Glock, C., et al. (2017). Activity-dependent spatially localized miRNA maturation in neuronal dendrites. *Science* 355, 634–637. doi: 10.1126/science.aaf8995

Scheetz, A. J., Nairn, A. C., and Constantine-Paton, M. (2000). NMDA receptor-mediated control of protein synthesis at developing synapses. *Nat. Neurosci.* 3, 211–216. doi: 10.1038/72915

Schratt, G. M., Tuebing, F., Nigh, E. A., Kane, C. G., Sabatini, M. E., Kiebler, M., et al. (2006). A brain-specific microRNA regulates dendritic spine development. *Nature* 439, 283–289. doi: 10.1038/nature04367

Siegel, G., Saba, R., and Schratt, G. (2011). microRNAs in neurons: manifold regulatory roles at the synapse. *Curr. Opin. Genet. Dev.* 21, 491–497. doi: 10.1016/j.gde.2011.04.008

Smith, A. C. W., and Kenny, P. J. (2018). MicroRNAs regulate synaptic plasticity underlying drug addiction. *Genes Brain Behav.* 17:e12424. doi: 10.1111/gbb.12424

Snoek-van Beurden, P. A., and Von den Hoff, J. W. (2005). Zymographic techniques for the analysis of matrix metalloproteinases and their inhibitors. *Biotechniques* 38, 73–83. doi: 10.2144/05381RV01

Szepesi, Z., Hosy, E., Ruszczycki, B., Bijata, M., Pyskaty, M., Bikbaev, A., et al. (2014). Synaptically released matrix metalloproteinase activity in control of structural plasticity and the cell surface distribution of GluA1-AMPA receptors. *PLoS One* 9:e98274. doi: 10.1371/journal.pone.0098274

Szklarczyk, A., Lapinska, J., Rylski, M., McKay, R. D., and Kaczmarek, L. (2002). Matrix metalloproteinase-9 undergoes expression and activation during dendritic remodeling in adult hippocampus. *J. Neurosci.* 22, 920–930. doi: 10.1523/JNEUROSCI.22-03-00920.2002

Tonnesen, J., and Nagerl, U. V. (2016). Dendritic Spines as Tunable Regulators of Synaptic Signals. *Front. Psychiatry* 7:101. doi: 10.3389/fpsyt.2016.00101

Vo, N. K., Cambronne, X. A., and Goodman, R. H. (2010). MicroRNA pathways in neural development and plasticity. *Curr. Opin. Neurobiol.* 20, 457–465. doi: 10.1016/j.conb.2010.04.002

Wanet, A., Tacheny, A., Arnould, T., and Renard, P. (2012). miR-212/132 expression and functions: within and beyond the neuronal compartment. *Nucleic Acids Res.* 40, 4742–4753. doi: 10.1093/nar/gks151

Wang, R. Y., Phang, R. Z., Hsu, P. H., Wang, W. H., Huang, H. T., and Liu, I. Y. (2013). In vivo knockdown of hippocampal miR-132 expression impairs memory acquisition of trace fear conditioning. *Hippocampus* 23, 625–633. doi: 10.1002/hipo.22123

Wiera, G., Szczot, M., Wojtowicz, T., Lebida, K., Koza, P., and Mozrzymas, J. W. (2015). Impact of matrix metalloproteinase-9 overexpression on synaptic excitatory transmission and its plasticity in rat CA3-CA1 hippocampal pathway. *J. Physiol. Pharmacol.* 66, 309–315.

Wilczynski, G. M., Konopacki, F. A., Wilczek, E., Lasiecka, Z., Gorlewicz, A., Michaluk, P., et al. (2008). Important role of matrix metalloproteinase 9 in epileptogenesis. *J. Cell Biol.* 180, 1021–1035. doi: 10.1083/jcb.200708213

Zalfa, F., Eleuteri, B., Dickson, K. S., Mercaldo, V., De Rubeis, S., di Penta, A., et al. (2007). A new function for the fragile X mental retardation protein in regulation of PSD-95 mRNA stability. *Nat. Neurosci.* 10, 578–587. doi: 10.1038/nn1893

frontiers | Frontiers in Molecular Neuroscience

TYPE Review
PUBLISHED 11 October 2022
DOI 10.3389/fnmol.2022.1006419

OPEN ACCESS

EDITED BY
Rochelle Marie Hines,
University of Nevada, Las Vegas,
United States

REVIEWED BY
Yue Zou,
University of Toledo, United States
Chi-Wai Cheng,
The University of Hong Kong,
Hong Kong SAR, China

*CORRESPONDENCE
Hekun Liu
fjlhk@163.com

SPECIALTY SECTION
This article was submitted to Molecular Signalling and Pathways, a section of the journal Frontiers in Molecular Neuroscience

RECEIVED 29 July 2022
ACCEPTED 20 September 2022
PUBLISHED 11 October 2022

CITATION
Chen Y, Hou X, Pang J, Yang F, Li A, Lin S, Lin N, Lee TH and Liu H (2022) The role of peptidyl-prolyl isomerase Pin1 in neuronal signaling in epilepsy. *Front. Mol. Neurosci.* 15:1006419. doi: 10.3389/fnmol.2022.1006419

The role of peptidyl-prolyl isomerase Pin1 in neuronal signaling in epilepsy

Yuwen Chen[1], Xiaojun Hou[1,2], Jiao Pang[1], Fan Yang[1,3], Angcheng Li[1], Suijin Lin[1], Na Lin[1], Tae Ho Lee[1] and Hekun Liu[1]*

[1]Institute of Basic Medicine, The School of Basic Medical Sciences, Fujian Medical University, Fuzhou, China, [2]Fuzhou Children's Hospital of Fujian Medical University, Fuzhou, China, [3]Department of Laboratory Medicine, Xiang'an Hospital of Xiamen University, School of Medicine, Xiamen University, Xiamen, China

Epilepsy is a common symptom of many neurological disorders and can lead to neuronal damage that plays a major role in seizure-related disability. The peptidyl-prolyl isomerase Pin1 has wide-ranging influences on the occurrence and development of neurological diseases. It has also been suggested that Pin1 acts on epileptic inhibition, and the molecular mechanism has recently been reported. In this review, we primarily focus on research concerning the mechanisms and functions of Pin1 in neurons. In addition, we highlight the significance and potential applications of Pin1 in neuronal diseases, especially epilepsy. We also discuss the molecular mechanisms by which Pin1 controls synapses, ion channels and neuronal signaling pathways to modulate epileptic susceptibility. Since neurotransmitters and some neuronal signaling pathways, such as Notch1 and PI3K/Akt, are vital to the nervous system, the role of Pin1 in epilepsy is discussed in the context of the CaMKII-AMPA receptor axis, PSD-95-NMDA receptor axis, NL2/gephyrin-GABA receptor signaling, and Notch1 and PI3K/Akt pathways. The effect of Pin1 on the progression of epilepsy in animal models is discussed as well. This information will lead to a better understanding of Pin1 signaling pathways in epilepsy and may facilitate development of new therapeutic strategies.

KEYWORDS

Pin1, neuronal signaling, neurodegeneration, epilepsy, synapses

Abbreviations: HFOs, high-frequency oscillations; rHFOSs, repetitive HFOs and spikes; PPIases, the peptidyl prolyl cis-trans isomerases; PPase, protein phosphatase; NIMA, never in mitosis, gene A; APP, amyloid precursor protein; Pin1, PPIase NIMA-interacting 1; LTP, long-term potentiation; TLE, temporal lobe epilepsy; CNS, central nervous system; SH3, Src homology 3; PDZ, PSD-95/Disks large/zona occludens-1; CaMKII, calcium/calmodulin-dependent protein kinase II; PKA, protein kinase A; PKCs, protein kinase C isoenzymes; GlyT-1, glycine transporter-1; NL2, Neuroligin2; CB, carotid body; CND, chemoreceptor discharge; SIK2, salt-induced kinase 2; NHERF, Na(+)/H(+) exchanger regulatory factor; NSC, neural stem cell; SMRT, silencing mediator of retinoic acid and thyroid hormone receptor; NICD1, Notch1 intracellular domain; pBMSCs, porcine bone marrow mesenchymal stem cells.

Introduction

Epilepsy is a common, chronic, and severe neurological disorder. Recurrent and unpredictable interruptions of normal brain function are the characteristic symptoms of epileptic seizures (Fisher et al., 2005; Moshé et al., 2015), which result from transient abnormal synchronization of neurons in the brain (Moshé et al., 2015). Many studies have demonstrated electrophysiological abnormalities in epilepsy. High-frequency oscillations (HFOs), repetitive HFOs and spikes (rHFOSs) and sleep spindles are typical electrophysiological biomarkers of epileptogenesis (Perucca et al., 2019). Neurotransmitters and neuroendocrine axes are critical in the onset of epilepsy (Camfield et al., 2017). Although the molecular mechanism of epilepsy has not been fully elucidated, there is growing evidence for synaptic transmission in the pathological process of epilepsy (Amador et al., 2020; Puhahn-Schmeiser et al., 2021), and altered dynamics of inhibitory synapses and excitatory synapses may be a critical signature of epileptic networks (Vannini et al., 2020).

The peptidyl prolyl *cis-trans* isomerase (PPIase) superfamily consists of four families characterized by their structural differences: cyclophilins, FK506-binding proteins (FKBPs), parvulins, and the protein phosphatase (PPase) 2A phosphatase activator (PTPA) (Li et al., 2021). Discovered in 1996 as a substrate of NIMA (never in mitosis, gene A), PPIase NIMA-interacting 1 (Pin1) protein is associated with mitosis (Lu et al., 1996; Fagiani et al., 2021). It consists of 163 amino acid residues with a relative molecular mass of 18 kDa and contains 1 nuclear localization signal and 2 functional domains (Li et al., 2021). Pin1-catalyzed isomerization, which is detected by cis and trans proline isomer-specific antibodies (Nakamura et al., 2012a; Kondo et al., 2015), has the ability to function as a molecular timer to synchronize cellular processes (Lu et al., 2007; Liou et al., 2011; Zhou and Lu, 2016).

Recently, emerging evidence has demonstrated that Pin1 is closely related to many cellular processes, such as the cell cycle, cell proliferation, cell motility, and apoptosis, by its isomerization phosphorylated substrates and postphosphorylation regulation (Ranganathan et al., 1997; Hilton et al., 2015; Lin et al., 2015; Feng et al., 2017; Risal et al., 2017). In addition, Pin1 also exerts a pivotal effect on multiple physiological processes, including the immune response, neuronal differentiation, and tumorigenesis (Sacktor, 2010; Tun-Kyi et al., 2011; Daza-Martin et al., 2019). Pin1 activity is tightly regulated through finely tuned cellular pathways downstream of phosphorylation signaling, and its dysregulation under pathological conditions is related to multiple diseases (Fagiani et al., 2021; Li et al., 2021). In particular, Pin1 regulates several neuronal proteins, such as Tau, amyloid precursor protein (APP), and α-synuclein (Li et al., 2021) and thus has a significant impact on the development of many neurodegenerative diseases.

Spontaneous seizures have been observed in Pin1-knockout mice without any induction, suggesting that Pin1 may be a neuroprotective gene in the development of epilepsy, and its function may be associated with the regulation of excitatory and inhibitory synapses (Antonelli et al., 2014, 2016; Tang et al., 2017). Specifically, Pin1 may be associated with excitatory glutamate receptors N-methyl-D-aspartic acid [(NMDA) receptors and alpha-amino-3-hydroxy-5-methyl-4-isoxazolepropionic acid (AMPA) receptors] as well as inhibitory neurotransmitter receptors gamma-aminobutyric acid [(GABA) receptors and glycine receptors], which can effectively regulate the release of neurotransmitters and are significant in the progression of epilepsy. Electrophysiological studies of ion channels have also revealed some of the pathophysiological mechanisms underlying Pin1 and epilepsy (Antonelli et al., 2014, 2016; Hu J. H. et al., 2020; Hou et al., 2021).

Given the critical role of Pin1 in neurological diseases, we discuss in this review the recent findings of the dysregulation, mechanisms, and biological functions of Pin1 in epilepsy.

The structure and function of Pin1

Pin1 was first found to be an essential PPIase that regulates mitosis, presumably by interacting with NIMA and attenuating its mitosis-promoting activity (Lu et al., 1996). Pin1 can specifically catalyze the isomerization of phosphorylated proline-directed serine or threonine (pS/T-P) (Wang et al., 2020; Li et al., 2021). The N-terminal WW domain (residues 1–39) and C-terminal PPIase domain (residues 50–163) are two main protein functional domains of Pin1. The WW domain performs the function of recognition and binding to the pSer/Thr-Pro motif of the substrate, while the PPIase domain is responsible for *cis-trans* isomerization and catalytic activity (Lu et al., 1999; Wang et al., 2020; Fagiani et al., 2021; Li et al., 2021). Since the WW domain specifically interacts with pSer-Pro or pThr-Pro motifs, which are the key phosphorylation sites of the substrates, Pin1 regulates diverse cellular processes in cell signaling pathways, such as cell cycle progression, cellular stress responses, development, neuronal function, immune responses, and cell death (Zhou et al., 2000; Lu and Zhou, 2007; Wang et al., 2020). Notably, Pin1 is expressed at very high levels in neurons (Nakamura et al., 2012b). Moreover, Pin1 function is inhibited in human central nervous system (CNS) disorders, including Alzheimer's disease, Parkinson's disease and schizophrenia, by multiple mechanisms (Driver et al., 2015; Fagiani et al., 2021), which supports the idea that it is an essential protective gene in the nervous system. The selected Pin1 substrates associated with the nervous system are summarized in **Table 1**.

TABLE 1 Selected Pin1 substrates.

Protein	Substrate regulation by Pin1	Pin1-binding motif	Cellular consequence of Pin1 substrates activation	References
PSD95	Structural rearrangements	T287/S290/S295	Negatively affecting its ability to interact with NMDARs	Antonelli et al., 2016
NMDAR	Altered NMDARs surface trafficking	NR2A and NR2B	Regulating hyper-excitability	Tang et al., 2017
CaMKII	Conformational change, auto-phosphorylation of Thr286.	T176	Activating CaMKII, increasing expression of total AMPA receptors and phosphorylating GluA1 Ser831	Hou et al., 2021
PKC	Phosphorylation Thr of the turn motif, converted PKC isozymes	The hydrophobic motif of conventional PKC isozymes	Dephosphorylating and ubiquitination PKC	Abrahamsen et al., 2012; Yang and Igumenova, 2013
PKA	Phosphorylation in the WW domain of Pin1	S16	Abolishing its binding capacity to a phosphorylated Tau peptide	Smet-Nocca et al., 2013
Neuroligin2	Phosphorylation	S714	Negatively modulating gephyrin–NL2 interaction	Antonelli et al., 2014

Pin1 and epilepsy

Pin1 has protective effects against the pathology of epilepsy

Although many signaling pathways have been reported to be involved in the pathology of epilepsy by participating in seizure-induced cognitive dysfunction or neuronal apoptosis (Cendes et al., 2005; Henshall and Engel, 2013), the exact molecular mechanism of epilepsy is still unclear. In addition, Pin1 is involved in many cellular processes because of its plentiful protein targets (Liou et al., 2011; Yuan et al., 2011; Tang et al., 2017). Pin1 interacts with many neuronal proteins, and its deficiency is implicated in neurodegeneration (Balastik et al., 2007; Driver and Lu, 2010; Rudrabhatla and Pant, 2010; Tang et al., 2017). Pin1 can inhibit the protein synthesis required to sustain the late phase of long-term potentiation (LTP) (Keeney et al., 2012; Tang et al., 2017). In addition, Pin1 regulates conformational changes in the neuronal protein gephyrin, which is involved in the development of temporal lobe epilepsy (TLE) (Fang et al., 2011), and it modulates glycine receptor function as well (Zita et al., 2007). Therefore, it is reasonable to hypothesize that Pin1 is associated with the development of epilepsy.

Pin1-deficient mice have significantly upregulated seizure susceptibility in chemically induced models and develop age-dependent spontaneous epilepsy without any induction, strongly suggesting that Pin1 may be an important neuroprotective gene and that deletion of Pin1 may contribute to the occurrence of epilepsy (Hou et al., 2021). Recent studies have shown that the expression of Pin1 is remarkably downregulated in epileptic patients as well as experimental epileptic mouse models (Tang et al., 2017). The expression of Pin1 is dramatically decreased in the neocortex of epilepsy patients. Additionally, a pilocarpine-induced epileptic mouse model has also been used to verify the expression of Pin1 in epilepsy, and the results are consistent with those in humans (Tang et al., 2017), which supports the antiepileptic effect of Pin1. This study provided direct evidence that Pin1 is essential in regulating epileptic seizures.

Pin1 regulates the synapses and ion channels in neurons

The imbalance of excitability and inhibition of a large number of neurons is a significant cause of epileptic seizures. Inhibitory and excitatory neurotransmitters are critical regulators of hyperexcitability in epilepsy (Van Liefferinge et al., 2013). Abnormal increases in excitability, inadequate inhibitory mechanisms, or a combination of both lead to the excitability of the neurons in the epileptic foci, resulting in the uncontrolled spontaneous abnormal synchronous discharge of these neurons, followed by repeated seizures (Moshé et al., 2015; Camfield et al., 2017). Among them, excitatory glutamate receptor NMDA receptors, AMPA receptors and inhibitory neurotransmitter receptor GABA receptors, which are all regulated by Pin1, are involved in the regulation of epileptic activity (He et al., 2011; Rogawski, 2013; Lippman-Bell et al., 2016). The proposed relationship between Pin1 and synapses is presented as a conceptual model in **Figure 1**.

N-methyl-D-aspartic acid receptors

Ionotropic glutamate NMDA receptors are important regulators of glutamatergic synaptic transmission in the CNS and modulate the maturation and plasticity of glutamate synapses (Ladépêche et al., 2014). Recent studies have suggested the possible role of lateral diffusion in the surface distribution of NMDA receptors, which provides a powerful way to rapidly

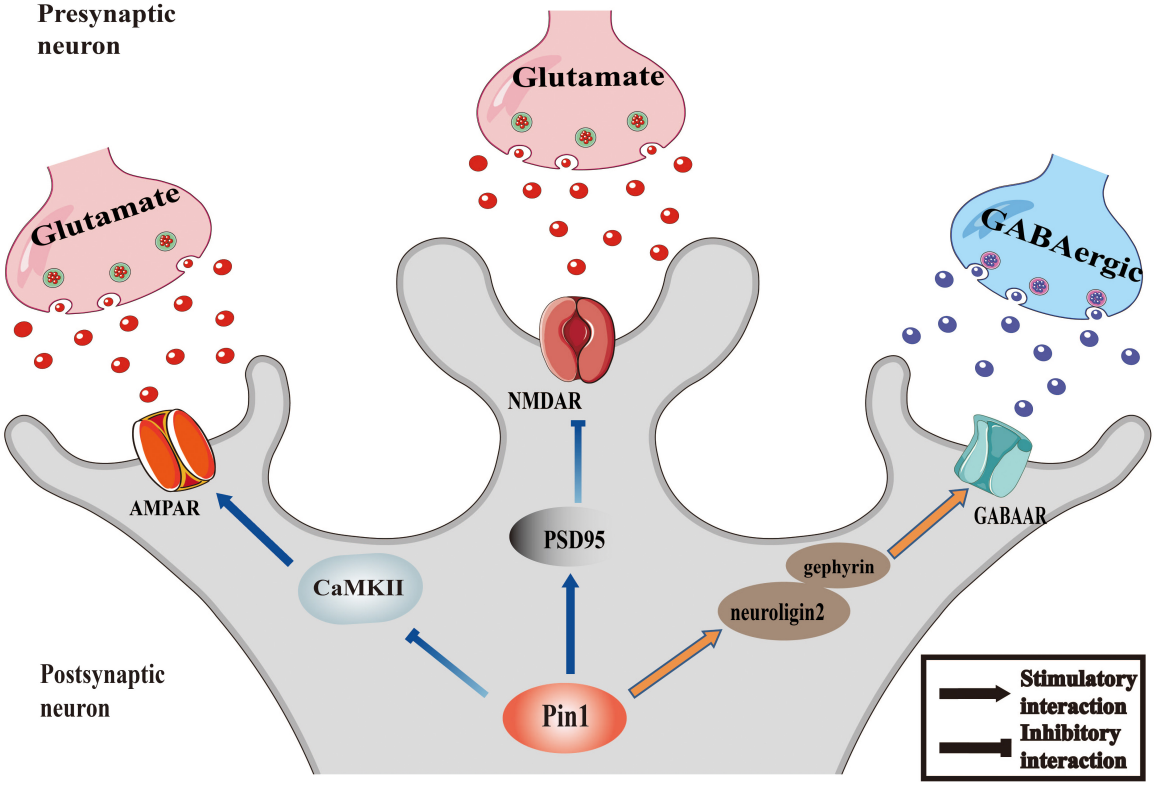

FIGURE 1
Pin1 as regulator of synaptic activity. The function of AMPAR could be inhibited by the interaction between Pin1 and CaMKII. Pin1 could down regulate the NMDA-mediated synaptic transmission by binding to PSD95. And the transmission of GABAergic will be modulated by Pin1 interfering the function of neuroligin2-gephyrin complex.

affect the content and composition of synaptic receptors (Peng et al., 2010; Ladépêche et al., 2014). The increased number of cell surface NMDARs is responsible for cell injury and neuronal death during epileptogenesis, and therapies that directly antagonize NMDA receptors may prevent excitotoxicity, which develops after various pro-epileptogenic brain injuries (Frasca et al., 2011; Naylor et al., 2013; Tang et al., 2017).

The relationship between Pin1 and NMDA receptors has recently been recognized. PSD-95 is a membrane-associated guanylate kinase with a catalytically inactive guanylate kinase domain, a Src homology 3 (SH3) domain and three PDZ (PSD-95/Disks large/zona occludens-1) domains, which allow it to anchor the NMDA receptors GluN2 and activate intracellular signaling complexes (Opazo et al., 2012). One study showed that Pin1 triggers structural changes in PSD-95 by interacting with PSD-95 at the T287, S290, and S295 consensus motifs and then negatively regulates its ability to interact with NMDARs (Antonelli et al., 2016). To be precise, Pin1 can bind with PSD-95 and then triggers its structural changes. Pin1-driven conformational rearrangements mainly impact on PDZ2, the domain involved in NMDAR recruitment. Larger NMDA-mediated synaptic currents in hippocampal slices were obtained from Pin1(–/–) mice compared with controls, and similar results were obtained in cultured hippocampal cells expressing a PSD-95 mutant unable to undergo prolyl-isomerization, further indicated the action of Pin1 on PSD-95 negatively regulates the ability of NMDARs. Furthermore, an increasing of dendritic spines was observed in Golgi-stained pyramidal neurons lacking Pin1 expression. Altogether, Pin1 could affect plasticity by determining the number of NMDARs initiating plasticity via PSD-95 prolyl-isomerization (Antonelli et al., 2016). Pin1 can also bind via its WW domain with phosphorylated threonine (T19) and serine (S25) in the N-terminal domain of PSD-95, and the binding reduces the palmitoylation of cysteine 3 and cysteine 5 in PSD-95 and then decreases its stability at excitatory synapses (Delgado, 2020; Delgado et al., 2020). This result indicates that Pin1 can modulate NMDARs via PSD-95 prolyl isomerization, suggesting that Pin1 plays a key role in synaptic transmission.

Alpha-amino-3-hydroxy-5-methyl-4-isoxazolepropionic acid receptors

AMPA receptors (AMPARs) are major regulators of excitatory synaptic transmission (Traynelis et al., 2010), and the expression of AMPARs at synapses is very dynamic

(Shepherd and Huganir, 2007). AMPA receptors consist of four subunits (GluA1–GluA4), and any of them can form both homo and heteromers (Traynelis et al., 2010) and possess multiple phosphorylation sites (He et al., 2011). The phosphorylation of its subunits can regulate AMPAR function effectively (Kittler and Moss, 2006; Lee, 2006b), which is significant for modulating different forms of synaptic plasticity (Turrigiano and Nelson, 2004). Research has highlighted the role of the GluA1 subunit on serine 845 (S845) in various forms of synaptic plasticity (Lee, 2006a). The phosphorylation of GluA1-S845 is a necessary prerequisite step for *in vivo* sensory experience-dependent homeostatic synaptic plasticity of visual cortical neurons (Goel et al., 2011). GluA1-S845 phosphorylation is critical for maintaining the perisynaptic population of AMPARs by trafficking AMPARs to extrasynaptic sites and subsequent delivery to synapses during LTP (Oh et al., 2006). In addition, the phosphorylation of Ser831 and Ser845 are also considered key factors in LTP (Shepherd and Huganir, 2007). Additional studies have shown the potential utility of AMPA receptors as targets for seizure protection and validated AMPA receptors as novel targets for epilepsy therapy (Rogawski and Donevan, 1999; French et al., 2012, 2013; Krauss et al., 2012; Rogawski, 2013).

Recent studies have indicated that Pin1 may negatively regulate AMPA receptors. Pin1 KO upregulates epileptic susceptibility in mice, which is associated with an increase in AMPA receptors (Hou et al., 2021). The specific mechanism may involve calcium/calmodulin-dependent protein kinase II (CaMKII), protein kinase A (PKA) and protein kinase C isoenzymes (PKCs), the phosphorylation of which can effectively alter the excitatory function of AMPA receptors and provides a novel mechanism for channel modulation through a variety of protein signaling cascades (Jenkins and Traynelis, 2012; Wang et al., 2013).

CaMKII is a key mediator of AMPA receptors through its GluA1 subunit (Hayashi et al., 2000) and plays a critical role in the process of epilepsy. The phosphorylation of GluA1 at Ser831 via CaMKII could increase the conductance of AMPA receptors (Derkach et al., 1999; Kristensen et al., 2011). The activity of CaMKII is modulated by its regulatory domains. The regulatory domain blocks the substrate binding site of the CaMKII kinase domain in its basal state structures (Krapivinsky et al., 2004; Rellos et al., 2010; Chao et al., 2011; Coultrap and Bayer, 2012), while Ca^{2+}/calmodulin can bind to the regulatory domain and then autophosphorylate CaMKII at Thr286 to keep the catalyst active (Partida et al., 2018). Recent studies using pull-down and immunoprecipitation assays have identified that Pin1 binds CaMKII in a phosphorylation-specific manner, which indicates the role of Pin1 in the phosphorylation-dependent signals involving CaMKII (Tatara et al., 2010). Additional research has demonstrated that the activity of CaMKII is significantly increased in Pin1 KO mice, and Pin1 can bind to phosphorylated CaMKII and decrease its activity (Shimizu et al., 2018; Hou et al., 2021). Moreover, restoration of the expression of Pin1 can reduce the phosphorylation of CaMKII and GluA1 (Hou et al., 2021), and Pin1 may regulate the phosphorylation of GluA1 Ser831 by acting on CaMKII, which supports the view that Pin1 effectively controls seizure susceptibility via the Pin1-CaMKII-AMPA receptor pathway.

Protein kinase C acts on a multitude of signal transduction pathways (Newton, 2001; Steinberg, 2008; Yang and Igumenova, 2013), and the relationship between PKC and AMPA receptors is significant in excitatory transmission. Some studies observed an increasing activity of PKC in the hippocampus of amygdala-kindled and hippocampus-kindled rats (Akiyama et al., 1995). PKC expression has also been detected to be decreased in pilocarpine induced epileptic rats, and further research has demonstrated that PKC can phosphorylate the GluA1 subunit of AMPA receptors at its S831 site (Roche et al., 1996; Kim et al., 2019). In addition, the C-terminal V5 domain is one of the most variable domains in PKCs due to cis-trans isomerization of the peptidyl-prolyl bonds (Yang and Igumenova, 2013). It has been shown that Pin1 binds to the hydrophobic motif of V5 and isomerizes the phosphorylated turn motif of conventional PKC, which primes it for subsequent ubiquitin-mediated degradation (Abrahamsen et al., 2012; Yang and Igumenova, 2013), to be specific, the study demonstrated that Pin1 could down regulate the conventional isozymes of PKC family. These studies highlight the role of the V5a-Pin1 interaction in neural function. Although PKC showed no change in Pin1 KO mice (Hou et al., 2021), studies have shown the effect of Pin1 on the PKCα subunit (Abrahamsen et al., 2012). Thus, the interaction between PKC and Pin1 and its function and molecular mechanism in the development of epilepsy is urgently needed.

Protein kinase A is crucial for both postsynaptic and presynaptic mechanisms underlying LTD and LTP (Kameyama et al., 1998; Banke et al., 2000), which supports its role in epilepsy. Previous studies have demonstrated that PKA can enhance neuronal AMPA receptor equilibrium response amplitude and upregulate channel opening frequency (Knapp et al., 1990; Greengard et al., 1991; Banke et al., 2000). Moreover, phosphorylation of AMPA is regulated by PKA, which increases the peak response open probability of the AMPA receptor by phosphorylating GluA1 Ser845 (Banke et al., 2000; Kim et al., 2019). In addition, the ratios of the expression of pPKA and pERK1/2 are decreased in epileptic rats, which further supports the phosphorylation function of activated PKA in epileptic rats (Kim et al., 2019). In terms of the relationship between PKA and Pin1, recent studies have supported the idea that PKA can modulate the phosphorylation of the WW domain of Pin1 at Ser16. The phosphorylation would reduce conformational heterogeneity and flexibility of the phospho-binding loop upon S16 phosphorylation and abrogates the binding capacity of Pin1 afterward, which would definitely affect the neuronal signaling in epilepsy (Luh et al., 2013; Smet-Nocca et al., 2013). Although there was no change in PKA in Pin1

knockout mice (Hou et al., 2021), the underlying mechanism of mutual regulation between Pin1 and PKA is still worth further study.

Gamma-aminobutyric acid receptors and glycine receptors

As previously discussed, synaptic inhibition is essential for shaping the dynamics of neuronal networks, and abnormal inhibition is closely associated with epilepsy (Macha et al., 2022). GABA receptors represent the most significant inhibitory system in the CNS (Barki and Xue, 2021). The receptors can be categorized as GABAA and GABAB. GABAA can modulate ligand-gated (or receptor-operated) ion channels, and GABAB can operate through second messengers. Both contribute to seizure-like discharge control when repetitive electrical stimulation is delivered to the limbic structure (Avoli and Lévesque, 2022). It has also been demonstrated that aberrant alternative GPHN splicing, leading to curtailed protein and diminished GABA receptors, is related to temporal lope lobe epilepsy (Förstera et al., 2010). Thus, GABAergic signaling is closely linked to the onset of epilepsy.

The glycine receptor (GlyR) is closely related to GABAA in the 'gene superfamily' of ligand-gated ion channels. It plays an essential role in mediating inhibitory neurotransmission in the spinal cord and brain stem, yet it also works as a coagonist with NMDARs in the CNS (Zafra et al., 2017). The malfunctions of GlyR are linked to temporal lobe epilepsy (Lynch et al., 2017), and it may contribute to the neuropsychiatric symptoms of the disease in a neuron type-specific way (Kankowski et al., 2017). Neuron type-specific expression of a gain-of-function variant of GlyR has been observed in the hippocampus of patients with temporal lobe epilepsy (Winkelmann et al., 2014). In addition, preclinical studies have shown that inhibition of its substrate selective transporter, glycine transporter-1 (GlyT-1), can promote neuroprotection and provide a pharmacotherapeutic strategy for epilepsy (Cioffi and Guzzo, 2016). These studies support the link between GlyR and epilepsy.

Accumulating evidence has demonstrated the interaction of Pin1 with GABA receptors and GlyR. It is known that Gephyrin is a central component of GABAergic signaling and plays a key role in α2 and γ2 subunit-containing GABAAR clustering (Kneussel et al., 1999; Tretter et al., 2012; Antonelli et al., 2014). The NL2 isoform is a kind of adhesion molecule that is present in GABAergic PSDs (Varoqueaux et al., 2004). The interaction of NL2 and gephyrin can modulate NL-scaffolding protein interactions and regulate excitatory and inhibitory synaptic transmission (Antonelli et al., 2014). Pin1 has been shown to interact with gephyrin and alter its overall structure, thereby enhancing its ability to bind GlyR (Zita et al., 2007; Antonelli et al., 2014). Additionally, Pin1 can mediate propyl isomerization of phosphorylated serine 714. Further studies have shown that Pin1 negatively regulates the interaction of the gephyrin–NL2 complex formation, which in turn downregulates GABAergic synaptic transmission (Antonelli et al., 2014), suggesting the existence of a Pin1/NL2/gephyrin signaling pathway in the regulation of GABAergic synapses. Moreover, ten putative Pin1 consensus motifs have been identified, mostly concentrated in the C-domain of gephyrin. The C-domain's cluster was responsible for Pin1 recruitment, following by Pin1-driven conformational changes of gephyrin substrate. Such structural remodeling of gephyrin could affect its binding affinity for the β subunit of the GlyR without affecting its oligomerization properties. Consistent with these findings, hippocampal neurons derived from Pin1 knockout mice show a loss in the number of GlyR immunoreactive puncta, corresponding to a reduction in amplitude of glycine-induced current (Zacchi et al., 2014). These studies further demonstrate the mechanism by which Pin1 regulates GlyR function.

Ion channels

Ion channels also participate in the occurrence of epilepsy. Approximately 25% of genes identified in epilepsy encode ion channels (Oyrer et al., 2018), and electrophysiological studies have shown not only pathophysiological mechanisms underlying epilepsy but also the mechanism of action of several antiepileptic drugs involve ion channels (Sugiura and Ugawa, 2017). Research has shown that when AMPA receptors are activated, they allow Na^+ to enter or leave, and extracellular Na^+ influx causes postsynaptic membrane depolarization and induces EPSP to participate in excitatory synaptic transmission. At the same time, membrane depolarization induced by the AMPA receptor causes Mg^{2+} to move away from the NMDA receptor channel and open the NMDA receptor channel. Activated NMDA receptors result in excessive Ca^{2+} influx and intracellular calcium overload, leading to cell death. In addition, activated GABA receptors can induce the opening of chloride ion channels, and the rapid influx of Cl^- causes hyperpolarization of the postsynaptic membrane and generates inhibitory postsynaptic potentials that inhibit neuronal excitation (Lippman-Bell et al., 2016).

In terms of the relationship between Pin1 and ion channels, a Pin1-dependent mechanism has been reported to regulate the association of the A-type K^+ channel subunit Kv4.2, suggesting a Pin1-mediated mechanism in the regulation of reversal learning (Hu J. H. et al., 2020). Recent studies have also hypothesized that hypoxia-induced changes in the flavoprotein (Fp)-mediated redox ratio of the carotid body (CB) modulate the Pin1/p47phox tandem to alter type I cell potassium channels and therefore chemoreceptor discharge (CND) (Bernardini et al., 2020). Pin1 also regulates Ca^{2+} influx by binding to salt-induced kinase 2 (SIK2) and decreasing the expression of p35, a negative regulator of Ca^{2+} influx (Nakatsu et al., 2017), yet the effect is induced by high glucose, which is not the same as the microenvironment of epilepsy. The association of Na(+)/H(+) exchanger regulatory factor (NHERF)-1 with Pin1 may also indicate the role of Pin1

in the Na(+)/H(+) channel (He et al., 2001). The mechanism by which Pin1 regulates epileptic ion channels may illuminate the underlying roles of Pin1 in epilepsy.

Pin 1 in neuronal signaling associated with epilepsy

Notch1 signaling pathway

Notch1 is a membrane receptor in the Notch family (Arumugam et al., 2018). Notch1 is tightly connected to cell proliferation, differentiation, and developmental fate switching (Arumugam et al., 2018). For neurons, Notch1 plays various roles in the development of the CNS, participating in the proliferation, survival, self-renewal and differentiation of neural stem cells (NSCs) (Lathia et al., 2008; Arumugam et al., 2018). In addition, Notch1 signaling may also affect synaptic plasticity and learning and memory in the adult brain (Lathia et al., 2008; Alberi et al., 2013; Sargin et al., 2013; Arumugam et al., 2018). In terms of epilepsy, Notch1 signaling has the ability to induce astrogliosis in glioma, which is critical in the occurrence of epilepsy. Notch signaling has been observed to be downregulated in a status epilepticus model, and the decrease may be associated with the disruption of the stem cell niche (Sibbe et al., 2012). Another study suggested that the Notch1 signaling pathway is activated in TLE mouse models and that its function is closely related to microglial phenotypic transformation (Deng et al., 2020). In addition, Notch1 was observed to increase in rats with status epilepticus and spontaneous recurrent seizures (Liu et al., 2014). Overall, the Notch1 signaling pathway is significant in the pathogenesis of epilepsy. Notch1 was found to modulate hippocampal plasticity via interaction with the reelin pathway, glutamatergic transmission and CREB signaling (Brai et al., 2015). CaMKII is closely related to Notch signaling activation by accelerating the degradation of the silencing mediator of retinoic acid and thyroid hormone receptor (SMRT), a corepressor of Notch signaling (Ann et al., 2012). In addition, the coaction of the PKA pathway and Notch1 expression is essential for the differentiation of C6 astrocytes (Angulo-Rojo et al., 2013). These studies highlight the interaction of CaMKII and PKA with the Notch1 signaling pathway.

Furthermore, Pin1 interacts with the Notch1 pathway. A strong correlation between Pin1 overexpression and high levels of activated Notch1 has been observed in breast cancer patients, and some studies have suggested that Notch1 may directly induce transcription of Pin1 (Rustighi et al., 2009). Resveratrol downregulates Pin1 and Notch1 intracellular domain (NICD1) at the same time and reverses cell dysfunction by inhibiting the Pin1/Notch1 signaling pathway (Yu and Fang, 2022). The relationship between NIC and Pin1 has also been analyzed in Pin1/p53 double-knockout mice, Pin1 deficiency might affect NIC stabilization, which is associated with the activity of presenilin1, a component of the gsecretase complex that would affect the releasing of NIC (Takahashi et al., 2008). Pin1 can also mediate cell death through the p53-NICD complex in ischemic stroke (Arumugam et al., 2018). The results indicated that the Pin1-p53-NIC system might be essential for preventing the pathogenesis and progression of epilepsy. Further research has demonstrated that Pin1 could bind with the crucial phosphorylated sites within the Ser-Thr-rich (STR) region of Notch1, then the conformational changes would lead to cleavage by γ-secretase and increased release of the active intracellular domain of Notch1, which explain the role of Pin1 in Notch1 pathway (Rustighi et al., 2009). Pin1 may promote proapoptotic function in neuronal death by promoting NICD1 stability (Baik et al., 2015), while other argue that Notch1 may increase the expression level of anti-apoptotic gene in rats with cerebral infarction and act an anti-apoptotic function in neuron (Zhao et al., 2019). Besides, Pin1 is closely associated with anti-apoptosis protein BCL-2 (Sultana et al., 2006; Li et al., 2007) and depict an anti-apoptotic effect in AD neurons (LaFerla et al., 1996; Rong et al., 2017; Wang et al., 2023). These findings strongly point to an anti-epileptic effect of Pin1 by antagonizing neuronal apoptosis in epilepsy, thus Pin1-Nocth1 complex may play anti-epileptic role.

Therefore, we can hypothesize that the interaction between Pin1 and Notch1 pathway may play a role in epilepsy and that Notch1 may participate in epileptogenesis via the function of CaMKII and PKA. The relevant characteristics of the Notch1 pathway are summarized in **Figure 2**.

PI3K/Akt signaling pathway

The PI3K/Akt pathway is significant for growth and survival and participates in many biological processes. It has been demonstrated that the PI3K/Akt pathway is associated with early ischemia/reperfusion injury (Fu et al., 2014), and it can regulate neuronal apoptosis and neuroinflammation in Alzheimer's disease (Liu and Li, 2020). Recent studies have shown that PI3K/Akt signaling improves the survival of neurons and axonal growth as well (Huang et al., 2017). For epilepsy, the PI3K/Akt signaling pathway can effectively inhibit the occurrence of epilepsy by attenuating neuronal apoptosis and autophagy (Duan et al., 2018; Wei et al., 2018; Hu F. et al., 2020). Moreover, the PI3K/Akt signaling pathway synergistically enhances adipogenesis and glucose uptake in porcine bone marrow mesenchymal stem cells (pBMSCs) through CaMKII (Zhang et al., 2018). Although few data describe the interaction between CaMKII and the PI3K/Akt pathway in neurons, it is logical to infer their role in epilepsy. In addition, fluoxetine elicited neuroprotection via PKA and PI3K/Akt (Zeng et al., 2016), which suggests the interaction of the PI3K/Akt signaling pathway and PKA in neurons. Furthermore, PKA-PI3K-Akt signaling has the ability to modulate the AMPA receptor GluA1 subunit to assist in learning and memory. These data demonstrate the coaction of

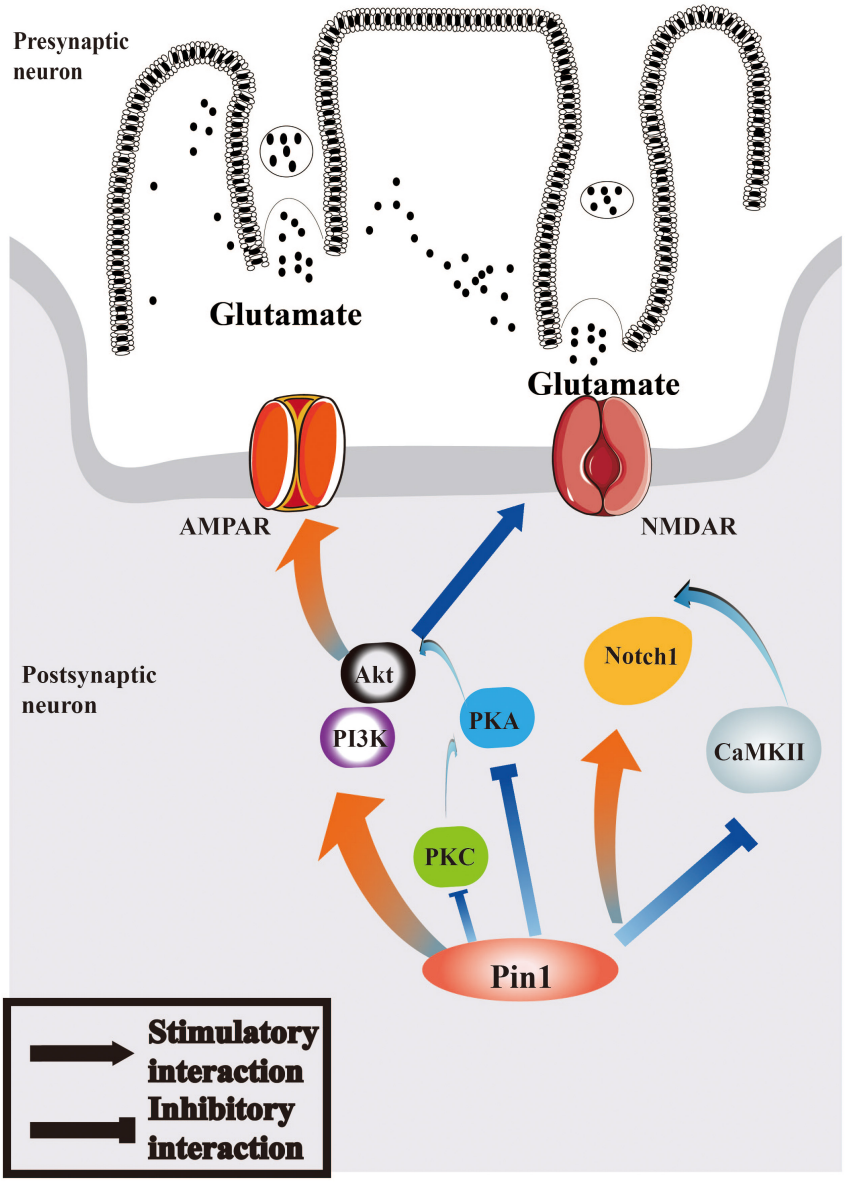

FIGURE 2
Pin1 may regulate Notch1 signaling and PI3K/Akt signaling pathways in epilepsy. Pin1 has an interaction with Notch1 pathways, and the function may associated with CaMKII. AMPAR and NMDAR can both be mediated by PI3K/Akt pathway, whose activation will be regulated by PKA, PKC, and Pin1. The relationship between Pin1 and PKA, PKC and CaMKII deserved further research.

PKA and PI3K/AKT and demonstrate their function on the AMPA receptor, which has a critical role in the progression of epilepsy (Chen M. W. et al., 2020). The relationship between PKC and PI3K/AKT has also been studied. PKC can regulate the activation of PKA-PI3K-Akt signaling, which effectively broadens the knowledge of the downstream signaling of GluA1 (Chen M. W. et al., 2020). Recent studies have also shown that the PI3K/Akt pathway may affect NMDA receptors via TrKB and BDNF (Srivastava et al., 2018), and activation of the PI3K-AKT-mTOR pathway can block NMDA-induced autophagy in neurons (Wang et al., 2014). The studies above have identified the interaction of PI3K/AKT and synaptic receptors and highlighted the effects of the PI3K/AKT pathway in epilepsy.

Pin1 can facilitate the activation of PI3K/Akt signaling. Some research has suggested that the expression of Pin1 is positively associated with activation of PI3K/Akt signaling (Yang et al., 2020), and that Pin1 can phosphorylate Akt at Ser434 and then increase Akt stability and subsequently activate PI3K/Akt (Nakatsu et al., 2011). The deletion of Pin1

can block the function of PI3K/Akt and suppress the growth of cells (Zhang et al., 2019). However, some studies have indicated an inhibitory effect of Pin1 on the PI3K/Akt pathway. Pin1 may downregulate the action of the PI3K/Akt/mTOR pathway and play a protective role in senescent cells (Zhang et al., 2021). The detailed mechanisms by which Pin1 acts on PI3K/Akt signaling may be useful to explain the role of Pin1 in neurons. Notably, Pin1 enables phosphatase PP2A to further mediate tau dephosphorylation in the AD brain (Ramakrishnan et al., 2003). PP2A is a special protein phosphatase that can dephosphorylate Akt. This function further supports the role of the Pin1/PI3K/Akt interaction in neurons. Therefore, it is valuable to study the mechanism by which Pin1 acts on the PI3K/Akt pathway, and PI3K/Akt may be another potential target for epilepsy treatment. The function of the PI3K/Akt pathway is shown in **Figure 2**.

Pin 1 and tau in epilepsy

Tau is an intrinsically disordered protein which has a closely relationship with microtubules. Its interaction with microtubules is characterized by a rapid "kiss-and-hop" process. It is most abundant in neuronal axons and the rapid interaction may explain how tau binding to microtubules without disturb axonal transport (Janning et al., 2014; Wang and Mandelkow, 2016; Chang et al., 2021b). Tau is also present in neuronal cell bodies, nuclei, synaptic specializations, glia and other cell types in the brain and peripheral organs (Wang and Mandelkow, 2016; Ittner and Ittner, 2018), which indicated that it may be involved in a variety of common and disabling brain diseases, including epilepsy. Reducing levels of endogenous tau has protective effects in epilepsy experimental models (DeVos et al., 2013; Gheyara et al., 2014). Tau deficit mice have an increased frequency of inhibitory postsynaptic currents in dentate granule cells (Roberson Halabisky et al., 2011), which may explain the beneficial effects of decreasing tau in epilepsy. Further study observed that Tau ablation could increase the excitability of inhibitory neurons, and structurally alters their axon initial segments, thus promote inhibition and suppress hypersynchrony (Chang et al., 2021a). Together, tau reduction prevents the occurrence of epilepsy. Hyperphosphorylated Tau protein might contribute to vulnerability to epileptogenesis, for excessive post-translational modifications of Tau creates a pathologic environment promoting epileptogenesis (Paudel et al., 2019). Therefore, therapy targeting Tau protein and p-tau anti-may be a viable epileptogenic strategy.

The interaction between Pin1 and tau has been demonstrated. Pin1 binds to pT231-tau and promotes tau dephosphorylation, and further study confirmed that the binding of Pin1 and p-tau could in turn isomerize phosphorylated tau proteins so that their conformation changes from *cis* to *trans*, thus favoring its recognition by the phosphatase PP2A. PP2A has conformational specificity and dephosphorylates only the trans pS/T-P motif (Zhou et al., 2000; Luna-Muñoz et al., 2007; Wang et al., 2020). *Cis* pT231-tau is associated with neuronal apoptosis under neuronal stress, thus is a key role in neurodegeneration, while Pin1 has the ability to decrease the level of abnormal p-tau and the regulation is a critical mechanism to protect against tau-related pathology (Wang et al., 2020).

Pin1 and the therapeutic application of epilepsy

The onset of seizure is mainly due to sudden abnormal discharge of neurons in the brain leading to temporary brain dysfunction. Thus, controlling or significantly reducing the abnormal charging of neurons is the main treatment for epilepsy. As mentioned above, Pin1 plays a critical role in preventing pathologies in epilepsy by regulating synapses; thus, it is reasonable to speculate that the upregulation and/or activation of Pin1 may be helpful for epilepsy treatment. However, Pin1 is a well-known oncogene, and overexpression of Pin1 has been reported to be associated with several cancers (Zhou and Lu, 2016). It can effectively activate a number of oncogenes and inactivate various tumor suppressors by modulating their functions to promote the development of cancer (Cheng and Tse, 2019; Yu et al., 2020). Therefore, treatment with Pin1 should be carried out with caution. Delivering the Pin1 activator to neurons specifically or therapies targeting the upstream regulators of Pin1 may be optional therapeutic strategies (Wang et al., 2020). In addition, although no drug candidates targeting Pin1 for neuronal diseases have been reported, specific antibodies targeting Thr231 of tau, which is the Pin1 binding site, have been developed, and such monoclonal antibodies could effectively prevent tau-related pathology development in AD and TBI patients by entering neurons and blocking the induction of pathological *cis* p-tau (Shahpasand et al., 2018; Chen D. et al., 2020; Wang et al., 2020), which is closely related to cognitive impairment and dementia (Albayram et al., 2017; Qiu et al., 2021). Moreover, aberrant p-tau aggregation has been reported in the epileptic human brain and in animal models of epilepsy (Machado et al., 2019; Liu et al., 2021; Canet et al., 2022), highlighting the role of pathological p-tau in the onset of epilepsy, suggesting that a therapy targeting the Pin1 binding site, especially p-tau, may also be a potential anti-epileptogenic therapy (Liu et al., 2016). Brivaracetam and the non-competitive antagonist of the AMPA glutamate receptor perampanel are the more recent antiseizure medications with a low risk of interaction, and have recently been approved for monotherapy and/or adjunctive treatment in the USA and Europe (Rohracher et al., 2021). Because of the close relationship between the AMPA receptor and Pin1, this novel therapy may broaden the spectrum of Pin1 in the treatment of epilepsy. More research in animal models and

technological innovation would be helpful to further boost the success of Pin1 in epilepsy treatment.

Conclusion

The evidence discussed in this review supports the idea that Pin1 is implicated in the onset and progression of epilepsy. Pin1 is identified as a unique enzyme and a crucial regulator that precisely regulates the *cis-trans* isomerization of a wide variety of phosphorylated proteins and alters the activity of its target proteins. Regulation of the phosphorylation and transcriptional landscapes by Pin1 makes this enzyme a central effector of many physiological and pathological activities related to neuronal cells (Zannini et al., 2019). In line with this hypothesis, Pin1 has been reported to take part in neuro-associated diseases (Fagiani et al., 2021), including epilepsy. In addition, emerging evidence supports the notion that Pin1 is a key molecule in epileptogenesis. Pin1 has strong neuroprotective effects in the progression of epilepsy, and the Pin1/NMDAR complex, Pin1-CaMKII-AMPA receptor axis and Pin1-NL2/gephyrin-GABAergic signaling may all be involved in the mechanism (Antonelli et al., 2014, 2016; Tang et al., 2017; Hou et al., 2021). The data strongly suggest the potential utility of Pin1 as a target for seizure protection (Hou et al., 2021). The function of Pin1 in epilepsy may be associated with some classical signaling pathways, such as the Notch1 signaling and PI3K/Akt signaling pathways. However, more evidence is needed to clarify the potential role of Pin1 in neuronal signaling, particularly in the occurrence of epilepsy. Finally, Pin1-related treatment is promising, and more research and technological innovation are needed to overcome its limitations in direct administration. We anticipate that the specific molecular mechanisms will be elucidated in the coming years, pushing Pin1 toward true clinical application.

Author contributions

All authors: conceptualization, substantive supervision, revision over the article, read and agreed to the published version of the manuscript. YC: collection the literature and writing—review and editing the manuscript. HL: project administration and funding acquisition.

Funding

This study was funded by Natural Science Foundation of Fujian Province (2020J01602).

Acknowledgments

We are grateful to Kun Ping Lu and Xiao Zhen Zhou for the guidance and valuable suggestions of our epilepsy-related projects.

Conflicts of interest

The authors declare that the research was conducted in the absence of any commercial or financial relationships that could be construed as a potential conflict of interest.

Conflict of interest

The authors declare that the research was conducted in the absence of any commercial or financial relationships that could be construed as a potential conflict of interest.

Publisher's note

All claims expressed in this article are solely those of the authors and do not necessarily represent those of their affiliated organizations, or those of the publisher, the editors and the reviewers. Any product that may be evaluated in this article, or claim that may be made by its manufacturer, is not guaranteed or endorsed by the publisher.

References

Abrahamsen, H., O'Neill, A. K., Kannan, N., Kruse, N., Taylor, S. S., Jennings, P. A., et al. (2012). Peptidyl-prolyl isomerase Pin1 controls down-regulation of conventional protein kinase C isozymes. *J. Biol. Chem.* 287, 13262–13278. doi: 10.1074/jbc.M112.349753

Akiyama, K., Ono, M., Kohira, I., Daigen, A., Ishihara, T., and Kuroda, S. (1995). Long-lasting increase in protein kinase C activity in the hippocampus of amygdala-kindled rat. *Brain Res.* 679, 212–220. doi: 10.1016/0006-8993(95)00221-b

Albayram, O., Kondo, A., Mannix, R., Smith, C., Tsai, C. Y., Li, C., et al. (2017). Cis P-tau is induced in clinical and preclinical brain injury and contributes to post-injury sequelae. *Nat. Commun.* 8:1000. doi: 10.1038/s41467-017-01068-4

Alberi, L., Hoey, S. E., Brai, E., Scotti, A. L., and Marathe, S. (2013). Notch signaling in the brain: In good and bad times. *Ageing Res. Rev.* 12, 801–814. doi: 10.1016/j.arr.2013.03.004

Amador, A., Bostick, C. D., Olson, H., Peters, J., Camp, C. R., Krizay, D., et al. (2020). Modelling and treating GRIN2A developmental and epileptic encephalopathy in mice. *Brain* 143, 2039–2057.

Angulo-Rojo, C., Manning-Cela, R., Aguirre, A., Ortega, A., and López-Bayghen, E. (2013). Involvement of the Notch pathway in terminal astrocytic differentiation: Role of PKA. *ASN neuro* 5:e00130. doi: 10.1042/AN20130023

Ann, E. J., Kim, H. Y., Seo, M. S., Mo, J. S., Kim, M. Y., Yoon, J. H., et al. (2012). Wnt5a controls Notch1 signaling through CaMKII-mediated degradation of the SMRT corepressor protein. *J. Biol. Chem.* 287, 36814–36829. doi: 10.1074/jbc.M112.356048

Antonelli, R., De Filippo, R., Middei, S., Stancheva, S., Pastore, B., Ammassari-Teule, M., et al. (2016). Pin1 modulates the synaptic content of NMDA receptors via prolyl-isomerization of PSD-95. *J. Neurosci.* 36, 5437–5447. doi: 10.1523/JNEUROSCI.3124-15.2016

Antonelli, R., Pizzarelli, R., Pedroni, A., Fritschy, J. M., Del Sal, G., Cherubini, E., et al. (2014). Pin1-dependent signalling negatively affects GABAergic transmission by modulating neuroligin2/gephyrin interaction. *Nat. Commun.* 5:5066. doi: 10.1038/ncomms6066

Arumugam, T. V., Baik, S. H., Balaganapathy, P., Sobey, C. G., Mattson, M. P., and Jo, D. G. (2018). Notch signaling and neuronal death in stroke. *Prog. Neurobiol.* 16, 103–116.

Avoli, M., and Lévesque, M. (2022). GABAB receptors: Are they missing in action in focal epilepsy research? *Curr. Neuropharmacol.* 20, 1704–1716. doi: 10.2174/1570159X19666210823102332

Baik, S. H., Fane, M., Park, J. H., Cheng, Y. L., Yang-Wei Fann, D., Yun, U. J., et al. (2015). Pin1 promotes neuronal death in stroke by stabilizing Notch intracellular domain. *Ann. Neurol.* 77, 504–516.

Balastik, M., Lim, J., Pastorino, L., and Lu, K. P. (2007). Pin1 in Alzheimer's disease: Multiple substrates, one regulatory mechanism? *Biochim. Biophys. Acta* 1772, 422–429. doi: 10.1016/j.bbadis.2007.01.006

Banke, T. G., Bowie, D., Lee, H., Huganir, R. L., Schousboe, A., and Traynelis, S. F. (2000). Control of GluR1 AMPA receptor function by cAMP-dependent protein kinase. *J. Neurosci.* 20, 89–102.

Barki, M., and Xue, H. (2021). GABRB2, a key player in neuropsychiatric disorders and beyond. *Gene* 809:146021. doi: 10.1016/j.gene.2021.146021

Bernardini, A., Wolf, A., Brockmeier, U., Riffkin, H., Metzen, E., Acker-Palmer, A., et al. (2020). Carotid body type I cells engage flavoprotein and Pin1 for oxygen sensing. *Am. J. Physiol. Cell Physiol.* 318:C719–C731. doi: 10.1152/ajpcell.00320.2019

Brai, E., Marathe, S., Astori, S., Fredj, N. B., Perry, E., Lamy, C., et al. (2015). Notch1 regulates hippocampal plasticity through interaction with the reelin pathway, glutamatergic transmission and CREB signaling. *Front. Cell. Neurosci.* 9:447. doi: 10.3389/fncel.2015.00447

Camfield, P., Camfield, C., Busiah, K., Cohen, D., Pack, A., and Nabbout, R. (2017). The transition from pediatric to adult care for youth with epilepsy: Basic biological, sociological, and psychological issues. *Epilepsy Behav.* 69, 170–176. doi: 10.1016/j.yebeh.2016.11.009

Canet, G., Zub, E., Zussy, C., Hernandez, C., Blaquiere, M., Garcia, V., et al. (2022). Seizure activity triggers tau hyperphosphorylation and amyloidogenic pathways. *Epilepsia* 63, 919–935. doi: 10.1111/epi.17186

Cendes, F., Kobayashi, E., and Lopes-Cendes, I. (2005). Familial temporal lobe epilepsy with auditory features. *Epilepsia* 46, 59–60.

Chang, C. W., Shao, E., and Mucke, L. (2021b). Tau: Enabler of diverse brain disorders and target of rapidly evolving therapeutic strategies. *Science* 371:eabb8255.

Chang, C. W., Evans, M. D., Yu, X., Yu, G. Q., and Mucke, L. (2021a). Tau reduction affects excitatory and inhibitory neurons differently, reduces excitation/inhibition ratios, and counteracts network hypersynchrony. *Cell Rep.* 37:109855. doi: 10.1016/j.celrep.2021.109855

Chao, L. H., Stratton, M. M., Lee, I. H., Rosenberg, O. S., Levitz, J., Mandell, D. J., et al. (2011). A mechanism for tunable autoinhibition in the structure of a human Ca2+/calmodulin- dependent kinase II holoenzyme. *Cell* 146, 732–745. doi: 10.1016/j.cell.2011.07.038

Chen, D., Wang, L., and Lee, T. H. (2020). Post-translational Modifications of the peptidyl-prolyl isomerase Pin1. *Front. Cell Dev. Biol.* 8:129. doi: 10.3389/fcell.2020.00129

Chen, M. W., Zhu, H., Xiong, C. H., Li, J. B., Zhao, L. X., Chen, H. Z., et al. (2020). PKC and Ras are involved in M1 muscarinic receptor-mediated modulation of AMPA receptor GluA1 subunit. *Cell. Mol. Neurobiol.* 40, 547–554. doi: 10.1007/s10571-019-00752-x

Cheng, C. W., and Tse, E. (2019). Targeting PIN1 as a therapeutic approach for hepatocellular carcinoma. *Front. Cell Dev. Biol.* 7:369. doi: 10.3389/fcell.2019.00369

Cioffi, C. L., and Guzzo, P. R. (2016). Inhibitors of Glycine Transporter-1: Potential therapeutics for the treatment of CNS disorders. *Curr. Topics Med. Chem.* 16, 3404–3437.

Coultrap, S. J., and Bayer, K. U. (2012). CaMKII regulation in information processing and storage. *Trends Neurosci.* 35, 607–618.

Daza-Martin, M., Starowicz, K., Jamshad, M., Tye, S., Ronson, G. E., MacKay, H. L., et al. (2019). Isomerization of BRCA1-BARD1 promotes replication fork protection. *Nature* 571, 521–527. doi: 10.1038/s41586-019-1363-4

Delgado, J. Y. (2020). An alternative Pin1 binding and isomerization Site in the N-terminus domain of PSD-95. *Front. Mol. Neurosci.* 13:31. doi: 10.3389/fnmol.2020.00031

Delgado, J. Y., Nall, D., and Selvin, P. R. (2020). Pin1 binding to phosphorylated PSD-95 regulates the number of functional excitatory synapses. *Front. Mol. Neurosci.* 13:10. doi: 10.3389/fnmol.2020.00010

Deng, X. L., Feng, L., Wang, Z. X., Zhao, Y. E., Zhan, Q., Wu, X. M., et al. (2020). The Runx1/Notch1 signaling pathway participates in M1/M2 microglia polarization in a mouse model of temporal lobe epilepsy and in BV-2 Cells. *Neurochem. Res.* 45, 2204–2216. doi: 10.1007/s11064-020-03082-3

Derkach, V., Barria, A., and Soderling, T. R. (1999). Ca2+/calmodulin-kinase II enhances channel conductance of alpha-amino-3-hydroxy-5-methyl-4-isoxazolepropionate type glutamate receptors. *Proc. Natl. Acad. Sci. U.S.A.* 96, 3269–3274. doi: 10.1073/pnas.96.6.3269

DeVos, S. L., Goncharoff, D. K., Chen, G., Kebodeaux, C. S., Yamada, K., Stewart, F. R., et al. (2013). Antisense reduction of tau in adult mice protects against seizures. *J. Neurosci.* 33, 12887–12897. doi: 10.1523/JNEUROSCI.2107-13.2013

Driver, J. A., and Lu, K. P. (2010). Pin1: A new genetic link between Alzheimer's disease, cancer and aging. *Curr. Aging Sci.* 3, 158–165.

Driver, J. A., Zhou, X. Z., and Lu, K. P. (2015). Pin1 dysregulation helps to explain the inverse association between cancer and Alzheimer's disease. *Biochim. Biophys. Acta* 1850, 2069–2076. doi: 10.1016/j.bbagen.2014.12.025

Duan, W., Chen, Y., and Wang, X. R. (2018). MicroRNA-155 contributes to the occurrence of epilepsy through the PI3K/Akt/mTOR signaling pathway. *Int. J. Mol. Med.* 42, 1577–1584. doi: 10.3892/ijmm.2018.3711

Fagiani, F., Govoni, S., Racchi, M., and Lanni, C. (2021). The peptidyl-prolyl isomerase Pin1 in neuronal signaling: From neurodevelopment to neurodegeneration. *Mol. Neurobiol.* 58, 1062–1073. doi: 10.1007/s12035-020-02179-8

Fang, M., Shen, L., Yin, H., Pan, Y. M., Wang, L., Chen, D., et al. (2011). Downregulation of gephyrin in temporal lobe epilepsy neurons in humans and a rat model. *Synapse* 65, 1006–1014. doi: 10.1002/syn.20928

Feng, D., Yao, J., Wang, G., Li, Z., Zu, G., Li, Y., et al. (2017). Inhibition of p66Shc-mediated mitochondrial apoptosis via targeting prolyl-isomerase Pin1 attenuates intestinal ischemia/reperfusion injury in rats. *Clin. Sci.* 131, 759–773. doi: 10.1042/CS20160799

Fisher, R. S., van Emde Boas, W., Blume, W., Elger, C., Genton, P., Lee, P., et al. (2005). epileptic seizures and epilepsy: Definitions proposed by the international league against epilepsy (ILAE) and the International Bureau for Epilepsy (IBE). *Epilepsia* 46, 470–472.

Förstera, B., Belaidi, A. A., Jüttner, R., Bernert, C., Tsokos, M., Lehmann, T. N., et al. (2010). Irregular RNA splicing curtails postsynaptic gephyrin in the cornu ammonis of patients with epilepsy. *Brain* 133, 3778–3794. doi: 10.1093/brain/awq298

Frasca, A., Aalbers, M., Frigerio, F., Fiordaliso, F., Salio, M., Gobbi, M., et al. (2011). Misplaced NMDA receptors in epileptogenesis contribute to excitotoxicity. *Neurobiol. Dis.* 43, 507–515. doi: 10.1016/j.nbd.2011.04.024

French, J. A., Krauss, G. L., Biton, V., Squillacote, D., Yang, H., Laurenza, A., et al. (2012). Adjunctive perampanel for refractory partial-onset seizures: Randomized phase III study 304. *Neurology* 79, 589–596.

French, J. A., Krauss, G. L., Steinhoff, B. J., Squillacote, D., Yang, H., Kumar, D., et al. (2013). Evaluation of adjunctive perampanel in patients with refractory partial-onset seizures: Results of randomized global phase III study 305. *Epilepsia* 54, 117–125. doi: 10.1111/j.1528-1167.2012.03638.x

Fu, H., Xu, H., Chen, H., Li, Y., Li, W., Zhu, Q., et al. (2014). Inhibition of glycogen synthase kinase 3 ameliorates liver ischemia/reperfusion injury via an energy-dependent mitochondrial mechanism. *J. Hepatol.* 61, 816–824. doi: 10.1016/j.jhep.2014.05.017

Gheyara, A. L., Ponnusamy, R., Djukic, B., Craft, R. J., Ho, K., Guo, W., et al. (2014). Tau reduction prevents disease in a mouse model of Dravet syndrome. *Ann. Neurol.* 76, 443–456. doi: 10.1002/ana.24230

Goel, A., Xu, L. W., Snyder, K. P., Song, L., Goenaga-Vazquez, Y., Megill, A., et al. (2011). Phosphorylation of AMPA receptors is required for sensory deprivation-induced homeostatic synaptic plasticity. *PLoS One* 6:e18264. doi: 10.1371/journal.pone.0018264

Greengard, P., Jen, J., Nairn, A. C., and Stevens, C. F. (1991). Enhancement of the glutamate response by cAMP-dependent protein kinase in hippocampal neurons. *Science* 253, 1135–1138.

Hayashi, Y., Shi, S. H., Esteban, J. A., Piccini, A., Poncer, J. C., and Malinow, R. (2000). Driving AMPA receptors into synapses by LTP and CaMKII: Requirement for GluR1 and PDZ domain interaction. *Science* 287, 2262–2267. doi: 10.1126/science.287.5461.2262

He, J., Lau, A. G., Yaffe, M. B., and Hall, R. A. (2001). Phosphorylation and cell cycle-dependent regulation of Na+/H+ exchanger regulatory factor-1 by Cdc2 kinase. *J. Biol. Chem.* 276, 41559–41565. doi: 10.1074/jbc.M106859200

He, K., Goel, A., Ciarkowski, C. E., Song, L., and Lee, H. K. (2011). Brain area specific regulation of synaptic AMPA receptors by phosphorylation. *Commun. Integr. Biol.* 4, 569–572.

Henshall, D. C., and Engel, T. (2013). Contribution of apoptosis-associated signaling pathways to epileptogenesis: Lessons from Bcl-2 family knockouts. *Front. Cell. Neurosci.* 7:110. doi: 10.3389/fncel.2013.00110

Hilton, B. A., Li, Z., Musich, P. R., Wang, H., Cartwright, B. M., Serrano, M., et al. (2015). ATR plays a direct antiapoptotic role at mitochondria, which is regulated by prolyl isomerase Pin1. *Mol. Cell* 60, 35–46.

Hou, X., Yang, F., Li, A., Zhao, D., Ma, N., Chen, L., et al. (2021). The Pin1-CaMKII-AMPA receptor axis regulates epileptic susceptibility. *Cereb. Cortex* 31, 3082–3095. doi: 10.1093/cercor/bhab004

Hu, F., Shao, L., Zhang, J., Zhang, H., Wen, A., and Zhang, P. (2020). Knockdown of ZFAS1 inhibits hippocampal neurons apoptosis and autophagy by activating the PI3K/AKT Pathway via Up-regulating miR-421 in Epilepsy. *Neurochem. Res.* 45, 2433–2441. doi: 10.1007/s11064-020-03103-1

Hu, J. H., Malloy, C., Tabor, G. T., Gutzmann, J. J., Liu, Y., Abebe, D., et al. (2020). Activity-dependent isomerization of Kv4.2 by Pin1 regulates cognitive flexibility. *Nat. Commun.* 11:1567. doi: 10.1038/s41467-020-15390-x

Huang, H., Liu, H., Yan, R., and Hu, M. (2017). PI3K/Akt and ERK/MAPK signaling promote different aspects of neuron survival and axonal regrowth following rat facial nerve axotomy. *Neurochem. Res.* 42, 3515–3524. doi: 10.1007/s11064-017-2399-1

Ittner, A., and Ittner, L. M. (2018). Dendritic tau in Alzheimer's disease. *Neuron* 99, 13–27.

Janning, D., Igaev, M., Sündermann, F., Brühmann, J., Beutel, O., Heinisch, J. J., et al. (2014). Single-molecule tracking of tau reveals fast kiss-and-hop interaction with microtubules in living neurons. *Mol. Biol. Cell* 25, 3541–3551. doi: 10.1091/mbc.E14-06-1099

Jenkins, M. A., and Traynelis, S. F. (2012). PKC phosphorylates GluA1-Ser831 to enhance AMPA receptor conductance. *Channels* 6, 60–64. doi: 10.4161/chan.18648

Kameyama, K., Lee, H. K., Bear, M. F., and Huganir, R. L. (1998). Involvement of a postsynaptic protein kinase A substrate in the expression of homosynaptic long-term depression. *Neuron* 21, 1163–1175. doi: 10.1016/s0896-6273(00)80633-9

Kankowski, S., Förstera, B., Winkelmann, A., Knauff, P., Wanker, E. E., You, X. A., et al. (2017). A novel RNA editing sensor tool and a specific agonist determine neuronal protein expression of RNA-edited glycine receptors and identify a genomic APOBEC1 dimorphism as a new genetic risk factor of epilepsy. *Front. Mol. Neurosci.* 10:439. doi: 10.3389/fnmol.2017.00439

Keeney, J. T., Swomley, A. M., Harris, J. L., Fiorini, A., Mitov, M. I., Perluigi, M., et al. (2012). Cell cycle proteins in brain in mild cognitive impairment: Insights into progression to Alzheimer disease. *Neurotox. Res.* 22, 220–230.

Kim, J. E., Choi, H. C., Song, H. K., and Kang, T. C. (2019). Perampanel affects up-stream regulatory signaling pathways of glua1 phosphorylation in normal and epileptic rats. *Front. Cell. Neurosci.* 13:80. doi: 10.3389/fncel.2019.00080

Kittler, J. T., and Moss, S. J. (eds) (2006). *The Dynamic Synapse: Molecular Methods in Ionotropic Receptor Biology*. Boca Raton, FL: CRC Press.

Knapp, A. G., Schmidt, K. F., and Dowling, J. E. (1990). Dopamine modulates the kinetics of ion channels gated by excitatory amino acids in retinal horizontal cells. *Proc. Natl. Acad. Sci. U.S.A.* 87, 767–771.

Kneussel, M., Brandstätter, J. H., Laube, B., Stahl, S., Müller, U., and Betz, H. (1999). Loss of postsynaptic GABA(A) receptor clustering in gephyrin-deficient mice. *J. Neurosci.* 19, 9289–9297.

Kondo, A., Shahpasand, K., Mannix, R., Qiu, J., Moncaster, J., Chen, C. H., et al. (2015). Antibody against early driver of neurodegeneration cis P-tau blocks brain injury and tauopathy. *Nature* 523, 431–436. doi: 10.1038/nature14658

Krapivinsky, G., Medina, I., Krapivinsky, L., Gapon, S., and Clapham, D. E. (2004). SynGAP-MUPP1-CaMKII synaptic complexes regulate p38 MAP kinase activity and NMDA receptor-dependent synaptic AMPA receptor potentiation. *Neuron* 43, 563–574. doi: 10.1016/j.neuron.2004.08.003

Krauss, G. L., Serratosa, J. M., Villanueva, V., Endziniene, M., Hong, Z., French, J., et al. (2012). Randomized phase III study 306: Adjunctive perampanel for refractory partial-onset seizures. *Neurology* 78, 1408–1415.

Kristensen, A. S., Jenkins, M. A., Banke, T. G., Schousboe, A., Makino, Y., Johnson, R. C., et al. (2011). Mechanism of Ca2+/calmodulin-dependent kinase II regulation of AMPA receptor gating. *Nat. Neurosci.* 14, 727–735. doi: 10.1038/nn.2804

Ladépêche, L., Dupuis, J. P., and Groc, L. (2014). Surface trafficking of NMDA receptors: Gathering from a partner to another. *Semin. Cell Dev. Biol.* 27, 3–13. doi: 10.1016/j.semcdb.2013.10.005

LaFerla, F. M., Hall, C. K., Ngo, L., and Jay, G. (1996). Extracellular deposition of beta-amyloid upon p53-dependent neuronal cell death in transgenic mice. *J. Clin. Invest.* 98, 1626–1632. doi: 10.1172/JCI118957

Lathia, J. D., Mattson, M. P., and Cheng, A. (2008). Notch: From neural development to neurological disorders. *J. Neurochem.* 107, 1471–1481.

Lee, H. K. (2006b). Synaptic plasticity and phosphorylation. *Pharmacol. Ther.* 112, 810–832.

Lee, H. K. (2006a). "Frontiers in Neuroscience AMPA Receptor Phosphorylation in Synaptic Plasticity: Insights from Knockin Mice," in *The Dynamic Synapse: Molecular Methods in Ionotropic Receptor Biology*, eds J. T. Kittler and S. J. Moss (Boca Raton, FL: CRC Press).

Li, J., Mo, C., Guo, Y., Zhang, B., Feng, X., Si, Q., et al. (2021). Roles of peptidyl-prolyl isomerase Pin1 in disease pathogenesis. *Theranostics* 11, 3348–3358.

Li, Q. M., Tep, C., Yune, T. Y., Zhou, X. Z., Uchida, T., Lu, K. P., et al. (2007). Opposite regulation of oligodendrocyte apoptosis by JNK3 and Pin1 after spinal cord injury. *J. Neurosci.* 27, 8395–8404.

Lin, C. H., Li, H. Y., Lee, Y. C., Calkins, M. J., Lee, K. H., Yang, C. N., et al. (2015). Landscape of Pin1 in the cell cycle. *Exp. Biol. Med.* 240, 403–408. doi: 10.1177/1535370215570829

Liou, Y. C., Zhou, X. Z., and Lu, K. P. (2011). Prolyl isomerase Pin1 as a molecular switch to determine the fate of phosphoproteins. *Trends Biochem. Sci.* 36, 501–514.

Lippman-Bell, J. J., Zhou, C., Sun, H., Feske, J. S., and Jensen, F. E. (2016). Early-life seizures alter synaptic calcium-permeable AMPA receptor function and plasticity. *Mol. Cell. Neurosci.* 76, 11–20. doi: 10.1016/j.mcn.2016.08.002

Liu, K., Zhu, J., Chang, Y., Lin, Z., Shi, Z., Li, X., et al. (2021). Attenuation of cerebral edema facilitates recovery of glymphatic system function after status epilepticus. *JCI Insight* 6:e151835. doi: 10.1172/jci.insight.151835

Liu, N. X., and Li, Q. H. (2020). LncRNA BC200 regulates neuron apoptosis and neuroinflammation via PI3K/AKT pathway in Alzheimer's disease. *J. Biol. Regul. Homeost. Agents* 34, 2255–2261. doi: 10.23812/20-498-L

Liu, S. J., Zheng, P., Wright, D. K., Dezsi, G., Braine, E., Nguyen, T., et al. (2016). Sodium selenate retards epileptogenesis in acquired epilepsy models reversing changes in protein phosphatase 2A and hyperphosphorylated tau. *Brain* 139, 1919–1938. doi: 10.1093/brain/aww116

Liu, X., Yang, Z., Yin, Y., and Deng, X. (2014). Increased expression of Notch1 in temporal lobe epilepsy: Animal models and clinical evidence. *Neural Regene. Res.* 9, 526–533. doi: 10.4103/1673-5374.130083

Lu, K. P., and Zhou, X. Z. (2007). The prolyl isomerase PIN1: A pivotal new twist in phosphorylation signalling and disease. *Nat. Rev. Mol. Cell Biol.* 8, 904–916. doi: 10.1038/nrm2261

Lu, K. P., Finn, G., Lee, T. H., and Nicholson, L. K. (2007). Prolyl cis-trans isomerization as a molecular timer. *Nat. Chem. Biol.* 3, 619–629.

Lu, K. P., Hanes, S. D., and Hunter, T. (1996). A human peptidyl-prolyl isomerase essential for regulation of mitosis. *Nature* 380, 544–547.

Lu, P. J., Zhou, X. Z., Shen, M., and Lu, K. P. (1999). Function of WW domains as phosphoserine- or phosphothreonine-binding modules. *Science* 283, 1325–1328.

Luh, L. M., Hänsel, R., Löhr, F., Kirchner, D. K., Krauskopf, K., Pitzius, S., et al. (2013). Molecular crowding drives active Pin1 into nonspecific complexes with endogenous proteins prior to substrate recognition. *J. Am. Chem. Soc.* 135, 13796–13803. doi: 10.1021/ja405244v

Luna-Muñoz, J., Chávez-Macías, L., García-Sierra, F., and Mena, R. (2007). Earliest stages of tau conformational changes are related to the appearance of

a sequence of specific phospho-dependent tau epitopes in Alzheimer's disease. *J. Alzheimers Dis.* 12, 365–375. doi: 10.3233/jad-2007-12410

Lynch, J. W., Zhang, Y., Talwar, S., and Estrada-Mondragon, A. (2017). Glycine receptor drug discovery. *Adv. Pharmacol.* 79, 225–253.

Macha, A., Liebsch, F., Fricke, S., Hetsch, F., Neuser, F., Johannes, L., et al. (2022). Biallelic gephyrin variants lead to impaired GABAergic inhibition in a patient with developmental and epileptic encephalopathy. *Hum. Mol. Genet.* 31, 901–913. doi: 10.1093/hmg/ddab298

Machado, R. A., Benjumea-Cuartas, V., Zapata Berruecos, J. F., Agudelo-Flóres, P. M., and Salazar-Peláez, L. M. (2019). Reelin, tau phosphorylation and psychiatric complications in patients with hippocampal sclerosis and structural abnormalities in temporal lobe epilepsy. *Epilepsy Behav.* 96, 192–199. doi: 10.1016/j.yebeh.2019.04.052

Moshé, S. L., Perucca, E., Ryvlin, P., and Tomson, T. (2015). Epilepsy: New advances. *Lancet* 385, 884–898.

Nakamura, K., Greenwood, A., Binder, L., Bigio, E. H., Denial, S., Nicholson, L., et al. (2012a). Proline isomer-specific antibodies reveal the early pathogenic tau conformation in Alzheimer's disease. *Cell* 149, 232–244. doi: 10.1016/j.cell.2012.02.016

Nakamura, K., Kosugi, I., Lee, D. Y., Hafner, A., Sinclair, D. A., Ryo, A., et al. (2012b). Prolyl isomerase Pin1 regulates neuronal differentiation via β-catenin. *Mol. Cell. Biol.* 32, 2966–2978. doi: 10.1128/MCB.05688-11

Nakatsu, Y., Mori, K., Matsunaga, Y., Yamamotoya, T., Ueda, K., Inoue, Y., et al. (2017). The prolyl isomerase Pin1 increases β-cell proliferation and enhances insulin secretion. *J. Biol. Chem.* 292, 11886–11895. doi: 10.1074/jbc.M117.780726

Nakatsu, Y., Sakoda, H., Kushiyama, A., Zhang, J., Ono, H., Fujishiro, M., et al. (2011). Peptidyl-prolyl cis/trans isomerase NIMA-interacting 1 associates with insulin receptor substrate-1 and enhances insulin actions and adipogenesis. *J. Biol. Chem.* 286, 20812–20822. doi: 10.1074/jbc.M110.206904

Naylor, D. E., Liu, H., Niquet, J., and Wasterlain, C. G. (2013). Rapid surface accumulation of NMDA receptors increases glutamatergic excitation during status epilepticus. *Neurobiol. Dis.* 54, 225–238. doi: 10.1016/j.nbd.2012.12.015

Newton, A. C. (2001). Protein kinase C: Structural and spatial regulation by phosphorylation, cofactors, and macromolecular interactions. *Chem. Rev.* 101, 2353–2364. doi: 10.1021/cr0002801

Oh, M. C., Derkach, V. A., Guire, E. S., and Soderling, T. R. (2006). Extrasynaptic membrane trafficking regulated by GluR1 serine 845 phosphorylation primes AMPA receptors for long-term potentiation. *J. Biol. Chem.* 281, 752–758. doi: 10.1074/jbc.M509677200

Opazo, P., Sainlos, M., and Choquet, D. (2012). Regulation of AMPA receptor surface diffusion by PSD-95 slots. *Curr. Opin. Neurobiol.* 22, 453–460. doi: 10.1016/j.conb.2011.10.010

Oyrer, J., Maljevic, S., Scheffer, I. E., Berkovic, S. F., Petrou, S., and Reid, C. A. (2018). Ion channels in genetic epilepsy: From genes and mechanisms to disease-targeted therapies. *Pharmacol. Rev.* 70, 142–173. doi: 10.1124/pr.117.014456

Partida, G. J., Fasoli, A., Fogli Iseppe, A., Ogata, G., Johnson, J. S., Thambiaiyah, V., et al. (2018). Autophosphorylated CaMKII facilitates spike propagation in rat optic nerve. *J. Neurosci.* 38, 8087–8105. doi: 10.1523/JNEUROSCI.0078-18.2018

Paudel, Y. N., Angelopoulou, E., Jones, N. C., O'Brien, T. J., Kwan, P., Piperi, C., et al. (2019). Tau related pathways as a connecting link between epilepsy and Alzheimer's disease. *ACS Chem. Neurosci.* 10, 4199–4212. doi: 10.1021/acschemneuro.9b00460

Peng, Y., Zhao, J., Gu, Q. H., Chen, R. Q., Xu, Z., Yan, J. Z., et al. (2010). Distinct trafficking and expression mechanisms underlie LTP and LTD of NMDA receptor-mediated synaptic responses. *Hippocampus* 20, 646–658. doi: 10.1002/hipo.20654

Perucca, P., Smith, G., Santana-Gomez, C., Bragin, A., and Staba, R. (2019). Electrophysiological biomarkers of epileptogenicity after traumatic brain injury. *Neurobiol. Dis.* 123, 69–74.

Puhahn-Schmeiser, B., Leicht, K., Gessler, F., and Freiman, T. M. (2021). Aberrant hippocampal mossy fibers in temporal lobe epilepsy target excitatory and inhibitory neurons. *Epilepsia* 62, 2539–2550. doi: 10.1111/epi.17035

Qiu, C., Albayram, O., Kondo, A., Wang, B., Kim, N., Arai, K., et al. (2021). Cis P-tau underlies vascular contribution to cognitive impairment and dementia and can be effectively targeted by immunotherapy in mice. *Sci. Transl. Med.* 13:eaaz7615. doi: 10.1126/scitranslmed.aaz7615

Ramakrishnan, P., Dickson, D. W., and Davies, P. (2003). Pin1 colocalization with phosphorylated tau in Alzheimer's disease and other tauopathies. *Neurobiol. Dis.* 14, 251–264. doi: 10.1016/s0969-9961(03)00109-8

Ranganathan, R., Lu, K. P., Hunter, T., and Noel, J. P. (1997). Structural and functional analysis of the mitotic rotamase Pin1 suggests substrate recognition is phosphorylation dependent. *Cell* 89, 875–886. doi: 10.1016/s0092-8674(00)80273-1

Rellos, P., Pike, A. C., Niesen, F. H., Salah, E., Lee, W. H., von Delft, F., et al. (2010). Structure of the CaMKIIdelta/calmodulin complex reveals the molecular mechanism of CaMKII kinase activation. *PLoS Biol.* 8:e1000426. doi: 10.1371/journal.pbio.1000426

Risal, P., Shrestha, N., Chand, L., Sylvester, K. G., and Jeong, Y. J. (2017). Involvement of prolyl isomerase PIN1 in the cell cycle progression and proliferation of hepatic oval cells. *Pathol. Res. Pract.* 213, 373–380. doi: 10.1016/j.prp.2017.01.005

Roberson, Halabisky, B., Yoo, J. W., Yao, J., Chin, J., Yan, F., et al. (2011). Amyloid-β/Fyn-induced synaptic, network, and cognitive impairments depend on tau levels in multiple mouse models of Alzheimer's disease. *J. Neurosci.* 31, 700–711. doi: 10.1523/JNEUROSCI.4152-10.2011

Roche, K. W., O'Brien, R. J., Mammen, A. L., Bernhardt, J., and Huganir, R. L. (1996). Characterization of multiple phosphorylation sites on the AMPA receptor GluR1 subunit. *Neuron* 16, 1179–1188. doi: 10.1016/s0896-6273(00)80144-0

Rogawski, M. A. (2013). AMPA receptors as a molecular target in epilepsy therapy. *Acta Neurol. Scand. Suppl.* 9–18. doi: 10.1111/ane.12099

Rogawski, M. A., and Donevan, S. D. (1999). AMPA receptors in epilepsy and as targets for antiepileptic drugs. *Adv. Neurol.* 79, 947–963.

Rohracher, A., Kalss, G., Kuchukhidze, G., Neuray, C., Leitinger, M., Höfler, J., et al. (2021). New anti-seizure medication for elderly epilepsy patients - a critical narrative review. *Expert Opin. Pharmacother.* 22, 621–634. doi: 10.1080/14656566.2020.1843636

Rong, X. F., Sun, Y. N., Liu, D. M., Yin, H. J., Peng, Y., Xu, S. F., et al. (2017). The pathological roles of NDRG2 in Alzheimer's disease, a study using animal models and APPwt-overexpressed cells. *CNS Neurosci. Ther.* 23, 667–679.

Rudrabhatla, P., and Pant, H. C. (2010). Phosphorylation-specific peptidyl-prolyl isomerization of neuronal cytoskeletal proteins by Pin1: Implications for therapeutics in neurodegeneration. *J. Alzheimers Dis.* 19, 389–403. doi: 10.3233/JAD-2010-1243

Rustighi, A., Tiberi, L., Soldano, A., Napoli, M., Nuciforo, P., Rosato, A., et al. (2009). The prolyl-isomerase Pin1 is a Notch1 target that enhances Notch1 activation in cancer. *Nat. Cell Biol.* 11, 133–142.

Sacktor, T. C. (2010). PINing for things past. *Sci. Signal.* 3:e9. doi: 10.1126/scisignal.3112pe9

Sargin, D., Botly, L. C., Higgs, G., Marsolais, A., Frankland, P. W., Egan, S. E., et al. (2013). Disrupting Jagged1-Notch signaling impairs spatial memory formation in adult mice. *Neurobiol. Learn. Mem.* 103, 39–49.

Shahpasand, K., Sepehri Shamloo, A., Nabavi, S. M., Ping Lu, K., and Zhen Zhou, X. (2018). Tau immunotherapy: Hopes and hindrances. *Hum. Vaccines Immunother.* 14, 277–284. doi: 10.1080/21645515.2017.1393594

Shepherd, J. D., and Huganir, R. L. (2007). The cell biology of synaptic plasticity: AMPA receptor trafficking. *Annu. Rev. Cell Dev. Biol.* 23, 613–643.

Shimizu, T., Kanai, K., Sugawara, Y., Uchida, C., and Uchida, T. (2018). Prolyl Isomerase Pin1 directly regulates calcium/calmodulin-dependent protein kinase II activity in mouse brains. *Front. Pharmacol.* 9:1351. doi: 10.3389/fphar.2018.01351

Sibbe, M., Häussler, U., Dieni, S., Althof, D., Haas, C. A., and Frotscher, M. (2012). Experimental epilepsy affects Notch1 signalling and the stem cell pool in the dentate gyrus. *Eur. J. Neurosci.* 36, 3643–3652. doi: 10.1111/j.1460-9568.2012.08279.x

Smet-Nocca, C., Launay, H., Wieruszeski, J. M., Lippens, G., and Landrieu, I. (2013). Unraveling a phosphorylation event in a folded protein by NMR spectroscopy: Phosphorylation of the Pin1 WW domain by PKA. *J. Biomol. NMR* 55, 323–337. doi: 10.1007/s10858-013-9716-z

Srivastava, P., Dhuriya, Y. K., Kumar, V., Srivastava, A., Gupta, R., Shukla, R. K., et al. (2018). PI3K/Akt/GSK3β induced CREB activation ameliorates arsenic mediated alterations in NMDA receptors and associated signaling in rat hippocampus: Neuroprotective role of curcumin. *Neurotoxicology* 67, 190–205. doi: 10.1016/j.neuro.2018.04.018

Steinberg, S. F. (2008). Structural basis of protein kinase C isoform function. *Physiol. Rev.* 88, 1341–1378.

Sugiura, Y., and Ugawa, Y. (2017). [Epilepsy and ion channels]. *Clin. Neurol.* 57, 1–8.

Sultana, R., Boyd-Kimball, D., Poon, H. F., Cai, J., Pierce, W. M., Klein, J. B., et al. (2006). Oxidative modification and down-regulation of Pin1 in Alzheimer's disease hippocampus: A redox proteomics analysis. *Neurobiol. Aging* 27, 918–925. doi: 10.1016/j.neurobiolaging.2005.05.005

Takahashi, K., Uchida, C., Shin, R. W., Shimazaki, K., and Uchida, T. (2008). Prolyl isomerase, Pin1: New findings of post-translational modifications and physiological substrates in cancer, asthma and Alzheimer's disease. *Cell. Mol. Life Sci.* 65, 359–375. doi: 10.1007/s00018-007-7270-0

Tang, L., Zhang, Y., Chen, G., Xiong, Y., Wang, X., and Zhu, B. (2017). Down-regulation of Pin1 in temporal lobe epilepsy patients and mouse model. *Neurochem. Res.* 42, 1211–1218. doi: 10.1007/s11064-016-2158-8

Tatara, Y., Terakawa, T., and Uchida, T. (2010). Identification of Pin1-binding phosphorylated proteins in the mouse brain. *Biosci. Biotechnol. Biochem.* 74, 2480–2483. doi: 10.1271/bbb.100580

Traynelis, S. F., Wollmuth, L. P., McBain, C. J., Menniti, F. S., Vance, K. M., Ogden, K. K., et al. (2010). Glutamate receptor ion channels: Structure, regulation, and function. *Pharmacol. Rev.* 62, 405–496.

Tretter, V., Mukherjee, J., Maric, H. M., Schindelin, H., Sieghart, W., and Moss, S. J. (2012). Gephyrin, the enigmatic organizer at GABAergic synapses. *Front. Cell. Neurosci.* 6:23. doi: 10.3389/fncel.2012.00023

Tun-Kyi, A., Finn, G., Greenwood, A., Nowak, M., Lee, T. H., Asara, J. M., et al. (2011). Essential role for the prolyl isomerase Pin1 in Toll-like receptor signaling and type I interferon-mediated immunity. *Nat. Immunol.* 12, 733–741. doi: 10.1038/ni.2069

Turrigiano, G. G., and Nelson, S. B. (2004). Homeostatic plasticity in the developing nervous system. *Nat. Rev. Neurosci.* 5, 97–107.

Van Liefferinge, J., Massie, A., Portelli, J., Di Giovanni, G., and Smolders, I. (2013). Are vesicular neurotransmitter transporters potential treatment targets for temporal lobe epilepsy? *Front. Cell. Neurosci.* 7:139. doi: 10.3389/fncel.2013.00139

Vannini, E., Restani, L., Dilillo, M., McDonnell, L. A., Caleo, M., and Marra, V. (2020). Synaptic vesicles dynamics in neocortical epilepsy. *Front. Cell. Neurosci.* 14:606142. doi: 10.3389/fncel.2020.606142

Varoqueaux, F., Jamain, S., and Brose, N. (2004). Neuroligin 2 is exclusively localized to inhibitory synapses. *Eur. J. Cell Biol.* 83, 449–456.

Wang, L., Zhou, Y., Chen, D., and Lee, T. H. (2020). peptidyl-prolyl Cis/trans isomerase Pin1 and Alzheimer's disease. *Front. Cell Dev. Biol.* 8:355. doi: 10.3389/fcell.2020.00355

Wang, Y., and Mandelkow, E. (2016). Tau in physiology and pathology. *Nat. Rev. Neurosci.* 17, 5–21.

Wang, S. C., Hu, X. M., and Xiong, K. (2023). The regulatory role of Pin1 in neuronal death. *Neural Regen. Res.* 18, 74–80.

Wang, Y., Wang, W., Li, D., Li, M., Wang, P., Wen, J., et al. (2014). IGF-1 alleviates NMDA-induced excitotoxicity in cultured hippocampal neurons against autophagy via the NR2B/PI3K-AKT-mTOR pathway. *J. Cell. Physiol.* 229, 1618–1629. doi: 10.1002/jcp.24607

Wang, Y., Wu, J., Guo, R., Zhao, Y., Wang, Y., Zhang, M., et al. (2013). Surgical incision induces phosphorylation of AMPA receptor GluR1 subunits at Serine-831 sites and GluR1 trafficking in spinal cord dorsal horn via a protein kinase Cγ-dependent mechanism. *Neuroscience* 240, 361–370. doi: 10.1016/j.neuroscience.2013.02.051

Wei, H., Duan, G., He, J., Meng, Q., Liu, Y., Chen, W., et al. (2018). Geniposide attenuates epilepsy symptoms in a mouse model through the PI3K/Akt/GSK-3β signaling pathway. *Exp. Therapeutic Med.* 15, 1136–1142. doi: 10.3892/etm.2017.5512

Winkelmann, A., Maggio, N., Eller, J., Caliskan, G., Semtner, M., Häussler, U., et al. (2014). Changes in neural network homeostasis trigger neuropsychiatric symptoms. *J. Clin. Investig.* 124, 696–711. doi: 10.1172/JCI71472

Yang, H., Zhang, P., Li, J., Gao, Y., Zhao, L., Li, J., et al. (2020). Targeting PIN-1 attenuates GCB DLBCL cell proliferation through inhibition of PI3K/AKT Signaling. *Onco Targets Ther.* 13, 8593–8600. doi: 10.2147/OTT.S247429

Yang, Y., and Igumenova, T. I. (2013). The C-terminal V5 domain of protein kinase Cα is intrinsically disordered, with propensity to associate with a membrane mimetic. *PLoS One* 8:e65699. doi: 10.1371/journal.pone.0065699

Yu, G. H., and Fang, Y. (2022). Resveratrol attenuates atherosclerotic endothelial injury through the Pin1/Notch1 pathway. *Toxicol. Appl. Pharmacol.* 446:116047. doi: 10.1016/j.taap.2022.116047

Yu, J. H., Im, C. Y., and Min, S. H. (2020). Function of PIN1 in cancer development and its inhibitors as cancer therapeutics. *Front. Cell Dev. Biol.* 8:120. doi: 10.3389/fcell.2020.00120

Yuan, W. C., Lee, Y. R., Huang, S. F., Lin, Y. M., Chen, T. Y., Chung, H. C., et al. (2011). A Cullin3-KLHL20 Ubiquitin ligase-dependent pathway targets PML to potentiate HIF-1 signaling and prostate cancer progression. *Cancer Cell* 20, 214–228. doi: 10.1016/j.ccr.2011.07.008

Zacchi, P., Antonelli, R., and Cherubini, E. (2014). Gephyrin phosphorylation in the functional organization and plasticity of GABAergic synapses. *Front. Cell. Neurosci.* 8:103. doi: 10.3389/fncel.2014.00103

Zafra, F., Ibáñez, I., Bartolomé-Martín, D., Piniella, D., Arribas-Blázquez, M., and Giménez, C. (2017). Glycine transporters and its coupling with NMDA receptors. *Adv. Neurobiol.* 16, 55–83.

Zannini, A., Rustighi, A., Campaner, E., and Del Sal, G. (2019). Oncogenic hijacking of the PIN1 signaling network. *Front. Oncol.* 9:94. doi: 10.3389/fonc.2019.00094

Zeng, B., Li, Y., Niu, B., Wang, X., Cheng, Y., Zhou, Z., et al. (2016). Involvement of PI3K/Akt/FoxO3a and PKA/CREB signaling pathways in the protective effect of fluoxetine against corticosterone-induced cytotoxicity in PC12 cells. *J. Mol. Neurosci.* 59, 567–578. doi: 10.1007/s12031-016-0779-7

Zhang, F., Ye, J., Meng, Y., Ai, W., Su, H., Zheng, J., et al. (2018). calcium supplementation enhanced adipogenesis and improved glucose homeostasis through activation of camkii and PI3K/Akt signaling pathway in porcine bone marrow mesenchymal stem cells (pBMSCs) and mice fed high fat diet (HFD). *Cell. Physiol. Biochem.* 51, 154–172. doi: 10.1159/000495171

Zhang, Y., Lv, Z., Liu, Y., Cao, H., Yang, J., and Wang, B. (2021). PIN1 protects hair cells and auditory HEI-OC1 cells against senescence by inhibiting the PI3K/Akt/mTOR pathway. *Oxid. Med. Cell. Longev.* 2021:9980444. doi: 10.1155/2021/9980444

Zhang, Z., Yu, W., Zheng, M., Liao, X., Wang, J., Yang, D., et al. (2019). Pin1 inhibition potently suppresses gastric cancer growth and blocks PI3K/AKT and Wnt/β-catenin oncogenic pathways. *Mol. Carcinog.* 58, 1450–1464. doi: 10.1002/mc.23027

Zhao, J. H., Wang, B., Wang, X. H., and Xu, C. W. (2019). Effect of lncRNA GAS5 on the apoptosis of neurons via the notch1 signaling pathway in rats with cerebral infarction. *Eur. Rev. Med. Pharmacol. Sci.* 23, 10083–10091. doi: 10.26355/eurrev_201911_19576

Zhou, X. Z., Kops, O., Werner, A., Lu, P. J., Shen, M., Stoller, G., et al. (2000). Pin1-dependent prolyl isomerization regulates dephosphorylation of Cdc25C and tau proteins. *Mol. Cell* 6, 873–883. doi: 10.1016/s1097-2765(05)00083-3

Zhou, X., and Lu, K. (2016). The isomerase PIN1 controls numerous cancer-driving pathways and is a unique drug target. *Nat. Rev. Cancer* 16, 463–478.

Zita, M. M., Marchionni, I., Bottos, E., Righi, M., Del Sal, G., Cherubini, E., et al. (2007). Post-phosphorylation prolyl isomerisation of gephyrin represents a mechanism to modulate glycine receptors function. *EMBO J.* 26, 1761–1771. doi: 10.1038/sj.emboj.7601625

frontiers | Frontiers in Molecular Neuroscience

TYPE Original Research
PUBLISHED 28 October 2022
DOI 10.3389/fnmol.2022.1028836

OPEN ACCESS

EDITED BY
Oliver Wirths,
University Medical Center Göttingen,
Germany

REVIEWED BY
Martin Fuhrmann,
Helmholtz Association of German Research Centers (HZ), Germany
Utpal Das,
University of California,
San Diego,
United States

*CORRESPONDENCE
Ulrike C. Müller
u.mueller@urz.uni-heidelberg.de

†These authors share senior authorship

SPECIALTY SECTION
This article was submitted to Brain Disease Mechanisms, a section of the journal Frontiers in Molecular Neuroscience

RECEIVED 26 August 2022
ACCEPTED 11 October 2022
PUBLISHED 28 October 2022

CITATION
Erdinger S, Amrein I, Back M, Ludewig S, Korte M, von Engelhardt J, Wolfer DP and Müller UC (2022) Lack of APLP1 leads to subtle alterations in neuronal morphology but does not affect learning and memory. *Front. Mol. Neurosci.* 15:1028836. doi: 10.3389/fnmol.2022.1028836

Lack of APLP1 leads to subtle alterations in neuronal morphology but does not affect learning and memory

Susanne Erdinger[1], Irmgard Amrein[2], Michaela Back[3], Susann Ludewig[4], Martin Korte[4,5], Jakob von Engelhardt[3], David P. Wolfer[2,6†] and Ulrike C. Müller[1*†]

[1]Department of Functional Genomics, Institute of Pharmacy and Molecular Biotechnology, Heidelberg University, Heidelberg, Germany, [2]Institute of Anatomy, University of Zurich and Institute of Human Movement Sciences, ETH Zurich, Zurich, Switzerland, [3]Institute of Pathophysiology, Focus Program Translational Neuroscience (FTN), University Medical Center of the Johannes Gutenberg University Mainz, Mainz, Germany, [4]Zoological Institute, Division of Cellular Neurobiology, TU Braunschweig, Braunschweig, Germany, [5]Helmholtz Centre for Infection Research, AG NIND, Braunschweig, Germany, [6]Zurich Center for Integrative Human Physiology, University of Zurich, Zurich, Switzerland

The amyloid precursor protein APP plays a crucial role in Alzheimer pathogenesis. Its physiological functions, however, are only beginning to be unraveled. APP belongs to a small gene family, including besides APP the closely related amyloid precursor-like proteins APLP1 and APLP2, that all constitute synaptic adhesion proteins. While APP and APLP2 are ubiquitously expressed, APLP1 is specific for the nervous system. Previous genetic studies, including combined knockouts of several family members, pointed towards a unique role for APLP1, as only APP/APLP1 double knockouts were viable. We now examined brain and neuronal morphology in APLP1 single knockout (KO) animals, that have to date not been studied in detail. Here, we report that APLP1-KO mice show normal spine density in hippocampal CA1 pyramidal cells and subtle alterations in dendritic complexity. Extracellular field recordings revealed normal basal synaptic transmission and no alterations in synaptic plasticity (LTP). Further, behavioral studies revealed in APLP1-KO mice a small deficit in motor function and reduced diurnal locomotor activity, while learning and memory were not affected by the loss of APLP1. In summary, our study indicates that APP family members serve both distinct and overlapping functions that need to be considered for therapeutic treatments of Alzheimer's disease.

KEYWORDS

Alzheimer disease, APP, APLP1, amyloid precursor like protein, synaptic plasticity, behavior, learning, memory

Introduction

The amyloid precursor protein (APP) is best known for its crucial role in Alzheimer's disease pathogenesis (De Strooper and Karran, 2016; Haass and Selkoe, 2022), whereas its physiological functions are only beginning to be unraveled (Mockett et al., 2017; Müller et al., 2017). APP belongs to a small gene family of type I transmembrane proteins, which includes in mammals the amyloid precursor like protein 1 and 2 (APLP1 and APLP2) (reviewed in (Müller et al., 2017)). The APP family members show several common features, including complex proteolytic processing by α-, β- and γ-secretase (Scheinfeld et al., 2002; Eggert et al., 2004; Endres et al., 2005; Kuhn et al., 2016; Müller et al., 2017). In addition, APP family proteins share a similar structural organization with conserved E1 and E2 regions located in their large extracellular domains and a highly conserved cytoplasmic tail that links them to a rich network of interacting factors implicated in signaling (Müller et al., 2017). The Aβ peptide, located at the juxtamembrane region is, however, unique for APP.

APP family proteins are highly expressed in neurons, in somata, axons and dendrites and are localized to pre- and postsynaptic sites (Lassek et al., 2013; DeBoer et al., 2014; Del Turco et al., 2016; Schilling et al., 2017), where they function as transsynaptic adhesion molecules that undergo homotypic and heterotypic dimerization (Soba et al., 2005; Kaden et al., 2008; Baumkotter et al., 2014; Stahl et al., 2014; Schilling et al., 2017). Consistent with this, APP family proteins are upregulated both at central and peripheral synapses during postnatal development coinciding with synaptogenesis (Schilling et al., 2017). Whereas APP and APLP2 are ubiquitously expressed in most tissues, APLP1 expression is restricted to neurons (Slunt et al., 1994; Lorent et al., 1995; Thinakaran et al., 1995). At the neuromuscular junction for example, APP and APLP2 are expressed in nerve and muscle, whereas APLP1 is located specifically at innervating axons (Wang et al., 2005, 2009; Caldwell et al., 2013; Klevanski et al., 2014; Schilling et al., 2017).

Gene knockout studies yielded important insights into physiological functions of the APP family for a variety of processes, notably synapse formation, maintenance and plasticity *in vivo*. While mouse mutants lacking only a single family member are fully viable, combined germline APP/APLP2 double knockout (DKO), APLP1/APLP2-DKO and APP/APLP1/APLP2 triple knockout (TKO) mice die shortly after birth (Li et al., 1996; von Koch et al., 1997; Steinbach et al., 1998; Heber et al., 2000; Herms et al., 2004) due to impairments at the neuromuscular junction (Wang et al., 2005, 2009; Weyer et al., 2011; Klevanski et al., 2014; Han et al., 2017) revealing genetic evidence for partially overlapping functions. This is further corroborated by studies of conditional, brain-specific combined mutants (Hick et al., 2015; Richter et al., 2018; Mehr et al., 2020; Steubler et al., 2021). Interestingly, while constitutive germline APLP1/APLP2-DKO mice are lethal, constitutive APLP1/APP-DKO mice proved viable, indicating specific, unique functions for APLP1 (Heber et al., 2000). APLP2-KO mice exhibit normal body weight, grip strength, motor coordination and cognition (von Koch et al., 1997; Weyer et al., 2014). In contrast, APP-KO mice show reduced body weight, reduced grip strength, impaired locomotor activity, impaired passive avoidance and spatial learning, as well as impaired synaptic plasticity (Dawson et al., 1999; Seabrook et al., 1999; Fitzjohn et al., 2000; Ring et al., 2007; Senechal et al., 2008; Zou et al., 2016; Galanis et al., 2021).

Compared to APP, much less is known about the functions of APLP1. Recently, we showed that APLP1 functions as a synaptic cell adhesion molecule with, compared to APP and APLP2, increased transcellular binding and elevated cell-surface levels (Schilling et al., 2017). Interestingly, in AD patients secreted fragments of APLP1 arising due to β-secretase (BACE) processing have recently been identified as a sensitive cerebrospinal fluid biomarker (Dislich et al., 2015; Simoes et al., 2020). In addition, APLP1 has recently been implicated as a possible receptor for α-synuclein fibrils mediating their cell-to-cell transmission (Zhang et al., 2021). As therapeutics targeting APP processing (e.g., BACE and other secretase inhibitors) may also affect APP/APLPs physiological functions, it is thus important to elucidate possible consequences for each APP family member. Here, we studied neuronal morphology in the hippocampus of APLP1-KO mice, examined basal synaptic transmission and synaptic plasticity at the CA3/CA1 pathway, performed a detailed analysis of neuromotor behavior and assessed their performance in various tasks for learning and memory. APLP1-KO mice revealed no deficit in spine density of CA1 neurons and only subtle alterations in dendritic branching. At the behavioral level we report reduced grip strength and impaired locomotor activity, whereas no significant deficits were found in cognitive tasks, consistent with normal synaptic plasticity.

Results

Hippocampal pyramidal cells of APLP1-KO mice exhibit normal spine density and only subtle deficits in dendritic branching

Consistent with previous studies (Heber et al., 2000; Steubler et al., 2021), brain slices of APLP1-KO mice (age at analysis: 5–6 months) showed no gross morphological abnormalities in cortex and hippocampus (Figure 1A) and no astrogliosis and microgliosis as unspecific signs of neurodegeneration. As analysis of APP-KO mice had previously revealed impairments in neuronal morphology of cortical and hippocampal pyramidal cells (Seabrook et al., 1999; Lee et al., 2010; Tyan et al., 2012; Weyer et al., 2014), we first evaluated spine density as a correlate of excitatory synapse numbers. To this end CA1 neurons were filled with biocytin and stained with Alexa594-conjugated Streptavidin. Spine density analysis (age: 4–5 months; see Figure 1B for examples of dendritic segments) revealed no significant differences between APLP1-KO CA1 pyramidal cells, as compared to wild

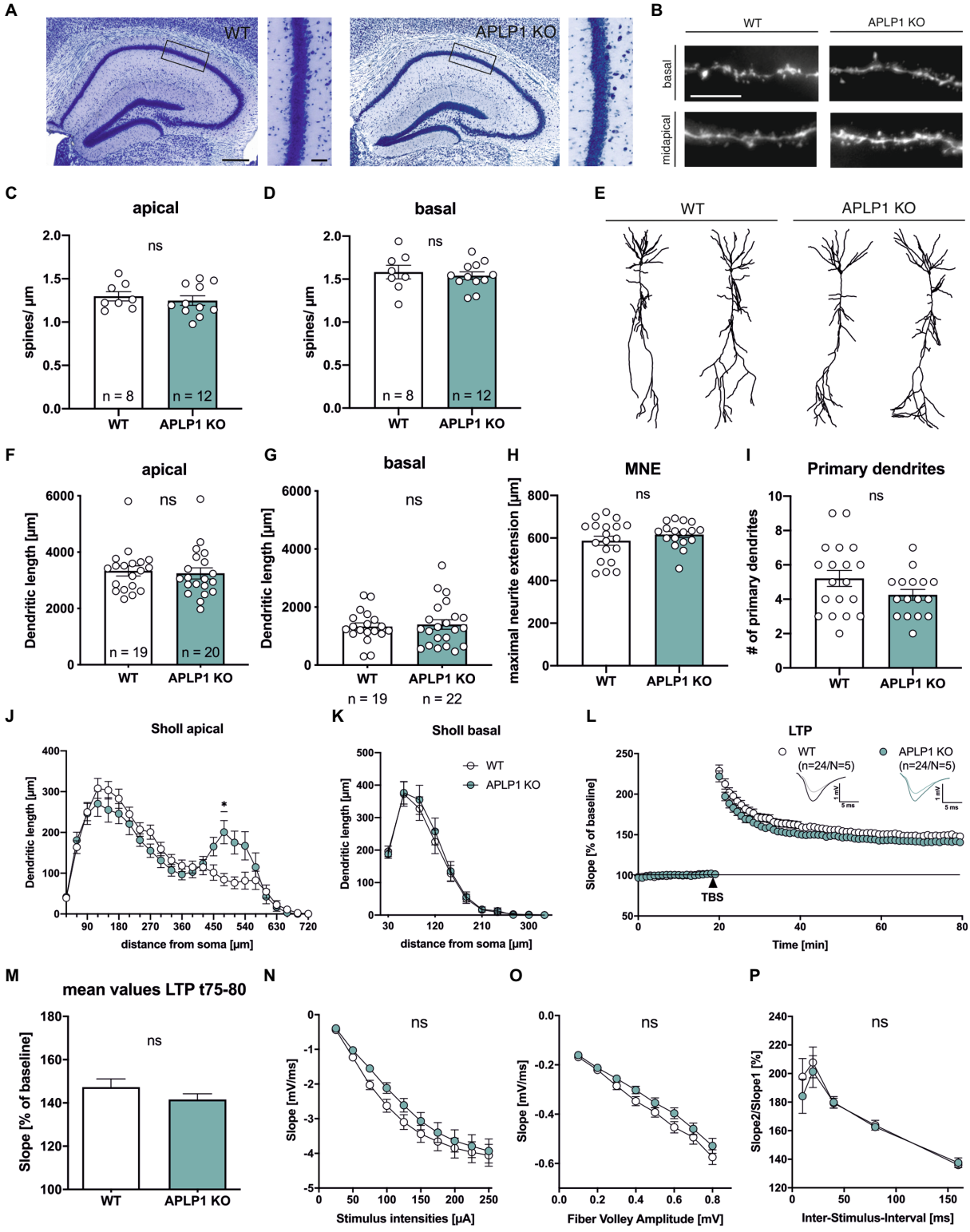

FIGURE 1
APLP1-KOs show no gross morphological defects and only subtle deficits in neuronal morphology. **(A)**: Giemsa-stained, glycolmethacrylate-embedded coronal brain sections (bregma –1.9) displaying the hippocampus and adjacent callosal fiber tracts of a wildtype WT, left and a APLP1-KO (right; age: 5–6months). Scale bar: 200µm, close-up: 50µm. **(B)**: Representative images of basal and midapical dendritic segments. Brightness and contrast were adjusted to ensure a uniform appearance. Scale bar: 5µm. **(C, D)**: Spine density of CA1 pyramidal cells is not significantly altered in midapical dendritic segments (C; unpaired Student's *t*-test, $^{ns}p=0.5306$), as well as in basal dendritic segments (D; unpaired Student's t-test, $^{ns}p=0.6281$). **(E)**: Representative 3D reconstructions of CA1 pyramidal neurons from both genotypes. **(F)**: Compared to wildtype controls, CA1 neurons of APLP1-KO

(Continued)

FIGURE 1 (Continued)
animals show no significant reduction in total dendritic length in apical dendrites (Mann–Whitney test, $^{ns}p=0.6667$). **(G)**: Compared to wildtype controls, CA1 neurons of APLP1-KO animals show no significant reduction in total dendritic length in basal dendrites (unpaired Student's t-test, $^{ns}p=0.7506$). **(H)**: APLP1-KO neurons show no altered maximal neurite extension (MNE) of apical dendrites compared to wildtype controls (unpaired Student's *t*-test, $^{ns}p=0.283$). **(I)**: The number of primary basal dendrites is significantly unchanged in APLP1-KO animals compared to WT in CA1 (unpaired Student's *t*-test, $^{ns}p=0.1137$). **(J)**: Sholl analysis reveals no genotype effect on apical dendritic segments of CA1 pyramidal neurons (WT: n =19, N =3; APLP1-KO: n=20/N =4). **(K)**: Sholl analysis reveals no genotype effect on basal dendritic segments of CA1 pyramidal neurons (WT: n =19, N =3; APLP1-KO: n =22/N =4). **(L)**: After 20min baseline recording, LTP was induced by application of Theta burst stimulation (TBS, arrowhead). Acute slices of APLP1-KO mice displayed an LTP curve that is statistical indistinguishable in induction and maintenance to that of wildtype controls. **(M)**: Averaged potentiation levels of the last 5min of LTP (55–60min after TBS) were 147.31±3.79% in wildtype slices compared to 141.59±2.66% in APLP1-KOs (Student's *t*-test, $^{ns}p=0.23$). **(N)**: Neuronal excitability was comparable at all stimulus intensities (25–250μA) between genotypes. **(O)**: Analyzing the Input–Output (IO) strength revealed no alterations between groups at any FV amplitude. **(P)**: PPF was unaltered between wildtype and APLP1-KO mice. Data information: n =number of neurons, N=number of animals. Age of animals **(B)–(K)**: 4–5months. Age of animals **(L)–(P)**: 3–4months. Data are represented as mean±SEM.

type (WT) neurons in both apical (1.24 ± 0.05 in APLP1-KO vs. 1.30 ± 0.05 in WT, ns, see Figure 1C) and basal dendrites (1.54 ± 0.05 in APLP1-KO vs. 1.58 ± 0.08 in WT, ns, see Figure 1D).

Subsequently, biocytin filled neurons were imaged and their dendritic tree was reconstructed for Sholl analysis (Figures 1E–K). Due to their different connectivity, the apical and basal dendrites of CA1 neurons were analyzed separately. Overall, pyramidal CA1 neurons of APLP1-KO mice showed no significant alteration in the total dendritic length of apical (3,246 ± 197 μm for APLP1-KO vs. 3,333 ± 179 μm for WT, see Figure 1F) or basal dendrites (1,399 ± 165 μm for APLP1-KO vs. 1,330 ± 125 μm for WT, see Figure 1G), similar maximal extension of apical dendrites (Figure 1H) and similar number of primary basal dendrites (Figure 1I).

Next, we performed a more detailed analysis by plotting the dendritic length (measured within circles centered on the soma), against the distance from the soma. In this analysis, an increased dendritic length per Sholl sphere corresponds to an increase in dendritic complexity. Apical dendrites of APLP1-KO CA1 neurons showed reduced branching towards more distant dendritic segments, with a significant decrease in complexity in dendritic segments at 480 μm from the soma (200.8 vs. 84.18 μm, Figure 1J). In contrast to this rather subtle difference in branching observed for apical dendrites, basal dendrites of CA1 neurons from APLP1-KO mice showed no difference in dendritic complexity (Figure 1K).

APLP1-KO mice exhibit normal basal synaptic transmission and no alterations in synaptic plasticity

To study potential functional differences at the level of the hippocampal network we performed extracellular field recordings in acute hippocampal slices from mice of both genotypes. We first assessed long-term potentiation (LTP), a cellular process believed to underly learning and memory (Bliss and Lomo, 1973; Korte and Schmitz, 2016). After 20 min of stable baseline recording LTP was induced by Thetaburst stimulation (TBS) of the Schaffer collaterals and monitored for 60 min (Figure 1L). LTP was not significantly altered between APLP1-KO and WT controls resulting in closely overlapping LTP curves shortly after TBS and during the LTP maintenance phase (Figure 1L). Averaged potentiation levels of the last 5 min of LTP (t75-80, 55–60 min after TBS; see Figure 1M) were 147.31 ± 3.79% in wildtype control slices compared to 141.59 ± 2.66% in APLP1-KOs (Student's t-test, $p = 0.23$). We also examined basal synaptic transmission and studied pre- and postsynaptic functionality. No significant differences between genotypes were detected when comparing the strength of fEPSP responses resulting from defined, increasing stimulus intensities (Figure 1N). Likewise, we failed to detect significant differences when correlating fiber volley amplitudes with fEPSP responses (input–output curves; Figure 1O), together indicating no major alterations at the postsynaptic side. Finally, to study putative presynaptic changes in APLP1-KO mice, we investigated short-term plasticity using the paired pulse facilitation (PPF) paradigm. APLP1-KO mice revealed no significant alteration in facilitation, when analyzing the ratio of fEPSP slopes resulting from two closely separated afferent stimuli (Figure 1P). Together, these data suggest normal basal synaptic transmission and synaptic plasticity in the hippocampus of mice lacking APLP1.

APLP1-KO mice show deficits in grip strength and impairments in locomotor and exploratory activity

We first studied body weight, that was unaltered in APLP1-KO mice (Figure 2A). As a baseline for subsequent cognitive tests, we started by examining the neuromotor performance of APLP1-KO mice. Compared to WT controls, APLP1-KO mice showed a small (about 14%) but significant deficit in forelimb grip strength (97.32 ± 3.05 vs. 83.66 ± 3.027, Figure 2B). On the rotarod that assesses motor coordination APLP1-KO mice showed slightly reduced motor learning during early trials (trial 2–4, see Figure 2C), but improved to levels undistinguishable from WTs at the final trial, with overall performance across trials not significantly different from WT animals (Figure 2C). Monitoring of the diurnal activity profile in a familiar home cage, we observed for APLP1-KO mice no difference in activity during the light phase, but severely reduced activity during the dark phase (35.75 vs. 22.66 s, Figure 2D). Similarly, also in the open field mutant

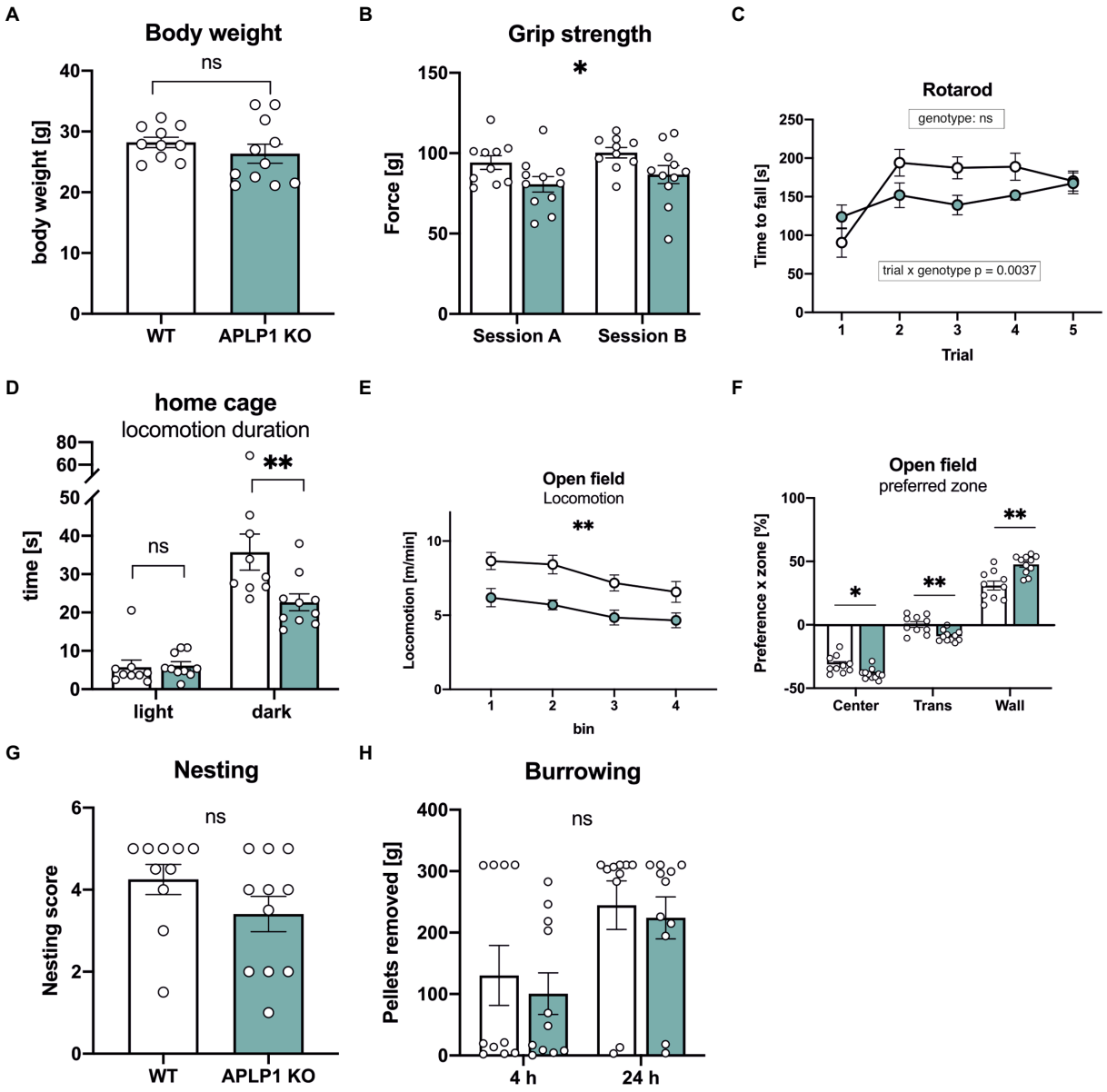

FIGURE 2
APLP1-KOs exhibit small impairments in innate and locomotor behavior. **(A)**: Bodyweight of APLP1-KOs is not different from wildtype controls (unpaired Student's t-test, ^{ns}p=0.3272). **(B)**: Grip force of APLP1-KO animals is slightly reduced comparted to wildtype controls in two test sessions. [geno F (1, 19)=5.079, p =0.0362; session F (1, 19)=5.282, p =0.0331; session × geno F (1, 19)=7.387e-005ns]. **(C)**: Rotarod performance is comparable between APLP1-KO animals and wildtype controls. [geno F (1, 19)=1.768ns; trial F (2.875, 54.63)=11.18, p <0.0001; trial × geno F (4, 76)=4.259, p =0.0037]. **(D)**: Locomotion in the home cage. APLP1-KOs showed reduced activity in the dark phase. [geno F (1, 17)=3.615, p =0.0743; phase F (1, 17)=144.8, p < 0.0001; phase × geno F (1, 17)=12.29, p =0.0027]. **(E)**: Open Field activity of APLP1-KOs is reduced compared to controls during exploration of a novel open field arena [geno F (1, 19)=13.38 p =0.0017; bin F (2.186, 41.54)=11.20, p < 0.0001; bin × geno F (3, 57)=0.4333, ns]. **(F)**: Open Field, APLP1-KOs showed an increased avoidance of the center field and a higher preference for the wall zone. [zone F (1.317, 25.03)=387.5, p < 0.0001; zone × geno F (2, 38)=14.60, p < 0.0001]. **(G)**: The nest score of APLP1-KOs is not significantly different from that of wildtype controls (unpaired Student's t-test, ^{ns}p=0.1577). **(H)**: Burrowing: Pellets removed from tube after 4 and 24h. Maximum to be removed=310g. Burrowing behavior was not significantly different between genotypes [geno F (1, 19)=0.2828, ns; time F (1, 19)=16.82, p =0.0006; time × geno F (1, 19)=0.02605, ns]. Data information: **(A–C; E–H)** number of animals: N = 10 WT, N = 11 APLP1-KO, age of animals 5months. **(D)** number of animals: N = 9 WT, N = 10 APLP1-KO, age of animals 3–4months. Data were analyzed using a mixed ANOVA model and are represented as mean±SEM. $*p < p$ <0.05, $**p$ <0.01, $***p$ <0.001, $****p$ <0.0001, ns not significant.

mice showed deficits in basal locomotion throughout testing (7.709 vs. 5.349 m/min, Figure 2E). Both groups showed, however, habituation in the second 10 min of testing, with reduced activity as compared to the first 10 min. In addition, APLP1-KO mice spent more time along the wall of the open field arena (Figure 2F) at the expense of time spent in the center or intermediate zones,

which may indicate reduced exploratory activity or increased anxiety. Next, mice were tested in the nesting and burrowing paradigms, two innate species-typic behaviors that are highly sensitive to hippocampal dysfunction (Deacon, 2006a, b). In both tests, APLP1-KO mice showed no significant impairments (Figures 2G, H).

APLP1-KO mice show no significant deficits in spatial working memory

To assess possible deficits in learning and memory, mice underwent testing in a series of hippocampus dependent tasks. Working memory was studied in an unbaited T-maze that exploits the natural tendency of mice to show alternating visits between the two arms of the maze. Spontaneous alternation rates of APLP1-KO mice in the T-maze were indistinguishable from those of WT controls (Figure 3A).

Next, to assess spatial working memory, mice underwent testing in an 8-arm fully baited radial maze. Overall, APLP1-KO mice showed normal performance and collected on average all 8 baits, similar to WT mice (Figure 3B). More detailed analysis of performance over trials indicated that APLP1-KO mice have a stronger tendency to use a non-spatial strategy to solve the task. As such, they showed an increase in chaining choices visiting adjacent arms of the maze more frequently (Figure 3C), paradoxically earning them superior performance scores compared to WT mice during the first 2 days of training (Figure 3D). In both groups, the number of reentry errors increased with the number of baits already collected, reflecting the increasing challenge of working memory. APLP1-KO mice showed fewer reentry errors when collecting the last two baits (Figure 3E), likely due to their increased use of chaining choices. In this regard, and consistent with their impaired spontaneous locomotor activity, APLP1-KO mice also spend more time resting and lingering (walking: movement bouts >5 cm and > 8.5 cm/s, resting: >2 s <2.5 cm/s, lingering: rest + any deceleration deeper than 15 cm/s) in the center zone of the maze (Figure 3F), which may prevent them from performing inadvertent reentry errors (Figure 3F). In summary, APLP1-KO mice showed no impairments in spatial working memory, but showed a more pronounced use of a non-spatial strategy.

APLP1-KO mice show no significant deficits in spatial reference memory

Next, mice were tested in the Morris water maze place navigation task with 3 days of acquisition learning, followed by 2 days of reversal learning (Figure 4). Both groups of mice showed similar learning curves, with a similar decline of path length required to reach the platform (Figure 4B). Also escape latency was indistinguishable between groups during the acquisition phase (Figure 4A), despite slightly increased swim speed in APLP1-KO mice (Figure 4C). When the platform was relocated to the opposite quadrant on day 4 of testing APLP1-KO mice showed, unlike WT mice, no reversal effect (e.g., increase) in swim path (Figure 4A). To assess whether this may indicate less persistent searching in the trained quadrant or maybe due to differences in search strategy, we also analyzed the path length parallel to wall of the arena (Figure 4D). Indeed, APLP1-KO mice showed an increased percentage of their overall pathlength parallel to the border, which increases the likelihood to find the platform by chance. During the probe trial (first trial after platform relocation), both groups of mice showed a clear and statistically indistinguishable preference for the trained target quadrant (Figure 4E), indicating normal spatial reference memory in APLP1-KO mice. After place navigation, the platform was labelled with a flag to test for cued navigation. Both groups of mice showed similar performance with similar path length and escape latency, excluding visual problems in APLP1 mutant mice (Figures 4F, G).

Finally, mice underwent testing in the Barnes maze that consists of a brightly lit circular table with 20 circular holes around its circumference. Under one of the holes is an "escape box" which the mouse can reach through the corresponding hole on the table top. The test exploits the rodents' aversion to open spaces, motivating them to seek shelter in the escape box. Both lines of mice rapidly learned the task and showed an indistinguishable decline in escape latency (Figure 5A). Further, no difference was detectable in the number of errors that declined in a similar manner during the five consecutive days of training (Figure 5B). As APLP1-KO had a higher tendency for a non-spatial strategy in the radial maze, we also analyzed the percentage of trials with a direct spatial strategy, versus serial and mixed approaches to find the escape hole. However, no significant difference between groups was detectable (Figure 5C). Likewise, during the probe trial, that was conducted 24 h after the last training session to test for spatial reference memory, APLP1-KO mice showed robust spatial retention of the goal position, with the number of correct pokes indistinguishable from WT mice (Figure 5D, correct pokes = angle 0°). We also failed to detect any difference in the number of pokes into adjacent or further distant holes between APLP1-KO and WT mice (Figure 5D). Taken together our data indicate largely normal cognition in APLP1-KO mice, with unimpaired spatial learning and normal short term and spatial reference memory.

Discussion

Brain architecture and neuronal morphology

In contrast to APP, that constitutes the precursor of Aβ peptides that accumulate as extracellular plaques in the brains of AD patients, the functions of APLP1 have been studied in much

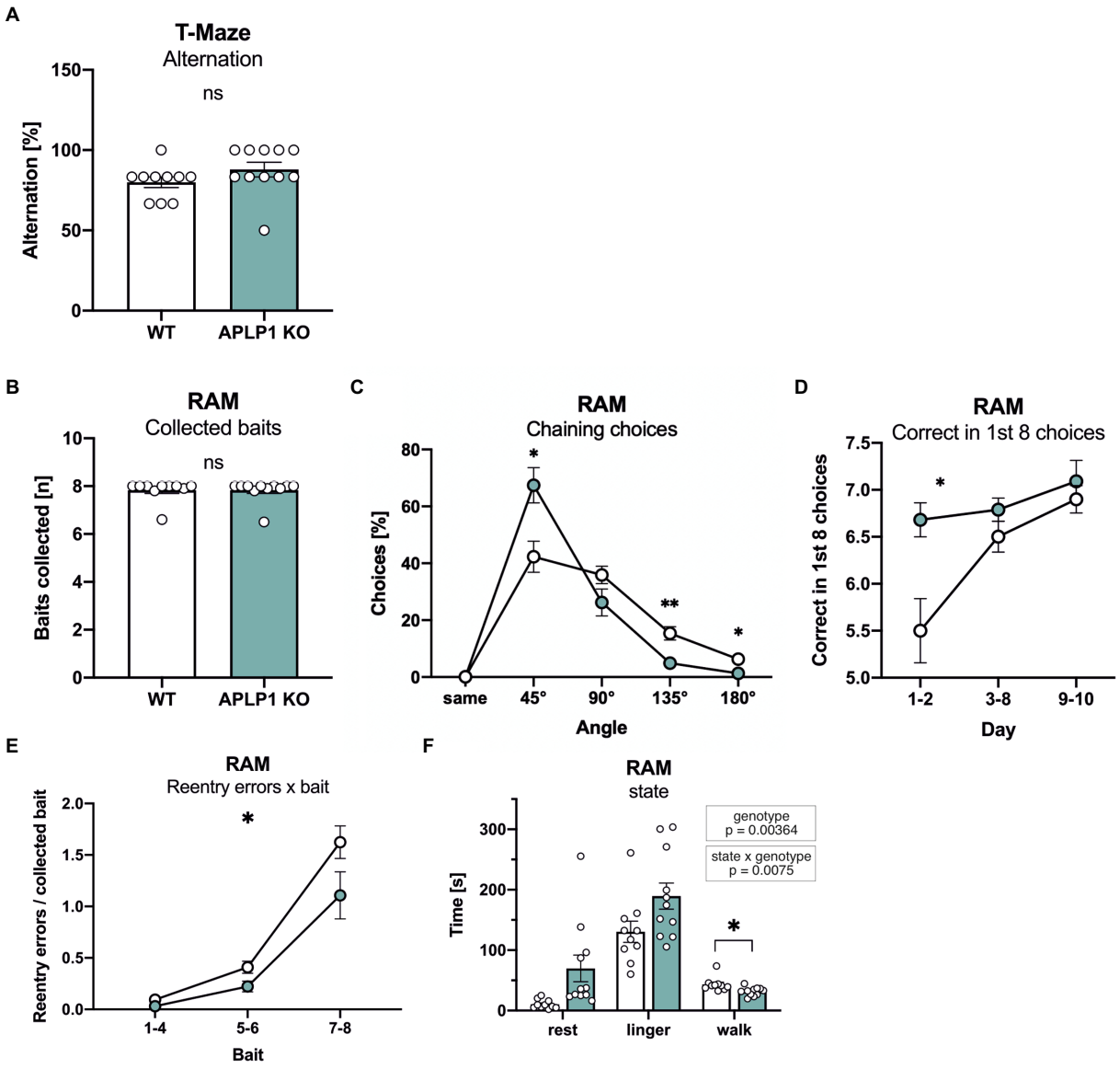

FIGURE 3
APLP1-KO mice exhibit normal short-term memory but use non-spatial search strategies more frequently. **(A)**: T-Maze alternation test shows no significant difference between genotypes (Mann–Whitney test, $^{ns}p=0.1149$). **(B)**: Radial Arm Maze (RAM). Almost all animals from both genotypes collected all baits during the test (Mann–Whitney test, $^{ns}p=0.8565$). **(C)**: RAM, APLP1-KOs showed a higher tendency for chaining choices than wildtype controls. [geno F (1, 19)=1.791, ns; angle F (1.141, 21.68)=74.31, p <0.0001; angle × geno F (4, 76)=7.631, p <0.0001]. **(D)**: RAM, during training, APLP1-KO mice made more correct among the first 8 choices than wildtype controls, especially at the first two days of training. [geno F (1, 19)=9.792, p =0.0055; day F (1.405, 26.69)=10.20, p =0.0015; day × geno F (2, 38)=3.660, p =0.0352]. **(E)**: RAM, APLP1-KO animals made less reentry errors than controls during training. [geno F (1, 19)=5.474, p =0.0304; bait F (1.110, 21,09)=74.62, p <0.0001; bait × geno F (2, 38)=2.131ns]. **(F)**: RAM, APLP1-KO mice spent less time walking, but more time resting and lingering than wildtype controls [geno F (1, 19)=5.069, p =0.00364; state F (1.918, 36.43)=65.03, p <0.0001; state × geno F (2, 38)=5.576, p =0.0075 Data information: number of animals: N = 10 WT, N = 11 APLP1-KO, age of animals 5months. Data were analyzed using a mixed ANOVA model and are represented as mean±SEM. $*p$ <0.05, $**p$ <0.01, $***p$ <0.001, $****p$ <0.0001, ns not significant.

less detail. Recent studies however, revived the interest in APLP1, as it may serve as a (co)-receptor for α-synuclein fibrils (Zhang et al., 2021) and can be classified as a synaptic adhesion molecule (Schilling et al., 2017). Moreover, recently generated triple knockout mice lacking the whole APP gene family in the forebrain indicated an essential role of APP and the APLPs for brain development and function, as evidenced by severe impairments in synaptic function, plasticity and behavior, in particular completely disrupted learning and memory (Steubler et al., 2021). To generate these cTKO mice we had used a NexCre driver line that was crossed with $APP^{flox/flox}APLP2^{flox/flox}$APLP1-KO mice (designated as APLP1-KO) to generate conditional NexCre-cTKO

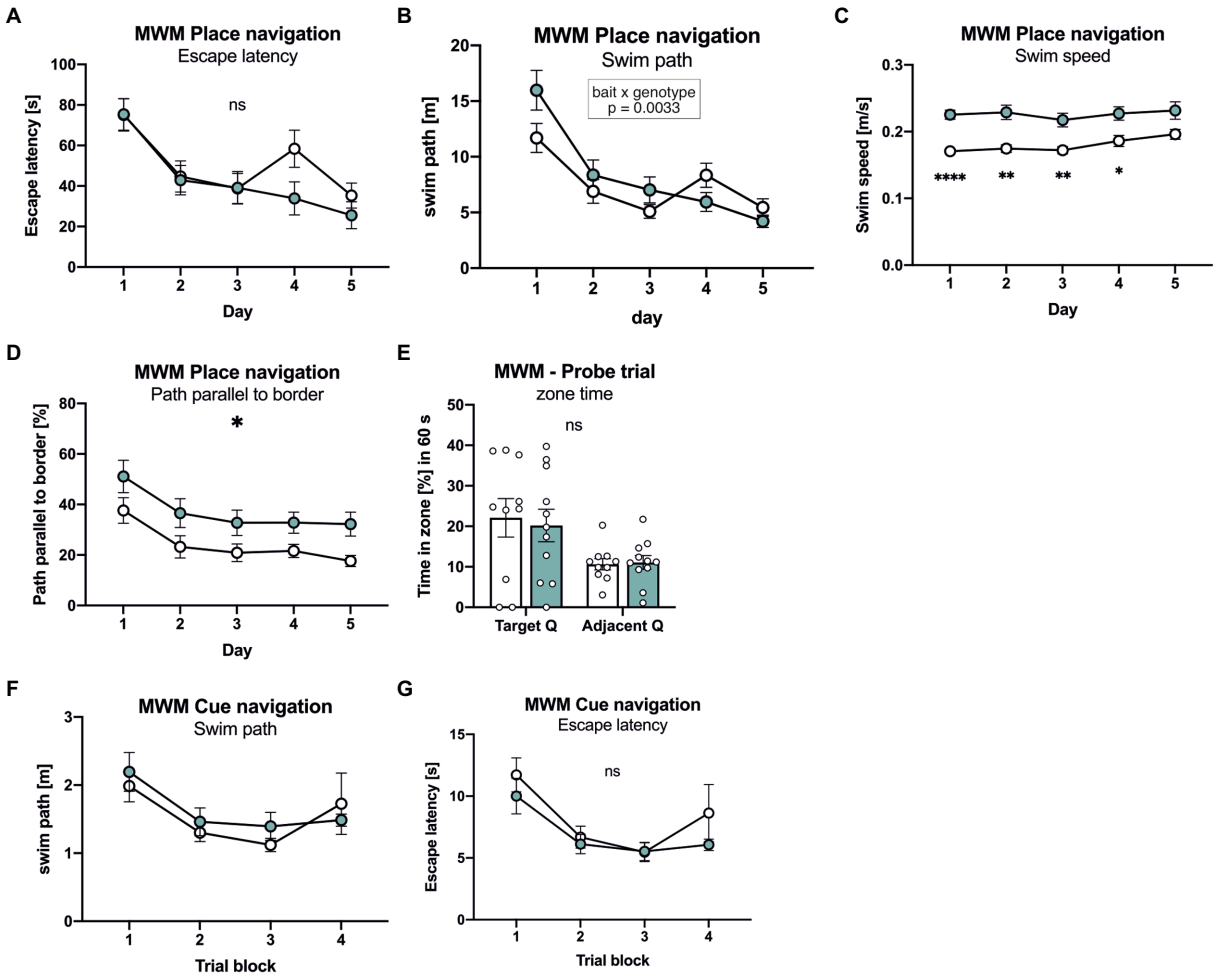

FIGURE 4
APLP1-KOs show no deficits in spatial learning and spatial reference memory. **(A)**: MWM, escape latency. During place navigation training, both genotypes showed evidence of learning. [geno F (1, 19)=0.6471ns; day F (3.455, 65.64)=22.86, p <0.0001; day × geno F (4, 76)=2.228ns]. **(B)**: Morris Water Maze (MWM), swim path. Both genotypes shortened their swim path over trials. Of note, wildtype controls showed a reversal effect while APLP1-KOs did not [geno F (1, 19)=0.5215ns; day F (2.871, 54.54)=29.73, p <0.0001; day × geno F (4, 76)=4.321, p =0.0033]. **(C)**: MWM, Swim speed of APLP1-KO animals was higher than in wildtype controls. [geno F (1, 19)=20.47, p =0.0002; day F (3.020, 57.39)=3.562, p =0.0194; day × geno F (4, 76)=1.113ns]. **(D)**: MWM, path parallel to the border. APLP1-KOs spent more time parallel to the border of the basin than wildtype controls. [geno F (1, 19)=6.912, p =0.0165; day F (2.286, 43.44)=10.47, p =0.0001; day × geno F (4, 76)=0.07723ns]. **(E)**: MWM, both genotypes preferred the trained target quadrant over the adjacent quadrant [geno F (1, 19)=0.04617ns; day F (1, 19)=10.55, p =0.0042; day × geno F (1, 19)=0.1404ns]. **(F)**: MWM, during cue navigation task, both genotypes do not differ in length of their swim path [geno F (1, 18)=0.2342ns; trial block F (2.596, 46.72)=5.613, p =0.0034; trial block × geno F (3, 54)=0.5595ns]. **(G)**: MWM, during cue navigation task, escape latency is not different between genotypes. [geno F (1, 18)=1.139ns; trial block F (2.581, 46.46)=9.433, p=0.0001; trial block × geno F (3, 54)=0.5880ns]. Data information: **(A)–(E)** number of animals: N = 10 WT, N = 11 APLP1-KO, age of animals 5months. **(F, G)** number of animals: N = 10 WT, N = 11 APLP1-KO, age of animals 6months. Data were analyzed using a mixed ANOVA model and are represented as mean±SEM. $*p$ <0.05, $**p$ <0.01, $***p$ <0.001, $****p$ <0.0001, ns not significant.

mice and APLP1-KO littermate controls. Here, we now performed a detailed characterization of APLP1-KO mice as compared to WT mice to delineate potential APLP1 specific deficits.

We had previously shown that APLP1-KO mice show no gross alterations in brain morphology, with unaltered neocortical volume and normal layering of the cortex and hippocampus (Steubler et al., 2021). Unlike NexCre-cTKO mice, that showed a high incidence of callosal agenesis/dysgenesis, APLP1-KO mice were indistinguishable from WT controls (Steubler et al., 2021), indicating that APLP1 is not essential for normal development of this fiber tract connecting both brain hemispheres. Likewise, single deficiency of APP or APLP2 was not sufficient to cause agenesis of the corpus callosum, which points towards compensation within the gene APP family that may serve overlapping functions with regard to axonal outgrowth (Wang et al., 2017; Steubler et al., 2021).

Sholl analysis of hippocampal CA1 cells from APLP1-KO mice revealed rather subtle deficits in neuronal morphology, as evidenced by reduced dendritic branching in distal segments of the apical dendrite, while branching of basal dendrites and total

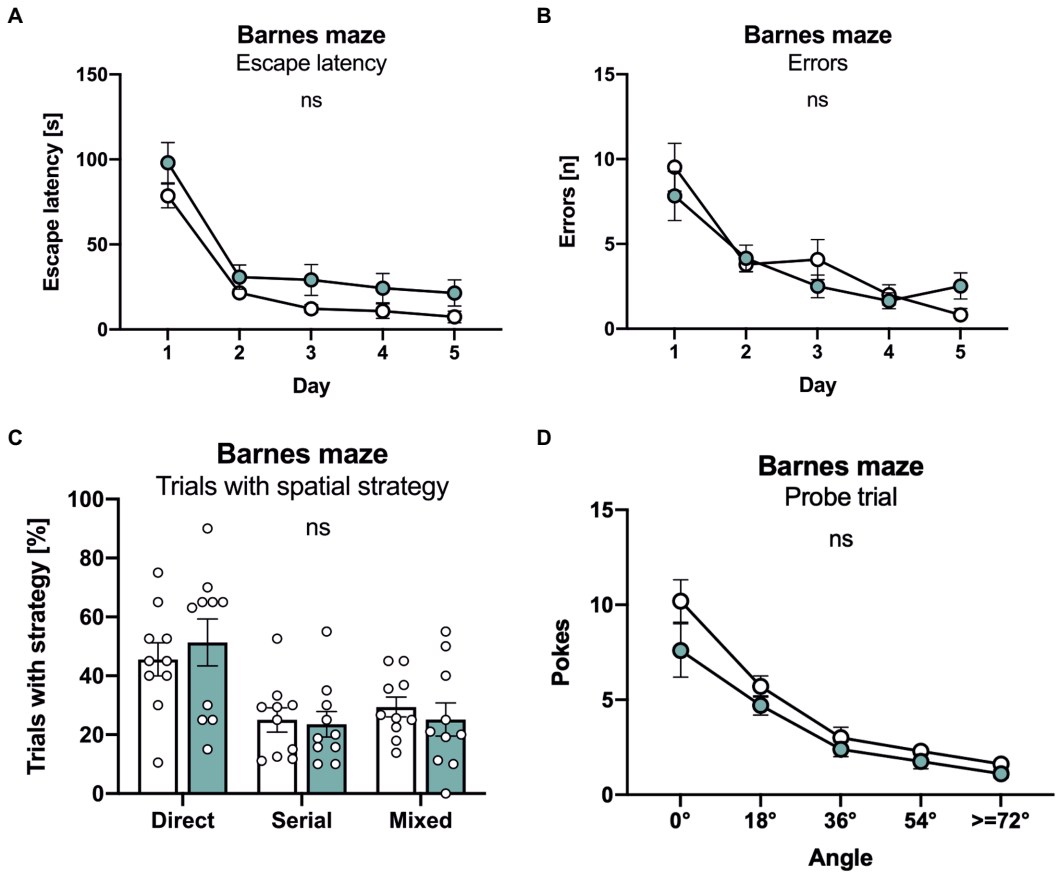

FIGURE 5
APLP1-KOs show no deficits in the Barnes maze. **(A)**: Barnes Maze (BM), throughout training, latency to escape the maze decreased similarly in APLP1-KO and control animals. [geno F (1, 18)=4.271ns; day F (2.347, 42.24)=61.08, p <0.0001; day × geno F (4, 72)=0.2359ns]. **(B)**: BM, APLP1-KO animals reduced their number of errors during training to the same extent as wildtype controls. [geno F (1, 18)=0.1351ns; day F (2.279, 41.03)=29.47, p <0.0001; day × geno F (4, 72)=1.812ns]. **(C)**: BM, trials of APLP1-KO mice with a direct spatial strategy was not significantly altered compared to wildtype controls. [strategy F (1.412, 25.42)=7.964ns; geno x strategy F (2, 36)=0.3051ns]. **(D)**: BM, during the probe trial, APLP1-KO animals performed as well as wildtype controls. [geno F (1, 18)=3.113ns; angle F (1.465, 26.37)=54.39, p <0.0001; angle × geno F (4, 72)=1.129ns]. Data information: number of animals: N = 10 WT, N = 11 APLP1-KO, age of animals 6months. Data were analyzed using a mixed ANOVA model and are represented as mean±SEM. $*p$ <0.05, $**p$ <0.01, $***p$ <0.001, $****p$ <0.0001, ns not significant.

dendritic length were unaffected. As APP family proteins have also been implicated in axonal outgrowth (Müller et al., 2017; Wang et al., 2017; Steubler et al., 2021) it is possible that the subtle reduction in dendritic complexity in distal regions of apical dendrites of APLP1-KO mice might also be related to changes in axonal projections from CA3, although this deserves further studies. Similar to APLP2-KO mice (Weyer et al., 2011; Midthune et al., 2012), young adult APLP1-KO mice did not show deficits in spine density at either apical or basal dendrites of CA1 pyramidal cells. Consitent with this, extracellular field recordings showed no alteration of basal excitatory synaptic transmission. Although APP and APLPs are upregulated postnatally during synaptogenesis and can potently induce pre-synaptic specializations *in vitro* (Schilling et al., 2017), our findings indicate that (1) they are not essential for initial synaptogenesis during development and/or (2) may have overlapping functions that require combined knockouts to reveal more severe phenotypes. Indeed, decreases in spine density were found in both aged APP-KO mice (Lee et al., 2010; Tyan et al., 2012), as well as in aged APLP1-KO mice together with reduced frequency of miniature EPSCs (Schilling et al., 2017). In contrast, APLP2 deficient mice had normal spine density even upon aging (Weyer et al., 2011; Midthune et al., 2012). Together, this indicates an essential role for spine maintenance for APLP1 and APP, although the underlying mechanism still needs to be unraveled. Together, normal brain architecture and only subtle alterations in neuronal morphology are also consistent with largely normal cognition in young APLP1-KO mice (see below). Consistent with overlapping physiological functions in the APP family, mice with brain-specific combined APP/APLP2 double KO mice revealed pronounced impaired spine density and morphology already in young adult mice *in vivo* (Hick et al., 2015; Richter et al., 2018; Steubler et al., 2021) that was associated with impaired LTP, learning and memory.

Neuromotor functions and cognition

Our analysis of APLP1-KO mice indicated normal motor learning and coordination on the accelerating rotarod, but subtle deficits in grip strength, similar to APP-KO mice (Ring et al., 2007). Although newborn APLP1-KO mice exhibit, like APP-KOs, normal neuromuscular innervation and morphology with unaltered size of axonal presynaptic terminals and postsynaptic boutons (Klevanski et al., 2014), this does not exclude functional impairments. In this regard, electrophysiological analysis in neonatal (p18-22) APP-KO mice showed that grip strength deficits are associated with increased depression of synaptic transmission at the neuromuscular junction after high frequency stimulation of the phrenic nerve (Yang et al., 2007). This decrease in maximal grip strength of APLP1-KO mice contrasts, however, with an increase in swim speed during water maze testing, although the underlying reason for this discrepancy is currently unclear. Further, locomotor activity of APLP1-KO mice was impaired in the home cage and the open field, indicating together subtle impairments in neuromotor function in the absence of APLP1.

Interestingly, APLP1-KO mice proved unimpaired in all cognitive tasks (T maze, radial maze, Morris water maze, Barnes maze), as well as in nesting and burrowing tasks that are sensitive to hippocampal dysfunction. As such, they showed normal escape latency and normal probe trial performance both in the Barnes maze and in the Morris water maze, indicating normal spatial learning and spatial reference memory. This is further corroborated by normal synaptic plasticity. Similarly, performance of APLP1-KO mice on the radial- and T-mazes suggest normal spatial working memory. Refined analysis revealed increased use of a non-spatial chaining strategy by APLP1-KO mice both in the water-maze and radial-maze. While this could in principle reflect compensation of a subtle memory deficit, intact performance in the water-maze probe trial and in the T-maze - that does not allow chaining - render this unlikely and speak in favor of mere motivational differences. It will now be interesting to see whether aged APLP1-KO mice may develop behavioral impairments as observed for APP-KO mice (Dawson et al., 1999; Seabrook et al., 1999; Ring et al., 2007). In contrast to APP-KO mice, however, that not only showed aged dependent deficits in learning but also in synaptic plasticity at the CA3/CA1 pathway (Dawson et al., 1999; Seabrook et al., 1999; Ring et al., 2007), LTP impairments were absent in aged APLP1-KO mice (Schilling et al., 2017), indicating nonoverlapping specific functions for APP and APLP1 with regard to synaptic plasticity. This may be due to the absence of the CTα16 domain, located at the very C-terminus of APPsα, that was recently identified as the major LTP-enhancing region (Hick et al., 2015; Richter et al., 2018; Morrissey et al., 2019) and is not conserved in APLP1 and APLP2. In summary, our study indicates that APP family members serve both distinct and overlapping functions that are essential for nervous system development, synaptic plasticity and behavior. When targeting APP in the course of therapeutic intervention for AD, or APLP1 to inhibit α-synuclein propagation in Parkinson's Disease, it will therefore be crucial to avoid compromising shared physiological functions within the APP family.

Materials and methods

Mice

APLP1-KO mice used in this study carry in addition floxed APP and APLP2 alleles and express APP and APLP2 at wild type level (Heber et al., 2000; Mallm et al., 2010). Genotyping was performed as described (Heber et al., 2000; Mallm et al., 2010). These $APP^{flox/flox}APLP2^{flox/flox}$APLP1-KO mice (referred to as APLP1-KO mice) had been generated as controls in a previous study of conditional APP/APLP1/APLP2 cTKO mice (Steubler et al., 2021). Here, we studied APLP1-KO mice as compared to C57Bl/6J mice as the age-matched control group (further referred to as WT). Experiments involving animals were performed in accordance with the guidelines and regulations set forth by the German Animal Welfare Act, the Regierungspräsidium Karlsruhe and the Niedersächsiches Landesamt für Verbraucherschutz und Lebensmittelsicherheit Germany. Behavioral procedures were approved by the Veterinary Office of the Canton of Zurich (license ZH044/15, #26394). Animals were housed in the same room with a 12 h/12 h light/dark-cycle in Makrolon Type II (360 cm^2) cages with standard bedding, either alone or in groups, and had *ad libitum* access to standard chow and water.

Neuronal morphology and spine density analysis

CA1 pyramidal neurons used for morphological analysis were filled with a solution containing 0.1–0.5% biocytin (Sigma Aldrich) through a patch pipette. Acute slices were fixed in 4% Histofix (Carl Roth). After 2–10 days, the slices were washed in 1x PBS (phosphate-buffered saline) for 3× 10 min. Permeabilization was performed for 1 h in 0.2% PBST (0.2% Triton X-100 in 1x PBS). Slices were stained overnight with Alexa 594-conjugated Streptavidin directed against biocytin (Life Technologies). On the next day, the slices were washed again for 3× 10 min in 1x PBS. After air-drying the slices at RT for 1 h, they were mounted with a coverslip in ProLong Gold Antifade (Life Technologies).

Image acquisition

Images of filled neurons were acquired at the inverted fluorescence microscope Axio Observer Z1 using Plan Apo 20x/0.8 DICII and Plan Apo 63x/1.4 Oil DICII objectives (Zeiss). Overview images of the whole neuron for reconstruction were taken with a 20x objective and a z-step size of 0.5 µm. Basal and apical dendrites were imaged individually with two overlapping stacks. More detailed images of basal and apical dendritic segments for spine density analysis were acquired with a 63x oil objective and a z-step size of

130 nm. Exposure time was individually set for each cell so that the complete range of the grayscale was used.

Neuronal morphology and spine counts

Sholl analyisis and spine density analysis was performed as decribed (Steubler et al., 2021). Biocytin filled hippocampal CA1 neurons were manually reconstructed using the Neurolucida software (MicroBrightField) by an experimenter blind to genotype. Neurons were only included in Sholl analysis if they showed a completely filled apical or basal tree and well-defined dendritic endings. The morphometric Sholl analysis was done using the NeuroExplorer software (MicroBrightField). In short, a series of concentric spheres (centered on the soma) was drawn with an intersection interval of 30 µm and the number of dendrites crossing each sphere as well as the dendritic length in between each sphere was calculated. This analysis was done separately for basal and apical dendrites of CA1 pyramidal cells and was plotted against the distance from the soma.

For evaluation of basal dendritic spine density, at least 3 different dendritic segments of the basal dendritic arbor were imaged. They had to fulfill the following criteria: (1) Lie mostly horizontally to the slice surface, (2) be at least 20 µm away from the soma, (3) have a comparable thickness. The minimum basal dendritic length imaged per neuron was 100 µm. For evaluation of midapical dendritic spine density, at least 3 different dendritic segments of the apical tree were imaged. Midapical was defined as the middle third of the length of the apical dendrite measured from the origin of the apical dendrite from the soma to the endpoint of the tufts. Dendritic segments used for evaluation had to fulfil the following criteria: (1) be of second or third order to assure comparable shaft thickness, (2) lie in the middle third of the main apical dendrite (3) be longer than 10 µm. The minimum midapical dendritic length imaged per neuron was 100 µm. Files in the zvi format were imported into ImageJ (NIH) using the BioFormats Importer. After adjusting, images were saved in the TIFF format. Dendritic spines were manually counted using the Neurolucida and NeuroExplorer software (MicroBrightField) following the criteria of Holtmaat (Holtmaat et al., 2009) with minor modifications: (1) All spines that protruded laterally from the dendritic shaft and exceeded a length of 0.4 µm were counted. (2) Spines that protruded into the z-plane were only counted if they exceeded the dendritic shaft more than 0.4 µm to the lateral side. (3) Spines that bisected were counted as two spines. (4) Spines had to be at least 10 µm away from branching points and the soma. Spine density was expressed as spines per µm of dendrite. Prior to statistical analysis and blind to genotype, neurons were excluded if the image quality (poor signal to noise ratio) was not sufficient for counting of spines. Data acquisition and analysis were performed blind to genotype.

Preparation of acute hippocampal slices and extracellular field recordings

Extracellular recordings were performed on acute hippocampal slices of WT littermates and APLP1 KO animals ($N = 5$), as previously described (Schilling et al., 2017; Steubler et al., 2021). Acute hippocampal transversal slices were prepared from individuals at an age of 3–4 months Mice were anesthetized with isoflurane and decapitated. The brain was removed and quickly transferred into ice-cold carbogenated (95% O_2, 5% CO_2) artificial cerebrospinal fluid (ACSF) containing 125.0 mM NaCl, 2.0 mM KCl, 1.25 mM NaH_2PO_4, 2.0 mM $MgCl_2$, 26.0 mM $NaHCO_3$, 2.0 mM $CaCl_2$, 25.0 mM glucose. The hippocampus was sectioned into 400 µm thick transversal slices with a vibratome (Leica, VT1200S) and maintained in carbogenated ACSF at room temperature for at least 1.5 h before transferred into a submerged recording chamber. Slices were placed in a submerged recording chamber and perfused with carbogenated ACSF (32°C) at a rate of 1.2 to 1.5 ml/min. Field excitatory postsynaptic potentials (fEPSPs) were recorded in stratum radiatum of CA1 region with a borosilicate glass micropipette (resistance 2–5 MΩ) filled with 3 M NaCl at a depth of ~150–200 µm. Monopolar tungsten electrodes were used for stimulating the Schaffer collaterals at a frequency of 0.1 Hz. Stimulation intensity was adjusted to ~40% of maximum fEPSP slope for 20 min baseline recording. LTP was induced by applying theta-burst stimulation (TBS: 10 trains of 4 pulses at 100 Hz in a 200 ms interval, repeated 3 times) and recorded for 60 min.

Basal synaptic transmission properties were analyzed *via* input–output-(IO) measurements and short-term plasticity was examined *via* paired pulse facilitation (PPF). The IO-measurements were performed either by application of defined current values (25–250 µA) or by adjusting the stimulus intensity to certain fiber volley (FV) amplitudes (0.1–0.8 mV). PPF was performed by applying a pair of two closely spaced stimuli in different inter-stimulus-intervals (ISI) ranging from 10 to 160 ms.

Behavioral analysis

Neuromotor behavior and cognitive tests

Animals

Twenty-one Mice were tested in total: 11 APLP1 KO animals (APP $^{flox/flox}$/APLP2 $^{flox/flox}$/APLP1$^{-/-}$; 5 females, 6 males) and 10 WT controls (C57Bl/6 J; 2 females, 8 males). Animals were housed under a 12/12 h light–dark cycle (lights on at 20:00) in groups of 2–5, unless individual housing was required by experimental protocols or to prevent fighting. Testing occurred during the dark phase under dim light (approximately 22 lux) if not stated otherwise, identity of genotype was blinded to the experimenter. Mice were transferred to the testing room 30 min before testing. Procedures were approved by the Veterinary Office of the Canton of Zurich (license ZH044/15, #26394).

Animals were aged 5 months at the beginning of behavioral testing. Test sequence was as follows: Open field, grip test, rotarod, water maze place navigation, burrowing, nesting, T-maze, radial maze, Barnes maze and water maze cue navigation. Tests including recovery periods in-between lasted 7 weeks.

Homecage, diurnal, and repetitive behavior

Home cage activity was recorded as described previously (Madani et al., 2003; Steubler et al., 2021) using a cage rack equipped with one passive IR sensor per mouse (ActiviScope, New Behavior Inc.,).[1] The sensors detected any locomotion and remained silent only when the mice were sleeping or grooming. Recording started after a habituation period of at least 18 h, and circadian activity profiles were calculated by averaging data from 11 recording days.

Open field

Activity was tested as described previously (Madani et al., 2003; Steubler et al., 2021). In brief, animals were tested on two consecutive days for 10 min in the open field, a circular arena of 150 cm in diameter. Mice were tracked using Noldus EthoVision 11.5 software.[2] For analysis of movement patterns, the arena was divided into a wall zone (18% of surface, 7 cm wide), a center zone (50%), and a transition zone in between.

Motor behavior, grip strength

Forepaw grip strength was measured as described previously (Ring et al., 2007; Steubler et al., 2021). using a newton meter (max. Force: 300 g). Animals had to hold on a metallic bar (4 cm long, 2.5 mm in diameter) attached to the horizontally positioned newton meter. Mice were held by the tail and allowed to grasp the bar with both forepaws. They were then gently pulled back until they released the bar. Mice were tested on two consecutive days for five trials each. For analysis, values of maximal pulling force were averaged.

Motor behavior, RotaRod

The RotaRod (Ugo Basile, model 47,600, Comerio, Italy) consisted of a rotating drum with a minimum speed of 2 round per minute (rpm) to maximal 40 rpm. Rotation speed was increased linearly until maximum speed was reached after 290 s. Animals were tested as previously described (Steubler et al., 2021) for 5 sessions on the same day, each session was terminated once the animal fell down the drum, or after 300 s the latest. Time at which animals for the first time clung to the drum (full circle ride), and time and acceleration at which the animals dropped off the drum was evaluated. For analysis, values were averaged.

Species-specific behavior, burrowing

The burrowing test was done as described previously (Deacon, 2006b; Steubler et al., 2021). In short, a grey plastic tube was filled with 310 g standard diet food pellets and placed at a slight angle into a Type III standard mouse cage equipped with normal bedding, a mouse shelter and water *ad libitum*. The lower end of the tube was closed, resting on the cage floor. The open end was supported 3.5 cm above the floor by two metal bolts. At the beginning of the dark period, mice were placed individually in the test cages, which were placed in their familiar animal room. At 4 h, and again at 24 h after experimental start the amount of non-displaced food (food still in the tube) was weighted. Consumed food by the animals (2 ± 0.5 g) was a very small proportion of the 310 g available and approximately equal across groups.

Species-specific behavior, nesting test

Nest building was studied as described (Deacon, 2006b; Steubler et al., 2021). At the beginning of the dark phase, mice were placed in individual testing cages (Type II) in their familiar animal room containing regular bedding and a Nestlet of 3 g compressed cotton (Ancare, Bellmore, USA). After 24 h, the nest-building activity of the mice was assessed on a rating scale of 1 to 5: 1 = Nestlet >90% intact, 2 = Nestlet 50–90% intact, 3 = Nestlet mostly shredded but no identifiable nest site, 4 = identifiable but flat nest, 5 = crater-shaped nest. Remaining intact parts of the Nestlet were weighted.

Water maze place navigation

Place navigation was assessed as described previously (Ring et al., 2007; Steubler et al., 2021). A white circular pool (150 cm diameter) contained milky water (24–26°C). Acquisition training consisted of 18 trials (6 per day, inter-trial interval 30–60 min) during which the submerged platform (14×14 cm) was left in the same position. Trials lasted a maximum of 120 s. To monitor reversal learning, the platform was moved to the opposite position for 2 additional days of testing (6 trials per day). Trials were video-tracked using a Noldus EthoVision. Raw data were transferred to the software Wintrack for analysis.[3] Results were plotted in bins of 3 trials. Passive floating episodes were defined as immobility or decelerations with speed minimum <0.06 m/s and removed from the data before calculating swim speed. A slightly modified version of Whishaw's error was calculated as path (%) outside a 18.5 cm wide corridor connecting release point and goal. Cumulative search error was determined by summing the distances to target measured at 1 s intervals and subtracting value that would be obtained for an ideal direct swim. Finally, wall-hugging was quantified by time (%) spent in a 10 cm wide wall zone. The first 30 s of the reversal trial served as probe trial to test for spatial retention.

Water maze cue navigation

On two consecutive days, mice were tested with the cued variant of the Morris water maze. For this, the location of the platform was marked with a black-and-white striped inverted pyramid (height 11 cm, base of pyramid 11x11cm) above the water. Animals were again tested in 6 trials per day, position of the flagged platform changed with each trial. Trials were video-tracked and analyzed as in place navigation.

T-maze

Spontaneous alternation on the T-maze was assessed as described (Deacon and Rawlins, 2006; Steubler et al., 2021). The T-maze was made of grey PVC. Each arm measured 30×10 cm. A removable central partition extended from the center of the back-goal wall of the T to 7 cm into the start arm. This prevented the

1 www.newbehavior.com
2 www.noldus.com
3 www.dpwolfer.ch/wintrack

mouse from seeing or smelling the non-chosen arm during the sample run, thus minimizing interfering stimuli. The entrance to each goal arm was fitted with a guillotine door. Each trial consisted of an information-gathering, sample run, followed immediately by a choice run. For the sample run a mouse was placed in the start arm, facing away from the choice point with the central partition in place. The mouse was allowed to choose a goal arm and was confined there for 30 s by lowering the guillotine door. Then the central partition was removed, the mouse replaced in the start arm, and the guillotine door was raised. Alternation was defined as entering the opposite arm to that entered on the sample trial (whole body, including tail). Three trials were run per day with an inter-trial interval of approximately 60 min. Each mouse received 6 trials in total and for data analysis the percentage of correct choices was calculated.

Radial maze

The working memory procedure on the 8-arm radial maze was carried out as described previously (Weyer et al., 2011; Steubler et al., 2021). Eight arms (7 × 38 cm) with clear Perspex tunnels (5 cm high) extended from an octagonal center platform (diameter 18.5 cm, distance platform center to end of arm 47 cm). The maze was placed 38 cm above the floor in a room rich in salient extramaze cues (same room as for open field testing). At the end of each arm, a metal cup (3 cm diameter) was lowered 1 cm to floor recess containing one millet-seed as bait (total ca 0.05 g), thus mice could not see the bait without completely entering the arm. Prior to the test, mice were gradually reduced to 85% of their free-feeding body weight for 2 days using a premeasured amount of chow, body weight was measured daily and 85% body weight was maintained throughout the test period. Water was available *ad libitum*. One day before test begin, mice were placed for 10 min into the baited radial maze for habituation. For testing, each mouse performed 1 session per day of maximally 10 min or until all eight seeds were collected. Test duration was 10 days. Mice were released in the center platform, performance of the animals was video-tracked, first visits to each arm and consumption of seeds were recorded manually. Using the video-tracking information, we calculated the number of correct choices among the first eight, as well as the number of reentry errors as a function of trial and of baits already collected. In addition, preferences for arm visits were analyzed. Error-free trials with one visit to each of the eight arms yielded preferred arm visits of 12.5%, corresponding to chance level without a preference for any arm. Reentries into already visited arms would yield values between 12.5–25%. Scores higher than 25% indicated excessive entry into one particular, preferred arm.

Barnes maze

The Barnes maze was made of a circular arena (1 m in diameter), placed 64 cm above ground. Twenty holes (5 cm in diameter) were evenly distributed at the margin of the platform. A black escape/goal box attached to the underside of a hole, equipped with a ramp inside, provided easy access to the dark escape. Tests were run in a brightly lit room for 5 days as previously described (Steubler et al., 2021). Each day, animals were trained in 4 trials, 3 min each, with a fixed position of the escape box. On the last day, one additional trial without escape box (probe trial) was run for 3 min. For each trial, animals were placed under a circular opaque start box in the platform center for 30 s. Trial started with removing the start box. If the animal successfully escaped into the goal box, the start box was placed over the whole with the goal box for another 30 s to prevent re-emergence of the mouse. Mice that did not succeed in finding the escape box within the given time were gently guided to the escape box during the first day of testing. Trials were video-tracked. Tracking data were used to calculate start delay (trial start until exit of start area), escape latency (exit of start area until disappearance of the animal), and number of errors (nosepokes into incorrect holes until first poke into the correct hole). In addition, trials were categorized according to search strategy: direct (max 1 error with absolute deviation angle <27°), serial (no center crosses and > 33% pokes to consecutive holes) or mixed (all remaining trials). During the probe trial, pokes were categorized according to deviation from the target hole.

Data availability statement

The raw data supporting the conclusions of this article will be made available by the authors, without undue reservation.

Author contributions

UM and DW designed and conceived the study. SE performed Sholl analysis, spine density analysis, and interpreted data. MB and JE performed biocytin fillings of neurons. IA and DW conducted, analyzed, and interpreted neuromotor and cognitive behavioral experiments. SL performed electrophysiological recordings, analyzed data, and interpreted data with MK. UM wrote the manuscript with help and input from all authors. All authors approved the final manuscript.

Funding

We acknowledge funding by the Deutsche Forschungsgemeinschaft (MU 1457/15–1 and MU 1457/17–1 to UM and KO 1674/28–1 to MK). DW is a member of the Neuroscience Center Zurich (ZNZ) and of the Zurich Center for Integrative Human Physiology (ZIHP).

Acknowledgments

We are grateful to Julia Gobbert and Sonia Matos for excellent technical assistance.

Conflict of interest

The authors declare that the research was conducted in the absence of any commercial or financial relationships that could be construed as a potential conflict of interest.

Publisher's note

References

Baumkotter, F., Schmidt, N., Vargas, C., Schilling, S., Weber, R., Wagner, K., et al. (2014). Amyloid precursor protein dimerization and synaptogenic function depend on copper binding to the growth factor-like domain. *J. Neurosci.* 34, 11159–11172. doi: 10.1523/JNEUROSCI.0180-14.2014

Bliss, T. V., and Lomo, T. (1973). Long-lasting potentiation of synaptic transmission in the dentate area of the anaesthetized rabbit following stimulation of the perforant path. *J. Physiol.* 232, 331–356. doi: 10.1113/jphysiol.1973.sp010273

Caldwell, J. H., Klevanski, M., Saar, M., and Muller, U. C. (2013). Roles of the amyloid precursor protein family in the peripheral nervous system. *Mech. Dev.* 130, 433–446. doi: 10.1016/j.mod.2012.11.001

Dawson, G. R., Seabrook, G. R., Zheng, H., Smith, D. W., Graham, S., O'Dowd, G., et al. (1999). Age-related cognitive deficits, impaired long-term potentiation and reduction in synaptic marker density in mice lacking the beta-amyloid precursor protein. *Neuroscience* 90, 1–13. doi: 10.1016.S0306-4522(98)00410-2

Deacon, R. M. (2006a). Assessing nest building in mice. *Nat. Protoc.* 1, 1117–1119. doi: 10.1038/nprot.2006.170

Deacon, R. M. (2006b). Burrowing in rodents: a sensitive method for detecting behavioral dysfunction. *Nat. Protoc.* 1, 118–121. doi: 10.1038/nprot.2006.19

Deacon, R. M., and Rawlins, J. N. (2006). T-maze alternation in the rodent. *Nat. Protoc.* 1, 7–12. doi: 10.1038/nprot.2006.2

DeBoer, S. R., Dolios, G., Wang, R., and Sisodia, S. S. (2014). Differential release of beta-amyloid from dendrite- versus axon-targeted APP. *J. Neurosci.* 34, 12313–12327. doi: 10.1523/JNEUROSCI.2255-14.2014

Del Turco, D., Paul, M. H., Schlaudraff, J., Hick, M., Endres, K., Muller, U. C., et al. (2016). Region-specific differences in amyloid precursor protein expression in the mouse hippocampus. *Front. Mol. Neurosci.* 9:134. doi: 10.3389/fnmol.2016.00134

De Strooper, B., and Karran, E. (2016). The cellular phase of Alzheimer's disease. *Cells* 164, 603–615. doi: 10.1016/j.cell.2015.12.056

Dislich, B., Wohlrab, F., Bachhuber, T., Muller, S. A., Kuhn, P. H., Hogl, S., et al. (2015). Label-free quantitative proteomics of mouse cerebrospinal fluid detects beta-site APP cleaving enzyme (BACE1) protease substrates in vivo. *Mol. Cell. Proteomics* 14, 2550–2563. doi: 10.1074/mcp.M114.041533

Eggert, S., Paliga, K., Soba, P., Evin, G., Masters, C. L., Weidemann, A., et al. (2004). The proteolytic processing of the amyloid precursor protein gene family members APLP-1 and APLP-2 involves alpha-, beta-, gamma-, and epsilon-like cleavages: modulation of APLP-1 processing by n-glycosylation. *J. Biol. Chem.* 279, 18146–18156. doi: 10.1074/jbc.M311601200M311601200

Endres, K., Postina, R., Schroeder, A., Mueller, U., and Fahrenholz, F. (2005). Shedding of the amyloid precursor protein-like protein APLP2 by disintegrin-metalloproteinases. *FEBS J.* 272, 5808–5820. doi: 10.1111/j.1742-4658.2005.04976.x

Fitzjohn, S. M., Morton, R. A., Kuenzi, F., Davies, C. H., Seabrook, G. R., and Collingridge, G. L. (2000). Similar levels of long-term potentiation in amyloid precursor protein -null and wild-type mice in the CA1 region of picrotoxin treated slices. *Neurosci. Lett.* 288, 9–12. doi: 10.1523/JNEUROSCI.21-13-04691.2001

Galanis, C., Fellenz, M., Becker, D., Bold, C., Lichtenthaler, S. F., Muller, U. C., et al. (2021). Amyloid-Beta mediates homeostatic synaptic plasticity. *J. Neurosci.* 41, 5157–5172. doi: 10.1523/JNEUROSCI.1820-20.2021

Haass, C., and Selkoe, D. (2022). If amyloid drives Alzheimer disease, why have anti-amyloid therapies not yet slowed cognitive decline? *PLoS Biol.* 20:e3001694. doi: 10.1371/journal.pbio.3001694

Han, K., Muller, U. C., and Hulsmann, S. (2017). Amyloid-precursor like proteins APLP1 and APLP2 are dispensable for Normal development of the neonatal respiratory network. *Front. Mol. Neurosci.* 10:189. doi: 10.3389/fnmol.2017.00189

Heber, S., Herms, J., Gajic, V., Hainfellner, J., Aguzzi, A., Rulicke, T., et al. (2000). Mice with combined gene knock-outs reveal essential and partially redundant functions of amyloid precursor protein family members. *J. Neurosci.* 20, 7951–7963.

Herms, J., Anliker, B., Heber, S., Ring, S., Fuhrmann, M., Kretzschmar, H., et al. (2004). Cortical dysplasia resembling human type 2 lissencephaly in mice lacking all three APP family members. *EMBO J.* 23, 4106–4115. doi: 10.1038/sj.emboj.7600390

Hick, M., Herrmann, U., Weyer, S. W., Mallm, J. P., Tschape, J. A., Borgers, M., et al. (2015). Acute function of secreted amyloid precursor protein fragment APPsalpha in synaptic plasticity. *Acta Neuropathol.* 129, 21–37. doi: 10.1007/s00401-014-1368-x

Holtmaat, A., Bonhoeffer, T., Chow, D. K., Chuckowree, J., De Paola, V., Hofer, S. B., et al. (2009). Long-term, high-resolution imaging in the mouse neocortex through a chronic cranial window. *Nat. Protoc.* 4, 1128–1144. doi: 10.1038/nprot.2009.89

Kaden, D., Munter, L. M., Joshi, M., Treiber, C., Weise, C., Bethge, T., et al. (2008). Homophilic interactions of the amyloid precursor protein (APP) ectodomain are regulated by the loop region and affect beta-secretase cleavage of APP. *J. Biol. Chem.* 283, 7271–7279. doi: 10.1074/jbc.M708046200

Klevanski, M., Saar, M., Baumkotter, F., Weyer, S. W., Kins, S., and Muller, U. C. (2014). Differential role of APP and APLPs for neuromuscular synaptic morphology and function. *Mol. Cell. Neurosci.* 61C, 201–210. doi: 10.1016/j.mcn.2014.06.004

Korte, M., and Schmitz, D. (2016). Cellular and system biology of memory: timing, molecules, and beyond. *Physiol. Rev.* 96, 647–693. doi: 10.1152/physrev.00010.2015

Kuhn, P. H., Colombo, A. V., Schusser, B., Dreymueller, D., Wetzel, S., Schepers, U., et al. (2016). Systematic substrate identification indicates a central role for the metalloprotease ADAM10 in axon targeting and synapse function. *elife* 5:e12748. doi: 10.7554/eLife.12748

Lassek, M., Weingarten, J., Einsfelder, U., Brendel, P., Muller, U., and Volknandt, W. (2013). Amyloid precursor proteins are constituents of the presynaptic active zone. *J. Neurochem.* 127, 48–56. doi: 10.1111/jnc.12358

Lee, K. J., Moussa, C. E., Lee, Y., Sung, Y., Howell, B. W., Turner, R. S., et al. (2010). Beta amyloid-independent role of amyloid precursor protein in generation and maintenance of dendritic spines. *Neuroscience* 169, 344–356. doi: 10.1016/j.neuroscience.2010.04.078

Li, Z. W., Stark, G., Gotz, J., Rulicke, T., Gschwind, M., Huber, G., et al. (1996). Generation of mice with a 200-kb amyloid precursor protein gene deletion by Cre recombinase-mediated site-specific recombination in embryonic stem cells. *Proc. Natl. Acad. Sci. U. S. A.* 93, 6158–6162.

Lorent, K., Overbergh, L., Moechars, D., De Strooper, B., Van Leuven, F., and Van den Berghe, H. (1995). Expression in mouse embryos and in adult mouse brain of three members of the amyloid precursor protein family, of the alpha-2-macroglobulin receptor/low density lipoprotein receptor-related protein and of its ligands apolipoprotein E, lipoprotein lipase, alpha-2-macroglobulin and the 40,000 molecular weight receptor-associated protein. *Neuroscience* 65, 1009–1025.

Madani, R., Kozlov, S., Akhmedov, A., Cinelli, P., Kinter, J., Lipp, H. P., et al. (2003). Impaired explorative behavior and neophobia in genetically modified mice lacking or overexpressing the extracellular serine protease inhibitor neuroserpin. *Mol. Cell. Neurosci.* 23, 473–494. doi: 10.1016/s1044-7431(03)00077-0

Mallm, J. P., Tschape, J. A., Hick, M., Filippov, M. A., and Muller, U. C. (2010). Generation of conditional null alleles for APP and APLP2. *Genesis* 48, 200–206. doi: 10.1002/dvg.20601

Mehr, A., Hick, M., Ludewig, S., Muller, M., Herrmann, U., von Engelhardt, J., et al. (2020). Lack of APP and APLP2 in GABAergic forebrain neurons impairs synaptic plasticity and cognition. *Cereb. Cortex*. 30, 4044–4063. doi: 10.1093/cercor/bhaa025

Midthune, B., Tyan, S. H., Walsh, J. J., Sarsoza, F., Eggert, S., Hof, P. R., et al. (2012). Deletion of the amyloid precursor-like protein 2 (APLP2) does not affect hippocampal neuron morphology or function. *Mol. Cell. Neurosci.* 49, 448–455. doi: 10.1016/j.mcn.2012.02.001

Mockett, B. G., Richter, M., Abraham, W. C., and Muller, U. C. (2017). Therapeutic potential of secreted amyloid precursor protein APPsalpha. *Front. Mol. Neurosci.* 10:30. doi: 10.3389/fnmol.2017.00030

Morrissey, J. A., Mockett, B. G., Singh, A., Kweon, D., Ohline, S. M., Tate, W. P., et al. (2019). A C-terminal peptide from secreted amyloid precursor protein-alpha enhances long-term potentiation in rats and a transgenic mouse model of Alzheimer's disease. *Neuropharmacology* 157:107670. doi: 10.1016/j.neuropharm.2019.107670

Müller, U. C., Deller, T., and Korte, M. (2017). Not just amyloid: physiological functions of the amyloid precursor protein family. *Nat. Rev. Neurosci.* 18, 281–298. doi: 10.1038/nrn.2017.29

Richter, M. C., Ludewig, S., Winschel, A., Abel, T., Bold, C., Salzburger, L. R., et al. (2018). Distinct in vivo roles of secreted APP ectodomain variants APPsalpha and APPsbeta in regulation of spine density, synaptic plasticity, and cognition. *EMBO J.* 37:e98335. doi: 10.15252/embj.201798335

Ring, S., Weyer, S. W., Kilian, S. B., Waldron, E., Pietrzik, C. U., Filippov, M. A., et al. (2007). The secreted beta-amyloid precursor protein ectodomain APPs alpha is sufficient to rescue the anatomical, behavioral, and electrophysiological abnormalities of APP-deficient mice. *J. Neurosci.* 27, 7817–7826. doi: 10.1523/JNEUROSCI.1026-07.2007

Scheinfeld, M. H., Ghersi, E., Laky, K., Fowlkes, B. J., and D'Adamio, L. (2002). Processing of beta-amyloid precursor-like protein-1 and -2 by gamma-secretase regulates transcription. *J. Biol. Chem.* 277, 44195–44201. doi: 10.1074/jbc.M208110200

Schilling, S., Mehr, A., Ludewig, S., Stephan, J., Zimmermann, M., August, A., et al. (2017). APLP1 is a synaptic cell adhesion molecule, supporting maintenance of dendritic spines and basal synaptic transmission. *J. Neurosci.* 37, 5345–5365. doi: 10.1523/JNEUROSCI.1875-16.2017

Seabrook, G. R., Smith, D. W., Bowery, B. J., Easter, A., Reynolds, T., Fitzjohn, S. M., et al. (1999). Mechanisms contributing to the deficits in hippocampal synaptic plasticity in mice lacking amyloid precursor protein. *Neuropharmacology* 38, 349–359. doi: 10.1016/s0028-3908(98)00204-4

Senechal, Y., Kelly, P. H., and Dev, K. K. (2008). Amyloid precursor protein knockout mice show age-dependent deficits in passive avoidance learning. *Behav. Brain Res.* 186, 126–132. doi: 10.1016/j.bbr.2007.08.003

Simoes, S., Neufeld, J. L., Triana-Baltzer, G., Moughadam, S., Chen, E. I., Kothiya, M., et al. (2020). Tau and other proteins found in Alzheimer's disease spinal fluid are linked to retromer-mediated endosomal traffic in mice and humans. *Sci. Transl. Med.* 12:eaba6334. doi: 10.1126/scitranslmed.aba6334

Slunt, H. H., Thinakaran, G., Von Koch, C., Lo, A. C., Tanzi, R. E., and Sisodia, S. S. (1994). Expression of a ubiquitous, cross-reactive homologue of the mouse beta-amyloid precursor protein (APP). *J. Biol. Chem.* 269, 2637–2644.

Soba, P., Eggert, S., Wagner, K., Zentgraf, H., Siehl, K., Kreger, S., et al. (2005). Homo- and heterodimerization of APP family members promotes intercellular adhesion. *EMBO J.* 25:653. doi: 10.1038/sj.emboj.7600956

Stahl, R., Schilling, S., Soba, P., Rupp, C., Hartmann, T., Wagner, K., et al. (2014). Shedding of APP limits its synaptogenic activity and cell adhesion properties. *Front. Cell. Neurosci.* 8:410. doi: 10.3389/fncel.2014.00410

Steinbach, J. P., Muller, U., Leist, M., Li, Z. W., Nicotera, P., and Aguzzi, A. (1998). Hypersensitivity to seizures in beta-amyloid precursor protein deficient mice. *Cell Death Differ.* 5, 858–866.

Steubler, V., Erdinger, S., Back, M. K., Ludewig, S., Fassler, D., Richter, M., et al. (2021). Loss of all three APP family members during development impairs synaptic function and plasticity, disrupts learning, and causes an autism-like phenotype. *EMBO J.* 40:e107471. doi: 10.15252/embj.2020107471

Thinakaran, G., Kitt, C. A., Roskams, A. J., Slunt, H. H., Masliah, E., von Koch, C., et al. (1995). Distribution of an APP homolog, APLP2, in the mouse olfactory system: a potential role for APLP2 in axogenesis. *J. Neurosci.* 15, 6314–6326.

Tyan, S. H., Shih, A. Y., Walsh, J. J., Maruyama, H., Sarsoza, F., Ku, L., et al. (2012). Amyloid precursor protein (APP) regulates synaptic structure and function. *Mol. Cell. Neurosci.* 51, 43–52. doi: 10.1016/j.mcn.2012.07.009S1044-7431(12)00125-X

von Koch, C. S., Zheng, H., Chen, H., Trumbauer, M., Thinakaran, G., van der Ploeg, L. H., et al. (1997). Generation of APLP2 KO mice and early postnatal lethality in APLP2/APP double KO mice. *Neurobiol. Aging* 18, 661–669.

Wang, B., Li, H., Mutlu, S. A., Bowser, D. A., Moore, M. J., Wang, M. C., et al. (2017). The amyloid precursor protein is a conserved receptor for slit to mediate axon guidance. *eNeuro* 4:ENEURO.0185-17.2017. doi: 10.1523/ENEURO.0185-17.2017

Wang, Z., Wang, B., Yang, L., Guo, Q., Aithmitti, N., Songyang, Z., et al. (2009). Presynaptic and postsynaptic interaction of the amyloid precursor protein promotes peripheral and central synaptogenesis. *J. Neurosci.* 29, 10788–10801. doi: 10.1523/JNEUROSCI.2132-09.2009

Wang, P., Yang, G., Mosier, D. R., Chang, P., Zaidi, T., Gong, Y. D., et al. (2005). Defective neuromuscular synapses in mice lacking amyloid precursor protein (APP) and APP-like protein 2. *J. Neurosci.* 25, 1219–1225. doi: 10.1523/JNEUROSCI.4660-04.2005

Weyer, S. W., Klevanski, M., Delekate, A., Voikar, V., Aydin, D., Hick, M., et al. (2011). APP and APLP2 are essential at PNS and CNS synapses for transmission, spatial learning and LTP. *EMBO J.* 30, 2266–2280. doi: 10.1038/emboj.2011.119

Weyer, S. W., Zagrebelsky, M., Herrmann, U., Hick, M., Ganss, L., Gobbert, J., et al. (2014). Comparative analysis of single and combined APP/APLP knockouts reveals reduced spine density in APP-KO mice that is prevented by APPsalpha expression. *Acta Neuropathol. Commun.* 2:36. doi: 10.1186/2051-5960-2-36

Yang, L., Wang, B., Long, C., Wu, G., and Zheng, H. (2007). Increased asynchronous release and aberrant calcium channel activation in amyloid precursor protein deficient neuromuscular synapses. *Neuroscience* 149, 768–778. doi: 10.1016/j.neuroscience.2007.08.025

Zhang, S., Liu, Y. Q., Jia, C., Lim, Y. J., Feng, G., Xu, E., et al. (2021). Mechanistic basis for receptor-mediated pathological alpha-synuclein fibril cell-to-cell transmission in Parkinson's disease. *Proc. Natl. Acad. Sci. U. S. A.* 118:e2011196118. doi: 10.1073/pnas.2011196118

Zou, C., Crux, S., Marinesco, S., Montagna, E., Sgobio, C., Shi, Y., et al. (2016). Amyloid precursor protein maintains constitutive and adaptive plasticity of dendritic spines in adult brain by regulating D-serine homeostasis. *EMBO J.* 35, 2213–2222. doi: 10.15252/embj.201694085

frontiers | Frontiers in Molecular Neuroscience

TYPE Original Research
PUBLISHED 11 November 2022
DOI 10.3389/fnmol.2022.1006455

OPEN ACCESS

EDITED BY
Haiyun Xu,
Wenzhou Medical University, China

REVIEWED BY
Francois Rouyer,
UMR 9197 Institut des Neurosciences Paris Saclay (Neuro-PSI), France
Hrvoje Augustin,
Royal Holloway University of London, United Kingdom

*CORRESPONDENCE
Hsin-Ping Liu
hpliu@mail.cmu.edu.tw

SPECIALTY SECTION
This article was submitted to Molecular Signaling and Pathways, a section of the journal Frontiers in Molecular Neuroscience

RECEIVED 29 July 2022
ACCEPTED 24 October 2022
PUBLISHED 11 November 2022

CITATION
Lin W-Y, Liu C-H, Cheng J and Liu H-P (2022) Alterations of RNA-binding protein *found in neurons* in *Drosophila* neurons and glia influence synaptic transmission and lifespan.
Front. Mol. Neurosci. 15:1006455.
doi: 10.3389/fnmol.2022.1006455

Alterations of RNA-binding protein *found in neurons* in *Drosophila* neurons and glia influence synaptic transmission and lifespan

Wei-Yong Lin[1,2], Chuan-Hsiu Liu[3], Jack Cheng[1,2] and Hsin-Ping Liu[4]*

[1]Graduate Institute of Integrated Medicine, College of Chinese Medicine, China Medical University, Taichung, Taiwan, [2]Department of Medical Research, China Medical University Hospital, Taichung, Taiwan, [3]School of Chinese Medicine, College of Chinese Medicine, China Medical University, Taichung, Taiwan, [4]Graduate Institute of Acupuncture Science, College of Chinese Medicine, China Medical University, Taichung, Taiwan

The *found in neurons* (*fne*), a paralog of the RNA-binding protein *ELAV* gene family in *Drosophila*, is required for post-transcriptional regulation of neuronal development and differentiation. Previous explorations into the functions of the FNE protein have been limited to neurons. The function of *fne* in *Drosophila* glia remains unclear. We induced the knockdown or overexpression of *fne* in *Drosophila* neurons and glia to determine how *fne* affects different types of behaviors, neuronal transmission and the lifespan. Our data indicate that changes in *fne* expression impair associative learning, thermal nociception, and phototransduction. Examination of synaptic transmission at presynaptic and postsynaptic terminals of the larval neuromuscular junction (NMJ) revealed that loss of *fne* in motor neurons and glia significantly decreased excitatory junction currents (EJCs) and quantal content, while flies with glial *fne* knockdown facilitated short-term synaptic plasticity. In muscle cells, overexpression of *fne* reduced both EJC and quantal content and increased short-term synaptic facilitation. In both genders, the lifespan could be extended by the knockdown of *fne* in neurons and glia; the overexpression of *fne* shortened the lifespan. Our results demonstrate that disturbances of *fne* in neurons and glia influence the function of the *Drosophila* nervous system. Further explorations into the physiological and molecular mechanisms underlying neuronal and glial *fne* and elucidation of how *fne* affects neuronal activity may clarify certain brain functions.

KEYWORDS

***fne*, RNA-binding protein, neuron, glia, synaptic plasticity**

Introduction

The embryonic lethal abnormal visual system-like (ELAVL/Hu) proteins are a family of RNA-binding proteins (RBPs) with three highly conserved RNA recognition motifs (RRMs) that mediate the post-transcriptional regulation of gene expression through alternative RNA splicing, localization, stability, translation, and metabolism (Colombrita et al., 2013). Humans possess four ELAVL/Hu protein-encoding genes; specifically, a ubiquitous member (*ELAVL1/HuR*) and three predominantly neuronal members (*ELAVL2/HuB*, *ELAVL3/HuC*, and *ELAVL4/HuD*), which are often used as reliable biomarkers for neurons. The *Drosophila* ELAV family comprises three members: *elav*, *RNA-binding protein 9* (*Rbp9*), and *found in neurons* (*fne*). These proteins are highly enriched in neurons, and RBP9 is also found in gonads (Colombrita et al., 2013). The ELAV protein is encoded by *elav,* and deletion of *elav* leads to defects in the visual system and to embryonic lethality (Jimenez and Campos-Ortega, 1987). ELAV is mostly found in the neuronal nucleus and is involved in the stability of mRNA, alternative splicing, and in the cleavage of the polyadenylation site of the 3' untranslated region (3'-UTR) (Koushika et al., 1996; Carrasco et al., 2020). The RBP9 protein encoded by *Rbp9* is present not only in neuronal nuclei but also in the cytoplasm of cystocytes during oogenesis for the necessity of germ cell differentiation (Kim-Ha et al., 1999). No gross neural developmental defects have been observed in *Rbp9* null mutation, but reduced locomotor activity, shorter lifespan, and defects in the blood-brain barrier and female sterility have been observed (Kim-Ha et al., 1999; Kim et al., 2010).

The third *elav*-related gene in *Drosophila*, *fne*, is present throughout development but after *elav* expression. The FNE protein is cytoplasmic and is restricted to neurons of the central and peripheral nervous systems (PNS) (Samson and Chalvet, 2003). The functional necessity of ELAV and FNE proteins to performing neural 3'-UTR alternative polyadenylation (APA) has been demonstrated, and in the absence of *elav*, FNE can rescue ELAV-mediated APA (Carrasco et al., 2020; Wei et al., 2020). Null mutants of *fne* were viable in adults: morphological defects were not apparent, but overexpression of *fne* in neurons resulted in an extreme decrease in the viability and phenotypic defects in the wings and legs (Samson, 2008). *fne* is also involved in the male courtship performance and the development of sex-specific nervous systems, and is required to restrict axonal extension of the beta lobes in adult mushroom body, a brain structure essential for the learning and memory (Zanini et al., 2012; Sun et al., 2015).

The physiological function of glia in *Drosophila* has been documented (Yildirim et al., 2019). In the central nervous system (CNS), similar with mammalian glia interacting with neurons, *Drosophila* glia are required for the regulation of neuronal development and differentiation in the brain and in the visual system (Edwards and Meinertzhagen, 2010). Glial cells also provide various supportive functions to neurons, including the modulation of electrical transmission or ion homeostasis, metabolic support of neurons, BBB formation, and responses to neuronal injury or infection (Logan, 2017; Nagai et al., 2021). In the PNS, the peripheral glia play an important role in coordinating synaptogenesis and shaping the synaptic connection in the neuromuscular junction (NMJ) by releasing glia-derived factors (Ou et al., 2014).

Studies on *fne* have mainly focused on neurons. However, the function of *fne* in glia has not yet been identified. In the present study, we investigated the physiological and molecular effects of *fne* in both neurons and glia, and our results revealed that changes in *fne* expression impaired phototransduction, learning performance, and thermal nociception. Changes in *fne* expression also affected the synaptic transmission and plasticity of the larval NMJ and preferentially acted at the presynaptic terminal, while knockdown of *fne* in the glia was highly influential. Our results suggest that expression of *fne* in the glia is essential for neurotransmission and elucidate the mechanism of *fne* in flies, possibly by extension, in mammals.

Materials and methods

Fly culture and strains

Drosophila strains were raised on regular cornmeal food under a 12-hr light/dark cycle with consistent 50–60% humidity at 25°C unless otherwise noted. The wild-type strain was w^{1118}. The fly strains used in this study, including *GMR-GAL4* (photoreceptor-specific, stock #1104), *tub-Gal80^{ts}* (stock #7018 and 7019), *TrpA1*^{1} (stock #26504), and *UAS-fne* (stock #6897) (Chalvet and Samson, 2002) were obtained from the Bloomington *Drosophila* Stock Center (BDSC), and *fne*-knockdown strain (*UAS-fne-IR*, stock #101508) (Alizzi et al., 2020) was obtained from the Vienna *Drosophila* Resource Center (VDRC). The strains, *elav^{C155}-GAL4* (neuron-specific), *C57-GAL4* (muscle cell-specific), and *repo^{7415}-GAL4* (glia-specific), which were outcrossed with w^{1118} (*isoCJ1*) for at least five generations, were provided by Dr. Hui-Fu Guo. Functioning of *UAS-fne* and *UAS-fne-IR* lines was verified in **Supplementary Figure 1**.

Because overexpressing *fne* under *repo-GAL4* and *C57-GAL4* drivers results in larval/pupal lethality, we used the TARGET expression system to temporally control *fne* expression under the specific *GAL4* drivers combined with temperature-sensitive *GAL80^{ts}* (*tub-GAL80^{ts}*) (McGuire et al., 2004). The flies were reared at the permissive temperature (18°C) during the developmental stages and shifted to the non-permissive temperature (25 or 29°C) after eclosion to initiate *GAL4* transcription of *UAS* transgenes.

Electroretinogram analysis

The Electroretinogram (ERG) test was performed as previously described (Cosens and Manning, 1969). Briefly, each fly was captured in a pipette tip. A reference electrode was contacted with the head and a recording electrode was attached to the fly's compound eye. The fly eye was exposed to a 1.5 W white-light LED which is programmed to a repetitive on-off cycle of 2–6 s. Signals were recorded by Axon Instruments GeneClamp 500 Voltage Patch Clamp Amplifier (Molecular Devices, USA) and analyzed by Axon Instruments pCLAMP software (Molecular Devices, USA). The ERG was recorded from males which were reared at 18°C and shifted to 29°C after eclosion for 5 days to induce *fne* and *fne-IR* expression in photoreceptors and glia under *GMR-GAL4* and *repo-GAL4* combined with *tub-GAL80^{ts}* (referred as *GMR^{ts}* and *repo^{ts}*), respectively. Data were collected and analyzed at least 6 on-off cycles per fly.

Olfactory associative learning assay

The flies with *fne* and *fne-IR* were reared at 18°C and after eclosion, shifted to 25 or 29°C to induce transgenes expression in neurons and glia under *elav^{ts}* and *repo^{ts}*, respectively. A single training trial was performed according to previous studies (Dubnau et al., 2001). Briefly, approximately 100 flies were exposed sequentially to two odors, either 3-octanol (OCT, Sigma-Aldrich) or 4-methylcyclohexanol (MCH, Sigma-Aldrich). Flies exposed to the first odor (conditioned stimulus, CS +) were paired with 80 V electric shocks and then received a second odor (CS-) without shocks. Learning ability was determined immediately after training. To perform the test, the trained flies were trapped into the choice point of a T-maze in which they were exposed simultaneously to OCT and MCH. A performance index (PI) was calculated to represent the conditioned odor avoidance. The PI = (# of CS- – # of CS +)/(# of total flies), and the final PI was calculated by averaging the PI in which OCT was the shock-paired odor and one in which MCH was the shock-paired odor. A PI of zero (no learning) indicated a 50:50 distribution, and a PI of 100 showed a 0:100 distribution away from the CS + odor.

Nociceptive test

For the avoidance of noxious heat, we used the behavior paradigm as previously described (Neely et al., 2011). Briefly, approximately 20 male flies were placed in a sealed peri dish chamber. The chamber was then floated on a 46°C water bath for 1 min 30 s. The bottom of the chamber was heated to 46°C, whereas the top of chamber was measured to be 31°C. All tests were performed under red light. Flies that move away from the 46°C bottom surface were considered to be capable of avoidance of heat challenge. The percentage of avoidance in response to noxious temperature was calculated by counting the number of flies that avoid the noxious temperature compared to the total number of flies in the chamber. The flies with *fne* and *fne-IR* were maintained at 18°C and the newly *eclosed* adult males were shifted to 29°C for 5 days and 25°C for 10 days to induce transgene expression in neurons and glia under *elav^{ts}* and *repo^{ts}* control, respectively.

Electrophysiology of the larval neuromuscular junction

Electrophysiological recordings of two-electrode voltage clamp were performed as previously described (Guo and Zhong, 2006). Wall climbing third-instar larvae were chosen for dissection at 25°C in Ca^{2+}-free hemolymph-like (HL-3) solution containing the following (in mM): 70 NaCl, 5 KCl, 4 $MgCl_2$, 10 $NaHCO_3$, 5 trehalose, 5 HEPES, and 115 sucrose. For recordings, HL-3 solution was supplemented with 0.2 mM $CaCl_2$. All recordings were made at the longitudinal muscle fiber 12 (M12) of segments A3-A5. To elicit evoked excitatory junction currents (EJCs), the segmental nerve was stimulated with a suction electrode at 1.5 times of the stimulus voltage required for a threshold response. Continuous recordings were made to measure the EJCs and miniature EJCs (mEJCs) while the nerve was stimulated at the baseline frequency of 0.05 Hz. For induction of short-term facilitation (STF), short trains of 20 repetitive stimulation were delivered at the frequency of 0.5–25 Hz. Current signals were amplified with an Axoclamp 2A amplifier (Molecular Devices, USA), filtered at 0.1 kHz on-line, and converted to a digital signal using a Digidata 1320A interface (Molecular Devices, USA) and pCLAMP software (Molecular Devices, USA). Stimulation of nerves was achieved by a Grass Instruments S88 Stimulator (Grass Instruments, USA). EJCs were determined by averaging consecutive EJCs in 0.05 Hz during the 5 min recording period, while mEJCs were analyzed from continuous recordings of 1 min. Values of average mEJC amplitudes were determined and quantal content is calculated as dividing average EJC amplitude by average mEJC amplitude. For STF, the EJC amplitudes of the last 10 responses in each train were averaged and normalized to the average EJC amplitudes at 0.5 Hz. The experiments were performed at 25°C. For overexpressing *fne* under *C57^{ts}* and *repo^{ts}*, the flies were reared at 18°C started from embryonic stages, shifted to 29°C for 1 day, and performed electrophysiology.

Longevity assay

The flies were expressed *fne* and *fne-IR* under *elav^{ts}* and *repo^{ts}* drivers. All flies were maintained at 18°C and shifted to 25°C after eclosion. Emerging adult flies were collected and separated by sex. Around thirty to thirty-five flies were kept in a

vial. Four repeat vials, comprising at least 120 flies in total were conducted for each genotype. Food vials were replaced every 3–4 days, and dead flies were counted at that time.

Data analyses and statistics

Statistical analysis of associate learning and longevity assay were performed by a Student's *t*-test and Log-rank test, respectively. For multiple comparisons of ERG, nociceptive test, and electrophysiology, data were performed using the one-way analysis of variance (ANOVA) followed by Turkey *post-hoc* test. The results represent as mean ± standard error mean (SEM) from at least three biological replicates. *p*-value less than 0.05 was considered statistical significance.

Results

Electroretinogram amplitudes are influenced by *fne*

Photoreceptors respond to periodic light exposure by converting light signals into electric currents. A periodic electric signal can thus be recorded by an extracellular ERG (**Figure 1A**). The typical ERG waveform of a wild-type fly can be divided into four components (**Figure 1B**). The receptor potential amplitude (RPA) reflects the depolarization of the photoreceptors during stimulation with light. The on- and off-transient spikes, which occur at the beginning and end of a flash of light, respectively, indicate the successful transmission of a signal from photoreceptors to their postsynaptic partners in the lamina (Montell, 1999). The quantity ΔV represents the amplitude between on- and off-transient spikes.

To test whether *fne* affected light-evoked responses in the retina, we used GMR^{ts} and $repo^{ts}$ to temporally control *fne* and *fne-IR* expression in the photoreceptors and glia, respectively (**Figures 1C–G**). The photoreceptors expressing *fne* and *fne-IR* (GMR^{ts} > *fne* and GMR^{ts} > *fne-IR*) revealed slightly affected electric potential, as indicated by the smaller ΔV and off-transient amplitudes. The flies with *fne* and *fne-IR* expression in glia ($repo^{ts}$ > *fne* and $repo^{ts}$ > *fne-IR*) exhibited decreased ΔV, on- and off-transient amplitudes. These results indicate that *fne* affects neurotransmission in both photoreceptors and glia and that changes in *fne* expression in glia cause more severe ERG defect than in neurons.

Overexpression of *fne* in neurons and glia impairs cognitive ability

Because changes in *fne* expression affect photoreceptor transmission, we attempted to determine the effects of *fne* on behavior. A single cycle of olfactory associative training was conducted to evaluate the learning performance index (PI; **Figure 2A**). After eclosion, the temperature was raised from 18 to 29°C for 10 days, and the flies started to overexpress ($elav^{ts}$ > *fne*) or knockdown ($elav^{ts}$ > *fne-IR*) *fne* in neurons. The PI of the $elav^{ts}$ > *fne-IR* flies was similar to that of the control group ($elav^{ts}$ > +, 55.5 ± 3.8 vs. 53.5 ± 1.1), but the $elav^{ts}$ > *fne* flies exhibited a lower PI than did the control (31.1 ± 4.0, $p < 0.01$). We also evaluated learning ability when *fne* expression in glia began to change during the adult stage. Because the overexpression of *fne* in glia at 29°C caused extremely low viability, we kept the flies at a lower non-permissive temperature of 25°C for 14 days. Our data revealed that the $repo^{ts}$ > *fne* flies had significantly lower PIs than did the control flies (39.8 ± 2.5 vs. 68.4 ± 4.6, $p < 0.001$), but $repo^{ts}$ > *fne-IR* flies showed non-significant difference. These results indicate that the overexpression but not knockdown of *fne* both in neurons and glia impairs learning behavior.

Changes in *fne* expression reduce thermal sensation

Having determined that changing *fne* expression impairs cognitive ability, we tested another behavior, thermal nociception. When the flies were exposed to a noxious temperature (46°C) at the bottom surface of a peri dish chamber, they rapidly moved to the top, which had a subnoxious temperature, to avoid being harmed by the heat. A low percentage of avoidance indicated that the flies were less sensitive to the noxious heat (Neely et al., 2011). When *fne* and *fne-IR* were expressed in neurons at 29°C for 5 days, the percentages of avoidance appeared lower in the $elav^{ts}$ > *fne-IR* and $elav^{ts}$ > *fne* groups (69.4 ± 2.7% and 51.7 ± 3.3%, respectively) than in the control groups ($elav^{ts}$ > +, 86.5 ± 1.0%; $fne\text{-}IR^{ts}$ > +, 92.1 ± 1.0%; fne^{ts} > +, 94.1 ± 1.6%; **Figure 2B**). After eclosion, the flies were kept at 25°C for 10 days to express *fne* in the glia, and the percentage of avoidance for the $repo^{ts}$ > *fne* flies was 20.5 ± 5.8%, which were lower than the controls ($repo^{ts}$ > +, 91.8 ± 0.8%; fne^{ts} > +, 91.1 ± 1.0%; **Figure 2B**). In addition, knockdown of *fne* ($repo^{ts}$ > *fne-IR*) did not affect thermal sensation. *Transient receptor potential cation channel A1* (*TrpA1*) is a nociceptor-related gene (Neely et al., 2011), and we used a *TrpA1* mutant ($TrpA1^{1}$) as a positive control (avoidance rate was 17.3 ± 4.0%). Our data indicated that changes in *fne* expression in neurons and glia caused defects in thermal nociception, particularly in the flies with *fne* overexpression in glia.

Impaired synaptic transmission of the larval neuromuscular junction in *fne*-knockdown flies

Changes in *fne* expression impaired phototransduction and adult behaviors, which might result from defective synaptic

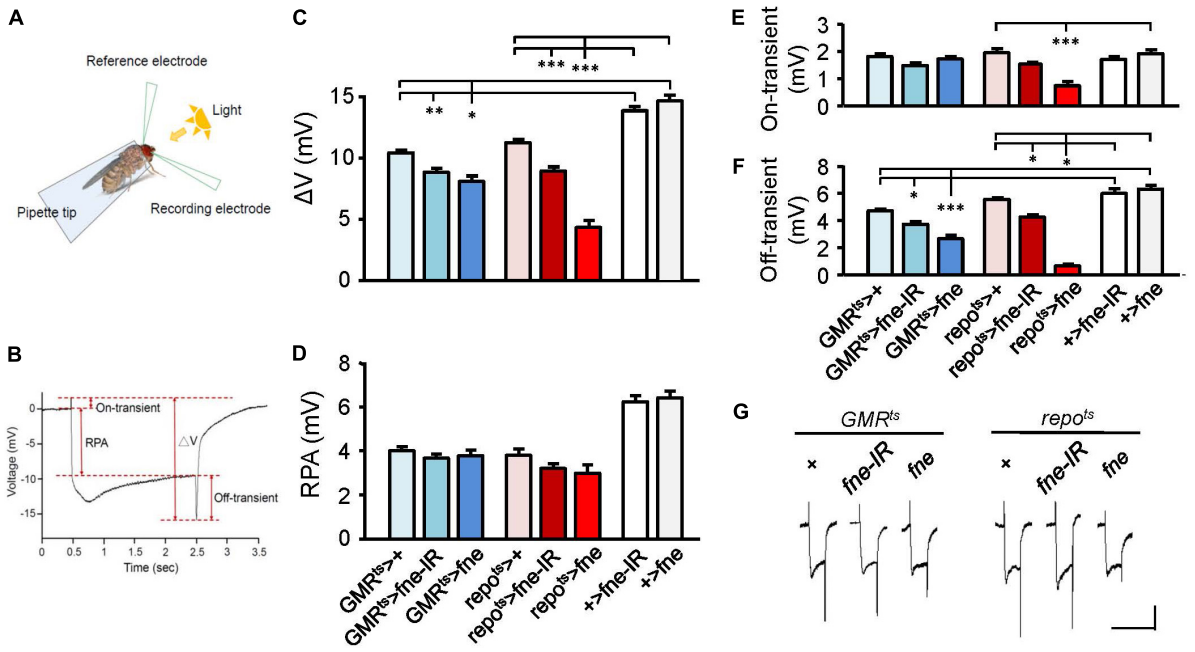

FIGURE 1
fne is involved in the light-induced synaptic transmission in neurons and glia. **(A)** A schematic diagram of ERG recording. **(B)** The components of a representative ERG signal contain the ΔV (the difference between on- and off-transient spikes), receptor potential amplitude (RPA), and on-transient (highest peak from baseline) and off-transient (lowest peak from baseline) spikes. Quantification of **(C)** ΔV, **(D)** RPA, **(E)** on-transient, and **(F)** off-transient spikes. **(G)** The ERG trace of each genotype. Calibration: 2 mV, 5 s. Error bars represent SEM. $n = 10$ for each group. $^{*}p < 0.05$, $^{**}p < 0.01$, $^{***}p < 0.001$.

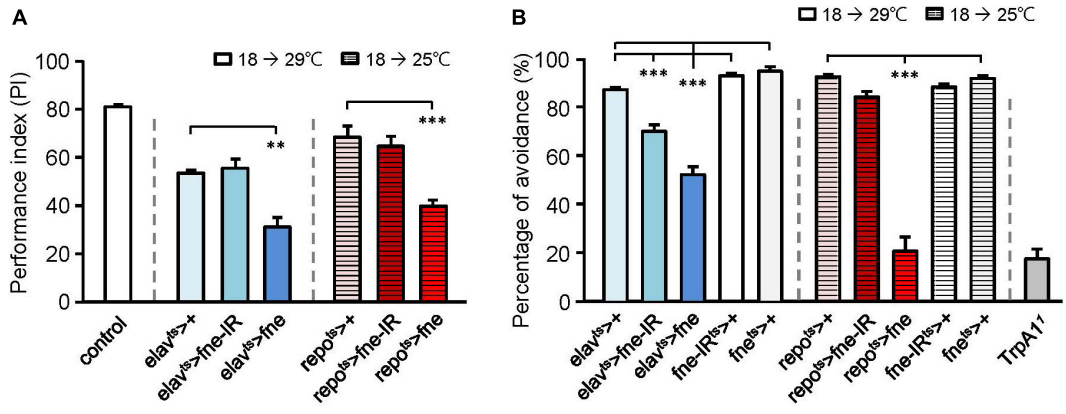

FIGURE 2
Effects of *fne* on cognitive behavior and thermal nociception. **(A)** The learning PI of *fne* and *fne-IR* expressing in neurons and glia. The control fly is 25°C 5-day-old *Canton-S* strain for experimental calibration. $n = 5–6$ for each group. **(B)** The percentages of avoidance in response to noxious temperature of *fne* and *fne-IR* expressing in neurons and glia. The *TrpA1* mutant ($TrpA1^{1}$) fly is a positive control (25°C, 5-day-old). $n = 10$ for each group. Error bars represent SEM. $^{**}p < 0.01$, $^{***}p < 0.001$.

transmission. Thus, we performed an electrophysiological study of the third-instar larval NMJ for the effects of *fne* on synaptic transmission. Continuous recordings were made while the muscle fiber M12 was voltage clamped at –80 mV and segmental nerves innervating the muscle cell were stimulated by 0.05 Hz in a HL-3 solution containing 0.2 mM Ca^{2+} (Guo and Zhong, 2006). We examined an evoked EJC in the *fne*-knockdown flies (Figures 3A,C). The knockdown of *fne* in neurons (*elav* > *fne-IR*), which represents a presynaptic site of synaptic transmission, caused significantly smaller EJC amplitude (10.70 ± 1.16 nA) than the control flies (*elav* > + and *fne-IR* > +, 25.96 ± 3.13, and 22.31 ± 3.66 nA, respectively, $p < 0.05$). The knockdown of *fne*

in muscle cells (*C57* > *fne-IR*), which represents a postsynaptic site of synaptic transmission, caused no difference in the EJC amplitudes among the control flies (*C57* > + and *fne-IR* > +). Because EJC amplitudes decreased only in the *elav* > *fne-IR* flies, it implies that their presynaptic function was affected.

Subsequently, we examined the amplitude and frequency of mEJCs to determine whether the spontaneous release of synaptic vesicles had changed (**Figures 3B,D,E**). The knockdown of *fne* in neurons did not alter the amplitude or frequency of the mEJCs. Only the mEJC amplitudes in the muscle cells expressing *fne-IR* (*C57* > *fne-IR*) significantly decreased compared to the control flies (*C57* > + and *fne-IR* > +, 0.40 ± 0.02 vs. 0.54 ± 0.03, and 0.52 ± 0.01 nA, respectively, $p < 0.05$). We also determined the quantal content, which reflects the number of vesicles released in response to a nerve impulse. A significant reduction in quantal content was observed in the *elav* > *fne-IR* flies (*elav* > *fne-IR*, 23.13 ± 2.50; *elav* > +, 50.99 ± 7.23; *fne-IR* > +, 42.53 ± 6.07, $p < 0.05$; **Figure 3F**).

Impaired synaptic function of the larval neuromuscular junction in *fne*-overexpressed flies

We attempted to determine whether the overexpression of *fne* also affected synaptic transmission (**Figures 4A,C**). The overexpression of *fne* in muscle cells ($C57^{ts}$ > *fne*) caused significantly smaller EJCs (8.20 ± 1.02 nA) than the control flies ($C57^{ts}$ > + and fne^{ts} > +, 17.60 ± 1.39, and 21.36 ± 0.86 nA, respectively, $p < 0.001$). A significant reduction in quantal content was also observed in the $C57^{ts}$ > *fne* flies ($C57^{ts}$ > *fne*, 16.11 ± 1.99; $C57^{ts}$ > +, 30.90 ± 2.91; fne^{ts} > +, 33.95 ± 3.30, $p < 0.01$; **Figure 4F**). The overexpression of *fne* in neurons (*elav* > *fne*) resulted in the EJC amplitudes and quantal content being similar with those of the control flies (*elav* > + and *fne* > +). In addition, the amplitude and frequency of mEJCs in the flies overexpressing *fne* in neurons and muscle cells did not differ from those of the controls (**Figures 4B,D,E**), suggesting that spontaneous synaptic transmission and constitutive synaptic vesicle fusion was not affected by *fne* overexpression.

Knockdown of *fne* in the larval neuromuscular junction did not affect short-term synaptic plasticity

To determine whether *fne* is involved in short-term synaptic plasticity, we induced a short train of repetitive stimulation at 25 Hz after 5 min of baseline stimulation. The repetitive impulses affected the probability of neurotransmitter release and resulted in changes to synaptic efficacy over time, which reflected the electrical activity of the presynaptic terminals. Normal STF was observed in neurons and muscle cells expressing *fne-IR* (*elav* > *fne-IR* and *C57* > *fne-IR*; control groups: *elav* > *fne-IR* vs. *elav* > + and *fne-IR* > + ; *C57* > *fne-IR* vs. *C57* > +, and *fne-IR* > +, respectively; **Figure 5A**). We also induced the frequency dependence of STF by delivering various frequencies (0.5–20 Hz). The synaptic transmission properties were normal with increasing stimulation frequency in the knockdown of *fne* in neurons and muscle cells (*elav* > *fne-IR* and *C57* > *fne-IR*; **Figure 5B**).

Overexpression of *fne* in muscle cells affected short-term synaptic plasticity

To determine whether the overexpression of *fne* was involved in short-term synaptic plasticity, we induced a short train of repetitive stimulation at 25 Hz in the *fne*- overexpressing flies. Normal STF was observed in the neurons expressing *fne* (*elav* > *fne*), but facilitation increased significantly for *fne*-expressing muscle cells, by approximately 5.1-fold after repetitive stimulation, relative to the controls ($C57^{ts}$ > *fne* vs. $C57^{ts}$ > + and fne^{ts} > + ; **Figure 6A**). A frequency-dependent facilitation was also obtained by stimulating muscle cells ($C57^{ts}$ > *fne*), where the stimulation gradually increased in frequency from 0.5 to 20 Hz; however, no difference was observed in the neuronal *fne*-expressing flies (*elav* > *fne*; **Figure 6B**).

These results indicated that the knockdown of *fne* in neurons reduced the amplitude of EJCs and quantal content, whereas the overexpression of *fne* in muscle cells reduced the amplitude of EJCs and quantal content and increased STF, suggesting that *fne* plays an important role in synaptic transmission and plasticity.

Knockdown of *fne* in glia affected synaptic transmission and short-term synaptic plasticity in the larval neuromuscular junction

Subsequently, we attempted to determine whether changes in *fne* expression in glia regulate synaptic transmission. The knockdown of *fne* in glia, rather than the overexpression of *fne* (*repo* > *fne-IR*), significantly reduced the amplitude of the EJCs in comparison with those of the EJCs of the controls (*repo* > + and *fne-IR* > +, 9.89 ± 1.03 vs. 18.53 ± 1.67 and 22.31 ± 3.66 nA, respectively, $p < 0.05$; **Figures 7A,C**). A significant reduction in quantal content was observed in the *repo* > *fne-IR* flies (*repo* > *fne-IR*, 20.83 ± 2.54 vs. *repo* > +, 35.35 ± 2.30; *fne-IR* > +, 42.53 ± 6.07, $p < 0.05$; **Figure 7F**). Changes in *fne* expression (*repo* > *fne-IR* and $repo^{ts}$ > *fne*) in glia did not cause the amplitude or frequency of the mEJCs to differ from those of the controls (**Figures 7B,D,E**).

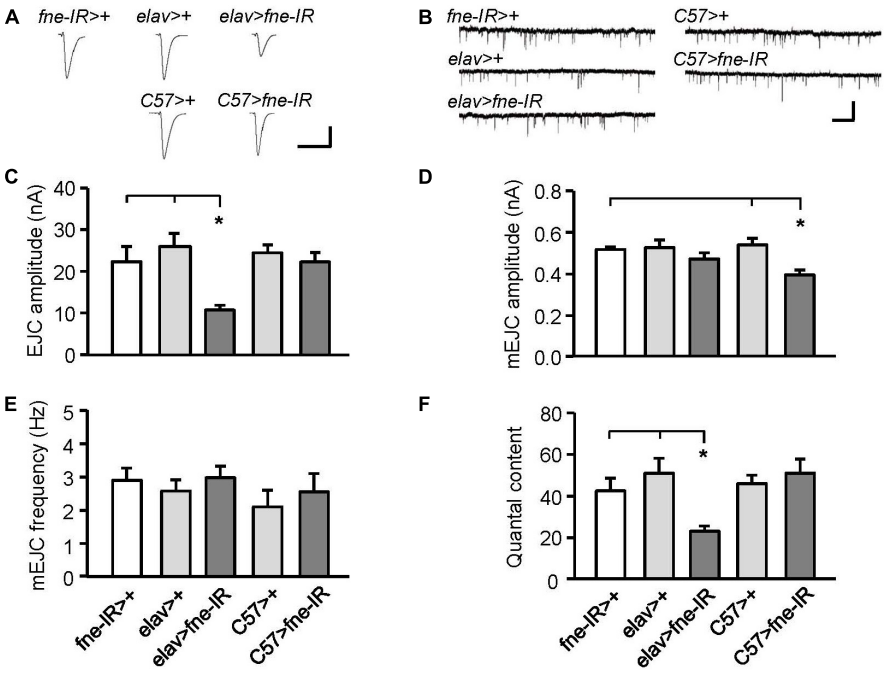

FIGURE 3
Knockdown of *fne* in neurons and muscle cells altered synaptic transmission in the larval NMJ. **(A)** Representative traces of EJC in the indicated genotypes. Calibration: 10 nA, 50 ms. **(B)** Representative traces of mEJC in the indicated genotypes. Calibration: 1 nA, 1 s. Quantification of **(C)** EJC amplitude, **(D)** mEJC amplitude, **(E)** mEJC frequency, and **(F)** quantal content. Error bars represent SEM. $*p < 0.05$, $n = 8$ for each group.

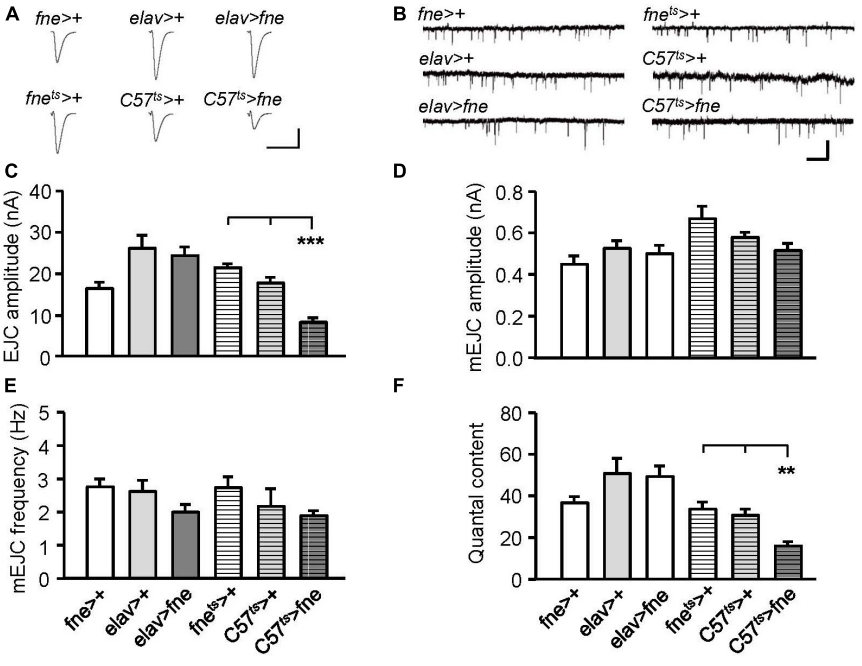

FIGURE 4
Overexpression of *fne* in muscle cells altered synaptic transmission in the larval NMJ. **(A)** Representative traces of EJC in the indicated genotypes. Calibration: 10 nA, 50 ms. **(B)** Representative traces of mEJC in the indicated genotypes. Calibration: 1 nA, 1 s. Quantification of **(C)** EJC amplitude, **(D)** mEJC amplitude, **(E)** mEJC frequency, and **(F)** quantal content. Bars with horizontal lines represented the flies that were reared at 18°C and shifted to 29°C for 1 day to induce *fne* expression. Error bars represent SEM. $**p < 0.01$, $***p < 0.001$, $n = 8$ for each group.

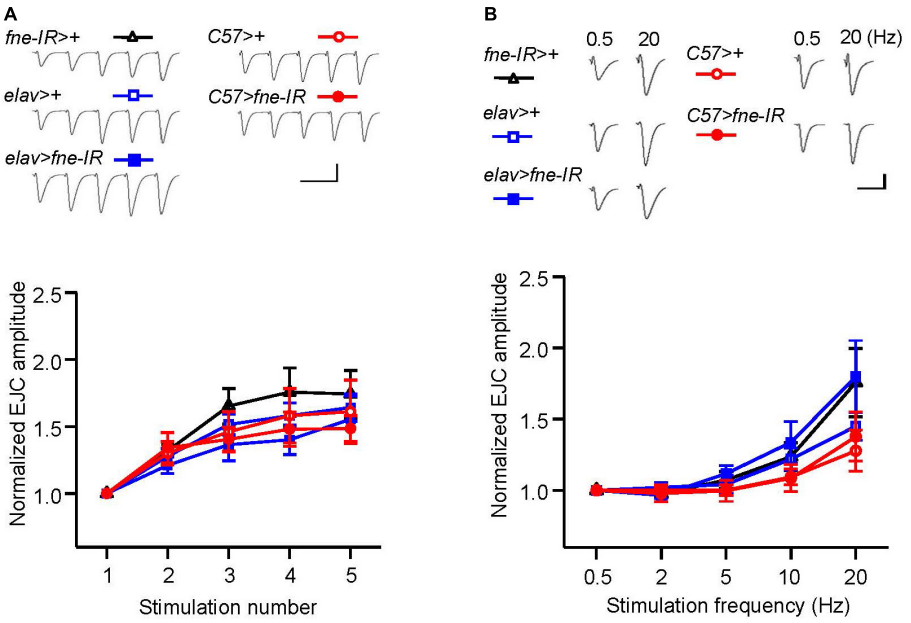

FIGURE 5
Knockdown of *fne* in neurons and muscle cells did not affect short-term synaptic facilitation in the larval NMJ. **(A)** STF during a short train of repetitive stimulation at 25 Hz in the wild type and in the knockdown of *fne* strains. Top, representative traces in the indicated genotypes. Bottom, summary of normalized EJC amplitude. **(B)** STF were determined at the various stimulation frequency of 0.5–20 Hz in the control and in the knockdown of *fne* strains. Top, representative traces of the EJCs for 0.5 and 20 Hz in the indicated genotypes. Bottom, summary of normalized EJC amplitude. Calibration: 10 nA, 50 ms. *N* = 8 for each group. Error bars represent SEM.

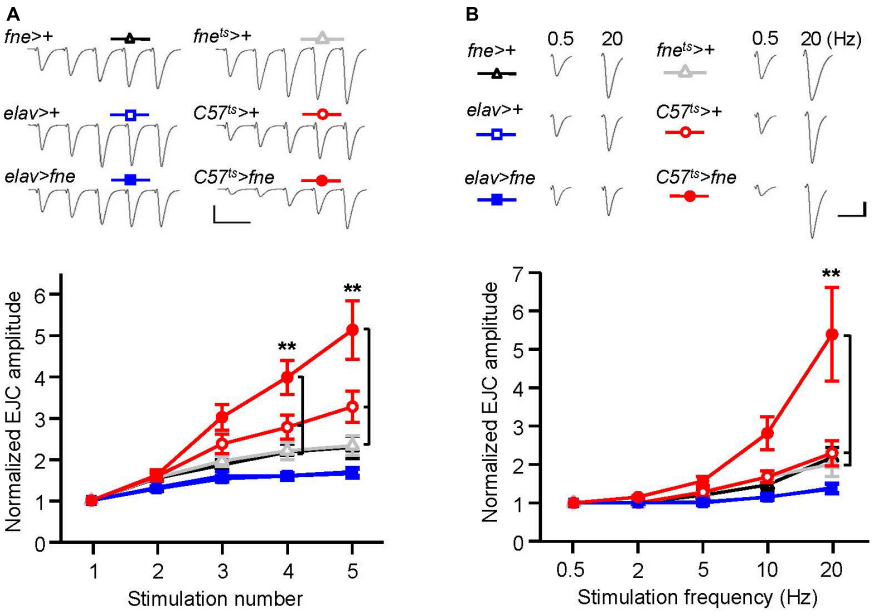

FIGURE 6
Overexpression of *fne* in muscle cells altered short-term synaptic facilitation in the larval NMJ. **(A)** STF during a short train of repetitive stimulation (25 Hz) in the wild type and in the overexpression of *fne* strains. Top, representative traces. Bottom, summary of normalized EJC amplitude. **(B)** STF were determined at the various stimulation frequency (0.5–20 Hz) in the control and in the overexpression of *fne* strains. Top, representative traces of the EJCs for 0.5 and 20 Hz in the indicated genotypes. Bottom, summary of normalized EJC amplitude. The $C57^{ts} > fne$, $C57^{ts} > +$, and $fne^{ts} > +$ flies were reared at 18°C and shifted to 29°C for 1 day to induce *fne* expression. Calibration: 10 nA, 50 ms. $n = 8$ for each group. Error bars represent SEM. $^{**}p < 0.01$.

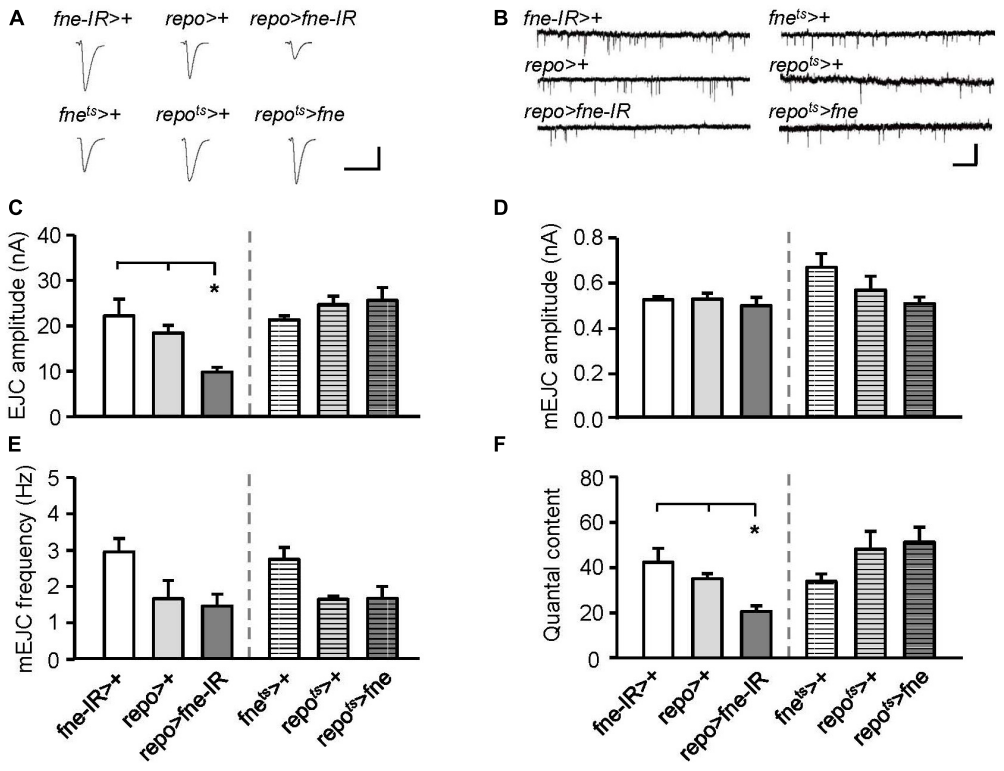

FIGURE 7
Change of *fne* expression in glia altered the synaptic transmission in the larval NMJ. **(A)** Representative traces of EJC while the glia expressing *fne* and *fne-IR*. Calibration: 10 nA, 50 ms. **(B)** Representative traces of mEJC in the indicated genotypes. Calibration: 1 nA, 1 s. Quantification of **(C)** EJC amplitude, **(D)** mEJC amplitude, **(E)** mEJC frequency, and **(F)** quantal content. Bars with horizontal lines represented the flies that were reared at 18°C and shifted to 29°C for 1 day to induce *fne* expression. Error bars represent SEM. $*p < 0.05$, $n = 8$ for each group.

To determine whether changes in *fne* in glia are involved in short-term synaptic plasticity, we induced a short train of repetitive stimulation at 25 Hz. A significant increase in STF, approximately 4.5-fold, occurred after repetitive stimulation for *fne-IR* expression in glia (*repo* > *fne-IR*). However, a normal STF was observed in the *fne*-overexpressing flies ($repo^{ts}$ > *fne*; Figure 8A). In addition, when STF was induced at 0.5–20 Hz, synaptic transmission revealed a frequency-dependent facilitation in the glial *fne*-knockdown flies (*repo* > *fne-IR*). This phenomenon was not observed in flies with *fne* overexpression in glia ($repo^{ts}$ > *fne*; Figure 8B). The results indicated that the knockdown rather than overexpression of *fne* in glia reduced the amplitudes of EJCs and quantal content and increased STF, suggesting that *fne* in glia has an important role in synaptic transmission and plasticity.

Changes of *fne* expression altered fly lifespan

To examine whether changes of *fne* expression can alter fly lifespan, we expressed *fne* and *fne-IR* in neurons and glia started at adult stage under $elav^{ts}$ and $repo^{ts}$ drivers, respectively, and measured their lifespan. Expression pattern of *elav-GAL4* and *repo-GAL4* lines was verified by crossing to a *UAS-GFP* (Supplementary Figure 2). As shown in Figures 9A,B, the mean lifespan decreased by 10.7 and 8.3% when overexpressing *fne* in neurons of male and female flies, respectively. Conversely, knockdown of *fne* expression in neurons increased up to 15.0 and 16.9% lifespan in both males and females, respectively. Similar results also observed when changing *fne* expression in glia (Figures 9C,D). The mean lifespan of $repo^{ts}$ > *fne* flies significantly decreased by 33.2 and 53.2% in males and females, respectively, and in $repo^{ts}$ > *fne-IR* flies, the mean lifespan was extended in both gender by 13.2% (males) and 13.6% (females). Our results suggest that changes of *fne* expression could alter fly lifespan. In particular, knockdown of *fne* expression in both neurons and glia started from the adult stage seems to appear a beneficial effect on longevity in both male and female flies.

Discussion

The ELAV family of proteins have been determined to perform post-transcriptional processes and mediate important

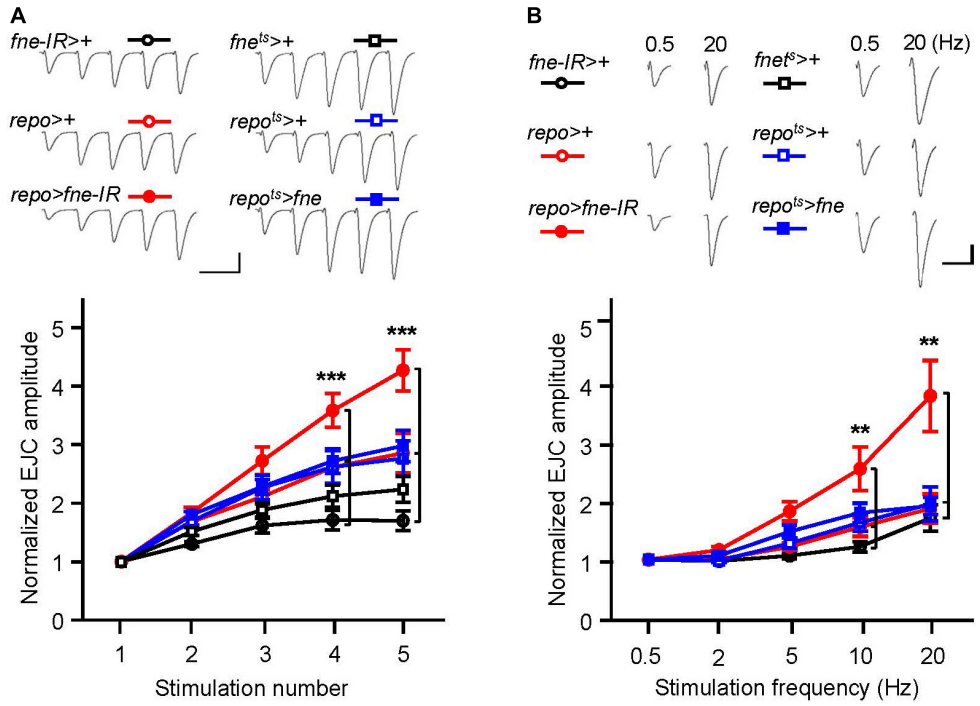

FIGURE 8
Change of *fne* expression in glia altered short-term synaptic facilitation in the larval NMJ. **(A)** STF during a short train of repetitive stimulation (25 Hz) in the control and in the glia expressing *fne* and *fne-IR*. Top, representative traces. Bottom, summary of normalized EJC amplitude. **(B)** STF were determined at the various stimulation frequency (0.5–20 Hz) in the control and in the glia expressing *fne* and *fne-IR*. Top, representative traces of the EJCs for 0.5 and 20 Hz in the indicated genotypes. Bottom, summary of normalized EJC amplitude. The $repo^{ts}$ > *fne*, $repo^{ts}$ > +, and fne^{ts} > + flies were reared at 18°C and shifted to 29°C for 1 day to induce *fne* expression. Calibration: 10 nA, 50 ms. n = 8 for each group. Error bars represent SEM. $^{**}p < 0.01$, $^{***}p < 0.001$.

roles in the *Drosophila* nervous system. For example, neural-specific target transcripts, *erect wing*, *neuroglian*, and *armadillo*, which can interact with ELAV's RRMs, are essential for the development and maintenance of neuronal function (Koushika et al., 2000). At least two target transcripts, *extramacrochaetae* and *bag-of-marbles*, are regulated by the RBP9 protein and regulate neuron and germ cell differentiation, respectively (Park et al., 1998; Kim-Ha et al., 1999). Few reports have identified the target transcripts of the FNE protein, and one target, *Basigin*, which encodes a cell adhesion molecule, accounts for the dendritic growth, and arborization in class IV da neurons during larval development (Alizzi et al., 2020). Little is known about the function of *fne* in neuronal plasticity. Recently, the knockdown of *fne* in muscle cells decreased the mEJC amplitudes. Changes in mEJCs can occur presynaptically (e.g., change in the number of neurotransmitters packed into a vesicle) or postsynaptically (e.g., change in the sensitivity of postsynaptic receptors). The overexpression of *fne* in muscle cells decreased the EJC amplitudes and quantal content and increased STF (all occurred presynaptically). Muscle-specific changes in *fne* expression affected neurotransmission, majorly on the presynaptic side. One possible mechanism is that FNE regulates the postsynaptic activity of calcium/calmodulin-dependent protein kinase II (*CaMKII*) through 3'UTR APA (Tiruchinapalli et al., 2008; Kuklin et al., 2017; Wei and Lai, 2022) and indirect alteration of CaMKII activity affects retrograde control of homeostasis of neurotransmitter release (Haghighi et al., 2003).

In addition, the loss of neuronal and glial *fne* resulted in presynaptic defects in neurotransmission, including smaller EJC amplitudes and quantal content, whereas normal transmission was observed in the overexpression of neuronal and glial *fne*. The loss of glial *fne* also increased STF (a presynaptic property), suggesting that *fne* is a critical regulator of neuronal transmission and synaptic plasticity. Several reports have characterized the role of glia in the PNS of *Drosophila*. The perineurial glial cells clear presynaptic debris through phagocytosis to modulate neuronal branching and shape synaptic connections during development or to do so in an activity-dependent manner (Fuentes-Medel et al., 2009). One purposed mechanism of glial *fne* in the regulation of synaptic transmission is through *genderblind* (*gb*). *fne* mutant affects 3'UTR APA of *gb* (Wei et al., 2020). Disruption of perineurial glial *gb* causes a reduction in extracellular free glutamate and results in increased postsynaptic glutamate receptor clustering and long-term strengthening of glutamatergic synapses at

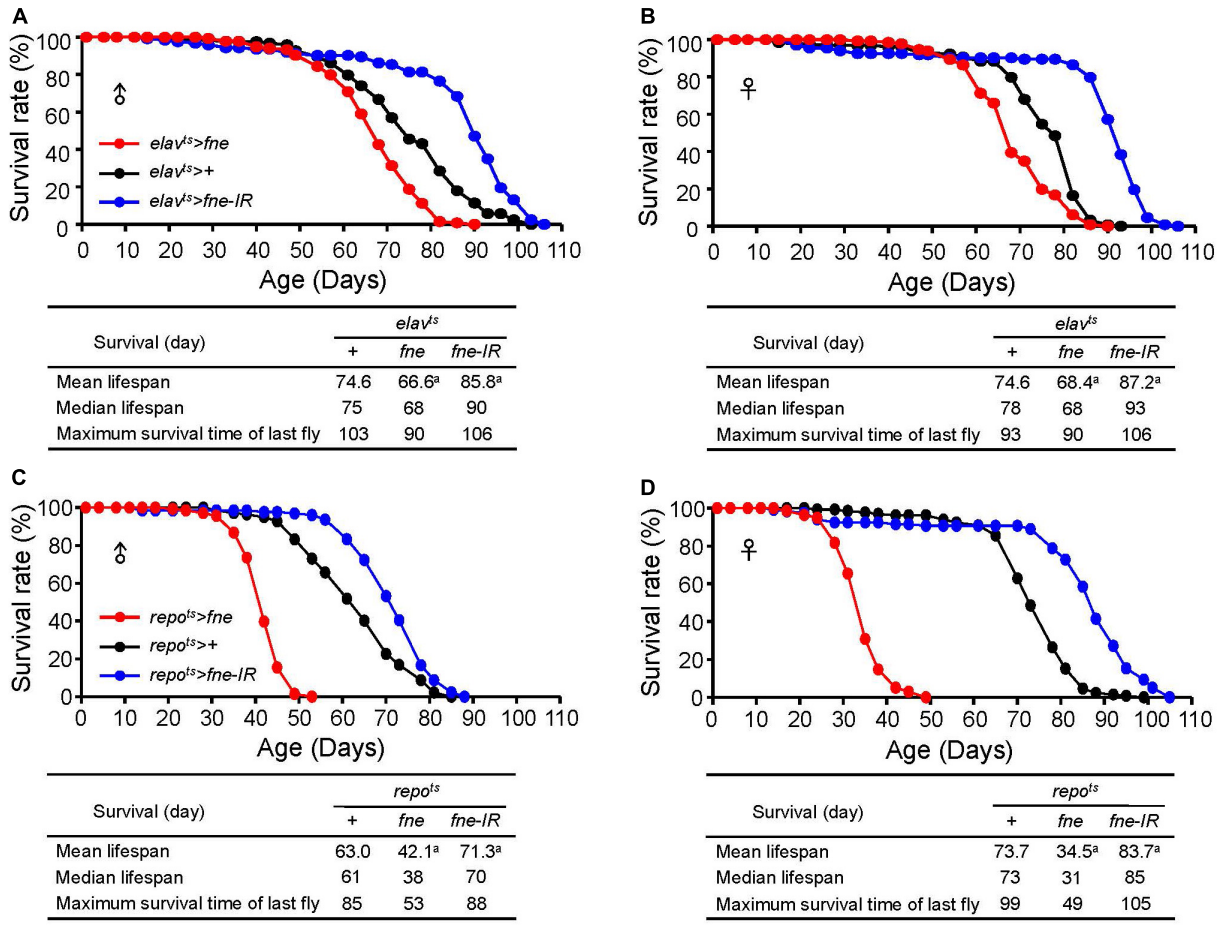

Survival (day)	$elav^{ts}$ +	$elav^{ts}$ *fne*	$elav^{ts}$ *fne-IR*
Mean lifespan	74.6	66.6[a]	85.8[a]
Median lifespan	75	68	90
Maximum survival time of last fly	103	90	106

Survival (day)	$elav^{ts}$ +	$elav^{ts}$ *fne*	$elav^{ts}$ *fne-IR*
Mean lifespan	74.6	68.4[a]	87.2[a]
Median lifespan	78	68	93
Maximum survival time of last fly	93	90	106

Survival (day)	$repo^{ts}$ +	$repo^{ts}$ *fne*	$repo^{ts}$ *fne-IR*
Mean lifespan	63.0	42.1[a]	71.3[a]
Median lifespan	61	38	70
Maximum survival time of last fly	85	53	88

Survival (day)	$repo^{ts}$ +	$repo^{ts}$ *fne*	$repo^{ts}$ *fne-IR*
Mean lifespan	73.7	34.5[a]	83.7[a]
Median lifespan	73	31	85
Maximum survival time of last fly	99	49	105

FIGURE 9
Effects of *fne* expression on the lifespan in neurons and glia. The survival curve of overexpression and knockdown of *fne* in neurons. Data represent the total lifespan of examined **(A)** male and **(B)** female flies. The genotypes of each group are $elav^{ts}$ > *fne* (red circle), $elav^{ts}$ > + (black circle), and $elav^{ts}$ > *fne-IR* (blue circle). The total lifespan of overexpression and knockdown of *fne* in glia represents in **(C)** male and **(D)** female flies. The genotypes of each group are $repo^{ts}$ > *fne* (red circle), $repo^{ts}$ > + (black circle), and $repo^{ts}$ > *fne-IR* (blue circle). Flies were reared at 18°C and transferred to 25°C after eclosion to induce *fne* and *fne-IR* expression. Total n = 120–130 for each group. Data are significantly different from the control at $^{a}p < 0.001$.

the NMJ (Sigrist et al., 2002; Augustin et al., 2007). Thus, glial cells also contribute to homeostatic plasticity, a process that modulates the presynaptic release of neurotransmitters, which is considered a compensatory response to the loss or inhibition of postsynaptic receptors (Wang et al., 2020). By converging the modulation of synaptic transmission with neurons, glial *fne* expression can influence neurotransmission between presynaptic and postsynaptic cells.

Although the ELAVL/Hu protein family has been determined to regulate neuronal development and differentiation, few reports have described their function in the retina. Amato et al. (2005) demonstrated the distribution of three members of the ELAVL/Hu family in *Xenopus* retinogenesis during retinal development, and Pacal and Bremner (2012) identified the expression patterns of Elavl2/3/4 in a developing murine retina. Elavl2 was also identified to express in retinal cells during retinogenesis and ablation of Elavl2 leads to deficit in ERG responses and visual acuity (Wu et al., 2021). The *elav* of *Drosophila* expresses in the imaginal disc of the larval eye and the adult optic lobe (Robinow and White, 1988). We found changes in the level of *fne* expression in both photoreceptors and glia beginning at the adult stage altered light-evoked synaptic potential. In the visual system of adult *Drosophila*, light stimuli depolarize photoreceptors to induce the release of histamines and activate postsynaptic receptors, histamine-gated Cl^{-} channels, on the lamina neurons (Chaturvedi et al., 2014). The ERG response can be modulated by the surrounding epithelial glia through the removal of histamines from the synaptic cleft (Stuart et al., 2007; Chaturvedi et al., 2014). Thus, for the retina, changes in *fne* expression in glia cause more severe defects than in neurons, particularly for the on- and

off-transient amplitudes, suggesting a significant role of glial *fne* in phototransduction.

A study from Ustaoglu et al. (2021) found that elavl2 is required for learning and memory consolidation in honey bees. Another study showed that ELAVL2-regulated transcriptional and splicing networks in human neurons including RBFOX1 and FMRP-related pathway are involved in synaptic function and neural development (Berto et al., 2016). These results highlight ELAVL/Hu's regulator of important neuronal pathways. For the lifespan experiment, our data showed that knockdown of *fne* in neurons and glia could cause the lifespan extension in both genders. However, genetic background effects might produce variable lifespan results, since we did not backcross at least 6 generations to produce the isogenic *UAS* strains (Piper and Partridge, 2016). Thus, we provided the tentative conclusion and further exploration need to be done for lifespan.

For the orthologs of *fne* in humans, FNE strongly shares its amino acid identity with ELAVL2/HuB and ELAVL4/HuD (Samson and Chalvet, 2003). Studies have indicated that ELAVL2/HuB and ELAVL4/HuD are highly enriched in the neuronal lineage but absent in glial cells (King et al., 1994; Mirisis and Carew, 2019; Hilgers, 2022). Defects in ELAVL2/HuB, ELAVL4/HuD, and their target transcripts can lead to abnormal neuronal proliferation and development and result in the pathogenesis of numerous CNS disorders, including seizures, autism, and schizophrenia (Yamada et al., 2011; Bronicki and Jasmin, 2013; Berto et al., 2016; Zybura-Broda et al., 2018). Silencing ELAVL1/HuR, which also shares high amino acid identity with FNE (Samson and Chalvet, 2003) in the activated microglia and astrocytes attenuate neuroinflammation and the occurrence of amyotrophic lateral sclerosis (Borgonetti et al., 2021). Thus, we conducted a bioinformatic analysis of *ELAVL2/HuB* and *ELAVL4/HuD* in neurons and glia from published gene expression datasets of human, mice, and rat samples. Two genes are expressed in all types of glia and neurons at similar levels (**Supplementary Table 1**). Similar human's results also observed in the database of The Human Protein Atlas (Digre and Lindskog, 2021).

In the present, we found changes in the level of *fne* expression in neurons and glia affected phototransduction, adult behaviors, synaptic transmission of larval NMJ, and could influence the lifespan. Although the *Drosophila* ELAV protein can be detected in the majority of neurons, Berger et al. (2007) demonstrated that ELAV can transiently express in early embryonic glial cells but not in adults. The expression of *fne* in glia has never been reported. Our findings highlighted the important *fne*'s function not only in neurons but also in glia. As FNE is an RNA-binding protein, homeostatic maintenance of FNE stability and its downstream multiple pathways through target transcripts is crucial for brain activities. Further explorations into the physiological and molecular functions of glial *fne* are expected to clarify certain *Drosophila* behaviors, which may also be a feature of mammal brains.

Data availability statement

The original contributions presented in this study are included in the article/**Supplementary material**, further inquiries can be directed to the corresponding author.

Author contributions

W-YL and H-PL wrote the manuscript. C-HL, W-YL, and H-PL performed the experiments. JC carried out the bioinformatic analysis. H-PL supervised the research and funding acquisition. All authors have read and approved the final manuscript.

Funding

This work was supported by the China Medical University (CMU108-MF-61, CMU109-MF-110, and CMU110-MF-92) and the National Science and Technology Council in Taiwan (MOST 108-2320-B-039-031-MY3, MOST 109-2314-B-039-030, and MOST 111-2314-B-039-017-MY3).

Conflict of interest

The authors declare that the research was conducted in the absence of any commercial or financial relationships that could be construed as a potential conflict of interest.

Publisher's note

Supplementary material

The Supplementary Material for this article can be found online at: https://www.frontiersin.org/articles/10.3389/fnmol.2022.1006455/full#supplementary-material

References

Alizzi, R. A., Xu, D., Tenenbaum, C. M., Wang, W., and Gavis, E. R. (2020). The ELAV/Hu protein Found in neurons regulates cytoskeletal and ECM adhesion inputs for space-filling dendrite growth. *PLoS Genet.* 16:e1009235. doi: 10.1371/journal.pgen.1009235

Amato, M. A., Boy, S., Arnault, E., Girard, M., Della Puppa, A., Sharif, A., et al. (2005). Comparison of the expression patterns of five neural RNA binding proteins in the *Xenopus* retina. *J. Comp. Neurol.* 481, 331–339. doi: 10.1002/cne.20387

Augustin, H., Grosjean, Y., Chen, K., Sheng, Q., and Featherstone, D. E. (2007). Nonvesicular release of glutamate by glial xCT transporters suppresses glutamate receptor clustering in vivo. *J. Neurosci.* 27, 111–123. doi: 10.1523/JNEUROSCI.4770-06.2007

Berger, C., Renner, S., Luer, K., and Technau, G. M. (2007). The commonly used marker ELAV is transiently expressed in neuroblasts and glial cells in the *Drosophila* embryonic CNS. *Dev. Dyn.* 236, 3562–3568. doi: 10.1002/dvdy.21372

Berto, S., Usui, N., Konopka, G., and Fogel, B. L. (2016). ELAVL2-regulated transcriptional and splicing networks in human neurons link neurodevelopment and autism. *Hum. Mol. Genet.* 25, 2451–2464. doi: 10.1093/hmg/ddw110

Borgonetti, V., Coppi, E., and Galeotti, N. (2021). Targeting the RNA-binding protein HuR as potential thera-peutic approach for neurological disorders: Focus on amyo-trophic lateral sclerosis (ALS), spinal muscle atrophy (SMA) and multiple sclerosis. *Int. J. Mol. Sci.* 22:10394. doi: 10.3390/ijms221910394

Bronicki, L. M., and Jasmin, B. J. (2013). Emerging complexity of the HuD/ELAVl4 gene; implications for neuronal development, function, and dysfunction. *RNA* 19, 1019–1037. doi: 10.1261/rna.039164.113

Carrasco, J., Rauer, M., Hummel, B., Grzejda, D., Alfonso-Gonzalez, C., Lee, Y., et al. (2020). ELAV and FNE determine neuronal transcript signatures through EXon-activated rescue. *Mol. Cell* 15:e156. doi: 10.1016/j.molcel.2020.09.011

Chalvet, F., and Samson, M. L. (2002). Characterization of fly strains permitting GAL4-directed expression of found in neurons. *Genesis* 34, 71–73. doi: 10.1002/gene.10108

Chaturvedi, R., Reddig, K., and Li, H. S. (2014). Long-distance mechanism of neurotransmitter recycling mediated by glial network facilitates visual function in *Drosophila*. *Proc. Natl. Acad. Sci. U.S.A.* 111, 2812–2817. doi: 10.1073/pnas.1323714111

Colombrita, C., Silani, V., and Ratti, A. (2013). ELAV proteins along evolution: Back to the nucleus? *Mol. Cell. Neurosci.* 56, 447–455. doi: 10.1016/j.mcn.2013.02.003

Cosens, D. J., and Manning, A. (1969). Abnormal electroretinogram from a *Drosophila* mutant. *Nature* 224, 285–287. doi: 10.1038/224285a0

Digre, A., and Lindskog, C. (2021). The human protein atlas-spatial localization of the human proteome in health and disease. *Protein Sci.* 30, 218–233. doi: 10.1002/pro.3987

Dubnau, J., Grady, L., Kitamoto, T., and Tully, T. (2001). Disruption of neurotransmission in *Drosophila* mushroom body blocks retrieval but not acquisition of memory. *Nature* 411, 476–480. doi: 10.1038/35078077

Edwards, T. N., and Meinertzhagen, I. A. (2010). The functional organisation of glia in the adult brain of *Drosophila* and other insects. *Prog. Neurobiol.* 90, 471–497. doi: 10.1016/j.pneurobio.2010.01.001

Fuentes-Medel, Y., Logan, M. A., Ashley, J., Ataman, B., Budnik, V., and Freeman, M. R. (2009). Glia and muscle sculpt neuromuscular arbors by engulfing destabilized synaptic boutons and shed presynaptic debris. *PLoS Biol.* 7:e1000184. doi: 10.1371/journal.pbio.1000184

Guo, H. F., and Zhong, Y. (2006). Requirement of Akt to mediate long-term synaptic depression in *Drosophila*. *J. Neurosci.* 26, 4004–4014. doi: 10.1523/JNEUROSCI.3616-05.2006

Haghighi, A. P., McCabe, B. D., Fetter, R. D., Palmer, J. E., Hom, S., and Goodman, C. S. (2003). Retrograde control of synaptic transmission by postsynaptic CaMKII at the *Drosophila* neuromuscular junction. *Neuron* 39, 255–267. doi: 10.1016/s0896-6273(03)00427-6

Hilgers, V. (2022). Regulation of neuronal RNA signatures by ELAV/Hu proteins. *Wiley Interdiscip. Rev. RNA* e1733. doi: 10.1002/wrna.1733 [Epub ahead of print].

Jimenez, F., and Campos-Ortega, J. A. (1987). Genes in subdivision 1B of the *Drosophila melanogaster* X-chromosome and their influence on neural development. *J. Neurogenet.* 4, 179–200.

Kim, J., Kim, Y. J., and Kim-Ha, J. (2010). Blood-brain barrier defects associated with Rbp9 mutation. *Mol. Cells* 29, 93–98. doi: 10.1007/s10059-010-0040-0

Kim-Ha, J., Kim, J., and Kim, Y. J. (1999). Requirement of RBP9, a *Drosophila* Hu homolog, for regulation of cystocyte differentiation and oocyte determination during oogenesis. *Mol. Cell Biol.* 19, 2505–2514. doi: 10.1128/mcb.19.4.2505

King, P. H., Levine, T. D., Fremeau, R. T. Jr., and Keene, J. D. (1994). Mammalian homologs of *Drosophila* ELAV localized to a neuronal subset can bind in vitro to the 3' UTR of mRNA encoding the Id transcriptional repressor. *J. Neurosci.* 14, 1943–1952. doi: 10.1523/JNEUROSCI.14-04-01943.1994

Koushika, S. P., Lisbin, M. J., and White, K. (1996). ELAV, a *Drosophila* neuron-specific protein, mediates the generation of an alternatively spliced neural protein isoform. *Curr. Biol.* 6, 1634–1641. doi: 10.1016/s0960-9822(02)70787-2

Koushika, S. P., Soller, M., and White, K. (2000). The neuron-enriched splicing pattern of *Drosophila* erect wing is dependent on the presence of ELAV protein. *Mol. Cell. Biol.* 20, 1836–1845. doi: 10.1128/mcb.20.5.1836-1845.2000

Kuklin, E. A., Alkins, S., Bakthavachalu, B., Genco, M. C., Sudhakaran, I., Raghavan, K. V., et al. (2017). The long 3'UTR mRNA of CaMKII is essential for translation-dependent plasticity of spontaneous release in *Drosophila melanogaster*. *J. Neurosci.* 37, 10554–10566. doi: 10.1523/JNEUROSCI.1313-17.2017

Logan, M. A. (2017). Glial contributions to neuronal health and disease: New insights from *Drosophila*. *Curr. Opin. Neurobiol.* 47, 162–167. doi: 10.1016/j.conb.2017.10.008

McGuire, S. E., Mao, Z., and Davis, R. L. (2004). Spatiotemporal gene expression targeting with the TARGET and gene-switch systems in *Drosophila*. *Sci. STKE* 2004:l6. doi: 10.1126/stke.2202004pl6

Mirisis, A. A., and Carew, T. J. (2019). The ELAV family of RNA-binding proteins in synaptic plasticity and long-term memory. *Neurobiol. Learn. Mem.* 161, 143–148. doi: 10.1016/j.nlm.2019.04.007

Montell, C. (1999). Visual transduction in *Drosophila*. *Annu. Rev. Cell Dev. Biol.* 15, 231–268. doi: 10.1146/annurev.cellbio.15.1.231

Nagai, J., Yu, X., Papouin, T., Cheong, E., Freeman, M. R., Monk, K. R., et al. (2021). Behaviorally consequential astrocytic regulation of neural circuits. *Neuron* 109, 576–596. doi: 10.1016/j.neuron.2020.12.008

Neely, G. G., Keene, A. C., Duchek, P., Chang, E. C., Wang, Q. P., Aksoy, Y. A., et al. (2011). TrpA1 regulates thermal nociception in *Drosophila*. *PLoS One* 6:e24343. doi: 10.1371/journal.pone.0024343

Ou, J., He, Y., Xiao, X., Yu, T. M., Chen, C., Gao, Z., et al. (2014). Glial cells in neuronal development: Recent advances and insights from *Drosophila melanogaster*. *Neurosci. Bull.* 30, 584–594. doi: 10.1007/s12264-014-1448-2

Pacal, M., and Bremner, R. (2012). Mapping differentiation kinetics in the mouse retina reveals an extensive period of cell cycle protein expression in post-mitotic newborn neurons. *Dev. Dyn.* 241, 1525–1544. doi: 10.1002/dvdy.23840

Park, S. J., Yang, E. S., Kim-Ha, J., and Kim, Y. J. (1998). Down regulation of extramacrochaetae mRNA by a *Drosophila* neural RNA binding protein Rbp9 which is homologous to human Hu proteins. *Nucleic Acids Res.* 26, 2989–2994. doi: 10.1093/nar/26.12.2989

Piper, M. D., and Partridge, L. (2016). Protocols to study aging in *Drosophila*. *Methods Mol. Biol.* 1478, 291–302. doi: 10.1007/978-1-4939-6371-3_18

Robinow, S., and White, K. (1988). The locus elav of *Drosophila melanogaster* is expressed in neurons at all developmental stages. *Dev. Biol.* 126, 294–303. doi: 10.1016/0012-1606(88)90139-x

Samson, M. L. (2008). Rapid functional diversification in the structurally conserved ELAV family of neuronal RNA binding proteins. *BMC Genomics* 9:392. doi: 10.1186/1471-2164-9-392

Samson, M. L., and Chalvet, F. (2003). found in neurons, a third member of the *Drosophila* elav gene family, encodes a neuronal protein and interacts with elav. *Mech. Dev.* 120, 373–383. doi: 10.1016/s0925-4773(02)00444-6

Sigrist, S. J., Thiel, P. R., Reiff, D. F., and Schuster, C. M. (2002). The postsynaptic glutamate receptor subunit DGluR-IIA mediates long-term plasticity in *Drosophila*. *J. Neurosci.* 22, 7362–7372. doi: 10.1523/JNEUROSCI.22-17-07362.2002

Stuart, A. E., Borycz, J., and Meinertzhagen, I. A. (2007). The dynamics of signaling at the histaminergic photoreceptor synapse of arthropods. *Prog. Neurobiol.* 82, 202–227. doi: 10.1016/j.pneurobio.2007.03.006

Sun, X., Yang, H., Sturgill, D., Oliver, B., Rabinow, L., and Samson, M. L. (2015). Sxl-Dependent, tra/tra2-independent alternative splicing of the *Drosophila melanogaster* X-linked gene found in neurons. *G3 (Bethesda)* 5, 2865–2874. doi: 10.1534/g3.115.023721

Tiruchinapalli, D. M., Ehlers, M. D., and Keene, J. D. (2008). Activity-dependent expression of RNA binding protein HuD and its association with mRNAs in neurons. *RNA Biol.* 5, 157–168. doi: 10.4161/rna.5.3.6782

Ustaoglu, P., Gill, J. K., Doubovetzky, N., Haussmann, I. U., Dix, T. C., Arnold, R., et al. (2021). Dynamically expressed single ELAV/Hu orthologue elavl2 of bees is required for learning and memory. *Commun. Biol.* 4:1234. doi: 10.1038/s42003-021-02763-1

Wang, T., Morency, D. T., Harris, N., and Davis, G. W. (2020). Epigenetic signaling in glia controls presynaptic homeostatic plasticity. *Neuron* 105, 491–505.e3. doi: 10.1016/j.neuron.2019.10.041

Wei, L., and Lai, E. C. (2022). Regulation of the alternative neural transcriptome by ELAV/Hu RNA binding proteins. *Front. Genet.* 13:848626. doi: 10.3389/fgene.2022.848626

Wei, L., Lee, S., Majumdar, S., Zhang, B., Sanfilippo, P., Joseph, B., et al. (2020). Overlapping activities of ELAV/Hu Family RNA binding proteins specify the extended neuronal 3' UTR landscape in *Drosophila*. *Mol. Cell* 14:e146. doi: 10.1016/j.molcel.2020.09.007

Wu, M., Deng, Q., Lei, X., Du, Y., and Shen, Y. (2021). Elavl2 regulates retinal function via modulating the differentiation of amacrine cells subtype. *Invest. Ophthalmol. Vis. Sci.* 62:1. doi: 10.1167/iovs.62.7.1

Yamada, K., Iwayama, Y., Hattori, E., Iwamoto, K., Toyota, T., Ohnishi, T., et al. (2011). Genome-wide association study of schizophrenia in Japanese population. *PLoS One* 6:e20468. doi: 10.1371/journal.pone.0020468

Yildirim, K., Petri, J., Kottmeier, R., and Klambt, C. (2019). *Drosophila* glia: Few cell types and many conserved functions. *Glia* 67, 5–26. doi: 10.1002/glia.23459

Zanini, D., Jallon, J. M., Rabinow, L., and Samson, M. L. (2012). Deletion of the *Drosophila* neuronal gene found in neurons disrupts brain anatomy and male courtship. *Genes Brain Behav.* 11, 819–827. doi: 10.1111/j.1601-183X.2012.00817.x

Zybura-Broda, K., Wolder-Gontarek, M., Ambrozek-Latecka, M., Choros, A., Bogusz, A., Wilemska-Dziaduszycka, J., et al. (2018). HuR (Elavl1) and HuB (Elavl2) stabilize matrix metalloproteinase-9 mRNA during seizure-induced Mmp-9 expression in neurons. *Front. Neurosci.* 12:224. doi: 10.3389/fnins.2018.00224

frontiers | Frontiers in Molecular Neuroscience

TYPE Original Research
PUBLISHED 22 December 2022
DOI 10.3389/fnmol.2022.1047801

OPEN ACCESS

EDITED BY
Muddanna Sakkattu Rao,
Kuwait University,
Kuwait

REVIEWED BY
Tushar Deshpande,
University Hospital Münster,
Germany
Mingxuan Xu,
University of Texas MD Anderson Cancer Center, United States

*CORRESPONDENCE
Weihua Yu
✉ yuweihua@cqmu.edu.cn

†These authors have contributed equally to this work

SPECIALTY SECTION
This article was submitted to Brain Disease Mechanisms, a section of the journal Frontiers in Molecular Neuroscience

RECEIVED 18 September 2022
ACCEPTED 02 December 2022
PUBLISHED 22 December 2022

CITATION
Zhong F, Gan Y, Song J, Zhang W, Yuan S, Qin Z, Wu J, Lü Y and Yu W (2022) The inhibition of PGAM5 suppresses seizures in a kainate-induced epilepsy model *via* mitophagy reduction. *Front. Mol. Neurosci.* 15:1047801. doi: 10.3389/fnmol.2022.1047801

The inhibition of PGAM5 suppresses seizures in a kainate-induced epilepsy model *via* mitophagy reduction

Fuxin Zhong[1†], Yunhao Gan[2†], Jiaqi Song[1], Wenbo Zhang[3], Shiyun Yuan[3], Zhangjin Qin[1], Jiani Wu[3], Yang Lü[3] and Weihua Yu[1*]

[1]Department of Human Anatomy, Institute of Neuroscience, Chongqing Medical University, Chongqing, China, [2]Department of Neurology, Children's Hospital of Chongqing Medical University, Chongqing, China, [3]Department of Geriatrics, The First Affiliated Hospital of Chongqing Medical University, Chongqing, China

Background: Epilepsy is a common neurological disease, and excessive mitophagy is considered as one of the major triggers of epilepsy. Mitophagy is a crucial pathway affecting reactive oxygen species. Phosphoglycerate mutase 5 (PGAM5) is a protein phosphatase present in mitochondria that regulates many biological processes including mitophagy and cell death. However, the mechanism of PGAM5 in epilepsy remains unclear. The purpose of the present study was to examine whether PGAM5 affects epilepsy through PTEN-induced putative kinase 1 (PINK1)-mediated mitophagy.

Methods: After the knockdown of PGAM5 expression by the adeno-associated virus, an epilepsy model was created by kainic acid. Next, the seizure activity was recorded by local field potentials before evaluating the level of mitochondrial autophagy marker proteins. Lastly, the ultrastructure of mitochondria, neuronal damage and oxidative stress levels were further observed.

Results: A higher PGAM5 level was found in epilepsy, and its cellular localization was in neurons. The interactions between PGAM5 and PINK1 in epilepsy were further found. After the knockdown of PGAM5, the level of PINK1 and light chain 3B was decreased and the expression of the translocase of the inner mitochondrial membrane 23 and translocase of the outer mitochondrial membrane 20 were both increased. Knockdown of PGAM5 also resulted in reduced neuronal damage, decreased malondialdehyde levels, decreased reactive oxygen species production and increased superoxide dismutase activity. In addition, the duration of spontaneous seizure-like events (SLEs), the number of SLEs and the time spent in SLEs were all reduced in the epilepsy model after inhibition of PGAM5 expression.

Conclusion: Inhibition of PGAM5 expression reduces seizures *via* inhibiting PINK1-mediated mitophagy.

KEYWORDS

epilepsy, seizure, PGAM5, PINK1, mitophagy, oxidative stress

Introduction

Epilepsy is a serious chronic neurological disease characterized by long-term vulnerability to seizures, affecting over 50 million people worldwide. Although dozens of antiseizure drugs (ASDs) have been applied to epilepsy treatment in clinical practice, still more than 30% of epilepsy patients experience recurrent seizures and undesirable side effects (Lopes et al., 2015). Therefore, there is currently an urgent need to explore the pathological mechanism of epilepsy to devise new therapeutic interventions. It is now well accepted the main pathology following epileptic seizures is the loss of neuronal cells, especially in the hippocampus (Lopes et al., 2015). Interestingly, recent studies have reported that neuronal loss may be attributed to autophagy (Wu et al., 2018).

Mitophagy shows an important role in removing damaged mitochondria and maintaining normal physiological processes in cells. However, over-mitophagy has been found in the kainic acid (KA)-induced epilepsy model (Zhang et al., 2020). It is reported that damaged mitochondria accumulate abnormally in the hippocampal region of patients with epilepsy, which may be a predisposing factor for epilepsy (Liang et al., 2000). Mitochondria are the primary site of reactive oxygen species (ROS) production. A high level of mitochondrial ROS contributes to neuronal damage in seizures, which plays a vital role in the pathogenesis of epilepsy (Das et al., 2010). In addition, Mitophagy is also an essential pathway for maintaining cellular homeostasis by selectively sequestering and removing damaged mitochondria. It is reported that PTEN-induced putative kinase protein 1 (PINK1) is one of the well-known indicators related to mitophagy (Geisler et al., 2010). The primary function of PINK1 is accumulating on the outer mitochondrial membrane (OMM) of damaged mitophagy and then recruiting the E3 ubiquitin ligase Parkin to induce damaged mitochondria degradation (Meyer et al., 2017). The dysfunction of the PINK1 pathway reduces the degradation of damaged mitochondria, which usually causes oxidative damage (Kim et al., 2008; Matsuda et al., 2010; Narendra et al., 2010). Moreover, if cells cannot eliminate oxidative damage, higher levels of oxidative stress can lead to the accumulation of damaged mitochondria and defects in mitophagy (Liesa et al., 2012).

Phosphoglycerate mutase family member 5 (PGAM5) plays a significant role in regulating mitochondrial homeostasis as a serine/threonine protein phosphatase in mitochondria (Takeda et al., 2009). On the one hand, PGAM5 can protects PINK1 from the degradation of the inner mitochondrial membrane (IMM), and stabilizes PINK1 in mitochondria as well as attenuates Parkinson-like dyskinesia (Lu et al., 2014; Park et al., 2018). Also, it can also enhance oxygen consumption through the inhibition of PGAM5 in adipocytes and mitophagy (Sugawara et al., 2020). However, the role of PGAM5 in epilepsy remains unclear. It is unclear whether PGAM5 is involved in epilepsy and is associated with PINK1-mediated mitophagy. Therefore, the purpose of this study was to observe the changes of mitophagy in the KA-induced epilepsy model after the inhibition of PGAM5 to clarify the potential mechanism. These findings indicate that regulating PGAM5 may be a new method to prevent epilepsy.

Materials and methods

Mice

Adult male C57BL/6J mice aged 5–8 weeks and weighing 24 g to 26 g were bred and maintained in the Laboratory Animal Center of Chongqing Medical University at specific pathogen-free conditions with a standardized environment, free eating, and drinking. Three mice were maintained in one cage. All procedures used on mice have been approved by the Commission of Chongqing Medical University for Ethics of Experiments on Animals and comply with the "Guidelines for the Care and Use of Laboratory Animals of the National Institute of Health." The mice were randomly assigned to different groups, and the experimenter only knew the group number of mice and did not know the grouping status.

Reagents

Rabbit PGAM5 antibody was purchased from Novus (NBP1, 92,257); Mouse PGAM5 (Santa, sc515880); Rabbit PINK1 (Proteintech, 23,274-1-AP) and translocase of the outer mitochondrial membrane 20 (TOMM20, Proteintech, 11,802-AP), translocase of the inner mitochondrial membrane 23 (TIMM23, Proteintech, 11,123-1-AP), light chain 3 (LC3, Proteintech, 14,600-1-AP); β-Actin (Proteintech, 20,536-1-AP); Mouse microtubule-associated protein 2 (MAP2, SAB, 38022) and glial fibrillary acidic protein (GFAP, SAB, 38014); Mouse ionized calcium-binding adapter molecule 1 (IBA1, Servicebio, O70200). The antibodies used in this study were used according to the instructions, and the molecular weights observed in WB were consistent with the literature (Wu et al., 2018; Wang et al., 2020; Gao et al., 2021; Brunelli et al., 2022).

Abbreviations: PGAM5, Phosphoglycerate mutase 5; PINK1, PTEN-induced putative kinase 1; ASDs, antiseizure drugs; KA, kainic acid; TLE, temporal lobe epilepsy; AAV, Adeno-associated virus; DG, dentate gyrus; SPF, specific pathogen-free; TOMM20, translocase of the outer mitochondrial membrane 20; TIMM23, translocase of the inner mitochondrial membrane 23; LC3 B, light chain 3 B; MAP2, microtubule-associated protein 2; GFAP, glial fibrillary acidic protein; IBA1, ionized calcium-binding adapter molecule 1; TBST, tris-buffered saline with Tween-20; PBST, pbs saline containing Tween-20; MDA, malondialdehyde; SOD, superoxide dismutase; ROS, reactive oxygen species; TEM, transmission electron microscope; RT-qPCR, Reverse transcription-quantitative polymerase chain reaction; LFPs, local field potentials; SE, status epilepticus; SLEs, spontaneous seizure-like events; OMM, outer mitochondrial membrane; IMM, inner mitochondrial membrane; DHE, dihydroethidium; OS, oxidative stress; PARL, presenilin-associated rhomboid-like protein.

Adeno-associated virus construction and Intrahippocampal injections of virus

An AAV carried a siRNA directed against PGAM5 to reduce hippocampal PGAM5 levels (AAV-RNAi-KA group). The vehicle for the control group was Con-AAV-KA. Mice without treatment were called the control group. Control siRNA and PGAM5 siRNAs were provided by Genechem (Shanghai). Three target sequences (PGAM5 siRNA-1: CAATGTCATCCGCTATATT; PGAM5 siRNA-2: AGAAGACGAGTTGACATCC; PGAM5 siRNA-3: AGTAGAGACCACAGACATC) were assessed for excluding off-target effects. The basic Local Alignment Search Tool (BLAST,[1]) was used to verify the off-target effects. The results showed no off-target effect of siRNA - 1: CAATGTCATCCGCTATATT. Therefore, the siRNA - 1 sequence was chosen to knock down the expression of PGAM5. The mice were placed in a stereotaxic apparatus (RWD Life Science Co. Ltd., Shenzhen, China) after being anesthetized with 0.8% pentobarbital sodium through intraperitoneal injection. One microliter virus particle was injected into the DG/CA1 region of the mouse hippocampus (anterior/posterior: −2.0 mm, medial/lateral: ±1.5 mm, and dorsal/ventral: −2.0/2.5 mm). The virus injection was performed through a 5 μl syringe (Hamilton-87900, Reno, NV) with an injection rate of 0.05 μl/min. After injection, the pipette was kept in place for 10 min to minimize reflux along the injection trace. The same operation was performed on the other hippocampus.

KA-induced mouse epileptic seizure model, behavioral video monitoring of seizure, and LFP recording

Seizures were induced by the stereotactic injection of 1.0 nmol KA (Sigma-K0250, Louis, MO) in 50 nl of saline, which was injected into the models' left hippocampus area (2.0 mm posterior to the bregma, 1.5 mm left lateral from the midline, and 1.5 mm deep from the dura) according to the atlas of Franklin and Paxinos. The KA model was established 3 weeks after intrahippocampal injection of the virus. The chronic mouse model of spontaneous seizures induced by intrahippocampal KA injection has been widely applied (Balosso et al., 2008; Maroso et al., 2010; Chen et al., 2012; Iori et al., 2013). Two hours after the KA injection, nonconvulsive SE was terminated by diazepam.

The video monitoring process was performed as described (Kohek et al., 2021). The monitoring process was 24 h recording. Spontaneous and recurrent seizure (SRS) refers to spontaneous seizures that are demonstrable at the gross visible level under behavioral monitoring, which can be graded using the Racine scale (Aguiar et al., 2013).

A month after SE induction, the local field potential (LFP) recording was performed as previously described (Yang et al., 2018). The skull was exposed after the mice were anesthetized and fixed on a stereotaxic apparatus. Mouse bregma was used as the anchor point, and a hole was drilled at 2.0 mm posteriorly and 1.5 mm to the left of the midline by a micro electric drill. Two stainless steel screws were placed in the frontal skull for alternate ground connection and then fixed the electrode face on the stereotaxic instrument. Next, the electrode was fixed with dental cement when the electrode slowly entered the hole in the vertical direction up to 1.5 mm. Sterile cotton balls were used to secure hemostasis during drilling. The head of the awake mouse was fixed to prevent the over-behavioral state induced by LFPs changes. MAP data acquisition system (Plexon, Dallas, TX) was used to record the LFPs. The signals were filtered (0.1 to 500 Hz), preamplified (1,000×), and digitized at 4 kHz. NeuroExplorer (Nex Technologies, Littleton, MA) was used to inspect the LFPs data. The seizure-like event (SLE) is identified as a cluster of spontaneous paroxysmal discharges that lasted for 5 s or more, which is characterized by a high-amplitude spike activity above 2 times the standard deviation (SD) and a frequency above 1 Hz. All subsequent analyses (including Western Blots, imaging, etc.) were performed in animals in which behavioral experiments were previously carried out.

Tissue collection

After anesthesia with 0.8% pentobarbital sodium through intraperitoneal injection, mice were rapidly decapitated. Twelve hippocampal tissues from each group were made into homogenates and stored at -80°C until analysis, and 6 hippocampal tissues (1mm^3) were observed by transmission electron microscopy (TEM), and 6 hippocampal tissues were fixed with 10% formalin for 12 h. Whole hippocampal tissues were dehydrated and cut into 16 μm thick sections in a cryostat (Leica-CM1850, Germany), followed by tissue staining.

Western blotting and coimmunoprecipitation

Western blot was performed as described previously (Biron-Shental et al., 2007). The bilateral whole hippocampus tissues of the Control group, Con-AAV-KA group, and PGAM5-RNAi-KA group were collected, and tissue proteins were extracted using lysis buffer (RIPA lysis buffer: Phenylmethanesulfonyl fluoride = 100:1, Beyotime, Shanghai, China). After centrifugation at 16,000 rpm (4°C), the supernatant was collected and stored at-20°C, followed by protein concentration determination with BCA Protein Assay Kit (Beyotime, Shanghai, China). The supernatant sample (40 μg heat-denatured protein) was separated by 12.5% SDS-PAGE gels and transferred onto 0.22 μm polyvinylidene fluoride membranes (Millipore-3,010,040,001, Billerica, MA, United States). Membranes were blocked with 5% nonfat dry milk in tris-buffered saline with Tween-20 (TBST) for 2 h at room temperature and then incubated with primary antibodies overnight at 4°C. On the next day, the membranes were washed 3 times for 5 min each with

1 https://blast.ncbi.nlm.nih.gov/Blast.cgi

PBS saline containing Tween-20 (PBST), and incubated with PBST secondary antibody (Proteintech, SA00001-4) for 1 h at room temperature, and then washed 3 times with PBST. And bands were visualized using enhanced chemiluminescence reagents (Thermo, Marina, CA, United States) and image analysis system (Bio-Rad, United States). Relative quantitative analysis was performed using image lab software and reference proteins. The image lab software (Bio-Rad, United States) was used to analyze the optical density value of the band.

For co-immunoprecipitation, protein extracts from mice hippocampal tissue were mixed with IP lysis buffer, incubated with 4 μl rabbit IgG (Biosharp, BL003A), 10 μl PGAM5 (Santa, sc515880), and 4 μl PINK1 antibodies (Proteintech, 23,274-1-AP) overnight at 4°C, and then incubated with 40 μl protein A/G agarose beads (MCE-HY-K0202) for 2 h at 4°C. The protein bead complexes were then washed three times and collected by centrifugation. Protein samples were mixed with 1 × loading buffer (Beyotime, P0015A) and subsequently subjected to Western blotting.

Nissl staining

Nissl staining was performed as described previously (Qin et al., 2022). Paraffin-embedded sections were dewaxed with 0.5% cresyl violet at room temperature (RT), hydrated, and stained with Nissl dye at RT for 10 min. The sections were dehydrated and sealed. Finally, each section was observed under an optical microscope (Nika A1*R. Japan), and the Nissl-positive cells were counted. For the Nissl staining, 5 images were used for statistical analysis of mice in the Con-AAV-KA group and AAV-RNAi-KA group. The number of Nissl bodies in stained tissue sections was observed in the hippocampus by light microscopy. Surviving neurons were assessed based on the presence or absence of Nissl bodies.

TEM observation

The hippocampal tissue sections at 1 mm^3 were fixed in 3% glutaraldehyde for 1 h. The tissue sections were fixed with 1% osmium acid for 3 h and were washed 3 times with 0.1 mol/l of phosphate buffer (pH 7.4) for 5 min each time. The tissue sections were dehydrated by acetone and embedded in Epon812. Thereafter, the sections were stained with 3% uranium acetate and lead citrate (all from Sangon Biotech) at room temperature for 15 min, respectively, and were observed and photographed under a TEM (JEM-1400PLUS. Japan).

Assay for malondialdehyde and superoxide dismutase

The levels of MDA and SOD in hippocampal tissues were measured using the MDA and SOD assay kits (Solarbio-BC0020; BC0170), respectively, following the manufacturer's instructions, including the use of all quality controls as well as negative controls. The Cell lysis buffer was added to each hippocampal tissue in the Control, Con-AAV-KA, and AAV-RNAi-KA groups for lysing the hippocampal tissues. (Tissue weight (mg): lysis buffer volume (μl) = 1: 9, Western and IP cell lysis buffer, Beyotime, Shanghai, China). Under ice-water bath conditions, mechanical homogenization was performed to prepare the hippocampal tissue into 10% homogenate. After homogenization, the mixture was centrifuged at 10,000 g-12,000 g for 10 min, and the supernatant was taken for subsequent MDA and SOD measurements. Briefly, after the experimental procedures were performed according to the instructions, the fluorescence (excitation at 550 nm for SOD and excitation at 532 nm for MDA was measured) with a microplate reader (Thermo Fisher) was measured with a microplate reader and values were saved for offline analysis.

Immunofluorescence staining

Immunofluorescence staining was performed as previously described (Qin et al., 2022). After anesthesia, mice were rapidly decapitated, and the brains were immediately postfixed in 4% paraformaldehyde for 24 h at 4°C. The brains were immersed in a 30% sucrose PBS solution for 48 h and subsequently sliced using a freezing microtome (Leica-CM1850); 16 μm sections were collected on glass slides. The sections were blocked with 10% goat serum (BOSTER Biological Technology) and 0.1% Triton X-100 in PBS for 2 h. The primary antibodies were diluted in 0.1% PBS added to the coverslip, and incubated overnight in a humidified chamber at 4°C. The coverslips were washed 3 times with PBS and incubated with the secondary fluorescent antibody diluted in 0.1% PBS at room temperature for 1 h. Images were captured using laser-scanning confocal microscopy (Andor-2000). The fluorescence intensity was analyzed using Image-Pro Plus software (Image-Pro Plus, v 6.0).

Immunohistochemistry assays

Immunohistochemical staining was performed as previously described (Lopes et al., 2015). We selected frozen sections with mouse hippocampal regions for immunohistochemistry. After incubation with the primary antibody at 4°C overnight, the tissues were treated with polymer helper (ZSGB-Bio, Beijing, China) for 20 min, and then treated with poly peroxidase-anti-goat IgG (ZSGB-Bio) for 20 min. Subsequently, the tissues were incubated with diaminobenzidine Horseradish Peroxidase Color Development Kit (ZSGB-Bio) for 2 min. Counterstaining was conducted with hematoxylin (ZSGB-Bio). After each incubation step, the sections were washed with TBST for 3 times, 5 min for each time. Five images per group were used for quantitative analysis. The PGAM5 immunoreactivity was quantified automatically by digital image procedures using Image-Pro Plus

software (Image-Pro Plus, v6.0). The detection threshold remained constant throughout the analysis. The percentage area occupied by PGAM5 was quantified.

Quantitative polymerase chain reaction analysis

qPCR analysis was performed as previously described (Cao et al., 2021). The bilateral hippocampal tissues of Control group, Con-AAV-KA group, and AAV-RNAi-KA group were collected for RT-qPCR analysis. Total RNA from hippocampal tissues was prepared with TRIzol reagent according to the manufacturer's protocol (TrizolTM Reagent, Thermo Scientific). The total RNA was reverse-transcribed to cDNA using a HiFi-MMLV cDNA first-strand synthesis kit (CW Bio, Beijing, China). qPCR was performed using GoTaq qPCR Master Mix (Promega) on the CFX96TM real-time system (Bio-Rad). The expression of the genes of interest was normalized to the levels of GAPDH. Primer sequences used for qPCR are listed below:

PGAM5: F: 5′-TGCCAATGTCATCCGCTAT-3′,
R: 5′-GGTGATACTGCCGTTGTTGA-3′.
PINK1: F: 5′-GGCTTCCGTCTGGAGGATTAT-3′,
R: 5′-AACCTGCCGAGATATTCCACA-3′.
GAPDH: F: 5′-AACTTTGGCATTGTGGAAGG-3′,
R: 5′-GGATGCAGGGATGATGTTCT-3′.

Statistical analysis

The Kolmogorov–Smirnov and Shapiro–Wilk tests were used to test whether the data conform to a normal distribution or not when two groups were compared to each other, and an unpaired t-test was used to show the statistical significance of the data. When multiple groups were compared, one-way analysis of variance (ANOVA) was used to determine statistical significance, followed by Bonferroni correction for multiple comparisons (*post hoc* test). Non-parametric tests were used when data did not follow a normal distribution and were presented by medians and interquartile ranges. Data were expressed mean ± SD. $p < 0.05$ in this experiment was considered as a statistically significant difference, and an asterisk was used to indicate a statistically significant difference.

Results

Expression and distribution of PGAM5 in the epileptic mice

The bilateral whole hippocampus tissues of the Epilepsy group were obtained at 30 days after intracranial KA injection. KA-induced temporal lobe epilepsy (TLE) model recapitulates human TLE patients with typical hippocampal sclerosis (Ben-Ari, 2001). Western blot, immunohistochemistry and qPCR analysis were used to verify the relationship between PGAM5 and epilepsy by measuring the PGAM5 levels between the KA-induced TLE model and normal control mice. PGAM5 protein expression in the KA-induced TLE model was higher than that in the control group (Figure 1A, Supplementary Figure 1). Besides, the result of the immunohistochemical semiquantitative analysis showed that a higher PGAM5 level was found in the epileptic group compared with the normal control group (Figure 1B). Compare with the control group, a higher PGAM5 mRNA level was found in the epileptic group (Figure 1C). To further verify the distribution of PGAM5 in epileptic brain tissue, we performed the IF staining that showed PGAM5 was concentrated in the hippocampal CA1, CA3 and DG regions (Figure 1D). Notably, PGAM5 was colocalized with MAP2 (a marker of dendrites), and there was no distinct PGAM5 colocalization in GFAP (a marker of astrocytes) and IBA1 (a marker of microglia). PGAM5 was also expressed at high levels in scattered neurons in the cerebral cortex (Figure 1E). Therefore, it could be seen that PGAM5 is mainly expressed in neurons.

PGAM5 inhibition mice decreased epileptic seizure activity and neuronal loss

Altered PGAM5 expression may be a phenomenon caused by epilepsy that indicates PGAM5 plays a causal role in seizures. Therefore, PGAM5 knockdown AAV was used to investigate whether PGAM5 level regulated epilepsy activity in the KA-induced TLE mouse model. After injecting AAV into the CA1 and DG regions of the hippocampus of mice (Figure 2A), we first used immunofluorescence for AAV expression (green) in the hippocampus of Con-AAV-KA and AAV-RNAi-KA injected mice (Figure 2B). Compared to the sham-operated groups, the knockdown efficiency of PGAM5 was 58% (Supplementary Figure 2). After 3 weeks, we created a model of epilepsy by KA injection.

Behavioral video monitoring was used to record the seizure in mice for a month after the KA injection. We compared the grade IV and V seizure behavior of mice in each group because grade III seizure behavior and below are prone to miss. Behavior video monitoring of mice revealed that the number of seizure frequency was reduced at 24–30 days in the AAV-RNAi-KA group (Figure 3B). Compared with Con-AAV-KA, the latency time of AAV-RNAi-KA was prolonged (Figure 3C). Next, behavior may have some limitations for seizures, we recorded seizure activity and SLE by LFPs after the induction of status epilepticus (SE) to obtain a more convincing judgment. Therefore, after the video behavioral analysis in the KA model, we performed LFPs to record seizures in each group of mice. Consistent with other studies, frequent and repetitive SLEs were observed in all mice with KA injection (Figure 3A). The results showed that mice in all groups had significant epileptiform discharges

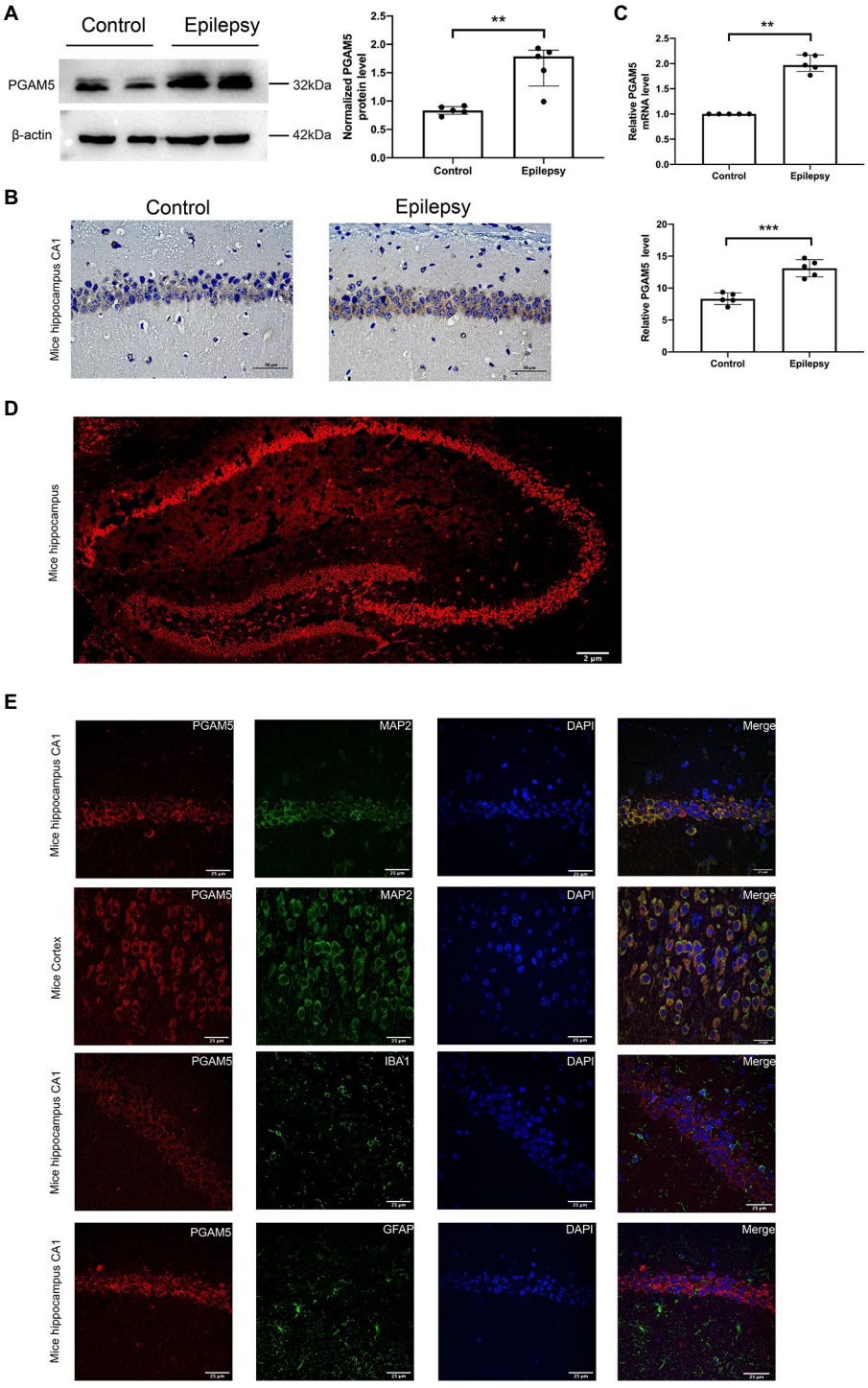

FIGURE 1
Expression and distribution of PGAM5 in the epileptic mice. **(A)** Quantitative analysis of the PGAM5/β-actin ratio, PGAM5 was increased in the hippocampus of the KA-induced epilepsy model (n =5). **(B)** Distribution and expression of PGAM5 in the CA1 region of hippocampus of control mice and temporal lobe epilepsy model mice (n =5). Data are expressed as Median with interquartile range. **(C)** Relative levels of PGAM5 detected by RT-qPCR analysis (n =5). Data are expressed as Means ± SD **(D)** In epileptic mice, PGAM5 is expressed in the whole hippocampus. Scale bar: 2μm. **(E)** In the hippocampus and cortex of the KA-induced epilepsy model, PGAM5 colocalizes with MAP2. Scale bar: 50μm. $^{**}p$ <0.01, $^{****}p$ <0.0001.

(Figures 3D–E). Compared with the AAV-RNAi-KA group, the increased number of SLEs and more total time of SLEs spent in 30 min were found in the Con-AAV-KA group (Figures 3F-H).

To further explore the effect of knockdown PGAM5 on neuronal survival, we performed the Nissl staining to identify Nissl bodies in nerve cells 1 month after SE induction. In the AAV-RNAi-KA group,

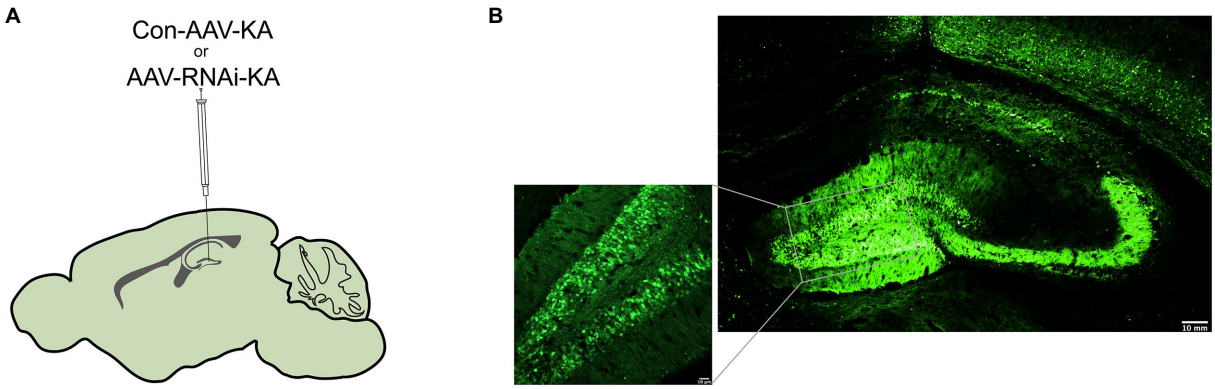

FIGURE 2
Intracranial injection of AAV with knockdown of PGAM5. **(A)** Inset of mouse hippocampal sections showing injection sites for Con-AAV-KA or AAV-RNAi-KA. **(B)** Immunofluorescence staining of AAV expression (green) in the hippocampus of mice injected with Con-AAV-KA.

most of the pyramidal cells in the CA1 and CA3 regions of the mouse hippocampus were clearly demarcated and morphologically normal, and a few neurons had blurred contours. Besides, a large number of dense vertebral cells were neatly arranged, and the edges and nucleoli were clear. There were abundant Nissl bodies in the cytoplasm, and the cytoplasm was clear.

In Con-AAV-KA, the neuronal cell structure in the mouse hippocampus was incomplete and ruptured. The contour and the boundary were blurred and unclear. The intercellular distance was increased, and the arrangement was disordered, and the chromatin clumping was observed at the edge. The cytoplasm was edematous, and fewer Nissl bodies could be found in it (Figure 4A). In summary, knockdown PGAM5 reduced the frequency and total time of seizures, and reduced the loss of neurons.

PGAM5 interacted with PINK1 in KA-induced mouse model, and knockdown of PGAM5 attenuated PINK1 expression

Previous studies have found that PGAM5 may protect PINK1 from the degradation of mitochondria (Imai et al., 2010). However, it has not been specifically studied in epilepsy. Compared with normal control brain tissue, the PINK1 level in the brain tissue of KA-induced epileptic mice was significantly up-regulated (Figures 4B,C). The result of the co-immunoprecipitation assay showed that PGAM5 co-immunoprecipitated with PINK1 in the KA-model mouse (Figure 4D). Western blot results showed that PGAM5 expression was inhibited in AAV-RNAi-KA mice compared with the Con-AAV-KA group (Figures 5B,C). PINK1 protein levels in the Con-AAV-KA group were higher than that in the control group in Figures 5B,D. After injecting AAV, the PINK1 level was significantly lower than that in the Con-AAV-KA group. These data suggested that the knockdown of PGAM5 may have the ability to strongly reduce PINK1 expression in the KA-injected mice model.

Knockdown of PGAM5 inhibited KA-induced mitophagy activity

To investigate the effect of PGAM5 on mitophagy, we selected electron microscopy to observe the morphology of neurocytes in the hippocampus. As shown in Figure 5A, clear and complete hippocampal neuron structure and the normal nuclear structure could be found in the control group. No double-membrane autophagosomes were detected. In the Con-AAV-KA group, apoptosis of most neuronal cells, shrunken nuclei, chromatin accumulation, rough endoplasmic reticulum, and mitochondrion swelling were clearly observed. Surprisingly, not only did the treatment with AAV make fewer neuronal cells undergo death but it also resulted in much mitochondrial morphology being restored. Besides, no significant vacuolar degeneration and cell membrane rupture were seen in the AAV-RNAi-KA group, which implies that neuronal morphology recovered after the knockdown of PGAM5. To further confirm these findings, protein expression of mitochondrial markers, including LC3 B (the autophagy-related marker), TIMM23 (an IMM protein), and TOMM20 (an OMM protein), was examined by Western blot. As shown in Figures 5B,E-G, compared with the Con group, LC3 B was increased, which was decreased after the AAV injection. The TIMM23 and TOMM20 protein expression were decreased in the Con-AAV-KA group, which was enhanced after AAV injection. Collectively, these data revealed that PGAM5 could reduce PINK1 expression to inhibit mitophagy activity during epilepsy after AAV intervention.

Increased oxidative stress level in KA-induced SE and knockdown of PGAM5 alleviated MDA, Sod, and ROS levels

To investigate the role of PGAM5 on oxidative stress in a KA-induced epilepsy model, we examined the ROS probe

10.3389/fnmol.2022.1047801

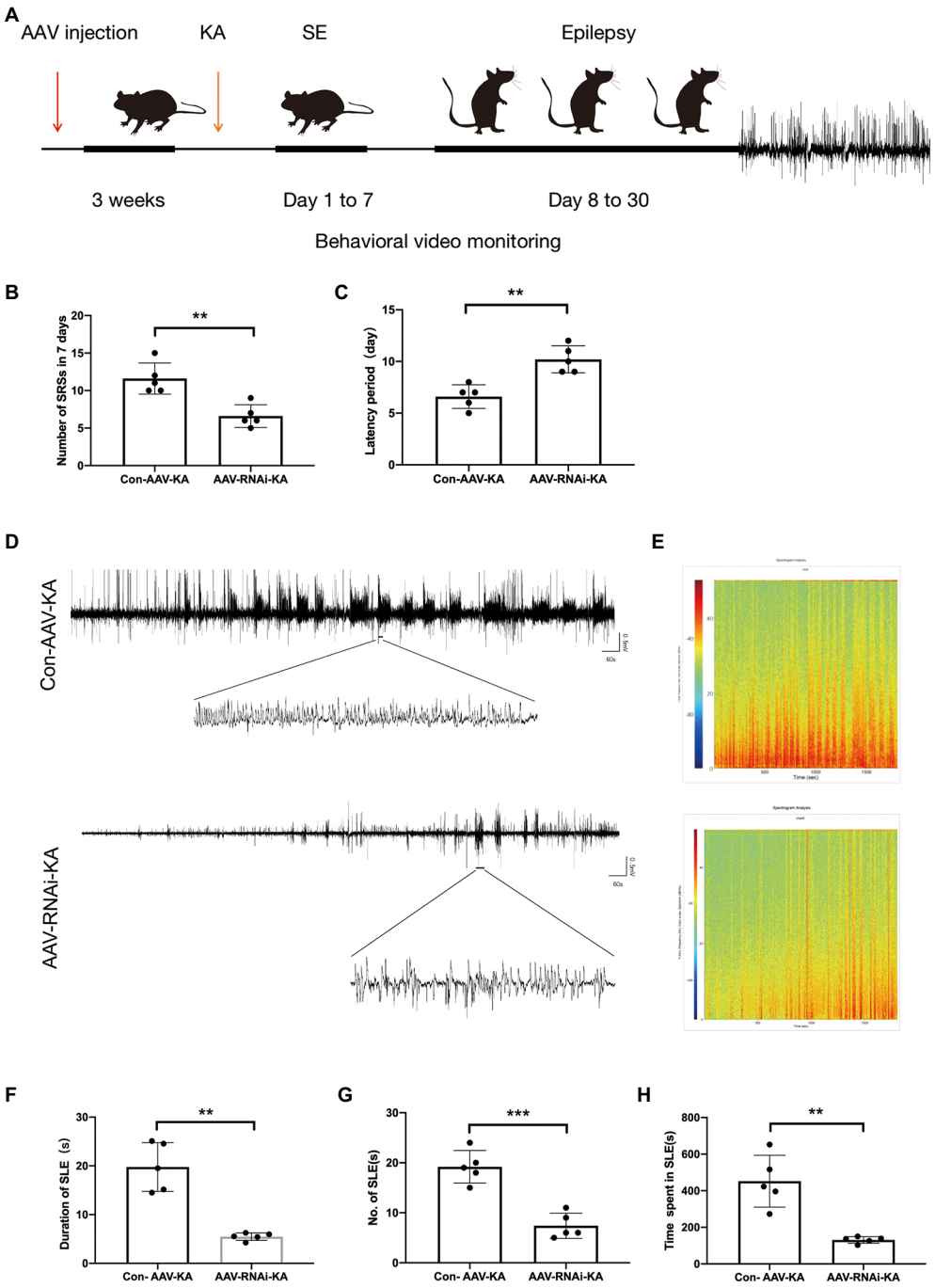

FIGURE 3
PGAM5 inhibition mice decreased epileptic seizure activity. **(A)** Graphical representation of the experimental timeline for the mouse KA injection model. Mice were injected with Con-AAV-KA and AAV-RNAi-treated mice in the hippocampus 3 weeks before KA injection. **(B)** Behavior video monitoring of mice revealed that the number of SRSs was reduced at 24–30days in AAV-RNAi-KA group. Compared with Con-AAV-KA, the latency time of AAV-RNAi-KA was prolonged (n =5). **(C)** Representative LFPs of Con-AAV-KA and AAV-RNAi-KA (n =5). **(D)** Spectrum of LFP corresponding to **(B)**. **(F–H)** During 30min, the duration of SLE, the number of SLEs and the total time spent in SLEs was reduced in the AAV-RNAi-KA group (n =5). Data are expressed as Means ± SD, *p <0.05, **p <0.01, ***p <0.001.

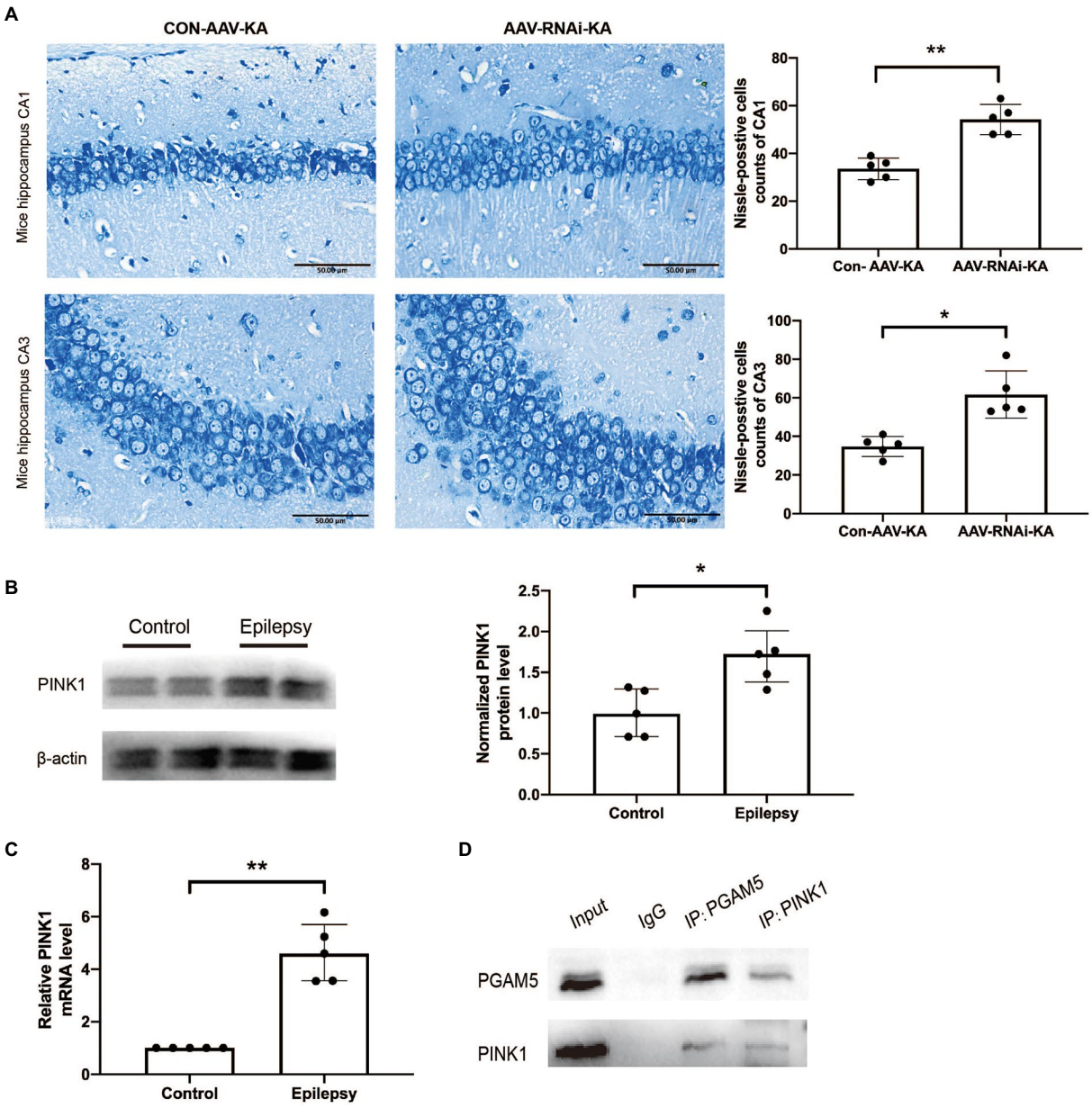

FIGURE 4
PGAM5 interacts with PINK1 in KA-induced mouse model and knockdown of PGAM5 inhibited mitophagy activity. **(A)** AAV-RNAi-KA group significantly increased the number of neuronal cell survival in the hippocampus after SE. Scale bar: 50μm, *n* =5. **(B)** Quantitative analysis of the PINK1/β-actin ratio, PINK1 was increased in the hippocampus of the KA-induced epilepsy model (*n* =5). **(C)** Relative levels of PINK1 detected by RT-qPCR analysis (*n* =5). Data are expressed as Median with interquartile range. **(D)** Co-immunoprecipitation between PGAM5 and PINK1 was demonstrated using anti-PGAM5 or anti-PINK1 antibodies.

dihydroethidium (DHE) to detect ROS accumulation in mouse hippocampal neurons. The results showed that ROS generation and red fluorescence intensity were increased in the CA1, CA3, and DG regions of the hippocampus of mice in the Con-AAV-KA group. After the AAV injection, ROS generation was significantly attenuated (Figure 6A). Next, we examined oxidative stress by spectrophotometry. However, MDA content decreased and SOD activity increased after the AAV injection. Our results stated that oxidative stress could be attenuated after injection (Figures 6B,C).

Discussion

The present study indicates that the expression of PGAM5 increases in neurons of epileptic mice, and increased mitophagy and ROS levels are also found in it. The knockdown of PGAM5 improves the ROS level, reduced neuronal damage and decreased the frequency of SLEs by inhibiting the PINK1-mediated mitophagy. More importantly, the interaction between PGAM5 and PINK1 is found in the epilepsy model. Therefore, we investigated the role of

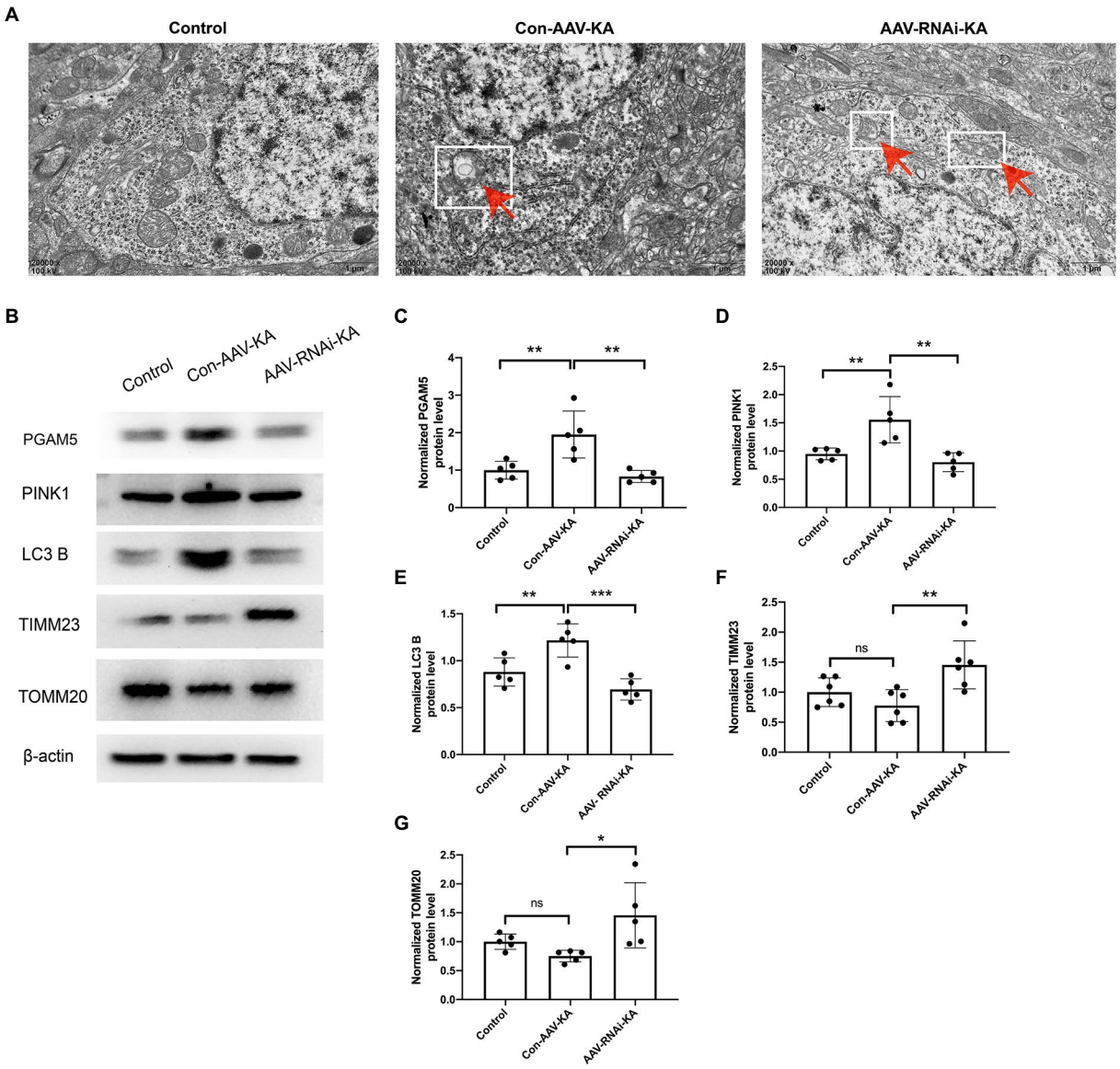

FIGURE 5
Knockdown of PGAM5 inhibited KA-induced mitophagy activity. **(A)** The representative images showed that the mitochondrial structure was normal in the Control group; mitochondria phagocytosed by double-membrane structures were labeled with red arrow and white square in the Con-AAV-KA group; no significant vacuolar degeneration and cell membrane rupture were observed in the AAV-RNAi-KA group by TEM. Scale bar: 1μm. **(B–G)** Protein levels of PGAM5, PINK1, LC3 B, TIMM23, TOMM20 in the hippocampus of three groups were measured by western blot (n =5). TEM, transmission electron microscope; PGAM5, phosphoglycerate mutase 5; PINK1, PTEN-induced putative kinase 1; LC3, light chain 3; TOMM20, translocase of the outer mitochondrial membrane 20; TIMM23, translocase of the inner mitochondrial membrane 23; IgG, immunoglobulin G. Data are expressed as Means ± SD *p <0.05, **p <0.01, ***p <0.001, ****p <0.0001.

PGAM5 in the development and progression of epilepsy as an important molecule role in regulating mitochondrial homeostasis.

In our study, the increased PGAM5 level is found in the hippocampus of epileptic mice, which is mostly located in the CA1, CA3, and DG neurons of the hippocampus. Neuronal cell death is the main pathological outcome after seizures, thus the results suggest that PGAM5 may play an important role in epilepsy (de Lanerolle et al., 2003; Dong et al., 2013; Park et al., 2018). The pathophysiological changes in epilepsy include the weakening of protective factors to prevent seizures as well as the strengthening of damaging factors to induce seizures (Pitkänen and Lukasiuk, 2011). The inhibition of PGAM5 is considered as a protective effect based on the following evidence. The previous study has demonstrated that LFHP-1c, an inhibitor of PGAM5, plays a significant role in protecting cerebral vessels and maintaining blood–brain barrier function (Gao et al., 2021). In addition, some studies have also reported the inhibition of PGAM5 has a positive role in reducing neuroinflammation,

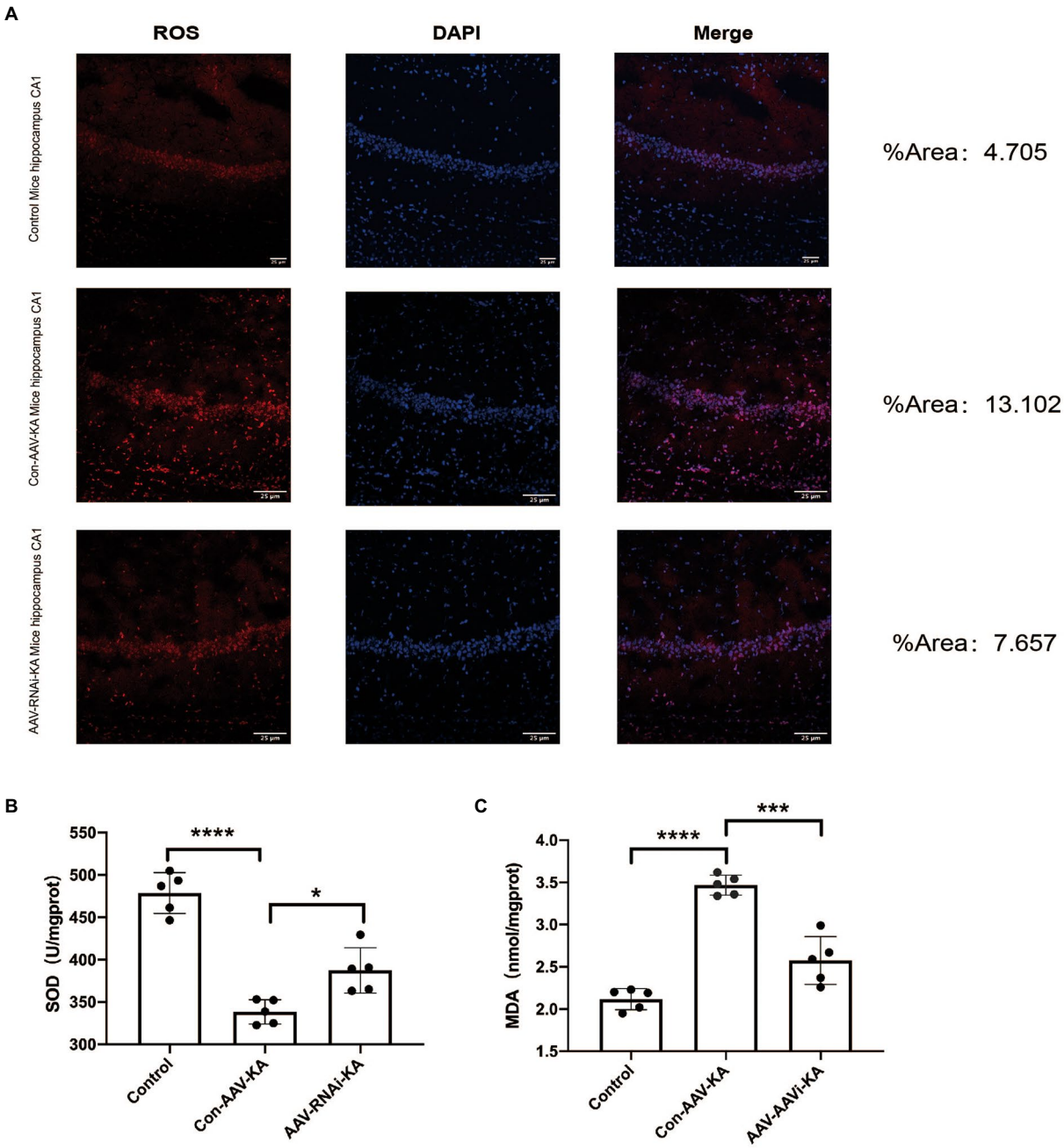

FIGURE 6
PGAM5 inhibition reduces ROS generation **(A)** Immunofluorescence staining of DHE expression in the hippocampus of mice in the Control, Con-AAV-KA and AAV-RNAi-KA groups (red). (*n* =5) **(B,C)** Relative MDA and SOD contents in Control, Con-AAV-KA and AAV-RNAi-KA groups measured by the TBA and WST-8 methods. (*n* =5); ROS, reactive oxygen species; DHE, dihydroethidium; MDA, malondialdehyde; SOD, superoxide dismutase; TBA, thiobarbituric acid; WST-8, water-soluble tetrazolium salt-8. Data are expressed as Means ± SD, **p* <0.05, ****p* <0.001, *****p* <0.0001.

rescuing mitochondrial function as well as improving oxidative stress (Johnson and Giulivi, 2005; Ooigawa et al., 2006; Chen et al., 2012). However, the role of PGAM5 in epilepsy remains unclear. Therefore, we explored the role of PGAM5 in seizures. Our results indicated that knockdown of PGAM5 reduced the frequency and total duration of seizures. This suggests that PGAM5 is a damaging factor based on the evidence presented above.

Next, we investigated whether PGAM5 is associated with mitophagy in a KA-induced epilepsy model. Previous studies have activated mitophagy participates in epilepsy development *via* mitochondrial dysfunction (Dilliogluglil et al., 2010; Wu et al., 2018). Mitophagy in TLE is activated after mitochondrial damage, which leads to the clearance of mitochondria themselves (Wu et al., 2018). It has been reported that mitochondrial dysfunction

in the CNS can not only lead to seizures, but also release harmful ROS and then result in neuronal degeneration or even death (Lin and Kang, 2010; Han et al., 2011; Sheng, 2014). Our results show that LC3 B level were significantly increased and TOMM20 and TIMM23 were significantly decreased in the epilepsy model, which indicates an enhanced level of mitophagy in our epileptic mice inducing by KA injection. However, reduced mitochondrial swelling and fragmentation are found after the inhibition of PGAM5, which suggests that the knockdown of PGAM5 is crucial for reducing mitophagy in epilepsy. In the previous study, the inhibition of mitophagy has a protective effect on acute neuronal injury (Cao et al., 2019; Gao et al., 2021). We revealed an increase in neuronal survival following PGAM5 knockdown. Therefore, according to these results, we speculated that PGAM5 might reduce neuron loss by inhibiting mitophagy.

Recent studies have shown that the hippocampus in the central nervous system (CNS) is vulnerable to abnormal mitophagy function by oxidative stress (Naziroğlu et al., 2008; Aguiar et al., 2013; Wu et al., 2018). Our results suggest that the aggravated oxidative damage, increased ROS as well as MDA contents and attenuated SOD activity in the epilepsy model. However, these results were reversed by PGAM5 inhibition. Moreover, decreased SOD levels are discovered in human epileptic cerebrospinal fluid, especially in patients with refractory epilepsy (Chen et al., 2012). Also, increasing fragile mitochondria, mitochondrial dysfunction and oxidative stress are found in a variety of animal models of acquired epilepsy (e.g., KA-induced epilepsy model, PTZ-induced epilepsy model, pilocarpine-induced epilepsy model) (Liang et al., 2000; Jarrett et al., 2008; Ryan et al., 2012). This demonstrates that the generation of ROS associated with mitochondrial defects can also affect epileptogenesis (Shekh-Ahmad et al., 2019). The oxidative stress during seizures may cause mitochondrial damage. Notably, ASDs with antioxidant properties have been proven to have neuroprotective effects (Bashkatova et al., 2003; Willmore, 2005). Our study suggests that the reduction in neuronal loss after the knockdown of PGAM5 is attributed to the attenuation of oxidative stress.

The PINK-mediated mitophagy pathway plays an important role in Parkinson's disease, aging rats, SH-SY5Y neuroblasts, cerebral ischemia–reperfusion injury (CIRI), and Alzheimer's disease (Pickrell and Youle, 2015; Martín-Maestro et al., 2016; Park et al., 2018; Yi et al., 2019; Ma et al., 2021; Wen et al., 2021; Mao et al., 2022). PINK1 expression is increased in our epilepsy model and decreased PINK1 levels are detected in the epilepsy model after inhibition of PGAM5. The co-immunoprecipitation shows the interaction between PGAM5 and PINK1, which suggests that PGAM5 may be involved in the PINK1-mediated mitophagy pathway. In previous studies, PGAM5 promote PINK1-mediated mitophagy and stabilized PINK1 on OMM (Sugo et al., 2018). Accordingly, PINK1 degradation induced by PGAM5 depletion causes a failure to initiate mitophagy. This suggests that PINK1 may be critical for increased mitophagy caused by PGAM5 in epilepsy. All these studies reveal that PGAM5 may regulate mitophagy in epilepsy *via* PINK1.

Herein, we address the possible mechanism of PGAM5 in epilepsy based on our study. During the progression of epilepsy, increased PGAM5 maybe contributes to mitochondrial damage. Meanwhile, mitophagy may further lead to excessive activation of oxidative stress. ROS production induces the enhancement of mitophagy and aggravates neuronal injury, which results in severe consequences including massive loss of epileptic neurons and increased SLEs (Tizon et al., 2010). After injection of AAV, rhomboid-like protein (PARL) directly combines with PINK1 based on inhibition of PGAM5, and degenerates PINK1 accumulation in IMM (Dilliogluglil et al., 2010). The inhibited PINK1 transport leads to the accumulation of PINK1 on the OMM. Accumulated PINK1 ubiquitinates OMM proteins by recruiting Parkin to damaged mitochondria, and finally causing a failure in the initiation of PINK1-mediated mitophagy (Imai et al., 2010; Lu et al., 2014; Park et al., 2018). The process ultimately leads to reducing PINK1-mitophagy. Following decreased PGAM5-PINK1-mediated mitophagy, subsequent attenuation of ROS and increased neuronal survival are demonstrated. Finally, sustained epileptic activity is significantly reduced. Our study suggests that the knockdown of PGAM5 has a significant attenuating effect on epilepsy *via* mitophagy (Figure 7). Therefore, PGAM5 is a potential target for epilepsy therapy.

The knockdown efficiency of AVV-RNAi has been confirmed in our experimental results, but the off-target effect of AVV failed to be completely excluded after detection. Therefore, more rigorous experiments may be needed to confirm it. Besides, PGAM5 is significantly up-regulated in the late stage of epilepsy. Considering that most of the neurons had died in this period, it may be necessary to find surviving neurons in epilepsy models to rule out the effect of dead neurons on PGAM5 expression. Lastly, although our results proved that PGAM5 can induce epileptogenesis by promoting PIN1-mediated mitophagy, the indirect effect of PGAM5 on PINK1-mediated mitophagy cannot be ruled out. Further work will be needed to verify this conjecture.

Conclusion

In conclusion, our findings report the unnoticed but important role of PGAM5 in epilepsy. We report that the knockdown of PGAM5 inhibits mitophagy, attenuates seizures, and improves neuronal survival in a KA-induced epilepsy model. These findings contribute to our understanding of the role of PGAM5 in epilepsy and provide a novel target for the treatment of epilepsy.

Data availability statement

The original contributions presented in the study are included in the article/Supplementary material, further inquiries can be directed to the corresponding author.

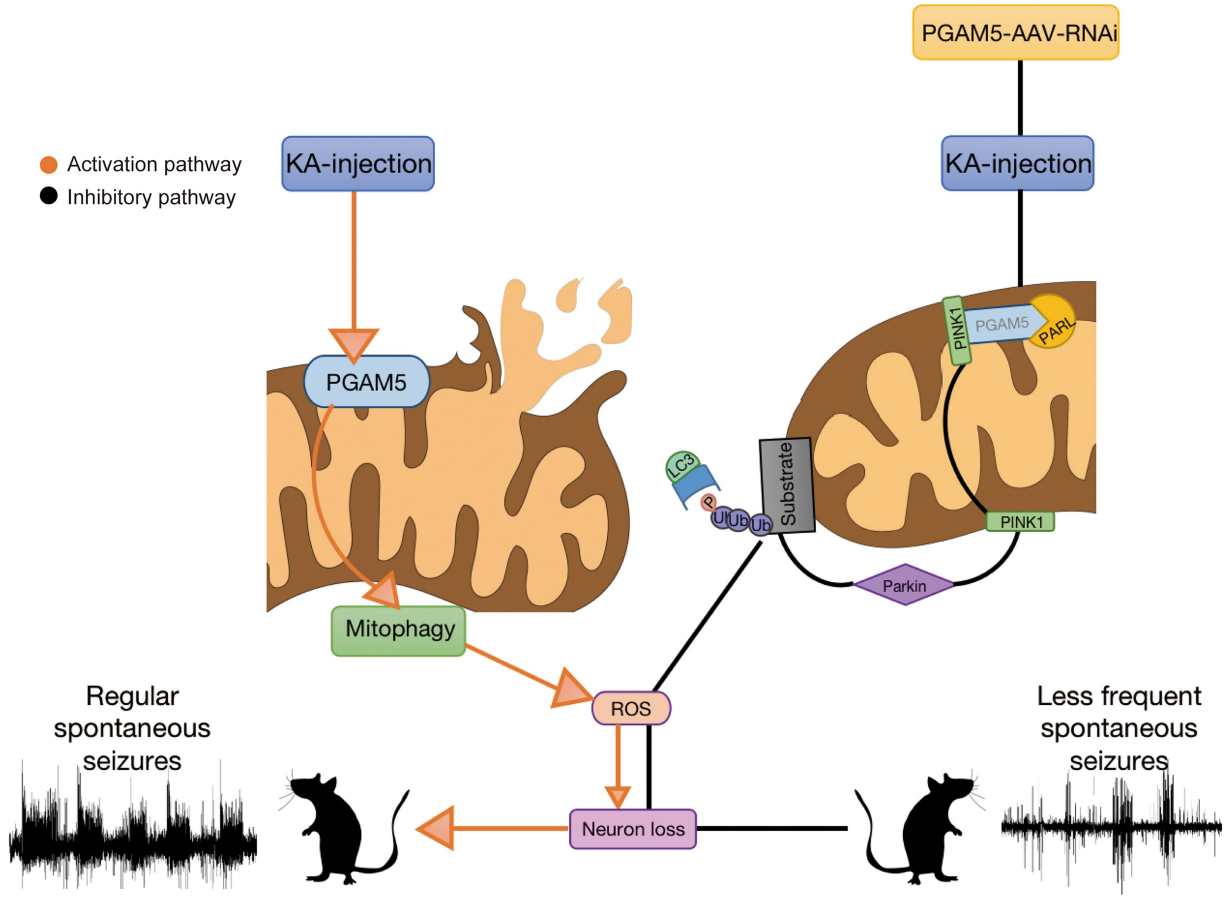

FIGURE 7
Seizures induce excessive activation of mitophagy and lead to oxidative stress. PGAM5 knockdown resists reactive oxygen species accumulation and protects neurons from mitophagy.

Ethics statement

The animal study was reviewed and approved by the Commission of Chongqing Medical University.

Author contributions

FZ was a major contributor in performing experiments and writing the manuscript. YG carried out the operation of tissue and related experiments. JS, WZ, and SY performed the tissue collection and analysis of the data. JW provided ideas for the experiments. YL and WY designed the study and revised the manuscript. All authors read and approved the final manuscript.

Funding

This study was supported by grants from the National Natural Science Foundation of China (81871019 and 81671286). Chongqing Postgraduate Scientific Research Innovation Project (CYS20188).

Conflict of interest

The authors declare that the research was conducted in the absence of any commercial or financial relationships that could be construed as a potential conflict of interest.

Publisher's note

All claims expressed in this article are solely those of the authors and do not necessarily represent those of their affiliated organizations, or those of the publisher, the editors and the reviewers. Any product that may be evaluated in this article, or claim that may be made by its manufacturer, is not guaranteed or endorsed by the publisher.

Supplementary material

The Supplementary material for this article can be found online at: https://www.frontiersin.org/articles/10.3389/fnmol.2022.1047801/full#supplementary-material

References

Aguiar, C. C., Almeida, A. B., Araújo, P. V., Vasconcelos, G. S., Chaves, E. M., Do Vale, O. C., et al. (2013). Effects of agomelatine on oxidative stress in the brain of mice after chemically induced seizures. *Cell. Mol. Neurobiol.* 33, 825–835. doi: 10.1007/s10571-013-9949-0

Balosso, S., Maroso, M., Sanchez-Alavez, M., Ravizza, T., Frasca, A., Bartfai, T., et al. (2008). A novel non-transcriptional pathway mediates the proconvulsive effects of interleukin-1beta. *Brain* 131, 3256–3265. doi: 10.1093/brain/awn271

Bashkatova, V., Narkevich, V., Vitskova, G., and Vanin, A. (2003). The influence of anticonvulsant and antioxidant drugs on nitric oxide level and lipid peroxidation in the rat brain during penthylenetetrazole-induced epileptiform model seizures. *Prog. Neuro-Psychopharmacol. Biol. Psychiatry* 27, 487–492. doi: 10.1016/s0278-5846(03)00037-x

Ben-Ari, Y. (2001). Cell death and synaptic reorganizations produced by seizures. *Epilepsia* 42, 5–7. doi: 10.1046/j.1528-1157.2001.042suppl.3005.x

Biron-Shental, T., Schaiff, W. T., Ratajczak, C. K., Bildirici, I., Nelson, D. M., and Sadovsky, Y. (2007). Hypoxia regulates the expression of fatty acid-binding proteins in primary term human trophoblasts. *Am. J. Obstet. Gynecol.* 197, 516.e1–516.e6. doi: 10.1016/j.ajog.2007.03.066

Brunelli, F., Torosantucci, L., Gelmetti, V., Franzone, D., Grünewald, A., Krüger, R., et al. (2022). PINK1 protects against Staurosporine-induced apoptosis by interacting with Beclin1 and impairing its pro-apoptotic cleavage. *Cells* 11, 1–15. doi: 10.3390/cells11040678

Cao, J., Gan, H., Xiao, H., Chen, H., Jian, D., Jian, D., et al. (2021). Key protein-coding genes related to microglia in immune regulation and inflammatory response induced by epilepsy. *Math. Biosci. Eng.* 18, 9563–9578. doi: 10.3934/mbe.2021469

Cao, S., Sun, Y., Wang, W., Wang, B., Zhang, Q., Pan, C., et al. (2019). Poly (ADP-ribose) polymerase inhibition protects against myocardial ischaemia/reperfusion injury via suppressing mitophagy. *J. Cell. Mol. Med.* 23, 6897–6906. doi: 10.1111/jcmm.14573

Chen, D., Lu, Y., Yu, W., Luo, J., Xiao, Z., Xiao, F., et al. (2012). Clinical value of decreased superoxide dismutase 1 in patients with epilepsy. *Seizure* 21, 508–511. doi: 10.1016/j.seizure.2012.05.003

Das, A., McDowell, M., O'Dell, C. M., Busch, M. E., Smith, J. A., Ray, S. K., et al. (2010). Post-treatment with voltage-gated Na(+) channel blocker attenuates kainic acid-induced apoptosis in rat primary hippocampal neurons. *Neurochem. Res.* 35, 2175–2183. doi: 10.1007/s11064-010-0321-1

de Lanerolle, N. C., Kim, J. H., Williamson, A., Spencer, S. S., Zaveri, H. P., Eid, T., et al. (2003). A retrospective analysis of hippocampal pathology in human temporal lobe epilepsy: evidence for distinctive patient subcategories. *Epilepsia* 44, 677–687. doi: 10.1046/j.1528-1157.2003.32701.x

Dilliоglugil, M. O., Kir, H. M., Demir, C., Ilbay, G., Sahin, D., Dilliоglugil, O., et al. (2010). Effect of pentylenetetrazole and sound stimulation induced single and repeated convulsive seizures on the MDA, GSH and NO levels, and SOD activities in rat liver and kidney tissues. *Brain Res. Bull.* 83, 356–359. doi: 10.1016/j.brainresbull.2010.09.007

Dong, Y., Wang, S., Zhang, T., Zhao, X., Liu, X., Cao, L., et al. (2013). Ascorbic acid ameliorates seizures and brain damage in rats through inhibiting autophagy. *Brain Res.* 16, 115–123. doi: 10.1016/j.brainres.2013.08.039

Gao, C., Xu, Y., Liang, Z., Wang, Y., Shang, Q., Zhang, S., et al. (2021). A novel PGAM5 inhibitor LFHP-1c protects blood-brain barrier integrity in ischemic stroke. *Acta Pharm. Sin. B* 11, 1867–1884. doi: 10.1016/j.apsb.2021.01.008

Geisler, S., Holmström, K. M., Skujat, D., Fiesel, F. C., Rothfuss, O. C., Kahle, P. J., et al. (2010). PINK1/Parkin-mediated mitophagy is dependent on VDAC1 and p62/SQSTM1. *Nat. Cell Biol.* 12, 119–131. doi: 10.1038/ncb2012

Han, Y., Lin, Y., Xie, N., Xue, Y., Tao, H., Rui, C., et al. (2011). Impaired mitochondrial biogenesis in hippocampi of rats with chronic seizures. *Neuroscience* 27, 234–240. doi: 10.1016/j.neuroscience.2011.07.068

Imai, Y., Kanao, T., Sawada, T., Kobayashi, Y., Moriwaki, Y., Ishida, Y., et al. (2010). The loss of PGAM5 suppresses the mitochondrial degeneration caused by inactivation of PINK1 in drosophila. *PLoS Genet.* 6:e1001229. doi: 10.1371/journal.pgen.1001229

Iori, V., Maroso, M., Rizzi, M., Iyer, A. M., Vertemara, R., Carli, M., et al. (2013). Receptor for advanced glycation Endproducts is upregulated in temporal lobe epilepsy and contributes to experimental seizures. *Neurobiol. Dis.* 58, 102–114. doi: 10.1016/j.nbd.2013.03.006

Jarrett, S. G., Liang, L. P., Hellier, J. L., Staley, K. J., and Patel, M. (2008). Mitochondrial DNA damage and impaired base excision repair during epileptogenesis. *Neurobiol. Dis.* 30, 130–138. doi: 10.1016/j.nbd.2007.12.009

Johnson, F., and Giulivi, C. (2005). Superoxide dismutases and their impact upon human health. *Mol. Asp. Med.* 26, 340–352. doi: 10.1016/j.mam.2005.07.006

Kim, Y., Park, J., Kim, S., Song, S., Kwon, S. K., Lee, S. H., et al. (2008). PINK1 controls mitochondrial localization of Parkin through direct phosphorylation. *Biochem. Biophys. Res. Commun.* 377, 975–980. doi: 10.1016/j.bbrc.2008.10.104

Kohek, S. R. B., Foresti, M. L., Blanco, M. M., Cavarsan, C. F., da Silva, C. S., et al. (2021). Anxious profile influences behavioral and Immunohistological findings in the pilocarpine model of epilepsy. *Front. Pharmacol.* 12:640715. doi: 10.3389/fphar.2021.640715

Liang, L. P., Ho, Y. S., and Patel, M. (2000). Mitochondrial superoxide production in kainate-induced hippocampal damage. *Neuroscience* 101, 563–570. doi: 10.1016/s0306-4522(00)00397-3

Liesa, M., Qiu, W., and Shirihai, O. S. (2012). Mitochondrial ABC transporters function: the role of ABCB10 (ABC-me) as a novel player in cellular handling of reactive oxygen species. *Biochim. Biophys. Acta* 1823, 1945–1957. doi: 10.1016/j.bbamcr.2012.07.013

Lin, W., and Kang, U. J. (2010). Structural determinants of PINK1 topology and dual subcellular distribution. *BMC Cell Biol.* 11:90. doi: 10.1186/1471-2121-11-90

Lopes, M. W., Lopes, S. C., Costa, A. P., Gonçalves, F. M., Rieger, D. K., Peres, T. V., et al. (2015). Region-specific alterations of AMPA receptor phosphorylation and signaling pathways in the pilocarpine model of epilepsy. *Neurochem. Int.* 87, 22–33. doi: 10.1016/j.neuint.2015.05.003

Lu, W., Karuppagounder, S. S., Springer, D. A., Allen, M. D., Zheng, L., Chao, B., et al. (2014). Genetic deficiency of the mitochondrial protein PGAM5 causes a Parkinson's-like movement disorder. *Nat. Commun.* 15:4930. doi: 10.1038/ncomms5930

Ma, K. Y., Fokkens, M. R., Reggiori, F., Mari, M., and Verbeek, D. S. (2021). Parkinson's disease-associated VPS35 mutant reduces mitochondrial membrane potential and impairs PINK1/Parkin-mediated mitophagy. *Transl. Neurodegener.* 10:19. doi: 10.1186/s40035-021-00243-4

Mao, Z., Tian, L., Liu, J., Wu, Q., Wang, N., Wang, G., et al. (2022). Ligustilide ameliorates hippocampal neuronal injury after cerebral ischemia reperfusion through activating PINK1/Parkin-dependent mitophagy. *Phytomedicine* 101:154111. doi: 10.1016/j.phymed.2022.154111

Maroso, M., Balosso, S., Ravizza, T., Liu, J., Aronica, E., Iyer, A. M., et al. (2010). Toll-like receptor 4 and high-mobility group box-1 are involved in ictogenesis and can be targeted to reduce seizures. *Nat. Med.* 16, 413–419. doi: 10.1038/nm.2127

Martín-Maestro, P., Gargini, R., Perry, G., Avila, J., and García-Escudero, V. (2016). PARK2 enhancement is able to compensate mitophagy alterations found in sporadic Alzheimer's disease. *Hum. Mol. Genet.* 25, 792–806. doi: 10.1093/hmg/ddv616

Matsuda, N., Sato, S., Shiba, K., Okatsu, K., Saisho, K., Gautier, C. A., et al. (2010). PINK1 stabilized by mitochondrial depolarization recruits Parkin to damaged mitochondria and activates latent Parkin for mitophagy. *J. Cell Biol.* 189, 211–221. doi: 10.1083/jcb.200910140

Meyer, J. N., Leuthner, T. C., and Luz, A. L. (2017). Mitochondrial fusion, fission, and mitochondrial toxicity. *Toxicology* 1, 42–53. doi: 10.1016/j.tox.2017.07.019

Narendra, D. P., Jin, S. M., Tanaka, A., Suen, D. F., Gautier, C. A., Shen, J., et al. (2010). PINK1 is selectively stabilized on impaired mitochondria to activate Parkin. *PLoS Biol.* 8:e1000298. doi: 10.1371/journal.pbio.1000298

Naziroğlu, M., Kutluhan, S., and Yilmaz, M. (2008). Selenium and topiramate modulates brain microsomal oxidative stress values, Ca2+-ATPase activity, and EEG records in pentylentetrazol-induced seizures in rats. *J. Membr. Biol.* 225, 39–49. doi: 10.1007/s00232-008-9132-6

Ooigawa, H., Nawashiro, H., Fukui, S., Otani, N., Osumi, A., Toyooka, T., et al. (2006). The fate of Nissl-stained dark neurons following traumatic brain injury in rats: difference between neocortex and hippocampus regarding survival rate. *Acta Neuropathol.* 112, 471–481. doi: 10.1007/s00401-006-0108-2

Park, Y. S., Choi, S. E., and Koh, H. C. (2018). PGAM5 regulates PINK1/Parkin-mediated mitophagy via DRP1 in CCCP-induced mitochondrial dysfunction. *Toxicol. Lett.* 1, 120–128. doi: 10.1016/j.toxlet.2017.12.004

Pickrell, A. M., and Youle, R. J. (2015). The roles of PINK1, parkin, and mitochondrial fidelity in Parkinson's disease. *Neuron* 85, 257–273. doi: 10.1016/j.neuron.2014.12.007

Pitkänen, A., and Lukasiuk, K. (2011). Mechanisms of epileptogenesis and potential treatment targets. *Lancet Neurol.* 10, 173–186. doi: 10.1016/s1474-4422(10)70310-0

Qin, Z., Song, J., Lin, A., Yang, W., Zhang, W., Zhong, F., et al. (2022). GPR120 modulates epileptic seizure and neuroinflammation mediated by NLRP3 inflammasome. *J. Neuroinflammation* 19:121. doi: 10.1186/s12974-022-02482-2

Ryan, K., Backos, D. S., Reigan, P., and Patel, M. (2012). Post-translational oxidative modification and inactivation of mitochondrial complex I in epileptogenesis. *J. Neurosci.* 32, 11250–11258. doi: 10.1523/jneurosci.0907-12.2012

Shekh-Ahmad, T., Lieb, A., Kovac, S., Gola, L., Christian Wigley, W., and Abramov, A. Y. (2019). Combination antioxidant therapy prevents epileptogenesis and modifies chronic epilepsy. *Redox Biol.* 26:101278. doi: 10.1016/j.redox.2019.101278

Sheng, Z. H. (2014). Mitochondrial trafficking and anchoring in neurons: new insight and implications. *J. Cell Biol.* 204, 1087–1098. doi: 10.1083/jcb.201312123

Sugawara, S., Kanamaru, Y., Sekine, S., Maekawa, L., Takahashi, A., Yamamoto, T., et al. (2020). The mitochondrial protein PGAM5 suppresses energy consumption in brown adipocytes by repressing expression of uncoupling protein 1. *J. Biol. Chem.* 295, 5588–5601. doi: 10.1074/jbc.RA119.011508

Sugo, M., Kimura, H., Arasaki, K., Amemiya, T., Hirota, N., Dohmae, N., et al. (2018). Syntaxin 17 regulates the localization and function of PGAM5 in mitochondrial division and mitophagy. *EMBO J.* 37. doi: 10.15252/embj.201798899

Takeda, K., Komuro, Y., Hayakawa, T., Oguchi, H., Ishida, Y., Murakami, S., et al. (2009). Mitochondrial phosphoglycerate mutase 5 uses alternate catalytic activity as a protein serine/threonine phosphatase to activate ASK1. *Proc. Natl. Acad. Sci. U. S. A.* 106, 12301–12305. doi: 10.1073/pnas.0901823106

Tizon, B., Sahoo, S., Yu, H., Gauthier, S., Kumar, A. R., Mohan, P., et al. (2010). Induction of autophagy by cystatin C: a mechanism that protects murine primary cortical neurons and neuronal cell lines. *PLoS One* 5:e9819. doi: 10.1371/journal.pone.0009819

Wang, Y. Y., Ke, C. C., Chen, Y. L., Lin, Y. H., Yu, I. S., Ku, W. C., et al. (2020). Deficiency of the Tbc1d21 gene causes male infertility with morphological abnormalities of the sperm mitochondria and flagellum in mice. *PLoS Genet.* 16:e1009020. doi: 10.1371/journal.pgen.1009020

Wen, H., Li, L., Zhan, L., Zuo, Y., Li, K., Qiu, M., et al. (2021). Hypoxic postconditioning promotes mitophagy against transient global cerebral ischemia via PINK1/Parkin-induced mitochondrial ubiquitination in adult rats. *Cell Death Dis.* 12:630. doi: 10.1038/s41419-021-03900-8

Willmore, L. J. (2005). Antiepileptic drugs and neuroprotection: current status and future roles. *Epilepsy Behav.* 7, S25–S28. doi: 10.1016/j.yebeh.2005.08.006

Wu, J. S., Li, L., Wang, S. S., Pang, X., Wu, J. B., Sheng, S. R., et al. (2018). Autophagy is positively associated with the accumulation of myeloid-derived suppressor cells in 4-nitroquinoline-1-oxide-induced oral cancer. *Oncol. Rep.* 40, 3381–3391. doi: 10.3892/or.2018.6747

Wu, M., Liu, X., Chi, X., Zhang, L., Xiong, W., Chiang, S. M. V., et al. (2018). Mitophagy in refractory temporal lobe epilepsy patients with hippocampal sclerosis. *Cell. Mol. Neurobiol.* 38, 479–486. doi: 10.1007/s10571-017-0492-2

Yang, Y., Tian, X., Xu, D., Zheng, F., Lu, X., Zhang, Y., et al. (2018). GPR40 modulates epileptic seizure and NMDA receptor function. *Sci. Adv.* 4:eaau2357. doi: 10.1126/sciadv.aau2357

Yi, M. H., Shin, J., Shin, N., Yin, Y., Lee, S. Y., Kim, C. S., et al. (2019). PINK1 mediates spinal cord mitophagy in neuropathic pain. *J. Pain Res.* 12, 1685–1699. doi: 10.2147/jpr.S198730

Zhang, Y., Zhang, M., Zhu, W., Yu, J., Wang, Q., Zhang, J., et al. (2020). Succinate accumulation induces mitochondrial reactive oxygen species generation and promotes status epilepticus in the kainic acid rat model. *Redox Biol.* 28:101365. doi: 10.1016/j.redox.2019.101365

frontiers | Frontiers in Molecular Neuroscience

TYPE Review
PUBLISHED 13 January 2023
DOI 10.3389/fnmol.2022.1116729

OPEN ACCESS

EDITED BY
Chen Gu,
The Ohio State University, United States

REVIEWED BY
Hee Jung Chung,
University of Illinois at Urbana-Champaign, United States
Martin Heine,
Johannes Gutenberg University Mainz, Germany

*CORRESPONDENCE
Karen L. Cunningham
✉ karen521@mit.edu

SPECIALTY SECTION
This article was submitted to Neuroplasticity and Development, a section of the journal Frontiers in Molecular Neuroscience

RECEIVED 05 December 2022
ACCEPTED 26 December 2022
PUBLISHED 13 January 2023

CITATION
Cunningham KL and Littleton JT (2023) Mechanisms controlling the trafficking, localization, and abundance of presynaptic Ca^{2+} channels.
Front. Mol. Neurosci. 15:1116729.
doi: 10.3389/fnmol.2022.1116729

Mechanisms controlling the trafficking, localization, and abundance of presynaptic Ca^{2+} channels

Karen L. Cunningham* and J. Troy Littleton

The Picower Institute for Learning and Memory, Department of Biology, Department of Brain and Cognitive Sciences, Massachusetts Institute of Technology, Cambridge, MA, United States

Voltage-gated Ca^{2+} channels (VGCCs) mediate Ca^{2+} influx to trigger neurotransmitter release at specialized presynaptic sites termed active zones (AZs). The abundance of VGCCs at AZs regulates neurotransmitter release probability (P_r), a key presynaptic determinant of synaptic strength. Given this functional significance, defining the processes that cooperate to establish AZ VGCC abundance is critical for understanding how these mechanisms set synaptic strength and how they might be regulated to control presynaptic plasticity. VGCC abundance at AZs involves multiple steps, including channel biosynthesis (transcription, translation, and trafficking through the endomembrane system), forward axonal trafficking and delivery to synaptic terminals, incorporation and retention at presynaptic sites, and protein recycling. Here we discuss mechanisms that control VGCC abundance at synapses, highlighting findings from invertebrate and vertebrate models.

KEYWORDS

voltage-gated calcium channel, synapse, active zone, neurotransmitter release, protein trafficking

Introduction

Electrical signaling within the nervous system provides a fast and robust mechanism for transmitting action potentials to synaptic terminals. Voltage-gated calcium channels (VGCCs) are essential for translating electrical propagation of action potentials into intracellular chemical signals. When the membrane voltage passes a critical threshold, VGCCs open and allow influx of Ca^{2+} ions into the cell. Baseline Ca^{2+} concentrations in the cytosol are kept extremely low through extensive buffering and fast extrusion *via* pumps, allowing Ca^{2+} to act as a potent intracellular signal to regulate a diversity of processes, such as vesicle fusion, phosphorylation, or transcriptional changes (Berridge et al., 2003). At chemical synapses, presynaptic VGCCs trigger neurotransmitter release from synaptic vesicles (SVs) by mediating Ca^{2+} influx, which activates the SV protein Synaptotagmin 1 (Syt1) to drive fusion of the SV and plasma membranes (Littleton et al., 1993, 1994; DiAntonio and Schwarz, 1994; Sauvola and Littleton, 2021).

Presynaptic neurotransmitter release lags behind intracellular Ca^{2+} influx by less than a millisecond (Katz and Miledi, 1965; Borst and Sakmann, 1996; Sabatini and Regehr, 1996; Neher, 1998). This incredible speed reflects the tight spatial organization of fusion-primed SVs near VGCCs. This spatial coordination occurs at active zones (AZs), specialized domains within the presynaptic membrane where a macromolecular complex of conserved scaffold proteins recruits SVs to clusters of VGCCs for efficient Ca^{2+} use (Kawasaki et al., 2004; Bucurenciu et al., 2008; Catterall and Few, 2008; Wang et al., 2008; Fouquet et al., 2009; Eggermann et al., 2011; Chen et al., 2015; Nakamura

et al., 2015). Although the opening of a single VGCC can trigger SV release at some synapses, VGCCs are typically clustered at AZs to produce a larger transient domain of intracellular Ca^{2+} (Jarsky et al., 2010; Bartoletti et al., 2011; Nakamura et al., 2015). AZs in different neurons and species differ in their ultrastructure. For example, AZs at the *Drosophila* neuromuscular junction (NMJ) show an electron dense "T-bar" structure composed primarily of the scaffold protein Bruchpilot (BRP) when viewed by EM (Figure 1A; Fouquet et al., 2009). In contrast, sensory synapses within photoreceptors and hair cells contain a long synaptic ribbon that is predicted to facilitate robust SV release at these terminals (Figure 1B). Mammalian CNS synapses lack such a striking dense projection but still have an increased electron density that corresponds to the dense network of AZ scaffold proteins (Figure 1C). Despite these ultrastructural differences, scaffolding proteins present at synapses are generally conserved. The major scaffolds that cluster VGCCs at AZs are Rab3-interacting molecules (RIMs), RIM-binding proteins (RBPs), ELKS/CAST, and Bassoon/Piccolo/Fife (Kittel et al., 2006; Müller et al., 2010; Han et al., 2011; Kaeser et al., 2011; Liu et al., 2011; Graf et al., 2012; Kiyonaka et al., 2012; Davydova et al., 2014; Bruckner et al., 2017; Xuan et al., 2017). These proteins form multiple binding interactions with VGCCs to provide functional redundancy in VGCC clustering at AZs.

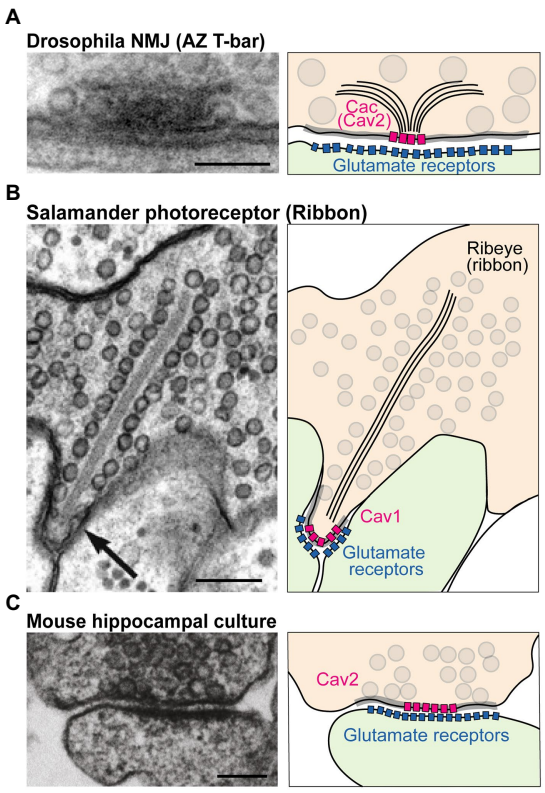

FIGURE 1
Structure and molecular composition of AZs. **(A)** Left: EM of an AZ at the *Drosophila* NMJ (modified from Fouquet et al., 2009; scale bar: 100nm). Right: molecular depiction of the AZ. The presynaptic terminal is colored in orange, and the postsynaptic cell green. Gray circles represent SVs. The gray highlighted zone along the presynaptic membrane marks the AZ area. Bruchpilot (BRP; black lines) forms the "T-bar" structure together with other scaffolds (not shown). The presynaptic Ca_v2 channel Cacophony (Cac) clusters at the base of the T-bar, while Glutamate Receptors cluster postsynaptically. **(B)** EM (modified from Thoreson et al., 2004; scale bar: 200nm) and depiction of a salamander photoreceptor ribbon synapse. The ribbon is an electron dense projection (formed by the protein Ribeye) and is lined with SVs. Ca_v1 family channels mediate fusion at this synapse. **(C)** EM (modified from Kaeser et al., 2011; scale bar: 100nm) and model of a mouse hippocampal cultured synapse. SV fusion at mammalian CNS neurons is primarily supported by $Ca_v2.1$ and $Ca_v2.2$ channels (pink).

Although AZs are specialized for SV fusion, not every AZ releases a SV following an action potential. Instead, neurons display a wide range of synaptic efficacies. Synaptic strength is a composite of both pre- and post-synaptic factors, and its regulation increases diversity for supporting circuit function and plasticity (Atwood and Karunanithi, 2002). A key presynaptic determinant of synaptic strength is neurotransmitter release probability (P_r), the likelihood of SV fusion after an action potential. Evoked P_r is partially regulated at the AZ-level and can vary dramatically across AZs formed by a single neuron (Figure 2A; Peled and Isacoff, 2011; Melom et al., 2013; Akbergenova et al., 2018; Sauvola et al., 2021; Newman et al., 2022). The amount of presynaptic Ca^{2+} influx at AZs, regulated in large part by the number of VGCCs clustered at the AZ, is a major determinant of P_r (Augustine et al., 1985; Borst and Sakmann, 1996; Wang et al., 2008; Bartoletti et al., 2011; Ariel et al., 2012; Sheng et al., 2012; Akbergenova et al., 2018; Newman et al., 2022). As such, VGCC function, regulation, and localization is central to how neurons control presynaptic output.

This review explores current models for how VGCC abundance is regulated at presynaptic AZs, with an emphasis on Ca_v2 family channels, which are the primary mediators of neurotransmission at most synapses (Dolphin and Lee, 2020). We focus exclusively on processes that mediate channel localization and abundance, as the structure and function of the channel has been extensively reviewed elsewhere (Catterall et al., 2020). We examine the regulation of VGCC localization at all stages of the channel's life, beginning with biosynthesis and progression through the ER and Golgi that requires auxiliary subunits. After axonal trafficking to synaptic terminals, channels are stabilized at AZs through multiple binding interactions with conserved AZ scaffold proteins including ELKS/CAST, RIM and RBP. We review evidence for the "slot" model of VGCC AZ abundance that suggests excess VGCCs compete for limited AZ localization through rate-limiting binding interactions downstream of channel biosynthesis (Cao et al., 2004; Cao and Tsien, 2010). Next, we focus on the channel's mobility once incorporated into AZs. Despite binding to multiple scaffolds, single-molecule tracking studies indicate VGCCs are highly mobile within the AZ (Mercer et al., 2011, 2012; Thoreson et al., 2013; Schneider et al., 2015; Voigt et al., 2016; Ghelani et al., 2022). In addition to VGCC mobility, we review molecular pathways facilitating endocytosis, although limited *in situ* information is available to contextualize these molecular pathways in intact circuits. Finally, we discuss how these processes are regulated during synaptic plasticity. Each of these steps—biosynthesis, trafficking, AZ scaffold-binding, mobility, and turnover, provide points of VGCC regulation that can be modulated to control presynaptic P_r.

The VGCC is a multisubunit complex

High resolution structures are available of the VGCC and its auxiliary subunits (Wu et al., 2015, 2016). Like other ion channels, VGCCs have a pore-forming α1 subunit that selectively fluxes Ca^{2+}, as well as several auxiliary subunits that regulate channel trafficking, stabilization, and function. The α1 subunit of the VGCC is closely related to voltage-gated sodium (Na_v) channels, and only several amino acid changes in the pore region are required to convert a Na_v channel

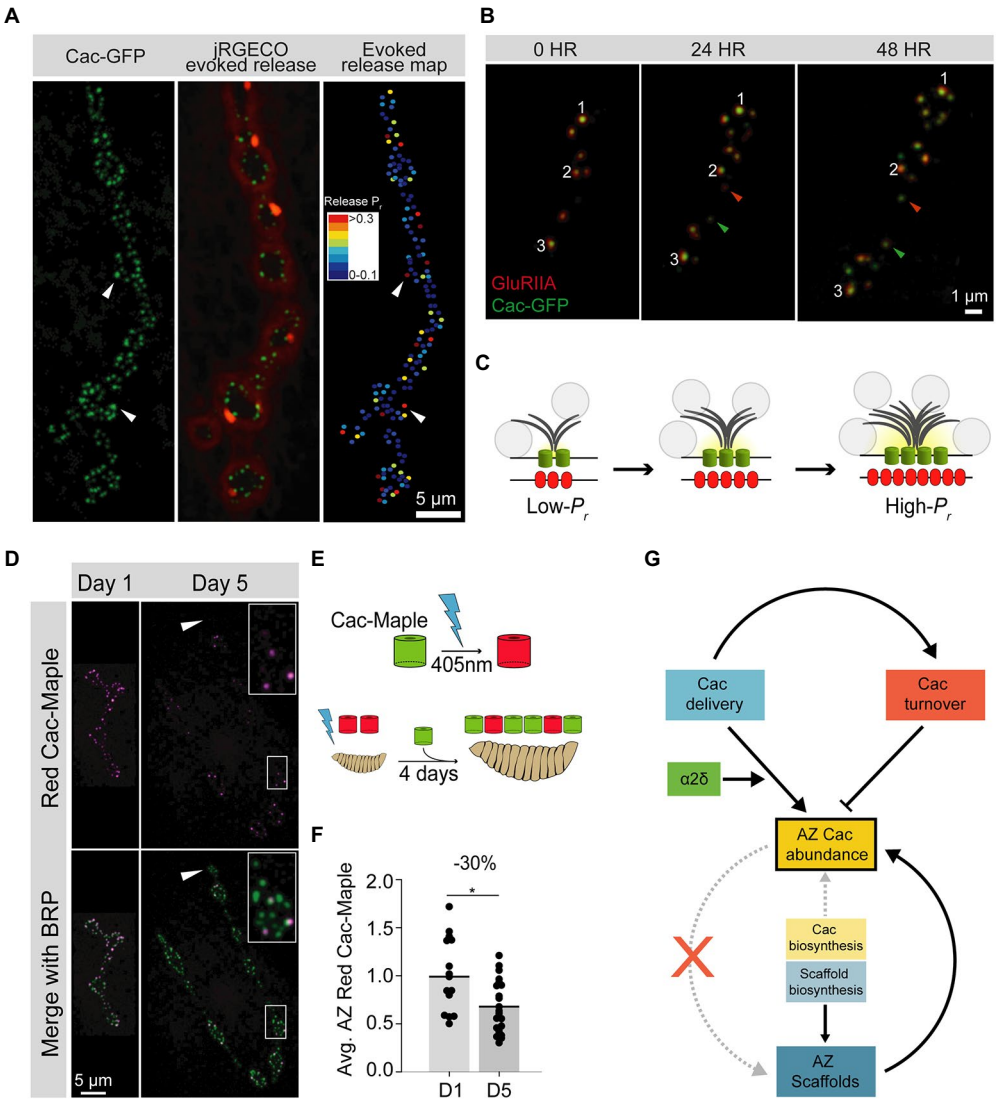

FIGURE 2
Cac regulation at the Drosophila third instar larval NMJ. **(A)** Representative image of a *Drosophila* larval NMJ. AZs are marked by clusters of Cac-GFP (green), and the jRGECO calcium sensor (red) is tethered to the postsynaptic membrane and indicates evoked release events at individual AZs. An evoked release heat map (right); generated from videos of jRGECO responses following a series of individual APs indicates P_r for each AZ, with high-P_r AZs in red and low-P_r sites in blue. **(B)** Sequential intravital imaging of a growing NMJ in an intact, anesthetized animal. Glutamate Receptor subunit GluRIIA-RFP marks postsynaptic densities and Cac-GFP marks presynaptic AZs. Arrows mark several new AZs formed after the 0-h timepoint, and white numbers track individual AZs through the image series. **(C)** Schematic of an AZ as it structurally and functionally matures from a young (low-P_r) site to an old (high-P_r) site through the multi-day acquisition of key components including BRP (gray), and Cac (green). Postsynaptic Glutamate Receptor abundance (red) also increases throughout maturation. SVs are marked as gray circles. **(D)** Representative images of Cac-Maple (magenta) and the AZ scaffold BRP (green) at AZs of the *Drosophila* NMJ, 1 day or 5 days after complete photoconversion. White arrows mark a bouton that formed after photoconversion, and is completely devoid of red Cac-Maple channels. The bouton outlined in white is enlarged in the upper right corner of each Day 5 image. **(E)** Schematic of Cac-Maple photoconversion (top panel) and experimental approach to measuring Cac turnover rate at AZs (bottom panel). Cac-Maple is green, and photoconverts permanently to red upon illumination with a 405nm light (blue lightning bolt). Photoconversion of an entire first instar larva, followed by 4 days of growth (during which time new green Cac-Maple channels are added to growing NMJs) results in a mixed pool of AZs with some AZs having only green channels (those that were added to the NMJ after the photoconversion event) and some AZs having red signal as well (representing channels present at the initial photoconversion timepoint). **(F)** Quantification of average red Cac-Maple abundance per AZ 1day and 5days post-photoconversion. A 30% reduction in red Cac-Maple levels occurs over this 4-day window. **(G)** Model of VGCC (Cac) regulation at the *Drosophila* NMJ. Cac delivery and turnover rates can be measured *in vivo* at this synapse. Both delivery (blue) and turnover (orange) cooperate to establish AZ Cac abundance. The α2δ subunit (green) positively regulates Cac delivery. AZ Cac abundance is only weakly regulated by Cac biosynthesis levels, as AZ Cac levels are highly buffered against changes in biosynthesis (yellow). In contrast, AZ scaffold biosynthesis plays a larger role in regulating AZ levels of the scaffold protein BRP (blue). While the presence of the AZ scaffold BRP is required for proper AZ Cac abundance (upward curved solid arrow), AZ Cac is not required for scaffold formation (red X). Figure panels **(A,B)** were adapted from Akbergenova et al. (2018). Figure panels **(D,G)** were adapted from Cunningham et al. (2022).

into one capable of fluxing Ca^{2+} (Tang et al., 2014). The VGCC α1 subunit contains four domains, each with six transmembrane spanning segments. Transmembrane segments I–IV comprise the voltage-sensing module of the channel, while segments V and VI form the Ca^{2+} selective pore (Figure 3A; Catterall et al., 2020). Despite conservation of α1 structure with other voltage-gated ion channels, the set of auxiliary subunits that regulates VGCCs are unique in the voltage-gated ion channel superfamily (Witcher et al., 1993; Yu et al., 2005). An

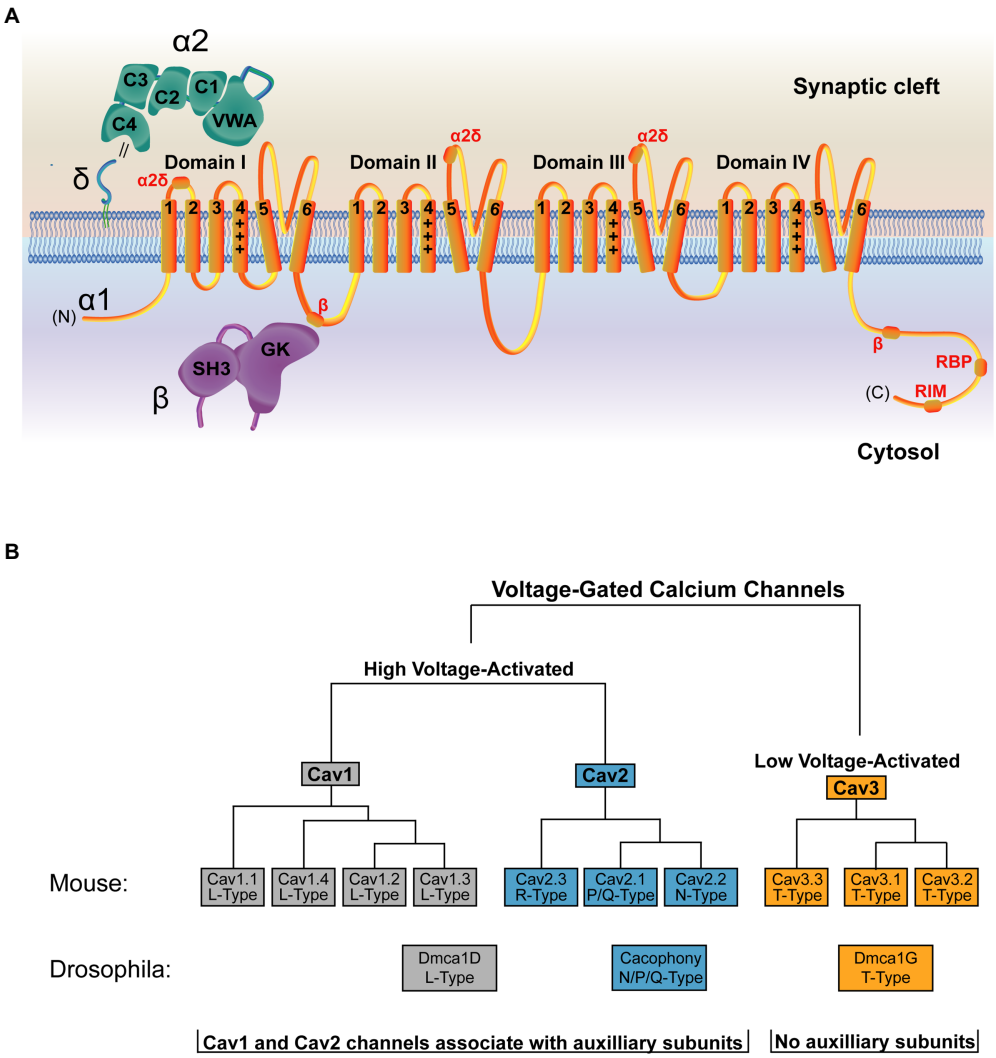

FIGURE 3
Structure and organization of the VGCC family. **(A)** Structure of a VGCC complex with the α1 pore-forming subunit in orange. VGCCs have four domains with six transmembrane segments each. Transmembrane segments I-IV comprise the voltage-sensing module, with transmembrane segment IV (marked +++) as the voltage sensing segment. Transmembrane segments V and VI form the ion-conducting pore. The cytoplasmic C-terminal tail interacts with multiple binding partners, including a secondary Cavß interaction site (Walker et al., 1998) and binding regions for RBP and RIM (Lübbert et al., 2017). The α2δ subunit (green) is extracellular and comprised of α2 and δ peptides linked *via* a disulfide bond (double black line) and anchored to the outer membrane leaflet *via* a lipid anchor (Davies et al., 2010; Wu et al., 2015). α2δ contains five domains, with the Von Willebrand Factor-A (VWA) and the first two Cache domains (C1 and C2) interacting with α1 (Wu et al., 2016). Sites of α2δ-interaction on the α1 subunit are marked in red. The Cavß subunit (purple) is cytosolic and comprised of an SH3 domain and a Guanylate Kinase (GK) domain. The primary α1 interaction site is mediated through an intracellular loop in domain I of the channel and the Cavß GK domain (Pragnell et al., 1994; Cantí et al., 2001; Chen et al., 2004; Opatowsky et al., 2004; Van Petegem et al., 2004; Wu et al., 2016). **(B)** The mammalian VGCC family is comprised of 7 high voltage-activated VGCCs (Ca_v1 and Ca_v2 family channels) and 3 low voltage-activated VGCCs (Ca_v3 family channels). *Drosophila* (shown below the mammalian tree) encodes one VGCC per class, with Dmca1D encoding the sole L-Type Ca_v1 channel (Eberl et al., 1998; Hara et al., 2015), Cacophony (Cac) encoding the sole N/Q/P type Ca_v2 channel that mediates synaptic transmission (Smith et al., 1996; Kawasaki et al., 2000, 2004), and Dmca1G encoding the sole T-Type Ca_v3 channel (Jeong et al., 2015). Ca_v1 and Ca_v2 channels associate with auxiliary subunits, while Ca_v3 channels do not.

extracellular α2δ subunit facilitates forward trafficking of the VGCC and modulates its gating and conductance properties (Dolphin, 2016). In addition, a cytosolic ß subunit acts as a chaperone during biosynthesis and is required for VGCC membrane expression (Figure 3A, Pragnell et al., 1994; Gregg et al., 1996; Cantí et al., 2001; Van Petegem et al., 2004; Weissgerber et al., 2006; Altier et al., 2011; Waithe et al., 2011; Dolphin, 2016). These subunits also support interactions between the channel and its signaling or scaffolding partners (Müller et al., 2010).

Mammals encode three VGCC families (Ca_v1–Ca_v3) defined by their pore-forming α1 subunit (Figure 3B; Dolphin, 2016). Of these, the four Ca_v1 channels (also called L-type based on initial current characterization) and the three Ca_v2 channels (P/Q-, N-, and R-type) are high-voltage activated and are the dominant contributors to synaptic transmission at presynaptic AZs (Luebke et al., 1993; Takahashi and Momiyama, 1993; Wheeler et al., 1994; Reuter, 1995; Reid et al., 1997; Wu et al., 1999; Dolphin and Lee, 2020). Ca_v2 channels mediate the majority of neurotransmission in the CNS, while Ca_v1 channels are important in sensory neurons like inner hair cells and photoreceptors. The three Ca_v3 channels (T-type) are low-voltage activated, do not play a central role in mediating evoked synaptic transmission, and do not require the canonical auxiliary subunits (Dolphin and Lee, 2020). Invertebrate VGCCs also mediate synaptic transmission but have less

redundancy. *Drosophila* encodes one family member from each of the three VGCC families, and the single Ca_v2 family VGCC (Cacophony; Cac) complexes with a single α2δ family member (Straightjacket) to mediate neurotransmission at synapses (Kawasaki et al., 2004; Ly et al., 2008; Ryglewski et al., 2012; Heinrich and Ryglewski, 2020; Figure 3B; Table 1).

VGCC auxiliary subunits promote cell surface expression

During biosynthesis, VGCCs are translated into the ER and move to the Golgi where they are extensively modified before delivery to the cell surface (Figure 4; step 2). The pore-forming α1 subunit requires co-expression of its auxiliary α2δ and Ca_vß subunits to reach the plasma membrane (Brice et al., 1997; Ball et al., 2002; Cassidy et al., 2014). Mammals encode 4 Ca_vß genes ($ß_1$-$ß_4$) that are essential for channel function and result in lethality or severe phenotypes when disrupted (Gregg et al., 1996; Burgess et al., 1997; Weissgerber et al., 2006). Four α2δ subunits ($α2δ_1$–$α2δ_4$) that are important for survival and display some functional redundancy are also expressed in mammals (Schöpf et al., 2021). While Ca_vß is essential for surface expression, α2δ plays a secondary trafficking role that rate-limits presynaptic expression of functional channels. In rodent cultured neurons, overexpression of either α2δ or Ca_vß alone dramatically increases presynaptic VGCC abundance, but only α2δ overexpression increases SV fusion (Hoppa et al., 2012). In addition to their requirements in promoting surface expression, these auxiliary subunits play extensive roles in modulating channel properties, including activation, inactivation, and gating, as well as mediating modulation by other regulatory pathways. In addition, α2δ subunits control synapse morphology independent of their role as channel subunits, and can localize to synapses without VGCCs (Kurshan et al., 2009; Dolphin, 2018; Held et al., 2020; Schöpf et al., 2021). These non-localizing or VGCC-independent roles of α2δ and Ca_vß subunits have been reviewed elsewhere (Buraei and Yang, 2010; Dolphin, 2018).

Ca_vß is a conserved intracellular subunit that controls channel progression through the biosynthetic pathway, determining whether nascent channels are destined for degradation or surface expression. Ca_vß contains SH3 and guanylate kinase (GK) domains through which it associates with an intracellular loop between domains I and II of the α1 subunit of Ca_v1 and Ca_v2 family VGCCs (Figure 3A; Pragnell et al., 1994; Cantí et al., 2001; Chen et al., 2004; Opatowsky et al., 2004; Van Petegem et al., 2004). Ca_vß binding at this site is predicted to promote proper folding of the channel (Opatowsky et al., 2004). In heterologous expression systems, α1 expression alone is insufficient for channel surface expression, but co-expression with Ca_vß promotes high levels of surface-expressed α1 (Brice et al., 1997; He et al., 2007; Cassidy et al., 2014). Likewise, *in vivo* knockdown of Ca_vß or disruption of the Ca_vß binding site on α1 inhibits VGCC surface expression (Berrow et al., 1995; Obermair et al., 2010). $Ca_v1.2$ α1 subunits are ubiquitinated and subsequently degraded without Ca_vß, and preventing this degradation by pharmacologically blocking the proteasome restores channel surface expression. This data suggests Ca_vß is not required for surface expression beyond its role in promoting protein stability in the ER (Altier et al., 2011; Waithe et al., 2011). A secondary Ca_vß-binding site is present in the VGCC C-terminal tail (Figure 3A). However structure–function studies at the calyx of Held demonstrated effective rescue of $Ca_v2.1$ function by $Ca_v2.1$ C-terminal truncation constructs lacking this Ca_vß-interaction domain (Walker et al., 1998; Lübbert et al., 2017). Overall these studies indicate Ca_vß functions as a chaperone by promoting α1 folding in the ER to prevent degradation.

The conserved VGCC subunit α2δ is also required for VGCC surface expression, though its mechanism of action is less clear. It is entirely extracellular, heavily glycosylated, and anchored to the external leaflet of the presynaptic membrane *via* a glycosyl-phosphatidyl inositol (GPI) anchor (Figure 3A; Davies et al., 2010; Wu et al., 2015). During processing, the α2δ precursor polypeptide is cleaved into α2 and δ subunits that are then linked together *via* disulfide bonds (De Jongh et al., 1990; Jay et al., 1991). Five domains have been identified in α2δ: a Von Willebrand Factor-A (VWA) domain and four Cache domains, with high-resolution structures suggesting multiple interactions between α2δ and the external face of the α1 channel (Figure 3A; Whittaker and Hynes, 2002; Wu et al., 2015, 2016; Cantí et al., 2001). The α2δ subunit can remain associated with the α1 subunit at synapses and modulate channel function, though it is unclear if continued α2δ- α1 interactions are absolutely essential for VGCC activity. Indeed, unlike Ca_vß that associates tightly to the α1 subunit with 1:1 stoichiometry, studies have reported a range of interaction strengths between α2δ and α1 ranging from stable to transient association modes (Pragnell et al., 1994; Müller et al., 2010; Cassidy et al., 2014; Voigt et al., 2016). Like Ca_vß, α2δ is required for proper surface expression of the channel. While the exact mechanism is unknown, this role of α2δ is likely performed by promoting forward trafficking rather than preventing channel endocytosis (Cantí et al., 2001; Dickman et al., 2008; Ly et al., 2008; Saheki and Bargmann, 2009; Hoppa et al., 2012; Cassidy et al., 2014; Cunningham et al., 2022). Understanding the structure and function of α2δ is of special importance due to its pharmacological targeting by the widely prescribed drugs gabapentin and pregabalin (Gee et al., 1996; Taylor et al., 2007; Eroglu et al., 2009; Dolphin, 2016).

Axonal trafficking and the "prefabricated synapse" hypothesis

After progression through the biosynthetic pathway, presynaptic VGCCs are trafficked down the axon to synaptic terminals (Figure 4; step 3). VGCC axonal trafficking is largely mysterious, but the trafficking of other presynaptic components such as AZ scaffolds and SV proteins has been extensively studied. Plus-end directed microtubule-based transport mediated by motor proteins of the Kinesin family is the dominant mode of trafficking to terminals (Vale et al., 1996; Goldstein et al., 2008; Hirokawa et al., 2010). Specifically, the anterograde Kinesin-3 family motor Unc-104/KIF1A plays a conserved role in the transport of many synaptic cargoes (Hall and Hedgecock, 1991; Okada et al., 1995; Yonekawa et al., 1998; Pack-Chung et al., 2007; Rivière et al., 2011; Maeder et al., 2014; Zhang et al., 2016, 2017). Kinesin-1 family members have also been implicated in synaptic transport (Gho et al., 1992; Hurd and Saxton, 1996; Gindhart et al., 1998). Since Kinesin diversity alone is insufficient to support the wide need of unique cellular trafficking processes, adaptor proteins that associate with cargo and Kinesins provide additional levels of regulation (Goldstein et al., 2008; Tempes et al., 2020). A conserved adaptor role for the GTPase Arl-8 in supporting Unc-104 mediated synaptic transport was first described in *C. elegans* where SV and AZ proteins are co-transported in an Unc-104/KIF1A dependent pathway (Hall and Hedgecock, 1991; Wu et al., 2013). In a forward genetic screen for genes involved in synapse formation, Arl-8 disruptions were found to deplete SV components from synapses

TABLE 1 Summary of AZ structure and VGCC localization/abundance phenotypes in *Mus musculus* (*M. mus*), *Caenorhabditis elegans* (*C. ele*), and *Drosophila melanogaster* (*D. mel*) AZ and VGCC mutants.

Function	Protein Family	Species	Gene name	Phenotype (VGCC)	References
AZ Scaffold	ELKS/CAST	*M. mus*	ELKS, CAST	Variable, from no effect to mild effect on VGCC abundance	Liu et al. (2014); Dong et al. (2018); Radulovic et al. (2020)
		C. ele	ELKS	Not required for VGCC clustering or synaptic transmission	Oh et al. (2021); Deken et al. (2005)
		D. mel	Bruchpilot (BRP)	*brp* nulls show a major loss of VGCCs, loss of T-bars; loss of channel stabilization, lower channel confinement, and failure to potentiate VGCC abundance during homeostatic plasticity	Kittel et al. (2006); Fouquet et al. (2009); Wagh et al. (2006); Ghelani et al. (2022); Matkovic et al. (2013)
	RIM	*M. mus*	RIM	*rim* nulls have ultrastructurally normal AZs with ~40% reduced $Ca_v2.1$ abundance, reduced release, and fewer docked SVs	Han et al. (2011); Kaeser et al. (2011)
		C. ele	RIM/Unc-10	Loss of Ca_v2 channels without ultrastructural changes	Oh et al. (2021); Koushika et al. (2001)
		D. mel	RIM	Loss of Ca_v2 channels without ultrastructural changes, decreased mobility of Ca_v2	Graf et al. (2012); Ghelani et al. (2022)
	RBP	*M. mus*	RBP	Reduced coupling of VGCCs to SVs, unaltered VGCC properties or abundance at calyx of Held but enhanced VGCC loss in *rim* mutants; 40% reduced Ca_v1 abundance in hair cell AZs	Acuna et al. (2015, 2016); Krinner et al. (2017)
		C. ele	RIMB-1	*rimb-1/rbp* mutants have normal VGCC localization and abundance but *rbp* enhances the loss of VGCCs in *rim* mutants	Kushibiki et al. (2019)
		D. mel	RBP	*rbp* mutants show depletion of VGCCs, disorganization of the BRP scaffold, and decreased mobility of Ca_v2 channels	Liu et al. (2011); Ghelani et al. (2022)
	Bassoon	*M. mus*	Bassoon	Loss of $Ca_v2.1$ (but not $Ca_v2.2$) at hippocampal synapses, loss of synaptic ribbons and reduction in VGCCs at sensory synapses	Altrock et al. (2003); Dick et al. (2003); Khimich et al. (2005); Frank et al. (2010); Jing et al. (2013); Davydova et al. (2014)
		C. ele	n/a		
		D. mel	n/a		
	Piccolo	*M. mus*	Piccolo	No reported involvement in VGCC abundance	
		C. ele	Clarinet	Piccolo-RIM homolog	Xuan et al. (2017)
		D. mel	Fife	Piccolo-RIM homolog, mutants have a modest reduction in VGCC abundance and reduced VGCC/SV coupling	Bruckner et al. (2017)

(Continued)

TABLE 1 (Continued)

Function	Protein Family	Species	Gene name	Phenotype (VGCC)	References
VGCC α1 subunits	Ca_v1 channels (high voltage activated)	*M. mus*	$Ca_v1.1$-$Ca_v1.4$ (L-type)	Required for synaptic transmission and ribbon stabilization in mammalian sensory synapses	Liu et al. (2013); Zabouri and Haverkamp (2013); Maddox et al. (2020)
		C. ele	egl-19 (L-type)	Muscle excitation and contraction, mechanosensation	Frøkjær-Jensen et al. (2006), Lainé et al. (2011), Lee et al. (1997)
		D. mel	Dmca1D (L-type)	Essential for viability, muscle calcium currents	Eberl et al. (1998); Hara et al. (2015)
	Ca_v2 channels (high voltage activated)	*M. mus*	$Ca_v2.1$ (P/Q-type) $Ca_v2.2$ (N-type) $Ca_v2.3$ (R-type)	Supports most neurotransmission in mammalian CNS. Triple conditional knockout of all Ca_v2s nearly abolishes evoked transmission without impacting AZ number or structure in CNS	Held et al. (2020)
		C. ele	Unc-2 (N/P/Q)	N/P/Q related channel required for evoked synaptic transmission	Schafer and Kenyon (1995); Mathews et al. (2003)
		D. mel	Cacophony (N/P/Q)	Sole VGCC responsible for evoked synaptic transmission	Smith et al. (1996); Kawasaki et al. (2000, 2004)
	Ca_v3 channels (low voltage activated)	*M. mus*	$Ca_v3.1$-$Ca_v3.3$. (T-type)	Mediates low threshold calcium currents in many excitable cell types	Lambert et al. (2014)
		C. ele	CCA-1 (T-type)	Muscle contraction	Shtonda and Avery (2005); Steger et al. (2005)
		D. mel	Dmca1G (T-type)	Expressed in brain, low voltage activated calcium currents, has a role in regulating sleep	Jeong et al. (2015)
VGCC auxilliary subunits	α2δ	*M. mus*	$\alpha2\delta_1$- $\alpha2\delta_4$	α2δ subunits interact with the VGCC and are required for VGCC surface expression in a semi-redundant manner	Kerov et al. (2018); Wang et al. (2017); Schöpf et al. (2021)
		C. ele	unc-36	Surface expression of VGCCs	Saheki and Bargmann (2009)
		D. mel	Straightjacket (stj), stol	Stj is required for surface expression of presynaptic VGCCs	Dickman et al. (2008); Ly et al. (2008)
	$Ca_vß$	*M. mus*	$ß_1$-$ß_4$	Required for channel surface expression by preventing proteasomal degradation in the biosynthetic pathway	Katiyar et al. (2015); Ball et al. (2002); Gregg et al. (1996); Weissgerber et al. (2006); Burgess et al. (1997); Obermair et al. (2010)
		C. ele	cbb-1	Cbb-1 is essential for viability and voltage dependent calcium currents in muscle	Lainé et al. (2011)
		D. mel	Ca-β		Kanamori et al. (2013)

and promote the ectopic accumulation of AZ and SV proteins along axons (Klassen et al., 2010). Likewise, Arl-8 co-traffics with several synaptic proteins, and its loss severely disrupts their synaptic localization as well as synapse growth in *Drosophila* (Vukoja et al., 2018). These studies demonstrate an important and conserved role for Unc-104 and its Arl-8 adaptor in axonal trafficking of synaptic proteins.

Do presynaptic proteins co-transport or arrive independently at developing synapses? Through studies of transport packets containing AZ and SV proteins, several synapse-specific transport organelles have been identified (Goldstein et al., 2008; Vukoja et al., 2018). In mammals, Golgi-derived ~80 nm dense core vesicles called Piccolo-Bassoon transport vesicles (PTVs) traffic many AZ proteins including Piccolo, Bassoon, RIM, CAST, N-Cadherin, Rab3, and Munc18, but lack the SV proteins Syt1 and VAMP (Zhai et al., 2001; Ohtsuka et al., 2002; Shapira et al., 2003; Dresbach et al., 2006; Cai et al., 2007; Maas et al., 2012). The α1 and $Ca_vß$ subunits of the $Ca_v2.2$ channel were biochemically

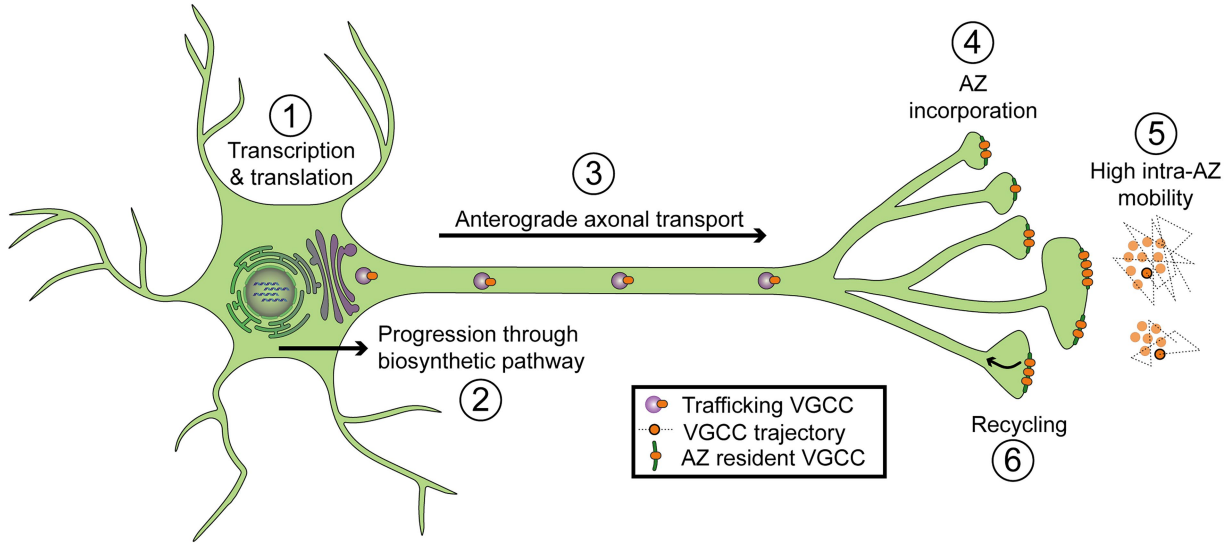

FIGURE 4
Diagram of regulatory steps involved in setting VGCC abundance at synaptic AZs. (1) Transcription and translation. (2) Progression through the biosynthetic pathway, including the endoplasmic reticulum and Golgi. (3) Forward axonal trafficking. (4) Incorporation into AZs through local interactions with scaffolding proteins. (5) High mobility within individual AZs (intra-AZ mobility) and low inter-AZ mobility. Cartoon on the right depicts a top-down view of VGCCs residing in two nearby AZs. Dotted lines represent short-term trajectories of VGCCs outlined in black. (6) Recycling of VGCCs.

suggested to reside on these compartments, but confirmation of their presence through microscopy was inaccessible due to technical limitations (Shapira et al., 2003). The other major transport organelle that has been identified is the Synaptic Vesicle Precursor (SVP), which carries SV markers including Synaptotagmin, Synaptophysin, and Rab3, and has not been shown to contain VGCCs (Okada et al., 1995; Maeder et al., 2014; Guedes-Dias et al., 2019; De Pace et al., 2020). SVP trafficking is primarily Kinesin-3 mediated (Okada et al., 1995). In addition to PTVs and SVPs, other transport organelles also likely exist. For example, mobile Neurexin puncta in axons do not colocalize with Bassoon but partially colocalize with other AZ proteins including CASK, RIM, and Mint, as well as the $Ca_v2.2$ channel, suggesting the identity of a third AZ transport packet that has so far been minimally studied (Fairless et al., 2008).

One hypothesis for the bulk transport of AZ proteins (on PTVs) and SV proteins (on SVPs) is that this packaging allows robust and efficient maturation of new AZs into functional release sites. It has even been suggested that AZ and SV transport packets may be coordinated and comprehensive enough to be considered "pre-fabricated synapses" (Ahmari et al., 2000; Shapira et al., 2003; Tao-Cheng, 2007; Bury and Sabo, 2011; Vukoja et al., 2018). Indeed, comparisons of Piccolo and Bassoon abundance at synaptic and non-synaptic puncta suggest that only several PTVs are required to populate an AZ with its full complement of these proteins (Shapira et al., 2003; Tao-Cheng, 2007). Additionally, live imaging of movement and pausing suggests that although PTVs and SVPs represent separate organelles, they partially co-transport and share defined pause sites along axons (Bury and Sabo, 2011). Evidence from EM also points to bundled transport organelles, as Bassoon/Piccolo-positive aggregates of proteins, dense core vesicles, and smaller clear vesicles carrying SV markers can be seen in axons (Ahmari et al., 2000; Tao-Cheng, 2007). Light microscopy suggests VGCC subunits may colocalize with these organelle aggregates, but the lack of spatial resolution precludes determination of whether channels are present on PTVs, SVPs or a separate (and perhaps co-bundled) compartment (Ahmari et al., 2000).

Invertebrates were long thought to lack Piccolo and Bassoon (although *Drosophila* and *C. elegans* encode Piccolo-RIM homologs called Fife and Clarinet, respectively), calling into question whether they use PTV-like organelles to transport AZ proteins (Bruckner et al., 2017; Xuan et al., 2017). Like mammalian neurons, imaging in *Drosophila* axons revealed coordinated transport of some presynaptic proteins. The core AZ scaffold BRP partially co-transports with the SV protein Syt1. Interestingly, these transport packets colocalize with markers of non-degradative lysosomes and have thus been termed presynaptic lysosome-related vesicles (PLVs; Vukoja et al., 2018). Consistent with the role of Arl-8 in mediating synaptic protein and lysosome transport, *arl-8* mutations block trafficking of these PLV packets, resulting in their buildup in the cell soma. EM visualization of these stalled packets indicate they are ~60–70 nm in diameter and have variable electron densities resembling a mix of dense-core and clear transport vesicles as seen in mammals (Khatter et al., 2015; Vukoja et al., 2018). In mammalian neurons, the SV marker VGlut1 and the AZ marker Bassoon also co-transport with the lysosome marker Lamp1, and reductions in Arl-8 caused a buildup of Bassoon in the soma, suggesting this lysosomal transport mechanism also occurs in mammals (Vukoja et al., 2018). In contrast to the "pre-fabricated synapse" hypothesis, sequential steps of AZ assembly are clearly temporally and genetically separable in *Drosophila*, as some proteins populate AZs ahead of others and *rab3* mutations produce a sub-population of AZs that have only early AZ scaffolds but not late scaffolds or VGCCs (Fouquet et al., 2009; Graf et al., 2009; Owald et al., 2010; Böhme et al., 2016; Ghelani and Sigrist, 2018). Though a picture is emerging for the trafficking of core AZ scaffolds and SV components, how VGCCs traffic to synapses is still a major unknown. Determining if VGCCs travel in association with PTV/SVP aggregates or other post-Golgi vesicles, and which motor proteins mediate their transport, will require developing new tools to visualize VGCC trafficking in live neurons.

The AZ clusters VGCCs

Once VGCCs arrive at the synaptic terminal, they are incorporated into an AZ (Figure 4 step 4). The AZ is a defined region of presynaptic membrane featuring a dense protein matrix that functions as a scaffold to cluster SVs near VGCCs for efficient Ca^{2+}-mediated fusion (Südhof, 2012). The structure of the AZ scaffold differs between species and neuron types, but it is comprised of several conserved proteins (including RIM, RIM-binding protein, and ELKS/CAST) that help cluster VGCCs (Table 1; Figure 1; Zhai and Bellen, 2004). The interactome of Ca_v2 channels has been analyzed in rodent brains using multi-epitope affinity purification and mass spectrometry, revealing a large cohort of ~200 proteins that interact with the channel (Müller et al., 2010). Multiple protein classes were identified, including known AZ scaffolds (CASK, RIM, RBP, Piccolo, etc) and other proteins that may regulate or function downstream of the channel. Given the multitude of proteins that bind VGCCs and contribute to their abundance and localization, a key question arises: which of these interactions is rate-limiting for VGCC accumulation? Identifying proteins that regulate VGCC abundance in a dosage-sensitive manner is critical, as these rate-limiting interactions may represent candidates for modulation during synaptic plasticity. The molecular constituents of the AZ and their roles in promoting VGCC clustering have been reviewed in depth (Dolphin and Lee, 2020; Gandini and Zamponi, 2022). Here we review the interactions of AZ proteins with VGCCs with a focus on distinguishing requirement versus rate-limiting roles.

RIM and RBP

RIM-interacting molecule and RBP are central scaffolds that semi-redundantly regulate VGCC abundance at AZs (Han et al., 2011; Kaeser et al., 2011; Liu et al., 2011; Graf et al., 2012; Jung et al., 2015; Oh et al., 2021). RIM was identified through its interaction with the SV protein Rab3 (Wang et al., 1997), but it also interacts with multiple AZ-resident proteins including Ca_v2 family VGCCs (*via* RIM's PDZ domain), ELKS/CAST, RBP, Munc-13, and Liprin-α (Wang et al., 2000; Betz et al., 2001; Coppola et al., 2001; Ohtsuka et al., 2002; Schoch et al., 2002; Kiyonaka et al., 2007; Müller et al., 2010; Kaeser et al., 2011). Conditional knock-out of all PDZ-domain-containing *rim* genes from mammalian neurons results in ultrastructurally normal AZs with ~40% reduced $Ca_v2.1$ channel abundance, similar to the partial loss of Ca_v2 channels in *Drosophila* and *C. elegans rim* mutants (Koushika et al., 2001; Kaeser et al., 2011; Graf et al., 2012; Oh et al., 2021). Mouse *rim* mutants show a dramatic reduction in evoked release that is secondary to a decrease in presynaptic Ca^{2+} influx and fewer docked SVs (Han et al., 2011; Kaeser et al., 2011). RIM's PDZ domain is required to rescue $Ca_v2.1$ AZ abundance, while its RBP-binding sequences are required for normal $[Ca^{2+}]$-dependence of release, indicating that both RIM's direct interaction with $Ca_v2.1$ and indirect interactions through RBP contribute to $Ca_v2.1$ channel localization (Hibino et al., 2002; Kaeser et al., 2011).

RBPs-interacting molecule-binding proteins were identified through their binding interaction with RIMs, but they also directly bind VGCCs and Liprin-α (Wang et al., 2000; Hibino et al., 2002; Müller et al., 2010; Liu et al., 2011). RBPs role in setting VGCC abundance varies between neuron types and is semi-redundant with RIM. In *C. elegans*, *rbp* deletion alone did not change VGCC abundance at AZs, but *rim/rbp* double nulls had more severe VGCC depletion than either individual mutation (Kushibiki et al., 2019). Similarly, conditional deletion of both neuronally-expressed *rbp* genes in mammalian neurons did not alter VGCC abundance, but removing both RIM and RBP families at the calyx of Held resulted in a more severe (~75%) disruption in presynaptic Ca^{2+} influx (and in AZ ultrastructure) than deletions of RIMs alone, suggesting partially redundant roles for RIM and RBP in localizing VGCCs (Acuna et al., 2015, 2016). Though *Drosophila rpb* mutations do independently disrupt VGCC clustering (possibly downstream of a disorganized BRP scaffold), *rim/rbp* double heterozygotes have severely reduced release despite normal function in each individual heterozygote, further suggesting functional redundancy (Kittel et al., 2006; Fouquet et al., 2009; Liu et al., 2011; Müller et al., 2015; Bruckner et al., 2017; Ortega et al., 2018). Though RBP plays a secondary role to RIM in many systems, RBP does independently regulate VGCCs in hair cells, where *rbp* mutants display ~40% reduction in presynaptic Ca^{2+} influx and a similarly reduced level of synaptic $Ca_v1.3$ immunofluorescence (Krinner et al., 2017).

These studies suggest that while RIM and RBP both bind to VGCCs, RIM is the dominant regulator of VGCC abundance at many synapses with partially redundant functions to RBP. This picture is complicated by *in vivo* structure–function studies at the calyx of Held, where $Ca_v2.1$ C-terminal truncation constructs lacking the known RIM and RBP binding domains rescue presynaptic currents in *$ca_v2.1$* conditional knockouts, suggesting these binding domains are dispensable for $Ca_v2.1$ localization (Lübbert et al., 2017). This finding likely reflects redundancy in binding interactions that localize the channel to presynaptic membranes and may indicate that the known binding interactions of RIM to Ca_vß, or perhaps direct or indirect binding to another unknown site on the α1 subunit, provides an additional mechanism of interaction (Kiyonaka et al., 2007). Functional redundancy in localizing VGCCs presents a challenge in deciphering whether RIMs or RBPs play a dosage-sensitive role in fine-tuning VGCC AZ abundance. Future experiments testing whether RIM or RBP levels can be bidirectionally modulated to fine-tune VGCC abundance at AZs would provide insights into whether the abundance of these components rate-limits VGCC clustering.

CAST/ELKS

In addition to RIM and RBP, the two semi-redundant CAST/ELKS family proteins (CAST and ELKS) are conserved core AZ scaffolds, initially discovered through biochemical analysis (Ohtsuka et al., 2002; Wang et al., 2002). In mammals, CAST/ELKS interacts directly with VGCCs, and other core AZ proteins including RIM, Munc13, and Liprin-α (Ohtsuka et al., 2002; Ko et al., 2003; Wang et al., 2009; Chen et al., 2011; Billings et al., 2012; Kiyonaka et al., 2012). Similarly, the *Drosophila* CAST/ELKS homolog BRP diverges from mammalian ELKS in its C-terminal domain but interacts with presynaptic Ca_v2 channels through its ELKS-homologous N-terminal domain (Wagh et al., 2006; Fouquet et al., 2009). Despite their presence at synapses and direct interactions with VGCCs, the role of CAST/ELKS proteins in regulating VGCC abundance varies across systems. In mouse hippocampal synapses, conditional knockout of both *elks* genes after synapse formation resulted in a 30% decrease in presynaptic Ca^{2+} influx without any change in presynaptic VGCC abundance or synaptic ultrastructure (Liu et al., 2014). However, this manipulation was made after Ca_v2 channels had already populated synapses, so whether this timeframe is long enough to see an ELKS-dependent effect on Ca_v2 levels

depends both on the AZ half-life of Ca_v2 channels and the role of the ELKS-VGCC binding interactions. At mature ($Ca_v2.1$-exclusive) and immature (Ca_v2-mixed) mouse calyx of Held synapses, conditional knockout of *elks* in the *cast* null line caused mildly decreased $Ca_v1.3$ abundance (Dong et al., 2018; Radulovic et al., 2020). In *C. elegans*, ELKS does not play a major role in clustering VGCCs at AZs (Deken et al., 2005; Oh et al., 2021). In contrast, the *Drosophila* CASK/ELKS homolog BRP plays a central role in forming the core of the AZ "T-bar" scaffold, promoting VGCC clustering and recruiting SVs to AZs (Kittel et al., 2006; Wagh et al., 2006; Fouquet et al., 2009). *Brp* mutants lack consolidated Ca_v2 clusters and have a large decrease in evoked synaptic transmission (Kittel et al., 2006; Fouquet et al., 2009). Unlike mammalian CAST/ELKS which is not always required for AZ morphology and structure (Dong et al., 2018), *brp* null mutants lack the AZ "T-bar" (Kittel et al., 2006; Fouquet et al., 2009). Despite this requirement for BRP in clustering VGCCs at the AZ, BRP is not a rate-limiting regulator of VGCC abundance, as ~35% reductions in AZ BRP have no impact on VGCC abundance and do not change single AP-evoked SV release (Müller et al., 2015; Cunningham et al., 2022).

Bassoon

The remaining core AZ proteins that are well characterized are Piccolo and Bassoon, Liprin-α, Syd-1, and Munc-13 (Cases-Langhoff et al., 1996; Tom Dieck et al., 1998; Fenster et al., 2000; Ackermann et al., 2015; Gundelfinger et al., 2015). Of these, Bassoon plays the most prominent role in VGCC localization, although Liprin-α is required for channel localization in *C. elegans* (Oh et al., 2021). Bassoon is a large multi-domain scaffolding protein that co-immunoprecipitates with $Ca_vß$ and promotes VGCC clustering in some systems (Frank et al., 2010; Chen et al., 2011; Davydova et al., 2014). Binding between Bassoon and the VGCC-interaction partner RBP is important for recruiting $Ca_v2.1$ (but not $Ca_v2.2$) channels to hippocampal synapses (Davydova et al., 2014). At ribbon synapses in mammalian sensory neurons, the major AZ phenotype in *bassoon* mutants is loss of the ribbons (Dick et al., 2003; Khimich et al., 2005;Frank et al., 2010; Jing et al., 2013). At inner hair cell synapses, $Ca_v1.3$ abundance is reduced even though some AZs have intact ribbons, indicating the *bassoon* VGCC-reduction phenotype is not completely downstream of ribbon loss (Frank et al., 2010; Jing et al., 2013). The Bassoon homolog Piccolo does not have an established role in promoting VGCC abundance, although it has been suggested to bind to VGCCs (Müller et al., 2010) and interacts with L-type VGCCs in pancreatic cells (Shibasaki et al., 2004). In contrast to the requirement of Bassoon for proper VGCC abundance and ribbon attachment at mammalian sensory synapses, Bassoon plays more minor roles in synaptic ultrastructure at mammalian central synapses (Altrock et al., 2003; Mukherjee et al., 2010). Although invertebrates were thought to lack Piccolo/Bassoon homologs, the Piccolo/Rim related proteins (Fife and Clarinet) were recently identified in *Drosophila* and *C. elegans*, respectively (Bruckner et al., 2017; Xuan et al., 2017). *Fife* mutants display a modest reduction in VGCC abundance at AZs (Bruckner et al., 2017). In summary, redundant interactions between the core AZ scaffolds (RIMs, RBPs, ELKS/CAST, and Bassoon) with each other and VGCCs provide a robust mechanism to ensure AZs are populated with VGCCs required to support synaptic transmission.

The slot model for VGCC accumulation at AZs

A popular slot model of VGCC AZ abundance was originally proposed to explain several observations of competition among VGCCs for AZ localization in cultured hippocampal neurons with mixed $Ca_v2.1$ and $Ca_v2.2$ synapses (Cao et al., 2004). Overexpressing $Ca_v2.1$ did not increase $Ca_v2.1$-mediated release at synaptic terminals, suggesting the number of $Ca_v2.1$ channels that localize to AZs is limited downstream of $Ca_v2.1$ biosynthesis. Overexpression of mutant Ca^{2+}-impermeant $Ca_v2.1$ channels reduced the contribution of $Ca_v2.1$ to total release, further indicating that mutant $Ca_v2.1$ channels compete with their wildtype counterparts for AZ localization "slots" (Cao et al., 2004). Because whole cell (somatodendritic) $Ca_v2.1$ currents were normal despite mutant channel overexpression, and were increased 5-fold by WT $Ca_v2.1$ overexpression, the rate-limiting factor in AZ localization is proposed to be downstream of channel biosynthesis and surface expression (Cao et al., 2004). Additionally, $Ca_v2.2$ influx was unaltered by $Ca_v2.1$ overexpression, suggesting the existence of "$Ca_v2.2$ specific slots" that cannot be occupied by $Ca_v2.1$ (Cao et al., 2004). In a similar series of experiments, overexpressing Ca^{2+}-impermeant $Ca_v2.2$ reduced synaptic release, further indicating competition for saturated VGCC "slots" (Cao and Tsien, 2010). While $Ca_v2.2$ overexpression failed to increase total presynaptic release, $Ca_v2.2$ channels could displace $Ca_v2.1$ channels, suggesting "$Ca_v2.1$-preferring slots" can accommodate $Ca_v2.2$ under conditions of $Ca_v2.2$ excess (Cao and Tsien, 2010).

Three key elements define the slot model for limiting VGCC accumulation at AZs. First, $Ca_v2.1$/$Ca_v2.2$ mixed synapses are proposed to have "$Ca_v2.1$-preferring slots" and "$Ca_v2.2$ specific slots" that limit the number of VGCCs at the AZ. Second, "slots" are typically saturated, supported by the observation that channel overexpression does not increase AZ channel levels (Cao et al., 2004). Third, "slots" may not represent a limited number of rigid locations at the AZ where VGCCs are physically tethered, but may instead include competition for binding partners at any stage of VGCC localization all the way from axonal trafficking to channel incorporation or stabilization at AZs. Since $Ca_v2.1$ and $Ca_v2.2$ overexpression increased cell body Ca^{2+} currents, the competition for rate-limiting binding partners ("slots") are proposed to be downstream of ER exit and cell surface expression (Cao and Tsien, 2010). The slot model predicts $Ca_v2.2$ channels should compensate for loss of $Ca_v2.1$ expression, whereas $Ca_v2.1$ channels should be unable to occupy $Ca_v2.2$-specific slots in $Ca_v2.2$ mutants. Indeed, $Ca_v2.2$ channels partially compensate in *$ca_v2.1$* knockout mice at the mature calyx of Held, but $Ca_v2.1$ does not increase in *$ca_v2.2$* mutant hippocampal neurons (Kim et al., 2001; Inchauspe et al., 2004; Ishikawa et al., 2005; Jeon et al., 2007). Additionally, Ca_v2 α1 subunit overexpression in dissociated rat neurons and *Drosophila* NMJs does not increase Ca_v2 levels at synapses, providing further support for a competition model (Hoppa et al., 2012; Cunningham et al., 2022).

Despite evidence supporting the slot model, its predictions partially fail at the calyx of Held. At immature ($Ca_v2.1$/$Ca_v2.2$ mixed) and mature ($Ca_v2.1$ exclusive) calyx neurons, $Ca_v2.1$ overexpression increased $Ca_v2.1$ number at AZs, indicating that if $Ca_v2.1$ slots exist, they are not saturated at this synapse (Lübbert et al., 2019). However, some evidence of competition was still observed, as $Ca_v2.1$ overexpression outcompeted $Ca_v2.2$ channels in the immature calyx. These data support an alternative model where $Ca_v2.1$ channels are not saturated at AZs, and $Ca_v2.2$ slots

are $Ca_v2.2$-preferred rather than $Ca_v2.2$-specific (Lübbert et al., 2019). Contrasting findings in hippocampal vs. calyx of Held neurons could be due to several factors. VGCC regulation could differ between cultured neurons vs. *in vivo* neurons embedded in native circuitry. In addition, rules for mixed synapses may differ and change during development. Finally, previous studies used human $Ca_v2.1$ and $Ca_v2.2$ overexpression in mouse neurons. Even though these constructs rescued their respective knockouts, human and mouse VGCCs could differ in their regulation (Cao et al., 2004; Cao and Tsien, 2010). Further experiments are needed to define which aspects of the slot model represent general principles versus synapse-specific regulation that reflect neuronal diversity.

Several important questions still need to be addressed in the classical slot model for AZ VGCC abundance. If slots exist, what do they physically represent? Is the slot mechanism implemented locally at AZs (by limiting incorporation or retention of channels) or upstream of AZ localization, perhaps through limited binding to axonal trafficking partners? The key criterion for identifying a protein that regulates competition is that the level of that protein should affect VGCC AZ abundance in a dosage sensitive manner. The conserved AZ scaffold proteins are attractive candidates for locally mediating slots at the AZ. *Drosophila* BRP is well situated to be a slot protein, as it binds directly to the Ca_v2 channel and is required for channel accumulation and stabilization at AZs (Fouquet et al., 2009; Ghelani et al., 2022). However, reductions in AZ BRP abundance have no effect on AZ VGCC levels, indicating this protein is likely not a rate-limiting regulator of VGCCs at AZs (Cunningham et al., 2022). RIMs and RBPs initially were compelling candidates for a slot protein because they both bind to VGCCs and are required (albeit redundantly at different synapses) for VGCC localization (Han et al., 2011; Kaeser et al., 2011; Liu et al., 2011; Graf et al., 2012; Jung et al., 2015; Oh et al., 2021). Additionally, RIM interacts stoichiometrically with Ca_v2 (Kaeser et al., 2011; Oh et al., 2021). However, in mammalian central synapses and *Drosophila* NMJs, loss of RIM and RBP binding to the C-terminal of VGCCs did not reduce channel AZ localization (Schneider et al., 2015; Lübbert et al., 2017; Ghelani et al., 2022). Indeed, several studies reported the lack of RIM and RBP interactions actually promotes channel stability at AZs, opposite to what would be expected for a protein functioning as a VGCC slot interactor (Schneider et al., 2015; Ghelani et al., 2022). Bassoon has also been proposed to contribute to defining $Ca_v2.1$ slots, as the Bassoon-RBP interaction recruits $Ca_v2.1$ (but not $Ca_v2.2$) channels to hippocampal synapses (Davydova et al., 2014). However, Bassoon does not appear to regulate VGCC abundance in all neurons (Altrock et al., 2003; Mukherjee et al., 2010). The α2δ subunit is another possible "slot" protein, as it plays a dosage-sensitive role in promoting AZ VGCC abundance. Overexpression of α2δ leads to increased VGCC levels at synapses, while heterozygous mutations in this subunit moderately decrease Ca_v2 levels at AZs (Hoppa et al., 2012; Cunningham et al., 2022). A role for α2δ as the slot factor would likely be in its capacity as a VGCC trafficking regulator, as *α2δ* mutants actually show increased Ca_v2 retention at synapses, arguing against AZ-localized α2δ as the regulator of slot number (Cunningham et al., 2022). Another possibility is the slot interaction is lipid-mediated, as cholesterol has been shown to restrict VGCC domain size at AZs in photoreceptors (Mercer et al., 2011). Deciphering which molecules and binding interactions are rate limiting for channel localization to AZs is an important goal but is complicated by functional redundancy and other potential compensatory mechanisms.

VGCCs are mobile within the AZ

Characterizing mobility of VGCCs within the AZ is a topic of interest, given positional coupling of VGCCs and docked SVs is a major determinant of P_r (Bucurenciu et al., 2008; Eggermann et al., 2011; Chen et al., 2015). VGCC mobility within the AZ could represent a fast method of P_r regulation by altering the channel's coupling distance to docked SVs. The idea that VGCCs occupy defined spots at the AZ arose from studies at the frog NMJ, where freeze fracture EM showed an array-like organization of particles, generating questions of whether these particles represent statically arranged VGCCs (Heuser et al., 1974; Pumplin et al., 1981; Cohen et al., 1991; Harlow et al., 2001). However modeling and experimental estimation of VGCC number at the frog NMJ suggests not all of these intramembrane particles can be channels, and Ca_v-immunogold EM reveal a less orderly, but non-randomly clustered, array of VGCCs (Luo et al., 2011; Holderith et al., 2012; Althof et al., 2015; Miki et al., 2017; Lübbert et al., 2019; Eguchi et al., 2022). The model of an orderly array of VGCCs is also at odds with more recent evidence from *in vivo* tracking of single VGCCs at synapses, showing that a fraction of AZ-resident VGCCs are mobile within a defined region of membrane, with low exit of channels from the AZ area (Mercer et al., 2011, 2012; Thoreson et al., 2013; Schneider et al., 2015; Figure 4; step 5).

At photoreceptor ribbon synapses of the salamander retina (populated with L-type VGCCs), quantum dots tagged to the extracellular α2δ-4 subunit of the channel revealed mobility within a defined ~0.18 μm^2 region of presynaptic membrane under the ribbon (Mercer et al., 2011, 2012). In addition to baseline VGCC movements, SV fusion briefly displaced VGCCs toward the outer rim of the membrane region (Mercer et al., 2011). In both photoreceptors and bipolar cells, actin restricts the size of the VGCC-mobile area, consistent with studies showing actin disruption promotes VGCC internalization (Cristofanilli et al., 2007; Mercer et al., 2011; Thoreson et al., 2013). Cholesterol levels also regulate VGCC mobility within photoreceptor synapses, as cholesterol depletion widened the VGCC-mobile area and reduced P_r without altering Ca^{2+} influx, suggesting mobility may be regulated to tune VGCC-SV coupling distances (Mercer et al., 2011, 2012). Additionally, movement of an open VGCC could spread Ca^{2+} over a larger area, reducing the effective peak Ca^{2+} concentration compared to influx from stabilized VGCCs. This "smearing" factor may be especially relevant at highly sensitive synapses in photoreceptors or bipolar cells where the opening of only one or a few VGCCs is sufficient to trigger SV fusion (Jarsky et al., 2010; Bartoletti et al., 2011; Kim et al., 2013). Though modeling suggests the expanded VGCC-domain size is sufficient to account for decreased release, the effect of cholesterol depletion on other proteins involved in SV fusion cannot be ruled out (Mercer et al., 2012). These tracking experiments provide insights into the mobility of VGCCs, but it is unclear if α2δ-4-QDot tagging is a robust proxy for VGCC α1 subunit localization and mobility, as α2δ subunits regulate synapse development independent of their canonical position as VGCC subunits and can localize to synaptic terminals independent of the VGCC (Kurshan et al., 2009; Dolphin, 2018; Held et al., 2020). Furthermore, studies in hippocampal cultured neurons suggest association of VGCC α1 and α2δ is dynamic, with α2δ showing more mobility than the VGCC α1 subunit (Voigt et al., 2016).

Direct single-particle tracking of VGCC α1 subunits in mammalian cultured neurons have circumvented this caveat. SptPALM imaging of cytoplasmic mEOS2-tagged $Ca_v2.1$ and $Ca_v2.2$ channels in hippocampal neurons revealed the population of VGCCs within clusters is comprised of a mobile fraction (~60% of channels) and a smaller immobile fraction

(Schneider et al., 2015). Channel mobility was largely confined within individual synapses, exhibited transient (~80 ms) confinement within synaptic nanodomains, and was similar for both $Ca_v2.1$ and $Ca_v2.2$, in contrast to mEOS2-tagged Syntaxin-1A (Schneider et al., 2015; Heck et al., 2019). Interestingly, reducing intracellular Ca^{2+} using BAPTA increased the fraction of immobile VGCCs, hinting at a possible mechanism to modulate VGCC mobility during plasticity (Schneider et al., 2015). In addition to regulation by Ca^{2+} buffering, VGCC mobility is activity-dependent, as blocking action potentials or postsynaptic glutamate receptors results in channel stabilization (Heck et al., 2019). Scaffold-channel interactions also regulate mobility; though surprisingly, the $Ca_v2.1$ splice variant lacking a C-terminal exon that encodes both RIM and RBP binding domains displays decreased mobility and supports more efficient SV release (Heck et al., 2019). These α1 tracking experiments in cell culture represent exciting steps forward in understanding channel mobility, as they reveal direct localization of the channel without relying on α2δ as a localization proxy. However, whether the lack of *in vivo* connections and a native synaptic environment abnormally influences channel mobility is currently unclear. Similar single-VGCC tracking experiments are currently being performed *in vivo* at *Drosophila* NMJs, where VGCCs appear to undergo high intra-AZ mobility as well (Ghelani et al., 2022). In addition, insights into longer-term VGCC mobility at *Drosophila* NMJs using photoconvertible Cac channels reveal they do not appear to laterally diffuse between neighboring AZs over multiple days, suggesting low inter-AZ movement despite high intra-AZ mobility (Cunningham et al., 2022).

VGCC internalization from AZs

The lifetime of surface expression for transmembrane proteins varies widely and is regulated in part by re-internalization through endocytosis (Figure 4; step 6). Most endocytosis is through a relatively slow Clathrin-mediated process, with adaptor proteins concentrating cargo and recruiting Clathrin, which assembles to deform the membrane into a pit. Subsequently, a burst of Actin to budding endocytic vesicles and membrane pinching by the GTPase Dynamin completes the endocytic process (Kaksonen and Roux, 2018). Faster Clathrin-independent modes of endocytosis have also been described at synapses. Bulk and ultrafast endocytosis are thought to quickly retrieve synaptic membrane after SV fusion (Watanabe and Boucrot, 2017). In addition, fast Endophilin mediated endocytosis (FEME) can be initiated to internalize specific membrane proteins, including some G Protein-Coupled Receptors (GPCRs; Moo et al., 2021). GPCRs are inhibited by their own agonist-stimulated endocytosis, a process which is canonically initiated by the binding of endocytic adaptor proteins of the Arrestin family, but that can also proceed through non-canonical pathways (Moo et al., 2021; von Zastrow and Sorkin, 2021). Receptor Tyrosine Kinases (RTKs) are also endocytosed after ligand binding, with internalization initiated either though RTK ubiquitination or binding to Clathrin-adapter proteins (von Zastrow and Sorkin, 2021). AMPA Receptors are glutamate-gated cation channels that mediate most excitatory neurotransmission in the mammalian CNS and their internalization regulates synaptic strength during several forms of synaptic plasticity (Citri and Malenka, 2008; Hastings and Man, 2018). AMPA Receptors can dissociate from scaffolds within the postsynaptic density and move into endocytic zones where they associate with Clathrin adaptor proteins and become internalized. In contrast to GPCRs, RTKs, and AMPA receptors, little is known about the role of internalization in VGCC regulation at AZs. How big of a role does VGCC internalization play in regulating synaptic strength? What regulates VGCC internalization and what molecular pathways facilitate this process? Does channel endocytosis occur within AZs or elsewhere on the presynaptic membrane?

Some evidence for GPCR-regulated VGCC internalization has come from studies of $Ca_v2.2$ channels in cultured neurons and DRG neurons involved in pain signaling (Bourinet et al., 2014). In this circuit, the GPCR opioid receptor (ORL1) forms a complex with $Ca_v2.2$ channels and its activation *via* the agonist nociceptin results in ORL1/$Ca_v2.2$ complex internalization (Beedle et al., 2004; Altier et al., 2006). This internalization can be directly visualized using GFP-tagged $Ca_v2.2$ α1 subunits and red-tagged ORL receptors. Upon ORL activation, $Ca_v2.2$ and ORL exclusively colocalize in intracellular puncta that label with a lysosomal marker (Altier et al., 2006). In acutely dissociated DRG neurons, $Ca_v2.2$ channels are internalized following nociceptin exposure, leading to a decrease in $Ca_v2.2$-mediated Ca^{2+} influx (Altier et al., 2006). Though lysosome marker colocalization suggests internalized channels may be degraded, the fate of these channels is unknown. Agonist washout results in loss of intracellular VGCCs after several hours, but whether channels were returned to the surface or targeted for degradation is unclear (Altier et al., 2006). Dopamine (DA) receptors are another family of GPCRs that regulate VGCCs in the mammalian CNS, and DA receptors can promote internalization of $Ca_v2.2$ through direct protein–protein interactions (Kisilevsky et al., 2008; Kisilevsky and Zamponi, 2008). Along with GPCR regulation, the Actin cytoskeleton plays a role in regulating presynaptic VGCC internalization in some systems (Furukawa et al., 1997; Cristofanilli et al., 2007; Mizuno et al., 2010; Tseng et al., 2017).

Studies of molecular mechanisms of VGCC internalization in cell culture is facilitated by molecular and imaging access, but *in vivo* experiments are required to understand the timescales and patterns of VGCC internalization at native synapses. Do AZ-localized VGCCs become internalized through similar pathways? How long do VGCCs remain at the presynaptic membrane and how is their internalization regulated? Animal-wide isotopic labeling has been employed as a high-throughput strategy for measuring protein half-lives *in vivo* (Price et al., 2010; Fornasiero et al., 2018; Heo et al., 2018). This approach can measure degradation rates of newly synthesized proteins across the entire proteome, but has limited spatial resolution to measure turnover in specific compartments or individual neuronal populations. Given degradation of VGCCs can occur in the biosynthetic pathway before channels reach the synapse, whole-brain turnover measurements may not accurately reflect rates of AZ-localized VGCCs dynamics. Despite these drawbacks, it is worth noting that VGCCs display a half-life of around 8 days when assayed by isotopic labeling (Fornasiero et al., 2018).

Studies of AZ-resident VGCC half-life and turnover have also been performed at the *Drosophila* NMJ, a synapse with hundreds of AZs that are individually resolvable by conventional light microscopy in intact animals, allowing multi-day experiments using intravital imaging (Figures 2B,C). Red-to-green photoconversion of endogenously Maple-tagged Cac (the sole VGCC mediating synaptic transmission in flies) allowed measurements of Cac removal from AZs over a multi-day period. On average, 30% of photoconverted Cac signal intensity was lost from AZs over 4 days, indicating turnover plays an important role in regulating the abundance of the channel at AZs (Figures 2D–G;

Cunningham et al., 2022). This 30% loss over 4 days predicts a half-life of about 8 days, consistent with isotopic labeling measurements of VGCC stability (Fornasiero et al., 2018; Cunningham et al., 2022). Measurements of new Cac delivery at individual AZs indicates turnover contributes to a leveling-off of Cac abundance at mature AZs. Furthermore, Cac loss from AZs is predicted to occur primarily through re-internalization of the channel, as lateral transfer of Cac channels was not observed (Cunningham et al., 2022). In mutants with either reduced levels of α2δ or reduced levels of the α1 subunit, turnover was reduced, indicating new channel delivery regulates channel turnover at this synapse rather than a fixed VGCC lifespan (Cunningham et al., 2022).

Presynaptic VGCCs: Beyond evoked neurotransmission

Aside from the canonical role of presynaptic VGCCs as mediators of evoked neurotransmission, non-AZ resident VGCCs can regulate other Ca^{2+}-dependent aspects of presynaptic function, including SV endocytosis and presynaptic plasticity. At presynaptic terminals, Ca^{2+}-dependent endocytosis immediately follows SV fusion (Hosoi et al., 2009; Wu et al., 2009, 2014). Temporal coordination between exo- and endocytosis ensures prompt recycling of SVs after fusion, and maintains presynaptic membrane homeostasis (for a detailed review of presynaptic exo-endocytic coupling, see Wu et al., 2014; Maritzen and Haucke, 2018). Ca^{2+} influx through VGCCs has been proposed to mediate this coupling (Wu et al., 2009, 2014; Xue et al., 2012; Krick et al., 2021). In addition to SV fusion and endocytosis, Ca^{2+} signaling through VGCCs can contribute to short term plasticity without altering baseline P_r, reflecting functional separation between VGCC subtypes within the presynaptic membrane (Jensen and Mody, 2001; Dietrich et al., 2003; Krick et al., 2021).

Given multiple processes—including neurotransmission, endocytosis, and plasticity—are controlled by VGCC-dependent Ca^{2+} signaling within a relatively small area, how are these Ca^{2+} signals separated to avoid crosstalk? Precise positioning of different VGCC subtypes within subdomains of the presynaptic membrane is one mechanism by which synapses can reduce crosstalk. This spatial separation of distinct VGCC populations in the presynaptic terminal is illustrated at the *Drosophila* NMJ, where the sole Ca_v2 channel (Cac) localizes to AZs and mediates neurotransmission, while the Ca_v1 channel (Dmca1D) localizes to non-AZ domains within the presynaptic membrane and regulates Ca^{2+}-dependent endocytosis and short-term plasticity (Krick et al., 2021). In addition to the distinct localizations of these channel types, cytosolic Ca^{2+} buffers and active extrusion of Ca^{2+} by the PMCA pump further reduces crosstalk between Ca_v1 and Ca_v2 signaling (Krick et al., 2021). Similar to AZ-resident VGCCs, the mechanisms that regulate the abundance and subcellular localization of other VGCC populations within the presynaptic membrane are unknown.

Modulation of VGCC abundance during plasticity: Insights from *Drosophila*

Voltage-gated Ca^{2+} channels are key regulators of presynaptic P_r, placing them in a prime position to be targeted by plasticity pathways that modulate synaptic strength (Augustine et al., 1985; Borst and Sakmann, 1996; Wang et al., 2008; Bartoletti et al., 2011; Ariel et al., 2012; Sheng et al., 2012; Newman et al., 2022). Indeed, acute modulation of VGCC activation, inactivation, and conductance have all been shown to contribute to various presynaptic plasticity pathways (Nanou and Catterall, 2018). More recently, studies at the *Drosophila* NMJ indicate plastic regulation of channel abundance and mobility at the presynaptic membrane can also occur. Due to robust genetic, imaging, and electrophysiological approaches that enable studies of individual AZs *in vivo*, this model has emerged as a key system for characterizing how presynaptic plasticity impinges on the abundance and mobility of AZ components. Indeed, changes in the abundance and organization of VGCCs and the AZ scaffold have been reported at the NMJ during expression of acute and chronic forms of plasticity.

When postsynaptic Glutamate Receptors are blocked acutely with a toxin or chronically *via* genetic mutations at *Drosophila* NMJs, the decrease in postsynaptic responsiveness to neurotransmitter (quantal size) triggers a compensatory upregulation of presynaptic P_r. Increased SV fusion precisely offsets the reduction in quantal size, homeostatically preserving overall synaptic strength. This homeostatic synaptic potentiation (HSP) can happen strikingly fast, occurring on the scale of minutes after application of a Glutamate Receptor toxin (Frank et al., 2006, 2009; Müller and Davis, 2012; Frank, 2014). The Cac channel is mechanistically implicated in HSP plasticity. Ca^{2+} imaging directly demonstrates an increase in presynaptic Ca^{2+} influx during HSP, and hypomorphic mutations in *cac* block potentiation of Ca^{2+} influx and homeostatic potentiation (Frank et al., 2006; Müller and Davis, 2012). Additionally, the extracellular Cac subunit α2δ is required for HSP, independent of its effect on baseline Ca^{2+} influx (Wang et al., 2016). An opposing form of presynaptic homeostatic plasticity is homeostatic synaptic depression (HSD). When quantal size is chronically increased through overexpression of the SV glutamate transporter VGlut, HSD compensates by reducing presynaptic P_r. Imaging of Ca^{2+} influx and AZ Cac-GFP abundance demonstrates this form of plasticity also targets the Cac channel by decreasing its abundance at AZs (Gaviño et al., 2015). Together these findings suggest Ca^{2+} influx through VGCCs is modulated bidirectionally to influence P_r during multiple forms of presynaptic plasticity.

While initial evidence for Cac involvement in HSP did not resolve whether channel properties or abundance were altered to trigger increased Ca^{2+} influx, several studies suggest AZ Cac abundance may increase during this form of potentiation (Gratz et al., 2019; Ghelani et al., 2022). Similarly, BRP puncta observed in AZ rings increased in number during HSP (Hong et al., 2020). Although these studies suggest elevated levels of BRP and Cac, studies employing STORM imaging indicate the increased fluorescent intensity is secondary to compaction of AZ material that occurs during plasticity rather than increases in protein content across AZs (Mrestani et al., 2021). Work in the *Drosophila* CNS indicates Cac transcription may also be a target for certain forms of presynaptic potentiation. In the *Drosophila* CNS, Kenyon Cell neurons form boutons along compartmentalized regions of the mushroom body to drive associative learning. Monitoring of presynaptic Ca^{2+} during behavior reveals compartment-specific modulation of Ca^{2+} influx along Kenyon Cell axons during learning that is mediated by neuromodulatory neuron dopamine release and presumed GPCR-mediated silencing of VGCC function (Bilz et al.,

2020). Although reducing VGCC biosynthesis by modest levels does not alter baseline transmission at these synapses, the same manipulation impairs presynaptic potentiation, indicating Cac biosynthesis becomes rate-limiting during certain forms of presynaptic plasticity (Stahl et al., 2022). Together, these studies suggest VGCC abundance, location, and mobility at AZs may represent important targets for fine-tuning of presynaptic output.

Conclusion and future directions

Pathways regulating the surface abundance of presynaptic VGCCs, including progression through the biosynthetic pathway, transport to the synapse, stabilization and mobility at AZs, and turnover by endocytosis, have emerged as important mechanisms to set baseline synaptic strength and as potential targets to change output during plasticity. Despite the importance of VGCC dynamics and regulation, many questions remain unsolved. In particular, identifying which VGCC-regulatory components are rate-limiting in setting channel abundance at AZs will provide insights into the fine-tuning and regulation of channel surface expression. Additionally, the precise mechanisms and timescales of channel delivery and turnover at individual presynaptic AZs are still unclear, precluding a clear understanding of how delivery and recycling modulate synaptic development and presynaptic strength in growing circuits.

Author contributions

All authors listed have made a substantial, direct, and intellectual contribution to the work and approved it for publication.

Funding

The authors' work has been funded by NIH grants NS40296, NS117588, and MH104536 and the JPB Foundation.

Conflict of interest

The authors declare that the research was conducted in the absence of any commercial or financial relationships that could be construed as a potential conflict of interest.

Publisher's note

References

Ackermann, F., Waites, C. L., and Garner, C. C. (2015). Presynaptic active zones in invertebrates and vertebrates. *EMBO Rep.* 16, 923–938. doi: 10.15252/embr.201540434

Acuna, C., Liu, X., Gonzalez, A., and Südhof, T. C. (2015). RIM-BPs mediate tight coupling of action potentials to Ca(2+)-triggered neurotransmitter release. *Neuron* 87, 1234–1247. doi: 10.1016/j.neuron.2015.08.027

Acuna, C., Liu, X., and Südhof, T. C. (2016). How to make an active zone: unexpected universal functional redundancy between RIMs and RIM-BPs. *Neuron* 91, 792–807. doi: 10.1016/j.neuron.2016.07.042

Ahmari, S. E., Buchanan, J., and Smith, S. J. (2000). Assembly of presynaptic active zones from cytoplasmic transport packets. *Nat. Neurosci.* 3, 445–451. doi: 10.1038/74814

Akbergenova, Y., Cunningham, K. L., Zhang, Y. V., Weiss, S., and Littleton, J. T. (2018). Characterization of developmental and molecular factors underlying release heterogeneity at drosophila synapses. *elife* 7. doi: 10.7554/eLife.38268

Althof, D., Baehrens, D., Watanabe, M., Suzuki, N., Fakler, B., and Kulik, Á. (2015). Inhibitory and excitatory axon terminals share a common nano-architecture of their Cav2.1 (P/Q-type) Ca(2+) channels. *Front. Cell. Neurosci.* 9:315. doi: 10.3389/fncel.2015.00315

Altier, C., Garcia-Caballero, A., Simms, B., You, H., Chen, L., Walcher, J., et al. (2011). The Cavβ subunit prevents RFP2-mediated ubiquitination and proteasomal degradation of L-type channels. *Nat. Neurosci.* 14, 173–180. doi: 10.1038/nn.2712

Altier, C., Khosravani, H., Evans, R. M., Hameed, S., Peloquin, J. B., Vartian, B. A., et al. (2006). ORL1 receptor-mediated internalization of N-type calcium channels. *Nat. Neurosci.* 9, 31–40. doi: 10.1038/nn1605

Altrock, W. D., tom Dieck, S., Sokolov, M., Meyer, A. C., Sigler, A., Brakebusch, C., et al. (2003). Functional inactivation of a fraction of excitatory synapses in mice deficient for the active zone protein bassoon. *Neuron* 37, 787–800. doi: 10.1016/s0896-6273(03)00088-6

Ariel, P., Hoppa, M. B., and Ryan, T. A. (2012). Intrinsic variability in Pv, RRP size, Ca(2+) channel repertoire, and presynaptic potentiation in individual synaptic boutons. *Front. Synap. Neurosci.* 4:9. doi: 10.3389/fnsyn.2012.00009

Atwood, H. L., and Karunanithi, S. (2002). Diversification of synaptic strength: presynaptic elements. *Nat. Rev. Neurosci.* 3, 497–516. doi: 10.1038/nrn876

Augustine, G. J., Charlton, M. P., and Smith, S. J. (1985). Calcium entry and transmitter release at voltage-clamped nerve terminals of squid. *J. Physiol. Lond.* 367, 163–181. doi: 10.1113/jphysiol.1985.sp015819

Ball, S. L., Powers, P. A., Shin, H. S., Morgans, C. W., Peachey, N. S., and Gregg, R. G. (2002). Role of the β2 subunit of voltage-dependent calcium channels in the retinal outer plexiform layer. *Invest. Ophthalmol. Vis. Sci.* 43, 1595–1603.

Bartoletti, T. M., Jackman, S. L., Babai, N., Mercer, A. J., Kramer, R. H., and Thoreson, W. B. (2011). Release from the cone ribbon synapse under bright light conditions can be controlled by the opening of only a few Ca(2+) channels. *J. Neurophysiol.* 106, 2922–2935. doi: 10.1152/jn.00634.2011

Beedle, A. M., McRory, J. E., Poirot, O., Doering, C. J., Altier, C., Barrere, C., et al. (2004). Agonist-independent modulation of N-type calcium channels by ORL1 receptors. *Nat. Neurosci.* 7, 118–125. doi: 10.1038/nn1180

Berridge, M. J., Bootman, M. D., and Roderick, H. L. (2003). Calcium signalling: dynamics, homeostasis and remodelling. *Nat. Rev. Mol. Cell Biol.* 4, 517–529. doi: 10.1038/nrm1155

Berrow, N. S., Campbell, V., Fitzgerald, E. M., Brickley, K., and Dolphin, A. C. (1995). Antisense depletion of beta-subunits modulates the biophysical and pharmacological properties of neuronal calcium channels. *J. Physiol. Lond.* 482, 481–491. doi: 10.1113/jphysiol.1995.sp020534

Betz, A., Thakur, P., Junge, H. J., Ashery, U., Rhee, J. S., Scheuss, V., et al. (2001). Functional interaction of the active zone proteins Munc13-1 and RIM1 in synaptic vesicle priming. *Neuron* 30, 183–196. doi: 10.1016/s0896-6273(01)00272-0

Billings, S. E., Clarke, G. L., and Nishimune, H. (2012). ELKS1 and Ca(2+) channel subunit β4 interact and colocalize at cerebellar synapses. *Neuroreport* 23, 49–54. doi: 10.1097/WNR.0b013e32834e7deb

Bilz, F., Geurten, B. R. H., Hancock, C. E., Widmann, A., and Fiala, A. (2020). Visualization of a distributed synaptic memory code in the drosophila brain. *Neuron* 106, 963–976.e4. doi: 10.1016/j.neuron.2020.03.010

Böhme, M. A., Beis, C., Reddy-Alla, S., Reynolds, E., Mampell, M. M., Grasskamp, A. T., et al. (2016). Active zone scaffolds differentially accumulate Unc13 isoforms to tune Ca(2+) channel-vesicle coupling. *Nat. Neurosci.* 19, 1311–1320. doi: 10.1038/nn.4364

Borst, J. G., and Sakmann, B. (1996). Calcium influx and transmitter release in a fast CNS synapse. *Nature* 383, 431–434. doi: 10.1038/383431a0

Bourinet, E., Altier, C., Hildebrand, M. E., Trang, T., Salter, M. W., and Zamponi, G. W. (2014). Calcium-permeable ion channels in pain signaling. *Physiol. Rev.* 94, 81–140. doi: 10.1152/physrev.00023.2013

Brice, N. L., Berrow, N. S., Campbell, V., Page, K. M., Brickley, K., Tedder, I., et al. (1997). Importance of the different beta subunits in the membrane expression of the alpha1A and alpha2 calcium channel subunits: studies using a depolarization-sensitive alpha1A antibody. *Eur. J. Neurosci.* 9, 749–759. doi: 10.1111/j.1460-9568.1997.tb01423.x

Bruckner, J. J., Zhan, H., Gratz, S. J., Rao, M., Ukken, F., Zilberg, G., et al. (2017). Fife organizes synaptic vesicles and calcium channels for high-probability neurotransmitter release. *J. Cell Biol.* 216, 231–246. doi: 10.1083/jcb.201601098

Bucurenciu, I., Kulik, A., Schwaller, B., Frotscher, M., and Jonas, P. (2008). Nanodomain coupling between Ca2+ channels and Ca2+ sensors promotes fast and efficient transmitter release at a cortical GABAergic synapse. *Neuron* 57, 536–545. doi: 10.1016/j.neuron.2007.12.026

Buraei, Z., and Yang, J. (2010). The ß subunit of voltage-gated Ca2+ channels. *Physiol. Rev.* 90, 1461–1506. doi: 10.1152/physrev.00057.2009

Burgess, D. L., Jones, J. M., Meisler, M. H., and Noebels, J. L. (1997). Mutation of the Ca2+ channel beta subunit gene Cchb4 is associated with ataxia and seizures in the lethargic (lh) mouse. *Cells* 88, 385–392. doi: 10.1016/s0092-8674(00)81877-2

Bury, L. A. D., and Sabo, S. L. (2011). Coordinated trafficking of synaptic vesicle and active zone proteins prior to synapse formation. *Neural Dev.* 6:24. doi: 10.1186/1749-8104-6-24

Cai, Q., Pan, P.-Y., and Sheng, Z.-H. (2007). Syntabulin-kinesin-1 family member 5B-mediated axonal transport contributes to activity-dependent presynaptic assembly. *J. Neurosci.* 27, 7284–7296. doi: 10.1523/JNEUROSCI.0731-07.2007

Cantí, C., Davies, A., Berrow, N. S., Butcher, A. J., Page, K. M., and Dolphin, A. C. (2001). Evidence for two concentration-dependent processes for beta-subunit effects on alpha1B calcium channels. *Biophys. J.* 81, 1439–1451. doi: 10.1016/S0006-3495(01)75799-2

Cao, Y.-Q., Piedras-Rentería, E. S., Smith, G. B., Chen, G., Harata, N. C., and Tsien, R. W. (2004). Presynaptic Ca2+ channels compete for channel type-preferring slots in altered neurotransmission arising from Ca2+ channelopathy. *Neuron* 43, 387–400. doi: 10.1016/j.neuron.2004.07.014

Cao, Y.-Q., and Tsien, R. W. (2010). Different relationship of N- and P/Q-type Ca2+ channels to channel-interacting slots in controlling neurotransmission at cultured hippocampal synapses. *J. Neurosci.* 30, 4536–4546. doi: 10.1523/JNEUROSCI.5161-09.2010

Cases-Langhoff, C., Voss, B., Garner, A. M., Appeltauer, U., Takei, K., Kindler, S., et al. (1996). Piccolo, a novel 420 kDa protein associated with the presynaptic cytomatrix. *Eur. J. Cell Biol.* 69, 214–223. PMID: 8900486

Cassidy, J. S., Ferron, L., Kadurin, I., Pratt, W. S., and Dolphin, A. C. (2014). Functional exofacially tagged N-type calcium channels elucidate the interaction with auxiliary α2δ-1 subunits. *Proc. Natl. Acad. Sci. U. S. A.* 111, 8979–8984. doi: 10.1073/pnas.1403731111

Catterall, W. A., and Few, A. P. (2008). Calcium channel regulation and presynaptic plasticity. *Neuron* 59, 882–901. doi: 10.1016/j.neuron.2008.09.005

Catterall, W. A., Lenaeus, M. J., and Gamal El-Din, T. M. (2020). Structure and pharmacology of voltage-gated sodium and calcium channels. *Annu. Rev. Pharmacol. Toxicol.* 60, 133–154. doi: 10.1146/annurev-pharmtox-010818-021757

Chen, J., Billings, S. E., and Nishimune, H. (2011). Calcium channels link the muscle-derived synapse organizer laminin β2 to bassoon and CAST/Erc2 to organize presynaptic active zones. *J. Neurosci.* 31, 512–525. doi: 10.1523/JNEUROSCI.3771-10.2011

Chen, Z., Das, B., Nakamura, Y., DiGregorio, D. A., and Young, S. M. (2015). Ca2+ channel to synaptic vesicle distance accounts for the readily releasable pool kinetics at a functionally mature auditory synapse. *J. Neurosci.* 35, 2083–2100. doi: 10.1523/JNEUROSCI.2753-14.2015

Chen, Y.-H., Li, M.-H., Zhang, Y., He, L.-L., Yamada, Y., Fitzmaurice, A., et al. (2004). Structural basis of the alpha1-beta subunit interaction of voltage-gated Ca2+ channels. *Nature* 429, 675–680. doi: 10.1038/nature02641

Citri, A., and Malenka, R. C. (2008). Synaptic plasticity: multiple forms, functions, and mechanisms. *Neuropsychopharmacology* 33, 18–41. doi: 10.1038/sj.npp.1301559

Cohen, M. W., Jones, O. T., and Angelides, K. J. (1991). Distribution of Ca2+ channels on frog motor nerve terminals revealed by fluorescent omega-conotoxin. *J. Neurosci.* 11, 1032–1039. doi: 10.1523/JNEUROSCI.11-04-01032.1991

Coppola, T., Magnin-Luthi, S., Perret-Menoud, V., Gattesco, S., Schiavo, G., and Regazzi, R. (2001). Direct interaction of the Rab3 effector RIM with Ca2+ channels, SNAP-25, and synaptotagmin. *J. Biol. Chem.* 276, 32756–32762. doi: 10.1074/jbc.M100929200

Cristofanilli, M., Mizuno, F., and Akopian, A. (2007). Disruption of actin cytoskeleton causes internalization of Cav1.3 (alpha 1D) L-type calcium channels in salamander retinal neurons. *Mol. Vis.* 13, 1496–1507.

Cunningham, K. L., Sauvola, C. W., Tavana, S., and Littleton, J. T. (2022). Regulation of presynaptic Ca2+ channel abundance at active zones through a balance of delivery and turnover. *elife* 11:e78648. doi: 10.7554/eLife.78648

Davies, A., Kadurin, I., Alvarez-Laviada, A., Douglas, L., Nieto-Rostro, M., Bauer, C. S., et al. (2010). The α2δ subunits of voltage-gated calcium channels form GPI-anchored proteins, a posttranslational modification essential for function. *Proc. Natl. Acad. Sci.* 107, 1654–1659. doi: 10.1073/pnas.0908735107

Davydova, D., Marini, C., King, C., Klueva, J., Bischof, F., Romorini, S., et al. (2014). Bassoon specifically controls presynaptic P/Q-type Ca(2+) channels via RIM-binding protein. *Neuron* 82, 181–194. doi: 10.1016/j.neuron.2014.02.012

De Jongh, K. S., Warner, C., and Catterall, W. A. (1990). Subunits of purified calcium channels. Alpha 2 and delta are encoded by the same gene. *J. Biol. Chem.* 265, 14738–14741. doi: 10.1016/S0021-9258(18)77174-3

De Pace, R., Britt, D. J., Mercurio, J., Foster, A. M., Djavaherian, L., Hoffmann, V., et al. (2020). Synaptic vesicle precursors and lysosomes are transported by different mechanisms in the axon of mammalian neurons. *Cell reports*. 31:107775.

Deken, S. L., Vincent, R., Hadwiger, G., Liu, Q., Wang, Z.-W., and Nonet, M. L. (2005). Redundant localization mechanisms of RIM and ELKS in Caenorhabditis elegans. *J. Neurosci.* 25, 5975–5983. doi: 10.1523/JNEUROSCI.0804-05.2005

DiAntonio, A., and Schwarz, T. L. (1994). The effect on synaptic physiology of synaptotagmin mutations in drosophila. *Neuron* 12, 909–920. doi: 10.1016/0896-6273(94)90342-5

Dick, O., tom Dieck, S., Altrock, W. D., Ammermüller, J., Weiler, R., Garner, C. C., et al. (2003). The presynaptic active zone protein bassoon is essential for photoreceptor ribbon synapse formation in the retina. *Neuron* 37, 775–786. doi: 10.1016/s0896-6273(03)00086-2

Dickman, D. K., Kurshan, P. T., and Schwarz, T. L. (2008). Mutations in a drosophila alpha2delta voltage-gated calcium channel subunit reveal a crucial synaptic function. *J. Neurosci.* 28, 31–38. doi: 10.1523/JNEUROSCI.4498-07.2008

Dietrich, D., Kirschstein, T., Kukley, M., Pereverzev, A., von der Brelie, C., Schneider, T., et al. (2003). Functional specialization of presynaptic Cav2. 3 Ca2+ channels. *Neuron* 39, 483–496. doi: 10.1016/S0896-6273(03)00430-6

Dolphin, A. C. (2016). Voltage-gated calcium channels and their auxiliary subunits: physiology and pathophysiology and pharmacology. *J. Physiol. Lond.* 594, 5369–5390. doi: 10.1113/JP272262

Dolphin, A. C. (2018). Voltage-gated calcium channel α 2δ subunits: an assessment of proposed novel roles. [version 1; peer review: 2 approved]. *F1000Res* 7:1830. doi: 10.12688/f1000research.16104.1

Dolphin, A. C., and Lee, A. (2020). Presynaptic calcium channels: specialized control of synaptic neurotransmitter release. *Nat. Rev. Neurosci.* 21, 213–229. doi: 10.1038/s41583-020-0278-2

Dong, W., Radulovic, T., Goral, R. O., Thomas, C., Suarez Montesinos, M., Guerrero-Given, D., et al. (2018). CAST/ELKS proteins control voltage-gated Ca2+ channel density and synaptic release probability at a mammalian central synapse. *Cell Rep.* 24, 284–293.e6. doi: 10.1016/j.celrep.2018.06.024

Dresbach, T., Torres, V., Wittenmayer, N., Altrock, W. D., Zamorano, P., Zuschratter, W., et al. (2006). Assembly of active zone precursor vesicles: obligatory trafficking of presynaptic cytomatrix proteins bassoon and piccolo via a trans-Golgi compartment. *J. Biol. Chem.* 281, 6038–6047. doi: 10.1074/jbc.M508784200

Eberl, D. F., Ren, D., Feng, G., Lorenz, L. J., Van Vactor, D., and Hall, L. M. (1998). Genetic and developmental characterization of Dmca1D, a calcium channel alpha1 subunit gene in Drosophila melanogaster. *Genetics* 148, 1159–1169. doi: 10.1093/genetics/148.3.1159

Eggermann, E., Bucurenciu, I., Goswami, S. P., and Jonas, P. (2011). Nanodomain coupling between Ca^{2+} channels and sensors of exocytosis at fast mammalian synapses. *Nat. Rev. Neurosci.* 13, 7–21. doi: 10.1038/nrn3125

Eguchi, K., Montanaro, J., Le Monnier, E., and Shigemoto, R. (2022). The number and distinct clustering patterns of voltage-gated calcium channels in nerve terminals. *Front. Neuroanat.* 16:846615. doi: 10.3389/fnana.2022.846615

Eroglu, C., Allen, N. J., Susman, M. W., O'Rourke, N. A., Park, C. Y., Ozkan, E., et al. (2009). Gabapentin receptor alpha2delta-1 is a neuronal thrombospondin receptor responsible for excitatory CNS synaptogenesis. *Cells* 139, 380–392. doi: 10.1016/j.cell.2009.09.025

Fairless, R., Masius, H., Rohlmann, A., Heupel, K., Ahmad, M., Reissner, C., et al. (2008). Polarized targeting of neurexins to synapses is regulated by their C-terminal sequences. *J. Neurosci.* 28, 12969–12981. doi: 10.1523/JNEUROSCI.5294-07.2008

Fenster, S. D., Chung, W. J., Zhai, R., Cases-Langhoff, C., Voss, B., Garner, A. M., et al. (2000). Piccolo, a presynaptic zinc finger protein structurally related to bassoon. *Neuron* 25, 203–214. doi: 10.1016/s0896-6273(00)80883-1

Fornasiero, E. F., Mandad, S., Wildhagen, H., Alevra, M., Rammner, B., Keihani, S., et al. (2018). Precisely measured protein lifetimes in the mouse brain reveal differences across tissues and subcellular fractions. *Nat. Commun.* 9:4230. doi: 10.1038/s41467-018-06519-0

Fouquet, W., Owald, D., Wichmann, C., Mertel, S., Depner, H., Dyba, M., et al. (2009). Maturation of active zone assembly by drosophila Bruchpilot. *J. Cell Biol.* 186, 129–145. doi: 10.1083/jcb.200812150

Frank, C. A. (2014). How voltage-gated calcium channels gate forms of homeostatic synaptic plasticity. *Front. Cell. Neurosci.* 8:40. doi: 10.3389/fncel.2014.00040

Frank, C. A., Kennedy, M. J., Goold, C. P., Marek, K. W., and Davis, G. W. (2006). Mechanisms underlying the rapid induction and sustained expression of synaptic homeostasis. *Neuron* 52, 663–677. doi: 10.1016/j.neuron.2006.09.029

Frank, C. A., Pielage, J., and Davis, G. W. (2009). A presynaptic homeostatic signaling system composed of the Eph receptor, ephexin, Cdc42, and CaV2.1 calcium channels. *Neuron* 61, 556–569. doi: 10.1016/j.neuron.2008.12.028

Frank, T., Rutherford, M. A., Strenzke, N., Neef, A., Pangršič, T., Khimich, D., et al. (2010). Bassoon and the synaptic ribbon organize Ca^{2}+ channels and vesicles to add release sites and promote refilling. *Neuron* 68, 724–738. doi: 10.1016/j.neuron.2010.10.027

Frøkjær-Jensen, C., Kindt, K. S., Kerr, R. A., Suzuki, H., Melnik-Martinez, K., Gerstbreih, B., et al. (2006). Effects of voltage-gated calcium channel subunit genes on calcium influx in cultured C. elegans mechanosensory neurons. *J. Neurobiol.* 66, 1125–1139. doi: 10.1002/neu.20261

Furukawa, K., Fu, W., Li, Y., Witke, W., Kwiatkowski, D. J., and Mattson, M. P. (1997). The actin-severing protein gelsolin modulates calcium channel and NMDA receptor activities and vulnerability to excitotoxicity in hippocampal neurons. *J. Neurosci.* 17, 8178–8186. doi: 10.1523/JNEUROSCI.17-21-08178.1997

Gandini, M. A., and Zamponi, G. W. (2022). Voltage-gated calcium channel nanodomains: molecular composition and function. *FEBS J.* 289, 614–633. doi: 10.1111/febs.15759

Gaviño, M. A., Ford, K. J., Archila, S., and Davis, G. W. (2015). Homeostatic synaptic depression is achieved through a regulated decrease in presynaptic calcium channel abundance. *elife* 4:e05473. doi: 10.7554/eLife.05473

Gee, N. S., Brown, J. P., Dissanayake, V. U., Offord, J., Thurlow, R., and Woodruff, G. N. (1996). The novel anticonvulsant drug, gabapentin (Neurontin), binds to the alpha2delta subunit of a calcium channel. *J. Biol. Chem.* 271, 5768–5776. doi: 10.1074/jbc.271.10.5768

Ghelani, T, Escher, M, Thomas, U, Esch, K, Lützkendorf, J, Depner, H, et al. (2022). An active zone state switch concentrates and immobilizes voltage-gated Ca2+ channels to promote long-term plasticity. Research Square [Preprint]. doi: 10.21203/rs.3.rs-1292687/v1

Ghelani, T., and Sigrist, S. J. (2018). Coupling the structural and functional assembly of synaptic release sites. *Front. Neuroanat.* 12:81. doi: 10.3389/fnana.2018.00081

Gho, M., McDonald, K., Ganetzky, B., and Saxton, W. M. (1992). Effects of kinesin mutations on neuronal functions. *Science* 258, 313–316. doi: 10.1126/science.1384131

Gindhart, J. G., Desai, C. J., Beushausen, S., Zinn, K., and Goldstein, L. S. (1998). Kinesin light chains are essential for axonal transport in drosophila. *J. Cell Biol.* 141, 443–454. doi: 10.1083/jcb.141.2.443

Goldstein, A. Y. N., Wang, X., and Schwarz, T. L. (2008). Axonal transport and the delivery of pre-synaptic components. *Curr. Opin. Neurobiol.* 18, 495–503. doi: 10.1016/j.conb.2008.10.003

Graf, E. R., Daniels, R. W., Burgess, R. W., Schwarz, T. L., and DiAntonio, A. (2009). Rab3 dynamically controls protein composition at active zones. *Neuron* 64, 663–677. doi: 10.1016/j.neuron.2009.11.002

Graf, E. R., Valakh, V., Wright, C. M., Wu, C., Liu, Z., Zhang, Y. Q., et al. (2012). RIM promotes calcium channel accumulation at active zones of the drosophila neuromuscular junction. *J. Neurosci.* 32, 16586–16596. doi: 10.1523/JNEUROSCI.0965-12.2012

Gratz, S. J., Goel, P., Bruckner, J. J., Hernandez, R. X., Khateeb, K., Macleod, G. T., et al. (2019). Endogenous tagging reveals differential regulation of Ca2+ channels at single active zones during presynaptic homeostatic potentiation and depression. *J. Neurosci.* 39, 2416–2429. doi: 10.1523/JNEUROSCI.3068-18.2019

Gregg, R. G., Messing, A., Strube, C., Beurg, M., Moss, R., Behan, M., et al. (1996). Absence of the beta subunit (cchb1) of the skeletal muscle dihydropyridine receptor alters expression of the alpha 1 subunit and eliminates excitation-contraction coupling. *Proc. Natl. Acad. Sci. U. S. A.* 93, 13961–13966. doi: 10.1073/pnas.93.24.13961

Guedes-Dias, P., Nirschl, J. J., Abreu, N., Tokito, M. K., Janke, C., Magiera, M. M., et al. (2019). Kinesin-3 responds to local microtubule dynamics to target synaptic cargo delivery to the Presynapse. *Curr. Biol.* 29, 268–282.e8. doi: 10.1016/j.cub.2018.11.065

Gundelfinger, E. D., Reissner, C., and Garner, C. C. (2015). Role of bassoon and piccolo in assembly and molecular Organization of the Active Zone. *Front. Synap. Neurosci.* 7:19. doi: 10.3389/fnsyn.2015.00019

Hall, D. H., and Hedgecock, E. M. (1991). Kinesin-related gene unc-104 is required for axonal transport of synaptic vesicles in C. elegans. *Cells* 65, 837–847. doi: 10.1016/0092-8674(91)90391-b

Han, Y., Kaeser, P. S., Südhof, T. C., and Schneggenburger, R. (2011). RIM determines Ca^2+ channel density and vesicle docking at the presynaptic active zone. *Neuron* 69, 304–316. doi: 10.1016/j.neuron.2010.12.014

Hara, Y., Koganezawa, M., and Yamamoto, D. (2015). The Dmca1D channel mediates Ca(2+) inward currents in drosophila embryonic muscles. *J. Neurogenet.* 29, 117–123. doi: 10.3109/01677063.2015.1054991

Harlow, M. L., Ress, D., Stoschek, A., Marshall, R. M., and McMahan, U. J. (2001). The architecture of active zone material at the frog's neuromuscular junction. *Nature* 409, 479–484. doi: 10.1038/35054000

Hastings, M. H., and Man, H.-Y. (2018). Synaptic capture of laterally diffusing AMPA receptors - an idea that stuck. *Trends Neurosci.* 41, 330–332. doi: 10.1016/j.tins.2018.03.016

He, L.-L., Zhang, Y., Chen, Y.-H., Yamada, Y., and Yang, J. (2007). Functional modularity of the beta-subunit of voltage-gated Ca2+ channels. *Biophys. J.* 93, 834–845. doi: 10.1529/biophysj.106.101691

Heck, J., Parutto, P., Ciuraszkiewicz, A., Bikbaev, A., Freund, R., Mitlöhner, J., et al. (2019). Transient confinement of CaV2.1 Ca2+-channel splice variants shapes synaptic short-term plasticity. *Neuron* 103, 66–79.e12. doi: 10.1016/j.neuron.2019.04.030

Heinrich, L., and Ryglewski, S. (2020). Different functions of two putative drosophila α2δ subunits in the same identified motoneurons. *Sci. Rep.* 10:13670. doi: 10.1038/s41598-020-69748-8

Held, R. G., Liu, C., Ma, K., Ramsey, A. M., Tarr, T. B., De Nola, G., et al. (2020). Synapse and active zone assembly in the absence of presynaptic ca2+ channels and ca2+ entry. *Neuron* 107, 667–683.e9. doi: 10.1016/j.neuron.2020.05.032

Heo, S., Diering, G. H., Na, C. H., Nirujogi, R. S., Bachman, J. L., Pandey, A., et al. (2018). Identification of long-lived synaptic proteins by proteomic analysis of synaptosome protein turnover. *Proc. Natl. Acad. Sci. U. S. A.* 115, E3827–E3836. doi: 10.1073/pnas.1720956115

Heuser, J. E., Reese, T. S., and Landis, D. M. (1974). Functional changes in frog neuromuscular junctions studied with freeze-fracture. *J. Neurocytol.* 3, 109–131. doi: 10.1007/BF01111936

Hibino, H., Pironkova, R., Onwumere, O., Vologodskaia, M., Hudspeth, A. J., and Lesage, F. (2002). RIM binding proteins (RBPs) couple Rab3-interacting molecules (RIMs) to voltage-gated Ca(2+) channels. *Neuron* 34, 411–423. doi: 10.1016/s0896-6273(02)00667-0

Hirokawa, N., Niwa, S., and Tanaka, Y. (2010). Molecular motors in neurons: transport mechanisms and roles in brain function, development, and disease. *Neuron* 68, 610–638. doi: 10.1016/j.neuron.2010.09.039

Holderith, N., Lorincz, A., Katona, G., Rózsa, B., Kulik, A., Watanabe, M., et al. (2012). Release probability of hippocampal glutamatergic terminals scales with the size of the active zone. *Nat. Neurosci.* 15, 988–997. doi: 10.1038/nn.3137

Hong, H., Zhao, K., Shiyan, H., Sheng, H., Yao, A., Jiang, Y., et al. (2020). Structural remodeling of active zones is associated with synaptic homeostasis. *J. Neurosci.* 40, 2817–2827. doi: 10.1523/JNEUROSCI.2002-19.2020

Hoppa, M. B., Lana, B., Margas, W., Dolphin, A. C., and Ryan, T. A. (2012). α2δ expression sets presynaptic calcium channel abundance and release probability. *Nature* 486, 122–125. doi: 10.1038/nature11033

Hosoi, N., Holt, M., and Sakaba, T. (2009). Calcium dependence of exo-and endocytotic coupling at a glutamatergic synapse. *Neuron* 63, 216–229. doi: 10.1016/j.neuron.2009.06.010

Hurd, D. D., and Saxton, W. M. (1996). Kinesin mutations cause motor neuron disease phenotypes by disrupting fast axonal transport in drosophila. *Genetics* 144, 1075–1085. doi: 10.1093/genetics/144.3.1075

Inchauspe, C. G., Martini, F. J., Forsythe, I. D., and Uchitel, O. D. (2004). Functional compensation of P/Q by N-type channels blocks short-term plasticity at the calyx of Held presynaptic terminal. *J. Neurosci.* 24, 10379–10383. doi: 10.1523/JNEUROSCI.2104-04.2004

Ishikawa, T., Kaneko, M., Shin, H.-S., and Takahashi, T. (2005). Presynaptic N-type and P/Q-type Ca2+ channels mediating synaptic transmission at the calyx of Held of mice. *J. Physiol. Lond.* 568, 199–209. doi: 10.1113/jphysiol.2005.089912

Jarsky, T., Tian, M., and Singer, J. H. (2010). Nanodomain control of exocytosis is responsible for the signaling capability of a retinal ribbon synapse. *J. Neurosci.* 30, 11885–11895. doi: 10.1523/JNEUROSCI.1415-10.2010

Jay, S. D., Sharp, A. H., Kahl, S., Vedvick, T. S., Harpold, M. M., and Campbell, K. P. (1991). Structural characterization of the dihydropyridine-sensitive calcium channel alpha 2-subunit and the associated delta peptides. *J. Biol. Chem.* 266, 3287–3293. doi: 10.1016/S0021-9258(18)49986-3

Jensen, K., and Mody, I. (2001). L-type Ca2+ channel-mediated short-term plasticity of GABAergic synapses. *Nat. Neurosci.* 4, 975–976. doi: 10.1038/nn722

Jeon, D., Kim, C., Yang, Y. M., Rhim, H., Yim, E., Oh, U., et al. (2007). Impaired long-term memory and long-term potentiation in N-type Ca2+ channel-deficient mice. *Genes Brain Behav.* 6, 375–388. doi: 10.1111/j.1601-183X.2006.00267.x

Jeong, K., Lee, S., Seo, H., Oh, Y., Jang, D., Choe, J., et al. (2015). Ca-α1T, a fly T-type Ca2+ channel, negatively modulates sleep. *Sci. Rep.* 5:17893. doi: 10.1038/srep17893

Jing, Z., Rutherford, M. A., Takago, H., Frank, T., Fejtova, A., Khimich, D., et al. (2013). Disruption of the presynaptic cytomatrix protein bassoon degrades ribbon anchorage, multiquantal release, and sound encoding at the hair cell afferent synapse. *J. Neurosci.* 33, 4456–4467. doi: 10.1523/JNEUROSCI.3491-12.2013

Jung, S., Oshima-Takago, T., Chakrabarti, R., Wong, A. B., Jing, Z., Yamanbaeva, G., et al. (2015). Rab3-interacting molecules 2α and 2β promote the abundance of voltage-gated CaV1.3 Ca2+ channels at hair cell active zones. *Proc. Natl. Acad. Sci. U. S. A.* 112, E3141–E3149. doi: 10.1073/pnas.1417207112

Kaeser, P. S., Deng, L., Wang, Y., Dulubova, I., Liu, X., Rizo, J., et al. (2011). RIM proteins tether Ca2+ channels to presynaptic active zones via a direct PDZ-domain interaction. *Cells* 144, 282–295. doi: 10.1016/j.cell.2010.12.029

Kaksonen, M., and Roux, A. (2018). Mechanisms of clathrin-mediated endocytosis. *Nat. Rev. Mol. Cell Biol.* 19, 313–326. doi: 10.1038/nrm.2017.132

Kanamori, T., Kanai, M. I., Dairyo, Y., Yasunaga, K. I., Morikawa, R. K., and Emoto, K. (2013). Compartmentalized calcium transients trigger dendrite pruning in drosophila sensory neurons. *Science* 340, 1475–1478. doi: 10.1126/science.1234879

Katiyar, R., Weissgerber, P., Roth, E., Dörr, J., Sothilingam, V., Garrido, M. G., et al. (2015). Influence of the β2-subunit of L-type voltage-gated Cav channels on the structural and functional development of photoreceptor ribbon synapses. *Invest. Ophthalmol. Vis. Sci.* 56, 2312–2324. doi: 10.1167/iovs.15-16654

Katz, B., and Miledi, R. (1965). The measurement of synaptic delay, and the time course of acetylcholine release at the neuromuscular junction. *Proc. R. Soc. Lond. B Biol. Sci.* 161, 483–495. doi: 10.1098/rspb.1965.0016

Kawasaki, F., Felling, R., and Ordway, R. W. (2000). A temperature-sensitive paralytic mutant defines a primary synaptic calcium channel in drosophila. *J. Neurosci.* 20, 4885–4889. doi: 10.1523/JNEUROSCI.20-13-04885.2000

Kawasaki, F., Zou, B., Xu, X., and Ordway, R. W. (2004). Active zone localization of presynaptic calcium channels encoded by the cacophony locus of drosophila. *J. Neurosci.* 24, 282–285. doi: 10.1523/JNEUROSCI.3553-03.2004

Kerov, V., Laird, J. G., Joiner, M.-L., Knecht, S., Soh, D., Hagen, J., et al. (2018). α2δ-4 is required for the molecular and structural Organization of rod and Cone Photoreceptor Synapses. *J. Neurosci.* 38, 6145–6160. doi: 10.1523/JNEUROSCI.3818-16.2018

Khatter, D., Sindhwani, A., and Sharma, M. (2015). Arf-like GTPase Arl8: moving from the periphery to the center of lysosomal biology. *Cell Logist.* 5:e1086501. doi: 10.1080/21592799.2015.1086501

Khimich, D., Nouvian, R., Pujol, R., Tom Dieck, S., Egner, A., Gundelfinger, E. D., et al. (2005). Hair cell synaptic ribbons are essential for synchronous auditory signalling. *Nature* 434, 889–894. doi: 10.1038/nature03418

Kim, C., Jun, K., Lee, T., Kim, S. S., McEnery, M. W., Chin, H., et al. (2001). Altered nociceptive response in mice deficient in the α1B subunit of the voltage-dependent calcium channel. *Mol. Cell. Neurosci.* 18, 235–245. doi: 10.1006/mcne.2001.1013

Kim, M.-H., Li, G.-L., and von Gersdorff, H. (2013). Single Ca2+ channels and exocytosis at sensory synapses. *J. Physiol. Lond.* 591, 3167–3178. doi: 10.1113/jphysiol.2012.249482

Kisilevsky, A. E., Mulligan, S. J., Altier, C., Iftinca, M. C., Varela, D., Tai, C., et al. (2008). D1 receptors physically interact with N-type calcium channels to regulate channel distribution and dendritic calcium entry. *Neuron* 58, 557–570. doi: 10.1016/j.neuron.2008.03.002

Kisilevsky, A. E., and Zamponi, G. W. (2008). D2 dopamine receptors interact directly with N-type calcium channels and regulate channel surface expression levels. *Channels* 2, 269–277. doi: 10.4161/chan.2.4.6402

Kittel, R. J., Wichmann, C., Rasse, T. M., Fouquet, W., Schmidt, M., Schmid, A., et al. (2006). Bruchpilot promotes active zone assembly, Ca2+ channel clustering, and vesicle release. *Science* 312, 1051–1054. doi: 10.1126/science.1126308

Kiyonaka, S., Nakajima, H., Takada, Y., Hida, Y., Yoshioka, T., Hagiwara, A., et al. (2012). Physical and functional interaction of the active zone protein CAST/ERC2 and the β-subunit of the voltage-dependent Ca(2+) channel. *J. Biochem.* 152, 149–159. doi: 10.1093/jb/mvs054

Kiyonaka, S., Wakamori, M., Miki, T., Uriu, Y., Nonaka, M., Bito, H., et al. (2007). RIM1 confers sustained activity and neurotransmitter vesicle anchoring to presynaptic Ca2+ channels. *Nat. Neurosci.* 10, 691–701. doi: 10.1038/nn1904

Klassen, M. P., Wu, Y. E., Maeder, C. I., Nakae, I., Cueva, J. G., Lehrman, E. K., et al. (2010). An Arf-like small G protein, ARL-8, promotes the axonal transport of presynaptic cargoes by suppressing vesicle aggregation. *Neuron* 66, 710–723. doi: 10.1016/j.neuron.2010.04.033

Ko, J., Na, M., Kim, S., Lee, J.-R., and Kim, E. (2003). Interaction of the ERC family of RIM-binding proteins with the liprin-alpha family of multidomain proteins. *J. Biol. Chem.* 278, 42377–42385. doi: 10.1074/jbc.M307561200

Koushika, S. P., Richmond, J. E., Hadwiger, G., Weimer, R. M., Jorgensen, E. M., and Nonet, M. L. (2001). A post-docking role for active zone protein rim. *Nat. Neurosci.* 4, 997–1005. doi: 10.1038/nn732

Krick, N., Ryglewski, S., Pichler, A., Bikbaev, A., Götz, T., Kobler, O., et al. (2021). Separation of presynaptic Cav2 and Cav1 channel function in synaptic vesicle exo-and endocytosis by the membrane anchored Ca2+ pump PMCA. *Proc. Natl. Acad. Sci.* 118:e2106621118. doi: 10.1073/pnas.2106621118

Krinner, S., Butola, T., Jung, S., Wichmann, C., and Moser, T. (2017). RIM-binding protein 2 promotes a large number of CaV1.3 Ca2+-channels and contributes to fast synaptic vesicle replenishment at hair cell active zones. *Front. Cell. Neurosci.* 11:334. doi: 10.3389/fncel.2017.00334

Kurshan, P. T., Oztan, A., and Schwarz, T. L. (2009). Presynaptic alpha2delta-3 is required for synaptic morphogenesis independent of its Ca2+−channel functions. *Nat. Neurosci.* 12, 1415–1423. doi: 10.1038/nn.2417

Kushibiki, Y., Suzuki, T., Jin, Y., and Taru, H. (2019). RIMB-1/RIM-binding protein and UNC-10/RIM redundantly regulate presynaptic localization of the voltage-gated Calcium Channel in Caenorhabditis elegans. *J. Neurosci.* 39, 8617–8631. doi: 10.1523/JNEUROSCI.0506-19.2019

Lainé, V., Frøkjær-Jensen, C., Couchoux, H., and Jospin, M. (2011). The alpha1 subunit EGL-19, the alpha2/delta subunit UNC-36, and the beta subunit CCB-1 underlie voltage-dependent calcium currents in Caenorhabditis elegans striated muscle. *J. Biol. Chem.* 286, 36180–36187. doi: 10.1074/jbc.M111.256149

Lambert, R. C., Bessaïh, T., Crunelli, V., and Leresche, N. (2014). The many faces of T-type calcium channels. *Pflugers Arch.* 466, 415–423. doi: 10.1007/s00424-013-1353-6

Lee, R. Y., Lobel, L., Hengartner, M., Horvitz, H. R., and Avery, L. (1997). Mutations in the alpha1 subunit of an L-type voltage-activated Ca2+ channel cause myotonia in Caenorhabditis elegans. *EMBO J.* 16, 6066–6076. doi: 10.1093/emboj/16.20.6066

Littleton, J. T., Stern, M., Perin, M., and Bellen, H. J. (1994). Calcium dependence of neurotransmitter release and rate of spontaneous vesicle fusions are altered in drosophila synaptotagmin mutants. *Proc. Natl. Acad. Sci. U. S. A.* 91, 10888–10892. doi: 10.1073/pnas.91.23.10888

Littleton, J. T., Stern, M., Schulze, K., Perin, M., and Bellen, H. J. (1993). Mutational analysis of drosophila synaptotagmin demonstrates its essential role in Ca(2+)-activated neurotransmitter release. *Cells* 74, 1125–1134. doi: 10.1016/0092-8674(93)90733-7

Liu, C., Bickford, L. S., Held, R. G., Nyitrai, H., Südhof, T. C., and Kaeser, P. S. (2014). The active zone protein family ELKS supports Ca2+ influx at nerve terminals of inhibitory hippocampal neurons. *J. Neurosci.* 34, 12289–12303. doi: 10.1523/JNEUROSCI.0999-14.2014

Liu, X., Kerov, V., Haeseleer, F., Majumder, A., Artemyev, N., Baker, S. A., et al. (2013). Dysregulation of Ca(v)1.4 channels disrupts the maturation of photoreceptor synaptic ribbons in congenital stationary night blindness type 2. *Channels* 7, 514–523. doi: 10.4161/chan.26376

Liu, K. S. Y., Siebert, M., Mertel, S., Knoche, E., Wegener, S., Wichmann, C., et al. (2011). RIM-binding protein, a central part of the active zone, is essential for neurotransmitter release. *Science* 334, 1565–1569. doi: 10.1126/science.1212991

Lübbert, M., Goral, R. O., Keine, C., Thomas, C., Guerrero-Given, D., Putzke, T., et al. (2019). Cav2.1 α1 subunit expression regulates presynaptic cav2.1 abundance and synaptic strength at a central synapse. *Neuron* 101, 260–273.e6. doi: 10.1016/j.neuron.2018.11.028

Lübbert, M., Goral, R. O., Satterfield, R., Putzke, T., van den Maagdenberg, A. M., Kamasawa, N., et al. (2017). A novel region in the CaV2.1 α1 subunit C-terminus regulates fast synaptic vesicle fusion and vesicle docking at the mammalian presynaptic active zone. *elife* 6. doi: 10.7554/eLife.28412

Luebke, J. I., Dunlap, K., and Turner, T. J. (1993). Multiple calcium channel types control glutamatergic synaptic transmission in the hippocampus. *Neuron* 11, 895–902. doi: 10.1016/0896-6273(93)90119-c

Luo, F., Dittrich, M., Stiles, J. R., and Meriney, S. D. (2011). Single-pixel optical fluctuation analysis of calcium channel function in active zones of motor nerve terminals. *J. Neurosci.* 31, 11268–11281. doi: 10.1523/JNEUROSCI.1394-11.2011

Ly, C. V., Yao, C.-K., Verstreken, P., Ohyama, T., and Bellen, H. J. (2008). Straightjacket is required for the synaptic stabilization of cacophony, a voltage-gated calcium channel alpha1 subunit. *J. Cell Biol.* 181, 157–170. doi: 10.1083/jcb.200712152

Maas, C., Torres, V. I., Altrock, W. D., Leal-Ortiz, S., Wagh, D., Terry-Lorenzo, R. T., et al. (2012). Formation of Golgi-derived active zone precursor vesicles. *J. Neurosci.* 32, 11095–11108. doi: 10.1523/JNEUROSCI.0195-12.2012

Maddox, J. W., Randall, K. L., Yadav, R. P., Williams, B., Hagen, J., Derr, P. J., et al. (2020). A dual role for Cav1.4 Ca2+ channels in the molecular and structural organization of the rod photoreceptor synapse. *elife* 9. doi: 10.7554/eLife.62184

Maeder, C. I., San-Miguel, A., Wu, E. Y., Lu, H., and Shen, K. (2014). In vivo neuron-wide analysis of synaptic vesicle precursor trafficking. *Traffic* 15, 273–291. doi: 10.1111/tra.12142

Maritzen, T., and Haucke, V. (2018). Coupling of exocytosis and endocytosis at the presynaptic active zone. *Neurosci. Res.* 127, 45–52. doi: 10.1016/j.neures.2017.09.013

Mathews, E. A., García, E., Santi, C. M., Mullen, G. P., Thacker, C., Moerman, D. G., et al. (2003). Critical residues of the Caenorhabditis elegans unc-2 voltage-gated calcium channel that affect behavioral and physiological properties. *J. Neurosci.* 23, 6537–6545. doi: 10.1523/JNEUROSCI.23-16-06537.2003

Matkovic, T., Siebert, M., Knoche, E., Depner, H., Mertel, S., Owald, D., et al. (2013). The Bruchpilot cytomatrix determines the size of the readily releasable pool of synaptic vesicles. *J. Cell Biol.* 202, 667–683. doi: 10.1083/jcb.201301072

Melom, J. E., Akbergenova, Y., Gavornik, J. P., and Littleton, J. T. (2013). Spontaneous and evoked release are independently regulated at individual active zones. *J. Neurosci.* 33, 17253–17263. doi: 10.1523/JNEUROSCI.3334-13.2013

Mercer, A. J., Chen, M., and Thoreson, W. B. (2011). Lateral mobility of presynaptic L-type calcium channels at photoreceptor ribbon synapses. *J. Neurosci.* 31, 4397–4406. doi: 10.1523/JNEUROSCI.5921-10.2011

Mercer, A. J., Szalewski, R. J., Jackman, S. L., Van Hook, M. J., and Thoreson, W. B. (2012). Regulation of presynaptic strength by controlling Ca2+ channel mobility: effects of cholesterol depletion on release at the cone ribbon synapse. *J. Neurophysiol.* 107, 3468–3478. doi: 10.1152/jn.00779.2011

Miki, T., Kaufmann, W. A., Malagon, G., Gomez, L., Tabuchi, K., Watanabe, M., et al. (2017). Numbers of presynaptic Ca2+ channel clusters match those of functionally defined vesicular docking sites in single central synapses. *Proc. Natl. Acad. Sci. U. S. A.* 114, E5246–E5255. doi: 10.1073/pnas.1704470114

Mizuno, F., Barabas, P., Krizaj, D., and Akopian, A. (2010). Glutamate-induced internalization of Ca(v)1.3 L-type Ca(2+) channels protects retinal neurons against excitotoxicity. *J. Physiol. Lond.* 588, 953–966. doi: 10.1113/jphysiol.2009.181305

Moo, E. V., van Senten, J. R., Bräuner-Osborne, H., and Møller, T. C. (2021). Arrestin-dependent and -independent internalization of G protein-coupled receptors: methods, mechanisms, and implications on cell signaling. *Mol. Pharmacol.* 99, 242–255. doi: 10.1124/molpharm.120.000192

Mrestani, A., Pauli, M., Kollmannsberger, P., Repp, F., Kittel, R. J., Eilers, J., et al. (2021). Active zone compaction correlates with presynaptic homeostatic potentiation. *Cell Rep.* 37:109770. doi: 10.1016/j.celrep.2021.109770

Mukherjee, K., Yang, X., Gerber, S. H., Kwon, H.-B., Ho, A., Castillo, P. E., et al. (2010). Piccolo and bassoon maintain synaptic vesicle clustering without directly participating in vesicle exocytosis. *Proc. Natl. Acad. Sci. U. S. A.* 107, 6504–6509. doi: 10.1073/pnas.1002307107

Müller, M., and Davis, G. W. (2012). Transsynaptic control of presynaptic Ca2+ influx achieves homeostatic potentiation of neurotransmitter release. *Curr. Biol.* 22, 1102–1108. doi: 10.1016/j.cub.2012.04.018

Müller, M., Genç, Ö., and Davis, G. W. (2015). RIM-binding protein links synaptic homeostasis to the stabilization and replenishment of high release probability vesicles. *Neuron* 85, 1056–1069. doi: 10.1016/j.neuron.2015.01.024

Müller, C. S., Haupt, A., Bildl, W., Schindler, J., Knaus, H.-G., Meissner, M., et al. (2010). Quantitative proteomics of the Cav2 channel nano-environments in the mammalian brain. *Proc. Natl. Acad. Sci. U. S. A.* 107, 14950–14957. doi: 10.1073/pnas.1005940107

Nakamura, Y., Harada, H., Kamasawa, N., Matsui, K., Rothman, J. S., Shigemoto, R., et al. (2015). Nanoscale distribution of presynaptic Ca(2+) channels and its impact on vesicular release during development. *Neuron* 85, 145–158. doi: 10.1016/j.neuron.2014.11.019

Nanou, E., and Catterall, W. A. (2018). Calcium channels, synaptic plasticity, and neuropsychiatric disease. *Neuron* 98, 466–481. doi: 10.1016/j.neuron.2018.03.017

Neher, E. (1998). Vesicle pools and Ca2+ microdomains: new tools for understanding their roles in neurotransmitter release. *Neuron* 20, 389–399. doi: 10.1016/s0896-6273(00)80983-6

Newman, Z. L., Bakshinskaya, D., Schultz, R., Kenny, S. J., Moon, S., Aghi, K., et al. (2022). Determinants of synapse diversity revealed by super-resolution quantal transmission and active zone imaging. *Nat. Commun.* 13:229. doi: 10.1038/s41467-021-27815-2

Obermair, G. J., Schlick, B., Di Biase, V., Subramanyam, P., Gebhart, M., Baumgartner, S., et al. (2010). Reciprocal interactions regulate targeting of calcium channel beta subunits and membrane expression of alpha1 subunits in cultured hippocampal neurons. *J. Biol. Chem.* 285, 5776–5791. doi: 10.1074/jbc.M109.044271

Oh, K. H., Krout, M. D., Richmond, J. E., and Kim, H. (2021). UNC-2 CaV2 channel localization at presynaptic active zones depends on UNC-10/RIM and SYD-2/Liprin-α in Caenorhabditis elegans. *J. Neurosci.* 41, 4782–4794. doi: 10.1523/JNEUROSCI.0076-21.2021

Ohtsuka, T., Takao-Rikitsu, E., Inoue, E., Inoue, M., Takeuchi, M., Matsubara, K., et al. (2002). Cast: a novel protein of the cytomatrix at the active zone of synapses that forms a ternary complex with RIM1 and munc13-1. *J. Cell Biol.* 158, 577–590. doi: 10.1083/jcb.200202083

Okada, Y., Yamazaki, H., Sekine-Aizawa, Y., and Hirokawa, N. (1995). The neuron-specific kinesin superfamily protein KIF1A is a uniqye monomeric motor for anterograde axonal transport of synaptic vesicle precursors. *Cells* 81, 769–780. doi: 10.1016/0092-8674(95)90538-3

Opatowsky, Y., Chen, C.-C., Campbell, K. P., and Hirsch, J. A. (2004). Structural analysis of the voltage-dependent calcium channel beta subunit functional core and its complex with the alpha 1 interaction domain. *Neuron* 42, 387–399. doi: 10.1016/s0896-6273(04)00250-8

Ortega, J. M., Genç, Ö., and Davis, G. W. (2018). Molecular mechanisms that stabilize short term synaptic plasticity during presynaptic homeostatic plasticity. *elife* 7. doi: 10.7554/eLife.40385

Owald, D., Fouquet, W., Schmidt, M., Wichmann, C., Mertel, S., Depner, H., et al. (2010). A Syd-1 homologue regulates pre- and postsynaptic maturation in drosophila. *J. Cell Biol.* 188, 565–579. doi: 10.1083/jcb.200908055

Pack-Chung, E., Kurshan, P. T., Dickman, D. K., and Schwarz, T. L. (2007). A drosophila kinesin required for synaptic Bouton formation and synaptic vesicle transport. *Nat. Neurosci.* 10, 980–989. doi: 10.1038/nn1936

Peled, E. S., and Isacoff, E. Y. (2011). Optical quantal analysis of synaptic transmission in wild-type and rab3-mutant drosophila motor axons. *Nat. Neurosci.* 14, 519–526. doi: 10.1038/nn.2767

Pragnell, M., De Waard, M., Mori, Y., Tanabe, T., Snutch, T. P., and Campbell, K. P. (1994). Calcium channel beta-subunit binds to a conserved motif in the I-II cytoplasmic linker of the alpha 1-subunit. *Nature* 368, 67–70. doi: 10.1038/368067a0

Price, J. C., Guan, S., Burlingame, A., Prusiner, S. B., and Ghaemmaghami, S. (2010). Analysis of proteome dynamics in the mouse brain. *Proc. Natl. Acad. Sci. U. S. A.* 107, 14508–14513. doi: 10.1073/pnas.1006551107

Pumplin, D. W., Reese, T. S., and Llinás, R. (1981). Are the presynaptic membrane particles the calcium channels? *Proc. Natl. Acad. Sci. U. S. A.* 78, 7210–7213. doi: 10.1073/pnas.78.11.7210

Radulovic, T., Dong, W., Goral, R. O., Thomas, C. I., Veeraraghavan, P., Montesinos, M. S., et al. (2020). Presynaptic development is controlled by the core active zone proteins CAST/ELKS. *J. Physiol. Lond.* 598, 2431–2452. doi: 10.1113/JP279736

Reid, C. A., Clements, J. D., and Bekkers, J. M. (1997). Nonuniform distribution of Ca2+ channel subtypes on presynaptic terminals of excitatory synapses in hippocampal cultures. *J. Neurosci.* 17, 2738–2745. doi: 10.1523/JNEUROSCI.17-08-02738.1997

Reuter, H. (1995). Measurements of exocytosis from single presynaptic nerve terminals reveal heterogeneous inhibition by Ca(2+)-channel blockers. *Neuron* 14, 773–779. doi: 10.1016/0896-6273(95)90221-x

Rivière, J.-B., Ramalingam, S., Lavastre, V., Shekarabi, M., Holbert, S., Lafontaine, J., et al. (2011). KIF1A, an axonal transporter of synaptic vesicles, is mutated in hereditary sensory and autonomic neuropathy type 2. *Am. J. Hum. Genet.* 89, 219–230. doi: 10.1016/j.ajhg.2011.06.013

Ryglewski, S., Lance, K., Levine, R. B., and Duch, C. (2012). Ca(v)2 channels mediate low and high voltage-activated calcium currents in drosophila motoneurons. *J. Physiol. Lond.* 590, 809–825. doi: 10.1113/jphysiol.2011.222836

Sabatini, B. L., and Regehr, W. G. (1996). Timing of neurotransmission at fast synapses in the mammalian brain. *Nature* 384, 170–172. doi: 10.1038/384170a0

Saheki, Y., and Bargmann, C. I. (2009). Presynaptic CaV2 calcium channel traffic requires CALF-1 and the alpha(2)delta subunit UNC-36. *Nat. Neurosci.* 12, 1257–1265. doi: 10.1038/nn.2383

Sauvola, C. W., Akbergenova, Y., Cunningham, K. L., Aponte-Santiago, N. A., and Littleton, J. T. (2021). The decoy SNARE Tomosyn sets tonic versus phasic release properties and is required for homeostatic synaptic plasticity. *elife* 10:e72841. doi: 10.7554/eLife.72841

Sauvola, C. W., and Littleton, J. T. (2021). SNARE regulatory proteins in synaptic vesicle fusion and recycling. *Front. Mol. Neurosci.* 14:733138. doi: 10.3389/fnmol.2021.733138

Schafer, W. R., and Kenyon, C. J. (1995). A calcium-channel homologue required for adaptation to dopamine and serotonin in Caenorhabditis elegans. *Nature* 375, 73–78. doi: 10.1038/375073a0

Schneider, R., Hosy, E., Kohl, J., Klueva, J., Choquet, D., Thomas, U., et al. (2015). Mobility of calcium channels in the presynaptic membrane. *Neuron* 86, 672–679. doi: 10.1016/j.neuron.2015.03.050

Schoch, S., Castillo, P. E., Jo, T., Mukherjee, K., Geppert, M., Wang, Y., et al. (2002). RIM1alpha forms a protein scaffold for regulating neurotransmitter release at the active zone. *Nature* 415, 321–326. doi: 10.1038/415321a

Schöpf, C. L., Ablinger, C., Geisler, S. M., Stanika, R. I., Campiglio, M., Kaufmann, W. A., et al. (2021). Presynaptic α2δ subunits are key organizers of glutamatergic synapses. *Proc. Natl. Acad. Sci. U. S. A.* 118. doi: 10.1073/pnas.1920827118

Shapira, M., Zhai, R. G., Dresbach, T., Bresler, T., Torres, V. I., Gundelfinger, E. D., et al. (2003). Unitary assembly of presynaptic active zones from piccolo-bassoon transport vesicles. *Neuron* 38, 237–252. doi: 10.1016/s0896-6273(03)00207-1

Sheng, J., He, L., Zheng, H., Xue, L., Luo, F., Shin, W., et al. (2012). Calcium-channel number critically influences synaptic strength and plasticity at the active zone. *Nat. Neurosci.* 15, 998–1006. doi: 10.1038/nn.3129

Shibasaki, T., Sunaga, Y., Fujimoto, K., Kashima, Y., and Seino, S. (2004). Interaction of ATP sensor, cAMP sensor, Ca2+ sensor, and voltage-dependent Ca2+ channel in insulin granule exocytosis. *J. Biol. Chem.* 279, 7956–7961. doi: 10.1074/jbc.M309068200

Shtonda, B., and Avery, L. (2005). CCA-1, EGL-19 and EXP-2 currents shape action potentials in the Caenorhabditis elegans pharynx. *J. Exp. Biol.* 208, 2177–2190. doi: 10.1242/jeb.01615

Smith, L. A., Wang, X., Peixoto, A. A., Neumann, E. K., Hall, L. M., and Hall, J. C. (1996). A drosophila calcium channel alpha1 subunit gene maps to a genetic locus associated with behavioral and visual defects. *J. Neurosci.* 16, 7868–7879. doi: 10.1523/JNEUROSCI.16-24-07868.1996

Stahl, A., Noyes, N. C., Boto, T., Botero, V., Broyles, C. N., Jing, M., et al. (2022). Associative learning drives longitudinally graded presynaptic plasticity of neurotransmitter release along axonal compartments. *elife* 11:11. doi: 10.7554/eLife.76712

Steger, K. A., Shtonda, B. B., Thacker, C., Snutch, T. P., and Avery, L. (2005). The C. elegans T-type calcium channel CCA-1 boosts neuromuscular transmission. *J. Exp. Biol.* 208, 2191–2203. doi: 10.1242/jeb.01616

Südhof, T. C. (2012). The presynaptic active zone. *Neuron* 75, 11–25. doi: 10.1016/j.neuron.2012.06.012

Takahashi, T., and Momiyama, A. (1993). Different types of calcium channels mediate central synaptic transmission. *Nature* 366, 156–158. doi: 10.1038/366156a0

Tang, L., Gamal El-Din, T. M., Payandeh, J., Martinez, G. Q., Heard, T. M., Scheuer, T., et al. (2014). Structural basis for Ca2+ selectivity of a voltage-gated calcium channel. *Nature* 505, 56–61. doi: 10.1038/nature12775

Tao-Cheng, J. H. (2007). Ultrastructural localization of active zone and synaptic vesicle proteins in a preassembled multi-vesicle transport aggregate. *Neuroscience* 150, 575–584. doi: 10.1016/j.neuroscience.2007.09.031

Taylor, C. P., Angelotti, T., and Fauman, E. (2007). Pharmacology and mechanism of action of pregabalin: the calcium channel alpha2-delta (alpha2-delta) subunit as a target for antiepileptic drug discovery. *Epilepsy Res.* 73, 137–150. doi: 10.1016/j.eplepsyres.2006.09.008

Tempes, A., Weslawski, J., Brzozowska, A., and Jaworski, J. (2020). Role of dynein-dynactin complex, kinesins, motor adaptors, and their phosphorylation in dendritogenesis. *J. Neurochem.* 155, 10–28. doi: 10.1111/jnc.15010

Thoreson, W. B., Mercer, A. J., Cork, K. M., and Szalewski, R. J. (2013). Lateral mobility of L-type calcium channels in synaptic terminals of retinal bipolar cells. *Mol. Vis.* 19, 16–24. PMID: 23335847

Thoreson, W. B., Rabl, K., Townes-Anderson, E., and Heidelberger, R. (2004). A highly Ca2+−sensitive pool of vesicles contributes to linearity at the rod photoreceptor ribbon synapse. *Neuron* 42, 595–605. doi: 10.1016/s0896-6273(04)00254-5

Tom Dieck, S., Sanmartí-Vila, L., Langnaese, K., Richter, K., Kindler, S., Soyke, A., et al. (1998). Bassoon, a novel zinc-finger CAG/glutamine-repeat protein selectively localized at the active zone of presynaptic nerve terminals. *J. Cell Biol.* 142, 499–509. doi: 10.1083/jcb.142.2.499

Tseng, P.-Y., Henderson, P. B., Hergarden, A. C., Patriarchi, T., Coleman, A. M., Lillya, M. W., et al. (2017). α-Actinin promotes surface localization and current density of the Ca2+ channel CaV1.2 by binding to the IQ region of the α1 subunit. *Biochemistry* 56, 3669–3681. doi: 10.1021/acs.biochem.7b00359

Vale, R. D., Funatsu, T., Pierce, D. W., Romberg, L., Harada, Y., and Yanagida, T. (1996). Direct observation of single kinesin molecules moving along microtubules. *Nature* 380, 451–453. doi: 10.1038/380451a0

Van Petegem, F., Clark, K. A., Chatelain, F. C., and Minor, D. L. (2004). Structure of a complex between a voltage-gated calcium channel beta-subunit and an alpha-subunit domain. *Nature* 429, 671–675. doi: 10.1038/nature02588

Voigt, A., Freund, R., Heck, J., Missler, M., Obermair, G. J., Thomas, U., et al. (2016). Dynamic association of calcium channel subunits at the cellular membrane. *Neurophotonics* 3:041809. doi: 10.1117/1.NPh.3.4.041809

von Zastrow, M., and Sorkin, A. (2021). Mechanisms for regulating and organizing receptor signaling by endocytosis. *Annu. Rev. Biochem.* 90, 709–737. doi: 10.1146/annurev-biochem-081820-092427

Vukoja, A., Rey, U., Petzoldt, A. G., Ott, C., Vollweiter, D., Quentin, C., et al. (2018). Presynaptic biogenesis requires axonal transport of lysosome-related vesicles. *Neuron* 99, 1216–1232.e7. doi: 10.1016/j.neuron.2018.08.004

Wagh, D. A., Rasse, T. M., Asan, E., Hofbauer, A., Schwenkert, I., Dürrbeck, H., et al. (2006). Bruchpilot, a protein with homology to ELKS/CAST, is required for structural integrity and function of synaptic active zones in drosophila. *Neuron* 49, 833–844. doi: 10.1016/j.neuron.2006.02.008

Waithe, D., Ferron, L., Page, K. M., Chaggar, K., and Dolphin, A. C. (2011). Beta-subunits promote the expression of Ca(V)2.2 channels by reducing their proteasomal degradation. *J. Biol. Chem.* 286, 9598–9611. doi: 10.1074/jbc.M110.195909

Walker, D., Bichet, D., Campbell, K. P., and De Waard, M. (1998). A beta 4 isoform-specific interaction site in the carboxyl-terminal region of the voltage-dependent Ca2+ channel alpha 1A subunit. *J. Biol. Chem.* 273, 2361–2367. doi: 10.1074/jbc.273.4.2361

Wang, Y., Fehlhaber, K. E., Sarria, I., Cao, Y., Ingram, N. T., Guerrero-Given, D., et al. (2017). The auxiliary Calcium Channel subunit α2δ4 is required for axonal elaboration, synaptic transmission, and wiring of rod photoreceptors. *Neuron* 93, 1359–1374.e6. doi: 10.1016/j.neuron.2017.02.021

Wang, X., Hu, B., Zieba, A., Neumann, N. G., Kasper-Sonnenberg, M., Honsbein, A., et al. (2009). A protein interaction node at the neurotransmitter release site: domains of Aczonin/piccolo, bassoon, CAST, and rim converge on the N-terminal domain of Munc13-1. *J. Neurosci.* 29, 12584–12596. doi: 10.1523/JNEUROSCI.1255-09.2009

Wang, T., Jones, R. T., Whippen, J. M., and Davis, G. W. (2016). α2δ-3 is required for rapid Transsynaptic homeostatic signaling. *Cell Rep.* 16, 2875–2888. doi: 10.1016/j.celrep.2016.08.030

Wang, Y., Liu, X., Biederer, T., and Südhof, T. C. (2002). A family of RIM-binding proteins regulated by alternative splicing: implications for the genesis of synaptic active zones. *Proc. Natl. Acad. Sci. U. S. A.* 99, 14464–14469. doi: 10.1073/pnas.182532999

Wang, L.-Y., Neher, E., and Taschenberger, H. (2008). Synaptic vesicles in mature calyx of Held synapses sense higher nanodomain calcium concentrations during action potential-evoked glutamate release. *J. Neurosci.* 28, 14450–14458. doi: 10.1523/JNEUROSCI.4245-08.2008

Wang, Y., Okamoto, M., Schmitz, F., Hofmann, K., and Südhof, T. C. (1997). Rim is a putative Rab3 effector in regulating synaptic-vesicle fusion. *Nature* 388, 593–598. doi: 10.1038/41580

Wang, Y., Sugita, S., and Sudhof, T. C. (2000). The RIM/NIM family of neuronal C2 domain proteins. Interactions with Rab3 and a new class of Src homology 3 domain proteins. *J. Biol. Chem.* 275, 20033–20044. doi: 10.1074/jbc.M909008199

Watanabe, S., and Boucrot, E. (2017). Fast and ultrafast endocytosis. *Curr. Opin. Cell Biol.* 47, 64–71. doi: 10.1016/j.ceb.2017.02.013

Weissgerber, P., Held, B., Bloch, W., Kaestner, L., Chien, K. R., Fleischmann, B. K., et al. (2006). Reduced cardiac L-type Ca2+ current in Ca(V)beta2−/− embryos impairs cardiac development and contraction with secondary defects in vascular maturation. *Circ. Res.* 99, 749–757. doi: 10.1161/01.RES.0000243978.15182.c1

Wheeler, D. B., Randall, A., and Tsien, R. W. (1994). Roles of N-type and Q-type Ca2+ channels in supporting hippocampal synaptic transmission. *Science* 264, 107–111. doi: 10.1126/science.7832825

Whittaker, C. A., and Hynes, R. O. (2002). Distribution and evolution of von Willebrand/integrin a domains: widely dispersed domains with roles in cell adhesion and elsewhere. *Mol. Biol. Cell* 13, 3369–3387. doi: 10.1091/mbc.E02-05-0259

Witcher, D. R., De Waard, M., Sakamoto, J., Franzini-Armstrong, C., Pragnell, M., Kahl, S. D., et al. (1993). Subunit identification and reconstitution of the N-type Ca2+ channel complex purified from brain. *Science* 261, 486–489. doi: 10.1126/science.8392754

Wu, L. G., Hamid, E., Shin, W., and Chiang, H. C. (2014). Exocytosis and endocytosis: modes, functions, and coupling mechanisms. *Annu. Rev. Physiol.* 76, 301–331. doi: 10.1146/annurev-physiol-021113-170305

Wu, Y. E., Huo, L., Maeder, C. I., Feng, W., and Shen, K. (2013). The balance between capture and dissociation of presynaptic proteins controls the spatial distribution of synapses. *Neuron* 78, 994–1011. doi: 10.1016/j.neuron.2013.04.035

Wu, X. S., McNeil, B. D., Xu, J., Fan, J., Xue, L., Melicoff, E., et al. (2009). Ca2+ and calmodulin initiate all forms of endocytosis during depolarization at a nerve terminal. *Nat. Neurosci.* 12, 1003–1010. doi: 10.1038/nn.2355

Wu, L. G., Westenbroek, R. E., Borst, J. G., Catterall, W. A., and Sakmann, B. (1999). Calcium channel types with distinct presynaptic localization couple differentially to transmitter release in single calyx-type synapses. *J. Neurosci.* 19, 726–736. doi: 10.1523/JNEUROSCI.19-02-00726.1999

Wu, J., Yan, Z., Li, Z., Qian, X., Lu, S., Dong, M., et al. (2016). Structure of the voltage-gated calcium channel Ca(v)1.1 at 3.6 Å resolution. *Nature* 537, 191–196. doi: 10.1038/nature19321

Wu, J., Yan, Z., Li, Z., Yan, C., Lu, S., Dong, M., et al. (2015). Structure of the voltage-gated calcium channel Cav1.1 complex. *Science* 350:aad2395. doi: 10.1126/science.aad2395

Xuan, Z., Manning, L., Nelson, J., Richmond, J. E., Colón-Ramos, D. A., Shen, K., et al. (2017). Clarinet (CLA-1), a novel active zone protein required for synaptic vesicle clustering and release. *elife* 6. doi: 10.7554/eLife.29276

Xue, L., Zhang, Z., McNeil, B. D., Luo, F., Wu, X. S., Sheng, J., et al. (2012). Voltage-dependent calcium channels at the plasma membrane, but not vesicular channels, couple exocytosis to endocytosis. *Cell Rep.* 1, 632–638. doi: 10.1016/j.celrep.2012.04.011

Yonekawa, Y., Harada, A., Okada, Y., Funakoshi, T., Kanai, Y., Takei, Y., et al. (1998). Defect in synaptic vesicle precursor transport and neuronal cell death in KIF1A motor protein-deficient mice. *J. Cell Biol.* 141, 431–441. doi: 10.1083/jcb.141.2.431

Yu, F. H., Yarov-Yarovoy, V., Gutman, G. A., and Catterall, W. A. (2005). Overview of molecular relationships in the voltage-gated ion channel superfamily. *Pharmacol. Rev.* 57, 387–395. doi: 10.1124/pr.57.4.13

Zabouri, N., and Haverkamp, S. (2013). Calcium channel-dependent molecular maturation of photoreceptor synapses. *PLoS One* 8:e63853. doi: 10.1371/journal.pone.0063853

Zhai, R. G., and Bellen, H. J. (2004). The architecture of the active zone in the presynaptic nerve terminal. *Physiology (Bethesda)* 19, 262–270. doi: 10.1152/physiol.00014.2004

Zhai, R. G., Vardinon-Friedman, H., Cases-Langhoff, C., Becker, B., Gundelfinger, E. D., Ziv, N. E., et al. (2001). Assembling the presynaptic active zone: a characterization of an active one precursor vesicle. *Neuron* 29, 131–143. doi: 10.1016/s0896-6273(01)00185-4

Zhang, Y. V., Hannan, S. B., Kern, J. V., Stanchev, D. T., Koç, B., Jahn, T. R., et al. (2017). The KIF1A homolog Unc-104 is important for spontaneous release, postsynaptic density maturation and perisynaptic scaffold organization. *Sci. Rep.* 7:38172. doi: 10.1038/srep38172

Zhang, Y. V., Hannan, S. B., Stapper, Z. A., Kern, J. V., Jahn, T. R., and Rasse, T. M. (2016). The drosophila KIF1A homolog unc-104 is important for site-specific synapse maturation. *Front. Cell. Neurosci.* 10:207. doi: 10.3389/fncel.2016.00207

frontiers | Frontiers in Molecular Neuroscience

TYPE Review
PUBLISHED 31 July 2023
DOI 10.3389/fnmol.2023.1183775

OPEN ACCESS

EDITED BY
Sandra Henriques Vaz,
Universidade de Lisboa, Portugal

REVIEWED BY
Edward Haig Beamer,
Nottingham Trent University, United Kingdom
Alberto Javier Ramos,
National Scientific and Technical Research Council (CONICET), Argentina

*CORRESPONDENCE
Filiz Onat
✉ filiz.onat@acibadem.edu.tr

RECEIVED 10 March 2023
ACCEPTED 12 July 2023
PUBLISHED 31 July 2023

CITATION
Çarçak N, Onat F and Sitnikova E (2023) Astrocytes as a target for therapeutic strategies in epilepsy: current insights.
Front. Mol. Neurosci. 16:1183775.
doi: 10.3389/fnmol.2023.1183775

Astrocytes as a target for therapeutic strategies in epilepsy: current insights

Nihan Çarçak[1,2], Filiz Onat[2,3]* and Evgenia Sitnikova[4]

[1]Department of Pharmacology, Faculty of Pharmacy, Istanbul University, Istanbul, Turkey, [2]Institute of Health Sciences, Department of Neuroscience, Acibadem Mehmet Ali Aydinlar University, Istanbul, Turkey, [3]Department of Medical Pharmacology, Faculty of Medicine, Acibadem Mehmet Ali Aydinlar University, Istanbul, Turkey, [4]Institute of Higher Nervous Activity and Neurophysiology of Russian Academy of Sciences, Moscow, Russia

Astrocytes are specialized non-neuronal glial cells of the central nervous system, contributing to neuronal excitability and synaptic transmission (gliotransmission). Astrocytes play a key roles in epileptogenesis and seizure generation. Epilepsy, as a chronic disorder characterized by neuronal hyperexcitation and hypersynchronization, is accompanied by substantial disturbances of glial cells and impairment of astrocytic functions and neuronal signaling. Anti-seizure drugs that provide symptomatic control of seizures primarily target neural activity. In epileptic patients with inadequate control of seizures with available anti-seizure drugs, novel therapeutic candidates are needed. These candidates should treat epilepsy with anti-epileptogenic and disease-modifying effects. Evidence from human and animal studies shows that astrocytes have value for developing new anti-seizure and anti-epileptogenic drugs. In this review, we present the key functions of astrocytes contributing to neuronal hyperexcitability and synaptic activity following an etiology-based approach. We analyze the role of astrocytes in both development (epileptogenesis) and generation of seizures (ictogenesis). Several promising new strategies that attempted to modify astroglial functions for treating epilepsy are being developed: (1) selective targeting of glia-related molecular mechanisms of glutamate transport; (2) modulation of tonic GABA release from astrocytes; (3) gliotransmission; (4) targeting the astrocytic Kir4.1-BDNF system; (5) astrocytic Na^+/K^+/ATPase activity; (6) targeting DNA hypo- or hypermethylation of candidate genes in astrocytes; (7) targeting astrocytic gap junction regulators; (8) targeting astrocytic adenosine kinase (the major adenosine-metabolizing enzyme); and (9) targeting microglia-astrocyte communication and inflammatory pathways. Novel disease-modifying therapeutic strategies have now been developed, such as astroglia-targeted gene therapy with a broad spectrum of genetic constructs to target astroglial cells.

KEYWORDS

temporal lobe epilepsy, absence epilepsy, epileptogenesis, gliotransmission, neuroglia, astrocytes, astrocyte-targeting therapy, ictogenesis

1. Introduction

Glial cells, also known as neuroglia, are non-neuronal cells of the central and peripheral nervous system (Kettenmann and Ransom, 2004a; Kettenmann and Verkhratsky, 2008; Verkhratsky and Butt, 2013). There is a great diversity of neuroglia in respect to their origin, localization, morphology, physiological, and functional properties. Traditionally, four types of

glial cell have been recognized in adults: (1) Astrocytes, (2) Microglia, (3) oligodendrocytes, and (4) their progenitors, neuron–glial antigen 2 (NG2) glia (Kettenmann and Ransom, 2004b; Kettenmann and Verkhratsky, 2008; Verkhratsky and Butt, 2013). Astrocytes, the most abundant type of glial cells in the brain, are very heterogeneous cells that provide physical and metabolic support for neurons, regulate the extracellular environment of neurons, are involved in blood-flow regulation, and have a close association with the microvasculature (Jabs et al., 2008; Lanerolle et al., 2010; Verhoog et al., 2020; Borodinova et al., 2021). Microglia are involved in first-line innate immunity to the central nervous system (Carson et al., 2007; Soulet and Rivest, 2008; Yang et al., 2010; Saijo and Glass, 2011). Oligodendrocytes synthesize myelin and wrap it around axons in the central nervous system and Schwann cells—in the peripheral nervous system. Damage or loss of the myelin sheath around axons is common in many neurological disorders (Kurosinski and Götz, 2002; Barres, 2008). The NG2-glia has been identified as a progenitor for mature oligodendrocytes within the oligodendrocyte lineage. NG2-glia keep generating mature myelinating oligodendrocytes throughout lifetime. Even though these cells have been the subject of a considerable amount of research, the function of NG2-glia in epileptogenesis has not been established yet (Dimou and Gallo, 2015).

Glial cells and neurons closely interact with each other (Kurosinski and Götz, 2002; Magistretti, 2006; Barres, 2008; Allen and Barres, 2009; Xu et al., 2016). According to the concept of the tripartite synapse, perisynaptic oligodendrocytes and synaptically associated astrocytes are thought to be integral elements involved in synaptic functions (Araque et al., 1999; Figure 1). A new morpho-functional concept of the "active milieu" of the brain refers to a close interaction between compartments of neurons, astrocytes, oligodendrocytes, microglia, blood vessels, the extracellular space, and the extracellular matrix (Semyanov and Verkhratsky, 2021). Neuron–glia interactions within the active milieu are more complex than those posited in the concept of the multipartite synapse. Dysfunction of neuron–glia interactions has been recognized and well documented in various neurological diseases (Verkhratsky and Butt, 2013), in particular, in neurodegenerative diseases (Lobsiger and Cleveland, 2007; Malva et al., 2007; Kim et al., 2020), brain tumors (Yang et al., 2010; Saijo and Glass, 2011), tuberous sclerosis complex (Wong, 2019), encephalopathy (Hamid et al., 2018), and epilepsy (Pollen and Trachtenberg, 1970; Glötzner, 1973; Bordey and Sontheimer, 1998; O'Connor et al., 1998; Heinemann et al., 2000; Perez Velazquez and Carlen, 2000; Steinhäuser and Seifert, 2002; D'Ambrosio, 2004; Tian et al., 2005; Binder and Steinhäuser, 2006; Li et al., 2007; Jabs et al., 2008; Wetherington et al., 2008; Lanerolle et al., 2010; Seifert et al., 2010; Aronica et al., 2012; Devinsky et al., 2013; Vezzani et al., 2013; Verhoog et al., 2020; Grigorovsky et al., 2021; Heuser et al., 2021; Lentini et al., 2021; Sano et al., 2021; Wang et al., 2021).

Although all glial cell types play a pivotal role in normal brain function, in this review we will focus on astrocytes, which are key homeostatic regulators in the central nervous system and play important roles in the pathophysiology of epilepsy.

According to the definition of the International League Against Epilepsy (ILAE) Commission, epilepsy is a disorder of the brain characterized by an enduring predisposition to generate epileptic seizures, and by the neurobiologic, cognitive, psychological, and social consequences of this condition (Fisher et al., 2005, 2017a,b). In addition, an epileptic seizure is a transient occurrence of signs and/or symptoms due to abnormal excessive or synchronous neuronal activity in the brain. Epilepsy has long been considered to result from a disorder of neuronal cells and neuronal circuits. This is mainly due to excessive neuronal firing (hyperexcitation) and abnormally strong synchronization in widespread neuronal populations (hypersynchronization). This idea was formulated by Ransom and Blumenfeld (2007): "*Modern neuroscience has demonstrated that seizures are the result of abnormal, synchronized paroxysms of electrical activity in a population of neurons (an epileptogenic focus) that are able to rapidly recruit other parts of the brain to share in its rhythmic, self-sustaining electrical discharge*." With this information in mind, abnormal activity of neurons has long been acknowledged as the primary source of epileptic activity. However, it has become evident that epilepsy, as a chronic disorder of the central nervous system, has been accompanied by dysfunction of glial cells and by impairment of communications between neurons and neighboring glial cells. The role of glial cells in epilepsy has attracted increasing attention over the last few decades, and many studies have shown that all types of glial cells are involved in epileptogenesis (Steinhäuser and Seifert, 2002; D'Ambrosio, 2004; Tian et al., 2005; Binder and Steinhäuser, 2006; Li et al., 2007; Jabs et al., 2008; Seifert et al., 2010; Steinhäuser et al., 2012; Grigorovsky et al., 2021; Heuser et al., 2021; Sano et al., 2021). A deeper understanding of the relationship between glial cells and epilepsy may provide insights into developing novel anti-seizure and anti-epileptogenic therapies (Brennan and Henshall, 2020; Peterson and Binder, 2020; Verhoog et al., 2020).

The clinical diagnosis of epilepsy relies on a detailed medical history and results of a thorough diagnostic evaluation (Fisher et al., 2017a; Devinsky et al., 2018). The classification of epilepsies considers clinical signs (semiology) of seizures as well as the underlying cause (etiology) of seizures. This review follows an etiology-based approach to epilepsy classification and extends this approach to astrocyte-related mechanisms. Considering the fact that changes in astrocytic functions may account for clinical signs of epilepsy, this review aims to bridge the gap between clinical and basic studies of epileptic disorders.

2. The etiologic categories of epilepsy

Major advances in molecular biology, cell biology, biochemistry, gene/protein functions contribute to a better understanding of underlying causes (or the etiologic basis) of epilepsy. The etiological classification of epilepsies was proposed based on epilepsies with genetic origins, epilepsies with structural/metabolic causes, and epilepsies of unknown cause (Berg et al., 2010). Then, in 2017, the International League Against Epilepsy (ILAE) Commission on Classification and Terminology defined six etiological categories: structural/metabolic/immune/infectious, genetic, and unknown (Fisher et al., 2017b; Scheffer et al., 2017). In this review, we will address structural/metabolic/immune/infectious and genetic etiological concepts. Nevertheless, the unknown etilogical category has not been addressed in this review because the concept has not been well defined.

1. Structural/metabolic/infectious/immune: Conceptually, there is a distinct other structural or metabolic condition or disease that has been demonstrated to be associated with a substantially

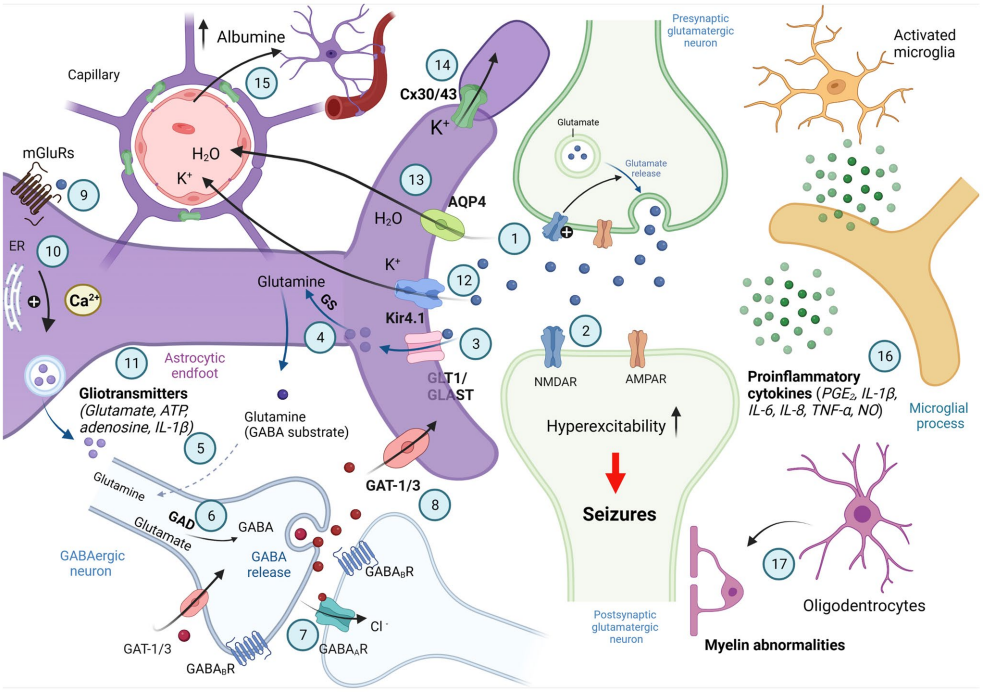

FIGURE 1
Involvement of astrocytes in synaptic excitability. Schematic illustration of signaling between astrocytes and neurons associated with active control of astrocytes of neuronal activity; synaptic neurotransmission is shown by two active synapses: one glutamatergic (light green) and the nother synapse is GABAergic (bottom); parts of reactive astrocytes shown as activated microglia and oligodentrocytes. Generated action potentials in the pre-synaptic glutamatergic neuron results in the excocytotic synaptic release of the neurotransmitter glutamate (1). Glutamate activates AMPA and NMDA receptors in the post-synaptic glutamatergicneuron, and excitatory postsynaptic potential is generated by influx of Na^+ and Ca^{2+} (2). Glutamate is taken up into astrocytes by the EAAT-1 and EAAT-2 transporters localized on the astrocytic membranes (GLAST and GLT-1 in rat; 3) and converted to glutamine by glutamine synthetase (GS; 4). Glutamine is taken up by GABAergic neurons (5) where it is converted to glutamate by glutaminase and then to GABA by glutamic acid decarboxylase (GAD; 6). When released from presynaptic vesicles into the synaptic cleft, GABA diffuses across and binds to postsynaptic $GABA_A$ and $GABA_B$ receptors. It may also bind to presynaptic $GABA_B$ receptors. GABA binds to specific recognition sites on the $GABA_A$ receptor, and this triggers a conformational change leading to opening of the intrinsic anion channel allowing chloride ions to flow through into the cell, resulting in hyperpolarization of the neuron (7). GABA is removed from the synaptic cleft into surrounding astrocytes or the presynaptic terminal by GABA transporters (GAT; 8). Neurotransmitters released by depolarized neurons activate the astrocytic G protein-coupled receptors (GPCRs; 9). The GPCRs activate the phospholipase C/inositol 1,4,5-triphosphate (PLC/IP3)-mediated pathway for the release of Ca^{2+} from intracellular calcium stores, such as the endoplasmatic reticulum (ER), resulting in an increase in intracelluar Ca^{2+} (10), intracellular Ca^{2+} elevations in astrocytes stimulate gliotransmitter release (11) that can influence neuronal excitability. K^+ released from neurons enters astrocytes via inward rectifying K^+ channels (Kir 4.1) and is distributed into capillaries (12). The astrocytic water channel Aquaporin-4 (AQP4) mediates the flow of water between the extracellular space and the blood to maintain osmotic balance (13). Astrocytes are connected to each other via gap junction channels composed of connexin 30 (Cx30) and connexin 43 (Cx43), which mediates spatial buffering of K^+ ions (14). Associated with the breakdown of the blood–brain barrier or with changes in blood flow and extravasation of molecules such as albumin microglia are activated (15). Activated microglia release proinflammatory cytokines involved in neuroinflammation and reactive gliosis (16). Oligodendrocytes and abnormalities in myelination of postsynaptic neuron are also involved in control of synaptic excitability (17; Created with BioRender.com).

increased risk of developing epilepsy in appropriately designed studies. Structural lesions of course include acquired disorders, such as stroke, trauma, and infection. They may also be of genetic origin (e.g., tuberous sclerosis, many malformations of cortical development); however, as we currently understand it, there is a separate disorder interposed between the genetic defect and the epilepsy. An immune etiology is related to autoimmune-mediated central nervous system inflammation against neuronal antigens such as receptors and synaptic proteins (Lancaster and Dalmau, 2012; Scheffer et al., 2017).

2. Genetic: The concept of genetic epilepsy is that epilepsy is, as best as understood, the direct result of a known or presumed genetic defect(s) in which seizures are the core symptom of the disorder. The knowledge regarding the genetic contributions may derive from specific molecular genetic studies that have been well replicated and even become the basis of diagnostic tests (e.g., SCN1A and Dravet syndrome) or the evidence for a central role of a genetic component may come from appropriately designed family studies. Designation of the fundamental nature of the disorder as genetic does not exclude the possibility that environmental factors (outside the individual) may contribute to the expression of disease.
3. Unknown cause: Unknown is meant to be viewed neutrally and to designate that the nature of the underlying cause is as yet unknown; it may have a fundamental genetic defect at its core or it may be the consequence of a separate as yet unrecognized disorder.

Astrocytes are the most abundant cells in the central nervous system (Araque et al., 1999; Kettenmann and Ransom, 2004a; Volterra and Meldolesi, 2005; Allen and Barres, 2009; Kaur and Ling, 2013; Verhoog et al., 2020; Borodinova et al., 2021). Astrocytes play a crucial

role in neuronal development and the anatomical and functional organization of neural circuits. More specifically, astrocytes are involved in neurogenesis and synaptogenesis, in maintaining extracellular ion balance, in controlling neuronal excitability, and in controlling the permeability of the blood–brain barrier (Araque et al., 1999; Angulo et al., 2004; Wallraff et al., 2006; Allen, 2013; Harada et al., 2016; Verhoog et al., 2020). They regulate synaptic transmission between the presynaptic and postsynaptic neurons, thus modulating synaptic transmission as the third part of the tripartite synapse (Araque et al., 1999; Xu et al., 2016). Astrocytes communicate with each other via gap junctions that permit direct cell–cell transfer of ions and small molecules (i.e., metabolites, catabolites, and second messengers). Upon the gap junctions, the calcium wave propagates from astrocyte to astrocyte (Figure 1). In addition, the membranes of astrocytes contain specific transport proteins involved in neurotransmitter reuptake from synaptic clefts (glutamate, GABA, and glycine). Apart from controlling the ionic environment of the neuropil and controlling the supply of neurotransmitters to synapses, astrocytes can directly activate neuronal receptors by releasing chemical transmitters called "gliotransmitters." These include peptides, chemokines, and cytokines (Halassa and Haydon, 2010; Seifert et al., 2010; Devinsky et al., 2013; Vezzani et al., 2013; Harada et al., 2016; Verhoog et al., 2020; Figure 1). Halassa et al. (2007) introduced the concept of the "astrocyte activation spectrum," in 2007, suggesting that enhanced gliotransmission might contribute to epilepsy, and reduced gliotransmission—to schizophrenia. Astrocytes effectively modulate synaptic transmission between neurons and the extracellular environment through the release of gliotransmitters (such as glutamate, d-serine, and ATP). In normal conditions, astrocytes are in a constant state in the neuronal circuits. However, insults to the nervous system in various pathological contidions shift their function to an "activated state." This process is called "*reactive astrogliosis*," and it is a key feature of the epileptic focus in both humans and experimental conditions (Binder and Steinhäuser, 2021). The multiple mechanisms by which astrocytes contribute to epilepsy will be examined in further detail in the next sections of this review, following an etiology-based approach.

3. The role of astrocytes in structural/metabolic/infectious/immune epilepsy

Structural/metabolic/infectious/immune epilepsies (Table 1) are caused by external/environmental/internal factors (such as perinatal/infantile causes, cerebral trauma, cerebral infection, hippocampal sclerosis, cerebral tumor, cerebrovascular disorder, cerebral immunologic disorder, degenerative, and other neurologic conditions). Temporal lobe epilepsy (TLE) is the most common epilepsy syndrome of acquired epilepsy that received the closest attention and is characterized by the prominent dysfunction of astrocytes (Ransom and Blumenfeld, 2007; Wetherington et al., 2008; Verhoog et al., 2020). Studies from TLE patients and related animal models have demonstrated the role of astrocytes in the onset and development of TLE. According to these studies, astrocyte dysfunction contributes to neuronal hyperexcitation, neurotoxicity, and epileptogenesis, or the seizure spread (Steinhäuser et al., 2012). Reactive astrogliosis in response to the initial insult, is frequently prominent and almost always coexists with hippocampal sclerosis, which is the most common histopathological finding in TLE (Twible et al., 2021). Proposed mechanisms of astrocyte involvement in structural/metabolic/infectious/immune epilepsy particularly in TLE will be summarized below.

3.1. Glutamate

In neurons, glutamate is the principal excitatory neurotransmitter, playing a key role in the initiation and spread of epileptic activity. Both neurons and astrocytes are capable of releasing glutamate (neurotransmitter and gliotransmitter, respectively; Harada et al., 2016). Astrocytes are known to be involved in many glutamate-mediated activities: glutamate synthesis, reuptake of released glutamate, and disposal of excess glutamate (Hertz and Zielke, 2004; Halassa and Haydon, 2010; Xu et al., 2016). As a part of the tripartite synapse, astrocytes can sense neural activity *via* metabotropic and ionotropic glutamate receptors. Once glutamate binds to an astrocytic metabotropic glutamate receptors (mGluRs), the astrocyte's second messenger systems are activated. Activation of mGluR3 affects cAMP accumulation, and activation of mGluR5 leads to an increase in intracellular Ca^{2+} (Binder and Steinhäuser, 2006). The initiation and the propagation of Ca^{2+} waves within the astrocytic network may induce glutamate release from astrocytes mediated by Ca^{2+}-dependent ion channels (Araque et al., 1999; Devinsky et al., 2013; Figure 1). Astrocytic glutamate may directly excite neighboring neurons and contribute to seizure generation (Kang et al., 2005). Electron-microscopic and immunohistochemical inspection of sclerotic hippocampal tissue from TLE patients revealed expression of mGluR2/3, mGluR4, mGluR5, and mGluR8 in reactive astrocytes, suggesting an involvement of these receptors in gliosis (see Binder and Steinhäuser, 2006; Lanerolle et al., 2010). Astrocytic mGluRs are upregulated in patients with mesial temporal sclerosis and with focal cortical dysplasia as a compensatory response to prevent seizures (see Lanerolle et al., 2010; Devinsky et al., 2013). Peterson and Binder (2020) published a review in 2020, in which they summarized the current knowledge regarding the astrocytic mGluRs in human TLE and animal models.

Secondly, astrocytic ionotropic glutamate receptors are also involved in the processes of epileptogenesis, as it has been shown in many studies (reviewed in Binder and Steinhäuser, 2006). Changes in the GluR1 and GluR2 subunits of AMPA receptors have been found in sclerotic hippocampi in patients with TLE. More specifically, an elevated flip-to-flop mRNA ratio of the GluR1 splice variant in reactive astrocytes may associate with an increase in responsiveness of these astrocytes to glutamate (see Binder and Steinhäuser, 2006; Lanerolle et al., 2010).

Glutamate transporters are expressed by several types of neurons and glia, but astrocytes are primarily responsible for glutamate uptake (Peterson and Binder, 2020). Glutamate transporters rapidly remove excess glutamate from the extrasynaptic space, resulting in termination of synaptic events and preventing excitotoxic injury of neurons (reviewed by Ransom and Blumenfeld, 2007; Verhoog et al., 2020). Astrocytes express Na^{+}-dependent glutamate transporters, such as glutamate transporter-1 (GLT-1) and glutamate aspartate transporter (GLAST; Figure 1). GLT-1 is responsible for ~90% of glutamate uptake in the adult dorsal forebrain and is crucial for the maintenance of low extracellular glutamate to permit efficient synaptic transmission (reviewed by Peterson and Binder, 2020). Downregulation of GLT-1 protein levels has been observed in the kainic acid-induced seizure

TABLE 1 Involvement of astrocytes in different etiologic categories of epilepsy (in patients with epilepsy and in animal models of epilepsy).

Etiologic category of epilepsy	Cell type	Functioning	References
Genetic	Astrocytes	Malfunction of the astrocytic GABA, transporter GAT-1	Crunelli et al. (2011)
		Lower expression of glutamate transporter (GLUT-1), increased expression of GFAP, and increased glutamine-glutamate cycle	Dutuit et al. (2002); Melø et al. (2006); Çavdar et al. (2019)
		Gap junction proteins (Cx30/43)	Çavdar et al. (2021)
		Induction of IL-1β in GAERS rats genetic absence epilepsy rats from strasbourg	Akin et al. (2011)
		In tuberous sclerosis: astrogliosis, changes in morphology, increased GFAP	Wong (2019)
		In focal cortical dysplasia: upregulation of astroglial metabotropic receptors mGluRs	Devinsky et al. (2013)
Structural/metabolic/ immune/infectious	Astrocytes	Activation of astrocytes	Tian et al. (2005); Devinsky et al. (2013); Sano et al., (2021)
		Glutamate: upregulation of astroglial metabotropic receptors mGluRs	Lanerolle et al. (2010); Devinsky et al. (2013); Peterson and Binder (2020)
		Glutamate: alterations in astroglial ionotropic receptor GluR1	Binder and Steinhäuser (2006)
		Glutamate: dysregulation of astrocytic glutamate transporters, GLT-1, and GLAST	Binder and Steinhäuser (2006); Peterson and Binder (2020)
		Potassium: downregulation of astroglial Kir4.1, and imbalance of normal extracellular potassium homeostasis	Ransom and Blumenfeld (2007); Kinboshi et al. (2020)
		Gliosis: proliferation of astroglia	Losi et al. (2012); Zamanian et al. (2012); Binder and Steinhäuser (2006)
		Electrolyte imbalance and osmolality: reduced expression of astroglial AQP4 and swelling of astrocytes	Binder et al. (2012); Murphy et al. (2017)
		BBB. Dysfunction of the BBB lead to epileptogenesis via astroglial TGF-bR	Ivens et al. (2007); Heinemann et al. (2012)
		Gap junctional contacts: enhanced astrocyte-astrocyte coupling mediated by proteins connexin-43 and connexin-30	Wallraff et al. (2006); Nagy and Rash (2000); Walrave et al. (2020)
		Gap junctional contacts: selective inhibition of astrocytic gap junctions suppress synchronization over astrocytic syncytium providing an anti-epileptic effect	Volnova et al. (2022)

GABA, gamma-aminobutyric acid; GAERS rats, genetic absence epilepsy rats from strasbourg; GFAP, glial-fibrillary acidic protein; mGluRs, metabotropic glutamate receptors; GluR1, ionotrotic glutamate receptor; GLT-1, astroglial glutamate transporter 1; GLAST, astroglial glutamate aspartate transporter; Kir4.1, inwardly rectifying K+ channels; AQP4, aquaporin-4 water channels; BBB, blood–brain barrier; TGF-bR, astroglial growth factor b receptor; TNF-α, tumor necrosis factor; IL-1β, interleukin 1β; and IL-6, interleukin 6.

mouse model (i.e., a pharmacological model of TLE). GLT-1 levels have been shown to have decreased levels in the hippocampus of TLE patients with hippocampal sclerosis (Peterson and Binder, 2020). Sha et al. (2017) demonstrated that upregulation of GLT-1 protein level had antiepileptic effects in the kainic acid model of TLE and in knockout mouse model of tuberous sclerosis complex ($T_{SC}1^{GFAP}$CKO mice). These authors showed that the substance 17AAG prevented degradation of GLT-1 by disrupting the association between Hsp90β and GLT-1. A reduction in the astrocytic glutamate transporter GLT-1 could have therapeutic potential for the treatment of epilepsy. Supporting this hypothesis, a novel mechanism of action on astrocytic GLT-1 has been described for gabapentin as an anti-seizure drug (Yoshizumi et al., 2012). *In vitro* and *in vivo* results confirmed that gabapentin increases extracellular glutamate by astroglial glutamate transporter-mediated mechanisms (Yoshizumi et al., 2012; Suto et al., 2014).

In addition to GLT-1 and GLAST, the cystine/glutamate exchanger (xCT; encoded by SLC7A11), which transports a cystine inside while exchanging for glutamate. This contributes to astrocyte glutamate release (Cuellar-Santoyo et al., 2023). The SLC7A11/xCT is an essential sodium-dependent glutamate transporter that is crucial for determining ambient glutamatergic concentration in the central nervous system (Augustin et al., 2007). Its expression occurs mainly in astrocytes (Ottestad-Hansen et al., 2018). SLC7A11/xCTprotein expression was elevated in about 50% of patient tumors, associated with faster growth, peritumoral glutamate excitotoxicity, seizures, and decreased survival. The use of sulfasalazine, an xCT inhibitor decreased the glutamate release from the tumor (Robert et al., 2015). Supporting this clinical data, sulfasalazine reduced the NMDA-induced current by 66.8% in mouse hippocampus slices (Koh et al., 2022) and decreased neuronal hyperexcitability *in vitro* (Alcoreza et al., 2019). Also, intraperitoneal administration of sulfasalazine

significantly reduced seizure burden in beta-1 integrin knockout mice, a model of astrogliosis-mediated epilepsy *in vivo* (Alcoreza et al., 2022). These data suggest that selective targeting of glia-associated molecular mechanisms of glutamate transport may be an effective pharmacological strategy to ameliorate tumor-associated seizures and develop novel anti-seizure drugs.

3.2. Gamma-aminobutyric acid

Tonic GABA release from astroctyes mediated by the reverse action of glial GABA transporter (GAT) subtypes, maintains the excitation/inhibition (E/I) balance within the central nervous system. The activity of the glutamate transporter triggers the reversal of GABA transporters through increasing astrocytic Na^+ concentration. Then, GABA causes tonic inhibition in a network activity-dependent way. This is an example of an *in situ* negative feedback mechanism by which astrocytes convert the glutamatergic excitation to GABA-ergic inhibition for modifying the excitability of neurons (Héja et al., 2012). Studies in experimental models of TLE reported that GABA released by reactive astrocytes from Bestrophin-1 channels strongly contributes to the compensatory shift of E/I balance in epileptic hippocampi. The tonic release of GABA from astrocytes is one of the key mechanisms by which astrocytes control epileptic seizures (Crunelli et al., 2011; Muller et al., 2020; Goisis et al., 2022). By modulating tonic GABA release from astrocytes, it might be possible to target epileptic seizures and other neurological disorders (Muller et al., 2020; Pandit et al., 2020).

3.3. Potassium

Astrocytes control neuronal hyperexcitability by regulating the release of K^+ ions from neurons into the extracellular space during action potentials. During neuronal hyperactivity, the extracellular [K^+] may increase from a resting level of around 3 mM to a ceiling of 10–12 mM and be taken up by astrocytes (Binder and Steinhäuser, 2006). The K^+ reuptake process is mediated by the inwardly rectifying K^+ channels (Kir channels) and other astrocyte K^+ transporters. Among the Kir channels (Kir1-Kir7), the subtype Kir4.1 has been most thoroughly investigated in brain astrocytes. Structural epilepsy with hippocampal sclerosis is known to be accompanied by a downregulation of Kir4.1 and a derangement of normal extracellular potassium homeostasis (Ransom and Blumenfeld, 2007). Kitaura et al. (2018) reported impairment of the potassium buffering system in astrocytes in mesial temporal lobe epilepsy. They suggested that a decreased activity of Kir4.1 channels in astrocytes induced hyperexcitability in the subiculum in sclerotic hippocampus.

Recently, the role of astrocytic Kir4.1 channels in epileptogenesis has been evaluated by Kinboshi et al. (2020) who concluded that reduction of Kir4.1 channels resulted in elevation of the level of extracellular K^+ and of the level of synaptic glutamate, and this facilitated the expression of brain-derived neurotrophic factor (BDNF) in astrocytes. BDNF is a key mediator of epileptogenesis that mediates synaptic plasticity, neuronal sprouting, neurogenesis and reactive astrogliosis (Scharfman, 2005; Ohno et al., 2018). BDNF is expressed in both pyramidal neurons and astrocytes (Saha et al., 2006). BDNF expression was upregulated in both neurons and astrocytes during epileptogenesis (Thomas et al., 2016). These findings support the concept that inhibition of Kir4.1 channels, which occurs under certain epileptic conditions, facilitates BDNF expression in astrocytes. The astrocytic Kir4.1-BDNF system has the potential to serve as a novel target for the treatment of epilepsy (Kinboshi et al., 2020). On top of that, growing evidence suggest the potential impact of astroglial functions through other neuromodulatory inputs such as endocannabinoid signaling (Eraso-Pichot et al., 2023).

Astrocytic K^+ buffering mediated by Na^+/K^+/ATPase is also critically involved in seizure susceptibility. In a model of focal cortical dysplasia (FCD) in rats, Zhao et al. (2022) found that *"the astrocytic Na^+/K^+/ATPase-mediated buffering of K+ contributes to activity-dependent inhibition of hyperexcitable pyramidal neurons during seizure and can attenuate neocortical seizures."* In this study, optogenetic activation of astrocytes exhibited anti-seizure effect on neocortical seizures following cortical kainic acid injection, in a Na^+/K^+/ATPase dependent manner (Zhao et al., 2022). The authors concluded that optogenetic control of astrocytic Na^+/K^+/ATPase activity can be considered as a promising therapeutic approach for the treatment of epilepsy. These experiments demonstrate that astrocytes can effectively control both seizure initiation and seizure spread.

3.4. Electrolyte imbalance and osmolality

Astrocytes are known to form the glymphatic system, or "pseudo-lymphatic" perivascular network, distributed throughout the brain (Reddy and van der Werf, 2020). The glymphatic system contributes to the transport of nutrients and signaling molecules into the brain parenchyma, meanwhile, promoting the clearance of proteins and interstitial waste solutes out of the brain (Natale et al., 2021). The glymphatic pathway is known to be impaired in different neurological pathologies, mainly neurodegenerative diseases (Alzheimer's disease), neurovascular disorders (hemorrhagic and ischemic), and other acute degenerative processes (normal pressure hydrocephalus or traumatic brain injury; Natale et al., 2021). In regard to the glymphatic system, changes in the aquaporin-4 (AQP4) water channels have been less clear, considering the following works: Eid et al. (2005), Binder et al. (2012), Peixoto-Santos et al. (2017), and Tice et al. (2020). These channels are located primarily on the astrocytic end-feet and are actively engaged in the circulation of interstitial and cerebrospinal fluids through the arterial perivascular spaces (Tice et al., 2020). The glial AQP4 plays an important role in modulating brain excitability and epilepsy, as reviewed by Binder and co-authors (Binder et al., 2012). These authors concluded: "*while many questions remain unanswered, the available data indicate that AQP4 and its molecular partners may represent important new therapeutic targets.*"

Another important issue is volume regulation in astrocytes. Cells may be swollen or shrunken by osmotic stress and return to their original volume even in the continued presence of the osmotic stress (Murphy et al., 2017). In animal models of structural epilepsy (i.e., induced by injections of pentilentetrazol, PTZ or electrical stimulation of hippocampus) astrocyte swelling was observed through specific targeting of AQP4 or Kir4.1 (see Murphy et al., 2017). Genetic mutations in the gene KCNJ10, which encodes Kir4.1, is known to cause seizures in humans (see Boni et al., 2020).

3.5. Blood–brain barrier

Astrocytes are key players in buffering neurons from the harmful effects of the bloodstream, such as oxidative stress and toxic chemicals. Astrocytes also form part of the blood–brain barrier (BBB) as the outer wall of the brain capillary endothelium is enclosed by pericytes and astrocyte end feet, anatomically assembled to guarantee barrier functions (Giannoni et al., 2018). The integrity of the BBB is impaired during epileptogenesis (Friedman et al., 2009). The primary dysfunction of the BBB is a hallmark of brain insults and brain inflammation, in which microglia play a major role (see below), and astrocytes are also responsible for some epileptogenic processes (Heinemann et al., 2012). Ivens et al. (2007) in a rat model confirmed the role of astrocytes in epileptogenesis after BBB opening and before development of epileptiform activity. In particular, they showed that "*epileptogenesis in the BBB-disrupted brain seems to be mediated by exposure of the brain cortex to serum albumin, mediated via its action on brain astrocytes*" (cited by Friedman et al., 2009). In addition, they also reported (Ivens et al., 2007) a cascade of events during this window period of epileptogenesis, and identified transforming growth factor b receptor (TGF-bR) as a key player in the cellular response resulting in abnormal accumulation of extracellular potassium and consequent activation of NMDA receptors. Therefore, amelioration of neural injury caused by disruption of BBB may be achieved via targeting the TGF-bRs.

Perivascular astrocytes are central to the structural and functional changes of the microvasculature in epilepsy through their combination of the roles in maintaining the BBB integrity and release of pro-inflammatory cytokines (including vascular endothelial growth factor, IL-1β, HMGB-1, and TNF), chemokines such as C-C motif ligand 2 (CCL2) as well as downstream effectors, which also activate receptors on pericytes and endothelial cells of microvessels (Giannoni et al., 2018; Yamanaka et al., 2021a). As a consequence of this neuroinflammatory state, peripheral immune cells, including monocytes, B and T cells, and neutrophils infiltrate into the brain and activate resident microglia (Yamanaka et al., 2021b). Experimental data demonstrated that infiltration of peripheral cells into the brain promote brain inflammation and exacerbate neuronal damage after status epilepticus (SE; Varvel et al., 2016). An increased expression of CCL2 which is an especially potent chemoattractant for cells of monocytic lineage (including macrophages, monocytes, and microglia) was observed in the astrocytes of the epileptic human and rat brain (Bozzi and Caleo, 2016; Broekaart et al., 2018). Supporting that, blocking the blood-derived cell invasion into the brain by knocking out CCR2, a receptor for CCL2 that affects monoycte migration, attenuated neuronal damage and suppress seizures in SE models (Varvel et al., 2016) and by knocking out of T and B cells leads to a decline in seizure activity in kainite model of (TLE) (Zattoni et al., 2011). Human data also revealed that seizure frequency was correlated with the number of infiltrating peripherally activated monocytes, but not microglia in intractable pediatric epilepsy (Xu et al., 2018). Experimental and human data supports the interplay among the astrocytes, microglia, and peripheral monocytes that can affect epileptogenesis and may lead to progression of epilepsy via increased leakage of the BBB. Neverthless, current understanding of this crosstalk between the microglia, blood-derived infiltrating cells, and astrocytes is still limited and relative importance of infiltrated cell types in epileptogenic process remain to be determined. Further studies needed to better understand the importance of the role of microglia and blood-derived-infiltrating monocytes and (perivascular) macrophages in the crosstalk with astrocytes and whether specific manipulations of this interaction can modify or prevent epileptogenesis. Rossi et al. (2017) have demonstrated that subacute treatment with gabapentin initiated immediately after the initial insult during the early latency period, successfully reduced reactive gliosis, macrophage infiltration and increased convulsive threshold in the long-term in post-SE model of pilocarpine. These results suggest that subsequent blood-derived macrophage interaction with resident microglia and astrocytes probably has an additional role on the microglial and astroglial activation during the latency period in acquired epilepsies.

3.6. Gap junctional contacts

Intercellular contacts between astrocytes have the nature of gap junctions (Nagy and Rash, 2000; Steinhäuser et al., 2012; Stephan et al., 2021). Astrocytes (and oligodendrocytes) form a non-synaptic communication called a glial syncytium through the connexin-based gap junctions in the membranes of neighboring cells. This allow ions, metabolites, and currents to pass (Stephan et al., 2021). In the adult brain, hippocampal astrocytes express two major gap junction proteins: connexin-43 (Cx43) and connexin-30 (Cx30; Nagy and Rash, 2000). As early as in 2006, Wallraff and co-authors (Wallraff et al., 2006) examined electrophysiological properties of the hippocampus in transgenic mice with conditional deletion of Cx43 in astrocytes and additional unrestricted deletion of Cx30. It appeared that hippocampal slices from mice with coupling-deficient astrocytes displayed a reduced threshold for the generation of epileptiform events. At the same time, an unexpectedly large capacity for K^+ clearance in these mice indicated that gap junction-dependent processes only partially account for K^+ buffering in the hippocampus. Connexin-based gap junctions have a complex and ambiguous role in epilepsy (Walrave et al., 2020). It is well documented that Cx43 mRNA levels, protein expression, phosphorylation state, distribution and/or functional coupling are altered in human epileptic tissue and experimental models (Walrave et al., 2020). In addition, Cx30/Cx43-based gap junctions are necessary for trafficking nutrients to neurons and initiating of astrocytic Ca^{2+} waves and hyper-synchronization, thereby supporting a proconvulsant effect.

Recently, Volnova et al. (2022) examined the role of gap junctions in epileptic activity *in vitro* using a 4-aminopyridin pharmacological model. These authors suggested a scheme in which astrocytes interconnected by gap junctions disperse the excessive release of neuronal K^+. The astrocytes absorb K^+ through the Kir1.4 channels and releasing it into the bloodstream. Moreover, they showed that a premedication with carbenoxolone (a gap junction blocker) in a 4-aminopyridin model of epilepsy decreased the latency period of seizure, decreased total seizure duration, and prevented the development of the status epilepticus (Volnova et al., 2022). Pharmacotherapy for epilepsy could also target astrocytic gap junction regulators. Levetiracetam as a clinically approved anti-seizure drug also exerts anti-inflammatory effects on glia, including reconstitution of gap junction coupling in cultured astrocytes (Bedner et al., 2015).

3.7. Adenosine

Adenosine functions as a neuromodulator functions as an endogenous anticonvulsant in the brain, and also act as a seizure terminator (Dragunow, 1991). Adenosine has an inhibitory effect on neuronal activity mediated by the activation of G_i-protein coupled adenosine receptors express on both neuronal and glial cells (Fredholm, 2012). Astrocytes play an important role in regulating adenosine levels. Nucleoside transporters expressed on the astrocyte membrane remove the adenosine form the extracellular space and stop adenosine-mediated signaling through the metobolising enzyme adenosine kinase (ADK), which is mainly localized to astrocytes (Boison et al., 2010). ADK overexpression as a general response to astroglial activation (Boison and Aronica, 2015) is considered a neuropathological feature of temporal lobe epilepsy (Aronica et al., 2011), focal cortical dysplasia (Guo et al., 2023), and contribute to the epileptogenic process itself (Gouder et al., 2004). In line with those observations in humans, ADK inhibitors showed an antiepileptogenic property in intrahippocampal kainic acid mouse model of temporal lobe epilepsy (Sandau et al., 2019). These findings support that an adenosine augmentation approach by using either adenosine receptor agonists or ADK inhibitors might be a promising treatment strategy for drug-resistant epilepsy.

3.8. DNA methylation

Maladaptive epigenetic changes, which include methylation of DNA and acetylation of histones play a functional role in the development of epilepsy and its progression. Methylation hypothesis for epileptogenesis suggested that seizures can induce epigenetic chromatin modifications, thereby aggravating the epileptogenic condition (Kobow and Blumcke, 2011). Supporting that, experimental and clinical studies provided some evidence epigenetic processes particularly increased DNA methyltransferase activity and abnormal DNA methylation contribute to seizures and epileptogenesis (Williams-Karnesky et al., 2013; Martins-Ferreira et al., 2022). As mentioned in the previous section, dysregulation of adenosine homeostasis due to overexpression of the key adenosine-metabolizing enzyme ADK leads to exacerbation of epilepsy and a general response to astrocyte activation (Boison and Aronica, 2015). Adenosine tone can directly modulate DNA methylation *in vivo* and thereby exert additional epigenetic effects via biochemical interference with the transmethylation pathway (Williams-Karnesky et al., 2013). Through enhanced DNA methylation, maladaptive increases in ADK expression in astrocytes drive the epileptogenic process (Williams-Karnesky et al., 2013). Therefore therapeutic adenosine augmentation or ADK inhibition preventing maladaptive DNA methylation can be considered as a rational approach to prevent epileptogenesis.

In a recent study, Boni et al. (2020) showed that DNA methylation can bidirectionally modulate transcription of the gene KCNJ10 representing *"a targetable molecular mechanism for the restoring astroglial Kir4.1 expression after central nervous system (CNS) insult."* Therefore, DNA hypo- or hypermethylation of candidate genes in astrocytes might be a promising genetic targets for therapeutic intervention of epileptogenesis (Williams-Karnesky et al., 2013). DNA methylation could potentially alter astrocyte reactivity and inflammatory status through controlling the signaling transducer and activator of transcription 3 (STAT3) pathway, along with other signaling pathways (O'Callaghan et al., 2014; Neal and Richardson, 2018).

The field of epigenetics is still relatively new and particularly few studies have examined astrocyte-specific DNA methylation in neurological diseases. There are still significant gaps in knowledge regarding how epigenetic mechanisms can influence astrocytes. Despite the fact that it is obvious that astrocytes in the adult brain express the numerous proteins required for the various epigenetic pathways including DNA methylation, histone modifications, and miRNAs, suggesting that these factors could be potentially involved in the astrocyte response to inflammation and epileptogenic process.

3.9. Astrogliosis

Reactive astrogliosis is a type of astrocyte response to an initial insult such as traumatic brain injury, stroke, status epilepticus, and viral infections. These activated astrocytes then contribute to the epileptogenic process (Binder and Steinhäuser, 2021; Purnell et al., 2023). Studies in humans and experimental models demonstrate that there is a bidirectional relationship between astrocytes and neuroinflammation: reactive astrocytes release cytokines such as inter-leukin (IL)-1b, IL-6, tumor necrosis factor (TNF)-a, transforming growth factor beta (TGF)-b, and chemokines, such as monocyte chemoattractant protein-1(MCP-1), chemokine, C-C motif, ligand 2 (CCL2; Aronica et al., 2012) that amplify epileptogenic inflammatory signaling. As above mentioned, astrocytes by releasing cytokines play a significant role in peripheral inflammation induced neuroinflammation by activating neighboring cells (pericytes and endothelial cells of microvessels) and amplify the local, initial innate immune response further; and also modify BBB permeability resulting in the recruitment of immune cells from the blood circulation into the neural tissue. This leads to an amplification of the initial innate immune reaction by activating microglia, and thus supporting an adaptive immune response (Farina et al., 2007; Riazi et al., 2010). On the other hand, inflammatory cytokine and chemokine release from astrocytes can also be triggered by a variety of cytokines, chemokines, and danger signals such as high mobility group box 1 (HMGB-1). The latter can be released by reactive microglia or the microvasculature after an initial insult (Maroso et al., 2010; Eyo et al., 2017). Microglia-astrocyte crosstalk is vital for normal neuronal function (Jha et al., 2019; Matejuk and Ransohoff, 2020). Microglia typically respond first to any pathological insult in the CNS, which is followed by astrocytic activation. Molecular mechanisms of microglia-astrocyte crosstalk in the CNS health and disease attract major attention (Jha et al., 2019; Matejuk and Ransohoff, 2020; Yang et al., 2020). Molecular therapy might target epilepsy-related aberrant communications between microglia and astrocytes.

A nuclear protein, HMGB-1, received particular attention, because it has an important role in models of non-infectious inflammation, such as autoimmunity, cancer, trauma, and ischemia reperfusion injury (Klune et al., 2008). HMGB-1 is known to be released from damaged neurons after, for example, traumatic brain injuries and serves as a prognostic biomarker and therapeutic target in patients (Parker et al., 2017). Animal models of acute and chronic seizures have shown that HMGB-1 receptors are expressed after experimental seizures (Maroso et al., 2010; Rossi et al., 2017) and HMGB-1/Toll-like

receptor-4 (TLR4) signaling plays a role in generating and perpetuating seizures and might be targeted to attain anticonvulsant effects in epilepsies (Maroso et al., 2010). Supporting this, inhibiting the inflammatory cytokine HMGB-1 in CNS by using monoclonal antibodies (Fu et al., 2017) and in the periphery by systemic application of glycyrrhizin (Rosciszewski et al., 2019) reduced inflammation and has demonstrated therapeutic value in numerous electrical and chemical animal models of TLE, as well as in human tissue (Zhao et al., 2017). Additionally, inflachromene had an anti-seizure potential as a small molecule HMGB-1 inhibitor, as was shown in different animal models of epilepsy (Dai et al., 2023). HMGB-1 may also be involved in the upregulation of P-glycoproteins during status epilepticus, which is linked to drug resistance (Xie et al., 2017). These findings suggest that HMGB-1 released after the initial insult acting on astrocytes and microglia activates TLRs and its downstream signaling pathways which are proposed as key early steps in epileptogenesis (Rosciszewski et al., 2019). Thus, either HMGB-1 blockage or TLR antagonist molecules would be able to reduce neuroinflammation and may be a novel target for developing anti-seizure drugs especially for drug-resistant epilepsies or anti-epileptogenic drugs.

4. The role of astrocytes in genetic generalized epilepsies

The term "genetic generalized epilepsies (GGEs)" describes all types of generalized epilepsies with a presumed genetic basis. Idiopathic generalized epilepsies (IGEs) can be recognized as a distinct subgroup of GGEs comprised of the following syndromes: childhood absence epilepsy, juvenile absence epilepsy, juvenile myoclonic epilepsy, and epilepsy with generalized tonic–clonic seizures alone (Hirsch et al., 2022). GGEs also include epilepsy with myoclonic-atonic seizures, epilepsy with eyelid myoclonia, epilepsy with myoclonic absences, and myoclonic epilepsy in infancy (MEI or Dravet Syndrome). Latter have a genetic basis and are associated with developmental and epileptic encephalopathy (Hirsch et al., 2022).

Among IGEs, the most knowledge about glia-related mechanisms was gained from animal models of generalized non-convulsive absence epilepsy (Crunelli and Leresche, 2002). Genetic rodent models of generalized epilepsy with spontaneous spike-and-wave discharges (SWDs) on the EEG exhibit defined periods of seizure onset followed by seizure progression. Absence seizure frequency increases in an age dependent manner (Crunelli and Leresche, 2002). Astrocytes get involved in disturbances of thalamic GABA-ergic and glutamatergic neurotransmission (Crunelli et al., 2020).

The astrocytic GABA transporter has been reported to be impaired in genetic models of absence seizures (Crunelli et al., 2011). More specifically, an enhanced GABA-ergic tonic inhibition in thalamic neurons, which is required for absence seizure generation, is associated with a malfunction of the astrocytic thalamic GABA transporter-1 (GAT-1). The neuro-glial relationships relating to glutamatergic transmission are also affected in an age-dependent manner in experimental absence epilepsy models. Lower expression of glutamate transporters (GLT1 and GLAST) in cortical primary astrocytes obtained from Genetic Absence Epilepsy Rats from Strasbourg (GAERS) suggests an impairment of turnover of transporter proteins, which leads to lower levels of glutamate uptake in the cortex and thalamus of GAERS (Dutuit et al., 2000; Touret et al., 2007). Another observation is the increased expression of glial fibrillary acidic protein (GFAP) as the first sign of reactive astrocytes in genetic absence epilepsy rat models. This suggests the presence and involvement of reactive astrocytes in the epileptogenesis of non-convulsive seizures (Dutuit et al., 2000; Çavdar et al., 2019). In addition, an increased cycling of glutamate and glutamine between astrocytes and glutamatergic neurons in the cortex of GAERS indicates a dysregulation of astrocyte-neuron interactions in the thalamo-cortical loop (Melø et al., 2006, 2007; Touret et al., 2007; Onat et al., 2013; Gobbo et al., 2021).

Astrocytic gap junctions formed by connexin (Cx) 30 and Cx43 (Figure 1) are also likely to play a role the pathogenesis of absence epilepsy. Astrocytic gap junction protein expressions increased in the thalamo-cortical circuitry in rat models of absence epilepsy (Gobbo et al., 2021). *In vivo*, gap junction blocker carbeoxolone reduced absence seizures (Gigout et al., 2006; Crunelli et al., 2015; Çavdar et al., 2019).

An astrocyte-modulating agent, ONO-2506 (arundic acid), appeared to have specific anti-epileptic properties in a mouse model of non-convulsive epilpesy (Yamamura et al., 2013). ONO-2506 was discovered by Ono Pharmaceutical Co as an agent inhibiting astrocytic S-100β (i.e., acidic calcium-binding protein produced mainly by astrocytes). ONO-2506 inhibited absence epilepsy in a genetic mouse model of absence epilepsy [Cacna1atm2Nobs/tm2Nobs mice, in which the conditional calcium channel (Cacna1a) gene was knocked-down], but it did not affect maximal electroshock seizures (MES) or pentylenetetrazol-induced seizures (PTZ; Yamamura et al., 2013). In fact, ONO-2506 did not affect convulsive seizures in traditional models of epilepsy, but markedly inhibited epileptic phenomena in a genetic epilepsy mouse model. These data suggest that enhancing gliotransmitter release might be the way to go for a novel glial-targeting drugs for non-convulsive seizures (Onat, 2013; İdrizoğlu et al., 2016).

The astrocytic interleukin-mediated mechanism has been identified, again, in a genetic model of absence seizures. In GAERS, the focal epileptic zone in the somatosensory cortex is characterized by induction of interleukin (IL)-1β in activated astrocytes (Akin et al., 2011). The authors of this study suggested a specific anti-inflammatory approach by blocking IL-1β biosynthesis, which may be helpful for managing this non-convulsive form of epilepsy. Cytokine (TNF-α, IL-1β) expression was associated with the development of absence seizures. The expression of these cytokines tended to increase before the seizure onset in GAERS and WAG/Rij (Wistar Albino Glaxo rats from Rijswijk) rat models. This might be considered as a form of neuroprotection toward adaptive mechanisms linked to generalized seizure activity (Akin et al., 2011; van Luijtelaar et al., 2012). This is also in line with results showing that a specific anti-inflammatory approach, the interruption of the IL-6 signaling pathway through administration of tocilizumab, a neutralizing humanized monoclonal antibody to the IL-6 receptor reduced the development of absence seizures and depressive-like comorbidity in the GAERS model (Leo et al., 2020). In agreement with that, IL-6 and IL-8 levels in the cerebrospinal fluid fluid have indeed been linked to human childhood absence epilepsy (Billiau et al., 2007) and valproic acid treatment lowers IL-6 serum levels in children with tonic–clonic generalized seizures (Steinborn et al., 2014). In order to treat this non-convulsive form of epilepsy and its

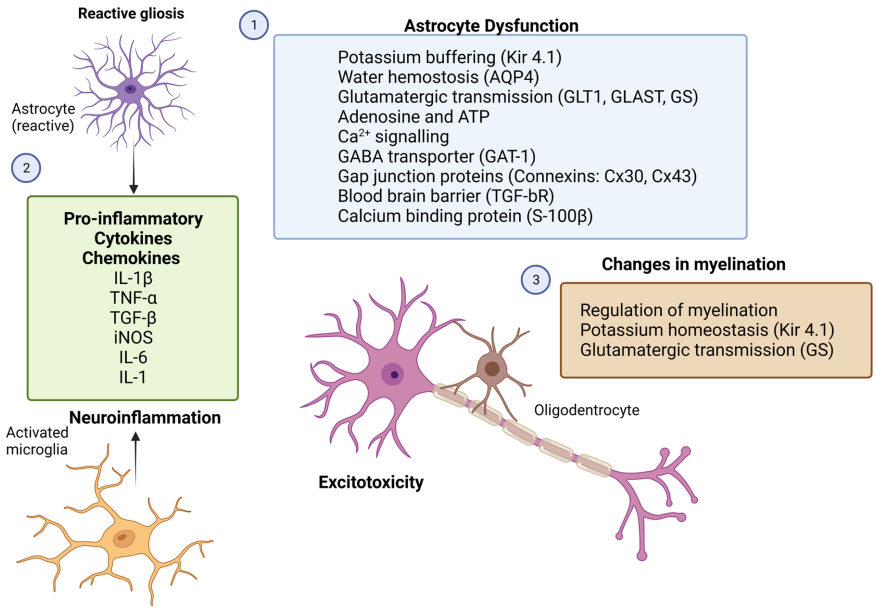

FIGURE 2
Potential therapeutic targets for glial cells in epilepsy. Rectangles with different colors represent the potential molecular candidates that can target astrocytes (1,2), microglia (2) and oligodendrocytes (3). GFAP, glial-fibrillary acidic protein; GLT-1, astroglial glutamate transporter 1; GLAST, astroglial glutamate aspartate transporter; GS, glutamine synthase; İNOS, inducible nitric oxide; Kir4.1, inwardly rectifying K+ channels; AQP4, aquaporin-4 water channels; BBB, blood–brain barrier; TGF-bR, astroglial growth factor b receptor; TNF-α, tumor necrosis factor; IL-1β, interleukin 1β; IL-1, interleukin 1; and IL-6, interleukin 6 (Created with BioRender.com).

associated neuropsychiatric comorbidities, targeting cytokines and chemokines may provide a new avenue for the development of targeted anti-epileptogenic therapies (Figure 2).

So far, evidence for linking the astroglial fine-tuning of the extracellular ion and transmitter homeostasis to absence seizures is still lacking. Yet, their involvement in controlling such network excitability is very likely, just as it is for other types of epileptiform activity. Therefore, more in-depths investigation is needed to determine the involvement of astroglial Kir4.1 channels in the occurrence of SWDs. Combining pharmacological models of absence epilepsy with cell-specific conditional knock-outs of these channels may shed new light on the subject.

Growing evidence also suggests that astrocytes are involved in the pathology of epileptic encephalopathies. Dravet syndrome (DS)or myoclonic epilepsy in infancy (MEI) is a rare, genetic epileptic encephalopathy which is linked to *de novo* loss of function mutations of the SCNA1 gene encoding for the α subunit of Nav1.1 voltage-dependent sodium channels (Claes et al., 2001). In experimental models of DS, during the development of seizures, changes in $GABA_A$ extrasynaptic receptor composition and GABA tonic currents have been recently shown to occur in parallel with an increase in microglia and astrocyte reactivity (Satta et al., 2021; Goisis et al., 2022). Moreover, GAT-1 is expressed in the nerve endings of GABAergic interneurons and astrocytes. A functional deficit in thalamic astrocytes may result in enhanced tonic inhibition in SLC6A1 variants associated with epilepsy (Mermer et al., 2022). Astrocyte reactivity was observed after the onset of spontaneous seizures in a mouse model of SCN8A encephalopathy. SCN8A encephalopathy is caused primarily by gain-of-function mutations in the neuronal sodium channel (Nav1.6) and causes severe, early-onset seizures. Reactive astrocytes have reduced Kir4.1 channel currents and reduced expression of GS protein, suggesting an impairment in K^+ ion uptake and glutamate homeostasis leading to the increase in seizure frequency in this mouse model (Thompson et al., 2022).

5. Conclusion and future directions: astroglial targets for treatment of epilepsy

Epilepsy is a chronic disorder of the central nervous system characterized not only by neuronal hyperexcitation and hypersynchronization, but also by substantial disturbances in large populations of glial cells and by impairment of neuron-glial interactions. A better understanding of glial pro-epileptic and epileptogenic mechanisms is helpful for the development of novel anti-seizure, anti-epileptogenic, and/or neuroprotective therapies. Astrocytes are the most prominent cell population within the glia, and they are deeply involved in controlling of neuronal excitability *via* releasing gliotransmitters, glutamate-dependent mechanisms (through astroglial metabotropic and ionotropic glutamate receptors), potassium-dependent mechanisms (through astroglial Kir4.1 and changes in gap junctional contacts), in controlling electrolyte balance and osmolality (through astroglial AQP4), in controlling the blood–brain barrier (through astroglial TGF-bR), regulation of blood flow and energy metabolism, and in supporting synapse formation (through the production of NG2; Figure 2). Since astrocytes involved in the variety of physiologic functions, it is not unexpected that

astrocytic dysfunction has been linked to many CNS pathologies including epilepsy. Data from experimental models and clinical studies indicate that astrocytes are both contribute to development of epilepsy (epileptogenesis) and seizure generation and recurrence (ictogenesis; Vezzani et al., 2022; Purnell et al., 2023).

In this review, we have presented the key functions of astrocytes contributing to neuronal hyperexcitability and synaptic activity following an etiology-based approach. In this part, we will analyze the role of astrocytes in both development (epileptogenesis) and generation of seizures (ictogenesis) and comment on the therapeutic strategies that attempted to modify astoglial responses in each time point of the epilepsy.

5.1. Role of astrocytes in epileptogenesis and anti-epileptogenic strategies

Epileptogenesis is a complex gradual process whereby healthy brain is transformed into an epileptic state occurring over months to years. It begins with a brain-damaging insult that triggers a cascade of molecular and cellular changes that lead to spontaneous recurrent seizures (Pitkänen and Lukasiuk, 2009; Maguire, 2016). Maguire (2016) considered the three stages of epileptogenesis: (1) the initial insult or precipitating event, (2) the latent period, and (3) the chronic epilepsy phase.

The reactive astogliosis is an essential processes of epileptogenesis during the latent period that likely to be applicable to a wide spectrum of structural epilepsies and is a hallmark of the epileptic focus in humans and experimental models (Devinsky et al., 2013; Binder and Steinhäuser, 2021). Astrocytes are known to be involved in inflammation via their interactions with microglia and other innate immune cells along with the BBB dysfunction (Vezzani and Friedman, 2011; Devinsky et al., 2013; Vezzani et al., 2013; Ismail et al., 2021). The permeability of the BBB is altered in acquired epilepsies and this alteration occurs early after the epileptogenic injury as a result of extravasation of serum albumin and activation of TGb-Rs (Friedman et al., 2009). Albumin can bind transforming growth factor beta (TGF-β) receptors in astrocytes and leads a downregulation of Kir 4.1 and AQP4 channels, which facilitates neuronal hyperexcitability during epileptogenesis (Löscher and Friedman, 2020). Pharmacological blockade of TGb-RII signaling after status epilepticus in rodents rescued some of the molecular changes in astrocytes and reduced the incidence of epilepsy (Vezzani et al., 2022). The angiotensin II type 1 receptor antagonist, losartan, blocks brain TGF-β signaling and prevents epilepsy in animal models of epileptogenesis (Bar-Klein et al., 2014; Hong et al., 2019). Moreover, the interplay among the astrocytes, microglia and peripheral monocytes may lead to progression of epilepsy via increased leakage of the BBB and can affect epileptogenesis. Immune cells in the blood such as macrophages and monocytes are highly activated after seizures. Importantly, inhibiting the chemotaxis of leukocytes across the BBB reduces the severity of seizures. Early gabapentin treatment during the latency period successfully reduced microglial reactivity, neuroinflammation, and macrophage infiltration in Lithium-Pilocarpine model of epileptogenesis (Rossi et al., 2013, 2017).

HMGB-1 as an inflammatory cytokine released after the initial insult acting on astrocytes and microglia activates TLRs and its downstream signaling pathways, which are proposed as key early steps in epileptogenesis (Rosciszewski et al., 2019). Thus, either HMGB-1 blockage or TLR antagonist molecules would be able to reduce neuroinflammation and may be a novel target for developing anti-epileptogenic drugs.

Specific anti-epileptogenic therapies in structural epilepsies may also target gliotransmission (blockage of TNF-α driven astrocyte prunergic signaling; Nikolic et al., 2018; Vezzani et al., 2022), astrocytic gap junctions (Wallraff et al., 2006; Carlen, 2012; Volnova et al., 2022), neurotrophic factors (Vezzani et al., 2013; Araki et al., 2021), the glymphatic pathway (Eid et al., 2005; Binder et al., 2012; Tice et al., 2020), microglia-astrocyte-immune system communication (Rosciszewski et al., 2019), astroglial inflammatory pathways (Wetherington et al., 2008; Vezzani and Friedman, 2011; Ismail et al., 2021), the astrocytic Kir4.1-BDNF system (Kinboshi et al., 2020), astrocytic adenosine tone by using either adenosine receptor agonists or ADK inhibitors (Boison and Aronica, 2015), and DNA hypo- or hypermethylation of candidate genes in astrocytes (Williams-Karnesky et al., 2013).

In genetic generalized epilepsies astrocyte involvement during the epileptogenesis still limited. Current data indicate that, astrocytes get involved in disturbances of thalamic GABA-ergic and glutamatergic gliotransmission during the epileptogenesis that influences thalamocortical circuitry (Crunelli et al., 2020). Reactive astrogliosis with an increased GFAP expression within the thalamocortical loop is observed in genetic rat models of absence epilepsy (Dutuit et al., 2000; Çavdar et al., 2019). Cytokine (TNF-α, IL-1β) expression was associated with the development of absence seizures and tended to increase before the seizure onset in GAERS and WAG/Rij (Wistar Albino Glaxo rats from Rijswijk) rat models (Akin et al., 2011; van Luijtelaar et al., 2012). This is also in line with results showing that a specific anti-inflammatory approach, the interruption of the IL-6 signaling pathway through administration of tocilizumab, a neutralizing humanized monoclonal antibody to the IL-6 receptor reduced the development of absence seizures and depressive-like comorbidity in the GAERS model (Leo et al., 2020). In humans, valproic acid treatment lowers IL-6 serum levels in children with tonic–clonic generalized seizures (Steinborn et al., 2014). In order to treat this non-convulsive form of epilepsy and its associated neuropsychiatric comorbidities, targeting cytokines and chemokines may provide a new avenue for the development of targeted anti-epileptogenic therapies.

5.2. Role of astrocytes in ictogenesis and anti-seizure strategies

Ictogenesis is a fast, short-term electrical/chemical event that generate recurrent seizures. At the molecular level, ictogenesis involves excessive brain electrical discharges propagated by a cascade of chemical events initiated by the transmembrane voltage gated Na + channels with subsequent involvement of K^+ channels and Ca^{2+} dependent release of neurotransmitters.

Recently, it was postulated that astrocytes play a significant role in ictogenesis. In structural epilepsies, astrocytes contribution in ictogenesis is relatively new area with limited data compared to what we know about epileptogenesis so far. However, growing evidence from experimental models and human studies suggests that reactive astrocytes play a key role in the initiation of seizures (Vezzani et al.,

2022; Purnell et al., 2023). First clue of direct contribution of astrocytes to the generation of an epileptic discharge was the glutamate release from astrocytes promotes local synchronous activity in hippocampal neurons by acting on extrasynaptic NMDA receptors (Fellin et al., 2004). *In vitro* study showed that during epileptiform activity, the frequency of Ca^{2+} oscillations in astrocytes is dramatically increased and it is reduced by anti-seizure drugs valproate, gabapentin, and phenytoin (Tian et al., 2005) suggesting that their another mechanism of action is inhibition of gliotransmission. Purinergic receptor antagonists MRS2179 and MRS2500 (Alves et al., 2019) and the Panx1 channel inhibitors probenecid and mefloquine (Dossi et al., 2018) has been shown to inhibit Ca^{2+}-mediated gliotransmission and have shown promise anti-seizure effect in experimental models. A study performed in *in vitro* model of focal seizures suggested that astrocytic Ca^{2+} elevation correlates with both the initial development and the maintenance of a ictal discharge but not interictal discharges, indicating that a recurrent excitatory loop (potentially including gliotransmission) between neurons and astrocytes increases seizure initiation and sustains the ictal discharge (Gómez-Gonzalo et al., 2010). In a recent study, optogenetic activation of astrocytes exhibited anti-seizure effect on neocortical seizures following cortical kainic acid injection, in a Na^+/K^+/ATPase dependent manner (Zhao et al., 2022). Authors investigated the anti-seizure mechanism of astrocyte stimulation and found that it was mediated by stimulation of the astrocytic Na^+/K^+/ATPase as a result of Na^+ influx independent from Ca^{2+} signaling. These findings show that astrocytes can effectively control seizure initiation as well as seizure spread.

In addition to the astrocytic gliotransmission, other astrocytic dysfunctions such as loss of astrocytic gap junction coupling, as well as the impaired K^+ clearance and glutamate homeostasis (Bedner et al., 2015), high levels of matrix metalloproteinases in astrocytes (Broekaart et al., 2021) are known to be involved in the initiation and progression of TLE.

So far, evidence showing the ictogenic involvement of astrocytes in genetic generalized epilepsies is still lacking. Observations from the rodent models of genetic absence epilepsy indicate that astrocyte modulation through inhibition of astrocytic acidic calcium-binding protein (S-100β) by a novel molecule ONO-2506 appeared to have specific anti-seizure properties in a genetic mouse model of absence epilepsy (Yamamura et al., 2013). The tonic GABA release of from astrocytes is one of the key mechanisms by which astrocytes play a key role in controlling absence seizures (Crunelli et al., 2011). Changes in GABAergic astrocyte-neuron signaling features in genetic rodent models of absence epilepsy may lead to the production of absence seizures. By modulating tonic GABA release from astrocytes, it might be possible to target absence seizures. Supporting this hypothesis putrescine which is a GABA precursor in astrocytes increased astrocytic GABA production and inhibited spontaneous SWDs in WAG/Rij rats (Kovács et al., 2022).

Despite these evidences, we are still far from understanding how astrocytes contribute to the generation of seizures, due to the many challenges in their investigation. First; astrocytes are diverse and have specific properties and functions in particular brain areas (Khakh and Deneen, 2019), second; reactive and compensatory phenotypes of astrocytes are not readily distinguishable and often coexist; third, difficult to distinguish the precise impact of astrocytes from that of neighboring neurons and fourth, individual astrocytes can even express both compensatory and pathological markers (Vezzani et al., 2022). Based on these facts we need selective tools as well as validated animal models to modulate astrocyte activity. Genetic approaches such as optogenetic, chemogenetic and Cre-technology have been largely used for selective activation or inhibition of astrocytes. Genetic mouse models generated by global and conditional gene deletion provide a platform for specifically targeting and manipulating astroctyes. There are several mouse lines, in which cre-lox system was used to conditionally delete genes in astrocytes by coupling cre with other reporters such as GFAP reporter, GLAST, or GLT-1 (Srinivasan et al., 2016). Another novel and promising alternative approach is to use viral vectors for gene delivery to astrocytes in specific brain regions (Nagai et al., 2019). Given the substantial insights made over the past decade, glial cells are attractive targets for new drug development for neurological disorders. However, there is an important challenge of delivering drugs across the BBB for targeting glial cells. Fortunately, new developments in drug delivery research can now address this challenge by describing synthetic nanoparticles that can be used for astrocyte-specific targeting, as well as developing non-invasive molecular delivery strategies that bypass the BBB including receptor-mediated transcytosis, neurotrophic viruses, and exosomes (Terstappen et al., 2021; Lee et al., 2022). All these abovementioned factors can help to understand the precise pathways by which astrocytes (and probably other glial cells) contribute to epileptogenesis and ictogenesis, and design novel therapeutic approaches that can be translated into the clinic.

Author contributions

NÇ: literature review, writing the manuscript, and drawing the figures. FO and ES: literature review and writing and editing the manuscript. All authors contributed to the article and approved the submitted version.

Funding

Research in the Onat's lab was supported by European Commission Horizon Europe Program under the call HORIZON-WIDERA-2021-ACCESS-03 (Grant Number 101078981-GEMSTONE).

Conflict of interest

The authors declare that the research was conducted in the absence of any commercial or financial relationships that could be construed as a potential conflict of interest.

Publisher's note

References

Akin, D., Ravizza, T., Maroso, M., Carcak, N., Eryigit, T., Vanzulli, I., et al. (2011). IL-1β is induced in reactive astrocytes in the somatosensory cortex of rats with genetic absence epilepsy at the onset of spike-and-wave discharges, and contributes to their occurrence. *Neurobiol. Dis.* 44, 259–269. doi: 10.1016/j.nbd.2011.05.015

Alcoreza, O., Jagarlamudi, S., Savoia, A., Campbell, S. L., and Sontheimer, H. (2022). Sulfasalazine decreases astrogliosis-mediated seizure burden. *Epilepsia* 63, 844–854. doi: 10.1111/epi.17178

Alcoreza, O., Tewari, B. P., Bouslog, A., Savoia, A., Sontheimer, H., and Campbell, S. L. (2019). Sulfasalazine decreases mouse cortical hyperexcitability. *Epilepsia* 60, 1365–1377. doi: 10.1111/epi.16073

Allen, N. J. (2013). Role of glia in developmental synapse formation. *Curr. Opin. Neurobiol.* 23, 1027–1033. doi: 10.1016/j.conb.2013.06.004

Allen, N. J., and Barres, B. A. (2009). Glia—more than just brain glue. *Nature* 457, 675–677. doi: 10.1038/457675a

Alves, M., De Diego, G. L., Conte, G., Jimenez-Mateos, E. M., D'Orsi, B., Sanz-Rodriguez, A., et al. (2019). Context-specific switch from anti- to pro-epileptogenic function of the P2Y1Receptor in experimental epilepsy. *J. Neurosci.* 39, 5377–5392. doi: 10.1523/JNEUROSCI.0089-19.2019

Angulo, M. C., Kozlov, A. S., Charpak, S., and Audinat, E. (2004). Glutamate released from glial cells synchronizes neuronal activity in the Hippocampus. *J. Neurosci.* 24, 6920–6927. doi: 10.1523/JNEUROSCI.0473-04.2004

Araki, T., Ikegaya, Y., and Koyama, R. (2021). The effects of microglia- and astrocyte-derived factors on neurogenesis in health and disease. *Eur. J. Neurosci.* 54, 5880–5901. doi: 10.1111/ejn.14969

Araque, A., Parpura, V., Sanzgiri, R. P., and Haydon, P. G. (1999). Tripartite synapses: glia, the unacknowledged partner. *Trends Neurosci.* 22, 208–215. doi: 10.1016/S0166-2236(98)01349-6

Aronica, E., Ravizza, T., Zurolo, E., and Vezzani, A. (2012). Astrocyte immune responses in epilepsy. *Glia* 60, 1258–1268. doi: 10.1002/glia.22312

Aronica, E., Zurolo, E., Iyer, A., de Groot, M., Anink, J., Carbonell, C., et al. (2011). Upregulation of adenosine kinase in astrocytes in experimental and human temporal lobe epilepsy. *Epilepsia* 52, 1645–1655. doi: 10.1111/j.1528-1167.2011.03115.x

Augustin, H., Grosjean, Y., Chen, K., Sheng, Q., and Featherstone, D. E. (2007). Nonvesicular release of glutamate by glial xCT transporters suppresses glutamate receptor clustering in vivo. *J. Neurosci.* 27, 111–123. doi: 10.1523/JNEUROSCI.4770-06.2007

Bar-Klein, G., Cacheaux, L. P., Kamintsky, L., Prager, O., Weissberg, I., Schoknecht, K., et al. (2014). Losartan prevents acquired epilepsy via TGF-beta signaling suppression. *Ann. Neurol.* 75, 864–875. doi: 10.1002/ana.24147

Barres, B. A. (2008). The mystery and magic of glia: a perspective on their roles in health and disease. *Neuron* 60, 430–440. doi: 10.1016/j.neuron.2008.10.013

Bedner, P., Dupper, A., Hüttmann, K., Müller, J., Herde, M. K., Dublin, P., et al. (2015). Astrocyte uncoupling as a cause of human temporal lobe epilepsy. *Brain* 138, 1208–1222. doi: 10.1093/brain/awv067

Berg, A. T., Berkovic, S. F., Brodie, M. J., Buchhalter, J., Cross, J. H., van Emde Boas, W., et al. (2010). Revised terminology and concepts for organization of seizures and epilepsies: report of the ILAE commission on classification and terminology, 2005-2009. *Epilepsia* 51, 676–685. doi: 10.1111/j.1528-1167.2010.02522.x

Billiau, A. D., Witters, P., Ceulemans, B., Kasran, A., Wouters, C., and Lagae, L. (2007). Intravenous immunoglobulins in refractory childhood-onset epilepsy: effects on seizure frequency, EEG activity, and cerebrospinal fluid cytokine profile. *Epilepsia* 48, 1739–1749. doi: 10.1111/j.1528-1167.2007.01134.x

Binder, D. K., Nagelhus, E. A., and Ottersen, O. P. (2012). Aquaporin-4 and epilepsy. *Glia* 60, 1203–1214. doi: 10.1002/glia.22317

Binder, D. K., and Steinhäuser, C. (2006). Functional changes in astroglial cells in epilepsy. *Glia* 54, 358–368. doi: 10.1002/glia.20394

Binder, D. K., and Steinhäuser, C. (2021). Astrocytes and epilepsy. *Neurochem. Res.* 46, 2687–2695. doi: 10.1007/s11064-021-03236-x

Boison, D., and Aronica, E. (2015). Comorbidities in neurology: is adenosine the common link? *Neuropharmacology* 97, 18–34. doi: 10.1016/j.neuropharm.2015.04.031

Boison, D., Chen, J.-F., and Fredholm, B. B. (2010). Adenosine signaling and function in glial cells. *Cell Death Differ.* 17, 1071–1082. doi: 10.1038/cdd.2009.131

Boni, J. L., Kahanovitch, U., Nwaobi, S. E., Floyd, C. L., and Olsen, M. L. (2020). DNA methylation: a mechanism for sustained alteration of KIR4.1 expression following central nervous system insult. *Glia* 68, 1495–1512. doi: 10.1002/glia.23797

Bordey, A., and Sontheimer, H. (1998). Properties of human glial cells associated with epileptic seizure foci. *Epilepsy Res.* 32, 286–303. doi: 10.1016/S0920-1211(98)00059-X

Borodinova, A. A., Balaban, P. M., Bezprozvanny, I. B., Salmina, A. B., and Vlasova, O. L. (2021). Genetic constructs for the control of astrocytes' activity. *Cells* 10:1600. doi: 10.3390/cells10071600

Bozzi, Y., and Caleo, M. (2016). Epilepsy, seizures, and inflammation: role of the C-C motif ligand 2 chemokine. *DNA Cell Biol.* 35, 257–260. doi: 10.1089/dna.2016.3345

Brennan, G. P., and Henshall, D. C. (2020). MicroRNAs as regulators of brain function and targets for treatment of epilepsy. *Nat. Rev. Neurol.* 16, 506–519. doi: 10.1038/s41582-020-0369-8

Broekaart, D. W. M., Anink, J. J., Baayen, J. C., Idema, S., de Vries, H. E., Aronica, E., et al. (2018). Activation of the innate immune system is evident throughout epileptogenesis and is associated with blood-brain barrier dysfunction and seizure progression. *Epilepsia* 59, 1931–1944. doi: 10.1111/epi.14550

Broekaart, D. W., Bertran, A., Jia, S., Korotkov, A., Senkov, O., Bongaarts, A., et al. (2021). The matrix metalloproteinase inhibitor IPR-179 has antiseizure and antiepileptogenic effects. *J. Clin. Invest.* 131:e138332. doi: 10.1172/JCI138332

Carlen, P. L. (2012). Curious and contradictory roles of glial connexins and pannexins in epilepsy. *Brain Res.* 1487, 54–60. doi: 10.1016/j.brainres.2012.06.059

Carson, M. J., Bilousova, T. V., Puntambekar, S. S., Melchior, B., Doose, J. M., and Ethell, I. M. (2007). A rose by any other name? The potential consequences of microglial heterogeneity during CNS health and disease. *Neurotherapeutics* 4, 571–579. doi: 10.1016/j.nurt.2007.07.002

Çavdar, S., Köse, B., Sur-Erdem, İ., and Özkan, M. (2021). Comparing astrocytic gap junction of genetic absence epileptic rats with control rats: an experimental study. *Brain Struct. Funct.* 226, 2113–2123. doi: 10.1007/s00429-021-02310-y

Çavdar, S., Kuvvet, Y., Sur-Erdem, I., Özgür, M., and Onat, F. (2019). Relationships between astrocytes and absence epilepsy in rat: an experimental study. *Neurosci. Lett.* 712:134518. doi: 10.1016/j.neulet.2019.134518

Claes, L., Del-Favero, J., Ceulemans, B., Lagae, L., Van Broeckhoven, C., and De Jonghe, P. (2001). De novo mutations in the Sodium-Channel gene SCN1A cause severe myoclonic epilepsy of infancy. *Am. J. Hum. Genet.* 68, 1327–1332. doi: 10.1086/320609

Crunelli, V., Carmignoto, G., and Steinhäuser, C. (2015). Novel astrocyte targets: new avenues for the therapeutic treatment of epilepsy. *Neuroscientist* 21, 62–83. doi: 10.1177/1073858414523320

Crunelli, V., Cope, D. W., and Terry, J. R. (2011). Transition to absence seizures and the role of GABA a receptors. *Epilepsy Res.* 97, 283–289. doi: 10.1016/j.eplepsyres.2011.07.011

Crunelli, V., and Leresche, N. (2002). Childhood absence epilepsy: genes, channels, neurons and networks. *Nat. Rev. Neurosci.* 3, 371–382. doi: 10.1038/nrn811

Crunelli, V., Lőrincz, M. L., McCafferty, C., Lambert, R. C., Leresche, N., Di Giovanni, G., et al. (2020). Clinical and experimental insight into pathophysiology, comorbidity and therapy of absence seizures. *Brain* 143, 2341–2368. doi: 10.1093/brain/awaa072

Cuellar-Santoyo, A. O., Ruiz-Rodríguez, V. M., Mares-Barbosa, T. B., Patrón-Soberano, A., Howe, A. G., Portales-Pérez, D. P., et al. (2023). Revealing the contribution of astrocytes to glutamatergic neuronal transmission. *Front. Cell. Neurosci.* 19:1037641. doi: 10.3389/fncel.2022.1037641

D'Ambrosio, R. (2004). The role of glial membrane ion channels in seizures and epileptogenesis. *Pharmacol. Ther.* 103, 95–108. doi: 10.1016/j.pharmthera.2004.05.004

Dai, S.-J., Shao, Y.-Y., Zheng, Y., Sun, J.-Y., Li, Z.-S., Shi, J.-Y., et al. (2023). Inflachromene attenuates seizure severity in mouse epilepsy models via inhibiting HMGB1 translocation. *Acta Pharmacol. Sin.* doi: 10.1038/s41401-023-01087-6. [Epub ahead of print].

Devinsky, O., Vezzani, A., Najjar, S., De Lanerolle, N. C., and Rogawski, M. A. (2013). Glia and epilepsy: excitability and inflammation. *Trends Neurosci.* 36, 174–184. doi: 10.1016/j.tins.2012.11.008

Devinsky, O., Vezzani, A., O'Brien, T. J., Jette, N., Scheffer, I. E., De Curtis, M., et al. (2018). Epilepsy. *Nat. Rev. Dis. Prim.* 4, 1–24. doi: 10.1038/nrdp.2018.24

Dimou, L., and Gallo, V. (2015). NG2-glia and their functions in the central nervous system. *Glia* 63, 1429–1451. doi: 10.1002/glia.22859

Dossi, E., Blauwblomme, T., Moulard, J., Chever, O., Vasile, F., Guinard, E., et al. (2018). Pannexin-1 channels contribute to seizure generation in human epileptic brain tissue and in a mouse model of epilepsy. *Sci. Transl. Med.* 10:eaar3796. doi: 10.1126/scitranslmed.aar3796

Dragunow, M. (1991). Adenosine and seizure termination. *Ann. Neurol.* 29:575. doi: 10.1002/ana.410290524

Dutuit, M., Didier-Bazès, M., Vergnes, M., Mutin, M., Conjard, A., Akaoka, H., et al. (2000). Specific alteration in the expression of glial fibrillary acidic protein, glutamate dehydrogenase, and glutamine synthetase in rats with genetic absence epilepsy. *Glia* 32, 15–24. doi: 10.1002/1098-1136(200010)32:1<15::AID-GLIA20>3.0.CO;2-#

Dutuit, M., Touret, M., Szymocha, R., Nehlig, A., Belin, M. F., and Didier-Bazès, M. (2002). Decreased expression of glutamate transporters in genetic absence epilepsy rats before seizure occurrence. *J. Neurochem.* 80, 1029–1038. doi: 10.1046/j.0022-3042.2002.00768.x

Eid, T., Lee, T.-S. W., Thomas, M. J., Amiry-Moghaddam, M., Bjørnsen, L. P., Spencer, D. D., et al. (2005). Loss of perivascular aquaporin 4 may underlie deficient water and K + homeostasis in the human epileptogenic hippocampus. *Proc. Natl. Acad. Sci.* 102, 1193–1198. doi: 10.1073/pnas.0409308102

Eraso-Pichot, A., Pouvreau, S., Olivera-Pinto, A., Gomez-Sotres, P., Skupio, U., and Marsicano, G. (2023). Endocannabinoid signaling in astrocytes. *Glia* 71, 44–59. doi: 10.1002/glia.24246

Eyo, U. B., Murugan, M., and Wu, L.-J. (2017). Microglia-neuron communication in epilepsy. *Glia* 65, 5–18. doi: 10.1002/glia.23006

Farina, C., Aloisi, F., and Meinl, E. (2007). Astrocytes are active players in cerebral innate immunity. *Trends Immunol.* 28, 138–145. doi: 10.1016/j.it.2007.01.005

Fellin, T., Pascual, O., Gobbo, S., Pozzan, T., Haydon, P. G., and Carmignoto, G. (2004). Neuronal synchrony mediated by astrocytic glutamate through activation of extrasynaptic NMDA receptors. *Neuron* 43, 729–743. doi: 10.1016/j.neuron.2004.08.011

Fisher, R. S., Cross, J. H., D'Souza, C., French, J. A., Haut, S. R., Higurashi, N., et al. (2017a). Instruction manual for the ILAE 2017 operational classification of seizure types. *Epilepsia* 58, 531–542. doi: 10.1111/EPI.13671

Fisher, R. S., Cross, J. H., French, J. A., Higurashi, N., Hirsch, E., Jansen, F. E., et al. (2017b). Operational classification of seizure types by the international league against epilepsy: position paper of the ILAE Commission for Classification and Terminology. *Epilepsia* 58, 522–530. doi: 10.1111/EPI.13670

Fisher, R. S., van Emde Boas, W., Blume, W., Elger, C., Genton, P., Lee, P., et al. (2005). Response: definitions proposed by the international league against epilepsy (ILAE) and the International Bureau for Epilepsy (IBE). *Epilepsia* 46, 1701–1702. doi: 10.1111/j.1528-1167.2005.00273_4.x

Fredholm, B. B. (2012). Rethinking the purinergic neuron–glia connection. *Proc. Natl. Acad. Sci.* 109, 5913–5914. doi: 10.1073/pnas.1203764109

Friedman, A., Kaufer, D., and Heinemann, U. (2009). Blood–brain barrier breakdown-inducing astrocytic transformation: novel targets for the prevention of epilepsy. *Epilepsy Res.* 85, 142–149. doi: 10.1016/j.eplepsyres.2009.03.005

Fu, L., Liu, K., Wake, H., Teshigawara, K., Yoshino, T., Takahashi, H., et al. (2017). Therapeutic effects of anti-HMGB1 monoclonal antibody on pilocarpine-induced status epilepticus in mice. *Sci. Rep.* 7:1179. doi: 10.1038/s41598-017-01325-y

Giannoni, P., Badaut, J., Dargazanli, C., De Maudave, A., Klement, V., Costalat, V., et al. (2018). The pericyte–glia interface at the blood–brain barrier. *Clin. Sci.* 132, 361–374. doi: 10.1042/CS20171634

Gigout, S., Louvel, J., and Pumain, R. (2006). Effects in vitro and in vivo of a gap junction blocker on epileptiform activities in a genetic model of absence epilepsy. *Epilepsy Res.* 69, 15–29. doi: 10.1016/j.eplepsyres.2005.12.002

Glötzner, F. L. (1973). Membrane properties of neuroglia in epileptogenic gliosis. *Brain Res.* 55, 159–171. doi: 10.1016/0006-8993(73)90495-2

Gobbo, D., Scheller, A., and Kirchhoff, F. (2021). From physiology to pathology of Cortico-Thalamo-cortical oscillations: Astroglia as a target for further research. *Front. Neurol.* 12:661408. doi: 10.3389/fneur.2021.661408

Goisis, R. C., Chiavegato, A., Gomez-Gonzalo, M., Marcon, I., Requie, L. M., Scholze, P., et al. (2022). GABA tonic currents and glial cells are altered during epileptogenesis in a mouse model of Dravet syndrome. *Front. Cell. Neurosci.* 16, 1–9. doi: 10.3389/fncel.2022.919493

Gómez-Gonzalo, M., Losi, G., Chiavegato, A., Zonta, M., Cammarota, M., Brondi, M., et al. (2010). An excitatory loop with astrocytes contributes to drive neurons to seizure threshold. *PLoS Biol.* 8:e1000352. doi: 10.1371/journal.pbio.1000352

Gouder, N., Scheurer, L., Fritschy, J. M., and Boison, D. (2004). Overexpression of adenosine kinase in epileptic hippocampus contributes to epileptogenesis. *J. Neurosci.* 24, 692–701. doi: 10.1523/JNEUROSCI.4781-03.2004

Grigorovsky, V., Breton, V. L., and Bardakjian, B. L. (2021). Glial modulation of electrical rhythms in a neuroglial network model of epilepsy. *IEEE Trans. Biomed. Eng.* 68, 2076–2087. doi: 10.1109/TBME.2020.3022332

Guo, M., Zhang, J., Wang, J., Wang, X., Gao, Q., Tang, C., et al. (2023). Aberrant adenosine signaling in patients with focal cortical dysplasia. *Mol. Neurobiol.* 60, 4396–4417. doi: 10.1007/s12035-023-03351-6

Halassa, M. M., Fellin, T., and Haydon, P. G. (2007). The tripartite synapse: roles for gliotransmission in health and disease. *Trends Mol. Med.* 13, 54–63. doi: 10.1016/j.molmed.2006.12.005

Halassa, M. M., and Haydon, P. G. (2010). Integrated brain circuits: astrocytic networks modulate neuronal activity and behavior. *Annu. Rev. Physiol.* 72, 335–355. doi: 10.1146/annurev-physiol-021909-135843

Hamid, S. H. M., Whittam, D., Saviour, M., Alorainy, A., Mutch, K., Linaker, S., et al. (2018). Seizures and encephalitis in myelin oligodendrocyte glycoprotein IgG disease vs aquaporin 4 IgG disease. *JAMA Neurol.* 75:65. doi: 10.1001/jamaneurol.2017.3196

Harada, K., Kamiya, T., and Tsuboi, T. (2016). Gliotransmitter release from astrocytes: functional, developmental, and pathological implications in the brain. *Front. Neurosci.* 9:499. doi: 10.3389/FNINS.2015.00499/BIBTEX

Heinemann, U., Gabriel, S., Jauch, R., Schulze, K., Kivi, A., Eilers, A., et al. (2000). Alterations of glial cell function in temporal lobe epilepsy. *Epilepsia* 41, S185–S189. doi: 10.1111/j.1528-1157.2000.tb01579.x

Heinemann, U., Kaufer, D., and Friedman, A. (2012). Blood-brain barrier dysfunction, TGFβ signaling, and astrocyte dysfunction in epilepsy. *Glia* 60, 1251–1257. doi: 10.1002/glia.22311

Héja, L., Nyitrai, G., Kékesi, O., Dobolyi, Á., Szabó, P., Fiáth, R., et al. (2012). Astrocytes convert network excitation to tonic inhibition of neurons. *BMC Biol.* 10, 1–21. doi: 10.1186/1741-7007-10-26

Hertz, L., and Zielke, H. R. (2004). Astrocytic control of glutamatergic activity: astrocytes as stars of the show. *Trends Neurosci.* 27, 735–743. doi: 10.1016/j.tins.2004.10.008

Heuser, K., de Curtis, M., and Steinhäuser, C. (2021). Editorial: glial dysfunction in Epileptogenesis. *Front. Neurol.* 12:716308. doi: 10.3389/fneur.2021.716308

Hirsch, E., French, J., Scheffer, I. E., Bogacz, A., Alsaadi, T., Sperling, M. R., et al. (2022). ILAE definition of the idiopathic generalized epilepsy syndromes: position statement by the ILAE task force on nosology and definitions. *Epilepsia* 63, 1475–1499. doi: 10.1111/epi.17236

Hong, S., He, J. C., Wu, J. W., Zhan, S. Q., Zhang, G. L., Wu, H. Q., et al. (2019). Losartan inhibits development of spontaneous recurrent seizures by preventing astrocyte activation and attenuating blood-brain barrier permeability following pilocarpine-induced status epilepticus. *Brain Res. Bull.* 149, 251–259. doi: 10.1016/j.brainresbull.2019.05.002

İdrizoğlu, M. G., Carcak, N., and Onat, F. Y. (2016). Managing epilepsy by modulating glia. *Anatomy* 10, 50–59. doi: 10.2399/ana.15.041

Ismail, F. S., Corvace, F., Faustmann, P. M., and Faustmann, T. J. (2021). Pharmacological investigations in glia culture model of inflammation. *Front. Cell. Neurosci.* 15:805755. doi: 10.3389/fncel.2021.805755

Ivens, S., Kaufer, D., Flores, L. P., Bechmann, I., Zumsteg, D., Tomkins, O., et al. (2007). TGF-receptor-mediated albumin uptake into astrocytes is involved in neocortical epileptogenesis. *Brain* 130, 535–547. doi: 10.1093/brain/awl317

Jabs, R., Seifert, G., and Steinhäuser, C. (2008). Astrocytic function and its alteration in the epileptic brain. *Epilepsia* 49, 3–12. doi: 10.1111/j.1528-1167.2008.01488.x

Jha, M. K., Jo, M., Kim, J. H., and Suk, K. (2019). Microglia-astrocyte crosstalk: an intimate molecular conversation. *Neuroscientist* 25, 227–240. doi: 10.1177/1073858418783959

Kang, N., Xu, J., Xu, Q., Nedergaard, M., and Kang, J. (2005). Astrocytic glutamate release-induced transient depolarization and epileptiform discharges in hippocampal CA1 pyramidal neurons. *J. Neurophysiol.* 94, 4121–4130. doi: 10.1152/jn.00448.2005

Kaur, C., and Ling, E. A. (2013). *Glial Cells: Embryonic Development, Types/Functions and Role in Disease*. New York, NY: Nova Science Publishers, Inc.

Kettenmann, H., and Ransom, B. R. (eds). (2004a) in *Neuroglia*. (New York, NY: Oxford University Press).

Kettenmann, H., and Ransom, B. R. (eds). (2004b). "The concept of neuroglia: a historical perspective" in *Neuroglia*. (New York, NY: Oxford University Press), 1–16.

Kettenmann, H., and Verkhratsky, A. (2008). Neuroglia: the 150 years after. *Trends Neurosci.* 31, 653–659. doi: 10.1016/j.tins.2008.09.003

Khakh, B. S., and Deneen, B. (2019). The emerging nature of astrocyte diversity. *Annu. Rev. Neurosci.* 42, 187–207. doi: 10.1146/annurev-neuro-070918-050443

Kim, Y. S., Choi, J., and Yoon, B.-E. (2020). Neuron-glia interactions in neurodevelopmental disorders. *Cells* 9:2176. doi: 10.3390/cells9102176

Kinboshi, M., Ikeda, A., and Ohno, Y. (2020). Role of astrocytic inwardly rectifying potassium (Kir) 4.1 channels in Epileptogenesis. *Front. Neurol.* 11:1832. doi: 10.3389/FNEUR.2020.626658/BIBTEX

Kitaura, H., Shirozu, H., Masuda, H., Fukuda, M., Fujii, Y., and Kakita, A. (2018). Pathophysiological characteristics associated with Epileptogenesis in human hippocampal sclerosis. *EBioMedicine* 29, 38–46. doi: 10.1016/j.ebiom.2018.02.013

Klune, J. R., Dhupar, R., Cardinal, J., Billiar, T. R., and Tsung, A. (2008). HMGB1: Endogenous Danger Signaling. *Mol. Med.* 14, 476–484. doi: 10.2119/2008-00034.Klune

Kobow, K., and Blumcke, I. (2011). The methylation hypothesis: do epigenetic chromatin modifications play a role in epileptogenesis? *Epilepsia* 52, 15–19. doi: 10.1111/j.1528-1167.2011.03145.x

Koh, W., Park, M., Chun, Y. E., Lee, J., Shim, H. S., Park, M. G., et al. (2022). Astrocytes render memory flexible by releasing D-serine and regulating NMDA receptor tone in the hippocampus. *Biol. Psychiatry* 91, 740–752. doi: 10.1016/j.biopsych.2021.10.012

Kovács, Z., Skatchkov, S. N., Szabó, Z., Qahtan, S., Méndez-González, M. P., Malpica-Nieves, C. J., et al. (2022). Putrescine intensifies Glu/GABA exchange mechanism and promotes early termination of seizures. *Int. J. Mol. Sci.* 23:8191. doi: 10.3390/ijms23158191

Kurosinski, P., and Götz, J. (2002). Glial cells under physiologic and pathologic conditions. *Arch. Neurol.* 59:1524. doi: 10.1001/archneur.59.10.1524

Lancaster, E., and Dalmau, J. (2012). Neuronal autoantigens–pathogenesis, associated disorders and antibody testing. *Nat. Rev. Neurol.* 8, 380–390. doi: 10.1038/nrneurol.2012.99

Lanerolle, N. C., Lee, T.-S., and Spencer, D. D. (2010). Astrocytes and epilepsy. *Neurotherapeutics* 7, 424–438. doi: 10.1016/j.nurt.2010.08.002

Lee, H. G., Wheeler, M. A., and Quintana, F. J. (2022). Function and therapeutic value of astrocytes in neurological diseases. *Nat. Rev. Drug Discov.* 21, 339–358. doi: 10.1038/s41573-022-00390-x

Lentini, C., D'Orange, M., Marichal, N., Trottmann, M.-M., Vignoles, R., Foucault, L., et al. (2021). Reprogramming reactive glia into interneurons reduces chronic seizure activity in a mouse model of mesial temporal lobe epilepsy. *Cell Stem Cell* 28, 2104–2121.e10. doi: 10.1016/j.stem.2021.09.002

Leo, A., Nesci, V., Tallarico, M., Amodio, N., Gallo Cantafio, E. M., De Sarro, G., et al. (2020). IL-6 receptor blockade by tocilizumab has anti-absence and anti-epileptogenic effects in the WAG/Rij rat model of absence epilepsy. *Neurotherapeutics* 17, 2004–2014. doi: 10.1007/s13311-020-00893-8

Li, T., Quan Lan, J., Fredholm, B. B., Simon, R. P., and Boison, D. (2007). Adenosine dysfunction in astrogliosis: cause for seizure generation? *Neuron Glia Biol.* 3, 353–366. doi: 10.1017/S1740925X0800015X

Lobsiger, C. S., and Cleveland, D. W. (2007). Glial cells as intrinsic components of non-cell-autonomous neurodegenerative disease. *Nat. Neurosci.* 10, 1355–1360. doi: 10.1038/nn1988

Löscher, W., and Friedman, A. (2020). Structural, molecular, and functional alterations of the blood-brain barrier during Epileptogenesis and epilepsy: a cause, consequence, or both? *Int. J. Mol. Sci.* 21:591. doi: 10.3390/ijms21020591

Losi, G., Cammarota, M., and Carmignoto, G. (2012). The role of astroglia in the epileptic brain. *Front. Pharmacol.* 3:132. doi: 10.3389/fphar.2012.00132

Magistretti, P. J. (2006). Neuron–glia metabolic coupling and plasticity. *J. Exp. Biol.* 209, 2304–2311. doi: 10.1242/jeb.02208

Maguire, J. (2016). Epileptogenesis: more than just the latent period. *Epilepsy Curr.* 16, 31–33. doi: 10.5698/1535-7597-16.1.31

Malva, J. O., Rego, A. C., Cunha, R. A., and Oliveira, C. R. (2007) in *Interaction Between Neurons and Glia in Aging and Disease*. eds. J. O. Malva, A. C. Rego, R. A. Cunha and C. R. O. Boston (MA: Springer US)

Maroso, M., Balosso, S., Ravizza, T., Liu, J., Aronica, E., Iyer, A. M., et al. (2010). Toll-like receptor 4 and high-mobility group box-1 are involved in ictogenesis and can be targeted to reduce seizures. *Nat. Med.* 16, 413–419. doi: 10.1038/nm.2127

Martins-Ferreira, R., Leal, B., Chaves, J., Li, T., Ciudad, L., Rangel, R., et al. (2022). Epilepsy progression is associated with cumulative DNA methylation changes in inflammatory genes. *Prog. Neurobiol.* 209:102207. doi: 10.1016/j.pneurobio.2021.102207

Matejuk, A., and Ransohoff, R. M. (2020). Crosstalk between astrocytes and microglia: an overview. *Front. Immunol.* 11:1416. doi: 10.3389/fimmu.2020.01416

Melø, T. M., Sonnewald, U., AinaBastholm, I., and Nehlig, A. (2007). Astrocytes may play a role in the etiology of absence epilepsy: a comparison between immature GAERS not yet expressing seizures and adults. *Neurobiol. Dis.* 28, 227–235. doi: 10.1016/j.nbd.2007.07.011

Melø, T. M., Sonnewald, U., Touret, M., and Nehlig, A. (2006). Cortical glutamate metabolism is enhanced in a genetic model of absence epilepsy. *J. Cereb. Blood Flow Metab.* 26, 1496–1506. doi: 10.1038/sj.jcbfm.9600300

Mermer, F., Poliquin, S., Zhou, S., Wang, X., Ding, Y., Yin, F., et al. (2022). Astrocytic GABA transporter 1 deficit in novel SLC6A1 variants mediated epilepsy: connected from protein destabilization to seizures in mice and humans. *Neurobiol. Dis.* 172:105810. doi: 10.1016/j.nbd.2022.105810

Muller, J., Timmermann, A., Henning, L., Muller, H., Steinhauser, C., and Bedner, P. (2020). Astrocytic GABA accumulation in experimental temporal lobe epilepsy. *Front. Neurol.* 11:614923. doi: 10.3389/fneur.2020.614923

Murphy, T. R., Binder, D. K., and Fiacco, T. A. (2017). Turning down the volume: astrocyte volume change in the generation and termination of epileptic seizures. *Neurobiol. Dis.* 104, 24–32. doi: 10.1016/j.nbd.2017.04.016

Nagai, J., Rajbhandari, A. K., Gangwani, M. R., Hachisuka, A., Coppola, G., Masmanidis, S. C., et al. (2019). Hyperactivity with disrupted attention by activation of an astrocyte Synaptogenic cue. *Cells* 177, 1280–1292.e20. doi: 10.1016/j.cell.2019.03.019

Nagy, J. I., and Rash, J. E. (2000). Connexins and gap junctions of astrocytes and oligodendrocytes in the CNS. *Brain Res. Rev.* 32, 29–44. doi: 10.1016/S0165-0173(99)00066-1

Natale, G., Limanaqi, F., Busceti, C. L., Mastroiacovo, F., Nicoletti, F., Puglisi-Allegra, S., et al. (2021). Glymphatic system as a gateway to connect neurodegeneration from periphery to CNS. *Front. Neurosci.* 15:92. doi: 10.3389/fnins.2021.639140

Neal, M., and Richardson, J. R. (2018). Epigenetic regulation of astrocyte function in neuroinflammation and neurodegeneration. *Biochim. Biophys. Acta Mol. basis Dis.* 1864, 432–443. doi: 10.1016/j.bbadis.2017.11.004

Nikolic, L., Shen, W., Nobili, P., Virenque, A., Ulmann, L., and Audinat, E. (2018). Blocking TNFα-driven astrocyte purinergic signaling restores normal synaptic activity during epileptogenesis. *Glia* 66, 2673–2683. doi: 10.1002/glia.23519

O'Connor, E. R., Sontheimer, H., Spencer, D. D., and Lanerolle, N. C. (1998). Astrocytes from human hippocampal epileptogenic foci exhibit action potential-like responses. *Epilepsia* 39, 347–354. doi: 10.1111/j.1528-1157.1998.tb01386.x

O'Callaghan, J. P., Kelly, K. A., Van Gilder, R. L., Sofroniew, M. V., and Miller, D. B. (2014). Early activation of STAT3 regulates reactive astrogliosis induced by diverse forms of neurotoxicity. *PLoS One* 9:e102003. doi: 10.1371/journal.pone.0102003

Ohno, Y., Kinboshi, M., and Shimizu, S. (2018). Inwardly rectifying potassium channel Kir4. 1 as a novel modulator of BDNF expression in astrocytes. *Int. J. Mol. Sci.* 19:3313. doi: 10.3390/ijms19113313

Onat, F. (2013). Astrocytes and absence epilepsy. *Br. J. Pharmacol.* 168, 1086–1087. doi: 10.1111/bph.12050

Onat, F. Y., van Luijtelaar, G., Nehlig, A., and Snead, O. C. (2013). The involvement of limbic structures in typical and atypical absence epilepsy. *Epilepsy Res.* 103, 111–123. doi: 10.1016/j.eplepsyres.2012.08.008

Ottestad-Hansen, S., Hu, Q. X., Follin-Arbelet, V. V., Bentea, E., Sato, H., Massie, A., et al. (2018). The cystine-glutamate exchanger (xCT, Slc7a11) is expressed in significant concentrations in a subpopulation of astrocytes in the mouse brain. *Glia* 66, 951–970. doi: 10.1002/glia.23294

Pandit, S., Neupane, C., Woo, J., Sharma, R., Nam, M., Lee, G., et al. (2020). Bestrophin1-mediated tonic GABA release from reactive astrocytes prevents the development of seizure-prone network in kainate-injected hippocampi. *Glia* 68, 1065–1080. doi: 10.1002/glia.23762

Parker, T. M., Nguyen, A. H., Rabang, J. R., Patil, A. A., and Agrawal, D. K. (2017). The danger zone: systematic review of the role of HMGB1 danger signaling in traumatic brain injury. *Brain Inj.* 31, 2–8. doi: 10.1080/02699052.2016.1217045

Peixoto-Santos, J. E., Kandratavicius, L., Velasco, T. R., Assirati, J. A., Carlotti, C. G., Scandiuzzi, R. C., et al. (2017). Individual hippocampal subfield assessment indicates that matrix macromolecules and gliosis are key elements for the increased T2 relaxation time seen in temporal lobe epilepsy. *Epilepsia* 58, 149–159. doi: 10.1111/epi.13620

Perez Velazquez, J. L., and Carlen, P. L. (2000). Gap junctions, synchrony and seizures. *Trends Neurosci.* 23, 68–74. doi: 10.1016/S0166-2236(99)01497-6

Peterson, A. R., and Binder, D. K. (2020). Astrocyte glutamate uptake and signaling as novel targets for Antiepileptogenic therapy. *Front. Neurol.* 11:1006. doi: 10.3389/fneur.2020.01006

Pitkänen, A., and Lukasiuk, K. (2009). Molecular and cellular basis of epileptogenesis in symptomatic epilepsy. *Epilepsy Behav.* 14, 16–25. doi: 10.1016/j.yebeh.2008.09.023

Pollen, D. A., and Trachtenberg, M. C. (1970). Neuroglia: gliosis and focal epilepsy. *Science* 167, 1252–1253. doi: 10.1126/science.167.3922.1252

Purnell, B. S., Alves, M. P., and Boison, D. (2023). Astrocyte-neuron circuits in epilepsy. *Neurobiol. Dis.* 179:106058. doi: 10.1016/j.nbd.2023.106058

Ransom, C. B., and Blumenfeld, H. (2007). "Acquired epilepsy: cellular and molecular mechanisms" in *Molecular Neurology*. ed. S. G. Waxman (Burlington (MA): Elsevier Academic Press), 347–370.

Reddy, O. C., and van der Werf, Y. D. (2020). The sleeping brain: harnessing the power of the Glymphatic system through lifestyle choices. *Brain Sci.* 10:868. doi: 10.3390/brainsci10110868

Riazi, K., Galic, M. A., and Pittman, Q. J. (2010). Contributions of peripheral inflammation to seizure susceptibility: cytokines and brain excitability. *Epilepsy Res.* 89, 34–42. doi: 10.1016/j.eplepsyres.2009.09.004

Robert, S. M., Buckingham, S. C., Campbell, S. L., Robel, S., Holt, K. T., Ogunrinu-Babarinde, T., et al. (2015). SLC7A11 expression is associated with seizures and predicts poor survival in patients with malignant glioma. *Sci. Transl. Med.* 7:289ra86. doi: 10.1126/scitranslmed.aaa8103

Rosciszewski, G., Cadena, V., Auzmendi, J., Cieri, M. B., Lukin, J., Rossi, A. R., et al. (2019). Detrimental effects of HMGB-1 require microglial-Astroglial interaction: implications for the status epilepticus -induced Neuroinflammation. *Front. Cell. Neurosci.* 13:380. doi: 10.3389/fncel.2019.00380

Rossi, A. R., Angelo, M. F., Villarreal, A., Lukin, J., and Ramos, A. J. (2013). Gabapentin administration reduces reactive gliosis and neurodegeneration after pilocarpine-induced status epilepticus. *PLoS One* 8:e78516. doi: 10.1371/journal.pone.0078516

Rossi, A., Murta, V., Auzmendi, J., and Ramos, A. J. (2017). Early gabapentin treatment during the latency period increases convulsive threshold, reduces microglial activation and macrophage infiltration in the Lithium-pilocarpine model of epilepsy. *Pharmaceuticals (Basel)* 10:93. doi: 10.3390/ph10040093

Saha, R. N., Liu, X., and Pahan, K. (2006). Up-regulation of BDNF in astrocytes by TNF-alpha: a case for the neuroprotective role of cytokine. *J. NeuroImmune Pharmacol.* 1, 212–222. doi: 10.1007/s11481-006-9020-8

Saijo, K., and Glass, C. K. (2011). Microglial cell origin and phenotypes in health and disease. *Nat. Rev. Immunol.* 11, 775–787. doi: 10.1038/nri3086

Sandau, U. S., Yahya, M., Bigej, R., Friedman, J. L., Saleumvong, B., and Boison, D. (2019). Transient use of a systemic adenosine kinase inhibitor attenuates epilepsy development in mice. *Epilepsia* 60, 615–625. doi: 10.1111/epi.14674

Sano, F., Shigetomi, E., Shinozaki, Y., Tsuzukiyama, H., Saito, K., Mikoshiba, K., et al. (2021). Reactive astrocyte-driven epileptogenesis is induced by microglia initially activated following status epilepticus. *JCI Insight* 6:e135391. doi: 10.1172/jci.insight.135391

Satta, V., Alonso, C., Díez, P., Martín-Suárez, S., Rubio, M., Encinas, J. M., et al. (2021). Neuropathological characterization of a Dravet syndrome Knock-in mouse model useful

for investigating cannabinoid treatments. *Front. Mol. Neurosci.* 13:602801. doi: 10.3389/fnmol.2020.602801

Scharfman, H. E. (2005). Brain-derived neurotrophic factor and epilepsy—a missing link? *Epilepsy Curr.* 5, 83–88. doi: 10.1111/j.1535-7511.2005.05312.x

Scheffer, I. E., Berkovic, S., Capovilla, G., Connolly, M. B., French, J., Guilhoto, L., et al. (2017). ILAE classification of the epilepsies: position paper of the ILAE Commission for Classification and Terminology. *Epilepsia* 58, 512–521. doi: 10.1111/epi.13709

Seifert, G., Carmignoto, G., and Steinhäuser, C. (2010). Astrocyte dysfunction in epilepsy. *Brain Res. Rev.* 63, 212–221. doi: 10.1016/j.brainresrev.2009.10.004

Semyanov, A., and Verkhratsky, A. (2021). Astrocytic processes: from tripartite synapses to the active milieu. *Trends Neurosci.* 44, 781–792. doi: 10.1016/j.tins.2021.07.006

Sha, L., Wang, X., Li, J., Shi, X., Wu, L., Shen, Y., et al. (2017). Pharmacologic inhibition of Hsp90 to prevent GLT-1 degradation as an effective therapy for epilepsy. *J. Exp. Med.* 214, 547–563. doi: 10.1084/jem.20160667

Soulet, D., and Rivest, S. (2008). Microglia. *Curr. Biol.* 18, R506–R508. doi: 10.1016/j.cub.2008.04.047

Srinivasan, R., Lu, T. Y., Chai, H., Xu, J., Huang, B. S., Golshani, P., et al. (2016). New transgenic mouse lines for selectively targeting astrocytes and studying calcium signals in astrocyte processes in situ and in vivo. *Neuron* 92, 1181–1195. doi: 10.1016/j.neuron.2016.11.030

Steinborn, B., Zarowski, M., Winczewska-Wiktor, A., Wójcicka, M., Młodzikowska-Albrecht, J., and Losy, J. (2014). Concentration of Il-1β, Il-2, Il-6, TNFα in the blood serum in children with generalized epilepsy treated by valproate. *Pharmacol. Rep.* 66, 972–975. doi: 10.1016/j.pharep.2014.06.005

Steinhäuser, C., and Seifert, G. (2002). Glial membrane channels and receptors in epilepsy: impact for generation and spread of seizure activity. *Eur. J. Pharmacol.* 447, 227–237. doi: 10.1016/S0014-2999(02)01846-0

Steinhäuser, C., Seifert, G., and Bedner, P. (2012). Astrocyte dysfunction in temporal lobe epilepsy: K + channels and gap junction coupling. *Glia* 60, 1192–1202. doi: 10.1002/glia.22313

Stephan, J., Eitelmann, S., and Zhou, M. (2021). Approaches to study gap junctional coupling. *Front. Cell. Neurosci.* 15:640406. doi: 10.3389/fncel.2021.640406

Suto, T., Severino, A. L., Eisenach, J. C., and Hayashida, K. I. (2014). Gabapentin increases extracellular glutamatergic level in the locus coeruleus via astroglial glutamate transporter-dependent mechanisms. *Neuropharmacology* 81, 95–100. doi: 10.1016/j.neuropharm.2014.01.040

Terstappen, G. C., Meyer, A. H., Bell, R. D., and Zhang, W. (2021). Strategies for delivering therapeutics across the blood–brain barrier. *Nat. Rev. Drug Discov.* 20, 362–383. doi: 10.1038/s41573-021-00139-y

Thomas, A. X., Cruz Del Angel, Y., Gonzalez, M. I., Carrel, A. J., Carlsen, J., Lam, P. M., et al. (2016). Rapid increases in proBDNF after pilocarpine-induced status epilepticus in mice are associated with reduced proBDNF cleavage machinery. *eneuro* 3:ENEURO.0020-15.2016. doi: 10.1523/ENEURO.0020-15.2016

Thompson, J. A., Miralles, R. M., Wengert, E. R., Wagley, P. K., Yu, W., Wenker, I. C., et al. (2022). Astrocyte reactivity in a mouse model of SCN8A epileptic encephalopathy. *Epilepsia Open* 7, 280–292. doi: 10.1002/epi4.12564

Tian, G.-F., Azmi, H., Takano, T., Xu, Q., Peng, W., Lin, J., et al. (2005). An astrocytic basis of epilepsy. *Nat. Med.* 11, 973–981. doi: 10.1038/nm1277

Tice, C., McDevitt, J., and Langford, D. (2020). Astrocytes, HIV and the Glymphatic system: a disease of disrupted waste management? *Front. Cell. Infect. Microbiol.* 10:521. doi: 10.3389/FCIMB.2020.523379/BIBTEX

Touret, M., Parrot, S., Denoroy, L., Belin, M. F., and Didier-Bazes, M. (2007). Glutamatergic alterations in the cortex of genetic absence epilepsy rats. *BMC Neurosci.* 8, 1–7. doi: 10.1186/1471-2202-8-69

Twible, C., Abdo, R., and Zhang, Q. (2021). Astrocyte role in temporal lobe epilepsy and development of mossy fiber sprouting. *Front. Cell. Neurosci.* 15:725693. doi: 10.3389/fncel.2021.725693

van Luijtelaar, G., Lyashenko, S., Vastyanov, R., Verbeek, G., Oleinik, A., van Rijn, C., et al. (2012). Cytokines and absence seizures in a genetic rat model. *Neurophysiology* 43, 478–486. doi: 10.1007/s11062-012-9252-6

Varvel, N. H., Neher, J. J., Bosch, A., Wang, W., Ransohoff, R. M., Miller, R. J., et al. (2016). Infiltrating monocytes promote brain inflammation and exacerbate neuronal damage after status epilepticus. *Proc. Natl. Acad. Sci. U. S. A.* 113, E5665–E5674. doi: 10.1073/pnas.1604263113

Verhoog, Q. P., Holtman, L., Aronica, E., and van Vliet, E. A. (2020). Astrocytes as guardians of neuronal excitability: mechanisms underlying epileptogenesis. *Front. Neurol.* 11:1541. doi: 10.3389/fneur.2020.591690

Verkhratsky, A., and Butt, A. (2013). *Glial Physiology and Pathophysiology*. Chichester, UK: John Wiley & Sons, Ltd

Vezzani, A., Aronica, E., Mazarati, A., and Pittman, Q. J. (2013). Epilepsy and brain inflammation. *Exp. Neurol.* 244, 11–21. doi: 10.1016/j.expneurol.2011.09.033

Vezzani, A., and Friedman, A. (2011). Brain inflammation as a biomarker in epilepsy. *Biomark. Med* 5, 607–614. doi: 10.2217/bmm.11.61

Vezzani, A., Ravizza, T., Bedner, P., Aronica, E., Steinhäuser, C., and Boison, D. (2022). Astrocytes in the initiation and progression of epilepsy. *Nat. Rev. Neurol.* 18, 707–722. doi: 10.1038/s41582-022-00727-5

Volnova, A., Tsytsarev, V., Ganina, O., Vélez-Crespo, G. E., Alves, J. M., Ignashchenkova, A., et al. (2022). The anti-epileptic effects of Carbenoxolone in vitro and in vivo. *Int. J. Mol. Sci.* 23:663. doi: 10.3390/ijms23020663

Volterra, A., and Meldolesi, J. (2005). Astrocytes, from brain glue to communication elements: the revolution continues. *Nat. Rev. Neurosci.* 6, 626–640. doi: 10.1038/nrn1722

Wallraff, A., Köhling, R., Heinemann, U., Theis, M., Willecke, K., and Steinhäuser, C. (2006). The impact of astrocytic gap junctional coupling on potassium buffering in the Hippocampus. *J. Neurosci.* 26, 5438–5447. doi: 10.1523/JNEUROSCI.0037-06.2006

Walrave, L., Vinken, M., Leybaert, L., and Smolders, I. (2020). Astrocytic connexin43 channels as candidate targets in epilepsy treatment. *Biomol. Ther.* 10, 1–32. doi: 10.3390/biom10111578

Wang, G., Wang, J., Xin, C., Xiao, J., Liang, J., and Wu, X. (2021). Inflammatory response in epilepsy is mediated by glial cell gap junction pathway (review). *Mol. Med. Rep.* 24:493. doi: 10.3892/mmr.2021.12132

Wetherington, J., Serrano, G., and Dingledine, R. (2008). Astrocytes in the epileptic brain. *Neuron* 58, 168–178. doi: 10.1016/j.neuron.2008.04.002

Williams-Karnesky, R. L., Sandau, U. S., Lusardi, T. A., Lytle, N. K., Farrell, J. M., Ignashchenkova, A., et al. (2013). Epigenetic changes induced by adenosine augmentation therapy prevent epileptogenesis. *J. Clin. Invest.* 123, 3552–3563. doi: 10.1172/JCI65636

Wong, M. (2019). The role of glia in epilepsy, intellectual disability, and other neurodevelopmental disorders in tuberous sclerosis complex. *J. Neurodev. Disord.* 11:30. doi: 10.1186/s11689-019-9289-6

Xie, Y., Yu, N., Chen, Y., Zhang, K., Ma, H. Y., and di, Q. (2017). HMGB1 regulates P-glycoprotein expression in status epilepticus rat brains via the RAGE/NF-κB signaling pathway. *Mol. Med. Rep.* 16, 1691–1700. doi: 10.3892/mmr.2017.6772

Xu, D., Robinson, A. P., Ishii, T., Duncan, D. S., Alden, T. D., Goings, G. E., et al. (2018). Peripherally derived T regulatory and gammadelta T cells have opposing roles in the pathogenesis of intractable pediatric epilepsy. *J. Exp. Med.* 215, 1169–1186. doi: 10.1084/jem.20171285

Xu, H., Zhang, H., Zhang, J., Huang, Q., Shen, Z., and Wu, R. (2016). Evaluation of neuron-glia integrity by in vivo proton magnetic resonance spectroscopy: implications for psychiatric disorders. *Neurosci. Biobehav. Rev.* 71, 563–577. doi: 10.1016/j.neubiorev.2016.09.027

Yamamura, S., Hoshikawa, M., Dai, K., Saito, H., Suzuki, N., Niwa, O., et al. (2013). ONO-2506 inhibits spike-wave discharges in a genetic animal model without affecting traditional convulsive tests via gliotransmission regulation. *Br. J. Pharmacol.* 168, 1088–1100. doi: 10.1111/j.1476-5381.2012.02132.x

Yamanaka, G., Morichi, S., Takamatsu, T., Watanabe, Y., Suzuki, S., Ishida, Y., et al. (2021b). Links between immune cells from the periphery and the brain in the pathogenesis of epilepsy: a narrative review. *Int. J. Mol. Sci.* 22:4395. doi: 10.3390/ijms22094395

Yamanaka, G., Takata, F., Kataoka, Y., Kanou, K., Morichi, S., Dohgu, S., et al. (2021a). The neuroinflammatory role of pericytes in epilepsy. *Biomedicine* 9:759. doi: 10.3390/biomedicines9070759

Yang, I., Han, S. J., Kaur, G., Crane, C., and Parsa, A. T. (2010). The role of microglia in central nervous system immunity and glioma immunology. *J. Clin. Neurosci.* 17, 6–10. doi: 10.1016/j.jocn.2009.05.006

Yang, L., Zhou, Y., Jia, H., Qi, Y., Tu, S., and Shao, A. (2020). Affective immunology: the crosstalk between microglia and astrocytes plays key role? *Front. Immunol.* 11:1818. doi: 10.3389/fimmu.2020.01818

Yoshizumi, M., Eisenach, J. C., and Hayashida, K. (2012). Riluzole and gabapentinoids activate glutamate transporters to facilitate glutamate-induced glutamate release from cultured astrocytes. *Eur. J. Pharmacol.* 677, 87–92. doi: 10.1016/j.ejphar.2011.12.015

Zamanian, J. L., Xu, L., Foo, L. C., Nouri, N., Zhou, L., Giffard, R. G., et al. (2012). Genomic analysis of reactive Astrogliosis. *J. Neurosci.* 32, 6391–6410. doi: 10.1523/JNEUROSCI.6221-11.2012

Zattoni, M., Mura, M. L., Deprez, F., Schwendener, R. A., Engelhardt, B., Frei, K., et al. (2011). Brain infiltration of leukocytes contributes to the pathophysiology of temporal lobe epilepsy. *J. Neurosci.* 31, 4037–4050. doi: 10.1523/JNEUROSCI.6210-10.2011

Zhao, J., Sun, J., Zheng, Y., Zheng, Y., Shao, Y., Li, Y., et al. (2022). Activated astrocytes attenuate neocortical seizures in rodent models through driving Na+-K+-ATPase. *Nat. Commun.* 13:7136. doi: 10.1038/s41467-022-34662-2

Zhao, J., Wang, Y., Xu, C., Liu, K., Wang, Y., Chen, L., et al. (2017). Therapeutic potential of an anti-high mobility group box-1 monoclonal antibody in epilepsy. *Brain Behav. Immun.* 64, 308–319. doi: 10.1016/j.bbi.2017.02.002

Frontiers in
Molecular Neuroscience

Leading research into the brain's molecular structure, design and function

Part of the most cited neuroscience series, this journal explores and identifies key molecules underlying the structure, design and function of the brain across all levels.

Discover the latest Research Topics

See more →

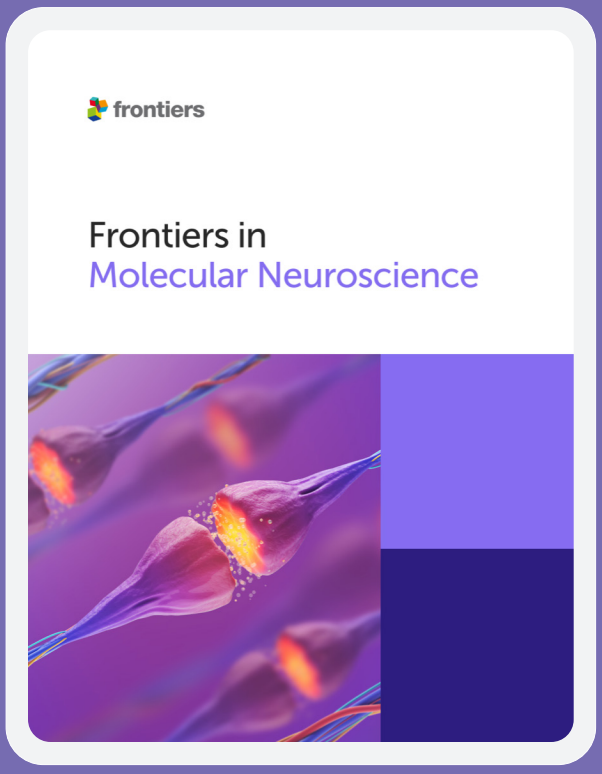

Frontiers

Avenue du Tribunal-Fédéral 34
1005 Lausanne, Switzerland
frontiersin.org

Contact us

+41 (0)21 510 17 00
frontiersin.org/about/contact